MICROWAVE ULTRASONICS
IN SOLID STATE PHYSICS

J. W. TUCKER
V. W. RAMPTON

NORTH-HOLLAND PUBLISHING COMPANY

microwave ultrasonics
in solid state physics

microwave ultrasonics
in solid state physics

J. W. TUCKER

University of Sheffield

and

V. W. RAMPTON

University of Nottingham

Publishers:

·NORTH-HOLLAND PUBLISHING COMPANY – AMSTERDAM

Sole distributors for the U.S.A. and Canada:

AMERICAN ELSEVIER PUBLISHING COMPANY, INC.
52 VANDERBILT AVENUE, NEW YORK, N.Y. 10017

Printed in The Netherlands

With the recent growth in the use of ultrasonics as a method of exploring the physics of the solid state, we feel that the time is right for the production of a book dealing exclusively with this topic. The greatest advances over the last few years have been in the microwave frequency range — frequencies in excess of 1 GHz — and for this reason we have limited discussion to those topics where waves of such frequencies have been, or may be gainfully employed. Hence some topics, for example acoustic paramagnetic resonance, are treated in greater depth than others. The chapter on metals is thus relatively short since many of the experiments on these materials utilize waves of much lower frequency and subjects such as the study of nuclear spins by acoustic excitation and the properties of surface waves have been omitted altogether.

We have divided the book broadly into two parts. The first part is concerned with the techniques used and the basic physical principles involved in the generation and detection of microwave ultrasonics. The second part, which is of most interest to the solid state physicist, deals in detail with the interaction of these high frequency waves with thermal phonons, paramagnetic centres, magnons, charged carriers in semiconductors and metals and with light waves. Introductory sections providing background to topics such as elasticity theory have also been included to enable the book to be read by the first year post-graduate student. The book is intended primarily for post-graduate students in solid state physics and the research worker who is new to the field of microwave ultrasonics and desires a text on the physical principles involved.

We are extremely grateful for many valuable discussions with friends and colleagues, especially Professor K. W. H. Stevens who first interested us in the subject of microwave ultrasonics. A number of

authors have kindly granted us permission to make use of figures from their original papers; to these acknowledgement has been made in the text.

The manuscript was completed in early 1971 and the bibliography includes references up to that time.

ERRATA

p. 181, the caption to fig. 5.9 should read (Reproduced from H. MATTHEWS and F.R. MORGENTHALER, Phys. Rev. Lett. 13, 616 (1964) with permission.).

p. 234, l. 25 should read "... and $A_4^2 H^2 |\langle S_z \rangle| / \hbar$ playing ...".

p. 235, l. 21 should read "... is replaced by $A_3^2 H^2 \omega_0 |\langle S_z \rangle| / \hbar$ and ...".

p. 275, l. 15 should read "... rate $\boldsymbol{\hat{u}} \cdot n_0 m(\langle \boldsymbol{v}_e \rangle - \boldsymbol{\hat{u}}) / \tau_{av}$".

CONTENTS

INTRODUCTION

During the last decade methods have become available for generating mechanical waves in solids at frequencies in excess of 1 GHz. The name 'microwave ultrasonics' has been adopted when discussing waves of this frequency because electromagnetic waves in the same frequency range have for a long time been termed microwaves. It should be realized though, that because the speed of sound in crystalline solids is generally about 10^5 times slower than that of light, the wavelength of microwave ultrasound is considerably shorter than the centimetre wavelength characteristic of these electromagnetic waves. In fact, for a velocity of sound of 2×10^5 cm/sec a wave of frequency 5 GHz has a wavelength of only 4×10^{-5} cm, that is, about a thousand lattice spacings.

As well as these bulk waves in solids it is also possible to generate mechanical waves on the surface of a solid whose amplitude decays rapidly as a function of depth within the solid. These Rayleigh waves have also been increasingly studied in recent years at high frequencies and show great promise for use in electronic devices as delay lines and filters. However this book will not discuss them further although methods are being developed to extend the study of surface waves into the gigahertz region. A useful review of surface waves on solids at high frequencies is by DRANSFELD and SALZMANN[1970].

In the following chapters an account is given of the propagation of microwave ultrasound in different types of solid and the interaction of the ultrasonic waves with thermal phonons, spins of paramagnetic centres and ferromagnetic ions, free electrons in metals and semi-conductors. There is, of course, an intrinsic interest in these phenomena for their own sake but the connection with the thermal properties of solids gives an added significance. For example, thermal conductivity measures the propagation of thermal phonons through a material and in the case of a paramagnetic dielectric at low temperature there is a magnetic field-dependent thermal resistivity; this is

closely related to the acoustic paramagnetic resonance attenuation of microwave ultrasound. Thermal conductivity employs a band of frequencies and thus the interpretation of results involves some sort of averaging but except at the lowest temperatures the dominant frequencies are much higher than can be achieved ultrasonically.

At very low frequencies – long wavelengths – the mechanical vibrations of a solid can be discussed within the framework of an elasticity theory that treats the solid as if it were a continuum rather than an array of discrete atoms. This picture is satisfactory as long as the variation in particle displacement from one atomic cell to the next is relatively small but it breaks down completely for very high frequency vibrations where the wavelength is relatively short. The relationship between frequency and wave-number is then no longer linear as predicted by elasticity theory but rather, dispersion occurs. More important though is that the periodicity of the lattice causes the appearance of frequency bands outside of which plane wave propagation through the lattice is not possible. This type of band structure occurs whenever periodicity is present, for example, it occurs in the band theory of the electronic structure of solids necessary to explain the difference between conductors, semiconductors and insulators and in the propagation of electromagnetic waves along periodic transmission lines. This distinction between an elasticity theory and a lattice dynamics treatment is more fully explained in the next chapter where an account of both theories is given. The upper end of the microwave frequency range roughly straddles the region where dispersion becomes important so both types of theory prove useful when discussing microwave ultrasonics.

Thermal excitation within the crystal causes the generation of lattice waves over the whole frequency spectrum. In quantum theory the vibrational energy associated with each frequency is quantized in discrete amounts each of magnitude $h\nu$ and these are known as phonons by analogy with the photons of electromagnetic radiation. As explained in ch. 2, although a lattice wave extends throughout the whole volume of the solid, wave packets which are highly localized in space may be constructed. The phonons associated with the excitation of these localized wave packets may then be regarded as particles moving through the solid. This would seem to be a more appropriate description for dealing with events of an essential local character such as the interaction of lattice vibrations with a localized impurity atom. On the other hand it is clear that as the wave packet travels through the lattice the presence of dispersion will cause it to be distorted so that it will spread out as it propagates. The idea of a local excitation then breaks down so there is obviously some limitation to the type of

problem for which the particle concept is useful. It turns out that the treatment of lattice vibrations on a wave and corpuscular basis both merit attention, the usefulness of each being dictated by the problem under consideration.

As has been indicated, in thermal excitation a distribution of frequencies rather than a mode of definite wave-number and polarization is excited. To get some idea of the mean frequency of the modes excited the quantity $h\nu$ can be set equal to the mean thermal energy KT. At room temperature the mean frequency, KT/h, is of the order of 6×10^{12} Hz, considerably higher than the microwave frequency range. However, many of the most interesting properties in solid-state physics occur in the liquid helium temperature range where the corresponding frequency will be much lower. For instance, at 1 K the mean value of ν will be ≈ 20 GHz, towards the upper end of the microwave frequency range. There is thus a considerable motivation for developing techniques whereby high frequency microwave phonons can be generated directly. Such methods enable the behaviour of these phonons to be studied in detail at separate fixed frequencies thereby eliminating the need to interpret data involving complicated thermal distributions of phonons as occurs in experiments involving measurements of specific heat, thermal conductivity etc. So far the most extensive investigation using microwave ultrasonics has been mainly concerned with frequencies below about 20 GHz but it is hoped that in the near future a wealth of information will come from experiments at higher frequencies since it is now feasible to generate coherent phonons at frequencies as high as 100 GHz.

The generation and detection of microwave ultrasonics is the topic treated in ch. 3. Basically the methods involve the conversion of microwave electromagnetic energy into acoustic energy by means of a transducer. Historically, the most widely used method for producing ultrasonic waves in the megacycle frequency range employed the use of piezoelectric materials such as quartz to form a resonant transducer. In certain crystallographic directions in a piezoelectric material the application of an electric field produces a strain proportional to the applied field. Whereas at low frequencies it is possible to generate ultrasonic waves by placing the piezoelectric material between the capacitor plates of a conventional resonant circuit, at microwave frequencies microwave circuits or transmission line techniques must be employed. For a resonant transducer its length must be chosen such that a standing wave pattern can be set up–that is its length must just contain an integral number of half-wavelengths of the ultrasonic wave. To get a good resonator the number of half-wavelengths, n, in its length must be small for if the wave loses energy by attenuation it will not be

possible to obtain a good standing wave pattern. In materials such as quartz the attenuation of the ultrasonics is severe at room temperatures so the wave generated at one end of the transducer will be to all intents and purposes lost before it reaches the opposite end. A standing wave pattern can therefore not be set up since the reflected wave will have an amplitude considerably reduced compared to that of the initial wave train. To avoid this the experiments at high frequencies must be performed at low temperatures in the liquid helium range and a low harmonic must be used. Because a relatively low harmonic must be used the extensive use of a normal quartz transducer into the microwave frequency range is prohibitive since the thickness of the transducer must be extremely small. For instance taking the velocity of sound in quartz as 5.7×10^5 cm/sec the wavelength at 1 GHz is 5.7×10^{-4} cm so a very thin wafer must be used. RINGO *et al.* [1947] performed experiments at frequencies up to 1·3 GHz using wafers of quartz only 0.038 cm thick. The technical difficulties involved in the preparation of these thin wafers is great because if the resonator is to work, the end faces must be flat and parallel to less than a wavelength of sound, which at frequencies around 10 GHz means that the preparation of the surfaces must be to optical standards. In the upper microwave frequency range, resonant transducer techniques can only be used with piezoelectric materials which may be deposited in the form of thin films. The most common example is cadmium sulphide although zinc oxide, zinc sulphide, lithium niobate and other piezoelectric materials have been used. The development and use of these transducers is discussed in ch. 3.

To avoid the difficulties associated with the production of these resonant transducers Baranskii, and Bömmel and Dransfeld developed a technique not requiring thin resonant thicknesses of quartz. The basic difference in the design of their experiments was that instead of the use of continuous ultrasonic waves, ultrasonic pulses of short duration were used. The transducer consists of a quartz rod, one end of which is placed in a microwave cavity. When the cavity is pulse excited with electromagnetic energy of a definite frequency an electromagnetic field is set up at the end of the rod and this, because of the piezoelectric properties of the quartz, causes a mechanical disturbance of the same frequency to be generated. In this way an ultrasonic pulse is launched from the end face of the quartz rod and propagates along it. When it has travelled the length of the rod it is reflected from the end face and on returning to the original end it will re-excite an electromagnetic pulse in the cavity by means of the inverse piezoelectric effect and can therefore be detected. To measure the velocity of the ultrasonic pulse, all that is required is a knowledge of the length of the rod and a measure

of the transit time between the launching and the arrival back of the first echo. For a good rod the pulse may continue to be reflected up and down the rod many times and a measure of the relative amplitudes of successive pulses as they reach the detector provides a means of measuring the ultrasonic attenuation. For the transducer to work successfully, accurate orientation of the crystallographic axis for plane wave propagation is required and again the end faces must be polished to a high degree of flatness and made accurately parallel. This is essential if the ultrasonic echo is to be detected, for the electric field generated by the inverse piezoelectric effect must be in step right across the end face of the rod if a true measure of the ultrasonic amplitude is to be obtained.

If experiments are to be performed on materials which are non-piezoelectric, then the sample has to be bonded onto a suitable transducer in some way. With a non-resonant bulk transducer an adhesive has to be found that will successfully transmit the ultrasonic wave from transducer to specimen without distortion. Alternatively if a thin film transducer is used, this may be deposited straight onto the sample. The relative merits of these two types of system are discussed in §3.6 of ch. 3.

Another method of producing microwave ultrasonics dispenses with piezoelectric generation and uses magnetostriction instead. A suitable ferromagnetic material is deposited on the end of the sample to be studied and this is placed in a microwave cavity which is pulse excited as before but now the generating surface is positioned in a region of strong magnetic field. A static magnetic field is also applied, usually perpendicular to the polished surface. The combination of these two fields causes the magnetization to precess about the static field direction and the amplitude of the precession is a maximum when the magnetic field is adjusted for resonance. Because of magnetostriction the precessing magnetization is accompanied by an alternating mechanical disturbance which launches an ultrasonic wave along the sample. The theory of this generation is given in ch. 3§4.2. For the geometry of magnetic fields normally employed it leads to the generation of shear waves. The generation of microwave ultrasonics by this method was initiated by the work of BÖMMEL and DRANSFELD[1959c] at 1 GHz and was later extended to 9 GHz by POMERANTZ[1961]. In addition to this work employing thin films, the generation of microwave ultrasonics in bulk ferromagnetic dielectrics is possible and this is discussed in ch. 5.

As soon as the successful generation and detection of microwave ultrasonics was achieved it was natural to see in what areas of research they could usefully be employed for probing the properties of the solid state. Naturally, if the ultrasonic wave is to act as a probe the prop-

erties of the solid that are of interest are those that are strongly depend-
ent upon the vibrational motion of the atoms. The first type of interac-
tion that springs to mind is the interaction between the different modes
of vibrations themselves. The normal modes of vibration of the lattice
are only independent within the framework of a harmonic theory. That
is to say it is assumed that the potential energy can be expanded in a
Taylor expansion about the equilibrium position with only the terms up
to those quadratic in the relative displacement of the neighbouring
atoms retained. In a continuum theory the equivalent statement is
that the elastic energy density is a quadratic function of the strain. In
other words this implies that in a discrete lattice model the force on a
particular atom depends linearly on its displacement relative to that of
the neighbouring atoms while in the continuum approach, Hooke's
law – stress is proportional to strain – is valid. In order to extend the
theory of elasticity to account for anharmonic effects, terms cubic in
the strain tensor should be included in the expression for the potential
energy function. It should be remembered though that in the classical
theory of elasticity the usual definition of the strain tensor is based on
the assumption of infinitesimal strains so that if a term cubic in the
strain tensor is to be included in the potential energy function, the full
deformation tensor for finite deformations should be used. This is
discussed in §1 of ch. 4. The new coefficients in the theory are known
as the third-order elastic moduli. It is clear that while it is the second-
order moduli that determine the velocity of the stress wave in a purely
elastic solid, it is the third- and higher-order moduli that determine the
velocity changes and attenuation due to the intermode coupling. Mea-
surements of the ultrasonic velocity and attentuation allow these con-
stants to be determined experimentally. A knowledge of these higher-
order elastic constants is important because they allow calculations of
quantities like thermal expansion to be made. In a lattice dynamics
theory, if the interaction between the different modes of vibration is to
be considered, the anharmonic terms must be retained in the expansion
of the potential energy term in the Hamiltonian. The first anharmonic
term will be cubic in the relative displacements of the atoms and leads
to processes in a phonon picture in which either a phonon can dissociate
into two phonons of lower energy or alternatively two phonons can
combine to give a third. In all these three-phonon processes energy
has to be conserved but the processes fall into two categories normal
or Umklapp, depending on whether the crystal momentum is conserved
or changes. The periodicity of the crystal lattice allows the crystal
momentum to change by an amount $\hbar G$, G being a reciprocal lattice
vector. The necessity of having to satisfy both the energy and the
momentum requirements leads to a number of selection rules that

restrict the types of three-phonon processes that can occur. For instance it is found that in a non-dispersive isotropic medium a longitudinal microwave phonon cannot decay by interaction with the thermal phonons. A lengthy account of these selection rules is given in ch. 4§2 and the relative importance of normal and Umklapp processes is discussed. In higher-order perturbation theory the four-phonon processes play a role and these are treated in ch. 4§2.7.

When discussing theoretically the attenuation of an impressed sound wave an important parameter that enters the theory is the ratio of the wavelength of the ultrasound to the mean free path of the phonons thermally excited in the crystal. It is shown in ch. 4 that the theory divides basically into two regimes depending on whether the product $\Omega\tau$ is greater or less than unity. Ω is the frequency of the sound wave and τ the collision time for the thermal phonons. In the low frequency regime the sound wave is treated as a slowly varying potential field that causes a periodic disturbance in the distribution of the thermal phonons. The perturbation in the distribution will tend to cause an increase in entropy and this leads to the absorption of the sound energy. The theory in this regime predicts an attenuation coefficient that is essentially independent of temperature. In the other regime, $\Omega\tau \gg 1$, the sound wave is considered as a highly excited phonon mode and the attenuation is regarded as arising from the collision of these phonons with the thermally excited phonons in the crystal. In this region the Landau–Rumer ωT^4 law is found. The theory for both of these regions is treated in depth in ch. 4 and a comparison of the theoretical predictions with experiment is made.

In addition to the interaction between the acoustic modes, an ultrasonic wave may interact with other entities in the crystal. For example in metals and semiconductors the conduction electrons are strongly coupled to the phonons through the electron–phonon interaction and in magnetic materials the coupling to the magnetic excitations is of interest. Also ultrasonic waves may be used to probe localized defects such as paramagnetic impurities where a strong coupling between the unpaired electron spins and the lattice exists. These interactions, together with the effect of ultrasonics on light waves, are the ones to be treated in this book because they are the main areas of research where the use of ultrasonics in the microwave frequency range has proven particularly fruitful. There are many other types of interaction that can be envisaged but many of these are only important at low frequencies or would occur at ultrasonic frequencies in excess of those at present attainable in the laboratory.

In ferromagnetic dielectrics where the Heisenberg model is applicable it is well known that the low-lying magnetic excitations have a

wave-like nature and these are known as spin waves. The dispersion relation that relates the frequency to the wave number for these waves is generally parabolic at long wavelengths as opposed to the linear relation characteristic of phonons. In a certain region therefore the dispersion curves may cross, which suggests that if an interaction exists between the two types of excitations, conditions should be ripe for an interchange of energy and momentum to occur. The interaction between the magnetic excitations and the vibrational motion of the lattice can occur in a variety of ways, the simplest of which is for the vibrations of the lattice to modulate the exchange interaction and hence the effective coupling between the magnetic moments. In the vicinity of the intersection of the two dispersion curves it is found that coupled excitations that belong to approximate normal modes of the total system can occur. These coupled modes are known as magnetoelastic modes and their excitation involves the excitation of both elastic and magnetic energy. The choice of frequency at which the magnetoelastic modes occur can be controlled to a limited extent by applying a d.c. magnetic field of a suitable magnitude in a chosen direction. The properties of these magnetoelastic waves have now been studied in acoustic experiments at microwave frequencies and the general features of the theory are now confirmed. Both the theory and the present experimental situation are fully described in ch. 5. The latter half of that chapter is concerned with non-linear effects at high power levels and discusses topics such as the parametric excitation of high frequency modes and the amplification of spin waves in phonon pumping experiments.

Soon after the first experiment in which microwave phonons were generated it was suggested that ultrasonics could be used to study the properties of paramagnetic ion defects. The more usual technique for probing the low-lying energy levels of paramagnetic ions in crystals is by electron–spin-resonance methods. In these experiments a large part of the linewidth arises from the spin–lattice interaction, an interaction in which the electron spin can exchange energy with the phonons of the lattice through the agency of the spin–orbit and orbit–lattice couplings. Because of the interest in these linewidths particularly with the search for suitable maser materials, a large amount of theoretical work has been carried out in the past to establish the details of this interaction. On the experimental side this interaction has been investigated in spin–lattice-relaxation experiments; but because the relaxation of the magnetization is due to a coupling of the electron spin to a distribution of phonon modes, a detailed quantitative analysis is exceedingly difficult. The use of microwave ultrasonics removes this difficulty in that the interaction of the electron spins with phonons of a definite fre-

quency and polarization can be studied. The spin–phonon coupling constants for various ions in suitable host lattices have now been measured and some qualitative features of the theory such as the variation of the transition probabilities with orientation of an applied magnetic field and the selection rules governing the interaction have now been checked in several cases. The selection rules for acoustic and electromagnetic excitation are different, so the ultrasonic and e.p.r. spectra are not the same. It is obvious that phonon-induced e.s.r. is particularly easy to observe in just those cases where the spin–lattice broadening of the linewidth prevents the observation of the photon-induced resonance. This has allowed the detection by ultrasonic methods of very low traces of paramagnetic ions which could not otherwise have been detected. However, a.p.r. has its own difficulties, one of which is the large inhomogeneous linewidths that accompany these spectra. These linewidths can arise from a variety of sources but are primarily thought to be due to the presence of local random strains in the host crystal. A discussion of these line-broadening mechanisms is given in ch. 6§6.

A particularly striking experiment was performed by TUCKER[1961b] who observed the passage of ultrasonic waves in a sample of ruby in which the spin populations were inverted in the way normally used for maser experiments. It was found that the ultrasonic wave was amplified due to stimulated emission of energy from the spins. This leads to the possibility of producing microwave ultrasonics by maser action.

Because the paramagnetic ions respond to ultrasonic waves in their immediate vicinity, they can be used to provide detectors of ultrasonic waves. A detecting technique based on a phonon–photon double quantum transition in Fe^{2+} ions was reported by SHIREN[1961].

In metals and semiconductors the coupling of the conduction electrons to the lattive vibrations is through the electron–phonon interaction. The source of this interaction can arise in a variety of ways. It may be due to a deformation potential, or may be of purely electromagnetic origin. Other sources that have already been mentioned are the piezoelectric and magnetoelastic interactions. It turns out that among the semiconducting materials those of most interest from the point of view of an ultrasonic experiment are those that also exhibit piezoelectricity. In piezoelectric materials the propagation of an ultrasonic wave is accompanied by an electromagnetic disturbance, the main effect of which is to modify the elastic constants of the crystal and hence change the velocity of the waves. In most piezoelectric materials this is not very interesting but when the crystal is also semiconducting some new features appear which have proved to be of technological importance. When the crystal is also semiconducting, attenuation and dispersion of the stress wave occur because of the

presence of space charges set up by the internal electric fields. For a strong effect high frequencies and low concentrations of the charged carriers are required. Similar effects would occur in a non-piezoelectric semiconductor when the coupling is through the deformation potential but the effect is then by no means as large. A significant advance was made when it was realized that if the electrons were given a drift velocity greater than the velocity of sound by the application of a d.c. electric field, then the attenuation of the ultrasonic waves would become negative, or rather, amplification should occur. The first experiment to demonstrate the amplification of ultrasonic waves in this way was made by HUTSON *et al.* [1961] with a specimen of cadmium sulphide, and the essential theoretical explanation of the effect was provided by WHITE [1962]. The amplification process applies to both ultrasonic waves which are introduced into the crystal using suitable transducers and to the lattice vibrations which are excited thermally within the crystal. An alternative scheme for observing ultrasonic amplification was proposed by DUMKE and HAERING [1962]. In their method a magnetic field is applied perpendicular to the d.c. electric field. This configuration limits the current flowing in the direction of the electric field and so enables higher concentrations of carriers to be used. The method is therefore more suitable when dealing with non-piezoelectric materials where the electron–phonon interaction is small. It is also suitable for semi-metals which have an equal number of holes and electrons as the drift velocity in crossed electric and magnetic fields is independent of the sign of the charge of the carriers.

The theory proposed by White to explain the amplification process was a linear theory that was valid for sound waves of small amplitude such that the bunched electrons were only a small fraction of the total free charge concentration. If the non-linear terms in the theory are examined, it is found that there is a non-linear contribution to the current arising from the interaction of the space charge with the alternating electric field. This can give rise to an additional d.c. component of the current which is referred to as the acoustoelectric current. This acoustoelectric current manifests itself in a variety of ways. For example it is found that if the current–voltage characteristic of a bar of semiconducting cadmium sulphide is measured, it shows an abrupt change in slope at some critical value of the electric field. This saturation effect is found to be due to energy being transferred from the drifting electrons to certain vibrational modes of the crystal lattice. A detailed account of these non-linear phenomena is given in ch. 7.

The use of ultrasonic waves at radio frequencies has been a very valuable tool in the study of metals both in the normal and superconducting states. However in the microwave frequency region the

attenuation becomes very high–often hundreds of dB/cm–in the normal state and thus very little work has been done in this region. Ch. 8 gives a summary of the reasons for the high attenuation of ultrasonic waves which is due to their interaction with the free electrons in the metal and a brief review of the magnetic field dependent phenomena that can be observed in ultrasonic studies. The motion of the free electrons in the metal is modified in the presence of a magnetic field and information about the Fermi surface of the metal can be obtained from a study of the magnetic field dependence of the ultrasonic attenuation.

When a metal becomes superconducting the free electrons become bound together in Cooper pairs and the ultrasonic attenuation is much reduced. The superconducting energy gap can be determined from the ratio of the attenuation in the superconducting phase to that in the normal phase. Type II superconductors in a magnetic field split into a fine scale mixture of superconducting and normal regions. Flux lines can exist in the normal regions so the material is threaded by lines of magnetic flux. The energy gap is then a function of position in the material. The ultrasonic attenuation is a function of magnetic field as the number of flux lines through the material varies when the field is changed.

Finally, the last chapter of this book deals with the interaction of microwave ultrasound with light waves. The diffraction of light by an ultrasonic beam is one of the means whereby it may be detected experimentally and in fact was the method used in the early experiments of Baranskii and of Bömmel and Dransfeld. The chapter discusses both the diffraction of light by a monochromatic beam of phonons and the scattering due to the thermal vibrations of the crystal lattice. The latter part of the chapter deals with the generation by parametric amplification of thermal phonons of intense beams of microwave ultrasound.

ELASTICITY AND LATTICE DYNAMICS

This book is concerned with the propagation of mechanical vibrations in solids. For vibrations of low frequencies, the wavelength is long and extends over many atomic sites of the crystal. The crystal may then be viewed as a homogeneous continuous medium rather than as a periodic array of atoms since the disturbance will not see the discrete nature of the lattice. The propagation of waves can then be understood on a macroscopic theory formulated in terms of the elastic constants of the solid. For higher frequencies the difference in wave disturbance at neighbouring atoms will be important and it is then necessary to work in terms of a microscopic theory. This is particularly true if the lattice has a basis, when the relative motion of the atoms in the unit cell will give rise to effects unobtainable in the macroscopic theory. The microscopic theory is generally expressed in terms of force constants which require a knowledge of the actual forces existing between the atoms of which the solid is composed. The major result of taking into account the periodicity of the lattice is that wave propagation is not possible for a continuous range of frequencies; rather, frequency bands occur, separated by regions where wave propagation is forbidden. This type of band structure is well known in many other branches of physics when periodicity is present: it is vital in the electron theory of solids to account for the difference between conductors, non-conductors and semiconductors and occurs in the theory of electrical networks, for example in transmission lines. This chapter gives an account of the main aspects of elasticity theory and the theory of lattice dynamics and illustrates the connection between the two in the limit of long wavelengths. It will also serve to establish the notation used in later chapters of the book.

1. Elasticity theory

1.1. *Concept of strain and the strain tensor*

A continuous medium is said to be strained when the relative positions of the points in the medium are altered. The change in the relative position of material particles is called a deformation. The position of particles within the medium will be given by reference to a set of orthogonal coordinate axes Ox_1, Ox_2, Ox_3. Focus attention on two particles P and Q at positions (x_1, x_2, x_3) and $(x_1 + \Delta x_1, x_2 + \Delta x_2, x_3 + \Delta x_3)$ respectively in the unstrained state. After deformation let the particles at x and $x + \Delta x$ be displaced to $x + u$ and $x + \Delta x + u + \Delta u$ respectively. Δu is therefore the difference between the displacement of the two particles P and Q. Since the components of u are functions of position, we can write

$$\Delta u_1 = \frac{\partial u_1}{\partial x_1} \Delta x_1 + \frac{\partial u_1}{\partial x_2} \Delta x_2 + \frac{\partial u_1}{\partial x_3} \Delta x_3 + \cdots,$$

$$\Delta u_2 = \frac{\partial u_2}{\partial x_1} \Delta x_1 + \frac{\partial u_2}{\partial x_2} \Delta x_2 + \frac{\partial u_2}{\partial x_3} \Delta x_3 + \cdots, \qquad (2.1)$$

$$\Delta u_3 = \frac{\partial u_3}{\partial x_1} \Delta x_1 + \frac{\partial u_3}{\partial x_2} \Delta x_2 + \frac{\partial u_3}{\partial x_3} \Delta x_3 + \cdots,$$

where the dots indicate terms containing higher powers of Δx_i above the first, which may be neglected provided $|\Delta x|$ is sufficiently small. If this is done it is seen that in a sufficiently small neighbourhood of any point the relative displacements are linear functions of the relative coordinates. In this case the strain about any point is said to be sensibly homogeneous. It will be found useful to use the condensed notation $\Delta u_i = \zeta_{ij} \Delta_j$ where $\zeta_{ij} = \partial u_i / \partial x_j$ $(i, j = 1, 2, 3)$. Since Δu and Δx are both vectors, ζ_{ij} is the component of a tensor. It is convenient to introduce the following notation,

$$\epsilon_{ij} = \tfrac{1}{2} (\zeta_{ij} + \zeta_{ji}); \qquad \omega_1 = \tfrac{1}{2} (\zeta_{32} - \zeta_{23}),$$

$$\omega_2 = \tfrac{1}{2} (\zeta_{13} - \zeta_{31}); \qquad \omega_3 = \tfrac{1}{2} (\zeta_{21} - \zeta_{12}).$$

In terms of these quantities eq. (2.1) may be rewritten as

$$\Delta u_1 = \epsilon_{11} \Delta x_1 + (\epsilon_{12} - \omega_3) \Delta x_2 + (\epsilon_{31} + \omega_2) \Delta x_3,$$

$$\Delta u_2 = (\epsilon_{12} + \omega_3) \Delta x_1 + \epsilon_{22} \Delta x_2 + (\epsilon_{23} - \omega_1) \Delta x_3, \qquad (2.2)$$

$$\Delta u_3 = (\epsilon_{31} - \omega_2) \Delta x_1 + (\epsilon_{23} + \omega_1) \Delta x_2 + \epsilon_{33} \Delta x_3.$$

Consider now the special case when the vector Δx is initially parallel to Ox_1, that is Δx_2 and Δx_3 are zero. The physical meaning of ϵ_{11} is now clear, for since $\epsilon_{11} = \Delta u_1 / \Delta x_1 = \partial u_1 / \partial x_1$, it is seen to be the exten-

sion per unit length of a vector initially parallel to the Ox_1 axis. Similarly ϵ_{22} and ϵ_{33} are the extensions per unit length of vectors parallel respectively to Ox_2 and Ox_3 in the unstrained state. For a general element of length $|\Delta x|$ having direction cosines l, m, n with respect to the axes, it is seen that

$$\Delta x_1 + \Delta u_1 = |\Delta x| \left[l(1 + \epsilon_{11}) + m(\epsilon_{12} - \omega_3) + n(\epsilon_{31} + \omega_2) \right],$$

$$\Delta x_2 + \Delta u_2 = |\Delta x| \left[l(\epsilon_{12} + \omega_3) + m(1 + \epsilon_{22}) + n(\epsilon_{23} - \omega_1) \right], \quad (2.3)$$

$$\Delta x_3 + \Delta u_3 = |\Delta x| \left[l(\epsilon_{31} - \omega_2) + m(\epsilon_{23} + \omega_1) + n(1 + \epsilon_{33}) \right].$$

Therefore, provided that powers of ϵ_{ij} and ω_i greater than the first may be neglected,

$$|\Delta x + \Delta u|^2 = |\Delta x|^2 [1 + 2\epsilon_{11}l^2 + 2\epsilon_{22}m^2 + 2\epsilon_{33}n^2 + 4lm\epsilon_{12}$$
$$+ 4mn\epsilon_{23} + 4ln\epsilon_{31}]. \quad (2.4)$$

In other words for small displacements the extension per unit length of a short element Δx having direction cosines l, m, n in the unstrained state is

$$\epsilon_{11}l^2 + \epsilon_{22}m^2 + \epsilon_{33}n^2 + 2\epsilon_{12}lm + 2\epsilon_{23}mn + 2\epsilon_{31}nl.$$

So far only the diagonal terms of the strain tensor have been discussed. To see the significance of the off-diagonal terms, for example ϵ_{12}, consider the line element initially along Ox_1 for which $l = 1$, $m = n = 0$. In the strained state the direction cosines of this element are 1, $\epsilon_{12} + \omega_3$, $\epsilon_{31} - \omega_2$ to first order in the ζ's. Likewise an element initially along Ox_2 will have direction cosines $\epsilon_{12} - \omega_3$, 1, $\epsilon_{23} + \omega_1$. Therefore the cosine of the angle between the two vectors is $\approx \epsilon_{12} - \omega_3 + \epsilon_{12} + \omega_3 = 2\epsilon_{12}$. The physical meaning of the off-diagonal term in the strain tensor is now evident: $2\epsilon_{12}$ is the cosine of the angle in the deformed state of the elements originally along the Ox_1 and Ox_2 axes. Therefore ϵ_{12} measures the shearing strain between the planes Ox_1-Ox_3 and Ox_2-Ox_3. It is also noted that after deformation, a line element initially along Ox_1 makes an angle $\theta \approx \tan \theta \approx \epsilon_{12} + \omega_3$ with Ox_1 in the Ox_1-Ox_2 plane. Similarly a line element initially parallel to Ox_2 makes an angle $-(\epsilon_{12} - \omega_3)$ with Ox_2 in the Ox_1-Ox_2 plane. If the material had simply undergone a pure rotation, these two angles would have been equal, implying that $\partial u_1/\partial x_2$ was equal to $\partial u_2/\partial x_1$. In this case ϵ_{12} would have been zero: ω_3 thus corresponds to a pure rotation.

It is recalled that in the derivation of eq. (2.4) it was assumed that ζ_{ij} was small so that powers of it greater than the first could be neglected. This is the usual assumption made in classical elasticity theory and physically it implies that one is dealing with infinitesimal strains. It will be found however, in ch. 4 that this approximation is insufficient

when one comes to deal with deviations from harmonicity where a more exact formalism is required. If the restriction that the ζ's are small is not made the following equation is obtained in the place of eq. (2.4)

$$\frac{|\Delta x + \Delta u|^2 - |\Delta x|^2}{|\Delta x|^2} = l^2[2\zeta_{11} + \zeta_{11}^2 + \zeta_{21}^2 + \zeta_{31}^2]$$

$$+ m^2[2\zeta_{22} + \zeta_{12}^2 + \zeta_{22}^2 + \zeta_{32}^2]$$

$$+ n^2[2\zeta_{33} + \zeta_{13}^2 + \zeta_{23}^2 + \zeta_{33}^2]$$

$$+ 2lm[\zeta_{12} + \zeta_{21} + \zeta_{11}\zeta_{12} + \zeta_{21}\zeta_{22} + \zeta_{31}\zeta_{32}]$$

$$+ 2mn[\zeta_{23} + \zeta_{32} + \zeta_{12}\zeta_{13} + \zeta_{22}\zeta_{23} + \zeta_{32}\zeta_{33}]$$

$$+ 2ln[\zeta_{13} + \zeta_{31} + \zeta_{11}\zeta_{13} + \zeta_{21}\zeta_{23} + \zeta_{31}\zeta_{33}].$$

The components of a tensor η are now defined by

$$\eta_{ij} = \tfrac{1}{2}(\zeta_{ij} + \zeta_{ji} + \zeta_{ki}\zeta_{kj}). \tag{2.5}$$

This definition of η_{ij} reduces to that of ϵ_{ij} if the second-order terms are neglected. In this form the expression for the strain tensor is valid for finite strains. Throughout this book, in order to distinguish between the quantities η and ϵ, the former will be referred to as the deformation tensor and the latter as the strain tensor. Strictly speaking of course η and ϵ are the same physical quantity, ϵ being merely an approximate expression for η.

To conclude this section an observation concerning notation should be made. In the literature it is found that the off-diagonal strain components, particularly in engineering usage, are sometimes defined as twice the values given above. To distinguish the engineering strains from the others a single subscript as indicated below is used in this book,

$$\epsilon_1 = \epsilon_{11}; \qquad \epsilon_4 = 2\epsilon_{23} = 2\epsilon_{32}$$

$$\epsilon_2 = \epsilon_{22}; \qquad \epsilon_5 = 2\epsilon_{13} = 2\epsilon_{31}$$

$$\epsilon_3 = \epsilon_{33}; \qquad \epsilon_6 = 2\epsilon_{12} = 2\epsilon_{21}.$$

1.2. Components of stress

Consider for simplicity a unit cube with body-edges parallel to the axes Ox_1, Ox_2 and Ox_3 and suppose that the stress is homogeneous. The stress components can be denoted by σ_{ij} which is the force exerted in the Ox_i direction on a face normal to Ox_j by the material on the outside of the cube upon the material inside. In a non-homogeneous situation, the stress varies from point to point. The stress component

σ_{ij} at a point can be defined as follows. The component of force in the Ox_i direction across a surface element dS perpendicular to Ox_j is $\sigma_{ij}dS$ as dS tends to zero. The sign convention is such that $\sigma_{ij}dS$ is the force in the $+Ox_i$ direction exerted by the material on the $+Ox_j$ side of the element upon the material on the $-Ox_j$ side. Consider the small volume element shown in fig. 2.1. The forces in the Ox_2 direction on the
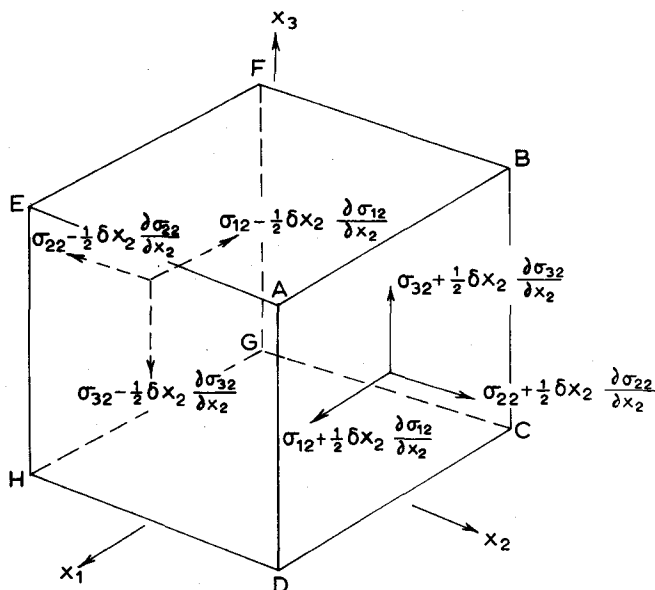
Fig. 2.1.

two faces ABCD and EFGH are as shown, where the σ's are the stress components at the centre of the element. The net force in the Ox_2 direction on these faces is $\delta x_1 \delta x_3 \delta x_2 \partial \sigma_{22}/\partial x_2$. Similarly the net force in the Ox_2 direction on the faces EADH and FBCG is $\delta x_1 \delta x_2 \times \delta x_3 \partial \sigma_{21}/\partial x_1$ and that on the faces EABF and HDCG is $\delta x_1 \delta x_2 \delta x_3 \times \partial \sigma_{23}/\partial x_3$. Thus the equation of motion for the Ox_2 direction is

$$\frac{\partial \sigma_{21}}{\partial x_1} + \frac{\partial \sigma_{22}}{\partial x_2} + \frac{\partial \sigma_{23}}{\partial x_3} + \rho f_2 = \rho \ddot{x}_2,$$

where ρ is the density of the medium. The term involving f_2 is included to allow for the presence of any body-forces with a component f_2 in the Ox_2 direction. Similar equations hold for motion directed along the other two axes. Therefore, in abbreviated form,

$$\frac{\partial \sigma_{ij}}{\partial x_j} + \rho f_i = \rho \ddot{x}_i \qquad (2.6)$$

is the fundamental equation connecting the motion of the element with the stress components acting upon it. Besides the equation for translational motion, equations for angular motion about the coordinate axis can be obtained. First consider rotations about the Ox_3 axis. The total couple about this axis is seen from fig. 2.2 to be

$$\left(\sigma_{21} + \frac{\partial \sigma_{21}}{\partial x_1} \frac{\delta x_1}{2}\right) \frac{\delta x_1}{2} \delta x_2 \delta x_3 + \left(\sigma_{21} - \frac{\partial \sigma_{21}}{\partial x_1} \frac{\delta x_1}{2}\right) \frac{\delta x_1}{2} \delta x_2 \delta x_3$$

$$- \left(\sigma_{12} + \frac{\partial \sigma_{12}}{\partial x_2} \frac{\delta x_2}{2}\right) \frac{\delta x_2}{2} \delta x_1 \delta x_3 - \left(\sigma_{12} - \frac{\partial \sigma_{12}}{\partial x_2} \frac{\delta x_2}{2}\right) \frac{\delta x_2}{2} \delta x_1 \delta x_3.$$
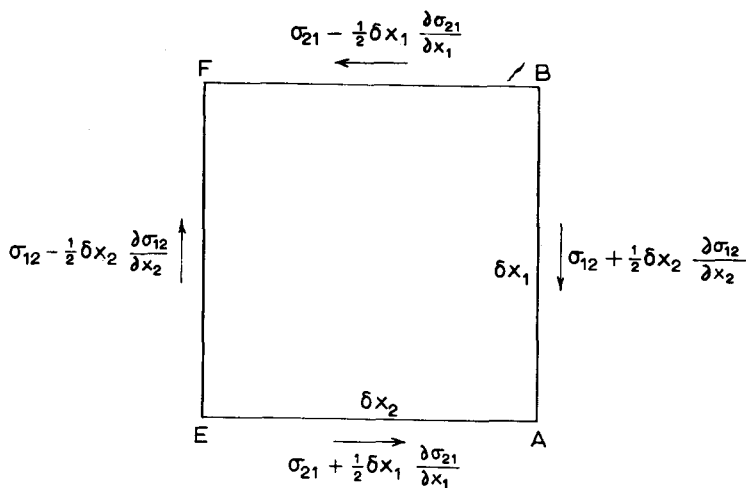
Fig. 2.2.

The angular motion about this axis is consequently described by

$$(\sigma_{21} - \sigma_{12}) \delta x_1 \delta x_2 \delta x_3 + G_3 \delta x_1 \delta x_2 \delta x_3 = I_3 \ddot{\theta}_3,$$

I_3 being the moment of inertia and $\ddot{\theta}_3$ the angular acceleration about Ox_3. G_3 represents the possible presence of a body-torque. For a non-homogeneous stress the interest is in the stress components at a point, that is, when the cubic element is very small. Since I_3 is of the order $\rho \delta x^5$, we must have in the limit of δx tending to zero, $\sigma_{21} - \sigma_{12} + G_3 = 0$. It therefore follows that in the absence of body-torques σ_{12} is equal to σ_{21}. Also by considering rotations about the other axes this can be generalised to $\sigma_{ij} = \sigma_{ji}$.

Unlike the strain tensor the engineering stresses are identical to the definitions given here and so the following identities hold,

$$\sigma_1 = \sigma_{11}; \qquad \sigma_4 = \sigma_{23} = \sigma_{32}$$

$$\sigma_2 = \sigma_{22}; \qquad \sigma_5 = \sigma_{13} = \sigma_{31}$$

$$\sigma_3 = \sigma_{33}; \qquad \sigma_6 = \sigma_{12} = \sigma_{21}.$$

1.3. *Elastic moduli and constants*

In the preceding subsections the concepts of stress and strain in a medium have been discussed. In order to know what deformations occur in a body under the action of stresses, it is necessary to have some physical law relating the two. Experimentally it is observed that when a body is subjected to an applied stress, for example a tension, the extension of the body is proportional to the stress for small displacements. This is known as Hooke's law. In elasticity theory it is assumed that a generalised Hooke's law holds. This states that the six components of stress at any point of a body are a linear function of the six components of strain. We may therefore write

$$\sigma_1 = c_{11}\epsilon_1 + c_{12}\epsilon_2 + c_{13}\epsilon_3 + c_{14}\epsilon_4 + c_{15}\epsilon_5 + c_{16}\epsilon_6$$

$$\sigma_2 = c_{21}\epsilon_1 + c_{22}\epsilon_2 + c_{23}\epsilon_3 + c_{24}\epsilon_4 + c_{25}\epsilon_5 + c_{26}\epsilon_6$$

$$\sigma_3 = c_{31}\epsilon_1 + c_{32}\epsilon_2 + c_{33}\epsilon_3 + c_{34}\epsilon_4 + c_{35}\epsilon_5 + c_{36}\epsilon_6$$

$$\sigma_4 = c_{41}\epsilon_1 + c_{42}\epsilon_2 + c_{43}\epsilon_3 + c_{44}\epsilon_4 + c_{45}\epsilon_5 + c_{46}\epsilon_6 \qquad (2.7)$$

$$\sigma_5 = c_{51}\epsilon_1 + c_{52}\epsilon_2 + c_{53}\epsilon_3 + c_{54}\epsilon_4 + c_{55}\epsilon_5 + c_{56}\epsilon_6$$

$$\sigma_6 = c_{61}\epsilon_1 + c_{62}\epsilon_2 + c_{63}\epsilon_3 + c_{64}\epsilon_4 + c_{65}\epsilon_5 + c_{66}\epsilon_6$$

or more briefly $\sigma_m = c_{mn}\epsilon_n$. The c's are the elastic moduli or stiffnesses. In tensor notation we may write

$$\sigma_{ij} = c_{ijkl}\epsilon_{kl}.$$

To go from one notation to the other ij may be replaced by m according to

$$1 \rightarrow 11; \qquad 4 \rightarrow 23 = 32$$
$$2 \rightarrow 22; \qquad 5 \rightarrow 13 = 31$$
$$3 \rightarrow 33; \qquad 6 \rightarrow 12 = 21.$$

The inverse equation defines the elastic constants or compliances

$$\epsilon_{ij} = s_{ijkl}\sigma_{kl}.$$

If it is desired to go over to the single suffix notation for the s's, care must be taken on account of the factor 2 appearing in the definition of the engineering strains. The relationship is

$$\epsilon_i = s_{ij}\epsilon_j,$$

where

$$s_{mn} = s_{ijkl} \text{ when } m,n \text{ are } 1, 2 \text{ or } 3$$

$$s_{mn} = 2s_{ijkl} \text{ when either } m, n \text{ is } 4, 5 \text{ or } 6$$

$$s_{mn} = 4s_{ijkl} \text{ when both } m, n \text{ are } 4, 5 \text{ or } 6.$$

The number of elastic constants is reduced from 81 to 36 because of the symmetry of the strain and stress tensor. A further reduction in the number follows from the expression for the internal energy and from the symmetry elements of the crystal as will now be demonstrated. It may be shown that the change in internal energy of an elastic body when the strains undergo a small change $d\epsilon_n$ is $dW = \sigma_m d\epsilon_m$. Eliminating the stress components with the aid of eq. (2.7) it follows immediately that $dW = c_{mn}\epsilon_n d\epsilon_m$ which, after partial differentiation with respect to ϵ_m, gives $\partial W/\partial\epsilon_m = c_{mn}\epsilon_n$. On further differentiation it follows that $c_{mn} = \partial^2 W/\partial\epsilon_n\partial\epsilon_m$. But since W is a single-valued function the order of differentiation may be changed. Thus the result is that $c_{mn} = c_{nm}$ or in tensor notation $c_{ijkl} = c_{klij}$. The number of elastic constants is thereby reduced from 36 to 21, the tensor components satisfying the conditions

$$c_{ijkl} = c_{jikl} = c_{ijlk} = c_{jikl} = c_{klij} = c_{lkij} = c_{klji} = c_{lkji}.$$

It should be remembered that it was possible to reduce the number of strain components from nine to six by separating them into two groups, pure strains and rotations and ignoring the latter. Similarly the number of stress components was reduced on the supposition that body-torques did not exist. Several authors, among them RAMAN and VISWANATHAN[1955] and LAVAL[1951], have expressed the view that rotations and body-torques should be included in the theory of elasticity. In this case the stress and strain tensors are not symmetric so they have nine independent constants. This would consequently raise the number of elastic constants to 45. Experimental evidence for this has not been forthcoming so it will not be considered further. It will be assumed that the conventional 21 elastic constant theory is valid.

A further reduction in the number of elastic constants occurs because of symmetry. As an illustration consider the example of a cubic crystal and suppose that the coordinate axes are chosen to be the four-fold axes of symmetry. Let the axes be rotated through 90° about Ox_3 such that $x_1 \rightarrow x_2$, $x_2 \rightarrow -x_1$, $x_3 \rightarrow x_3$. Now tensor components transform like the corresponding products of coordinates, which means for example that c_{2222} will transform to c_{1111}. But since a symmetry operation has been performed this implies that c_{2222} is equal to c_{1111}. Again, considering c_{1223}, it will be seen to transform to c_{2113} whilst on the other hand, c_{2113} will transform to $-c_{1223}$. Thus to satisfy the

symmetry requirements c_{1223} and c_{2113} must be identically zero. In this way, by considering rotations about other axes, the result, given in table 2.1 follows, showing that the non-zero elastic constants of a cubic crystal are just three. Similar arguments can be applied to all the point groups listed in table A1.1 and the results are given in table A1.2.

TABLE 2.1
Non-vanishing elastic stiffness
coefficients for cubic symmetry

c_{11}	c_{12}	c_{12}	0	0	0
	c_{11}	c_{12}	0	0	0
		c_{11}	0	0	0
			c_{44}	0	0
				c_{44}	0
					c_{44}

1.4. *Equations of motion and plane wave propagation*

In this subsection a few aspects of elastic wave propagation in a continuous medium are considered. Accordingly solutions of the force equation, eq. (2.6), are sought. One can use the relationship between the σ, ϵ and ζ to give, in the absence of body-forces,

$$\rho \ddot{u}_i = c_{ijkl} \frac{\partial^2 u_l}{\partial x_j \partial x_k}. \tag{2.8}$$

For crystals of high symmetry, where the number of independent elastic moduli is small, the number of terms on the right-hand side of eq. (2.8) reduces considerably. For instance, in the case of cubic crystals using table 2.1 the following three equations are obtained

$$\rho \ddot{u}_1 = c_{11} \frac{\partial^2 u_1}{\partial x_1^2} + c_{44} \left(\frac{\partial^2 u_1}{\partial x_2^2} + \frac{\partial^2 u_1}{\partial x_3^2} \right) + (c_{12} + c_{44}) \left(\frac{\partial^2 u_2}{\partial x_1 \partial x_2} + \frac{\partial^2 u_3}{\partial x_1 \partial x_3} \right), \tag{2.9}$$

$$\rho \ddot{u}_2 = c_{11} \frac{\partial^2 u_2}{\partial x_2^2} + c_{44} \left(\frac{\partial^2 u_2}{\partial x_1^2} + \frac{\partial^2 u_2}{\partial x_3^2} \right) + (c_{12} + c_{44}) \left(\frac{\partial^2 u_3}{\partial x_2 \partial x_3} + \frac{\partial^2 u_1}{\partial x_1 \partial x_2} \right), \tag{2.10}$$

$$\rho \ddot{u}_3 = c_{11} \frac{\partial^2 u_3}{\partial x_3^2} + c_{44} \left(\frac{\partial^2 u_3}{\partial x_2^2} + \frac{\partial^2 u_3}{\partial x_1^2} \right) + (c_{12} + c_{44}) \left(\frac{\partial^2 u_1}{\partial x_3 \partial x_1} + \frac{\partial^2 u_2}{\partial x_2 \partial x_3} \right). \tag{2.11}$$

Normally one is interested in the solutions of eq. (2.8) which represent plane monochromatic elastic waves for which the displacement vector has the form

$$u = Ae(q) \exp \left[i \left(\omega t - q \cdot x \right) \right]. \tag{2.12}$$

This is a plane wave because the phase, $\omega t - q \cdot x$ is a linear function of the coordinate x. The shape of the wave is determined by the surfaces

of constant phase and these at any instant of time are clearly plane surfaces perpendicular to the vector q. Of course, the displacement is a real physical quantity, so strictly speaking one should take the real or imaginary part of the exponential in eq. (2.12). However, provided that the equations are linear, one may use the exponential for ease of mathematical working. The vector q, components q_1, q_2, q_3, is known as the propagation vector since its direction is in the direction along which the wave is moving and its magnitude is 2π times the reciprocal of the wavelength. $e(q)$, components $e_i(q)$, is a unit vector known as the polarization vector and it denotes the direction in which the material particles are vibrating. If $e(q)$ is parallel to the propagation vector q the wave is called a *longitudinal wave*. When the polarization vector is perpendicular to q the wave is termed *transverse*. In order that the plane wave, eq. (2.12), may be a solution of eq. (2.8), a definite relationship must exist between the frequency ω and the wave number q. This relationship is known as the dispersion relationship and allows the phase velocity, $v = \omega/q$ and the group velocity $v_g = \partial\omega/\partial q$ to be determined. In an elastic medium it is found that ω is proportional to q so there is no dispersion and these two velocities are equal.

To illustrate the physics it is preferable to proceed by way of a specific example rather than to consider the general solutions of eq. (2.8). Consider the problem of wave propagation along the (110) direction in a cubic lattice. Putting $q_1 = q_2 = q/\sqrt{2}$ the desired direction is selected. From the symmetry of the crystal it may be expected that longitudinal wave propagation is possible in this direction. Such a wave must have $e \| q$ which implies that both $e_1(q)$ and $e_2(q)$ are $1/\sqrt{2}$ and $e_3(q)$ is zero. The particle displacement will then have components

$$u_{1,2} = 2^{-1/2}A \exp \{i[\omega t - q(x_1 + x_2)/\sqrt{2}]\}.$$

Direct substitution into eq. (2.9) shows that such a solution exists provided that

$$\rho\omega^2 = \tfrac{1}{2}(c_{11} + 2c_{44} + c_{12})q^2.$$

Thus a longitudinal wave can propagate along the (110) direction in a cubic crystal and will have a velocity

$$v_\ell = \omega/q = \{(c_{11} + 2c_{44} + c_{12})/2\rho\}^{1/2}.$$

In addition to the longitudinal wave, we might expect transverse wave propagation to be possible. By definition this requires that $e(q) \cdot q = 0$. Let us consider two particular cases when this relationship is satisfied: (a) a transverse wave plane polarized along (001) and (b) a transverse wave polarized along $(1\bar{1}0)$. For the former case it follows from eq. (2.11) that $v_{t_1} = (c_{44}/\rho)^{1/2}$ while for the latter, eq. (2.9) gives $v_{t_2} =$

$[(c_{11} - c_{12})/2\rho]^{1/2}$. Direct substitution has illustrated that both transverse and longitudinal waves may propagate along the (110) axis of a cubic crystal but that in general the velocities of the waves are different.

So far elastic wave propagation along a high symmetry direction in the crystal has been considered. Propagation in a general direction is now considered. Choosing the direction of q in eq. (2.12), we must substitute for u in eqs. (2.9)–(2.11). This will give three equations involving $e_1(q)$, $e_2(q)$, $e_3(q)$. For solubility the determinant of the coefficients of $e_1(q)$, $e_2(q)$, $e_3(q)$ must be equated to zero, which yields a cubic equation for ω^2 in terms of the components of q. This equation for a cubic crystal is found to be

$$\begin{vmatrix} c_{11}q_1^2 + c_{44}(q_2^2+q_3^2) - \omega^2\rho; & (c_{12}+c_{44})q_1q_2; & (c_{12}+c_{44})q_1q_3 \\ (c_{12}+c_{44})q_1q_2; & c_{11}q_2^2+c_{44}(q_1^2+q_3^2) - \omega^2\rho; & (c_{12}+c_{44})q_2q_3 \\ (c_{12}+c_{44})q_1q_3; & (c_{12}+c_{44})q_2q_3; & c_{44}(q_1^2+q_2^2)+c_{11}q_3^2 - \omega^2\rho \end{vmatrix} \equiv 0. \quad (2.13)$$

Each value of ω corresponds to a definite mode of vibration. To find the polarization directions for each mode the appropriate value of ω must be substituted back and the ratio $e_1(q):e_2(q):e_3(q)$ determined, that is the direction of $e(q)$. For directions of high symmetry it is found that one longitudinal and two transverse modes exist. However for any arbitrary direction the modes are neither purely longitudinal nor purely transverse: nevertheless, convention has it that the mode of highest velocity is referred to as the longitudinal mode and the other two as transverse.

In general the velocity of the waves will depend upon the direction of propagation in the crystal. However if $c_{11} - c_{12}$ is put equal to $2c_{44}$ it is easily checked that eq. (2.13) gives a longitudinal velocity $v_\ell = (c_{11}/\rho)^{1/2}$ and two transverse velocities $v_t = (c_{44}/\rho)^{1/2}$ independent of the direction of propagation. The medium is then said to be isotropic. The quantity $(c_{11} - c_{12})/2c_{44}$, known as the anisotropy factor, is a measure of the degree of anisotropy that exists in the crystal.

The above procedure which has been carried out for cubic crystals can be applied equally well to other symmetries. Direct substitution of the plane wave solution, eq. (2.12) into the equation of motion, eq. (2.8), gives the set of relations

$$(c_{ijkl}q_jq_k - \rho\omega^2\delta_{i,l})e_l = 0. \quad (2.14)$$

This fundamental equation of elasticity is known as Christoffel's equation. It is more conveniently expressed in the form

$$(\Lambda_{il} - v^2\delta_{i,l})e_l = 0, \quad (2.15)$$

where $\Lambda_{il} = c_{ijkl}\hat{q}_j\hat{q}_k/\rho$ and $\hat{q}_i = q_i/|q|$. In order to set up the determinantal equation like eq. (2.13) for a particular crystal symmetry only the six elements of Λ_{il} are needed. These are given in tables A2.1. For any direction of propagation in the crystal, Λ will have three eigenvalues corresponding to the three allowed values of v^2. Usually for crystals these are distinct, giving three linear polarized waves. In some cases two of the eigenvalues may be degenerate, the wave normal is then referred to as an acoustic axis. It is then possible to take linear combinations of the degenerate eigenvectors to form other types of polarizations. In an isotropic medium, whatever the direction of propagation, there is always one purely longitudinal and two degenerate transverse waves. In crystals, it is only in special directions that a pure longitudinal or transverse wave can exist. The special directions are usually, but not always, related to directions of high crystal symmetry. For instance there is always one purely transverse wave if $\hat{q}$ lies in a symmetry plane or in a plane perpendicular to a symmetry axis of even order.

2. Thermal, electric and magnetic variables

The elastic properties of a solid have so far been treated only in isolation from its electrical, magnetic and thermal properties. The generation of microwave ultrasonics in crystals frequently involves materials, such as piezoelectrics, in which there is a strong coupling between the elastic and electromagnetic field variables. A brief résumé will now be given of the basic relations governing the main interactions which exist between these variables. The processes that can occur are clearly illustrated in fig. 2.3. The elastic variables are the nine components of the strain tensor ϵ_{ij} and the nine components of stress σ_{ij}. The electric field variables will be the three components of the electric and displacement vectors E and D respectively. The corresponding quantities for the magnetic variables are the magnetic field H and the magnetic induction B. Finally, the thermal state of the body is described by its temperature T and its entropy S. Thus there is a total of sixteen independent variables needed to describe a state of the system. These may be taken as σ_{ij}, E_i, H_i, T leaving $\epsilon_{ij}, D_i, B_i, S$ to be the dependent variables. Of course, this is not the only choice; $\epsilon_{ij}, E_i, H_i, T$ can equally well be taken as the independent variables and so on. Using the first set the differentials of $\epsilon_{ij}, D_i, B_i, S$ may be written as follows:

$$d\epsilon_{ij} = \left(\frac{\partial \epsilon_{ij}}{\partial \sigma_{kl}}\right)_{EHT} d\sigma_{kl} + \left(\frac{\partial \epsilon_{ij}}{\partial E_k}\right)_{\sigma HT} dE_k + \left(\frac{\partial \epsilon_{ij}}{\partial H_k}\right)_{\sigma ET} dH_k + \left(\frac{\partial \epsilon_{ij}}{\partial T}\right)_{\sigma EH} dT,$$

$$dD_i = \left(\frac{\partial D_i}{\partial \sigma_{jk}}\right)_{EHT} d\sigma_{jk} + \left(\frac{\partial D_i}{\partial E_j}\right)_{\sigma HT} dE_j + \left(\frac{\partial D_i}{\partial H_j}\right)_{\sigma ET} dH_j + \left(\frac{\partial D_i}{\partial T}\right)_{\sigma EH} dT,$$

Fig. 2.3.

$$dB_i = \left(\frac{\partial B_i}{\partial \sigma_{jk}}\right)_{EHT} d\sigma_{jk} + \left(\frac{\partial B_i}{\partial E_j}\right)_{\sigma HT} dE_j + \left(\frac{\partial B_i}{\partial H_j}\right)_{\sigma ET} dH_j + \left(\frac{\partial B_i}{\partial T}\right)_{\sigma EH} dT,$$

$$dS = \left(\frac{\partial S}{\partial \sigma_{ij}}\right)_{EHT} d\sigma_{ij} + \left(\frac{\partial S}{\partial E_i}\right)_{\sigma HT} dE_i + \left(\frac{\partial S}{\partial H_i}\right)_{\sigma ET} dH_i + \left(\frac{\partial S}{\partial T}\right)_{\sigma EH} dT.$$

(2.16)

Thermodynamic arguments can now be used to obtain the relationship between the various coefficients. To illustrate the method consider the total energy of the body, that is the sum of its elastic, electric, magnetic and thermal energies. The first law of thermodynamics states that the change in internal energy of a body is $dU = dW + dQ$ when an amount of heat dQ flows into the system and an amount of work dW is done on the body by external forces. To be more explicit

$$dU = \sigma_{ij} d\epsilon_{ij} + E_i dD_i + H_i dB_i + T dS.$$ (2.17)

The first term on the right-hand side is the work done per unit volume on changing the strain by a small amount $d\epsilon_{ij}$ while the second term represents any electrical work that occurs due to a change in the polarization of the material. The third term is the corresponding quantity for the magnetic energy and the last term follows directly from the

second law of thermodynamics for a reversible process. It is convenient to introduce the Gibbs function G defined by

$$G = U - \sigma_{ij}\epsilon_{ij} - E_i D_i - H_i B_i - TS. \qquad (2.18)$$

Combining this with the expression for dU, for a reversible process,

$$dG = -\epsilon_{ij}d\sigma_{ij} - D_i dE_i - B_i dH_i - S\,dT. \qquad (2.19)$$

It is seen that G is a function of σ, E, H and T so that

$$dG = \left(\frac{\partial G}{\partial \sigma_{ij}}\right)_{EHT} d\sigma_{ij} + \left(\frac{\partial G}{\partial E_i}\right)_{\sigma HT} dE_i + \left(\frac{\partial G}{\partial H_i}\right)_{\sigma ET} dH_i + \left(\frac{\partial G}{\partial T}\right)_{\sigma EH} dT. \qquad (2.20)$$
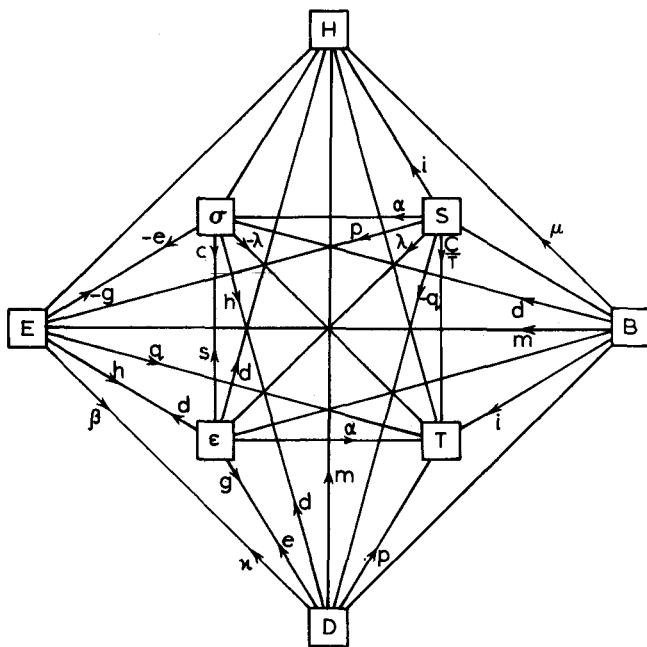
Comparison of eqs. (2.19) and (2.20) yields the following relationships

$$\epsilon_{ij} = -\left(\frac{\partial G}{\partial \sigma_{ij}}\right)_{EHT} \qquad D_i = -\left(\frac{\partial G}{\partial E_i}\right)_{\sigma HT}$$

$$B_i = -\left(\frac{\partial G}{\partial H_i}\right)_{\sigma ET} \qquad S = -\left(\frac{\partial G}{\partial T}\right)_{\sigma EH}.$$

After a straightforward partial differentiation it follows that $(\partial\epsilon_{ij}/\partial E_k)_{\sigma HT} = (\partial D_k/\partial\sigma_{ij})_{EHT}$. Similar expressions exist between the other coefficients. The results are conveniently tabulated in table 2.2 where x is the independent and y the dependent variable. The symbol in each box of the table denotes the value of $\partial y/\partial x$ corresponding to the column and row in which it is situated, for example $m_{ki}^{\sigma T} = (\partial B_i/\partial E_k)_{\sigma T}$. The superscripts indicate the variables which are to be held constant. The important point to note is that the matrix is diagonal in the symbols so that many relationships hold between the partial derivatives, for instance $(\partial B_i/\partial E_k)_{\sigma T} = (\partial D_k/\partial H_i)_{\sigma T}$. Using the notation introduced in table 2.2 eq. (2.16) may be rewritten as

$$\begin{aligned}
\epsilon_{ij} &= s_{ijkl}^{EHT}\sigma_{kl} + d_{kij}^{HT}E_k + d_{kij}^{ET}H_k + \alpha_{ij}^{EH}\Delta T, \\
D_i &= d_{ijk}^{HT}\sigma_{jk} + \kappa_{ij}^{\sigma HT}E_j + m_{ij}^{\sigma T}H_j + p_i^{\sigma H}\Delta T, \\
B_i &= d_{ijk}^{ET}\sigma_{jk} + m_{ji}^{\sigma T}E_j + \mu_{ij}^{\sigma ET}H_j + i_i^{\sigma E}\Delta T, \\
\Delta S &= \alpha_{ij}^{EH}\sigma_{ij} + p_i^{\sigma H}E_i + i_i^{\sigma E}H_i + (C^{\sigma EH}/T)\Delta T.
\end{aligned} \qquad (2.21)$$

TABLE 2.2

x \ y	ϵ_{ij}	D_i	B_i	S
σ_{kl}	s_{ijkl}^{EHT}	d_{ikl}^{TH}	d_{ikl}^{TE}	α_{kl}^{EH}
E_k	d_{kij}^{TH}	$\kappa_{ik}^{\sigma HT}$	$m_{ki}^{\sigma T}$	$p_k^{\sigma H}$
H_k	d_{kij}^{TE}	$m_{ik}^{\sigma T}$	$\mu_{ik}^{\sigma EH}$	$i_k^{\sigma E}$
T	α_{ij}^{EH}	$p_i^{\sigma H}$	$i_i^{\sigma E}$	$C^{\sigma EH}/T$

$$G = U - \epsilon_{ij}\sigma_{ij} - D_i E_i - B_i H_i - TS$$

Many other equations can be obtained by choosing a different set of independent variables. Other choices are shown in tables 2.3–2.6. The magnetic variables have been neglected, since in practice we are concerned with the presence of either electric or magnetic fields rather than both simultaneously. The magnetic case can be obtained from the electric case by replacing E and D by H and B respectively. The information in the tables is obtained in the same way as that obtained for table 2.2 but in each case a different thermodynamic function is used. The thermodynamic function needed is given with each table. The names of the various symbols for the partial differentials are listed in table 2.7.

In tables 2.3–2.6 it will be noticed that T has always been taken to be an independent variable, so that for constant T we have the iso-

TABLE 2.3

$x \backslash y$	ϵ_{ij}	D_i	S
σ_{kl}	s^{ET}_{ijkl}	d^T_{ikl}	α^E_{kl}
E_k	d^T_{kij}	$\kappa^{\sigma T}_{ik}$	p^σ_k
T	α^E_{ij}	p^σ_i	$C^{\sigma E}/T$

$$G = U - \epsilon_{ij}\sigma_{ij} - D_iE_i - TS$$

TABLE 2.4

$x \backslash y$	σ_{ij}	D_i	S
ϵ_{kl}	c^{ET}_{ijkl}	e^T_{ikl}	λ^E_{kl}
E_k	$-e^T_{kij}$	$\kappa^{\epsilon T}_{ik}$	p^ϵ_k
T	$-\lambda^E_{ij}$	p^ϵ_i	$C^{\epsilon E}/T$

$$G_2 = U - D_iE_i - TS$$

TABLE 2.5

$x \backslash y$	ϵ_{ij}	E_i	S
σ_{kl}	s^{DT}_{ijkl}	$-g^T_{ikl}$	α^D_{kl}
D_k	g^T_{kij}	$\beta^{\sigma T}_{ki}$	$-q^\sigma_k$
T	α^D_{ij}	q^σ_i	$C^{\sigma D}/T$

$$G_1 = U - \epsilon_{ij}\sigma_{ij} - TS$$

TABLE 2.6

$x \backslash y$	σ_{ij}	E_i	S
ϵ_{kl}	c^{DT}_{ijkl}	h^T_{ikl}	λ^D_{kl}
D_k	h^T_{kij}	$\beta^{\epsilon T}_{ki}$	$-q^\epsilon_k$
T	$-\lambda^D_{ij}$	q^ϵ_i	$C^{\epsilon D}/T$

$$A = U - TS$$

TABLE 2.7

Elastic stiffness coefficient	c
Elastic compliance constant	s
Dielectric permittivity	κ
Dielectric constant	K
Dielectric impermeability	β
Permeability constant	μ
Specific heat/unit volume	C
Piezoelectric constants if the magnetic-field variables are constant	$\begin{cases} d \\ e \\ g \\ h \end{cases}$
Piezomagnetic constants if the electric-field variables are constant	
Thermal expansion coefficient	α
Thermal stress constant	λ
Pyroelectric constants	$\begin{cases} p \\ q \end{cases}$
Pyromagnetic constant	i
Magnetodielectric constant	m
Temperature	T
Entropy	S

thermal, piezoelectric and dielectric constants. If the roles of S and T are interchanged, then S can be fixed to obtain the adiabatic constants. To find the relationship between the isothermal and adiabatic constants ΔS can be equated to zero in tables 2.3–2.6 and ΔT eliminated to give the results of table 2.8.

TABLE 2.8

Relationship between the adiabatic and isothermal coefficients

$$s_{ijkl}^{xS} = s_{ijkl}^{xT} - \frac{T}{C^{\sigma x}} \alpha_{ij}^{x} \alpha_{kl}^{x} \qquad g_{ijk}^{S} = g_{ijk}^{T} + \frac{T}{C^{\sigma D}} q_{i}^{q} \alpha_{jk}^{D}$$

$$c_{ijkl}^{xS} = c_{ijkl}^{xT} + \frac{T}{C^{\epsilon x}} \lambda_{ij}^{x} \lambda_{kl}^{x} \qquad h_{ijk}^{S} = h_{ijk}^{T} - \frac{T}{C^{\sigma D}} q_{i}^{q} \lambda_{jk}^{D}$$

$$d_{ijk}^{S} = d_{ijk}^{T} - \frac{T}{C^{\sigma E}} p_{i}^{\sigma} \alpha_{jk}^{E} \qquad \beta_{ij}^{yS} = \beta_{ij}^{yT} + \frac{T}{C^{yD}} q_{i}^{y} q_{j}^{y}$$

$$e_{ijk}^{S} = e_{ijk}^{T} - \frac{T}{C^{\epsilon E}} p_{i}^{\epsilon} \lambda_{jk}^{E} \qquad \kappa_{ij}^{yS} = \kappa_{ij}^{yT} - \frac{T}{C^{yE}} p_{i}^{y} p_{j}^{y}$$

where $x = E$ or D and $y = \epsilon$ or σ

3. Elements of lattice dynamics

The theory of elasticity which has been outlined so far is useful when dealing with the low frequency vibrations of solids. As has been noted

this macroscopic theory is then valid because the wavelength of the vibrations are very long compared to the interatomic spacings. This means that as far as wave propagation is concerned the discrete nature of the lattice is not important because the variation in amplitude of the wave in going from one lattice site to the next is small. To deal with high frequency vibrations such as those occuring thermally at high temperatures, a microscopic theory is needed. The discussion will begin with a few simple examples. This has the advantage of demonstrating the physics of the problem without confusing the issue with complicated mathematical notation. Later on, in ch. 2§3.5 a more general treatment of the problem is given.

3.1. *Monatomic linear chain*

One of the simplest systems that could be considered is a monatomic periodic chain of atoms each of mass m lying along the x-direction. If the lattice spacing is a the position of each atom may be denoted by na where the integer n numbers the position of the atom along the chain. The chain, for the moment, is of infinite extent so that end effects can be neglected. It is assumed that the atoms interact only with their nearest-neighbour atoms via an elastic force proportional to their relative displacements. If $u(n)$ denotes the displacement of the nth atom from equilibrium, the force acting on the atom n due to atoms $(n-1)$ and $(n+1)$ is $K[u(n+1)+u(n-1)-2u(n)]$, where K is the appropriate force constant. Newton's equation of motion for the nth atom is thus

$$m\ddot{u}(n) = K[u(n+1)+u(n-1)-2u(n)]. \qquad (2.22)$$

This equation is satisfied by the wave-like solution

$$u(n) = A \exp[i(\omega t - qna)]$$

provided ω and q satisfy the following dispersion relation

$$\omega = 2(K/m)^{1/2} \sin\tfrac{1}{2}qa. \qquad (2.23)$$

The dispersion curve is plotted in fig. 2.4. The important point to notice is that there is only a limited frequency range over which an elastic wave can propagate. Wave propagation above $2(K/m)^{1/2}$ is forbidden. Also dispersion occurs, that is, ω is no longer proportional to q. For long wavelengths, $qa \to 0$, a macroscopic theory should be valid. In this region it is seen that $\omega \to qa(K/m)^{1/2}$. This is the result which would be obtained from elasticity theory applied to the propagation of a compression wave along the one-dimensional chain regarded as a continuous medium. The dispersion curve of elasticity theory is a tangent to the true curve at $q=0$. It is also noted that according to
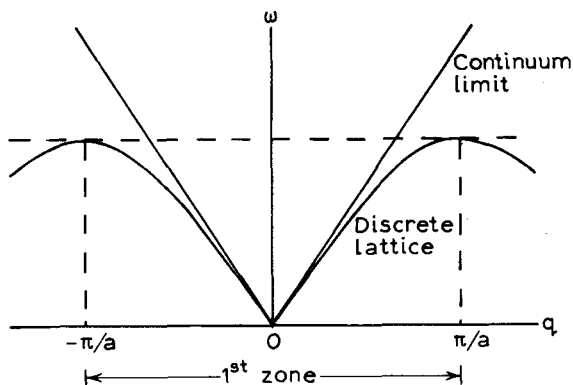
Fig. 2.4.

elasticity theory there is no upper limit to the frequency of the wave that may be propagated. It may be recalled that the model introduced by Debye to explain the low temperature specific heat of solids treated the solid as an elastic continuum. The reason for its success at low temperatures is obvious: at these temperatures the modes excited have frequencies close to that given by the continuum model. When the lattice is of finite extent the appropriate boundary conditions at the end of the chain must of course be taken into account. The usual method is to introduce Born–von Karman or periodic boundary conditions, as they are known. These state that the particle displacement at each end of the chain must be the same. If there are N atoms in the chain the displacement of the Nth atom must be the same as the first so that $\exp[i(N-1)qa] = 1$. Neglecting terms of order $1/N$ this implies that $q = 2l\pi/Na$ where l is an integer. Thus q does not take a continuous range of values but instead the allowed values occur in integer steps of $2\pi/Na$. Since in practice N is very large, the allowed values of q are close together. It will be noticed that the dispersion curve has only been plotted for q in the range $-\pi/a < q \leqslant \pi/a$. The reason for doing this is that the frequency of any q outside this range is equal to the frequency of the corresponding q in the first zone obtained by subtracting off a reciprocal lattice vector, in this case an integer multiple of $1/a$.

3.2. *Diatomic linear chain*

A more complicated model having two different types of atom, masses m_1 and m_2 respectively alternating along the chain, will now be considered. Let the separation of the atoms be a and suppose that the masses m_1 are on even integer sites $2n$ while the masses m_2 are on the

odd integer sites $(2n+1)$. It will again be assumed that short range forces exist so that each atom is only coupled to its immediate neighbour on either side with a force constant K. This time there are two equations of motion, one for m_1 and the other for m_2:

$$m_1\ddot{u}(2n) = K\left[u(2n+1)+u(2n-1)-2u(2n)\right],$$
$$m_2\ddot{u}(2n+1) = K\left[u(2n+2)+u(2n)-2u(2n+1)\right]. \tag{2.24}$$

Assuming wave-like solutions

$$u(2n)=A_1\exp\left[i(\omega t-2qna)\right], \quad u(2n+1)=A_2\exp\left[i(\omega t-[2n+1]qa)\right],$$

it follows on substituting in eq. (2.24)

$$(m\omega^2-2K)A_1+2K\cos(qa)A_2 = 0,$$
$$2K\cos(qa)A_1+(m_2\omega^2-2K)A_2 = 0. \tag{2.25}$$

For solubility the determinant of the coefficients of A_1 and A_2 in eq. (2.25) must be zero. This condition implies that

$$\omega^2 = (K/m_1m_2)[m_1+m_2\pm[(m_1+m_2)^2-4m_1m_2\sin^2 qa]^{1/2}]. \tag{2.26}$$

If this function is plotted, two frequency branches as shown in fig. 2.5 are obtained. The curve passing through the origin is called the acoustic branch and the other is known as the optical branch. Substituting back into eq. (2.25) it is found that for the acoustic mode A_1 and A_2 have the same sign, so that the atoms move in phase, whereas for the optical mode they have opposite signs, implying that the atoms move out of
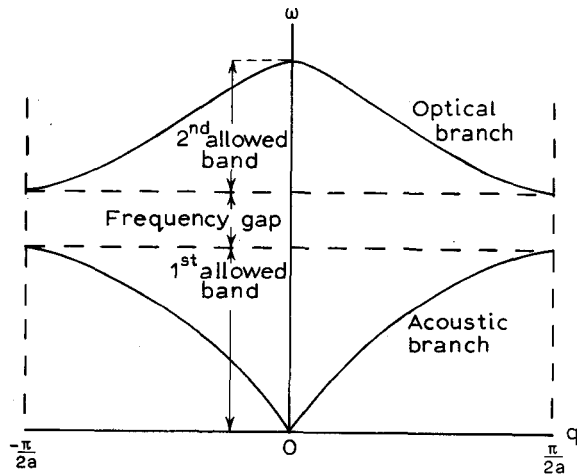

Fig. 2.5.

phase. The term 'optical mode' arises as follows: if m_1 and m_2 are charged ions, carrying positive and negative charges respectively, then their relative motion will give rise to an oscillating dipole which may be excited by the application of an oscillating field. The frequency is usually in the infra-red or optical range. The acoustic branch is so called simply because the acoustic frequencies are in this range. The main characteristic of the frequency curve is the presence of two branches separated by a frequency gap in which plane wave propagation is not possible. It is to be noted that each unit cell in the lattice contains two atoms. This is the reason for obtaining two branches to the dispersion curve. In general if there are p atoms per unit cell there will be $(p-1)$ optical branches and one acoustic branch. The same result holds for three dimensions, only in this case it will be found (ch. 2§3.5) that each of these branches will have three curves associated with it, corresponding to the three states of polarization of the lattice waves.

3.3. *Quantization of lattice vibrations*

Let us return to the discussion of the one-dimensional monatomic chain of atoms. The classical Hamiltonian of the system is

$$H = \sum_n \left\{ \frac{p^2(n)}{2m} + \tfrac{1}{2} K \left[u(n) - u(n+1) \right]^2 \right\}, \qquad (2.27)$$

where $p(n)$ is the momentum of the atom n. The first term is the kinetic energy and the second is the potential energy. (The reader may verify that Hamilton's equations of motion give the force equation used earlier.) In a quantum mechanical treatment the $p(n)$'s and $u(n)$'s must be treated as quantum mechanical operators obeying the usual commutation rules $[u(n), p(m)] = i\hbar\delta_{n,m}$. For the same site u and p are conjugate dynamical variables but for different sites they are dynamically independent. It will be noted that the Hamiltonian may be rewritten in the form

$$H = \sum_n \left[p^2(n)/2m + Ku^2(n) \right] - \sum_n Ku(n)u(n+1).$$

The first term describes a set of independent harmonic oscillators, one on each lattice site, while the second term is an interaction between pairs of neighbouring atoms. The system is therefore composed of a set of N interacting 'particles'. To solve the problem we try to transform the Hamiltonian by defining new coordinates so that it can be re-expressed as a sum of N one-particle Hamiltonians. In most problems of course this cannot be achieved. Nevertheless an attempt is made to transform away the interaction as far as is possible so that the small interactions which remain can be treated by a perturbation

method. In this problem it is fortunate that the interaction term can be removed. Because of the periodic nature of the lattice it is convenient to define normal mode operators through the Fourier transforms

$$u(q) = \frac{1}{\sqrt{N}} \sum_n u(n) \exp(iqna); \qquad p(q) = \frac{1}{\sqrt{N}} \sum_n p(n) \exp(-iqna).$$

$$(2.28)$$

The $u(q)$ and $p(q)$ satisfy the commutation rules

$$[u(q), p(q')] = \frac{1}{N} \sum_{n,m} [u(n), p(m)] \exp[i(qn - q'm)a]$$

$$= \frac{1}{N} \sum_{n,m} i\hbar \delta_{n,m} \exp[i(q-q')na] = i\hbar \delta_{q,q'}.$$

A canonical transformation has in fact been carried out since the new coordinates and momenta satisfy the same commutation rules as the old $u(n)$ and $p(n)$. Inverting the formulae eq. (2.28)

$$u(n) = \frac{1}{\sqrt{N}} \sum_q u(q) \exp(-iqna); \qquad p(n) = \frac{1}{\sqrt{N}} \sum_q p(q) \exp(iqna)$$

$$(2.29)$$

and substituting back into the Hamiltonian gives

$$H = \frac{1}{2m} \sum_q p(q)p(-q) + \sum_q 2Ku(q)u(-q) \sin^2 \tfrac{1}{2}qa. \quad (2.30)$$

Since $u(-q) = u^*(q)$ and letting $\omega(q)$ equal $2(K/m)^{1/2}|\sin \tfrac{1}{2}qa|$ it follows that

$$H = \frac{1}{2m} \sum_q [p(q)p^*(q) + m^2\omega^2(q)u(q)u^*(q)]. \quad (2.31)$$

Using Heisenberg's equations of motion $i\hbar\dot{u}(q) = [u(q), H]$ the Hamiltonian can then be written as

$$H = \tfrac{1}{2}m \sum_q [\dot{u}(q)\dot{u}^*(q) + \omega^2(q)u(q)u^*(q)]. \quad (2.32)$$

This verifies that the $u(q)$ are the normal coordinates since the Hamiltonian contains no cross terms involving products $u(q)u(q')$ etc. Also making use of $i\hbar\dot{p}(q) = [p(q), H]$ the equation $\ddot{u}(q) + \omega^2(q)u(q) = 0$ is obtained which shows that $u(q)$ varies harmonically with $\omega(q)$: $\omega(q)$ is therefore the frequency of a normal mode. It will be noted that $\omega(q)$ agrees with the frequency of the wave-like solution assumed earlier. A general displacement of the nth atom, $u(n)$, can be expressed as a linear superposition of these normal modes.

A more convenient expression for the Hamiltonian is found by introducing the creation and annihilation operators (sometimes referred

to as ladder operators) defined by

$$a(q) = (2m\hbar\omega(q))^{-1/2}(p(q) - im\omega(q)u^*(q)),$$
$$a^*(q) = (2m\hbar\omega(q))^{-1/2}(p^*(q) + im\omega(q)u(q)). \qquad (2.33)$$

An important property of these operators, as can be verified by direct substitution, is that they obey the simple commutation rules

$$[a(q), a^*(q')] = \delta_{q,q'}; \quad [a(q), a(q')] = 0; \quad [a^*(q), a^*(q')] = 0. \qquad (2.34)$$

Expressed in terms of these operators the Hamiltonian becomes

$$H = \sum_q \tfrac{1}{2}\hbar\omega(q)[a^*(q)a(q) + a(q)a^*(q)]. \qquad (2.35)$$

The importance of these creation and annihilation operators is clear from the following discussion. The Hamiltonian, as is evident from eq. (2.35), belongs to a set of harmonic oscillators. The eigenstates of a quantum mechanical oscillator are well known. Each harmonic oscillator of eq. (2.35) corresponding to a particular q will have a set of eigenfunctions $\psi_n(q)$ with eigenvalues $E_n(q) = [n(q) + \tfrac{1}{2}]\hbar\omega(q)$, where $n(q)$ takes values $0, 1, 2, 3,...$ up to infinity. The total energy of the lattice is thus

$$E = \sum_q \hbar\omega(q)[n(q) + \tfrac{1}{2}]$$

and the wave functions will be product functions of the individual $\psi_n(q)$'s. The sound wave may be treated as a harmonic oscillator which can only be excited in steps or quanta of energy $\hbar\omega(q)$. The lowest state of each harmonic oscillator contains an energy $\tfrac{1}{2}\hbar\omega(q)$. This is known as the zero-point energy. Returning now to eq. (2.35) it can be shown that if $\psi_0(q)$ is the lowest eigenfunction the other eigenfunctions are given by

$$\psi_n(q) = [n(q)!]^{-1/2}[a(q)]^{n(q)}\psi_0(q)$$

with energy $\hbar\omega(q)[n(q) + \tfrac{1}{2}]$.

Alternatively, instead of regarding the sound wave as one entity it can be regarded as $n(q)$ quanta, or particles, each having an energy $\hbar\omega(q)$ together with a ground state energy $\tfrac{1}{2}\hbar\omega(q)$. These quanta of energy are called phonons and it is convenient to specify the energy of the system by stating the number of phonons in each mode q. Because each phonon contains the smallest amount of energy possible above the ground state, they are referred to as elementary excitations. To think of elementary excitations of the lattice as phonons is in fact no different from describing the electromagnetic field in terms of photons. To bring out the concept of phonons, a more convenient notation follows. The

ground state of the system is denoted by $|0\rangle$ which means that there are no phonons excited in any of the modes. A state containing $n(q_1)$ particles in mode q_1, $n(q_2)$ in mode q_2 etc. is then written as

$$|n(q_1)n(q_2) \cdots n(q_r) \cdots\rangle.$$

The creation and annihilation operators then operate on these states according to the following rules

$$a^*(q_r)|n(q_1)n(q_2) \cdots n(q_r) \cdots\rangle = (n(q_r)+1)^{1/2}|n(q_1)\dots, n(q_r)+1,\dots\rangle,$$

(2.36)

$$a(q_r)|n(q_1)n(q_2) \cdots n(q_r) \cdots\rangle = (n(q_r))^{1/2}|n(q_1)\dots, n(q_r)-1,\dots\rangle.$$

It is clear from this how the operators get their name; $a^*(q_r)$ creates an extra phonon in the mode q_r while $a(q_r)$ destroys it. In thermal equilibrium the occupation number of each mode is given by the Bose–Einstein distribution function

$$n(q) = \{\exp[\hbar\omega(q)/KT-1]\}^{-1}.$$

It is often required to express the displacement of an ion in terms of creation and annihilation operators. From the definition of the a's it is seen that

$$u(n) = i \sum_q (\hbar/2mN\omega(q))^{1/2}[a(q)-a^*(-q)]\exp(iqna). \quad (2.37)$$

3.4. Wave packets

Frequently in transport phenomena it is convenient to think of phonons as being particles which are able to move through the solid transporting energy from one region to another. Strictly speaking this view is incorrect because the term phonon applies to the eigenstates of energy of the normal modes which, as has been seen, are plane waves occupying the whole volume of the solid. What can be done however is to build-up localized excitations by forming wave packets composed of plane waves. Therefore instead of working with pure normal modes it is preferable to work with wave packets localized in a small region δr, composed from vibrations having a small spread δq in wave number. It is known from the uncertainty principle that this is possible if the spread in wave number is such that $\delta r \cdot \delta q \approx 1$. The general theory of wave motion tells us that this localized wave packet will move through the crystal with the group velocity $\partial\omega/\partial q$ rather than with the mean phase velocity associated with the constituent individual plane waves. In order to know whether this idea of a localized wave packet is useful in phonon transport, an estimation is required of the rate at which the wave packet will broaden due to dispersion. The order of magnitude

of this dispersive broadening for the case of the simple monatomic lattice treated in this section may be estimated as follows.

A general wave packet may be expressed in the form

$$\phi(x, t) = \int\limits_{-\infty}^{\infty} A(q)\, e^{i(\omega t - qx)}\, dq.$$

For mathematical simplicity it is convenient to consider a Gaussian wave packet for which the amplitude factor $A(q)$ has the form $A(q) = A \exp[-\sigma(q-q_0)^2]$. The wave packet is composed of waves with wave vectors centred about q_0. The amplitudes of the waves fall-off rapidly as their wave numbers deviate from q_0 and reach a value e^{-1} of that corresponding to q_0 in a wave number spread $\Delta q = 1/\sqrt{\sigma}$, where $1/\sqrt{\sigma}$ is referred to as the half width of the distribution. To carry out the integration in order to find the resultant displacement a knowledge of the frequency ω as a function of q is required. If the dispersion is small it is useful to expand ω in a Taylor series about the frequency corresponding to the wave number q_0:

$$\omega = \omega_0 + \alpha(q-q_0) + \beta(q-q_0)^2 + \cdots,$$

with $\alpha = (\partial\omega/\partial q)_0$, $\beta = \frac{1}{2}(\partial^2\omega/\partial q^2)_0$. If ω is a slowly varying function of q this series may be terminated at the third term. Substitution of ω into the integrand gives, after performing the integration,

$$\phi(x, t) = A\left(\frac{\pi}{\sigma - i\beta t}\right)^{1/2} \exp\left[\frac{-(x-\alpha t)^2}{4(\sigma - i\beta t)}\right] \exp[i(\omega_0 t - q_0 x)].$$

[Note the integral can be turned into the standard form

$$\int\limits_{-\infty}^{\infty} \exp(-ax^2)\, dx = (\pi/a)^{1/2}.]$$

Neglecting for the moment β, the first exponential factor shows that there is a spatial wave packet having a Gaussian profile of half-width $2\sqrt{\sigma}$ and moving with the velocity α, that is with the group velocity. The last factor shows that the wave train has a velocity equal to the mean phase velocity ω_0/q_0. If β is non-zero, it is noticed that there is still a Gaussian wave packet moving with the velocity α but now its half-width increases with time: the wave packet spreads out as it propagates. The half-width at time t is given by $2[(\sigma^2 + \beta^2 t^2)/\sigma]^{1/2}$ and therefore the pulse width increases by a factor $\sqrt{2}$ in time $t = \sigma/\beta$, during which time the wave packet will have travelled a distance $s = \alpha\sigma/\beta$. To estimate the magnitude of this an expression for α and β is required. For the lattice under consideration the dispersion relation is

$$\omega = 2(K/m)^{1/2} \sin\tfrac{1}{2}qa = (2v_0/a)\sin\tfrac{1}{2}qa$$

where v_0 is the sound velocity in the limit of long wavelengths. From this it follows that

$$s = 8v_0[1 - (a\omega/2v_0)^2]^{1/2}\sigma/a^2\omega.$$

Using the representative values $v_0 = 5 \times 10^5$ cm/sec, $a = 2$ Å and $\omega = 10^{11}$ rad/sec it is found that $s \approx 10^{11}\sigma$. Thus a pulse of initial width 10^{-5} cm will travel a distance of 2.5 cm before its half-width increases by $\sqrt{2}$.

3.5. General theory of lattice dynamics

We now proceed to the general theory of lattice dynamics in three dimensions. The starting point is the assumption that the total potential energy function is a function of the instantaneous position of all the ions. If the primitive translation vectors of the lattice are a_1, a_2 and a_3 the position of each lattice cell may be denoted by $x(l) = l_1a_1 + l_2a_2 + l_3a_3$. If the lattice has p atoms per unit cell, the position of each atom within the unit cell can be denoted by $x(k)$ where k runs from 1 to p. The position of each atom in the lattice is thus described by

$$x\begin{pmatrix} l \\ k \end{pmatrix} = x(l) + x(k).$$

When the atoms are displaced from equilibrium we may write

$$x_\alpha\begin{pmatrix} l \\ k \end{pmatrix} = x_\alpha^0\begin{pmatrix} l \\ k \end{pmatrix} + u_\alpha\begin{pmatrix} l \\ k \end{pmatrix}.$$

The u's denote the displacement of the atoms from their equilibrium values x^0. The $\alpha(1, 2, 3)$ are the cartesian components of each vector. If the potential energy can be expanded in a Taylor series of the atomic displacements the Hamiltonian may be expressed in the form

$$H = \tfrac{1}{2}\sum_{lk\alpha} m_k \dot{u}_\alpha^2\begin{pmatrix} l \\ k \end{pmatrix} + \phi_0 + \sum_{lk\alpha} \phi_\alpha\begin{pmatrix} l \\ k \end{pmatrix} u_\alpha\begin{pmatrix} l \\ k \end{pmatrix}$$

$$+ \tfrac{1}{2}\sum_{\substack{lk\alpha \\ l'k'\beta}} \phi_{\alpha\beta}\begin{pmatrix} ll' \\ kk' \end{pmatrix} u_\alpha\begin{pmatrix} l \\ k \end{pmatrix} u_\beta\begin{pmatrix} l' \\ k' \end{pmatrix} + \cdots. \qquad (2.38)$$

The first term is simply the kinetic energy term, m_k being the mass of the individual atoms and ϕ_0 is the equilibrium potential energy. The coefficients $\phi_\alpha\begin{pmatrix} l \\ k \end{pmatrix}$ and $\phi_{\alpha\beta}\begin{pmatrix} ll' \\ kk' \end{pmatrix}$ in the Taylor expansion are

$$\phi_\alpha\begin{pmatrix} l \\ k \end{pmatrix} = \left[\frac{\partial\phi}{\partial u_\alpha\begin{pmatrix} l \\ k \end{pmatrix}}\right]_0; \quad \phi_{\alpha\beta}\begin{pmatrix} ll' \\ kk' \end{pmatrix} = \left[\frac{\partial^2\phi}{\partial u_\alpha\begin{pmatrix} l \\ k \end{pmatrix}\partial u_\beta\begin{pmatrix} l' \\ k' \end{pmatrix}}\right]_0. \qquad (2.39)$$

The subscript 0 indicates that the derivatives are to be evaluated in the equilibrium configuration. Only terms up to second power in the atomic displacement in the Taylor series expansion will be retained. This is the harmonic approximation when normal modes of the system can be found. To account for properties like thermal expansion and thermal resistance higher order terms would have to be included. Various symmetry properties between the ϕ's can be established. Clearly, by definition

$$\phi_{\alpha\beta}\begin{pmatrix} ll' \\ kk' \end{pmatrix} = \phi_{\beta\alpha}\begin{pmatrix} l'l \\ k'k \end{pmatrix}. \tag{2.40}$$

Also because of translational invariance $\phi_\alpha\begin{pmatrix} l \\ k \end{pmatrix}$ is independent of l and

$\phi_{\alpha\beta}\begin{pmatrix} ll' \\ kk' \end{pmatrix}$ depends only on $l - l'$ and not the individual l's. Suppose

now that the lattice undergoes a rigid translation. Then the displacement $u\begin{pmatrix} l \\ k \end{pmatrix}$ of all atoms will be equal, independent of l and k. Therefore

for the Hamiltonian to be invariant it is seen that

$$\sum_{lk} \phi\begin{pmatrix} l \\ k \end{pmatrix} \quad \text{and} \quad \sum_{lkl'k'} \phi\begin{pmatrix} ll' \\ kk' \end{pmatrix} = 0. \tag{2.41}$$

Also it is noticed that the α-component of force on the atom $\begin{pmatrix} l \\ k \end{pmatrix}$ is given by

$$-X_\alpha\begin{pmatrix} l \\ k \end{pmatrix} = \frac{\partial\phi}{\partial u_\alpha\begin{pmatrix} l \\ k \end{pmatrix}} = \phi_\alpha\begin{pmatrix} l \\ k \end{pmatrix} + \sum_{l'k'\beta} \phi_{\alpha\beta}\begin{pmatrix} ll' \\ kk' \end{pmatrix} u_\beta\begin{pmatrix} l' \\ k' \end{pmatrix}. \tag{2.42}$$

If, as before, it is assumed that the lattice has undergone a rigid translation so that the u's are independent of l and k the equation

$$\sum_{l'k'} \phi_{\alpha\beta}\begin{pmatrix} ll' \\ kk' \end{pmatrix} = 0$$

is obtained since the force on any atom could not have changed. From the Hamiltonian it is seen that the equation of motion is

$$m_k\ddot{u}_\alpha\begin{pmatrix} l \\ k \end{pmatrix} = -\frac{\partial\phi}{\partial u_\alpha\begin{pmatrix} l \\ k \end{pmatrix}} = -\sum_{l'k'\beta} \phi_{\alpha\beta}\begin{pmatrix} ll' \\ kk' \end{pmatrix} u_\beta\begin{pmatrix} l' \\ k' \end{pmatrix}. \tag{2.43}$$

As for the one-dimensional problem a solution of the form

$$u_\alpha\begin{pmatrix} l \\ k \end{pmatrix} = m_k^{-1/2} A_\alpha(k) \exp\left[i(\omega(q)t - q \cdot x(l))\right]$$

is chosen where $A_\alpha(k)$ is independent of l. Substituting in the equation of motion gives

$$\omega^2(q)A_\alpha(k) = \sum_{k'\beta} D_{\alpha\beta}\left(\begin{matrix}q\\kk'\end{matrix}\right)A_\beta(k'), \tag{2.44}$$

where

$$D_{\alpha\beta}\left(\begin{matrix}q\\kk'\end{matrix}\right) = \frac{1}{(m_k m_{k'})^{1/2}}\sum_l \phi_{\alpha\beta}\left(\begin{matrix}l\\kk'\end{matrix}\right)e^{iq\cdot x(l)}. \tag{2.45}$$

For this set of equations to have a solution the determinant of the coefficients of A must vanish. Thus the condition for solubility is

$$\left| D_{\alpha\beta}\left(\begin{matrix}q\\kk'\end{matrix}\right) - \omega^2(q)\delta_{\alpha,\beta}\delta_{k,k'}\right| \equiv 0, \tag{2.46}$$

α and k take 3 and p values respectively so that the equation is of $3p$ degree in $\omega^2(q)$. This equation is the analogue of Christoffel's equation, eq. (2.15). It will be noticed that for a lattice with a basis there are more than three eigenvalues because the detail structure within a unit cell has been accounted for. Also the eigenfrequencies $\omega(q)$ will no longer be proportional to q implying that dispersion occurs. The $3p$ eigenfrequencies for a particular q may be denoted by $\omega_j(q)$ with $j = 1$ to $3p$. Each value of j denotes a particular branch of the phonon spectrum. A mode is specified when the values of both q and j are given. From eq. (2.45) it is seen that

$$D^*_{\alpha\beta}\left(\begin{matrix}q\\kk'\end{matrix}\right) = D_{\beta\alpha}\left(\begin{matrix}q\\k'k\end{matrix}\right).$$

Thus the matrix obtained from the coefficients of

$$D_{\alpha\beta}\left(\begin{matrix}q\\kk'\end{matrix}\right)$$

by pairing indices (αk) and $(\beta k')$ is Hermitian. It follows that the values of $\omega_j^2(q)$ are real and so it may be assumed that the $\omega_j(q)$ are real. To each value of $\omega_j(q)$ corresponding to a particular q there is a vector $e\left(k\left|\begin{matrix}q\\j\end{matrix}\right.\right)$ whose components are the solutions of eq. (2.44)

$$\omega_j^2(q)e_\alpha\left(k\left|\begin{matrix}q\\j\end{matrix}\right.\right) = \sum_{k'\beta} D_{\alpha\beta}\left(\begin{matrix}q\\kk'\end{matrix}\right)e_\beta\left(k'\left|\begin{matrix}q\\j\end{matrix}\right.\right). \tag{2.47}$$

The eigenvectors may be chosen to satisfy the conditions

$$\sum_{k\alpha} e^*_\alpha\left(k\left|\begin{matrix}q\\j\end{matrix}\right.\right)e_\alpha\left(k\left|\begin{matrix}q\\j'\end{matrix}\right.\right) = \delta_{jj'}$$

$$\sum_j e^*_\beta\left(k'\left|\begin{matrix}q\\j\end{matrix}\right.\right)e_\alpha\left(k\left|\begin{matrix}q\\j\end{matrix}\right.\right) = \delta_{\alpha,\beta}\delta_{k,k'}. \tag{2.48}$$

It will be noticed that

$$D_{\alpha\beta}\binom{-q}{kk'} = D_{\alpha\beta}^*\binom{q}{kk'}.$$

Taking the conjugate complex of eq. (2.47), since the ω_j's are real, it can be assumed that

$$e_\alpha\left(k\Big|_j^q\right) = e_\alpha^*\left(k\Big|_j^{-q}\right) \quad \text{and} \quad \omega_j^2(q) = \omega_j^2(-q).$$

It is useful to expand the

$$u\binom{l}{k} \quad \text{and} \quad p\binom{l}{k}$$

in Fourier series as follows

$$u_\alpha\binom{l}{k} = \frac{1}{(Nm_k)^{1/2}} \sum_{qj} e_\alpha\left(k\Big|_j^q\right) e^{-iq\cdot x(l)} u\binom{q}{j},$$

$$p_\alpha\binom{l}{k} = \left(\frac{m_k}{N}\right)^{1/2} \sum_{qj} e_\alpha^*\left(k\Big|_j^q\right) e^{iq\cdot x(l)} p\binom{q}{j}. \tag{2.49}$$

Substituting these expansions into the Hamiltonian gives within the framework of the harmonic approximation

$$H = \tfrac{1}{2} \sum_{qj} p\binom{q}{j} p^*\binom{q}{j} + \tfrac{1}{2} \sum_{qj} \omega_j^2(q) u^*\binom{q}{j} u\binom{q}{j}. \tag{2.50}$$

Note that the mass does not appear explicitly as it is included in the definition of the p's and u's. As in the one-dimensional problem, using the Heisenberg equations of motion it is found that the $u\binom{q}{j}$ are the normal coordinates with frequencies given by

$$\ddot{u}\binom{q}{j} + \omega_j^2(q) u\binom{q}{j} = 0.$$

The displacement components of any atom are then a superposition of normal-mode coordinates multiplied by the factor

$$e_\alpha\left(k_j^q\right) \exp\left[-iq\cdot x(l)\right].$$

As in the one-dimensional problem it is possible to introduce creation and annihilation operators. The relations inverse to eq. (2.49) are

$$u\binom{q}{j} = \frac{1}{\sqrt{N}} \sum_{lk\alpha} e_\alpha^*\left(k\Big|_j^q\right) m_k^{1/2} u_\alpha\binom{l}{k} e^{iq\cdot x(l)},$$

$$p\binom{q}{j} = \frac{1}{\sqrt{N}} \sum_{lk\alpha} e_\alpha\left(k\Big|_j^q\right) m_k^{-1/2} p_\alpha\binom{l}{k} e^{-iq\cdot x(l)}. \tag{2.51}$$

Quantum mechanically these satisfy the commutation rules

$$\left[u\begin{pmatrix}q\\j\end{pmatrix}, p\begin{pmatrix}q'\\j'\end{pmatrix}\right] = i\hbar\delta_{q,q'}\,\delta_{j,j'}. \tag{2.52}$$

As in eq. (2.33) creation and annihilation operators are defined through the relations

$$a_j^*(q) = [2\hbar\omega_j(q)]^{-1/2}\left[p^*\begin{pmatrix}q\\j\end{pmatrix} + i\omega_j(q)u\begin{pmatrix}q\\j\end{pmatrix}\right]$$

$$a_j(q) = [2\hbar\omega_j(q)]^{-1/2}\left[p\begin{pmatrix}q\\j\end{pmatrix} - i\omega_j(q)u^*\begin{pmatrix}q\\j\end{pmatrix}\right] \tag{2.53}$$

obeying

$$[a_j(q), a_{j'}^*(q')] = \delta_{q,q'}\delta_{j,j'}$$

$$[a_j(q), a_{j'}(q')] = [a_j^*(q), a_{j'}^*(q')] = 0. \tag{2.54}$$

Expressed in terms of these operators the Hamiltonian is

$$H = \sum_{qj} \hbar\omega_j(q)\,[a_j^*(q)a_j(q) + a_j(q)a_j^*(q)] \tag{2.55}$$

and the displacement vector of the atom $\begin{pmatrix}l\\k\end{pmatrix}$ has components

$$u_\alpha\begin{pmatrix}l\\k\end{pmatrix} = i\sum_{qj}\left(\frac{\hbar}{2Nm_k\omega_j(q)}\right)^{1/2} e_\alpha^*\left(k\bigg|\begin{matrix}q\\j\end{matrix}\right) e^{iq\cdot x(l)}\,[a_j(q) - a_j^*(-q)]. \tag{2.56}$$

3.6. *Central forces and Cauchy relations*

What is the connection between the classical elasticity theory and the dynamical lattice treatment? At long wavelengths, since the wave disturbance may only vary slightly over an atomic spacing it may be expected that the behaviour of the discrete lattice is much the same as that of the continuum. In fact, under certain conditions it is found that the long wavelength behaviour of an acoustic mode is the same as that predicted by elasticity theory so that expressions may be obtained relating the elastic constants with the actual force constants between the atoms. To see this a simple example will be considered.

The model to be examined is a simple cubic lattice having only one type of atom. The subscript k may thus be dropped:

$$D_{\alpha\beta}(q) = \frac{1}{m}\sum_l \phi_{\alpha\beta}(l)\,e^{iq\cdot x(l)}, \tag{2.57}$$

where

$$\phi_{\alpha\beta}(l) = \left[\frac{\partial^2\phi}{\partial u_\alpha(l)\partial u_\beta(0)}\right]_0. \tag{2.58}$$

An additional assumption will now be made concerning the form of the potential energy. It will be assumed that it is the sum of pairwise inter-

actions between all the atoms in the lattice and that the potential function through which the atoms interact depends only on the magnitude of their separation:

$$\phi = \tfrac{1}{2} \sum_{ll'} \psi(|x(l) - x(l') + u(l) - u(l')|^2). \tag{2.59}$$

This particular form for the potential energy gives force constants

$$\phi_{\alpha\beta}(l) = [-2\delta_{\alpha,\beta}\psi' - 4x_\alpha x_\beta \psi'']_{x(l)}, \tag{2.60}$$

where it is understood that the case $l = 0$ is to be excluded. The subscript $x(l)$ means that the square brackets are to be evaluated at those lattice vectors. In addition, from eq. (2.41)

$$\phi_{\alpha\beta}(0) = \sum_{l \neq 0} [2\delta_{\alpha\beta}\psi' + 4x_\alpha x_\beta \psi'']_{x(l)}. \tag{2.61}$$

For a simple cubic lattice of lattice constant a the lattice vectors are given by $x(l) = l_1 a_1 + l_2 a_2 + l_3 a_3$, where l_1, l_2 and l_3 are integers and a_1, a_2, a_3 are vectors of length a along the cubic axes. Assuming a long wavelength limit the exponential in eq. (2.57) can be expanded retaining terms up to order q^2:

$$D_{\alpha\beta}(q) = \frac{1}{m} \sum_{l\gamma\delta} [2\delta_{\alpha\beta}\psi' + 4a^2 l_\alpha l_\beta \psi'']^{1/2} a^2 l_\gamma l_\delta q_\gamma q_\delta.$$

But if the lattice is initially free of stress it can be shown that

$$\sum_l x_\alpha(l) x_\beta(l) \psi'(|x(l)|^2) = 0.$$

Therefore

$$D_{\alpha\beta}(q) = (2a^4/m) \sum_{l\gamma\delta} l_\alpha l_\beta l_\gamma l_\delta q_\gamma q_\delta \psi''(l)$$

$$= \sum_{\gamma\delta} [\alpha\beta\gamma\delta] q_\gamma q_\delta, \tag{2.62}$$

where

$$[\alpha\beta\gamma\delta] = \frac{2a^4}{m} \sum_l l_\alpha l_\beta l_\gamma l_\delta \psi''(l). \tag{2.63}$$

Since ψ'' is symmetric and l_α etc. take equal positive and negative values, the only non-zero values of $[\alpha\beta\gamma\delta]$ which will occur will be those for which all the indices are the same or those for which the indices are equal in pairs. Also the order of $\alpha, \beta, \gamma, \delta$ cannot matter. In addition for a cubic lattice, because of the symmetry of the structure with respect to the three cartesian directions, $[1111] = [3333]$ and $[1122] = [1133]$ etc. The condition for solubility, eq. (2.46), thus reduces to

$$\begin{vmatrix} [1111]q_1^2 + [1122](q_2^2 + q_3^2) - \omega^2(q); & 2[1122]q_1q_2; & 2[1122]q_1q_3 \\ 2[1122]q_1q_2; & [1111]q_2^2 + [1122](q_1^2 + q_3^2) - \omega^2(q); & 2[1122]q_2q_3 \\ 2[1122]q_1q_3; & 2[1122]q_2q_3; & [1111]q_3^2 + [1122](q_1^2 + q_2^2) - \omega^2(q) \end{vmatrix} = 0.$$

This agrees with eq. (2.13) if the following identification is made:

$$c_{11} = \rho[1111]; \quad c_{44} = \rho[1122]; \quad c_{12} + c_{44} = 2\rho[1122].$$

Thus, noting that $\rho = M/a^3$ the elastic constants c may be expressed in terms of the force constants ψ'' by

$$c_{11} = 2a \sum_l l_1^4 \psi''(l), \qquad c_{44} = 2a \sum_l l_1^2 l_2^2 \psi''(l). \tag{2.64}$$

In addition, a further relation between the elastic constants of the cubic crystal is obtained, namely $c_{12} = c_{44}$. In the general case it is seen that because eq. (2.63) is independent of the order of α, β, γ, δ the number of independent constants is 15 rather than 21 as stated before in ch. 2 §1.3. The additional relations are

$$c_{23} = c_{44}, \quad c_{31} = c_{55}, \quad c_{12} = c_{66}, \quad c_{14} = c_{56}, \quad c_{25} = c_{64}, \quad c_{36} = c_{45}.$$

These are known as Cauchy relations. For cubic crystals they reduce, as has been seen, to $c_{12} = c_{44}$. It will be noted that in the model that has been treated, (a) each atom is at a centre of symmetry, (b) the atoms interact through pairwise central forces, (c) there is no initial stress in the crystal. Indeed, unless these conditions are satisfied, Cauchy relations will not hold. It is of interest to mention that in the early days of elasticity there was some controversy as to the maximum number of elastic moduli. Stokes and Green believed there were 21 while Cauchy and Poisson held that there were 15. The difference was due to the assumptions made about the microstructure of the crystal lattice. As has been noted above conditions (a), (b) and (c) lead to a 15 constant theory.

THE GENERATION AND DETECTION OF MICROWAVE ULTRASONICS

1. Introduction

Most experiments in microwave ultrasonics have used the pulse-echo technique. A short pulse of ultrasound, perhaps 1 μsec long, generated at one end of a delay rod specimen travels backwards and forwards along the rod as a series of echoes and may be detected at either end. The transducers which have been used have relied for their action on the piezoelectric effect or on magnetostriction, phenomena widely used at lower frequencies in ultrasonic work. The first experiments in the microwave frequency range using the piezoelectric effect were reported by BARANSKII[1957a] and those involving magnetostriction were successfully performed by BÖMMEL and DRANSFELD[1959a].

One of the main problems encountered in ultrasonic work at microwave frequencies is the short wavelength of the ultrasonic waves. Ultrasonic detectors using the piezoelectric or magnetostrictive effects depend on a coupling between the electromagnetic wave and the ultrasonic wave which is proportional to the strain in the transducer rather than to the intensity of the ultrasonic wave. When such a transducer is used as a detector it is necessary for maximum response that the ultrasonic wave arrives with its wavefront parallel to the surface of the detector to an accuracy of at least one ultrasonic wavelength. In most solid materials such as the hard dielectrics, magnesium oxide, corundum and quartz, the velocity of ultrasonic waves is more than 10^3 m·sec^{-1}. Taking as a representative value a velocity of 5×10^3 m·sec^{-1} the wavelength at a frequency of 1 GHz is 5×10^4 Å and at 10 GHz is 5×10^3 Å. This latter wavelength is the same as that of visible light and thus the surfaces of the transducers and delay rod specimens for microwave ultrasonics must be prepared to optical standards. Delay rod specimens must have end faces, whether for the attachment of transducers or as reflecting faces for pulse echoes, that are flat and mutually

parallel to at least ⅓ ultrasonic wavelength if satisfactory results are to be obtained.

Most crystalline solids are elastically anisotropic so the choice of direction along which we attempt to propagate an ultrasonic wave is important. In such substances the ultrasonic energy flow is only perpendicular to the wavefronts in certain special directions – usually axes of symmetry of the crystal. Thus the specimens must be accurately oriented before a delay rod is cut and its end faces polished to ensure that a suitable direction has been chosen for the propagation of the microwave ultrasound.

The attenuation of microwave ultrasonic waves rises rapidly with temperature in most materials due to interactions with thermal vibrations. For frequencies of 9 GHz and above this usually implies that experiments – especially of the pulse-echo type – must be done at low temperatures in the liquid hydrogen and liquid helium ranges below 20°K. The frequency- and temperature-dependence of ultrasonic attenuation in dielectrics is considered in detail in ch. 4 and so will not be discussed further here. We merely point out that in the discussion that follows it is understood that most of the methods mentioned are used at very low temperatures.

2. Specimen preparation

2.1. *Introduction*

This section is mainly concerned with the preparation of dielectric and semiconductor materials rather than metals which present additional complications. In metals the attenuation of the microwave ultrasound is very high at all temperatures so very short delay rods are necessary. Special methods each perhaps applicable only to a single metal must then be used. Because of this problem of very high attenuation very few experiments using microwave ultrasonics in metals have been reported.

Single crystal specimens must usually be employed to form microwave ultrasonic delay rod specimens to avoid the large scattering that would be present in polycrystalline materials due to the discontinuities at the crystalline boundaries. If the size of the scattering centres is small compared to the wavelength, that is $ka \ll 1$ where k is the ultrasonic wave number and a the radius of the spherical scattering centre, the Rayleigh approximation should hold and the scattering increase as the fourth power of the frequency. When the wavelength is shorter and it becomes comparable or less than the size of the crystallites the Rayleigh treatment is no longer valid. At each crystallite boundary reflection and refraction of the ultrasonic wave occur due to anisotropy

of the material and the wave is strongly scattered. Thus in the micro-
wave frequency range single crystal delay rods must be used. (See the
article by TRUELL and ELBAUM[1962] for a discussion of these
scattering mechanisms.)

2.2. *Orientation*

The method used to orient a single crystal sample before cutting out
a delay rod specimen depends on the material. If it has well-defined
cleavage planes or is optically birefringent these properties can be used
and are usually of great assistance, even if X-ray diffraction has to be
employed for the final accuracy required. It is very time consuming to
orient a sample entirely by X-ray diffraction so any guide to the approxi-
mate orientation is helpful. Whichever method is employed to establish
the sample orientation, it is clearly most important that the orientation
is maintained while the sample is cut or ground to define a surface from
which the delay rod specimen can be taken. Most X-ray goniometers
are not designed for holding large samples nor for holding them
sufficiently firmly for sawing or grinding. Suitably designed crystal
holders have been described by BOND[1961], WALKER *et al.*[1949]
and JEFKINS and HINES[1968]. An extensive discussion of X-ray
orientation methods with particular reference to quartz is given
by BOND and ARMSTRONG[1943].

2.3. *Polishing*

When the raw crystal sample is oriented it must be cut to size and the
end faces polished. The accuracy and surface finish required are
similar to those needed for laser crystals and the techniques used to
achieve them are the same. Many of the methods have been familiar
to optical workers for many years but some modifications need to be
made because the materials used for a particular experiment may be
available in only a limited quantity and may be delicate or brittle. The
traditional opticians' method with such materials involves much hand
working which can be an accurate and rapid procedure when employed
by an experienced worker; the methods are described by TWYMAN
[1952]. If an experienced optical hand-worker is not available excel-
lent results can be obtained using simple machine methods requiring
less skill and experience. A saw using a diamond-impregnated blade
for sawing oriented single crystals has been described by FYNN and
POWELL[1966]. Alternatively the crystal faces can be ground with a
diamond-impregnated wheel in a surface grinding machine. Polishing
of the specimen surfaces is then carried out on a flat rotating lap hold-
ing the crystal in a suitable holder to maintain the orientation of the
face being polished. Suitable crystal holders have been described by

BENNETT and WILSON[1966] and by FYNN and POWELL[1967]. The choice of lap material and polishing medium depends on the properties, especially hardness, of the specimen material. Alumina, diamond dust or cerium oxide (ceri-rouge) are the most used materials for polishing while lap materials may be brass, soft solder, pitch or a mixture of pitch and waxes. The choice is often a matter of trial and error for a material not polished before. Too soft a lap material usually produces an excellent surface finish but at the sacrifice of flatness, the surface becomes convex; while too hard a lap gives a flat surface with scratches. The most important requirement for polishing a flat surface is an initially flat lap surface. The authors already mentioned give methods of ensuring lap flatness and DICKINSON[1968] suggests a way of maintaining the flatness of a pitch lap during polishing.

2.4. Parallelism of ends

The end faces of the delay rod specimen must be polished parallel to each other as well as flat. The simplest way of polishing parallel faces is to polish three or more rods of the same length at the same time. The lengths can be compared with a sensitive length comparator (e.g. that described by FYNN[1950]) and if the rods are spaced apart in a holder this gives a sensitive test of the surface parallelism. If only one rod is available for polishing other methods must be used such as the auto-collimator technique of BENNETT and WILSON[1966].

3. Piezoelectric transducers

3.1. Introduction

Certain crystals when strained become electrically polarized and conversely when placed in an electric field become strained. This is the piezoelectric effect and its converse and is extensively employed to make ultrasonic transducers for a wide range of frequencies. In the lower frequency range below 1 GHz piezoelectric transducers are almost invariably operated in an acoustic resonance mode. However at 1 GHz and above the resonant transducer thickness becomes very small unless a high harmonic is used. At 10 GHz a quartz transducer half an ultrasonic wavelength thick generating a longitudinal wave would be about 2500 Å thick. Clearly such a thin slice is extremely difficult to cut and polish, nevertheless it is feasible, for example WILSON[1967] has cut a thin resonant transducer of cadmium sulphide.

Two methods have been employed to overcome this problem; firstly the use of non-resonant surface generation at the end of a long rod transducer and secondly the use of a thin evaporated film of piezo-electric material equivalent to the resonant thickness. These two

methods will be considered in turn in subsequent sections but first we shall deal with the properties of the materials usually employed as microwave ultrasonic transducers.

3.2. *Piezoelectric materials*

A piezoelectric transducer for generating and detecting ultrasonic waves should be mechanically strong and stable to facilitate handling. It should be made of a material in which the ultrasonic attentuation is low and should have an acoustic impedance close to that of the delay rod specimen material. Finally it should usually be an efficient power transducer although this latter requirement is not always desirable as has been discussed by DE KLERK[1966a]. If the attentuation of ultrasound is being measured in a material where it is low then it can be that a major contribution to the apparent attenuation is the power taken at each reflection of the ultrasonic pulse by the detecting transducer in the specimen delay rod. In the microwave frequency region this is rarely a serious problem because of the usually low efficiency of present transducers.

Materials which exhibit the phenomenon of piezoelectricity form crystals which are necessarily of low symmetry. The absence of a centre of symmetry is a necessary condition for the appearance of the piezoelectric effect. Thus only materials from a restricted number of crystal classes can be used as ultrasonic transducers and of these only a very small number have actually been employed in the microwave frequency range. The discussion will be restricted to these materials, a much more comprehensive discussion of piezoelectric materials appears in the article by BERLINCOURT *et al.*[1964].

Quartz has been used almost exclusively as a non-resonant transducer in the microwave frequency range because of its ready availability in large single crystals of good quality and its excellent mechanical properties. The main disadvantage of quartz is its high attenuation of microwave ultrasound at temperatures above about 20 K (BÖMMEL and DRANSFELD[1960]). The attenuation increases with frequency, see ch. 4, and thus at 10 GHz and above non-resonant quartz transducers can only be used in the liquid helium or liquid hydrogen temperature ranges. Quartz is a member of the crystal class 32 with a threefold symmetry axis, usually designated as the z-axis, and with three two-fold axes normal to it, one of which is taken as the x-axis. There are two independent piezoelectric constants usually taken as d_{11} and d_{14}, see appendix 1. The piezoelectric constants are defined by eqs. (2.21) which in the absence of a magnetic field and at constant temperature reduce to

$$\epsilon_{ij} = s^E_{ijkl}\sigma_{kl} + d_{kij}E_k, \qquad D_i = d_{ijk}\sigma_{jk} + \kappa^\sigma_{ij}E_j. \qquad (3.1)$$

In this notation i, j, k, l take the values 1 to 3. Alternatively the single suffix notation* can be used when

$$\epsilon_m = s_{mn}^E \sigma_n + d_{km} E_k, \qquad D_i = d_{im} \sigma_m + \kappa_{ij}^\sigma E_j.$$

Again i, j and k take the values 1 to 3 but m and n take values 1 to 6. For quartz it is found that, because of symmetry, the piezoelectric constants d_{14} and $-d_{25}$ are equal and this describes the interaction of an electric field in the plane normal to the three-fold axis with a shear strain in the plane normal to the field. Taking d_{11} as the other independent constant, as is customary, symmetry considerations give $d_{12} = -d_{11}$ and $d_{26} = -2d_{11}$. That is, an electric field along the two-fold axis, the X-axis, is coupled to a longitudinal strain along the same axis together with an equal strain of opposite sign along the Y-axis. Also, an electric field along the Y-axis causes a shear strain in the XY-plane. The values of the piezoelectric constants for quartz are given in table 3.1. The most useful parameter to describe a material which is used as

TABLE 3.1
Piezoelectric and elastic constants of quartz[a]) (low frequency values)

Density (kg·m⁻³)	Elastic compliances s_{ij}^E (10⁻¹² m²·N⁻¹)						
	s_{11}	s_{33}	s_{12}	s_{13}	s_{44}	s_{66}	s_{14}
2649	12.77	9.60	−1.79	−1.22	20.04	29.12	4.50

Piezoelectric constants (10⁻¹² C·N⁻¹)		Dielectric constants	
d_{11}	d_{14}	K_{11}^T	K_{33}^T
2.31	0.727	4.52	4.64

[a]) From BECHMANN[1958].

a piezoelectric ultrasonic transducer is the piezoelectric coupling factor. This may be defined as the ratio of the mutual elastic and dielectric energy density to the geometric mean of the two self-energy densities. The efficiency of a transducer is proportional to the square of this coupling factor as will be shown later. Generally the form of this coupling factor can be very complicated but for certain orientations of the crystal and particular directions of the electric field the expression may be quite simple. Some of these factors are given in the article by BERLINCOURT et al. [1964].

The most commonly used cuts of quartz are the X-cut and rotated

---

* In this notation $d_{im} = 2d_{ijk}$ if $m = 4, 5, 6$ and $= d_{ijk}$ otherwise.

Y-cuts. The former has surfaces cut normal to the *X*-axis along which the alternating electric field is applied. A longitudinal strain in the *X*-direction is produced, resulting in a longitudinal ultrasonic wave propagating in this direction since it is a pure mode axis for this type of wave. In this case the piezoelectric coupling factor K_{11} is given by $K_{11} = d_{11}/(\kappa_{11}s_{11}^E)^{1/2}$. The two rotated *Y*-cuts that are used are frequently called AC and BC and have the transducer axis, along which the electric field is applied, at angles of $-59°$ and $+31°$ respectively to the *Z*-axis in the *YZ*-plane. These are pure mode axes for shear waves and the ultrasonic energy propagates in a direction normal to the wave front, FARNELL[1961]. The wave front is determined by the transducer surface, see §3.3 below, which is cut normal to the transducer axis. Figure 3.1 illustrates the quartz cuts used. The shear wave transducers, the AC and BC cuts, have not been widely used at microwave frequencies because of the difficulty of making a bond to a delay rod specimen that efficiently transmits shear waves. They have been used however in investigations of the attenuation of shear waves in quartz itself when the transducer acts as the delay rod and no bonding is required (BÖMMEL and DRANSFELD[1960]).

The other materials that have been used as piezoelectric ultrasonic transducers at microwave frequencies are members of the crystal class
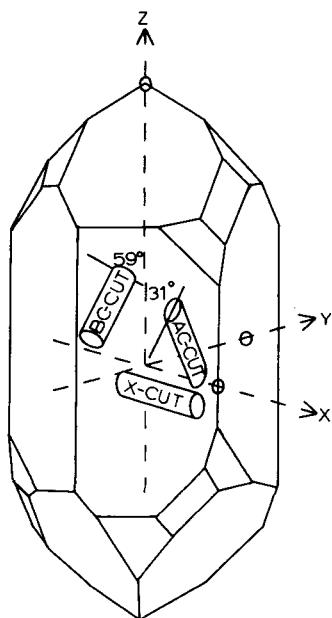

Fig. 3.1. Quartz cuts used as microwave ultrasonic transducers.

6 mm. They are cadmium sulphide, zinc sulphide, zinc oxide, cadmium selenide and zinc selenide: the first of these is the most extensively used, especially as an evaporated thin film. Materials of this class have a six-fold axis of symmetry chosen as the Z-axis. They possess three independent piezoelectric constants d_{33}, $d_{31} = d_{32}$ and $d_{15} = d_{24}$. An electric field parallel to the six-fold axis causes a longitudinal strain in this direction and also longitudinal strains along the X- and Y-directions. These latter two strains are equal to each other but are different, and often of opposite sign, from the strain along the Z-axis. These materials of class 6 mm are elastically and piezoelectrically isotropic in the plane perpendicular to the six-fold axis. An electric field in this plane causes a shear strain in the plane containing the field and the Z-axis irrespective of the direction of the field in that plane. Production by evaporation of thin films of these materials usually results in a film with the Z-axis normal to the substrate surface. An electric field normal to the substrate surface then generates a longitudinal wave into the substrate delay rod, while an electric field parallel to the substrate surface generates a shear wave. The piezoelectric coupling factor K_{33} for the generation of longitudinal waves is $K_{33} = d_{33}/(\kappa_{33} s_{33}^E)^{1/2}$. The values of the elastic and piezoelectric constants for some of these materials are listed in table 3.2.

Other materials have been used in piezoelectric transducers at microwave frequencies, for example, aluminium nitride and lithium niobate

TABLE 3.2
Piezoelectric and elastic constants of hexagonal crystals

Material	Density (kg·m⁻³)	Elastic compliances $(10^{-12}\,\mathrm{C\cdot N^{-1}})$					
		s_{11}	s_{33}	s_{12}	s_{13}	s_{44}	s_{66}
CdS[a]	4819	20.69	16.97	−9.99	−5.81	66.49	61.36
CdSe[a]	5684	23.38	17.35	−11.22	−5.72	75.95	69.20
ZnO[b]	5676	7.86	6.94	−3.43	−2.21	23.55	22.57
ZnS[c]	3980	11.12	8.47	−4.56	−1.4	34.4	31.4

Material	Piezoelectric constants $(10^{-12}\,\mathrm{C.\,N^{-1}})$			Dielectric constants	
	d_{31}	d_{33}	d_{15}	K_{33}^T	K_{11}^T
CdS[a]	−5.18	10.32	−13.98	10.33	9.35
CdSe[a]	−3.92	7.84	−10.51	10.65	9.70
ZnO[b]	−5.2	10.6	−13.9	11.0	9.26
ZnS[c]	−1.1	3.2	−2.8	8.7	8.7

[a] From BERLINCOURT et al. [1961].
[b] From BATEMAN [1962].
[c] From KOBYAKOV [1966].

(WAUK and WINSLOW[1968], GRACE et al.[1966]). As methods are developed for depositing these and other materials as thin films onto delay rods more information will become available leading to more efficient transducers and, perhaps especially, efficient and convenient shear wave transducers.

3.3. Generation of ultrasonic waves by non-resonant transducers

It has already been mentioned that a resonant piezoelectric ultrasonic transducer for microwave frequencies is very thin if a low harmonic is used and can in practice only be obtained by using an evaporated thin film. Long, non-resonant transducers have been used extensively at microwave frequencies; the generation of ultrasonic waves occurs at a single surface where there is a piezoelectric discontinuity.

A typical experimental arrangement for the generation of microwave ultrasound by a non-resonant transducer–usually quartz–is shown in fig. 3.2. A cylindrical re-entrant microwave cavity is used which provides a strong electric field across the end face of the transducer. The theory of the generation of ultrasound with this arrangement has been given by JACOBSEN[1960] and his treatment will be followed. It will be assumed that an X-cut quartz transducer is being used to generate longitudinal waves. The system of coordinates adopted for the discussion is shown in fig. 3.3. The polished end face of the quartz lies in the $x_1 = 0$ plane and the ultrasonic wave is propagating along the x_1-direction along which the microwave electric field $E_1(t)$ lies. The stress σ_1 in the quartz of density ρ is given by

$$\sigma_1 = c_{11}\epsilon_1 - e_{11}E_1(t), \qquad (3.2)$$

where c_{11} is the appropriate elastic stiffness constant, ϵ_1 the strain and e_{11} the piezoelectric stress constant. The equation of motion for the
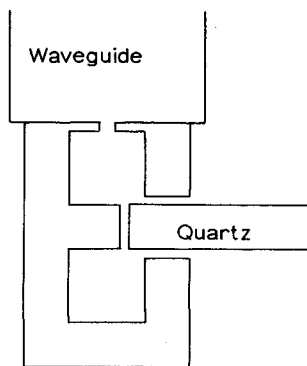

Fig. 3.2. Re-entrant co-axial resonant cavity used with a quartz transducer.
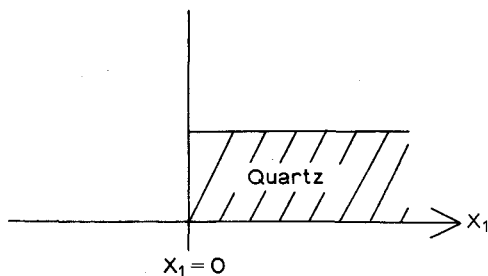
$X_1 = 0$

Fig. 3.3.

displacement u_1 is obtained from the usual force equation, eq. (2.6)

$$\rho \frac{\partial^2 u_1}{\partial t^2} = \frac{\partial \sigma_1}{\partial x_1} = c_{11} \frac{\partial \epsilon_1}{\partial x_1} - \frac{\partial}{\partial x_1}(e_{11}E_1)$$

or

$$\frac{\partial^2 u_1}{\partial x_1^2} - \frac{1}{v_\ell^2}\frac{\partial^2 u_1}{\partial t^2} = \frac{\partial}{\partial x}\left(\frac{e_{11}}{c_{11}}E_1\right), \tag{3.3}$$

where $(c_{11}/\rho)^{1/2}$ has been identified as the velocity of longitudinal elastic waves, see ch. 2§1.4, along the X-axis of quartz. It is clear from this equation that the gradient in the piezoelectric stress is the source of the ultrasonic waves. This gradient will only have a large value at the free end face of the quartz transducer as the electric field decays fairly slowly with distance inside the rod. To solve the equation, harmonic solutions of the form

$$E_1 = E_1^0 \exp(-i\omega t); \quad u_1 = u_1^0 \exp(-i\omega t) \tag{3.4}$$

are assumed. The equation then becomes

$$\frac{\partial^2 u_1^0}{\partial x_1^2} + k^2 u_1^0 = \frac{\partial}{\partial x_1}\left(\frac{e_{11}}{c_{11}}E_1^0\right)$$

where $k^2 = \omega^2/v_\ell^2$.

Using the fact that the solution to the homogeneous equation

$$\frac{\partial^2 G}{\partial x_1^2} + k^2 G = \delta(x_1 - x_1') \tag{3.5}$$

is the Green's function

$$G(x_1, x_1') = i\{\exp[i\,k|x_1 - x_1'|]\}/2k$$

it follows that

$$u_1^0(x_1) = \int \frac{i}{2k}e^{ik|x_1 - x_1'|}\frac{\partial}{\partial x_1'}\left[\frac{e_{11}}{c_{11}}E_1^0\right]dx_1'. \tag{3.6}$$

The spatial variation in the electric field is most rapid at the boundary so the source term approximates to a delta function there. To account for the boundary condition at the free end the source term is considered to be at a short distance x^0 inside the specimen. Waves travelling in the $-x_1$ direction will be reflected at the free end. The boundary condition can then be taken into account by considering a second source, an image source, at $x_1 = -x^0$ and by extending the rod to $-\infty$. The two sources are then brought into coincidence by taking the limit $x^0 \to 0$ to give the required result:

$$u_1^0(x_1) = \operatorname*{Lt}_{x_0 \to 0} \frac{iE_1^0}{2k} \frac{e_{11}}{c_{11}} \int e^{ik|x_1 - x_1'|} [\delta(x_1' - x_0) + \delta(x_1' + x_0)] \, dx_1'$$

$$= \frac{iE_1^0}{k} \frac{e_{11}}{c_{11}} e^{ikx_1} \qquad \text{for} \quad x_1 > 0.$$

Since the displacement is a real physical quantity the real part of this expression is required

$$u_1 = \frac{e_{11} E_1^0}{k c_{11}} \sin(\omega t - kx_1). \tag{3.7}$$

It is now a straightforward step to find the rate at which acoustic energy flows down the rod away from the generating surface and hence to calculate the efficiency of the transducer. The acoustic potential energy density in the quartz rod is $\frac{1}{2} c_{11}(\epsilon_1^0)^2$ and this is transmitted away from the end surface of area A at speed v_ℓ. The strain ϵ_1, from eq. (3.7), is given by

$$\epsilon_1 = \frac{\partial u_1}{\partial x_1} = -\frac{e_{11}}{c_{11}} E_1^0 \cos(\omega t - kx_1)$$

and so the strain amplitude is $e_{11} E_1^0/c_{11}$. Thus the acoustical power transmitted from the end face is

$$S = \frac{1}{2} e_{11}^2 (E_1^0)^2 A v_\ell / c_{11}. \tag{3.8}$$

To find the efficiency of the transducer this is to be compared with the input of electrical energy to the resonant cavity. The electrical power supplied to the cavity is

$$P = \frac{\omega}{Q} (\frac{1}{2} \kappa E_1^{02} V), \tag{3.9}$$

where Q is the quality factor and V is the volume of the cavity occupied by the quartz of dielectric permittivity κ. This expression follows from the definition of Q defined through the relation

$$Q = \frac{\omega \times \text{energy stored}}{\text{power input}}. \tag{3.10}$$

In the expression for the stored energy it has been assumed that the volume V is the only part of the resonant cavity to contain a microwave electric field. This is a reasonable approximation when using a resonant cavity of the form shown in fig. 3.2. It follows that the ratio of the acoustic power generated to the electrical input power is

$$\frac{S}{P} = \frac{e_{11}^2}{\kappa c_{11}} \frac{Av_\ell Q}{\omega V} = K_{11}^2 \frac{Av_\ell Q}{\omega V}, \tag{3.11}$$

where the piezoelectric coupling factor $K_{11} = [e_{11}^2/\kappa c_{11}]^{1/2}$ has been introduced. This is not quite the same as the piezoelectric factor discussed in §3.2 above, but the difference is small in practice and has been discussed by BECHMANN [1955].

In the derivation of eq. (3.11) two assumptions have been made. First that the quartz transducer is touching the central post in the resonant cavity and secondly that the fringing electric field around the quartz can be neglected. CARR [1967] has modified the expression to avoid these assumptions. He finds that the ratio of the acoustic power generated to the electrical power input is given by

$$\frac{S}{P} = \frac{\eta K_{11}^2 v_\ell Q}{\omega [d_0(K-1) + d_g]},$$

where d_0 is the distance between the central post of the cavity and the face of the quartz transducer, d_g is the distance between the post and the opposite wall of the cavity and η is a filling factor. The filling factor is given by the expression

$$\eta = \frac{2F(d_0)}{K-1} [d_0(K-1) + d_g],$$

where $F(d_0) = -(\Delta\omega/\Delta d)/\omega$ with $\Delta\omega$ the change in resonant frequency of the cavity on moving the quartz a distance Δd.

3.4. *Detection of ultrasonic waves by non-resonant transducers*

The efficiency of the reverse process can be shown to be equal to S/P by a thermodynamic argument due to BÖMMEL and DRANSFELD [1960]. That is to say, the efficiency of a transducer used to convert an ultrasonic wave into an electromagnetic wave is the same as of that used to convert an electromagnetic wave into an ultrasonic wave. Consider a resonant cavity with a quartz transducer as shown in fig. 3.4 where the waveguide, critically coupled to the cavity, is represented by a resistor R_L and the cavity losses are represented by a resistor R_c. In thermal equilibrium, the thermal energy flowing into the quartz from the two resistors is equal to that flowing in the reverse direction. Let A_{12} be
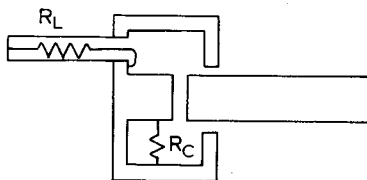
Fig. 3.4. Resonant cavity with resistors representing electrical losses.

the fraction of electrical power in the cavity converted to acoustic power in the quartz rod and A_{21} be the fraction of acoustic power in the rod appearing as an electrical power output in R_L. Only those longitudinal acoustic modes in the quartz rod at an angle of incidence of less than about $\lambda/\pi r$ to the quartz face will be coupled to the electric field in the cavity, because only for these modes will there be a large fraction of the quartz surface oscillating in phase. In this expression λ is the acoustic wavelength and r is the radius of the quartz rod. In an isotropic Debye model the density of longitudinal acoustic modes in the quartz in the frequency range $\Delta\nu$ determined by the cavity is $4\pi\nu^2\Delta\nu/v_\ell^3$. The number of modes within the solid angle $\lambda^2/\pi r^2$ is therefore given by

$$\Delta z = \frac{1}{4\pi}\left(\frac{\lambda^2}{\pi r^2}\right) 4\pi \left(\frac{\nu^2}{v_\ell^3}\right)\Delta\nu = \frac{\Delta\nu}{\pi r^2 v_\ell}. \qquad (3.12)$$

Each mode carries thermal energy KT so that the thermal power arriving at the surface of the quartz rod is $\Delta z KT v_\ell \pi r^2 = KT\Delta\nu$. Some of this power is coupled into the output load R_L and an equal power is dissipated in the cavity losses R_c. Thus the output power in R_L is $A_{21}KT\Delta\nu$ and so the total power leaving the quartz is $2A_{21}KT\Delta\nu$. Now the electrical power appearing in the cavity from thermal energy in each resistor is $KT\Delta\nu$, so that the total electrical power fed into the cavity is $2KT\Delta\nu$ giving rise to an acoustic output in the quartz rod of $2A_{12}KT \times \Delta\nu$. In thermal equilibrium the acoustic power entering and leaving the quartz must be equal and hence $A_{21} = A_{12} = K_{11}^2 A v_\ell Q/\omega V$. Thus the conversion efficiency for a transducer is the same for the conversion to or from acoustic power. For X-cut quartz operating at 10^{10} Hz in a resonant cavity at liquid helium temperatures, typical values for the parameters are $K_{11} \sim 10^{-1}$, $Q \sim 2000$, $v_\ell \sim 6 \times 10^3$ m·sec^{-1}. $V/A \sim 10^{-3}$ m and hence $A_{12} \sim 2 \times 10^{-3}$.

In the above discussion use has already been made of the fact that an ultrasonic wave must reach the end face of the transducer very close to normal incidence if a large electrical signal is to be generated in the cavity. This is because a large portion of the end face must be moving in phase; those parts of the end face moving out of phase with the rest will produce an electrical signal which is out of phase with the main

signal and by destructive interference the microwave electrical signals will cancel, or partially cancel, each other. The degree of tolerance allowed can be estimated from the value of $\lambda/\pi r$. For a quartz rod of diameter 3 mm used at a frequency of 10 GHz, when the wavelength of longitudinal waves along the X-axis is about 6000 Å, the angle $\lambda/\pi r$ is about 0.4 minutes of arc. The necessity for strict normal incidence is especially important when a pulse-echo experiment is performed in which a short pulse of ultrasonic waves is generated and allowed to echo backwards and forwards in a transducer and specimen delay rod system. The returning pulses must reach the detecting end with their wavefront parallel to within 0.4 minutes of the surface in order that they can be detected. Thus the reflecting surface must be parallel to the generating and detecting surface to within 0.2 minutes. To observe a train of many echoes, much smaller tolerances must be maintained in the parallelism of the surfaces. As the frequency rises the requirements become more severe. If the attenuation of ultrasound in a transducer delay rod system remained constant, an exponential decay of intensity in pulse echoes would be expected, but at microwave frequencies, especially at 9 GHz and above, this is rarely observed because of the non-parallel ends to the samples. Fig. 3.5 shows a typical set of pulse echoes at 9.5 GHz in a quartz transducer.

The effect of non-parallelism of the end faces of a quartz transducer has been considered by CARR and STRANDBERG [1962] who derived an expression for the intensity of the signal observed from a pulse echo in
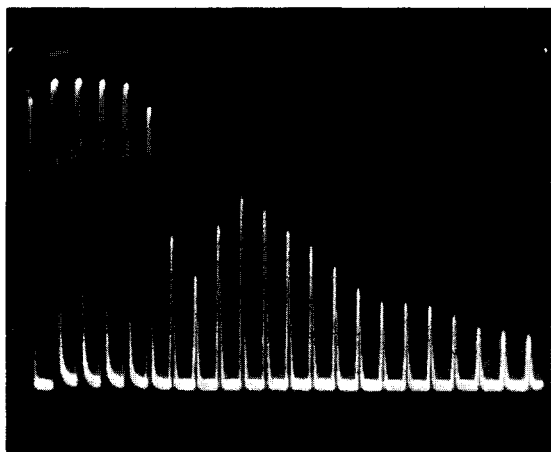

Fig. 3.5. Typical echo train from a quartz transducer at 9.5 GHz and at 4.2 K.

a quartz rod with non-parallel ends. TRUELL and OATES[1963] have investigated the problem experimentally at a sufficiently low frequency, 70 MHz, for polishing to reduce the non-parallelism to an insignificant degree. Then a controlled change in the angle between the ends was made and the resulting pulse-echo train envelope was very similar to that observed at higher microwave frequencies with the best available polishing. The expression given by Carr and Strandberg is

$$P = \frac{S}{z^2} [2J_1(z)]^2 A_{12}, \qquad (3.13)$$

where P, S and A_{12} have the same meaning as above and $z = \gamma k r$, where γ is the angle between the echo wavefront and the quartz face, k is 2π times the reciprocal of the wavelength and r is the radius of the quartz rod. Even the first echo will give a much reduced signal for a small error in parallelism of the faces. A comparison of experimentally observed pulse-echo envelopes with this expression, as has been made by Carr and Strandberg, shows that only an approximate fit can be obtained. There are probably several reasons for this; one of the most serious may be because amplitude variations occur across the wavefront of the generated ultrasonic wave because of the field configuration in the microwave cavity, LAMB and RICHTER [1967]. Slight misorientation of the quartz rod relative to its crystallographic axes may also change the echo train envelope; this effect is strongly dependent on the direction as well as the magnitude of the error, FARNELL [1961].

These problems have meant that measurements of the absolute attenuation of microwave ultrasonic waves in solids have not been possible except at the low-frequency end of the microwave region. Changes in attenuation with temperature, magnetic field, irradiation dose or some other parameter have been measured by assuming the effects of misorientation and non-parallelism are unchanged during the experiment. Direct comparisons between specimens cannot be made, nor even comparisons between different experiments with the same transducer unless it can be replaced in the microwave cavity in precisely the same position. However in many cases the changes in relative attenuation with, for example, temperature or magnetic field, are found to be consistent between different experiments and different specimens of the same material.

3.5. *Bonding of transducers to specimens*

In an experiment in which the propagation of microwave ultrasound is to be investigated in a non-piezoelectric solid and a long rod transducer is used, this must be bonded to the specimen material in such a way as

to transmit the ultrasonic wave efficiently into the specimen. Various materials have been used for bonding; many are successful in transmitting longitudinal waves but few have been consistently good for shear waves. BATEMAN [1967] has considered several oils, greases and resins, though using them at lower frequencies, SMITH [1965] and CARR [1965] have successfully used optical contact bonding at 3 GHz and 9 GHz.

The most widely used materials have been indium, epoxy resin and various brands of stopcock grease which freezes hard at the low temperatures normally used in microwave ultrasonic work. Indium and epoxy resin bonds have been used to transmit shear waves. The efficiency of the bonds in transmitting longitudinal waves is difficult to measure because of the effects of non-parallelism of the surfaces; usually much less than 50% of the ultrasonic power is transmitted. The transmission clearly depends on the acoustic impedances of the materials and the thickness of the bond. Apart from transmission of the ultrasonic waves, one of the problems of bonding is that most microwave ultrasonic experiments must be performed at liquid helium temperatures and then differential contraction of the transducer and specimen on cooling can often break the bond.

3.6. Thin film piezoelectric transducers

Evaporated piezoelectric thin films have recently been used increasingly as ultrasonic transducers for the generation and detection of microwave ultrasonic waves, DE KLERK and KELLY [1965], FOSTER [1965]. The main advantage of these thin film transducers is the elimination of the bond between the transducer and the delay rod specimen and hence the elimination, in a pulse-echo experiment, of echoes which have only travelled back and forth in the long rod transducer and have not passed through into the specimen. A further advantage is that in principle a more efficient transducer can be made by using a material with a high piezoelectric coupling factor and evaporated to a resonant thickness. However the quality of an evaporated thin film is strongly dependent on the evaporation technique and the substrate preparation so the results actually achieved in practice are not often as good as theory predicts. It must be noted moreover that it is not always desirable to produce a highly efficient transducer. DE KLERK [1966a] has pointed out that when measuring a very low ultrasonic attenuation by the pulse-echo method, an appreciable contribution to the fall in the intensity may be the power taken by an efficient detecting transducer.

Various materials have been used as thin film transducers, the most usual being cadmium sulphide but zinc sulphide, zinc oxide, aluminium

nitride, lithium niobate and others have also been used. Some of these were discussed in §3.2. The films are normally used in a microwave cavity similar to that used for quartz transducers and shown in fig. 3.2; that is, the oscillating electric field is applied normal to the plane of the film. Under conditions to be discussed below, a film of cadmium sulphide can be grown with its Z-axis normal to the substrate. This type of film will act in a similar way to X-cut quartz and will generate longitudinal ultrasonic waves. The expected efficiency of such a trans- ducer will now be calculated following the methods of HAYDL et al. [1964]. Fig. 3.6 shows a thin film of material of characteristic acoustic impedance Z attached to a material of acoustic impedance Z'. The film is of area A and thickness d and ultrasonic waves propagate in the x_3 direction into the delay rod material. The free surface of the thin film
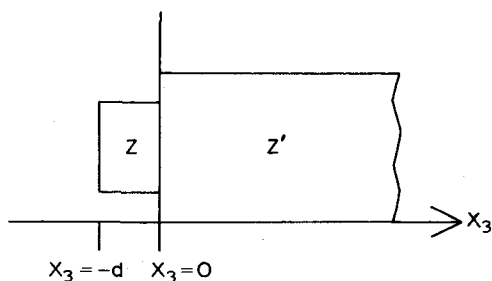
Fig. 3.6.

is at $x_3 = -d$ and the other surface is at $x_3 = 0$. From the discussion in §3.3, it is clear that the generation of ultrasonic waves occurs at the surface of the piezoelectric thin film. Consider ultrasonic waves

$$\left. \begin{array}{l} U = U_0 \exp\left[i(\omega t - kx_3)\right] \\ V = V_0 \exp\left[i(\omega t + kx_3)\right] \end{array} \right\} x_3 < 0,$$

$$W = W_0 \exp\left[i(\omega t - k'x_3)\right] \quad x_3 > 0, \tag{3.14}$$

in the transducer and specimen. Here U, V and W are longitudinal displacements parallel to the x_3 direction and k and k' are the wave numbers in the transducer and delay rod material. At the free surface of the thin film transducer the total stress vanishes. If $E = E_0 \exp(i\omega t)$ is the applied electric field then

$$c_{33}\left(\frac{\partial U}{\partial x_3}\right) + c_{33}\left(\frac{\partial V}{\partial x_3}\right) + e_{33}E = 0 \quad \text{at } x = -d, \tag{3.15}$$

where c_{33} is the appropriate elastic stiffness constant for the trans- ducer. At the junction between the transducer and the specimen, the

displacement and stress must be equal on the two sides. This gives the two equations

$$U + V = W, \tag{3.16}$$

$$c_{33}\left(\frac{\partial U}{\partial x_3}\right) + c_{33}\left(\frac{\partial V}{\partial x_3}\right) + e_{33}E = c_{33}'\left(\frac{\partial W}{\partial x_3}\right) \quad \text{at } x = 0, \tag{3.17}$$

where c_{33}' is the elastic stiffness constant of the delay rod medium. For sinusoidal waves of the form given by eq. (3.14), eqs. (3.15)–(3.17) give

$$(U_0 + V_0)k \sin kd - i(U_0 - V_0)k \cos kd + \frac{e_{33}}{c_{33}}E_0 = 0,$$

$$U_0 + V_0 = W_0,$$

$$ik(U_0 - V_0) - \frac{e_{33}}{c_{33}}E_0 = i\frac{c_{33}'}{c_{33}}k'W_0. \tag{3.18}$$

From this set of equations U_0 and V_0 can be eliminated to give for the amplitude of the wave in the delay rod specimen

$$W_0 = -\frac{e_{33}E_0[1 - \cos kd]}{kc_{33}[\sin kd - i(Z'/Z)\cos kd]}. \tag{3.19}$$

Here the ratio $Z'/Z = c_{33}'k'/c_{33}k$ has been introduced. The associated strain amplitude in the delay rod specimen will be ik' times the value of W_0 given by eq. (3.19) and from this the ultrasonic power S flowing from the transducer to the delay rod medium is readily obtained. It is

$$S = \frac{1}{2}\left(\frac{Z'}{Z}\right)^2 \frac{Av_\ell' e_{33}^2 E_0^2[1 - \cos kd]^2}{c_{33}'[\sin^2 kd + (Z'/Z)^2\cos^2 kd]}, \tag{3.20}$$

where v_ℓ' is the velocity of the longitudinal wave in the delay rod medium. An alternative expression for S is

$$S = \frac{1}{2}\left(\frac{Z'}{Z}\right) \frac{Av_\ell \kappa K^2 E_0^2[1 - \cos kd]^2}{\sin^2 kd + (Z'/Z)^2\cos^2 kd}, \tag{3.21}$$

where v_ℓ is the velocity of longitudinal waves in the thin film transducer, κ is the permittivity of the transducer material and K is the piezoelectric coupling factor. The ultrasonic power flowing away from the thin film is at a maximum if the thickness of the transducer corresponds to resonance, that is if $kd = (2n+1)\pi$ where n is an integer. In this case $\cos kd = -1$ and so S reduces to

$$S = 4(Z/Z')Av_\ell K^2(\tfrac{1}{2}\kappa E_0^2). \tag{3.22}$$

A comparison between this result and that of eq. (3.8) shows that the power of a resonant thin film transducer differs by the factor $4Z/Z'$

from that of the non-resonant single surface transducer of §3.3 with the same piezoelectric coupling factor. No account was taken there of transmission through the bond between the long non-resonant trans-ducer and the delay rod specimen, whereas here it has been included. It is, in fact, just at this point that the real advantage of the thin film transducer appears. There is no need for a separate bonding material which presents problems of parallelism, acoustic losses and in most cases the inability to transmit shear waves. A thin film transducer is evaporated or sputtered either directly onto the delay rod specimen itself or onto a thin evaporated gold or silver film. This metal film can be made very thin and by acting as one electrode it is used to provide a more uniform electric field in the transducer. In practice the perfor-mance of evaporated thin film transducers is rarely as good as that predicted by eq. (3.22), probably because of structural imperfections in the film. They are rarely single crystals, unless grown epitaxially on the substrate, but are usually formed of many crystallites at slightly different orientations. In addition, unless the evaporation conditions are very carefully controlled the film may not be of precisely uniform thickness and hence not exactly resonant over its whole area.

To summarize, an evaporated thin film transducer of cadmium sulphide, zinc sulphide or zinc oxide is likely to be at least as efficient a transducer for the generation of longitudinal waves as an X-cut quartz rod, and may be better. There will be no problem of bonding the transducer to the specimen and as a result no problem, in a pulse-echo experiment, of identifying echoes which have passed through the specimen from those which have travelled only through the trans-ducer. With special evaporation techniques, or a different electric field configuration, it is possible to use a thin film for shear wave generation where the bonding problem using a quartz transducer is particularly serious. Against these advantages must be set the need for evaporation or sputtering techniques to produce the oriented thin films.

3.7. *Production of thin film piezoelectric transducers*

The requirements of a piezoelectric thin film transducer are (i) a high resistivity to enable a high electric field to be used with low Joule heating losses, (ii) a good crystallographic orientation for generation of the desired acoustic mode, (iii) good acoustic matching to the delay rod specimen and (iv) a high piezoelectric coupling factor if an efficient transducer is needed. The last two of these depend on the choice of material for the transducer and delay rod and on the experiment that is planned. The matching between the transducer and delay rod can be improved by the use of an acoustic transformer which will be con-sidered later, §3.8. The requirements of high resistivity and good

orientation can be met by a suitable choice of evaporation conditions; in the case of cadmium sulphide the pressure of the chamber during evaporation, the angle between the substrate surface and the vapour beam and the substrate temperature appear to be the important factors. Similar factors are probably important in the production of thin film transducers of other materials.

Cadmium sulphide will now be considered in detail. The discussion of §3.2 shows that an electric field along the c- or Z-axis, the axis of six-fold symmetry, produces a longitudinal strain along all three axes. Thus in order to generate a longitudinal ultrasonic wave in a delay rod a film of CdS is needed on the end face of the rod with its c-axis and the applied oscillating electric field normal to the surface. An electric field normal to the c-axis of CdS produces a shear strain about an axis normal to the c-axis and the applied field. A shear wave transducer can therefore consist either of a film with its c-axis normal to the delay rod surface and with an electric field applied in the plane of the film, or it can consist of a film whose c-axis is inclined to the surface if the electric field is applied normal to the surface. Both methods have been used, DE KLERK [1966a], FOSTER *et al.* [1968]. As will be shown below there are special problems in producing films whose c-axis is not normal to the surface.

There is broad agreement among different workers on the conditions needed during evaporation of CdS to produce a satisfactory transducer for longitudinal ultrasonic waves. However the reasons given for the choice of these conditions are not always the same. The main problem in forming a thin film of high resistivity CdS by evaporation lies in the large difference in the vapour pressures of cadmium and sulphur. The vapour pressure of sulphur is greater than 10^{-5} Torr – a typical evaporation chamber pressure – at room temperature, whereas that of cadmium only reaches this value at 150°C. Even if the compound cadmium sulphide is evaporated, the vapour splits into cadmium and sulphur and recombines on the substrate. A cadmium-rich film will have a low resistivity while a film with excess sulphur has a high resistivity. Conditions for evaporation and deposition of the cadmium sulphide film must be chosen to favour the production of a stoichiometric or even of a sulphur-rich film in spite of the high vapour pressure which tends to cause re-evaporation of excess sulphur. These conditions have been achieved by evaporating from separate sources of cadmium and sulphur or from a source of cadmium sulphide with a separate sulphur source to provide excess sulphur to the vapour. The temperature of the substrate also affects the composition of the film as well as its crystallographic orientation and structural perfection. Thus the production of thin films of cadmium sulphide is usually carried out at pressures of

10^{-5} Torr and at a substrate temperature of about 200°C while an excess of sulphur in the vapour is ensured by controlling the temperatures of the evaporation sources. Fig. 3.7 shows the evaporation unit used by DE KLERK and KELLY[1965] in which these conditions were employed. The cadmium sulphide films form in the hexagonal phase with the c-axis normal to the substrate surface. Deposition rates must be slow for accurate oriented films of high crystallographic perfection. At substrate temperatures lower than 200°C there is a tendency for a mixture of the cubic and hexagonal phases of cadmium sulphide to be formed. In an evaporator chamber the substrate temperature is strongly influenced by the radiation falling on it. It will receive radiation from the heated evaporation sources, unless a cooled baffle is used as shown in fig. 3.7, and its temperature will rise as the evaporation begins. The baffle also prevents the direct splashing of molten cadmium or sulphur onto the substrate. The orientation of the film is to some extent affected by the substrate material; DE KLERK[1966a] has produced epitaxial growth on single crystal substrates of aluminium oxide and magnesium oxide, the c-axis of the film being normal to the surface and the a-axis aligned with one of the substrate crystal axes. Thoroughly clean substrate surfaces are needed if thin films of cadmium sulphide are to adhere strongly. The surface can be cleaned chemically followed by ion bombardment in the evaporation unit itself, HOLLAND[1961].

A slightly different evaporation system has been used by FOSTER [1965], [1967] and by FOSTER *et al.*[1968]. A diagram of his unit is
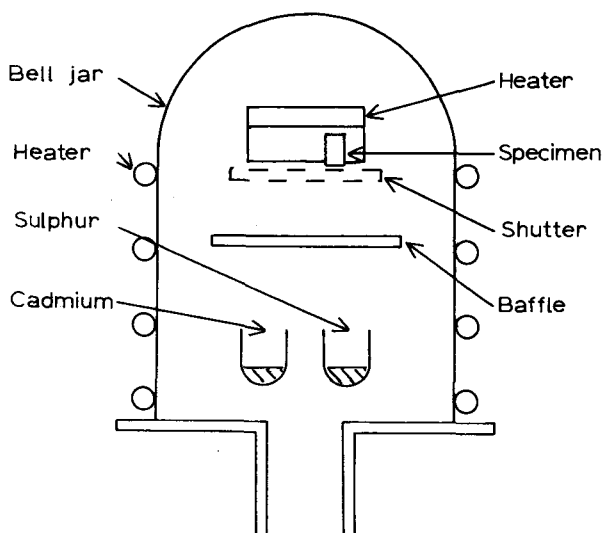
Fig. 3.7. Simplified diagram of a cadmium sulphide evaporator of de Klerk and Kelly.

shown in fig. 3.8. Similar conditions to those already described are used to form films with the c-axis normal to the surface. These transducers can then be used to generate longitudinal waves. To produce a shear wave transducer the c-axis has to be inclined to the surface; this is achieved as follows. It is found that on some metal substrate surfaces –silver and platinum–the c-axis of a thin film of cadmium sulphide can be oriented in a direction nearly parallel to the incident beam of vapour. If the incident vapour beam is arranged at an angle to the normal of the substrate surface the initial layer of cadmium sulphide, deposited at 0.2 μm/min is formed with its c-axis normal to the surface but subsequent layers, deposited at 0.03 μm/min will be formed with their c-axes in a direction between the surface normal and the vapour beam direction. The actual direction will be about 10° from that of the vapour beam.

The production of thin film transducers of zinc sulphide is similar to that already described for cadmium sulphide, DE KLERK [1966a].

Thin film transducers of zinc oxide have been produced by two different methods. In one method, MALBON et al. [1967] have used a reactive evaporation method similar to the technique described above. Zinc is evaporated from a heated source while a stream of oxygen at 10^{-3}–10^{-4} Torr, admitted to the evaporation unit, is allowed to impinge on the substrate at the same time as the zinc reaches it. In order that oriented films of zinc oxide may be deposited the substrate must be cooled. If it has a silver film on it then the temperature must be less
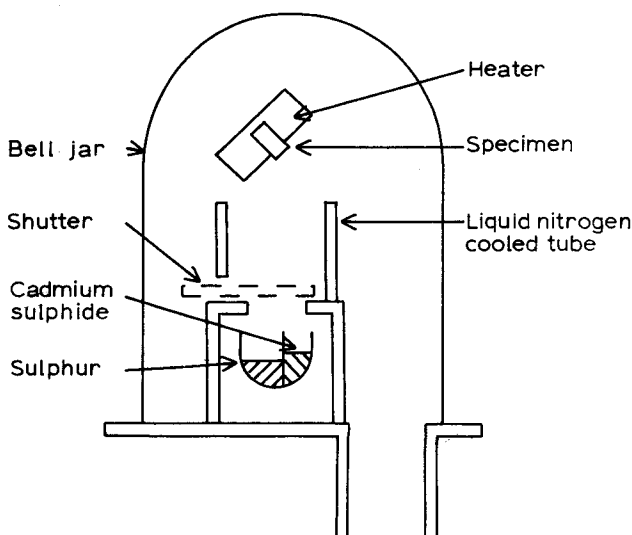
Fig. 3.8. Simplified diagram of a cadmium sulphide evaporator for angled films of Foster.

than 0°C but for a gold surface a temperature below −50°C is required. As in the case of cadmium sulphide, the films are oriented with their c-axes normal to the surface and thus provide transducers for longitudinal waves if an oscillating electric field is applied at right angles to the plane of the film. The method of sputtering has been used by FOSTER *et al.* [1968] and by ROZGONYI and POLITO [1966] to form thin film transducers of zinc oxide. The zinc oxide was sputtered onto the gold-plated surface of a corundum delay rod specimen held at 50°C in a mixture of 0.05 Torr of oxygen and 0.05 Torr of argon. An initial potential difference of 3 kV was used and the discharge current was kept at about 4 mA to give a deposition rate of about 2 μm/h when the substrate was 1.5 cm to 2.0 cm above the zinc oxide cathode. The films produced in this way also have the c-axis of the zinc oxide normal to the film surface and act as transducers for longitudinal waves.

To produce a transducer of maximum efficiency the film must be exactly a resonant thickness so some method of measuring its thickness as it is growing is needed. A quartz crystal oscillator has been used by DE KLERK [1966a] as a microbalance to monitor the thickness of the film during its preparation. This is done by depositing a film on the quartz crystal oscillator at the same time as it is forming on the experimental specimen. The change in resonant frequency of the quartz oscillator is proportional to the mass deposited and hence to the thickness of the film formed. Another method that has been employed is to observe light reflected from the film at normal incidence. Interference occurs between the light reflected from the front and back surfaces of the film. If monochromatic light is used–such as from a gas laser–the reflected intensity can be directly related to the thickness of the film. When the film is completed its thickness can be measured by the method of LYASHENKO and MILOSLAVSKII [1964] which can also give an indication of the quality of the film. The transmission spectrum of the film is measured away from the absorption edge and the thickness of the film deduced from the interference fringes obtained. If the spectrum includes the region of the absorption edge then the sharpness of this will give some indication of the purity of the material constituting the film. Fig. 3.9 shows a typical spectrum obtained with a film of cadmium sulphide.

Other materials and techniques have been used to produce thin film piezoelectric transducers but to a lesser extent than those already described. WINSLOW [1968] has used aluminium nitride and lithium niobate. FOSTER [1964] has described a cadmium sulphide diffusion layer transducer in which a thin layer of high resistivity cadmium sulphide, to act as the transducer, is formed at one surface of a single crystal of low resistivity cadmium sulphide by the diffusion in of copper.

Fig. 3.9. Transmission spectrum of a thin film of cadmium sulphide on quartz [P. J. King and B. G. Helme].

The main disadvantages of this type of transducer are the large series resistance of the bulk cadmium sulphide which forms one electrode and the need to bond the crystal onto the delay rod material. The same disadvantages appear in the depletion layer transducer of WHITE [1961] and described also by HOGARTH [1964]. A reverse d.c. bias is applied to a rectifying p–n junction in a piezoelectric semiconductor–cadmium sulphide or gallium arsenide–to produce a depletion layer. This will act as an ultrasonic transducer if an a.c. modulation is applied on the d.c. bias. The thickness of the depletion layer can be adjusted to acoustic resonance by varying the magnitude of the bias.

3.8. *Multilayer transducers*

The efficiency of a thin film piezoelectric transducer can be increased in two ways by using a multilayer structure. The first is that a multilayer acoustic transfc...aer can be used to match acoustically the transducer to the delay rod. The second way of increasing the efficiency is to use a multiple transducer formed of successive resonant thin film transducers spaced by inactive layers each half an acoustic wavelength thick. The ultrasonic waves produced by each transducer are then in phase. An extension of this method is to use a multilayer transducer consisting of successive resonant piezoelectric layers but with each alternate c-axis (if CdS is used) reversed, DE KLERK [1968].

An acoustic transformer used to match a transducer to a delay rod is now considered. The treatment follows the method of FRY and DUNN [1962] and of HAYDL *et al.* [1964]. Consider two materials p and r

attached to each other as in fig. 3.10. A length L_p of material p of density ρ_p will present to an ultrasonic wave of frequency ω an acoustic impedance

$$Z_p = R_p \left[\frac{Z_r + j R_p \tan (\omega L_p/v_p)}{R_p + j Z_r \tan (\omega L_p/v_p)} \right]. \tag{3.23}$$

In this formula Z_r is the acoustic impedance of the material r and R_p, equal to $v_p \rho_p$, is the characteristic acoustic impedance of p: v_p is the velocity of sound in this material. It follows that the acoustic impedance of a specimen of material p whose length is equal to one quarter of
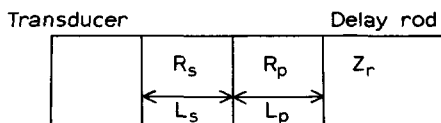
Fig. 3.10.

an ultrasonic wavelength is R_p^2/Z_r and that the acoustic impedance of two successive quarter wavelengths of materials p and s is $(R_s/R_p)^2 Z_r$. The double layer therefore transforms the acoustic impedance by the ratio $(R_s/R_p)^2$. For N successive double layers the impedance can be stepped by a factor $(R_s/R_p)^{2N}$. In this way any desired acoustic impedance can in principle be produced at the transducer surface. Clearly as the number of layers increases the bandwidth of the system is reduced so that the gain in conversion efficiency is only obtained at the expense of the latter, HAYDL et al. [1964]. It should also be stated that the technical problems of forming a large number of thin films of accurate thickness are, of course, considerable.

The other type of multilayer transducer consists of several active piezoelectric layers spaced by passive layers. For instance, DE KLERK et al. [1965] made a structure with three layers of cadmium sulphide each half a wavelength thick separated by layers of silicon oxide each of this thickness. For two and three layers the improvement in conversion efficiency over that of a single layer transducer was 6 and 9.5 dB respectively. For a small number of layers the conversion efficiency should be proportional to the square of their number since in this case the ultrasonic amplitides add if the waves are precisely in phase. DE KLERK [1968] has subsequently made a multilayer transducer of several layers of cadmium sulphide and with alternate layers having the c-axis in the reverse direction. At each interface there is then a piezoelectric discontinuity which is twice as large as that present when alternate passive layers are being used. These multilayer transducers can be considered to give an improved conversion efficiency by

improved impedance matching, only now it is the electrical impedance of the transducer which is reduced by having several layers in parallel. The electrical impedance of a waveguide or co-axial line is typically very much less than that of a piezoelectric ultrasonic transducer and a transducer of reduced impedance is more easily matched by means of the resonant cavity which acts as a transformer.

3.9. *Resistive-layer transducers*

In addition to the evaporated or sputtered thin film piezoelectric transducers considered above, transducers have also been formed in piezoelectric semiconductors by producing a thin layer of high resistivity at the surface of a material of much lower resistivity. This has been done in two ways, either by diffusing a compensating impurity into the surface layer of the piezoelectric semiconductor or by using the depletion layer at a p–n junction and applying a reverse d.c. bias. Neither of these methods has yet been used extensively at microwave frequencies although experiments have been performed up to 1 GHz and could be extended to higher frequencies. In both types of transducer the ultrasonic waves must propagate through the low resistivity region of the crystal and this can either act as the delay medium or it must be bonded to the delay rod specimen. Against this possible disadvantage must be set the better crystallographic orientation of the transducer that is possible as compared with an evaporated thin film, FOSTER[1964]. WHITE[1964].

Fig. 3.11 shows the two types of transducer. Diffusion layer transducers have been made from zinc oxide with lithium as the diffusant and also from cadmium sulphide, cadmium selenide and gallium arsenide all with a diffusant of copper, FOSTER[1963], HICKERNELL and ALLEN[1965], HICKERNELL[1968]. In the diffusion process a highly resistive layer whose thickness is half the wavelength of the required ultrasonic waves is produced. The problem of making uniform and very thin high resistance layers may restrict the frequency at which diffusion layer transducers can be efficiently used to below 1 GHz. Depletion layer transducers have been described by WHITE[1964]. A rectifying junction was formed on a crystal of gallium arsenide by evaporating a gold film onto one face and the depletion layer was formed at the metal–semiconductor boundary. This system was used as a transducer at a frequency of 830 MHz. The thickness of the depletion layer formed in typical samples of cadmium sulphide or gallium arsenide is likely to be of the order of 10^{-4} cm. This corresponds to a half-wavelength resonant transducer operating above 1 GHz. Thus it is likely that depletion layer transducers may become useful in the microwave region.
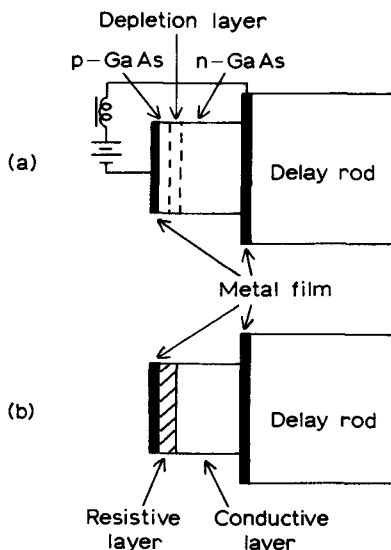
Fig. 3.11. (a) Depletion layer transducer. (b) Diffusion layer transducer.

4. Magnetostrictive transducers

4.1. *Introduction*

The magnetostrictive transducer is the other device which has been used extensively to generate ultrasonic waves at microwave frequencies. The basic experimental arrangement is shown in fig. 3.12. A thin ferromagnetic film is deposited on the surface of the delay rod specimen in which the ultrasonic wave will propagate. It is magnetized by the application of a steady magnetic field usually directed normal to the plane of the film and an oscillating field is then applied. The latter field is usually in the plane of the film. The magnetization oscillations due to the presence of the microwave field generates a strain in the ferromagnetic film and an ultrasonic wave propagates into the delay rod. This method of generating microwave ultrasonic waves was first
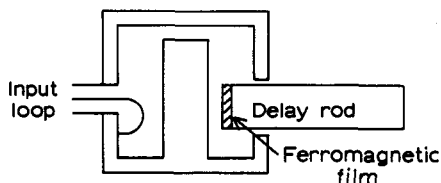
Fig. 3.12. Re-entrant co-axial resonant cavity used with a thin film ferromagnetic transducer.

demonstrated by Bömmel and Dransfeld [1960] and has been used especially for the generation of shear waves. The orientation of the magnetic fields described above leads to the most efficient generation of shear waves. As the diagram of fig. 3.12 shows, the film is usually excited in a resonant cavity which can be very similar to that used for piezoelectric transducers but in this case the film is positioned in a region of strong magnetic field. An alternative arrangement is shown in fig. 3.13 in which the film is held against the wall of a rectangular TE 101 resonant cavity in the position of maximum magnetic field.
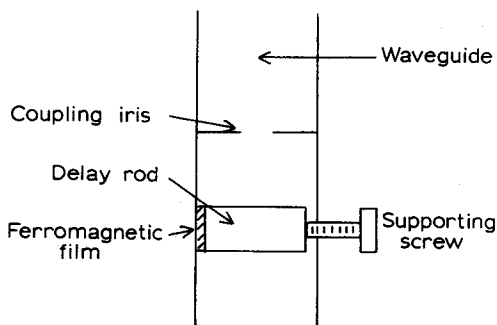
Fig. 3.13. Rectangular TE₁₀₁ resonant cavity used with a thin film paramagnetic transducer.

4.2. *Generation of ultrasonic waves by thin ferromagnetic films*

The theory of the generation of ultrasonic waves by a thin ferromagnetic film has been given by Seavey [1963] whose treatment will be followed. Here we are only interested in the theory of the generation of ultrasonic waves by a thin film, typically of nickel, evaporated onto the surface of a delay rod specimen. At this stage the treatment of ultrasonic wave propagation near the crossover frequency, when the spin-wave and ultrasonic wavelengths are equal does not concern us. The discussion of these phenomena is deferred until ch. 5.

Consider a thin ferromagnetic film deposited on the end surface of a delay rod specimen and having a steady magnetic field applied. This will produce a uniform saturation magnetization M_0 in the film at an angle, say of α, to the normal of the plane of the film. Because of demagnetization effects, see ch. 5§1.3, the magnetization is only parallel to the applied field if α is zero or $\frac{1}{2}\pi$. A set of axes is chosen as shown in fig. 3.14, where the ferromagnetic film lies in the xz-plane and the ultrasonic waves propagate down the rod along the y-axis. It is assumed that the material of the film is polycrystalline so that there is no restriction on the choice of the direction of the x- and z-axes in the plane of the film. Then, without loss of generality, the magnetiza-
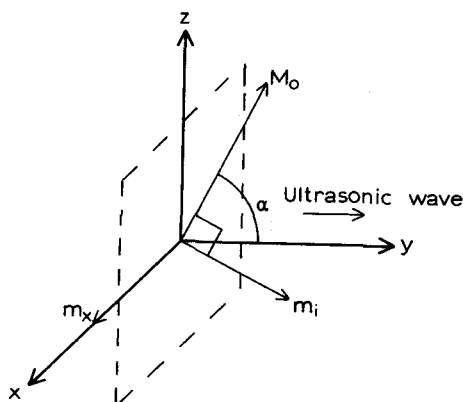
Fig. 3.14.

tion M_0 can be taken to lie in the yz-plane. The incident microwave radiation produces magnetization components m_x in the x-direction and m_i in the yz-plane as shown in fig. 3.14.

The magnetoelastic energy density in a cubic ferromagnetic material is discussed in ch. 5§2.2. It is, see eq. (5.61),

$$W_{\text{m-p}} = \frac{b_1}{M_0^2} [M_x^2 \epsilon_{xx} + M_y^2 \epsilon_{yy} + M_z^2 \epsilon_{zz}]$$

$$+ \frac{2b_2}{M_0^2} [M_x M_y \epsilon_{xy} + M_y M_z \epsilon_{yz} + M_z M_x \epsilon_{zx}]. \qquad (3.24)$$

The elastic potential energy density for a cubic material, see ch. 2, is

$$W_L = \tfrac{1}{2} c_{11} [\epsilon_{xx}^2 + \epsilon_{yy}^2 + \epsilon_{zz}^2] + c_{12} [\epsilon_{xx}\epsilon_{yy} + \epsilon_{yy}\epsilon_{zz} + \epsilon_{zz}\epsilon_{xx}]$$

$$+ 2c_{44} [\epsilon_{xy}^2 + \epsilon_{xz}^2 + \epsilon_{yz}^2]. \qquad (3.25)$$

Nickel and iron form cubic crystals but cobalt crystals are hexagonal; however an evaporated thin film of one of these materials will probably be polycrystalline and some suitable average elastic constants and magnetoelastic constants must be used. The components of stress are found in the usual way by differentiating the free energy with respect to the appropriate strain components:

$$\sigma_{xy} = 2c_{44}\epsilon_{xy} + \frac{b_2}{M_0^2} M_x M_y,$$

$$\sigma_{yy} = c_{11}\epsilon_{yy} + c_{12}[\epsilon_{xx} + \epsilon_{zz}] + \frac{b_1}{M_0^2} M_y^2, \qquad (3.26)$$

$$\sigma_{zy} = 2c_{44}\epsilon_{yz} + \frac{b_2}{M_0^2} M_y M_z.$$

In terms of the saturation magnetization M_0 and the microwave components m_i and m_x the cartesian components M_x, M_y and M_z are

$$M_x = m_x; \quad M_y = M_0 \cos \alpha + m_i \sin \alpha;$$

$$M_z = M_0 \sin \alpha - m_i \cos \alpha. \tag{3.27}$$

In this notation the stress components become

$$\sigma_{xy} = 2c_{44}\epsilon_{xy} + \frac{b_2}{M_0^2} m_x (M_0 \cos \alpha + m_i \sin \alpha),$$

$$\sigma_{yy} = c_{11}\epsilon_{yy} + c_{12}(\epsilon_{xx} + \epsilon_{zz})$$

$$+ \frac{b_1}{M_0^2} (M_0^2 \cos^2 \alpha + m_i^2 \sin^2 \alpha + m_i M_0 \sin 2\alpha), \tag{3.28}$$

$$\sigma_{zy} = 2c_{44}\epsilon_{yz} + \frac{b_2}{M_0^2} (\tfrac{1}{2}M_0^2 \sin 2\alpha - \tfrac{1}{2}m_i^2 \sin 2\alpha - M_0 m_i \cos 2\alpha).$$

For wave propagation in the y-direction the force equation, eq. (2.6), gives

$$\frac{\partial^2 u_x}{\partial y^2} - \frac{1}{v_t^2} \frac{\partial^2 u_x}{\partial t^2} = -\frac{b_2}{M_0^2 c_{44}} \left[M_0 \cos \alpha \frac{\partial m_x}{\partial y} + \sin \alpha \frac{\partial}{\partial y} (m_x m_i) \right],$$

$$\frac{\partial^2 u_y}{\partial y^2} - \frac{1}{v_\ell^2} \frac{\partial^2 u_y}{\partial t^2} = -\frac{b_1}{M_0^2 c_{11}} \left[\sin^2 \alpha \frac{\partial}{\partial y} (m_i^2) + M_0 \sin 2\alpha \frac{\partial m_i}{\partial y} \right], \tag{3.29}$$

$$\frac{\partial^2 u_z}{\partial y^2} - \frac{1}{v_t^2} \frac{\partial^2 u_z}{\partial t^2} = -\frac{b_2}{2M_0^2 c_{44}} \left[-\sin 2\alpha \frac{\partial}{\partial y} (m_i^2) - 2M_0 \cos 2\alpha \frac{\partial m_i}{\partial y} \right],$$

where $v_t^2 = c_{44}/\rho$ and $v_\ell^2 = c_{11}/\rho$ are the velocities of the transverse and longitudinal ultrasonic waves in the film. These equations are inhomogeneous wave equations similar to that of eq. (3.3) for a piezoelectric ultrasonic transducer. It will be noted that in this case there are two types of driving terms on the right-hand side of each equation; the first depends linearly on the microwave magnetization and generates an ultrasonic wave at the same frequency as the incident microwave field while the second term, quadratic in the microwave magnetization, generates an ultrasonic wave at twice the frequency of the incident radiation. However this second type of term is a factor m/M_0 smaller than the first and so it may be neglected in a first approximation. This approximation will be made in the following discussion.

It can be seen that if the steady magnetization M_0 is either parallel to the plane of the film or perpendicular to it, that is $\alpha = 90°$ or 0, the driving term in the second of the eqs. (3.29) is zero; only transverse waves are generated. A longitudinal ultrasonic wave is generated at maximum efficiency when $\alpha = 45°$ as then the driving term in the

second equation is a maximum. To illustrate the nature of the solution consider the first of eqs. (3.29) which gives rise to a transverse wave polarized in the x-direction. The method of solution is similar to that used in §3.3 to solve eq. (3.3):

$$u_x = e^{-i\omega t} \int\limits_{-\infty}^{\infty} G(yy') \left[-\frac{b_2}{M_0 c_{44}} \cos \alpha \left(\frac{\partial m_x}{\partial y'} \right) \right] dy',$$

where $G(yy')$ is the appropriate Green's function. This Green's function is made up of two parts, a propagation $(i/2k) \exp(ik|y-y'|)$ arising from a source at y' and moving in the $+y$ direction and a part $(i/2k) \exp(ik|y+y'|)$ corresponding to a propagation originating at the same point but in the reverse direction (see fig. 3.15). The total Green's function is therefore

$$G(yy') = \frac{i}{k} \exp(iky) \cos ky'. \tag{3.30}$$

In this expression k is ω/v_t. Hence

$$u_x = -\frac{ib_2 \cos \alpha}{k M_0 c_{44}} e^{i(ky-\omega t)} \int\limits_{0}^{d} \cos ky' \left(\frac{\partial m_x}{\partial y'} \right) dy'. \tag{3.31}$$
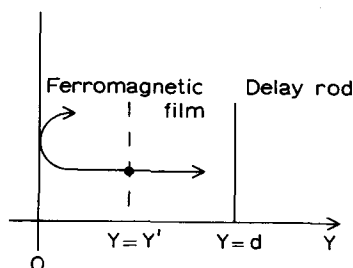
Fig. 3.15. Ferromagnetic film transducer showing direct and reflected contribution to the ultrasonic wave.

It has been assumed that the ferromagnetic film and the delay rod are acoustically matched. The limits of integration are from 0 to d, the thickness of the film. It is only in this region that the magnetization m_x is different from zero. In order to complete the solution the spatial variation of the magnetization m_x through the film is required. This can be of two types. In the case of a spin-wave resonance the magnetization varies throughout the film. The value of the integral in eq. (3.31) depends upon the spin-wave mode that is excited and on the spin pinning at the surfaces. These factors have been considered by KOOI [1963] and by WIGEN et al. [1965] but will not be discussed further

here. For ferromagnetic resonance, on the other hand, all the spins precess uniformly so that m_x will be a constant in the interior of the film and will drop to zero at each surface. In this situation it is reasonable to take $(\partial m_x / \partial y) \approx m_x^0 [\delta(y) - \delta(y-d)]$. Substitution of this value of the gradient into eq. (3.31) gives the result

$$u_x = -\frac{ib_2 \cos \alpha}{kM_0 c_{44}} e^{i(ky-\omega t)} m_x^0 [1 - \cos kd]. \tag{3.32}$$

If the acoustic matching of the delay rod to the ferromagnetic film is perfect the power flow away from the film is given by the product of the energy density and the velocity of the propagation,

$$S = \frac{b_2^2 \cos^2 \alpha}{2c_{44}} \left(\frac{m_x^0}{M_0}\right)^2 [1 - \cos kd] A v_t, \tag{3.33}$$

where A is the area of the film, cf. eq. (3.8).

In the usual arrangement for the generation of transverse ultrasonic waves, that is with the steady magnetic field applied perpendicular to the film and with $\alpha = 0$ there is also a contribution from the third equation of eq. (3.29). This is a transverse wave with the polarization in the z-direction. Combining this solution with that of the first equation it can be seen that a circularly polarized ultrasonic shear wave is generated by y-variations in the circularly polarized magnetization $m_x + im_z$. If the amplitude of this precessional magnetization is m_0 the acoustic power flowing away from the film is

$$S = \frac{b_2^2}{2c_{44}} \left(\frac{m_0}{M_0}\right)^2 [1 - \cos kd]^2 A v_t. \tag{3.34}$$

The efficiency of a thin ferromagnetic film as an ultrasonic transducer, that is the ratio of the input microwave electromagnetic power to the input acoustic power can be found in a similar way to that used in §3.3 for piezoelectric transducers

$$P = \tfrac{1}{2}\mu_0 h^2 \omega V / Q, \tag{3.35}$$

where h is the average microwave magnetic field in the cavity of volume V. In the usual cavity configuration the ferromagnetic film only occupies a small fraction of the total volume V in contrast to the piezoelectric transducer for which it is possible to design a resonant cavity where the electric field only has a large value in the region of the transducer. Equations (3.34) and (3.35) give for the ratio of S/P in the case of $\alpha = 0$

$$\frac{S}{P} = \frac{b_2^2 Q A v_t [1 - \cos kd]^2}{\mu_0 c_{44} M_0^2 \omega V} \left(\frac{m_0}{h}\right)^2. \tag{3.36}$$

By analogy with eq. (3.11) this equation can be written in the form

$$\frac{S}{P} = K_m^2 \frac{A v_t Q}{\omega V},\qquad(3.37)$$

where K_m^2 is $\mu_0 b_2^2 [1 - \cos kd]^2 |\chi|^2 / c_{44} M_0^2$ and $|\chi|^2 = (m_0/\mu_0 h)^2$. K_m is the magnetomechanical coupling factor for the film.

The arrangement considered so far in which the steady magnetic field is applied perpendicular to the plane of the film and $\alpha = 0$, is the most efficient geometry for magnetostrictive generation of microwave ultrasonic waves. It is found that the arrangement with the steady magnetic field parallel to the plane of the film, $\alpha = 90°$, is less efficient by a factor of about 10^{-2}, SEAVEY [1963]. This is because the amplitude of the microwave magnetization that can be achieved is much less for a given microwave magnetic field even if the effective susceptibility is the same. When $\alpha = 0$ the microwave magnetization must lie in the plane

TABLE 3.3
Magnetostriction constants at room temperature

Cubic materials		
Material	λ_{100}	λ_{111}
Fe[a])	20.3×10^{-6}	-21.1×10^{-6}
Ni[b])	-50.8×10^{-6}	-22.6×10^{-6}
Permalloy 78% Ni–Fe[b])	13.0×10^{-6}	1.8×10^{-6}

Hexagonal materials			
λ_a	λ_b	λ_c	λ_d
Co[c]) -45×10^{-6}	-95×10^{-6}	110×10^{-6}	-100×10^{-6}

[a]) CARR and SMOLUCHOWSKI [1951].
[b]) BOZORTH and HAMMING [1953].
[c]) BOZORTH [1954].

For a cubic crystal the magnetostriction in the direction $(\beta_1 \beta_2 \beta_3)$ due to the saturation magnetization in the direction $(\alpha_1 \alpha_2 \alpha_3)$ is given by

$$\lambda = dl/l \approx \tfrac{3}{2}\lambda_{100}(\alpha_1^2\beta_1^2 + \alpha_2^2\beta_2^2 + \alpha_3^2\beta_3^2 - \tfrac{1}{3}) + 3\lambda_{111}(\alpha_1\alpha_2\beta_1\beta_2 + \alpha_2\alpha_3\beta_2\beta_3 + \alpha_3\alpha_1\beta_3\beta_1),$$

λ_{100} and λ_{111} are related to the magnetoelastic constants of ch.5 by $\lambda_{100} = \tfrac{2}{3}b_1/(c_{11} - c_{12})$, $\lambda_{111} = -\tfrac{1}{3}b_2/c_{44}$, LEE [1955]. For a hexagonal crystal,

$$\lambda = \lambda_a[(\alpha_1\beta_1 + \alpha_2\beta_2)^2 - (\alpha_1\beta_1 + \alpha_2\beta_2)\alpha_3\beta_3] + \lambda_b[(1 - \alpha_3^2)(1 - \beta_3^2)$$
$$- (\alpha_1\beta_1 + \alpha_2\beta_2)^2] + \lambda_c[(1 - \alpha_3)^2\beta_3^2 - (\alpha_1\beta_1 + \alpha_2\beta_2)\alpha_3\beta_3] + 4\lambda_d(\alpha_1\beta_1 + \alpha_2\beta_2)\alpha_3\beta_3.$$

of the film while for $\alpha = 90°$ it must be in a direction normal to the film; the boundary conditions relating the magnetic field in the resonant cavity to the magnetization of the film account for the difference in efficiency. For the generation of longitudinal waves the effect is less marked; an arrangement with $\alpha = 45°$ can be used, and the microwave magnetization is also in a direction making an angle of $45°$ with the plane of the film.

Table 3.3 gives the magnetostrictive constants of some ferromagnetic materials. Nickel exhibits the largest magnetostriction and is usually employed for the generation of microwave ultrasonic waves by the techniques described above. Cobalt films have been used by DOBROV [1964] because of their very broad ferromagnetic resonance. This enabled the effect of small variations in the applied magnetic field on the propagation of the ultrasonic waves in a ruby delay rod specimen to be studied without drastically altering the performance of the transducer. The applied steady magnetic field is always liable to limit the usefulness of thin film ferromagnetic transducers to those applications where the applied field does not affect any other aspect of the experiment. BIALAS and WEIS[1968] have shown however that for nickel films the field for ferromagnetic resonance can be reduced to zero by mechanical strain or by applying a magnetic field during evaporation to produce magnetic anisotropy.

5. Resonant cavities and microwave circuits

5.1. *Resonant cavity designs*

All the microwave ultrasonic transducers discussed so far need a high intensity electric or magnetic field oscillating at the frequency of the ultrasonic waves to be generated. These fields are normally produced in a microwave resonant cavity. The requirements of a high efficiency of generation are, see for example eq. (3.37), that the cavity should have a high Q-factor and that the ratio of the area of the transducer to the volume of the region of the cavity occupied by the field should be as large as possible. The re-entrant coaxial cavity as shown in fig. 3.2 has been the most widely used type when piezoelectric transducers have been employed. The electric field is confined to a small region of the cavity if a quarter wavelength cavity is used, thus ensuring a large value for A/V, and the Q-factor at X-band frequencies (9.5 GHz) can be about 2000. The design of these cavities is discussed by MORENO [1958]. The cavity can be regarded as having an inductance due to the short length of coaxial line which is tuned by the capacitance formed between the post and the opposite wall. The resonant free space wave-

length of such a cavity is approximately given by

$$\lambda_0 = 2\pi \left[\frac{Kl\rho_1^2}{2\delta} \log \left(\frac{\rho_2}{\rho_1} \right) \right]^{1/2}, \tag{3.38}$$

where K is the dielectric constant of the medium filling the gap, and the other symbols are defined in fig. 3.16. The expression, as given by eq. (3.38), neglects fringing fields and gives a slight overestimate of the
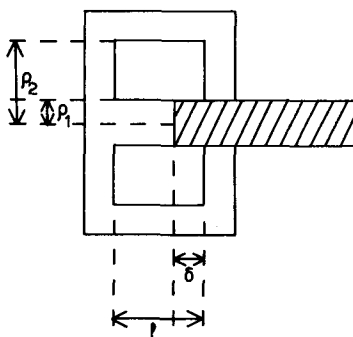
Fig. 3.16. Re-entrant co-axial resonant cavity.

resonant frequency. A cavity with $l = 2.7$ mm, $\delta = 1.44$ mm, $\rho_1 = 1.5$ mm and $\rho_2 = 6.6$ mm gives a calculated resonance frequency of 11.1 GHz for quartz where K is 3.8, whereas experimentally this cavity is resonant at about 9.5 GHz. Equation (3.38) nevertheless provides a guide to cavity design. It is often desirable for the resonant cavity to be tunable over a small range. With the re-entrant coaxial cavity this can be achieved in several ways. The value of δ is adjustable as the back wall of the cavity is made of flexible copper foil so that the post can be moved backwards and forwards. A similar effect is obtained if the transducer is moved in and out, the effective dielectric constant in the gap then varies and the resonant frequency changes. There is, of course, a limit to the extent of the movement of the transducer; otherwise it will move right out of the electric field of the cavity. Another method of tuning the cavity is described by STEPHENSON [1963]. A dielectric or metal discontinuity, such as a collar round the post, is moved to and fro to tune the cavity. This method does not move the transducer and so does not affect the efficiency of generation.

A slightly different form of re-entrant resonant cavity has been described by LAMB and RICHTER[1967] and is shown in fig. 3.17. There are two resonant modes of this cavity which can be used. The one at lower frequency gives an electric field tangential to the surface
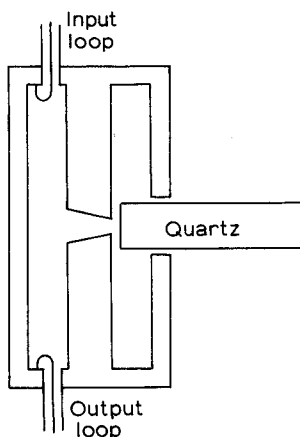
Fig. 3.17. Co-axial cavity of Lamb and Richter.

of the transducer and the resonant frequency is the same as that of a single re-entrant cavity, as in fig. 3.16, which could be formed by dividing the double cavity with a metal sheet down the centre through the gap in the centre electrode. The higher frequency mode gives an electric field normal to the transducer surface and occurs at a frequency as if the cavity consisted of a half wavelength of co-axial line with no gap in the centre electrode. This type of cavity is useful because these two orientations of the electric field can be produced. The mode with the electric field tangential to the surface is especially useful for the generation of shear waves, DE KLERK [1966b].

The single re-entrant co-axial cavity has also been used with thin ferromagnetic film transducers by BÖMMEL and DRANSFELD [1959b]. In this case the delay rod specimen is inserted through the side wall of the cavity into the region of high magnetic field. This is shown in fig. 3.12. Rectangular cavities have also been used, SEAVEY [1963]. The whole of the delay rod specimen was inside the cavity with the ferromagnetic film pressed against one wall where the magnetic field is of the greatest intensity. A TE 101 mode was used, for which the resonant free space wavelength is given by $\lambda_0 = 4[l/a + m/b + n/c]^{-1/2}$, where $2a$, $2b$ and $2c$ are the dimensions of the cavity and $l = n = 1$ and $m = 0$, see fig. 3.13.

5.2. Microwave circuits

The microwave and electronic circuits required for the generation and detection of ultrasonic waves, using piezoelectric or ferromagnetic transducers, are almost entirely conventional and so will only be described briefly. At the low frequency end of the range, about 1 GHz,

co-axial cable circuits are usually used while waveguides are employed for the higher frequencies. A block diagram indicating a typical arrangement with a waveguide at 9.5 GHz is shown in fig. 3.18. A pulse-echo system is shown in which the same transducer is used for generating the ultrasonic waves and for detecting the returning pulse echoes. The final recording arrangement depends upon the type of experiment and the information sought. For example, if the absolute attenuation constant in a delay rod specimen is required the exponential decay of the echo train can be compared on an oscilloscope screen with a trace decaying at a known rate. This type of measurement is only possible at the lower frequencies when the effects of non-parallel ends of the specimen are not serious, see §3.4. The change in attenuation with temperature can be examined by comparing the relative amplitudes of two echoes seen on the oscilloscope at each temperature.
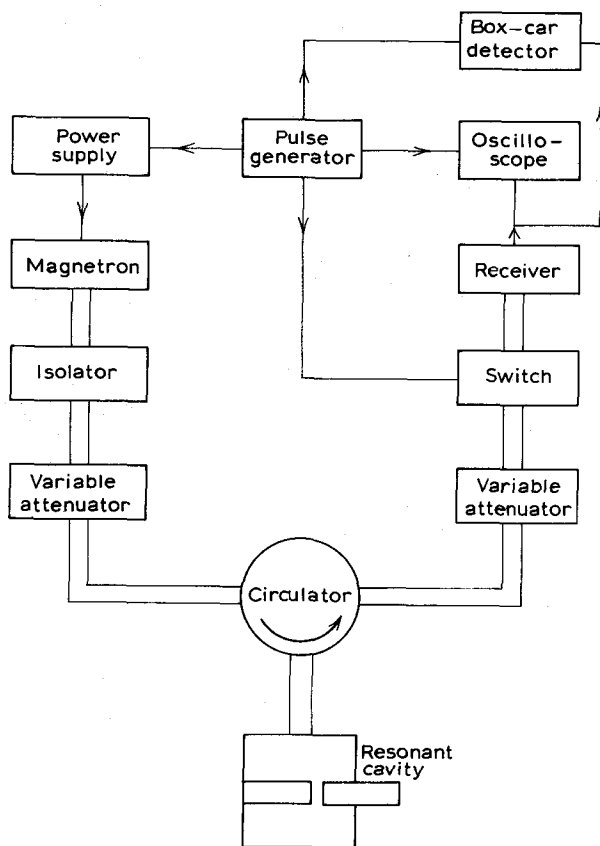
Fig. 3.18. Block diagram of a typical 9.5 GHz microwave ultrasonics pulse-echo system.

When the ultrasonic attenuation is required as a function of an applied magnetic field, as in acoustic paramagnetic resonance experiments, the amplitude of a chosen echo is observed for different field strengths. If a gated amplifier is used to select the chosen echo in conjunction with an integrating peak recording voltmeter, LEWIS and STONEHAM[1967], the attenuation can be plotted directly on a chart recorder. This gives an improvement in the signal-to-noise ratio because of the very narrow bandwidth of the recording system. A further improvement in the signal-to-noise ratio has been obtained by TITTMANN and BÖMMEL [1967] by using the technique of time averaging.

TITTMANN and BÖMMEL[1968] have also described an apparatus for investigating ultrasonic waves in the frequency range 0.4 to 4 GHz which uses quartz transducers but not resonant cavities. Co-axial lines, widened in the vicinity of the sample to accommodate the transducers, are used. Double stub tuners match the transducer impedance onto the line.

6. Other methods

6.1. *Heat pulses and bolometers*

There are several other methods of generating and detecting microwave ultrasonic waves which have been used to a lesser extent than those already described. Some of these will now be briefly mentioned.

Heat pulses have been used to extend effectively the frequency range to very high frequencies. A thin metal film is evaporated onto the end surface of a specimen rod and then rapidly heated by passing a high current pulse, VON GUTFELD and NETHERCOT[1964]. Alternatively, one may shine a short laser pulse on to the metal film or allow an *X*-band microwave pulse to fall upon it, ANDREWS and STRANDBERG [1967]. Provided that the temperature of the film is low enough for the phonon–phonon collisions to be rare, the heat pulse propagates along the bar as a set of high frequency ultrasonic waves with many frequencies and polarizations. Sometimes three components can be detected corresponding to a longitudinal and two transverse waves. The principal frequencies are those corresponding to the modes populated at the temperature of the pulse. The high frequency thermometer that is used to detect the heat pulses is usually a superconducting bolometer. A superconducting alloy is evaporated onto the end of the specimen rod and is then held at its superconducting transition temperature where there is a rapid change of electrical resistance over several millidegrees Kelvin. An alloy is used for which the critical temperature is not quite so sharp as it is for an elementary superconductor. The temperature at which the bolometer operates can be adjusted by applying

a magnetic field to lower the critical temperature of the superconductor. The choice of superconducting alloy controls the highest temperature at which the bolometer will work; for most materials this is in, or just above, the liquid helium temperature range. This of course is not a serious limitation in heat pulse experiments because in any case they must be done at sufficiently low temperatures for the mean free path of the phonons to be greater than the length of the specimen.

Superconducting bolometers have also been used by ANDREWS and STRANDBERG[1967] to detect microwave ultrasonic waves at 9 GHz in quartz which had been generated piezoelectrically. The advantage of bolometer detection over piezoelectric detection is that the output signal depends on the ultrasonic intensity rather than the amplitudes of the waves; thus the relative phase of the wave across the detecting surface is unimportant. The problems with bolometer detection are the precise temperature control which is required and the dependence of the detector on the applied magnetic field. A change in the magnetic field alters the transition temperature and hence the temperature at which the detector can operate. Materials which have been used as bolometers include the alloys of 98% tin 2% copper at 3.5 K; 94% indium 6% tin at 3.8 K; 65% lead 35% bismuth at 8.5 K. The films used varied in thickness from 1000 Å to 1500 Å.

6.2. *Semiconductor avalanche*

An alternative high frequency thermometer which has been used to detect heat pulses as well as microwave ultrasonic pulses at 9.5 GHz is the semiconductor avalanche detector of ZYLBERSZTEJN[1967] and WIGMORE[1968]. Electrodes are connected to a piece of doped germanium or silicon which is polished on one face and cemented to the specimen delay rod. A steady voltage is applied to bias the material until avalanche breakdown is just occurring. The current then varies rapidly with temperature and the device acts as a rapidly responding thermometer. The active region is very small because only over a small region is the electric field at the appropriate value to give the slight impact ionization required. This is one of the reasons for the rapid response.

6.3. *Optical methods*

The diffraction of light by the microwave ultrasonic waves provides another means of detection that does not depend on the accurate polishing of the end face. The ultrasonic wave causes a sinusoidal variation of the refractive index along the specimen delay rod which can then act as a diffraction grating to light entering the side of the rod. This method was used by BARANSKII[1957a] and by BÖMMEL and DRANSFELD[1958]. It is necessary for the sides of the specimen to be

optically polished and for the specimen to be transparent to the light used.

An optical method of generating microwave ultrasonic waves is the inverse of this detection method. Brillouin scattering of light by a solid involves a change in frequency of the light and the production of a lattice vibration. The whole topic of the interaction between light and lattice vibrations is considered in more detail in ch. 9.

6.4. *Paramagnetic resonance methods*

There are other methods of detecting ultrasonic waves based on acoustic paramagnetic resonance which is discussed in ch. 6. LEWIS[1965] has used the partial saturation of the electron paramagnetic resonance of ferrous ions in magnesium oxide to detect ultrasonic waves at 9.5 GHz. The specimen delay rod consisted of a sample of ferrous doped magnesium oxide in the resonance cavity of an electron paramagnetic resonance spectrometer. The resonance absorption was observed at a frequency equal to that of the ultrasonic waves to be detected. When an ultrasonic pulse passed through the specimen the ferrous resonance was partially saturated and a change in the resonance absorption was observed. Lewis carried out the experiment at 10 K and 4 K. At lower temperatures because the spin–lattice relaxation time of the ferrous ions was much longer than the ultrasonic pulse length the perturbed resonance absorption persisted so that the ultrasonic pulse shape could not be observed.

Another detection method employing acoustic paramagnetic resonance is due to SHIREN[1961]. Again the delay rod specimen is a sample of ferrous doped magnesium oxide in the resonance cavity of an electron paramagnetic resonance spectrometer. Under the appropriate conditions a transition between the energy levels of the ferrous ion can be induced by a photon and a phonon simultaneously; hence a change in the microwave electromagnetic absorption will occur when ultrasonic waves of the correct frequency are present. This detector gives an indication of the ultrasonic pulse shape, unlike the saturation method of LEWIS[1965]. However it appears to be somewhat specimen dependent; not all samples of ferrous doped magnesium oxide will function as double quantum detectors.

SABISKY and ANDERSON[1968] have also employed a paramagnetic crystal to detect microwave ultrasonic waves. A change in the circular dichroism associated with a change in the spin populations during the passage of an ultrasonic wave was observed optically.

Further consideration of acoustic paramagnetic resonance is deferred to ch. 6 where the generation of ultrasonic waves in the phonon maser is described, TUCKER[1964].

ATTENUATION OF ULTRASONIC WAVES IN DIELECTRICS

This chapter is concerned with the interaction between phonons and with the absorption of ultrasound in dielectric crystals. An important parameter which will enter the theory is the ratio of the wavelength of the ultrasound to the mean free path of the phonons thermally excited in the crystal. If the wavelength of the ultrasound is small compared to the mean free path of the phonons the attenuation of the sound waves may be regarded as arising from collisions with lattice phonons which are in thermal equilibrium. If the collision time between the thermal phonons is denoted by τ then the above condition will be realised when $\Omega\tau$ is much greater than unity, Ω being the frequency of the sound wave that is present. The second regime, which was first discussed in detail by AKHIESER[1939], is when $\Omega\tau$ is very much less than unity. In this case it is more realistic to treat the phonons as particles moving about in the slowly varying potential field produced by the presence of the sound wave.

Before any of these problems can be discussed it is necessary to know the nature of the interactions that take place between phonons or between elastic waves in crystals. These interactions do not occur in a harmonic theory so elasticity theory and the theory of lattice dynamics has to be extended beyond this framework by the inclusion of higher powers of the displacement and deformation tensor in the expansion of the potential energy function.

1. Anharmonic interactions

1.1. *Third-order elastic constants*

In the discussion of classical elasticity theory in ch. 2 it was remarked that, assuming Hooke's law to be valid, the elastic potential energy was quadratic in the components of the strain tensor

$$W = \tfrac{1}{2} c_{ijkl} \epsilon_{ij} \epsilon_{kl}.$$

83

To obtain interactions between elastic waves terms cubic in ζ_{ij} have to be included in the potential energy function W. This may be achieved by adding to W a term of third order in the strain components ϵ_{ij}. It should be recalled however that in the usual definition of ϵ_{ij} terms quadratic in ζ_{ij} have already been dropped. Therefore, as mentioned in ch. 2 if terms cubic in ζ_{ij} are of interest the deformation tensor η rather than the conventional strain tensor ϵ must be used. Consequently to account for terms cubic in ζ_{ij} the potential energy function is written in the form

$$W = \tfrac{1}{2}c_{ijkl}\eta_{ij}\eta_{kl} + c_{ijklmn}\eta_{ij}\eta_{kl}\eta_{mn}. \qquad (4.1)$$

The c_{ijklmn} are known as the third-order elastic constants and form the components of a sixth-order tensor. It might be expected that there should be a factor 1/3! in the last term of eq. (4.1) but it is omitted in the convention adopted by many authors in their definition of elastic constants. A sixth-order tensor will have 729 components, but the use of symmetry arguments similar to those employed in ch. 2§1.3 for the c_{ijkl} enables the number of independent third-order elastic constants to be considerably reduced in the case of crystals with high symmetry. The non-zero independent third-order elastic constants for the different classes of crystal symmetry are listed in table A1.3.

As an example consider an isotropic crystal. It is well known, e.g. MURNAGHAN[1951], that η has three invariants, namely, trace η, trace co. η and det. η. By this it is meant that the above three quantities are independent of the rotation of the initial coordinate axes. Written in full the invariants are

$$
\begin{aligned}
I_1 &= \text{Trace } \eta = \text{sum of diagonal elements of } \eta \\
&= \eta_{11} + \eta_{22} + \eta_{33} \\[4pt]
I_2 &= \text{Trace co. } \eta = \text{sum of the three diagonal minors of } \eta \\
&= \eta_{22}\eta_{33} + \eta_{11}\eta_{33} + \eta_{11}\eta_{22} - (\eta_{23}^2 + \eta_{13}^2 + \eta_{12}^2) \\[4pt]
I_3 &= \text{determinant of } \eta \\
&= \eta_{11}\eta_{22}\eta_{33} + 2\eta_{23}\eta_{13}\eta_{12} - (\eta_{11}\eta_{23}^2 + \eta_{22}\eta_{13}^2 + \eta_{33}\eta_{12}^2).
\end{aligned}
\qquad (4.2)
$$

Making use of these invariants the general expression for the energy of an isotropic medium can be obtained by writing

$$W = AI_1^2 + BI_2 + CI_1^3 + DI_1I_2 + EI_3. \qquad (4.3)$$

Some authors find it convenient to use, instead of the invariants above, the quantities

$$J_1 = \text{Trace } (\eta); \quad J_2 = \text{Trace } (\eta^2); \quad J_3 = \text{Trace } (\eta^3) \qquad (4.4)$$

related to the I's by

$$J_1 = I_1; \quad J_2 = I_1^2 - 2I_2; \quad J_3 = I_1^3 + 3I_3 - 3I_1 I_2.$$

Employing the fact that $\eta_{ij} = \eta_{ji}$ and that $c_{ijklmn} = c_{mnijkl}$ etc. it is found that on comparing the coefficients of η_{11}, $\eta_{11}\eta_{22}$, η_{11}^3, $\eta_{11}\eta_{13}^2$ and $\eta_{13}\eta_{23}\eta_{12}$ in eqs. (4.3) and (4.1)

$$W = \tfrac{1}{2}c_{1111}I_1^2 - (c_{1111} - c_{1122})I_2 + c_{111111}I_1^3$$
$$- 12c_{111313}I_1 I_2 + 24c_{121323}I_3. \tag{4.5}$$

An alternative notation is obtained by pairing the suffices and making the following replacements*

$$11 \to 1, \ 22 \to 2, \ 33 \to 3, \ 23 \to 4, \ 13 \to 5, \ 12 \to 6.$$

In this scheme

$$W = \tfrac{1}{2}c_{11}I_1^2 - (c_{11} - c_{12})I_2 + c_{111}I_1^3 - 12c_{155}I_1 I_2 + 24c_{456}I_3.$$

To obtain an expression for the energy density which accounts for the cubic anharmonic interactions, the I's are expressed in terms of the ζ's and terms up to third order in ζ retained. The terms cubic in ζ are those responsible for the interactions between the elastic waves. The resultant expression is

$$W = \tfrac{1}{8}(c_{11} - c_{12})(\zeta_{ik} + \zeta_{ki})^2 + \tfrac{1}{2}c_{12}\zeta_{ii}\zeta_{jj} + (\tfrac{1}{2}c_{12} + 3c_{155} - 6c_{456})\zeta_{ii}\zeta_{jk}^2$$
$$+ (\tfrac{1}{2}c_{11} - \tfrac{1}{2}c_{12} + 6c_{456})\zeta_{ij}\zeta_{ki}\zeta_{kj} + (3c_{155} - 6c_{456})\zeta_{ii}\zeta_{jk}\zeta_{kj}$$
$$+ (c_{111} - 6c_{155} + 4c_{456})\zeta_{ii}\zeta_{jj}\zeta_{kk} + 2c_{456}\zeta_{ij}\zeta_{jk}\zeta_{ki}. \tag{4.6}$$

It should be noted that the third and fourth terms of eq. (4.6) show that even in the absence of the third-order elastic constants the potential energy function contains cubic terms in ζ. This is because the deformation tensor rather than the strain tensor has been used and implies that Hooke's law is only valid for small deformations. Interactions between elastic waves can occur even if only quadratic terms in the deformation tensor are retained in the expression for the energy density.

Before proceeding with a discussion of how these anharmonic terms account for the attenuation of ultrasonic waves the equivalent anharmonic terms on the basis of a lattice theory will be obtained.

1.2. Anharmonic interactions in lattice dynamics

In ch. 2§3 an outline of the theory of lattice dynamics in the harmonic approximation was given. That is to say the total potential energy was

---

* This notation is not to be confused with that of HEARMON [1953] and that of BIRCH [1947] where their c_{pqr} are only defined for $p \geqslant q \geqslant r$.

expanded in a Taylor series of the particle displacements and only terms up to those quadratic in the displacement retained. This chapter is concerned with the interaction of ultrasonic waves with thermal phonons and also the interaction of phonons with each other. To effect these interactions it is necessary to go further than the harmonic approximation and consider the higher-order terms in the expansion of the potential energy. The first two anharmonic terms are

$$\phi_3 = \sum_{\substack{l_1 k_1 \alpha \\ l_2 k_2 \beta \\ l_3 k_3 \gamma}} \phi_{\alpha\beta\gamma} \begin{pmatrix} l_1 l_2 l_3 \\ k_1 k_2 k_3 \end{pmatrix} u_\alpha \begin{pmatrix} l_1 \\ k_1 \end{pmatrix} u_\beta \begin{pmatrix} l_2 \\ k_2 \end{pmatrix} u_\gamma \begin{pmatrix} l_3 \\ k_3 \end{pmatrix}$$

$$\phi_4 = \sum_{\substack{l_1 k_1 \alpha \\ l_2 k_2 \beta \\ l_3 k_3 \gamma \\ l_4 k_4 \delta}} \phi_{\alpha\beta\gamma\delta} \begin{pmatrix} l_1 l_2 l_3 l_4 \\ k_1 k_2 k_3 k_4 \end{pmatrix} u_\alpha \begin{pmatrix} l_1 \\ k_1 \end{pmatrix} u_\beta \begin{pmatrix} l_2 \\ k_2 \end{pmatrix} u_\gamma \begin{pmatrix} l_3 \\ k_3 \end{pmatrix} u_\delta \begin{pmatrix} l_4 \\ k_4 \end{pmatrix}$$

(4.7)

where the coupling coefficients $\phi_{\alpha\beta\gamma}$ and $\phi_{\alpha\beta\gamma\delta}$ are the third- and fourth-order derivatives of the potential energy function with respect to the displacements evaluated at the equilibrium atomic positions*. Introducing the normal coordinates defined in eq. (2.49) the anharmonic terms can be transformed to

$$\phi_3 = \frac{1}{3!} \frac{1}{\sqrt{N}} \sum_{\substack{q_1 q_2 q_3 \\ j_1 j_2 j_3}} \phi \, {}^{q_1 q_2 q_3}_{j_1 j_2 j_3} \, u \begin{pmatrix} q_1 \\ j_1 \end{pmatrix} u \begin{pmatrix} q_2 \\ j_2 \end{pmatrix} u \begin{pmatrix} q_3 \\ j_3 \end{pmatrix}$$

$$\phi_4 = \frac{1}{4!} \frac{1}{\sqrt{N}} \sum_{\substack{q_1 q_2 q_3 q_4 \\ j_1 j_2 j_3 j_4}} \phi_{j_1 j_2 j_3 j_4}^{q_1 q_2 q_3 q_4} \, u \begin{pmatrix} q_1 \\ j_1 \end{pmatrix} u \begin{pmatrix} q_2 \\ j_2 \end{pmatrix} u \begin{pmatrix} q_3 \\ j_3 \end{pmatrix} u \begin{pmatrix} q_4 \\ j_4 \end{pmatrix}$$

(4.8)

with

$$\phi \, {}^{q_1 q_2 q_3}_{j_1 j_2 j_3} = \frac{1}{N} \sum_{\substack{l_1 k_1 \alpha \\ l_2 k_2 \beta \\ l_3 k_3 \gamma}} \frac{\phi_{\alpha\beta\gamma} \begin{pmatrix} l_1 l_2 l_3 \\ k_1 k_2 k_3 \end{pmatrix}}{(m_{k_1} m_{k_2} m_{k_3})^{1/2}} e_\alpha \left(k_1 \middle| \begin{matrix} q_1 \\ j_1 \end{matrix} \right) e_\beta \left(k_2 \middle| \begin{matrix} q_2 \\ j_2 \end{matrix} \right) e_\gamma \left(k_3 \middle| \begin{matrix} q_3 \\ j_3 \end{matrix} \right)$$

$$\times \exp \{-\mathrm{i}[q_1 \cdot x(l_1) + q_2 \cdot x(l_2) + q_3 \cdot x(l_3)]\}$$ (4.9)

and a similar type of expression for $\phi \, {}^{q_1 q_2 q_3 q_4}_{j_1 j_2 j_3 j_4}$. Now $\phi_{\alpha\beta\gamma} \begin{pmatrix} l_1 l_2 l_3 \\ k_1 k_2 k_3 \end{pmatrix}$ is invariant if a translation by an arbitrary lattice vector is made. This implies that $q_1 + q_2 + q_3 = 0$ or G where G is a reciprocal lattice vector. It must therefore be remembered that in ϕ_3 and ϕ_4 it is understood that $q_1 + q_2 + q_3 = 0$ or G and $q_1 + q_2 + q_3 + q_4 = 0$ or G respectively. Using the fact that

$$u \begin{pmatrix} q \\ j \end{pmatrix} = \mathrm{i} \left(\frac{\hbar}{2\omega_j(q)} \right)^{1/2} [a_j(-q) - a_j^*(q)],$$

---

* In this chapter subscripts on the l, k and q do not indicate cartesian components.

ϕ_3 and ϕ_4 can be expressed in terms of creation and annihilation operators. It is clear that ϕ_3 contains triplet products of creation and annihilation operators. For example a typical term might involve the factor $a_{j_1}^*(q_1)a_{j_2}^*(q)a_{j_3}(q_3)$ which destroys a phonon in the mode $(j_3 q_3)$ and creates one in each of the modes $(j_1 q_1)$ and $(j_2 q_2)$. It should be emphasized though that the term is only present provided that

$$q_1 + q_2 - q_3 = 0 \text{ or } G. \tag{4.10}$$

Processes for which G is zero are referred to as *normal processes* while for non-zero G they are known as *Umklapp processes*. The restriction expressed by eq. (4.10) in the case of $G = 0$ is often referred to as the momentum conservation condition. This statement is misleading in that it implies that a phonon with wave vector q carries with it a momentum $\hbar q$. This is evidently not true because the theory of lattice vibrations which has been discussed only accounts for vibrations of atoms about fixed equilibrium positions so that on the average there is no mass motion of the atoms. Strictly speaking therefore a phonon in a lattice does not carry momentum. Nevertheless as is customary, we shall still refer to the conservation of momentum when what is really meant is crystal momentum.

Suppose that ϕ_3 is small enough to be treated as a small perturbation on the harmonic crystal. If the lattice is initially in a definite state $|i\rangle$ then from lowest-order time-dependent perturbation theory, (appendix 3) the probability of ϕ_3 causing a transition to a state $|j\rangle$ in time t is

$$\frac{2|\phi_3(ji)|^2}{(E_j - E_i)^2}[1 - \cos(E_j - E_i)t/\hbar] \tag{4.11}$$

where E_j and E_i are the energies of the two states and $|\phi_3(ij)|^2$ is the square of the matrix element between them. It is seen that the transition probability selects those terms for which $E_i = E_j$. Thus the term involving $a_{j_1}^*(q_1)a_{j_2}^*(q_2)a_{j_3}(q_3)$ will only give rise to a significant scattering provided that

$$\omega_{j_1}(q_1) + \omega_{j_2}(q_2) = \omega_{j_3}(q_3). \tag{4.12}$$

Eqs. (4.10) and (4.12) taken together severely restrict the number of scattering processes that may occur. It leads to a number of selection rules which will be discussed in detail shortly. Naturally there will also be present a term conjugate to that above which creates a phonon in the mode $(j_3 q_3)$ and destroys one in each of the modes $(j_1 q_1)$ and $(j_2 q_2)$. It is the difference in transition rates for these two processes that is important.

2. Phonon interactions

2.1. *Selection rules for three-phonon processes*

A typical term in the anharmonic interaction will consist of a product of three or more creation and annihilation operators. This means that for three-phonon processes involving the destruction of a phonon in the mode $(j_1 q_1)$ there will be present terms involving $a_{j_1}(q_1)a_{j_2}^*(q_2)a_{j_3}^*(q_3)$ or $a_{j_1}(q_1)a_{j_2}(q_2)a_{j_3}^*(q_3)$. These processes are indicated in fig. 4.1. The

(a)   (b)
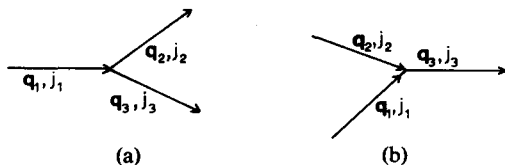
Fig. 4.1.

energy conservation and interference conditions, eqs. (4.12) and (4.10), imply that for processes (a) and (b) of fig. 4.1

$$\omega_{j_1}(q_1) = \omega_{j_2}(q_2) + \omega_{j_3}(q_3) \qquad \omega_{j_1}(q_1) = \omega_{j_3}(q_3) - \omega_{j_2}(q_2)$$

$$q_1 = q_2 + q_3 + G \qquad\qquad q_1 = q_3 - q_2 + G \qquad (4.13)$$

(a)   (b)

where G is a reciprocal lattice vector. For the present only normal processes where G is zero, will be considered.

The simplest example to treat is an isotropic medium without dispersion for which the frequency $\omega(q)$ varies linearly with the wave vector q. As seen in ch. 2§1.4 for any direction of propagation in the crystal there is always one longitudinal branch and two degenerate transverse branches. The velocity, v_ℓ, of the longitudinal modes is greater than the corresponding velocities, v_t, of the transverse modes. Normal processes of the type (a) have $q_1 = q_2 + q_3$ which implies that q_1 is less than $q_2 + q_3$. An equality would occur if the three q's were collinear but discussion of this special case will be deferred to §2.5. Because of the absence of dispersion these processes will therefore occur if $\omega_1/v_1 < \omega_2/v_2 + \omega_3/v_3$. However energy conservation dictates that $\omega_1 = \omega_2 + \omega_3$ so consequently the velocity v_1 must be greater than either v_2 or v_3. This implies that the three phonons which interact cannot all belong to the same branch of polarization. Now since v_ℓ is greater than v_t it is clear from these conditions that process (a) is only possible if $v_1 = v_\ell$ and either one or both of v_2 and v_3 must equal v_t. The allowed processes of the type (a) are therefore governed by the following selection rules

(i) $\omega_\ell(q_1) \rightarrow \omega_t(q_2) + \omega_t(q_3),$

(ii) $\omega_\ell(q_1) \rightarrow \omega_t(q_2) + \omega_\ell(q_3),$ (4.14)

(iii) $\omega_\ell(q_1) \rightarrow \omega_\ell(q_2) + \omega_t(q_3).$

The subscripts ℓ and t denote longitudinal and transverse modes respectively. The three-phonon interaction of the type (b) can be analysed in a similar manner and leads to the following selection rules

(iv) $\omega_\ell(q_1) + \omega_t(q_2) \rightarrow \omega_\ell(q_3),$

(v) $\omega_t(q_1) + \omega_\ell(q_2) \rightarrow \omega_\ell(q_3),$ (4.15)

(vi) $\omega_t(q_1) + \omega_t(q_2) \rightarrow \omega_\ell(q_3).$

From the point of view of this book the three-phonon process of major interest is the decay of a microwave phonon arising from its interaction with thermal phonons of the lattice. The decay rate will of course depend to a large extent on the number of thermal phonons excited at a particular temperature. In the Debye approximation, $\omega(q)$ is proportional to q, so the number of thermal phonons having frequencies between $\omega(q)$ and $\omega(q) + d\omega(q)$ is proportional to the factor $\omega^2(q)d\omega(q)/\{\exp[\hbar\omega(q)/KT] - 1\}$. For fixed temperature this quantity, plotted in fig. 4.2, is strongly peaked about the value of $\omega(q)$ satisfying $\hbar\omega(q) \approx 1.6KT$. Now energies of 1 cm^{-1} correspond to a temperature of about 1.4 K so that the frequency of microwave phonons is generally considerably smaller than that of the bulk of the thermal phonons
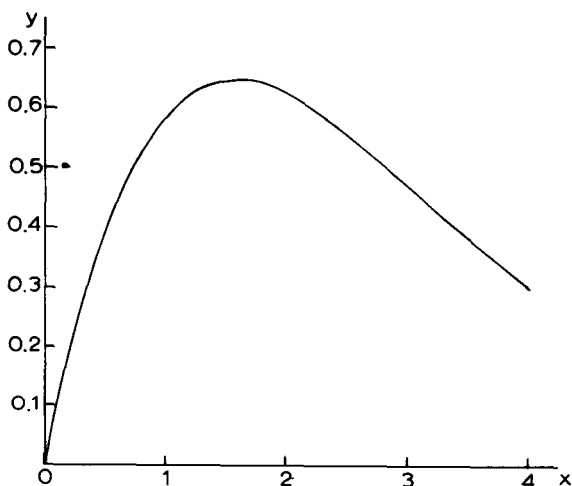
Fig. 4.2. Graph showing the variation of $y = \hbar^2\omega^2(q)/\{\exp[\hbar\omega(q)/KT] - 1\}$ as a function of $x = \hbar\omega(q)/KT$.

present in the crystal. In microwave ultrasonics we are therefore usually interested in the decay of low frequency phonons through their interaction with phonons of much higher frequencies. Thus in the range of frequencies of major interest processes (i)–(iii) are not of prime importance at most temperatures since it is not possible to have $\omega(q_1)$ small and at the same time $\omega(q_2)$ or $\omega(q_3)$ much larger than $\omega(q_1)$. Consider now processes (iv)–(vi). In terms of velocities the energy and momentum conservation requirements are

$$v_1 q_1 + v_2 q_2 = v_3 q_3, \quad q_1^2 + q_2^2 + 2 q_1 q_2 \cos \theta = q_3^2,$$

where θ is the angle between the vectors q_1 and q_2. Elimination of q_3 from these equations gives

$$\frac{q_2}{q_1} = \frac{v_1 v_2 - v_3^2 \cos \theta \pm [(v_3^2 \cos \theta - v_1 v_2)^2 - (v_3^2 - v_2^2)(v_3^2 - v_1^2)]^{1/2}}{v_3^2 - v_2^2}, \quad (4.16)$$

For process (iv), $v_1 = v_3 = v_\ell$ and $v_2 = v_t$ yields

$$\frac{v_t q_2}{v_\ell q_1} = \frac{\omega_2}{\omega_1} = \frac{2 v_t (v_t - v_\ell \cos \theta)}{v_\ell^2 - v_t^2}. \quad (4.17)$$

Clearly for no value of the angle θ can ω_2 be much greater than ω_1. The maximum ratio of ω_2 to ω_1 is obtained when $\theta = 180°$. At this angle, in the case of an isotropic medium satisfying the Cauchy relation, ch. 2§3.6, $\omega_2/\omega_1 = 2v_t/(v_\ell - v_t) = 2.732$. Since this number is small it can therefore be concluded that a longitudinal microwave phonon *cannot* decay by interacting with high frequency thermal phonons. On the other hand, process (v) of eq. (4.15) has $v_1 = v_t$ and $v_2 = v_3 = v_\ell$. In this case the solution of eq. (4.16) is

$$\frac{\omega_2}{\omega_1} = \frac{v_\ell^2 - v_t^2}{2 v_t (v_t - v_\ell \cos \theta)}. \quad (4.18)$$

It follows that in this process it is possible for ω_2 to be much greater than ω_1 over a reasonable range of angles; thus a transverse microwave phonon can decay through its interaction with high frequency thermal phonons.

In order to ascertain the number of vectors q_2 satisfying the eq. (4.16) it is necessary to know the area of the surface which contains the end-point of q_2 for a fixed vector q_1. The condition, eq. (4.17), has the form $q_2 = q_1 a (1 - b \cos \theta)$ where b is greater than unity. For fixed q_1, the end-point of q_2 will lie on two ovals as shown in fig. 4.3. The dotted oval indicates q_2 is negative and hence for these values it has no physical significance. The surface swept out by rotating this curve about an axis lying along q_1 contains all the possible end-points of the vector q_2 allowed to participate in the three-phonon interaction. Since the
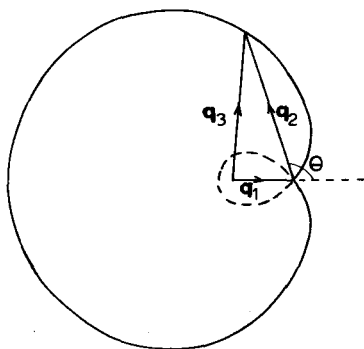
Fig. 4.3.

surface traced out is closed the area will be proportional to q_1^2. Thus longitudinal phonons of long wavelength can only take part in processes of which the total number is inversely proportional to the square of the wavelength. On the other hand eq. (4.18) is of the form $q_2 = q_1 c (1 - d \cos \theta)^{-1}$ with $d > 1$. This is the polar equation of a hyperbola as shown in fig. 4.4. This time there is no limit to the size of q_2 and hence no limit to the area of the surface generated by rotating the hyperbola about the axis along q_1. The number of phonons that can participate in the three-phonon interaction is consequently much greater.
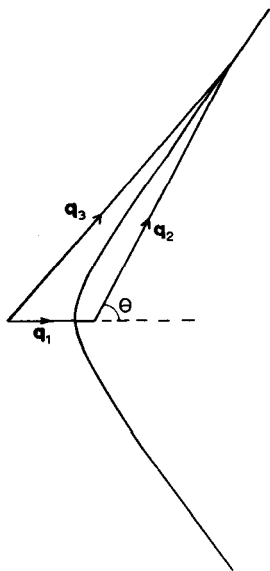
Fig. 4.4.

The rules which have been obtained above are for a non-dispersive medium with $\omega(q)$ proportional to q. Fortunately, when dispersion is accounted for, it is found that the dispersion curves are convex upwards so that the phase velocity of the higher frequency modes is reduced to a greater extent than the velocity of the lower frequency modes. The rules already derived are therefore still valid. The other major factor which has not been included in the theory is the anisotropy. This was accounted for in the work of HERRING [1954] which is now described. It is found that the rules are relaxed to a certain extent because there are points in q-space where two or more modes of wave vector q may have the same frequency. These are referred to as degenerate points. To illustrate the basic ideas surface contours at constant frequency are drawn in q-space. In order to see whether the process (a) of eq. (4.13) is possible put $\omega(q_1) = \omega_1$, $\omega(q_2) = \omega_2$, $\omega(q_3) = \omega_3 = \omega_1 + \omega_2$. In fig. 4.5 the curve labelled (a) represents the constant frequency surface ω_2 and curve (b) the contour of ω_3. If the interaction under consideration is allowed it must be possible to get from a point q_3 on curve (b) to a point q_2 on curve (a) by translation through a vector q_1. In other words if the origin of curve (b) is shifted by a vector q_1 with respect to the origin of curve (a), the intersection of the two curves will give the allowed values of q_2 and q_3. This is what has been done in figs. 4.6 and 4.7. The solid lines representing the constant frequency surfaces $\omega(q_2)$ are drawn with respect to the origin O_2 and the surfaces $\omega(q_3)$ with respect to the origin O_3. There will be three curves in each case corresponding to the different acoustic branches. Fig. 4.6 shows
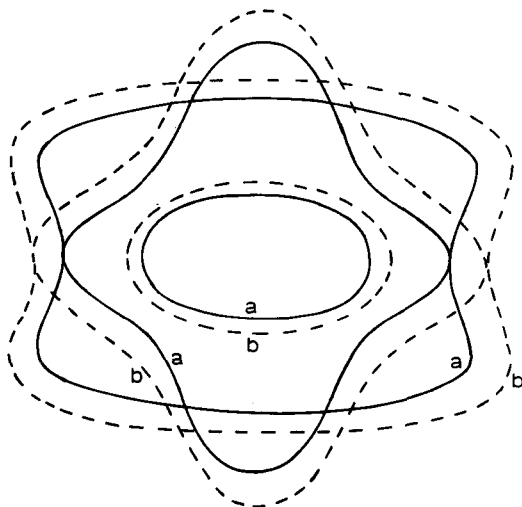
Fig. 4.5.
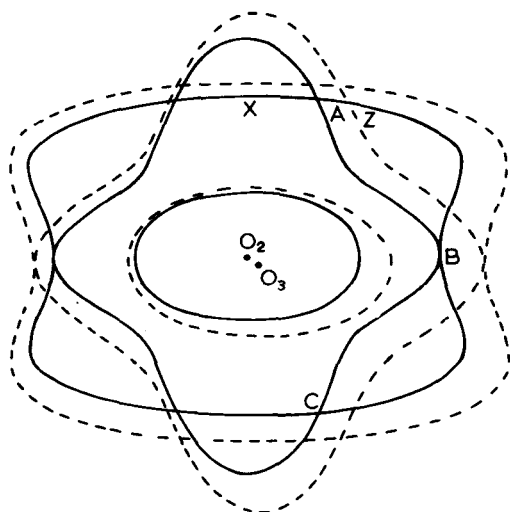
Fig. 4.6.
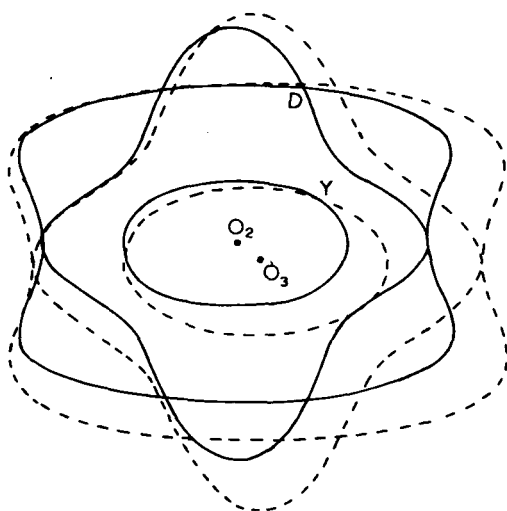
Fig. 4.7.

a typical set of curves when the mode q_1 is a longitudinal mode and fig. 4.7 the case when q_1 is a transverse mode. In both cases q_2 is considered to be large compared to q_1. The degenerate points which have been referred to above are the points such as A, B, C, D etc. where two branches of the $\omega(q_2)$ curve intersect or touch. These points may be single points or they may extend to form a line or a plane of

degeneracy. When q_1 is a transverse mode points such as Y occur where the dotted curve intersects the solid curve. This points corresponds to the allowed process (v) in which a transverse microwave phonon may decay. Referring now to fig. 4.6 it is seen that well away from any points of degeneracy process (iv) is forbidden since the solid curve does not intersect the dotted curve at any point such as X. However in the neighbourhood of a degeneracy, for example in the neighbourhood of A, there can be an interaction: the point Z. This point corresponds to a process in which a longitudinal microwave phonon can decay, therefore relaxing the selection rule obtained above. This process was not included in eq. (4.16) because there the transverse modes were degenerate. Denoting the non-degenerate transverse modes by t_1 and t_2 the process is of the form

$$\omega_\ell(q_1) + \omega_{t_1}(q_2) \rightarrow \omega_{t_2}(q_3).$$

Near a degenerate point where $v_{t_1} \approx v_{t_2}$ eq. (4.16) has a solution

$$\frac{\omega_2}{\omega_1} = \frac{v_{t_1}}{v_\ell} \frac{v_\ell - v_t \cos \theta}{v_{t_2} - v_{t_1}}.$$

Therefore by keeping near a degenerate point a longitudinal microwave phonon can relax to higher frequency phonons. The degree to which the process can take place is of course dependent on the number and type of the degeneracies that exist in q-space. In three-dimensional solids degenerate points or planes of degeneracy in q-space arise mainly because of crystal symmetry although they may occur accidentally. The extent to which the selection rules are relaxed thus depends on the crystal symmetry. An example of the importance of anisotropy is provided by the measurements of KING[1970] on quartz, discussed in §4.2.

2.2. *Transition rates for three-phonon interactions*

As has been seen the anharmonic term ϕ_3 in the Hamiltonian is responsible for processes in which two phonons suffer a collision and decay to create a third phonon or one phonon spontaneously decays into two. In this section the time dependence of the occupation number of a particular mode due to this interaction is calculated. To do this, ϕ_3 is first of all expressed in terms of creation and annihilation operators so that the non-zero matrix elements of the perturbation between the eigenstates of the system can be found. From eq. (4.8) it is found directly that

$$\phi_3 = -\frac{i}{3!} \frac{\hbar^{3/2}}{2^{3/2} N^{1/2}} \sum_{\substack{q_1 q_2 q_3 \\ j_1 j_2 j_3}} M_{j_1 j_2 j_3}^{q_1 q_2 q_3} A_{j_1 j_2 j_3}^{q_1 q_2 q_3}$$

where

$$M_{j_1 j_2 j_3}^{q_1 q_2 q_3} = \phi_{j_1 j_2 j_3}^{q_1 q_2 q_3} [\omega_{j_1}(q_1) \omega_{j_2}(q_2) \omega_{j_3}(q_3)]^{-1/2}$$

and

$$A_{j_1 j_2 j_3}^{q_1 q_2 q_3} = [a_{j_1}(-q_1) - a_{j_1}^*(q_1)][a_{j_2}(-q_2) - a_{j_2}^*(q_2)]$$
$$\times [a_{j_3}(-q_3) - a_{j_3}^*(q_3)].$$

ϕ_3, in addition to having matrix elements in which the occupation numbers of three different modes change, will also have non-zero elements connecting states differing in the occupation numbers of only two modes, for example when $(j_1 q_1) = (j_2 q_2)$. However the number of these matrix elements will be a factor N smaller and can be neglected. Therefore only processes in which all the j's and q's are different will be considered. The non-zero matrix elements of $A_{j_1 j_2 j_3}^{q_1 q_2 q_3}$ which satisfy the momentum conservation condition, eq. (4.10), are the following

$$\langle n_{j_1}(q_1) - 1, n_{j_2}(q_2) - 1, n_{j_3}(-q_3) + 1, \cdots | A | n_{j_1}(q_1), n_{j_2}(q_2), n_{j_3}(-q_3), \cdots \rangle$$
$$= -\{n_{j_1}(q_1) n_{j_2}(q_2)[n_{j_3}(-q_3) + 1]\}^{1/2}$$

$$\langle n_{j_1}(q_1) - 1, n_{j_2}(-q_2) + 1, n_{j_3}(q_3) - 1, \cdots | A | n_{j_1}(q_1), n_{j_2}(-q_2), n_{j_3}(q_3), \cdots \rangle$$
$$= -\{n_{j_1}(q_1)[n_{j_2}(-q_2) + 1] n_{j_3}(q_3)\}^{1/2}$$

$$\langle n_{j_1}(q_1) - 1, n_{j_2}(-q_2) + 1, n_{j_3}(-q_3) + 1, \cdots | A | n_{j_1}(q_1), n_{j_2}(-q_2), n_{j_3}(-q_3), \cdots \rangle$$
$$= +\{n_{j_1}(q_1)[n_{j_2}(-q_2) + 1][n_{j_3}(-q_3) + 1]\}^{1/2}$$

$$\langle n_{j_1}(q_1) + 1, n_{j_2}(-q_2) - 1, n_{j_3}(-q_3) - 1, \cdots | A | n_{j_1}(q_1), n_{j_2}(-q_2), n_{j_3}(-q_3), \cdots \rangle$$
$$= -\{[n_{j_1}(q_1) + 1] n_{j_2}(-q_2) n_{j_3}(-q_3)\}^{1/2}$$

$$\langle n_{j_1}(q_1) + 1, n_{j_2}(-q_2) - 1, n_{j_3}(q_3) + 1, \cdots | A | n_{j_1}(q_1), n_{j_2}(-q_2), n_{j_3}(q_3), \cdots \rangle$$
$$= +\{[n_{j_1}(q_1) + 1] n_{j_2}(-q_2)[n_{j_3}(q_3) + 1]\}^{1/2}$$

$$\langle n_{j_1}(q_1) + 1, n_{j_2}(q_2) + 1, n_{j_3}(-q_3) - 1, \cdots | A | n_{j_1}(q_1), n_{j_2}(q_2), n_{j_3}(-q_3), \cdots \rangle$$
$$= +\{[n_{j_1}(q_1) + 1][n_{j_2}(q_2) + 1] n_{j_3}(-q_3)\}^{1/2}$$

with $q_1 + q_2 + q_3 + G = 0$. In order to calculate the rate at which ϕ_3 may create or destroy a phonon in the mode $(j_1 q_1)$ use is made of standard lowest-order time-dependent perturbation theory, eq. (4.11). It is desirable to remove the energy denominator in this expression by introducing a delta function. This standard procedure in quantum mechanics is outlined in appendix 3 for the benefit of those not familiar

with it. The net rate of change of $n_{j_1}(q_1)$ will be the difference between reaction rates for the process going in the two directions. Making use of eq. (A3.6) it is found that the net transition probability per unit time for the mode $(j_1 q_1)$ is

$$
\begin{aligned}
\dot{n}(q_1) = -\frac{\pi\hbar}{4N} \sum_{q_2 q_3} |M_{j_1 j_2 j_3}^{q_1 q_2 q_3}|^2 \{ & [n_{j_2}(-q_2)n_{j_3}(-q_3) - n_{j_1}(q_1)n_{j_2}(-q_2) \\
& - n_{j_1}(q_1)n_{j_3}(-q_3) - n_{j_1}(q_1)]\delta(\omega_{j_1}(q_1) - \omega_{j_2}(q_2) - \omega_{j_3}(q_3)) \\
& + [n_{j_1}(q_1)n_{j_2}(-q_2) + n_{j_2}(-q_2)n_{j_3}(q_3) + n_{j_2}(-q_2) \\
& - n_{j_1}(q_1)n_{j_3}(q_3)]\delta(\omega_{j_1}(q_1) - \omega_{j_2}(q_2) + \omega_{j_3}(q_3)) \\
& + [n_{j_1}(q_1)n_{j_3}(-q_3) + n_{j_2}(q_2)n_{j_3}(-q_3) + n_{j_3}(-q_3) \\
& - n_{j_1}(q_1)n_{j_2}(q_2)]\delta(\omega_{j_1}(q_1) + \omega_{j_2}(q_2) - \omega_{j_3}(q_3)) \}.
\end{aligned}
\tag{4.19}
$$

If the n's are replaced by their thermal equilibrium values,

$$
n_j^0(q) = \{\exp[\hbar\omega_j(q)/KT] - 1\}^{-1}.
$$

the transition rate reduces to zero because of the delta functions, as clearly it must by definition of equilibrium. A finite probability will occur however if some of the n's deviate from equilibrium, as will be illustrated in the following sections.

2.3. *Attenuation of ultrasound in the region $\Omega\tau \gg 1$*

In the introduction to this chapter it was explained that there were two regions to be discussed depending upon the relative magnitude of the frequency of the ultrasound and the mean free path of the phonons excited in the crystal. The region which will first be discussed is where $\Omega\tau$ is greater than unity. This is the low temperature region where the phonon mean free path is greater than the ultrasonic wavelength. For most materials this is below 50 K at ultrasonic frequencies of 1 GHz. The model which will be adopted is that of an isotropic medium in which dispersion may be neglected. Calculations along this line were first carried out by LANDAU and RUMER [1937] and by SLONIMSKII [1937].

It has been shown, eq. (4.6) that for this model the third-order terms in the energy density are

$$
\begin{aligned}
(\tfrac{1}{2}c_{12} + 3c_{155} - 6c_{456})\zeta_{ii}\zeta_{jk}^2 + (\tfrac{1}{2}c_{11} - \tfrac{1}{2}c_{12} + 6c_{456})\zeta_{ij}\zeta_{ki}\zeta_{kj} \\
+ (3c_{155} - 6c_{456})\zeta_{ii}\zeta_{jk}\zeta_{kj} + (c_{111} - 6c_{155} + 4c_{456})\zeta_{ii}\zeta_{jj}\zeta_{kk} + 2c_{456}\zeta_{ij}\zeta_{jk}\zeta_{ki}.
\end{aligned}
\tag{4.20}
$$

As was done in the case of the discrete lattice the elastic waves may

be quantized by expressing the particle displacement in the form

$$u_\alpha(x) = i \sum_q (\hbar/2\rho V\omega(q))^{1/2} e_\alpha(q) \, e^{iq \cdot x} [a(q) - a^*(-q)]. \quad (4.21)$$

Substituting this expression into eq. (4.20) it is noted that each ζ_{ij} will give rise to a factor $e_i q_j$. As explained above the processes of interest are those where the three phonons that interfere come from different modes; hence the only terms that will be retained will be those in which the three q's are different. In this case there is no difficulty with the non-commutation of the a's. Direct substitution of eq. (4.21) gives the following expression for the energy density*

$$
\begin{aligned}
W = -i \sum_{q_1 q_2 q_3} &(\hbar/2M)^{3/2} (\omega(q_1)\omega(q_2)\omega(q_3))^{-1/2} [a(q_1) - a^*(-q_1)] \\
&\times [a(q_2) - a^*(-q_2)][a(q_3) - a^*(-q_3)]\{\exp[i(q_1 + q_2 + q_3) \cdot x]\} \\
&\times \{A_1[(e_1 \cdot q_1)(e_2 \cdot e_3)(q_2 \cdot q_3) + (e_2 \cdot q_2)(e_1 \cdot e_3)(q_1 \cdot q_3) \\
&+ (e_3 \cdot q_3)(e_1 \cdot e_2)(q_1 \cdot q_2)] \\
&+ A_2[(e_1 \cdot q_2)(q_1 \cdot q_3)(e_2 \cdot e_3) + (e_2 \cdot q_3)(q_1 \cdot q_2)(e_1 \cdot e_3) \\
&+ (e_3 \cdot q_1)(q_2 \cdot q_3)(e_1 \cdot e_2) + (e_1 \cdot q_3)(q_1 \cdot q_2)(e_2 \cdot e_3) \\
&+ (e_2 \cdot q_1)(q_2 \cdot q_3)(e_1 \cdot e_3) + (e_3 \cdot q_2)(q_1 \cdot q_3)(e_1 \cdot e_2)] \\
&+ A_3[(e_1 \cdot q_3)(e_2 \cdot q_1)(e_3 \cdot q_2) + (e_1 \cdot q_2)(e_2 \cdot q_3)(e_3 \cdot q_1)] \\
&+ A_4[(e_1 \cdot q_1)(e_2 \cdot q_3)(e_3 \cdot q_2) + (e_2 \cdot q_2)(e_1 \cdot q_3)(e_3 \cdot q_1) \\
&+ (e_3 \cdot q_3)(e_1 \cdot q_2)(e_2 \cdot q_1)] + A_5[(e_1 \cdot q_1)(e_2 \cdot q_2)(e_3 \cdot q_3)]\} \quad (4.22)
\end{aligned}
$$

where

$$A_1 = (c_{12} + 6c_{155} - 12c_{456}); \quad A_2 = \tfrac{1}{2}(c_{11} - c_{12} + 12c_{456})$$
$$A_3 = 6c_{456}; \quad A_4 = 6(c_{155} - 2c_{456})$$
$$A_5 = 6(c_{111} - 6c_{155} + 4c_{456})$$

It has been seen that one of the processes of interest is process (v), eq. (4.15). This was the one considered by Landau and Rumer, $\omega_t(q_1) + \omega_\ell(q_2) \to \omega_\ell(q_3)$. Let us single out that part of the energy function which gives rise to this interaction. The required part will have $e_1 \cdot q_1 = 0$, $e_2 \cdot q_2 = q_2$, $e_3 \cdot q_3 = q_3$ and must contain a creation operator for the mode q_3 and annihilation operators for modes q_1 and q_2. The required perturbation is

$$
\begin{aligned}
V_{t+\ell \to \ell} = -i \sum_{q_1 q_2} &(\hbar/2M)^{3/2} V[\omega(q_1)\omega(q_2)\omega(q_3)]^{-1/2} \\
&\times a(q_1)a(q_2)a^*(-q_3)\{(A_1 + A_4)[q_2(e_1 \cdot q_3)(q_1 \cdot q_3)/q_3 \\
&+ q_3(e_1 \cdot q_2)(q_1 \cdot q_2)/q_2] + (3A_2 + A_3)[(e_1 \cdot q_2)(q_1 \cdot q_3) \\
&\times (q_2 \cdot q_3)/q_2 q_3 + (e_1 \cdot q_3)(q_1 \cdot q_2)(q_2 \cdot q_3)/q_2 q_3]\}.
\end{aligned}
$$

* In this section we shall use the abbreviated notation e_i for $e(q_i)$.

The volume V arises from the integration of the energy density over the volume of the material. Denoting the factor in the curly brackets by F and using the relevant part of the eq. (4.19) it follows that

$$\dot{n}(q_1)_{l+l'\to l'} = -\frac{\pi\hbar}{4M^3}V^2\sum_{q_2q_3}F^2[\omega(q_1)\omega(q_2)\omega(q_3)]^{-1}[n(q_1)n(-q_3)$$
$$+ n(q_2)n(-q_3) + n(-q_3) - n(q_1)n(q_2)]$$
$$\times \delta(\omega(q_1)+\omega(q_2)-\omega(q_3)).$$

As has already been remarked if all the n's have their thermal equilibrium value, $\dot{n}(q_1)$ reduces to zero. In this work it will be assumed that $n(q_2)$ and $n(-q_3)$ are kept in thermal equilibrium by the presence of the thermal phonons but that $n(q_1)$ is equal to $n^0(q_1)+\Delta n(q_1)$, $\Delta n(q_1)$ being a small deviation from equilibrium. It then follows that

$$\dot{n}(q_1)_{l+l'\to l'} = -\frac{\pi\hbar}{4M^3}V^2\sum_{q_2q_3}F^2[\omega(q_1)\omega(q_2)\omega(q_3)]^{-1}[n(q_1)-n^0(q_1)]$$
$$\times [n^0(-q_3)-n^0(q_2)]\delta(\omega(q_1)+\omega(q_2)-\omega(q_3)). \quad (4.23)$$

Now if q_2 and q_3 are high energy thermal phonons and q_1 is a low frequency microwave phonon the conservation of energy and momentum conditions imply that $q_2 \approx q_3$ and $\omega(q_2) \approx \omega(q_3)$. Because of this

$$n^0(-q_3) - n^0(q_2) = \{\exp[\hbar(\omega(q_2)+\omega(q_1))/KT]-1\}^{-1}$$
$$- \{\exp[\hbar\omega(q_2)/KT]-1\}^{-1}$$
$$\approx \omega(q_1)\frac{\partial n^0(q_2)}{\partial\omega(q_2)}. \quad (4.24)$$

Therefore

$$\frac{\dot{n}(q_1)}{\Delta n(q_1)} = -\frac{\pi\hbar V^2}{4M^3}\sum_{q\cdot q}\frac{F^2}{\omega(q_2)\omega(q_3)}\frac{\partial n^0(q_2)}{\partial\omega(q_2)}\delta(v_tq_1+v_{l'}q_2-v_{l'}q_3)$$

or because $q_2 \approx q_3$, $q_3 = q_2 + q_1\cos\theta$

$$\frac{\dot{n}(q_1)}{\Delta n(q_1)} = -\frac{\pi\hbar V^2}{4M^3}\sum_{q_2q_3}\frac{F^2}{\omega(q_2)\omega(q_3)}\frac{\partial n^0(q_2)}{\partial\omega(q_2)}\delta(v_tq_1-v_{l'}q_1\cos\theta).$$

It is convenient to introduce cartesian coordinates such that q_1 and e_1 are respectively parallel to the z- and x-axes. If an approximation is made by replacing q_3 by q_2 the factor F^2 becomes

$$\approx [2(A_1+A_4)+2(3A_2+A_3)]^2 q_2^4 q_1^2\cos^2\theta\sin^2\theta\cos^2\phi$$

where θ and ϕ are the polar angles of q_2 with respect to the chosen axes. In this way it is found, on replacing the sum over q_2 by an integral, that

$$\frac{\dot{n}(q_1)}{\Delta n(q_1)} = -\frac{\pi\hbar V^2}{4M^3}\left(\frac{V}{8\pi^3}\right)\int_0^{\omega_D}\int_0^{\pi}\int_0^{2\pi}\frac{[2(A_1+A_4)+2(3A_2+A_3)]^2}{\omega^2(q_2)}$$

$$\times\frac{\partial n^0(q_2)}{\partial\omega(q_2)}\frac{1}{v_\ell q_1}\delta(v_t/v_\ell-\cos\theta)$$

$$\times q_2^6 q_1^2\cos^2\theta\sin^3\theta\cos^2\phi\,d\phi\,d\theta\,dq_2 \tag{4.25}$$

where ω_D is the Debye cut-off frequency. After taking into account the delta function this gives

$$-\frac{\hbar\omega(q_1)\pi}{32\pi^2\rho^3 v_t v_\ell^8}[2(A_1+A_4)+2(3A_2+A_3)]^2\frac{v_t^2}{v_\ell^2}\left[1-\frac{v_t^2}{v_\ell^2}\right]$$

$$\times\int_0^{\omega_D}\omega^4(q_2)\frac{\partial n^0(q_2)}{\partial\omega(q_2)}\,d\omega(q_2).$$

For temperatures well below the Debye temperature the limit of integration may be extended to infinity because of the exponential factor in the denominator of the integrand. Finally using the result that

$$\int_0^{\infty}x^n\exp(\alpha x)/[\exp(\alpha x)-1]^2\,dx = n!(\alpha)^{-(n+1)}\epsilon(n)$$

where ϵ is the Riemann zeta function it follows that the right-hand side is

$$\frac{\hbar\omega(q_1)\pi}{32\pi^2\rho^3 v_t v_\ell^8}[2(A_1+A_4)+2(3A_2+A_3)]^2\frac{v_t^2}{v_\ell^2}\left[1-\frac{v_t^2}{v_\ell^2}\right]4!\left(\frac{KT}{\hbar}\right)^4\epsilon(4).$$

If a relaxation time defined by $\tau_{t+\ell\to\ell}^{-1}=\dot{n}(q_1)/\Delta n(q_1)$ is introduced it is seen that, for the process under consideration, it is inversely proportional to the frequency $\omega(q_1)$ and to the fourth power of the absolute temperature.

A comparison must now be made between the relaxation time for this process and that obtained for the processes (i) to (iii) and the processes (iv) and (vi). As an example process (iv) will be considered. This was originally calculated by SLONIMSKII [1937], but as pointed out by ORBACH [1960], the temperature behaviour of $\tau_{\ell\cdot t\to\ell}$ which was obtained was in fact incorrect. The relaxation time of this process will again be governed by an equation similar to that of eq. (4.23) the only difference being in the geometric factor F^2. The new expression is found by putting $e_1\cdot q_1=q_1$, $e_2\cdot q_2=0$, $e_3\cdot q_3=q_3$ in eq. (4.22). The main difference in the result obtained for this process with that obtained above arises because of the need to satisfy the conservation of energy and momentum conditions. As already has been shown, pro-

cess (iv) requires that $q_2 \approx q_1 \approx q_3$. This means that for $\omega(q_1) \ll KT$ the factor $n^0(-q_3) - n^0(q_2)$ now approximates to

$$-KT\omega(q_1)/[\hbar\omega(q_2)(\omega(q_1)+\omega(q_2))].$$

Since $\omega(q_1) \approx \omega(q_2) \approx \omega(q_3)$ the factor F^2 which involves $(q_1 q_2 q_3)^2$ will under these conditions be roughly proportional to $\omega^6(q_1)$. The factor $[\omega(q_1)\omega(q_2)\omega(q_3)]^{-1}$ clearly goes as $\omega^{-3}(q_1)$. The factor $n^0(-q_3) - n^0(q_2)$ is proportional to $KT/\hbar\omega(q_1)$ and finally there will be an additional $\omega^2(q_1)$ coming from the density of states when the summation is replaced by an integral. The net result is that $\tau^{-1}_{\ell'+t \to \ell}$ is proportional to $KT\omega^4(q_1)/\hbar$ in contrast to $\omega(q_1)(KT/\hbar)^4$ for $\tau^{-1}_{t+t \to \ell}$. Thus the relaxation time is increased by a factor $[KT/\hbar\omega(q_1)]^3$. In a similar way all the other processes can be considered and Orbach has found that they all have relaxation times that go as $\hbar/KT\omega^4(q_1)$.

It is noted that in all the processes considered to date the sum of the powers of $\omega(q_1)$ and $KT/\hbar$ in τ^{-1} is five. Therefore in general for three-phonon processes well below the Debye temperature and for wave vectors in the acoustic range, $\tau^{-1} \propto \omega^a(KT/\hbar)^{5-a}$ a fact which was first pointed out by HERRING[1954]. In the processes considered, a was 1 or 4 but other values are possible when anisotropy and a possible degeneracy of modes are accounted for. As was mentioned in §2.1 Herring pointed out that this is because the selection rules are relieved to a certain extent. For transverse waves a is normally 1 as was found above but for longitudinal waves a is 2 for crystals of the highest symmetry, 3 and perhaps 4 for those of lowest symmetry. The detailed results obtained by Herring for various symmetries are given in table 4.1. These asymptotic values of a are estimated by Herring to be valid in the case of $a = 2$ and 3 for $\hbar\omega(q_1)$ below 0.15 KT and for $a = 4$ in the range less than 0.03 KT.

It will be seen later, in §2.7, that for four-phonon processes there will be an extra power of ω in the square of the matrix element of the perturbation and an extra ω^3 coming from the additional summation over phase space; in this case $\tau^{-1} \propto \omega^a(KT/\hbar)^{9-a}$.

So far the only cases to be considered have been those for which the energy of the microwave phonon is very much less than KT. Recently, it has been possible to observe the lifetime of phonons with $\hbar\omega \gg KT$. Experiments which produce these high energy phonons via non-radiative transitions in paramagnetic salts have shown that at least some of these phonons have anomalously long lifetimes. A theoretical investigation of the lifetime of these phonons has been carried out by ORBACH and VREDEVOE[1964]. It might be expected that these high energy phonons would decay spontaneously via a three-phonon process into two phonons each of energy of the order of $\frac{1}{2}\hbar\omega$. However by referring

TABLE 4.1

Asymptotic values of a for longitudinal acoustic modes in various crystal classes

System	Class	Dominant value of a for most directions	
		With dispersion	Without dispersion
Orthorhombic			
Monoclinic		4	3 or 4
Triclinic			
Tetragonal	C_4	4	2
	S_4	2	2
	C_{4h}	2	2
	C_{4v}	2	2
	V_d	2	2
	D_4	4	2
	D_{4h}	2	2
Trigonal	C_3	4	3
	C_{3i}	3	3
	C_{3v}	3	3
	D_3	4	3
	D_{3d}	3	3
Hexagonal	C_{3h}	4	3
	C_6	4	2
	C_{6h}	2	2
	D_{3h}	3	3
	C_{6v}	2	2
	D_6	4	2
	D_{6h}	2	2
Cubic	T	4	2
	T_h	3	2
	T_d	2	2
	O	4	2
	O_h	2	2

to the selection rules that are given in eq. (4.14) it is seen that only a longitudinal phonon can decay in this way. How then can transverse phonons decay? One possibility is that they could combine with a thermal phonon through processes (v) and (vi) of eq. (4.15) to give a high frequency longitudinal phonon which then decays rapidly via the process of eq. (4.14). Orbach and Vredevoe have calculated the relaxation time for this mechanism in the case of an isotropic medium without dispersion and have found that the lifetimes of the high energy transverse phonons are in fact very long. To see the reason for this, suppose that q_1 is the high energy phonon with energy $\hbar\omega(q_1)$ and q_2 is a thermal phonon with energy of the order of KT. If it is assumed that

$\hbar\omega(q_1) \gg KT$ this implies that $\omega(q_1)/\omega(q_2) \gg 1$. However it is evident from eq. (4.18) that this is not possible for any angle θ between q_1 and q_2 if the interaction is via process (v) of eq. (4.15). A similar situation is also found in the case of process (vi). The decay of a high energy transverse phonon via the three-phonon interactions (v) and (vi) necessitates the presence of longitudinal or transverse phonons of energy of the order of $\hbar\omega(q_1)$. One would expect this to reduce the relaxation rate by a factor exp $[\hbar\omega(q_1)/KT]$ below that which would be possible if thermal phonons could participate in the interaction. Orbach and Vredevoe have calculated the relaxation times in detail and find the following results:

for process, eq. (4.14) $\tau_{\ell \to \ell + t} \propto \omega^{-5}(q_1)$ (4.26)
for process, eq. (4.15)

$$\tau_{t + \ell \leftrightarrow \ell} \propto \omega(q_1)^{-3} \left(\frac{KT}{\hbar}\right)^{-2} \exp\left[\frac{\hbar\omega(q_1)}{2KT}\left(\frac{v_\ell - v_t}{v_t}\right)\right] \qquad (4.27)$$

$$\tau_{t + t \leftrightarrow \ell} \propto \omega(q_1)^{-5} \exp\left[\frac{\hbar\omega(q_1)}{KT}\left(\frac{v_\ell - v_t}{v_\ell + v_t}\right)\right]. \qquad (4.28)$$

The constants of proportionality, which need not be given in detail, contain simple products of various elastic constants and velocities. They have estimated, using representative values for the constants, that eq. (4.26) gives a lifetime of 5×10^{-8} sec for a longitudinal phonon of energy 30 cm^{-1}. For a transverse phonon of the same energy at a temperature of 1 K, eq. (4.28) gives 3.8×10^{-2} sec, that is a relaxation time six orders of magnitude greater.

The discussion given above is based on an isotropic continuum model. If the energy – momentum relation of the lowest branch is not isotropic, then three-phonon processes of the type t → t + t are allowed, Maris[1965]. Such splitting processes may take place only within some parts of the Brillouin zone and are characterized by a strong anisotropy and temperature independent decay.

2.4. Umklapp processes

The discussion until now has been centred on normal processes where the reciprocal lattice vector G of eq. (4.13) is zero. In this section this restriction will be lifted and the effect of the Umklapp processes on the absorption of ultrasound considered. For an isotropic medium the selection rules of eqs. (4.14) and (4.15) for three-phonon processes are still valid. As an example of the difference that U-processes can make to the relaxation time process (v) of eq. (4.15) which has already been studied in some depth in §2.3 will be reconsidered. In the presence of Umklapp processes the conservation laws become

$$\omega_t(q_1) + \omega_\ell(q_2) \rightarrow \omega_\ell(q_3)$$

$$q_1 + q_2 \rightarrow q_3 + G$$

(4.29)

Again the decay of a microwave phonon whose energy is small compared to KT will be examined which means we are interested in the situation where $|q_1|$ and consequently $\omega(q_1)$ are small. If $\omega(q_1)$ is small the first conservation condition of eq. (4.29) implies that $\omega_\ell(q_2) \approx \omega_\ell(q_3)$ and hence to satisfy the second requirement the wave vectors of the phonons must be such that $q_2 \approx -q_3 \approx \frac{1}{2}G$. It was seen when calculating the relaxation time due to normal processes that a factor $\omega(q_1)\partial n^0(q_2)/\partial\omega(q_2)$, eq. (4.24) occurred. If $|q_2| \approx \frac{1}{2}G$ this factor becomes equal to $-(\hbar\omega(q_1)/KT)\exp(\hbar x)/[\exp(\hbar x)-1]^2$ where $x = v_\ell G/2KT$. Now the radius of the Debye sphere in q-space for an isotropic medium is $q_m = (6\pi^2 N/V)^{1/3}$ which is of the order of half a reciprocal lattice vector. Therefore for temperatures well below the Debye temperature the above factor will approximate to $(\hbar\omega(q_1)/KT)x\exp(-\hbar x)$. The importance of U-processes on the attenuation of microwave phonons at low temperatures is consequently relatively small compared to that of the normal processes. Calculations of the relaxation times for the processes of eq. (4.15) have been made by ORBACH[1960] who gives the following results

process (iv) $\dfrac{1}{\tau_u} \propto \dfrac{\omega(q_1)^2}{KT}\exp\left[-\dfrac{\hbar G v_t v_\ell}{KT(v_\ell + v_t)}\right],$

process (v) $\dfrac{1}{\tau_u} \propto \dfrac{\omega^2(q_1)}{KT}\exp\left[-\dfrac{\hbar G v_\ell}{2KT}\right],$ (4.30)

process (vi) $\dfrac{1}{\tau_u} \propto \dfrac{\omega^2(q_1)}{KT}\exp\left[-\dfrac{\hbar G v_t v_\ell}{KT(v_\ell + v_t)}\right].$

Transverse and longitudinal microwave phonons have the same general form for their relaxation times although processes (iv) and (vi) might dominate at low temperatures due to the different factor in the exponential.

2.5. Collinear longitudinal phonons

As demonstrated in §2.1, for a medium without dispersion the process $\ell + \ell \rightarrow \ell$ is possible only in the special case of the interaction between three collinear phonons, that is, for three phonons whose q-vectors are parallel. If the conservation laws of energy and momentum are to be strictly enforced this is the only situation where the process is allowed and therefore the number of phonons that can participate in the process is severely limited. However, by relaxing the condition for the exact conservation of energy, CICCARELLO and DRANSFELD[1964]

have shown that a longitudinal acoustic wave can in fact interact in three-phonon processes with almost as many thermal phonons as a transverse wave can. Consequently, they find under certain conditions that the absorption of longitudinal waves by three-phonon processes is of a similar magnitude to the absorption of transverse waves. Experimental evidence for this was obtained in the work of NAVA et al. [1964].

To relax the energy conservation condition a small quantity Δ may be added to $\omega(q_3)$. The new requirements are that

$$\omega(q_1) + \omega(q_2) = \omega(q_3) + \Delta \qquad q_1 + q_2 = q_3.$$

Δ may be regarded as an inverse relaxation time which causes a fuzziness in the frequency surface $\omega(q_3)$. The angle between q_1 and q_2 will again be denoted by θ and as before it is assumed that $\omega(q_1)$ is much smaller than $\omega(q_2)$. Then in the place of eq. (4.18) it is found that for process (v)

$$\cos\theta = \frac{v_t}{v_\ell}\left\{1 - \frac{\omega(q_1)}{2\omega(q_2)}\frac{v_\ell^2}{v_t^2} + \frac{\omega(q_1)}{2\omega(q_2)} - \Delta\left[\frac{1}{\omega(q_1)} + \frac{1}{\omega(q_2)}\right] + \frac{\Delta^2}{2\omega(q_1)\omega(q_2)}\right\}.$$

(4.31)

In the absence of Δ, $\cos\theta \equiv \cos\theta_0 \approx v_t/v_\ell$ for $\omega(q_1) \ll \omega(q_2)$

(4.32)

in the presence of Δ, $\theta_{max} - \theta_{min} \equiv \delta\theta \approx \frac{2|\Delta|}{\omega(q_1)}\cot\theta_0$.

The corresponding equation for the process $\ell + \ell \to \ell$ is

$$\cos\theta = 1 - \Delta\left[\frac{1}{\omega(q_1)} + \frac{1}{\omega(q_2)}\right] + \frac{\Delta^2}{2\omega(q_1)\omega(q_2)} \qquad (4.33)$$

which implies that in the absence of the energy spread Δ, the wave vectors of the phonons that participate must be collinear. If the necessity of exact conservation of energy is relaxed it is seen that Δ must be positive since the cosine of the angle θ must be less than unity. In the situation where $\omega(q_2)$ is much greater than $\omega(q_1)$

$$\cos\theta_{max} \approx 1 - \tfrac{1}{2}\theta_{max}^2 \approx 1 - |\Delta|/\omega(q_1).$$

Therefore for this process $(\tfrac{1}{2}\delta\theta)^2 = |\Delta|/\omega(q_1)$. On referring to fig. 4.8 it is seen that the three-phonon process governed by eq. (4.31) takes place if the end-point of the vector q_3 lies on the arc P. By considering the diagram rotated about q_1 it is evident that the relative solid angle containing the end-point of q_3 is

$$\frac{2\pi\sin\theta_0}{4\pi}\frac{2\cos\theta_0}{\sin\theta_0}\frac{|\Delta|}{\omega(q_1)} = \frac{|\Delta|}{\omega(q_1)}\cos\theta_0.$$

This is to be compared with the corresponding result, $\tfrac{1}{2}|\Delta|/\omega(q_1)$
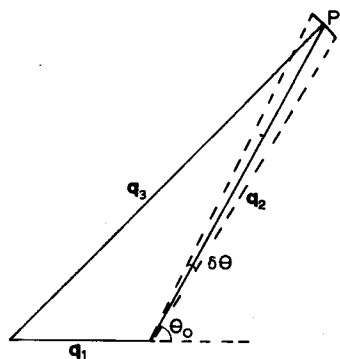
Fig. 4.8.

which would be obtained for the process $\ell + \ell \rightarrow \ell$. These two solid angles are much the same for any lifetime $1/\Delta$. In the analysis it has been assumed that Δ is less than $\omega(q_1)$ and that dispersion may be neglected. Nava *et al.* have shown that the neglect of dispersion is permissible provided that $\omega(q_1)/\Delta \lesssim 3\pi(\theta_D/T)^2$, where θ_D is the Debye temperature. Using the method of Landau and Rumer, which was outlined in §2.3 in the case of transverse waves, Ciccarello and Dransfeld find that the absorption of longitudinal waves due to their interaction with collinear thermal phonons is proportional to ωT^4, as was the case for process (v) of eq. (4.15), and is also of the same order of magnitude.

2.6. *Finite lifetime effects*

In the calculation of the relaxation time of the three-phonon process $q_1 + q_2 \rightarrow q_3$, use was made of the formula, eq. (A3.6), of time dependent perturbation theory outlined in appendix 3. The delta function in the expression leads to the requirement of the conservation of energy. Eq. (A3.6) can only be used however if the energy deficit between the initial and final states for the process is very much greater than the energy uncertainty of the phonons with wave vector q_2 and q_3. If this condition is not fulfilled the lifetime of the phonons in modes q_2 and q_3 must be accounted for in the theory. A fuller treatment of the three-phonon process which attempted to incorporate the influence of the finite lifetimes of the other phonons was first attempted in detail by SIMONS[1964]. In his method, instead of using eq. (A3.6) he made use of the more exact expression given by eq. (A3.4). In this the transition rate is not constant but is given by $2|V_{mm'}|^2 \sin(\Delta_E t/\hbar)/\hbar\Delta_E$ which is dependent upon t, the duration of the process. In this expression the energy difference between the initial and final states, that is, the energy

deficit, has been written as Δ_E. Since the case of interest is where q_1 is very much smaller than q_2 and q_3 Simons argues that the time to be used is the time taken for the phonon of wave vector q_2 to be created by other interactions, since the relaxation time of the mode q_1 will be much greater than that of the modes q_2 or q_3. Because all the phonons of wave vector q_2 are not created at the same time, he argues that $\sin \Delta_E t/\hbar$ should be averaged over t from 0 to ∞ after having been weighted by a factor $\exp(-t/\tau_2)$, this factor being the probability that the phonon in mode q_2 has been present for a time t. τ_2 is the life-time of this phonon. Replacing $\sin \Delta_E t/\hbar$ by this average value it follows that the transition rate is given by

$$\frac{dT}{dt} = \frac{2|V_{mm'}|^2}{\hbar \Delta_E} \overline{\sin(\Delta_E t/\hbar)} = \frac{2|V_{mm'}|^2}{\hbar \Delta_E} \frac{\int_0^\infty e^{-t/\tau_2} \sin(\Delta_E t/\hbar)\, dt}{\int_0^\infty e^{-t/\tau_2} dt}$$

$$= \frac{2|V_{mm'}|^2}{\hbar^2} \frac{\tau_2}{1 + \Delta_E^2 \tau_2^2/\hbar^2}. \qquad (4.34)$$

Let us now use this expression to calculate the probability of occur-rence of the process $\ell + \ell' \to \ell'$. As already seen, this process can occur under certain circumstances in the case of nearly mutually collinear phonons. $\omega(q_1)$, q_1 will refer to the frequency and wave vector of the sound wave and the corresponding quantities for the thermal phonons will be denoted by $\omega(q_2)$, q_2 and $\omega(q_3)$, q_3. Since the phonons of interest are those for which q_2 and q_3 are much greater than q_1 and the angle θ between q_1 and q_2 is small it may be assumed that q_2 is parallel to q_3. In the case of an isotropic solid the relevant expression representing the interaction can be obtained from eq. (4.22). For the process defined above, the curly bracket in the expression reduces to $Fq_1 q_2 q_3$ where F is $[c_{12} + 6c_{111} - 24c_{155}] + \cos^2 \theta [24c_{155} + 3c_{11}]$. Following the method of §2.3 it is found on replacing the delta function by the expression in eq. (4.34) that

$$\frac{1}{\tau_{\ell+\ell'\to\ell'}} = \left(\frac{\hbar}{2M}\right)^3 \frac{V^3}{(2\pi)^3} 2\pi \int \int \frac{2\omega(q_1) q_2^2 \beta \cos \theta}{v_1^4 \beta^2}$$

$$\times \frac{F^2 \tau_2 [\beta \omega(q_1) \cos \theta \, (\partial n^0(q_2)/\partial \omega(q_2)) q_2^2 \, dq_2 \, d \cos \theta]}{\hbar^2 [1 + \tau_2^2 \omega^2(q_1)(1 - \beta \cos \theta)^2]}.$$

Here use has been made of the fact that $\omega(q_3) - \omega(q_2) = \beta \omega(q_1) \cos \theta$ where $\beta = v_2/v_1 \approx v_3/v_1$ is the ratio of the velocity of the thermal phonons to those of the acoustic wave. The expression is valid under the assumption made that q_2 and q_3 were very much greater than q_1. The integral over q_2 may be readily evaluated and gives

$$\frac{1}{\tau_{\ell+\ell\to\ell}} = \frac{\hbar\pi^2\omega^2(q_1)\tau}{60\rho^3 v_1^9\beta^5}\left(\frac{KT}{\hbar}\right)^4 \int_{-1}^{+1}\frac{F^2\cos^2\theta\,\mathrm{d}\cos\theta}{1+\omega^2(q_1)\tau^2(1-\beta\cos\theta)^2}.$$

The frequency dependence of τ_2 is not known but as $q_2^4\partial n(q_2)/\partial\omega(q_2)$ has a maximum of $\omega(q_2) \sim 3KT/\hbar$ we approximate by replacing it by its value τ at this frequency and withdrawing it outside the integral. The remaining integral over $\cos\theta$ can then be evaluated since it is of the standard form

$$\int\frac{Ax+B}{ax^2+2bx+c}\,\mathrm{d}x = \frac{A}{2a}\log\,(ax^2+2bx+c) + \frac{aB-bA}{a(ac-b^2)^{1/2}}$$

$$\times\arctan\frac{(ax+b)}{(ac-b^2)^{1/2}}\quad\text{when } b^2-ac<0.$$

For $\omega(q_1)\tau \gg 1$ the result may be written in a power series of $1/\omega(q_1)\tau$ of which the leading term is

$$\tau_{\ell+\ell\to\ell}^{-1} = \frac{\hbar\pi^2\omega(q_1)\tau}{60\rho^3 v_\ell^9\beta^5}\left(\frac{KT}{\hbar}\right)^4\frac{1}{\omega(q_1)\tau\beta^7}\{[c_{12}+3c_{11}+6c_{111}]$$
$$+(\beta^2-1)[c_{12}+6c_{111}-24c_{155}]\}^2$$
$$\times\{\arctan\,[\omega(q_1)\tau(1+\beta)$$
$$-\arctan\,[\omega(q_1)\tau(1-\beta)]\}.$$

Under the conditions $\omega(q_1)\tau \gg 1 \gg \omega(q_1)\tau(1-\beta)$ it follows that $\tau_{\ell+\ell\to\ell}^{-1}\propto \omega(q_1)T^4$ which is identical to the result obtained by Landau and Rumer in the case of transverse waves. For $\beta=1$ the result depends only on c_{111} and not on c_{155}. The next term in the expansion, the coefficient of $1/(\omega(q_1)\tau)^2$, contains both c_{111} and c_{155}. SHIREN [1966] has pointed out that if $c_{155} > c_{111}$ which implies that there is a large third-order elastic anisotropy, it is possible for this term to be comparable to the first. In this case, since τ is temperature dependent, it can give rise to a higher power of T than T^4 in $\tau_{\ell+\ell\to\ell}^{-1}$. KLEIN [1967] has suggested another reason why a temperature dependence greater than T^4 may be obtained. In some cases, he has pointed out that it may be possible for $\omega(q_1)\tau(1-\beta)$ to be of the order of or greater than unity in which case the difference of the arctangents in the above expression is $\arctan\{2\beta/\omega(q_1)\tau(1-\beta^2)\}$. This factor may then give rise to a temperature dependence of $\tau_{\ell+\ell\to\ell}^{-1}$ greater than T^4.

To conclude, it has been seen that there are two possible explanations of deviations from the Landau–Rumer ωT^4 law in the region $\omega\tau \gg 1$. One, as pointed out by Shiren, is due to the large third-order anisotropy and the second may be regarded as due to dispersion. The latter case requires fairly high values of $\omega\tau$ and materials with relatively

low Debye temperatures. Klein believes that the deviations from the Landau–Rumer law observed by NAVA *et al.* [1964] are due to dispersion. This is because even though there is quite a large third-order anisotropy the higher-order terms in the expansion for $\tau_{\ell+\ell\rightarrow\ell}^{-1}$ fortuitously cancel the large contribution from the second term. On the other hand it is felt that the results of DE KLERK [1965] on Al_2O_3 may be due to anisotropy because the Debye temperature in that material is relatively high and deviations from T^4 occur even around 50 K.

2.7. *Four-phonon processes*

In §2.1–2.6 of this chapter the interaction processes involving three phonons have been considered. The interactions involving four phonons will now be discussed. Naturally, since the four-phonon processes arise from the quartic term in the expansion of the potential energy function or from the cubic term in second-order perturbation theory, it is expected that the associated relaxation times will be much longer than those obtained for the three-phonon processes. This may be seen as follows. From eq. (4.21) the displacement of an atom at position x can be written as

$$u_\alpha(x) = i \sum_q (\hbar/2M\omega(q))^{1/2} e_\alpha(q) \exp(iq \cdot x)[a(q) - a^*(-q)].$$

Therefore since the strain components at any point involve $\partial u_\alpha/\partial x_\beta$ the average of the square of the matrix element of the strain is given by

$$|\epsilon|^2 \approx \sum_q \tfrac{1}{3}[\hbar/(2M\omega(q)]\bar{n}(q)q^2.$$

The factor $\tfrac{1}{3}$ is included as the mean square value of the direction cosine between $e(q)$ and q. Evaluating this in the Debye approximation

$$|\epsilon|^2 \approx \hbar/[4\pi^2\rho v^5] \int_0^{\omega_D} \omega^3(q)/[\exp(\hbar\omega(q)/KT) - 1] \, d\omega(q).$$

Letting $x = \hbar\omega(q)/KT$ and $\theta_D = \hbar\omega_D/K$ it follows that

$$|\epsilon|^2 \approx (KT)^4/(4\pi^2\rho v^5\hbar^3) \int_0^{\theta_D/T} x^3/[\exp(x) - 1] \, dx.$$

The integral is easily evaluated for temperatures much lower than the Debye temperature when the upper limit of the integral can be taken as infinity. The result is that $|\epsilon|^2 \approx (KT)^4/\tfrac{1}{15}[4\pi^2\rho v^5\hbar^3]\pi^2 \approx 10^{-14}T^4$ for typical values of v and ρ. Since the relaxation time of the four-phonon process will involve something like an additional factor of $|\epsilon|^{-2}$ over that of the three-phonon process, it is seen that in general it will be very much greater. This need not be true of course in the case of

longitudinal microwave phonons with energy much less than KT; in this case it was found that, except in special circumstances, the three-phonon process is forbidden. Here the major contribution might come from the four-phonon interactions since in these it is always possible for phonons with energy of the order of KT to participate in the process. In the case of an isotropic medium without dispersion, the decay of a longitudinal microwave phonon with energy $\hbar\omega(q_1) \ll KT$ can take place via the following processes,

$$\omega_\ell(q_1) + \omega_\ell(q_2) \rightarrow \omega_\ell(q_3) + \omega_\ell(q_4)$$

$$\omega_\ell(q_1) + \omega_\ell(q_2) \rightarrow \omega_t(q_3) + \omega_\ell(q_4)$$

$$\omega_\ell(q_1) + \omega_\ell(q_2) \rightarrow \omega_t(q_3) + \omega_t(q_4)$$

$$\omega_\ell(q_1) + \omega_t(q_2) \rightarrow \omega_\ell(q_3) + \omega_\ell(q_4)$$

$$\omega_\ell(q_1) + \omega_t(q_2) \rightarrow \omega_t(q_3) + \omega_\ell(q_4)$$

$$\omega_\ell(q_1) + \omega_t(q_2) \rightarrow \omega_t(q_3) + \omega_t(q_4)$$

$$\omega_\ell(q_1) + \omega_t(q_2) + \omega_t(q_3) \rightarrow \omega_\ell(q_4)$$

$$\omega_\ell(q_1) + \omega_t(q_2) + \omega_\ell(q_3) \rightarrow \omega_\ell(q_4).$$

The relaxation time of the phonons due to these processes has been estimated by POMERANCHUK [1942] who found that the main feature was that τ^{-1} varied as $\omega^2(q_1)(KT/\hbar)^7$. This is in accord with the general argument given earlier in §2.3 that $\tau^{-1} \propto \omega^a(KT/\hbar)^{9-a}$.

It was noted in §2.3 that it is now possible to observe the decay of phonons having energies very much greater than KT. In that section an argument due to ORBACH and VREDEVOE [1964] was followed which showed that the lifetime of the phonons in the lowest branch is very long if only three-phonon processes are considered. Because of this it is of interest to examine the decay due to four-phonon processes. Such processes can occur in two ways. They may arise from the quartic anharmonic terms of the Hamiltonian or from the cubic terms treated in second-order perturbation theory. The processes have been considered in detail by KWOK and MILLER [1966]. For the discussion it is convenient to denote the lowest branch of the phonon spectrum by T and the other *two* branches by L. The four-phonon processes can be divided into three types, E standing for either T or L.

$$T \rightarrow E + E' + E'' \tag{4.35}$$

$$T + E \rightarrow E' + E'' \tag{4.36}$$

$$T + E + E' \rightarrow E'' \tag{4.37}$$

Kwok and Miller assumed an isotropic dispersion relation of the form $\omega_j(q) = c_j q(1 - \lambda_j q^2)$ where λ was a dispersion parameter. With

an isotropic dispersion relation the process of eq. (4.35) is forbidden because of energy and momentum conservation requirements. In the process given in eq. (4.37) only $E'' = L$ is allowed. Obviously this is a higher-order type of process than that of the form $T + E \rightarrow L$ considered by Orbach and Vredevoe and so can be ignored. Likewise for the interaction of eq. (4.36) the only processes which do not represent small corrections to lower-order processes are

$$T_q + T_{q_2} \rightarrow T_{q-q_1} + T_{q_1+q_2} \tag{4.38}$$

$$T_q + L_{q_2} \rightarrow T_{q-q_1} + T_{q_1+q_2} \tag{4.39}$$

$$T_q + T_{q_2} \rightarrow L_{q-q_1} + T_{q_1+q_2} \tag{4.40}$$

$$T_q + L_{q_2} \rightarrow L_{q-q_1} + T_{q_1+q_2} \tag{4.41}$$

Of these it was found by Kwok and Miller that those of eqs. (4.38) and (4.39) are the fastest. The decay due to these processes is found to be comparable in magnitude to the three-phonon processes(v) and (vi) of eq. (4.15) but has a different frequency and temperature dependence. It is pointed out that in special circumstances the process of eq. (4.38) may in fact disappear because the coupling constant vanishes. This occurs if an elastically isotropic continuum model is used or in some cases when wave propagation is along a direction of high crystal symmetry. The following results have been obtained by Kwok and Miller. The contribution to τ^{-1} arising from the cubic anharmonic term taken to second order in the perturbation is most important in the case of the process of eq. (4.38). It is found that

$$\begin{aligned} \tau^{-1} &\propto q^2 T^5 \quad \text{if} \quad 8KT/\hbar c \lambda q^3 \gg 1 \\ &\propto q^{-4} T^7 \quad \text{if} \quad 8KT/\hbar c \lambda q^3 \ll 1. \end{aligned} \tag{4.42}$$

Processes of eq. (4.40) and (4.41) are much less important because $(q - q_1)$ of the longitudinal phonon in the final state is restricted by the energy–momentum conservation laws to the range $0 < |q - q_1| \leqslant q_2$. The process of eq. (4.39) plays a smaller role in the decay than that of eq. (4.38) when $\hbar c \lambda q^3 \ll 8KT$ because the energy deficit for the intermediate state is larger for eq. (4.39) than for eq. (4.38). On the other hand in the range $\hbar c \lambda q^3 \gg 8KT$ the roles played by the processes of eqs. (4.39) and (4.38) are comparable. It is found that when the contributions from the quartic terms are considered the decay due to the processes contained in eqs. (4.40) and (4.41) are again of minor importance compared to those of eq. (4.38) for the same reasons as before. Those of eqs. (4.38) and (4.39) are comparable and lead to

relaxation times of the form

$$\tau^{-1} \propto q^5 T^4 \quad \text{if} \quad \hbar c \lambda q^3 \ll 8KT$$
$$\tau^{-1} \propto q^{-4} T^7 \quad \text{if} \quad \hbar c \lambda q^3 \gg 8KT. \tag{4.43}$$

3. Attenuation of ultrasound in the region $\Omega\tau \ll 1$

A discussion of the second of the two regimes mentioned in the intro-
duction to this chapter will now be given. This is when the wavelength
of the ultrasound exceeds that of the mean free path of the thermal
phonons, $\Omega\tau \ll 1$. For most materials this region lies above 50 K at
ultrasonic frequencies of 1 GHz.

A well-known source of energy loss due to thermal phonons is the
thermoelastic loss. This occurs because the compressed regions become
slightly hotter than the expanded regions resulting in the occurrence of
temperature gradients. Because of these temperature gradients irrevers-
ible processes of thermal conduction occur resulting in energy being ab-
stracted from the sound wave. The idea behind this absorption process
has been known for a long time, in fact it was calculated as far back as
1868 by KIRCHHOFF [1868] for the case of fluids. As will be seen later this
process is insufficient to explain the experimentally observed attenua-
tion coefficients in dielectrics so other mechanisms must be invoked. It
is though, likely to be important in metals where the thermal conductivi-
ties are high. Because the thermoelastic effect is quite well known and
because it is of more general applicability than to the problem we are
discussing we have chosen to defer the theory to appendix 4. Also appen-
dix 5 is devoted to the general discussion of internal friction on a phe-
nomenological basis in terms of viscosity coefficients. It also serves to
define important quantities like the Q-factor and attenuation constant
which are frequently used in the discussion of absorption.

A major step forward in the theory was provided by AKHIESER
[1939]. He pointed out that a sound wave passing through a crystal
causes a disturbance of the distribution of phonons so that the thermal
phonons corresponding to the thermal lattice vibrations have no
longer an equilibrium Planck distribution. The increase in entropy
required to restore these phonons to thermal equilibrium leads to an
absorption of the acoustical energy. The treatment of this phenomenon
as given by Akhieser will now be presented.

3.1. *The Akhieser mechanism of sound absorption*

The presence of a sound wave causes a change in the elastic properties
of the medium and hence in the frequency of the Debye phonons. For
small deformations, assuming that classical elasticity theory can be

used, the change in phonon frequency may be expanded in terms of a power series of the strain and rotation tensors. Thus the phonon frequency to first order in these tensors may be written as

$$\omega_j(q) = \omega_j^0(q)[1 + \gamma_{ij}(q)\epsilon_{ij} + \gamma_i'(q)w_i] \qquad (4.44)$$

where $\omega_j^0(q)$ is the frequency of the phonons in the absence of the applied sound wave. γ_{ij} may be regarded as a Gruneisen constant, appendix 4. In general it will be a function of q but if dispersion can be neglected it depends only on the direction of the wave vector and not its magnitude. Akhieser's method of calculating the attenuation coefficients involved computing the amount of heat dissipated per unit volume in unit time. That is, he calculated the rate of entropy change of the phonon gas and multiplied it by the temperature. From standard statistical mechanics, see for example the book by TER HAAR[1954], the entropy of the phonons can be expressed in the form

$$S = K \sum_{qj} \{(n_j(q) + 1) \log (n_j(q) + 1) - n_j(q) \log n_j(q)\}.$$

A straightforward differentiation gives

$$T\dot{S} = KT \sum_{qj} \dot{n}_j(q) \log [(n_j(q) + 1)/n_j(q)]. \qquad (4.45)$$

The rate of change of the phonon occupation numbers arising from collisions due to anharmonic terms in the potential energy has already been calculated in eq. (4.19). Thus the rate of change of $n(q_1)$ due to the presence of the sound field under stationary conditions may be calculated by equating the sum of the two time derivatives to zero

$$[\dot{n}(q_1)]_{\text{collisions}} + [\dot{n}(q_1)]_{\text{sound}} = 0. \qquad (4.46)$$

Let the deviation of the phonon occupation numbers from thermal equilibrium be given by $n(q) = n^0(q) + \Delta n(q)$. Substituting for $n(q)$ into eq. (4.19) and keeping only the terms linear in the deviation $\Delta n(q)$, it follows that

$$[\dot{n}(q_1)]_{\text{coll}} = \frac{-\pi\hbar}{4N} \sum_{q,q_2} |M|^2 \left\{ 2 \sinh \frac{\hbar\omega(q_1)}{2KT} \sinh \frac{\hbar\omega(q_2)}{2KT} \sinh \frac{\hbar\omega(q_3)}{2KT} \right\}^{-1}$$

$$\times \left\{ \left[-\Delta n(q_1) \sinh^2 \frac{\hbar\omega(q_1)}{2KT} + \Delta n(-q_2) \sinh^2 \frac{\hbar\omega(q_2)}{2KT} \right. \right.$$

$$\left. + \Delta n(-q_3) \sinh^2 \frac{\hbar\omega(q_3)}{2KT} \right] \delta(\omega(q_1) - \omega(q_2) - \omega(q_3))$$

$$+ \left[-\Delta n(q_1) \sinh^2 \frac{\hbar\omega(q_1)}{2KT} + \Delta n(-q_2) \sinh^2 \frac{\hbar\omega(q_2)}{2KT} \right.$$

$$\left. - \Delta n(q_3) \sinh^2 \frac{\hbar\omega(q_3)}{2KT} \right] \delta(\omega(q_1) - \omega(q_2) + \omega(q_3))$$

$$+ \left[-\Delta n(q_1) \sinh^2 \frac{\hbar \omega(q_1)}{2KT} - \Delta n(q_2) \sinh^2 \frac{\hbar \omega(q_2)}{2KT} \right.$$

$$\left. + \Delta n(-q_3) \sinh^2 \frac{\hbar \omega(q_3)}{2KT} \right] \delta(\omega(q_1) + \omega(q_2) - \omega(q_3)) \Big\}. \quad (4.47)$$

Akhieser expressed the small deviation $\Delta n(q)$ in the form $\Delta n(q) = -\phi(q) \partial n^0(q)/\partial \hbar \omega(q)$ where $\phi(q)$ is now the unknown quantity to be determined. Using this, it follows immediately that

$$n(q) = n^0(q) + \frac{\phi(q)}{KT} n^0(q)(n^0(q)+1) = n^0(q) + \frac{\phi(q)}{4KT} \sinh^{-2} \frac{\hbar \omega(q)}{2KT}.$$
$$(4.48)$$

Therefore

$$[\dot{n}(q_1)]_{\text{coll}} = -\frac{\pi \hbar}{32N} \sum_{q_i q_s} |M|^2 \left\{ KT \sinh \frac{\hbar \omega(q_1)}{2KT} \sinh \frac{\hbar \omega(q_2)}{2KT} \sinh \frac{\hbar \omega(q_3)}{2KT} \right\}^{-1}$$

$$\times \{ [-\phi(q_1) + \phi(-q_2) + \phi(-q_3)] \delta(\omega(q_1) - \omega(q_2) - \omega(q_3))$$
$$+ [-\phi(q_1) + \phi(-q_2) - \phi(q_3)] \delta(\omega(q_1) - \omega(q_2) + \omega(q_3))$$
$$+ [-\phi(q_1) - \phi(q_2) + \phi(-q_3)] \delta(\omega(q_1) + \omega(q_2) - \omega(q_3)) \}.$$
$$(4.49)$$

Returning to eq. (4.45) after substituting for $n(q)$ from eq. (4.48) it follows that

$$T\dot{S} = KT \sum_{q_i} \dot{n}(q_1) \log \left[(n^0(q_1)+1)/n^0(q_1) \right]$$

$$+ KT \sum_{q_i} \dot{n}(q_1) \log (1 - \phi(q_1)/KT).$$

Replacing $\dot{n}(q_1)$ by the quantity $-[\dot{n}(q_1)]_{\text{coll}}$ given in eq. (4.49), the first term gives zero while the second term, on writing $\log(1-x) \approx -x$ for small x, gives to second order in ϕ

$$T\dot{S} = -\frac{\pi \hbar}{32N} \sum_{q_1 q_2 q_3}$$

$$\times \frac{|M|^2] \phi(q_1) - \phi(-q_2) - \phi(-q_3)]^2 \delta(\omega(q_1) - \omega(q_2) - \omega(q_3))}{KT \sinh(\hbar \omega(q_1)/2KT) \sinh(\hbar \omega(q_2)/2KT) \sinh(\hbar \omega(q_3)/2KT)}.$$
$$(4.50)$$

The result has been simplified by cyclic permutation of some of the indices in the triple summation. Akhieser determined in the long wavelength limit how this dissipative function varied with temperature in the case of high and low temperatures. As indicated already the presence of the sound wave alters the frequency of the phonons. In addition it also changes the temperature T of the phonon gas. To account for this Akhieser wrote $\dot{n}(q_1)$ in the form

$$\dot{n}(q_1) = \frac{\partial n(q_1)}{\partial \omega(q_1)} \dot{\omega}(q_1) + \frac{\partial n(q_1)}{\partial T} \dot{T}.$$

The kinetic equation then becomes

$$[\dot{n}(q_1)]_{\text{coll}} = \frac{\hbar\omega^0(q_1)}{4KT} \sinh^{-2}\frac{\hbar\omega^0(q_1)}{2KT} \left[\gamma_{ij}\dot{\epsilon}_{ij} + \gamma'\dot{\omega}_i - \frac{\dot{T}}{T}\right]. \quad (4.51)$$

First of all, to determine $\dot{T}$ it is noted that

$$\sum_{q_1} [\hbar\omega^0(q_1)\dot{n}(q_1)]_{\text{coll}} = 0.$$

This follows directly from the expression of eq. (4.49). If $\dot{n}(q_1)]_{\text{coll}}$ as given by eq. (4.51) is substituted into this result it is seen that $\dot{T}/T$ is determined by some average over wave numbers of the quantity $[\gamma_{ij}\dot{\epsilon}_{ij} + \gamma'_i\dot{\omega}_i]$. A solution of this kinetic equation cannot be found exactly but the main features of the temperature dependence of ϕ can be extracted. At temperatures high compared to the Debye temperature, when the Planck distribution function approximates to $KT/\hbar\omega$, it is found that ϕ is inversely proportional to T. On the other hand at low temperatures it can be shown by replacing the summation by an integral that the temperature dependence of ϕ is inversely proportional to T^4. The constants of proportionality will involve quantities like the matrix elements of $|M|^2$. To estimate these Akhieser considered the process of thermal conduction in which the same constants enter. In the place of the kinetic equation, eq. (4.46), one has

$$[\dot{n}(q_1)]_{\text{collisions}} + [\dot{n}(q_1)]_{\text{conduction}} = 0$$

where the change in occupation number due to thermal conduction is given by $[\dot{n}(q_1)]_{\text{cond}} = v\partial n^0(q_1)/\partial T$. The deviation in $\dot{n}(q_1)$ can be expressed in terms of a quantity $[\phi(q)]_{\text{cond}}$ as in eq. (4.48) and an expression for it obtained from the conduction equation. The same parameters will enter this expression as occurred in the equation for $[\phi(q)]_{\text{sound}}$. The energy density flux for thermal conduction is given by

$$\frac{1}{V}\sum_{q_1}\hbar\omega(q_1)v\Delta n(q_1)$$

so that, if this is expressed in the form κ grad T, an expression relating the required parameters to the thermal conductivity coefficient κ can be obtained. Substituting these results into eq. (4.50) causes the dissipative function $T\dot{S}$ to be independent of temperature at high temperatures and to be inversely proportional to temperature for small T. From $T\dot{S}$ the sound absorption coefficient may be deduced, see appendix 4. $T\dot{S}$ also involves the quantity $(\gamma_{ij}(q)\epsilon_{ij} + \gamma'_i(q)\omega_i - \dot{T}/T)$. An expression for this may be obtained by relating γ_{ij} to the average Gruneisen constant γ which in turn may be expressed, for an isotropic medium, in terms of the bulk modulus B. With these approximations

Akhieser found that the sound absorption coefficient at high temperatures was

$$A = B^2 \left(\frac{3\alpha}{C}\right)^2 \frac{\kappa T}{\rho v^5} \omega^2 \qquad (4.52)$$

while at low temperatures it is

$$A = B^2 \left(\frac{3\alpha}{C}\right)^2 \frac{\kappa_\theta \theta^2}{\rho v^5 T} \omega^2 \qquad (4.53)$$

θ is the Debye temperature. Note at high temperatures Akhieser finds that κ is proportional to $1/T$ so that A is independent of temperature.

3.2. The work of Woodruff and Ehrenreich

An extension to the work of Akhieser on the attenuation of sound was made by WOODRUFF and EHRENREICH[1961] whose work will now be described. The method is based upon the technique used by BLOUNT[1959] for treating the attenuation of ultrasound by electrons in metals. It is convenient to consider three systems, the driving sound wave, the dissipative system which is taken to be the phonon gas occupying the dielectric in which the sound wave is propagating, and the external heat bath. The attenuation of the acoustic wave is then regarded as being due to the transfer of energy from the wave to the phonon gas which in turn transfers an equal amount of energy to the heat bath in contact with the dielectric. As pointed out by Blount one can either calculate the rate at which the sound wave loses energy to the phonons or the equivalent rate at which the phonons lose energy to the bath. Woodruff and Ehrenreich calculate the latter quantity. The starting point is to write down the Boltzmann transport equation for the system.

It has already been indicated in ch. 2§3.4 that when dealing with transport properties it is convenient to formulate the theory in terms of localized wave packets. This is necessary for example in thermal conduction where a spatial temperature gradient exists, for we must be able to describe the state of the system at different points in space where the temperature is different. The phonons are regarded as being localized particles so that their distribution function is a function of position as well as of their wave vector and polarization. Because one is not now dealing with states of the system which are strictly stationary, that is, with normal modes, a slight spread of energy should be allowed for in the energy conservation condition for phonon collisions, eq. (4.12), since the energy of the waves is not sharply defined. This is not important however, if the other energy dependent factors in the equations are almost constant over the region of this uncertainty. This

idea of localized phonons moving through the lattice with the group velocity is convenient in the regime where the sound wave may be regarded as a slowly varying spatial perturbation. It is convenient to divide the crystal up into small regions, small compared to the wavelength of the sound wave but nevertheless large enough to contain many phonons. To each region a distribution function $n(qrt)$ may be assigned.

In the absence of external fields the probabilities of occupation of the phonon modes with wave vectors q and $-q$ are the same. Since the group velocities for these two modes are oppositely directed no net transport of energy takes place. In the presence of an externally applied acoustic field or a thermal gradient, the distribution function of the phonons will become modified. Let $n(qrt)$ be the distribution function of the thermal phonons in mode q at position r at time t. Then if the phonons are regarded as classical particles, when a force acts on the phonons, the value of q will change at a rate given by $\hbar \dot{q} = F$ while the position vector of the phonons will in a short time dt change from r to $r + \dot{r} dt$. Therefore the new distribution function for the phonons is $n(q + \dot{q} dt, r + \dot{r} dt, t + dt)$. Consequently the rate of change of the occupation number n is given by

$$\frac{dn}{dt} = \frac{\partial n}{\partial t} + \dot{q}_x \frac{\partial n}{\partial q_x} + \dot{q}_v \frac{\partial n}{\partial q_v} + \dot{q}_z \frac{\partial n}{\partial q_z} + \dot{x} \frac{\partial n}{\partial x} + \dot{y} \frac{\partial n}{\partial y} + \dot{z} \frac{\partial n}{\partial z}.$$

This total rage of change of n must be brought about by collisions. Therefore it follows that

$$\left[\frac{dn}{dt}\right]_{\text{coll}} = \frac{\partial n}{\partial t} + \dot{q} \cdot \nabla_q n + \dot{r} \cdot \nabla_r n.$$

A more convenient form for this expression can be obtained by using Hamilton's equations of motion

$$\dot{r}_i = \hbar^{-1} \partial H/\partial q_i, \qquad \dot{q}_i = -\hbar^{-1} \partial H/\partial r_i,$$

to give

$$\left[\frac{dn}{dt}\right]_{\text{coll}} = \frac{\partial n}{\partial t} + \hbar^{-1} \sum_i \left[\frac{\partial n}{\partial r_i} \frac{\partial H}{\partial q_i} - \frac{\partial n}{\partial q_i} \frac{\partial H}{\partial r_i}\right].$$

If the perturbation is considered to be due to a plane sound wave propagating along the z-axis then the dependence of n on x and y will drop out and the equation reduces to

$$\left[\frac{dn}{dt}\right]_{\text{coll}} = \frac{\partial n}{\partial t} + \hbar^{-1} \left[\frac{\partial n}{\partial z} \frac{\partial H}{\partial q_z} - \frac{\partial n}{\partial q_z} \frac{\partial H}{\partial z}\right]. \qquad (4.54)$$

The rate at which energy is transferred from the phonon system to the heat bath is $\dot{E} = -\Sigma_{qj} \langle H [\partial n/\partial t]_{\text{coll}} \rangle$ where the angular brackets indi-

cate a time average over a cycle. H is the total time-dependent Hamiltonian for a single phonon in the presence of the sound field. Making use of the Boltzmann equation, eq. (4.54), and slightly rearranging the terms it follows that

$$\dot{E} = + \sum_{qj} \left\langle n \frac{\partial H}{\partial t} - \frac{\partial}{\partial t}(nH) - \hbar^{-1} \frac{\partial}{\partial z}\left(nH \frac{\partial H}{\partial q_z}\right) + \hbar^{-1} \frac{\partial}{\partial q_z}\left(nH \frac{\partial H}{\partial z}\right)\right\rangle.$$

The second term on the right-hand side is just the time derivative of the total energy which averages to zero and the last two terms give zero when summed over the Brillouin zone. Therefore $\dot{E}$ reduces to $\sum_{qj} \langle n \partial H / \partial t \rangle$. It is found convenient to write H as $H_0 + H_1$ where H_1 is the periodic perturbation. Also putting $n = n_0(H_0 + H_1) + n_1$ it follows, since $\partial H_0 / \partial t = 0$, that

$$\dot{E} = \sum \langle n_0(H_0 + H_1) \partial H_1 / \partial t \rangle + \sum \langle n_1 \partial H_1 / \partial t \rangle$$
$$= \sum \langle [n_0(H_0) + n_0' H_1 + \cdots] \partial H_1 / \partial t \rangle + \sum \langle n_1 \partial H_1 / \partial t \rangle$$

Therefore because $\partial H_1 / \partial t$ and $H_1 \partial H_1 / \partial t$ are zero when averaged over a cycle

$$\dot{E} = \sum \langle n_1 \partial H_1 / \partial t \rangle. \tag{4.55}$$

As before it will be assumed that the change in the eigen-frequency of the phonon q is given by the expression of eq. (4.44). To simplify matters we follow Woodruff and Ehrenreich and consider a particular example, that of a longitudinal sound wave propagating along the z-direction. Further if the discussion is restricted to a consideration of an isotropic medium where the velocity is independent of the direction of propagation the term involving the rotation part of the strain tensor will vanish. From eq. (2.12) the sound wave under consideration gives rise to a displacement $u = u_0 e_3(k) \exp[i(\Omega t - kz)]$ with $|e_3(k)| = 1$. Therefore the change in phonon frequency arising from the presence of the sound wave is

$$\omega_j(q) = \omega_j^0(q)[1 - i\gamma_{33}ku_0 \exp[i(\Omega t - kz)]].$$

The Hamiltonian for a single phonon in the mode q can then be written as $H = H_0 + H_1$ with

$$H_0 = \hbar\omega_j^0(q) \quad \text{and} \quad H_1 = -i\hbar\omega_j^0(q)\gamma_{33}ku_0 \exp[i(\Omega t - kz)].$$

In the absence of any perturbation let the thermal equilibrium distribution function be denoted by* $n^0(\omega^0)$, the usual Planck distribution function. In the perturbed lattice, since the frequency $\omega_j(q)$ of the phonons varies spatially, it is necessary to define for each small region

---

* For ease of printing the suffice q and j on the ω will be dropped in $n(\omega)$.

of the crystal a new local equilibrium distribution $n^0(\omega)$. For small perturbations we can write to first order

$$n^0(\omega) = n^0(\omega^0) + \frac{\hbar\omega^0(q) i\gamma_{33} k u_0 \exp[i(\Omega t - kz)]}{4KT \sinh^2 \hbar\omega^0(q)/2KT}. \qquad (4.56)$$

The sound wave will perturb the local distribution away from its equilibrium value by a small amount Δn so that $n(qzt) = n^0(\omega) + \Delta n$. After introducing a function ϕ as in eq. (4.48) it follows that

$$n(qzt) \approx n^0(\omega) + \frac{\phi(qzt)}{4KT} \sinh^{-2}(\hbar\omega^0(q)/2KT)$$

$$\approx n^0(\omega) + \frac{\phi}{4KT} \sinh^{-2}(\hbar\omega^0(q)/2KT) \exp[i(\Omega t - kz)] \qquad (4.57)$$

where ϕ is now a function of q, k and Ω. Combining eqs. (4.56) and (4.57)

$$n(qzt) = n^0(\omega^0) + [4KT \sinh^2 \hbar\omega(q)/2KT]^{-1}[i\hbar\omega^0(q)\gamma_{33}ku_0 + \phi]$$

$$\times \exp[i(\Omega t - kz)]. \qquad (4.58)$$

The last term on the right-hand side of this equation is the function n_1 to be used in the calculation of the heat dissipation $\dot{E}$. If reference is made back to the Boltzmann equation it is seen to contain a collision term depending upon the interaction that each phonon makes with the phonons present in all the other modes. Clearly such an equation is not directly solvable. The approximation which is frequently made is to replace the collision term by a relaxation time which characterizes the return of the distribution function to its equilibrium value. The collision term describes interactions of two distinct types, normal collisions in which momentum is conserved and Umklapp processes. It was pointed out, originally by Peierls, that because energy and momentum are conserved in normal collisions these processes by themselves cannot lead to a finite thermal resistance. For these processes the distribution need not relax to that given by the Planck distribution function but can relax to a displaced distribution of the form $\{\exp[(\hbar\omega(q) + \Lambda \cdot q)/KT] - 1\}^{-1}$. This fact can be readily verified by checking that this distribution function does indeed give zero on the right-hand side of eq. (4.19). It is seen that $\Lambda = \Lambda_0 \exp[i(\Omega t - kz)]$ has the dimension of a velocity. Once the phonon gas has been given a drift velocity, normal processes by themselves cannot remove it. Because of this fundamental difference in the role of normal and Umklapp processes it is necessary to introduce two relaxation times, one for each type of process. This was the method adopted by CALLAWAY [1959] in his discussion of thermal conductivity. We write

$$\left[\frac{dn}{dt}\right]_{\text{coll}} = -\frac{n(qzt) - n^0(\omega T'\Lambda)}{\tau_N(q)} - \frac{n(qzt) - n^0(\omega T')}{\tau_U(q)} \quad (4.59)$$

with

$$n^0(\omega T') = \{\exp(\hbar\omega(q)/KT') - 1\}^{-1}$$

and

$$n^0(\omega T'\Lambda) = \{\exp[(\hbar\omega(q) - \Lambda \cdot q)/KT'] - 1\}^{-1}.$$

$T' = T + \Delta T \exp[i(\Omega t - kz)]$ is the temperature which would finally be obtained in a small region around a point at position z, if at time t the region were isolated from the remainder of the solid but maintained in the state of strain existing in it at that time. As before it is convenient to expand the distribution functions in a Taylor series and retain only the leading terms

$$n^0(\omega T') = n^0(\omega) + \sinh^{-2}\left(\frac{\hbar\omega^0(q)}{2KT}\right)\frac{\hbar\omega^0(q)}{4KT}\frac{\Delta T}{T}\exp[i(\Omega t - kz)]$$

$$(4.60)$$

$$n^0(\omega T'\Lambda) = n^0(\omega) + \sinh^{-2}\left(\frac{\hbar\omega^0(q)}{2KT}\right)\frac{1}{4KT}$$

$$\times\left\{\frac{\Delta T}{T}\hbar\omega^0(q)\exp[i(\Omega t - kz)] + \Lambda \cdot q\right\}. \quad (4.61)$$

Eqs. (4.60) and (4.61) may be substituted into $[dn/dt]_{\text{coll}}$ of eq. (4.59). This together with $n(qzt)$ given by eq. (4.58) can then be put into the Boltzmann equation, eq. (4.54), which may then be linearized. This equation will involve the unknown quantities ΔT, Λ and ϕ. Two more expressions involving ΔT and Λ may be obtained by using the following subsidiary conditions. For normal processes the wave vector is conserved so

$$\sum_j \int q(\partial n/\partial t)_{\text{coll,N}} dq = 0.$$

The second condition is that to first order the total rate of change of the energy of the system must vanish. That is

$$\sum_j \int \hbar\omega^0(q)(\partial n/\partial t)_{\text{coll}}^{\bullet} dq = 0,$$

Use of these two conditions in conjunction with the linearized Boltzmann equation allows the elimination of ΔT and Λ and hence an expression for ϕ. A knowledge of ϕ allows n_1 to be determined and hence $\dot{E}$ may be evaluated from eq. (4.55). Finally the coefficient of absorption A may be found from eq. (A4.18). To obtain an explicit relationship for A Woodruff and Ehrenreich considered a simple model in which τ_N and τ_U were assumed independent of q, and for which the frequencies had the simple Debye form $\omega(q_j) = v|q|$ with

v an average velocity. In addition they considered the case when τ_N was very much greater than τ_U so that the term involving Λ, see eq. (4.59), could be eliminated from the discussion. The following result was obtained in the region $\Omega\tau \ll 1$

$$A = C_v T \gamma_{33}^2 \Omega^2 \tau / 3\rho v^3. \tag{4.62}$$

If τ is identified as the relaxation time which enters the result, $\kappa = \frac{1}{3}C_v v^2 \tau$, of the simple kinetic theory of thermal conduction then

$$A = \kappa T \gamma_{33}^2 \Omega^2 / \rho v^5. \tag{4.63}$$

At temperatures greater than the Debye temperature κ is proportional to $1/T$ so the absorption coefficient is independent of temperature in agreement with the work of Akhieser.

Two other regimes have been considered by Woodruff and Ehrenreich. In the region $\Omega\tau \gg 1$ they find

$$A = \pi \gamma_{33}^2 \Omega C_v T / 4\rho v^3. \tag{4.64}$$

Strictly speaking the analysis is not valid in this region as has been discussed earlier in this chapter. Nevertheless it is interesting to observe, remembering that $C_v \propto T^3$, that this result gives the same temperature and frequency dependence for the attenuation coefficient as the quantum mechanical theory of Landau and Rumer outlined in §2.3. They also examined the question of what happens if the temperature difference ΔT is ignored. That is, when it is assumed the phonon distribution relaxes to the unperturbed thermal equilibrium value rather than to a perturbed distribution at temperature T'. The result for ΔT and Λ both being zero is

$$A = \frac{3\gamma_{33}^2 \Omega^2 T \kappa}{\rho v^5} \frac{\tan^{-1}(2\Omega\tau)}{2\Omega\tau}. \tag{4.65}$$

For $\Omega\tau \ll 1$ this gives a value of A three times that of eq. (4.62) whereas for $\Omega\tau \gg 1$ it is the same as that given by eq. (4.63).

3.3. *Further extensions to the Akhieser effect*

An extension to the work of Akhieser has been given by BÖMMEL and DRANSFELD [1960]. It will be recalled that in his analysis Akhieser introduced an average Gruneisen constant defined by eq. (A4.9) and related through eq. (A4.10) to the coefficient of thermal expansion. Instead of doing this Bömmel and Dransfeld proceeded as follows. For each group of phonons with the same polarization vector p and propagation vector q they defined a Gruneisen constant $\gamma_p(q)$. Groups of phonons with a common value of q and p were referred to as comprising a branch. For each branch the relative velocity change under a

compression is related to the relative density change by

$$\left(\frac{\Delta v}{v}\right)_{qp} = \gamma_p(q)\left(\frac{\Delta\rho}{\rho}\right). \qquad (4.66)$$

Bömmel and Dransfeld neglected dispersion and assumed that the γ-values did not depend upon frequency so that phonons of all frequencies which belonged to the same branch suffered the same velocity change and hence the same temperature change, given by

$$\left(\frac{\Delta T}{T}\right)_{\hat{q}p} = \gamma_p(\hat{q})\frac{\Delta\rho}{\rho} \qquad (4.67)$$

cf. eq. (A4.11). To proceed further requires detailed knowledge of the values of γ for all the branches. The magnitudes of γ for the branches may differ considerably and even suffer a change of sign. Experimental evidence for this is given in the work of SUSSE [1955]. Because of insufficient data concerning these values Bömmel and Dransfeld made the following simplification. They divided all the branches into two main groups, one group containing all the branches that suffered a large positive temperature change and the other group containing the remainder. The average fractional temperature change between the two groups was then taken as

$$\left(\frac{\Delta T}{T}\right)_{av} = \left(\frac{\Delta T}{T}\right)_1 - \left(\frac{\Delta T}{T}\right)_2$$

and this is used to define an average γ through the equation

$$\left(\frac{\Delta T}{T}\right)_{av} = \gamma_{av}\left(\frac{\Delta\rho}{\rho}\right). \qquad (4.68)$$

When a compressional sound wave propagates through the crystal a time-dependent temperature difference is produced between these two groups of phonons. Heat exchange will occur between them leading to an increase in entropy and thus a consequent absorption of sound. This effect is clearly different from the thermal conduction effect described in appendix 4. In that case heat conduction from one region to another occurred in contrast to the mechanism examined here which depends on the fact that different phonon modes in the *same* spatial region are affected differently by the presence of the sound field. Nevertheless in both cases the heat exchange is governed by the same relaxation time τ characterising the time required for the thermal phonons to interact. Because of this, the formula for the attenuation coefficient in the two cases will have the same structure, both processes being governed by the usual relaxation equations of internal friction. Assuming that both groups of phonons have about the same specific

heat, the attenuation coefficient is

$$A = \frac{C_v T \gamma_{av}^2}{4\rho v^3} \left(\frac{\omega^2 \tau}{1 + \omega^2 \tau^2} \right) \tag{4.69}$$

see eq. (A5.20). The factor 1.1 in the work of Bömmel and Dransfeld comes from the conversion of nepers to decibels. Also there is a difference of a factor of $\frac{1}{2}$ between their definition of the attenuation coefficient and ours.

Another expression for the attenuation due to the Akhieser mechanism has been obtained by MASON and BATEMAN[1964]. The idea is to relate the attenuation to the known third-order elastic constants. It is shown in appendix 5 that the attenuation coefficient arising from internal friction may be expressed in terms of the relaxed and unrelaxed elastic moduli. In the case of interest here the attenuation will be given by

$$A = \frac{\Delta c \omega^2 \tau}{2\rho v^3 (1 + \omega^2 \tau^2)} \tag{4.70}$$

where Δc is the instantaneous increase in the modulus caused by the separation of the phonon modes. To calculate Δc an expression for the thermal energy is required. This is $U = \Sigma \, \hbar \omega_p(q) n_p(q)$ where $\omega_p(q)$ is the angular frequency of the mode with wave vector q and polarization p, and $n_p(q)$ is its occupation number which in thermal equilibrium is given by $\{\exp [\hbar \omega_p(q)/KT] - 1\}^{-1}$. If dispersion can be neglected a Debye model may be used to convert the summation over states to an integral over frequencies

$$U = 3\hbar \sum_i \frac{N_i}{\omega_{m_i}^3} \int_0^{\omega_{m_i}} \frac{\omega^3 d\omega}{e^{\hbar \omega/KT} - 1} \tag{4.71}$$

with $\omega_{m_i} = 2\pi v_i m_i/l$. To account for anisotropy an anisotropic Debye model has been used in which ω_{m_i} is the cut-off frequency for each mode i and N_i is the number of modes of this type. Here i denotes the direction and polarization of the modes. m_i is a constant determined by the number of modes for the direction i and l is the pathlength. As before, the change in frequency of the modes on deformation may be described in terms of Gruneisen constants

$$\omega_p(q) = \omega_p^0(q) \left[1 - \sum_{j=1}^6 \gamma_p^j(q) \epsilon_j \right]. \tag{4.72}$$

Now if dispersion is ignored the γ's will depend only on p and the direction of q, that is on i. Therefore

$$\gamma_i^j = -\frac{1}{\omega_i^0} \frac{\partial \omega_i}{\partial \epsilon_j} \tag{4.73}$$

is independent of the magnitude of q. Suppose now that a strain ϵ_j is suddenly applied. The stress associated with this strain is given by the derivative of the total energy

$$\sigma_j = c_{jj}^S \epsilon_j + \frac{\partial}{\partial \epsilon_j} \left\{ 3\hbar \sum_i \frac{N_i}{\omega_{m_i}^3} \int_0^{\omega_{m_i}} \frac{\omega^3 d\omega}{e^{\hbar\omega/KT}-1} \right\}$$

$$= c_{jj}^S \epsilon_j - 9\hbar \sum_i \frac{N_i}{\omega_{m_i}^3} \left(\frac{1}{\omega_{m_i}} \frac{\partial \omega_{m_i}}{\partial \epsilon_j} \right) \int_0^{\omega_{m_i}} \frac{\omega^3 d\omega}{e^{\hbar\omega/KT}-1}$$

$$= c_{jj}^S \epsilon_j + 3 \sum_i \frac{E_i \gamma_i^j}{1 - \gamma_i^j \epsilon_i}$$

where E_i is the thermal energy associated with the modes i and c_{jj}^S is the elastic modulus which results when there is no entropy exchange between the modes. Therefore

$$\sigma_j \approx \left[c_{jj}^S + 3 \sum_i (\gamma_i^j)^2 E_i \right] \epsilon_j + 3 \sum_i E_i \gamma_i^j. \tag{4.74}$$

The last term on the right-hand side of this equation is the stress required to keep the volume constant as the temperature varies. It is noted that there is an increase in the elastic modulus by an amount

$$\Delta c = 3 \sum_i E_i (\gamma_i^j)^2. \tag{4.75}$$

This modulus relaxes down to the adiabatic value in a time which is short compared to the adiabatic–isothermal transition time. Therefore in the case of a longitudinal mode where the average temperature increase is not zero we must subtract from Δc the Δc arising from the temperature difference ΔT of eq. (A4.8). From eqs. (A4.7) and (A4.10) this is $\gamma^2 C_v T$. The total change in elastic modulus for a longitudinal wave is therefore

$$\Delta c = 3 \sum_i E_i (\gamma_i^j)^2 - \gamma^2 C_v T \tag{4.76}$$

which gives rise to an attenuation coefficient

$$A = \left[3 \sum_i E_i (\gamma_i^j)^2 - \gamma^2 C_v T \right] \omega^2 \tau / 2\rho v^3 (1 + \omega^2 \tau^2). \tag{4.77}$$

Mason and Bateman write this in the form

$$\tfrac{1}{3} E_0 D \omega^2 \tau / 2\rho v^3 (1 + \omega^2 \tau^2)$$

where E_0 is the thermal energy per unit volume. For a shear wave the second term in the square brackets must be equated to zero. To evaluate the absorption coefficients the quantities γ_i^j are required. Analytic

expressions for them in terms of the second- and third-order elastic constants of the crystal have been derived by BRUGGER[1965].

4. Comparison of theory and experiment

In this section a comparison between the experimentally determined values of the attenuation coefficients and those given by the theories discussed in this chapter is made.

4.1. *The region where* $\Omega\tau \ll 1$

One of the earliest measurements of hypersonic attenuation was made at a frequency of 1 GHz by BÖMMEL and DRANSFELD[1960] on a specimen of quartz. Their experimental results for the absorption of transverse waves are displayed in fig. 4.9. To explain these results they made use of the formula of eq. (4.69) which had been derived by them in the same publication. It was assumed that the exchange of energy between the two groups of phonons occurred through Umklapp processes. To estimate the relaxation time τ they assumed that it could be identified with that occurring in the usual kinetic theory result for
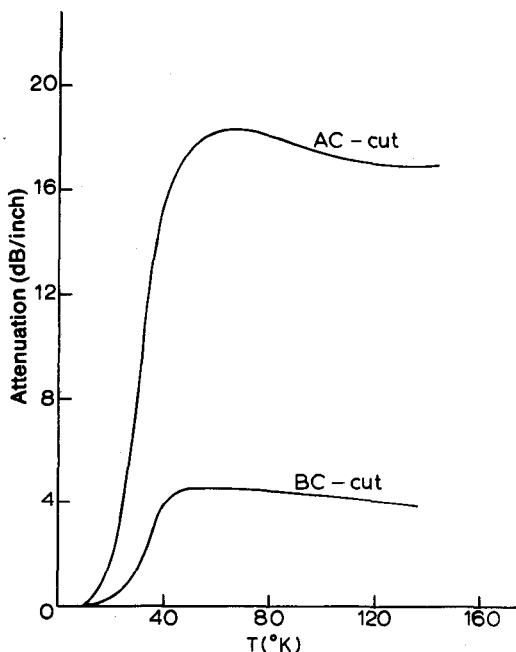
Fig. 4.9. Absorption of 1 GHz transverse waves propagating along the AC and BC directions in quartz. (After Bömmel and Dransfeld.)

the thermal conductivity, $\tau = 3\kappa/C_v v^2$. At temperatures above 40 K, known measurements of the specific heat and the thermal conductivity indicated that they were proportional to the temperature T and to $1/T$ respectively. This implied that the relaxation time τ should vary as the inverse square of the temperature. In the high temperature region where the product $\omega\tau$ is very much less than unity, the absorption coefficient reduces to $3\kappa T\gamma_{av}^2\omega^2/4\rho v^5$ and is therefore independent of temperature. This agrees with the experimental results for temperatures about 60 K. Measurements of the specific heat and the thermal conductivity suggested in fact that $\omega\tau$ would be about unity around 40 K. At this temperature agreement with the experimental value of the attenuation is obtainable if γ_{av} is taken to be 2, a value which does not sound unreasonable.

Experimental measurements of the ultrasonic attenuation in pure silicon and germanium have been made by MASON and BATEMAN [1964] and explained satisfactorily on the basis of the Akhieser mechanism. It was shown in fact that the thermoelastic effect was virtually unimportant, giving rise to only 4% of the total attenuation in the case of longitudinal waves and of course, none for shear waves. Attempts to explain the results in terms of eq. (4.69) with τ equal to the thermal relaxation time $3\kappa/C_v v^2$ proved unsatisfactory. The amount of discrepancy can be seen in fig. 4.10 where γ_{av} is chosen so that the
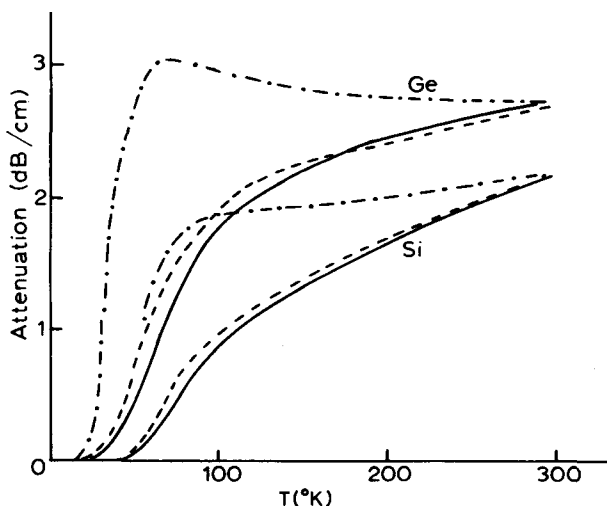
Fig. 4.10. Attenuation of longitudinal ultrasonic waves along the [100] axis in Ge and Si at frequencies of 0.306 and 0.48 GHz respectively. (After Mason and Bateman.) -·-·-·- Theory of eq. (4.69) with $\gamma_{av} = 4.85$, Ge and $\gamma_{av} = 4.15$, Si. -------- Theory of eq. (4.77) with $D = 5,1$, Ge and $D = 4.5$, Si. ———Experiment.

theoretical curves agree with the experimental measurements at 300 K. A much better fit was obtained by using eq. (4.77) with D picked to give the best overall agreement with experiment, figs. 4.10 and 4.11. For the shear wave attenuation τ was taken as the thermal relaxation time but in the case of the longitudinal waves it was taken as twice this value. The best fit to the experimental results occurred when D was chosen as 5.1 and 4.5 for the longitudinal wave in Ge and in Si respectively and unity for the shear waves. These 'experimentally' determined values of D were compared with theoretical values, obtained as follows. The expression for D involves the summation over all γ_i^j. This summation over all modes was cut down to a practicable size by carrying out a partial summation over just the waves propagating along the $\langle 100 \rangle$, $\langle 110 \rangle$ and $\langle 111 \rangle$ directions. This accounted in an approximate way for the angularity in the Gruneisen constants. The expressions for these constants involve the third-order elastic constants which have been measured for germanium by BATEMAN *et al.* [1961] and by DRABBLE and GLUYAS [1963] for both materials. The theoretical values of D obtained by using these constants are shown in table 4.2. It is seen that the formula is quite successful in explaining the temperature variation of the attenuation and that the agreement between the theoretical and experimental values of D is reasonable; in particular it predicts the large difference in the attenuation of the longitudinal and shear waves. A check on the values of D is to compare their average values with the known Gruneisen constants for these materials. Agreement to within 9% for Ge and 15% for Si is found.
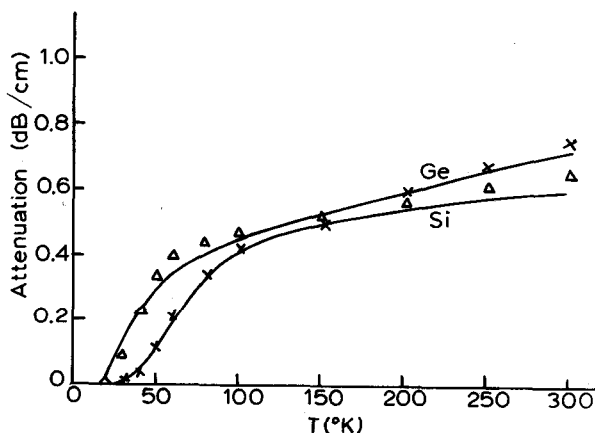
Fig. 4.11. Attenuation of ultrasonic shear waves along the [100] axis in Ge and Si at frequencies of 0.306 and 0.48 GHz respectively. (After Mason and Bateman.) $\triangle$ = theory for Ge and $\times$ theory for Si with $D = 1$. ——— = experiment.

TABLE 4.2

	Experiment	Theory[a]	Theory[b]
Ge (long)	5.1	6.7	5.8
Si (long)	4.5		5.15
Ge (trans)	1	1.46	1.47
Si (trans)	1		0.94

[a] BATEMAN et al. [1961].
[b] DRABBLE and GLUYAS [1963].

A similar comparison of the 'experimental' and theoretical values of the constant D has been made by MASON and BATEMAN [1966] for samples of NaCl, KCl, MgO and YIG. Table 4.3 is a summary of their results. In that table the references under the heading 'D_{expt}' cite the authors of the attenuation measurements whilst those in the column headed 'D_{calc}' give the source of the elastic constants used to calculate the γ_i^j. In the case of YIG no attenuation measurements were available so those pertaining to YAG, a similar structure, were used.

TABLE 4.3

		D_{expt}			D_{calc}
NaCl	L	30	MERKULOV [1959]	42	CHANG [1965]
	T	2.4		2.1	
KCl	L	25		36	
	T	1.8		1.4	
MgO	L	26	DE KLERK [1966b]	24	BOGARDUS [1965]
	T	—		1.8	
YIG	L	4.5 YAG		6.0	EASTMAN [1965]
	T	< 0.91	LECRAW AND COMSTOCK [1965]	0.26	

The Mason and Bateman formulation of the Akhieser mechanism has recently been applied by LEWIS [1968] to calculate the attenuation in quartz and in fused silica. Interest in these materials lies in their technological applications. Quartz is frequently used in the study of the acoustical properties of other materials and finds wide applications in frequency stable oscillators and wave filters, while fused silica is often used in megahertz delay lines. The calculation of the average of $(\gamma_i^j)^2$ was performed over the 57 modes lying along the z-axis, the 3 x-axes, the 3 y-axes, the 3 AC axes, the 3 BC axes and the 6 axes defined by $(x \pm z)/\sqrt{2}$. The results of Lewis's calculations for

quartz are presented in table 4.4 where it is seen that the calculated values of D for the transverse and longitudinal waves are of similar magnitudes. Lewis claims this to be the first quantitative explanation of the experimental fact that the attenuations of transverse and longitudinal waves in trigonal crystals are much the same. It will be noted that there is some discrepancy in the calculated values for the two transverse modes in the [001] direction which is rather hard to understand. Lewis believes that this may be partially due to the particular phonon distribution he has chosen. Another puzzling feature is that the averages of the Gruneisen constants are in poor agreement with those obtained from the thermal expansion coefficient.

TABLE 4.4

Propagation direction	Polarization direction	D_{calc}	D_{expt}
[001]	[001]	12.56	9.32
[001]	[010]	8.24	7.44
[001]	[100]	5.60	7.44
[100]	[100]	10.18	8.75
[100]	[0, −0.5150, 0.8572]	4.69	7.05
[100]	[0, 0.8572, 0.5150]	4.47	7.05
[010]	[100]	3.56	6.17

Calculations performed for fused silica using the elastic constants of BOGARDUS[1965] give $D_\ell = 27$ and $D_t = 2.4$ compared to the experimental values of $D_\ell = 214$ deduced from the measurements of LAMB et al.[1959] and $D_t = 85$ from those of FRASER et al.[1967]. The discrepancy arises mainly because of the low value of τ as deduced from the thermal conductivity measurements. Lewis concludes that the Akhieser mechanism accounts for less than 10% of the room temperature attenuation in this material, the rest being due to another mechanism. This is partly supported by the fact that the temperature dependence of the attenuation is different from that of quartz and most other single crystals.

4.2. The region where $\Omega\tau \gg 1$

POMERANTZ[1965] has carried out a series of experiments at 9 GHz on several materials including crystals of quartz, CdS, GaAs, Ge, Si, CaF_2, Al_2O_3 and MgO to determine the temperature dependence of the microwave ultrasonic attenuation in the region $\Omega\tau > 1$. The attenuation of the microwave phonons was observed for wave propagation in several directions and for different modes of polarization. The transducers used were ferromagnetic films evaporated onto the ends of the

single crystal samples and the change in the attenuation of several acoustic pulse echoes was observed as the temperature was raised from 4 K. Measurements of the attenuation as a function of temperature were made for fast transverse, slow transverse and longitudinal waves. 'Fast transverse' refers to the transverse wave of highest velocity along a given axis. For the particular cases where the two transverse waves are degenerate these waves were classed as fast. The following results were obtained. In all cases except for fast transverse waves in Al_2O_3 the attenuation was proportional to T^n. The average values of n for the fast transverse, slow transverse and longitudinal waves were $\bar{n} = 4.1$, 4.0 and 4.8 with standard deviations $\sigma = 1.2$, 1.7 and 1.4 respectively. The standard deviation σ was calculated from

$$\left\{ \Sigma \left[(n - \bar{n})^2 / N \right] \right\}^{1/2}$$

where N was the number of samples. The results for transverse waves are therefore in reasonable agreement with the theory of Landau and Rumer described in §2.3 which predicted a T^4 temperature dependence. The results for the longitudinal waves are in fair agreement with the work of CICCARELLO and DRANSFELD[1964] and that of MARIS [1964] who accounted for the finite lifetimes of the thermal phonons. It was seen in §§2.5 and 2.6 that these theories lead to a temperature dependence for longitudinal waves similar to that for transverse waves. The results for MgO and Al_2O_3 were compared with earlier measurements of Ciccarello and Dransfeld carried out at 3 GHz. The attenuation was approximately three times higher at 9 GHz again in agreement with the theories of §§2.3 and 2.5 which predicted that the attenuation is proportional to the frequency.

The attenuation at a particular temperature varied considerably from specimen to specimen. In order to be able to predict the amount of attenuation expected for a particular crystal Pomerantz attempted to find a correlation between the attenuations and the Debye temperature θ of the crystal. Such a correlation is to be expected because in the Debye theory the number of thermally excited phonons is proportional to $(T/\theta)^3$ and these are the phonons which provide the scattering for the microwave wave. In the case of the longitudinal and the fast transverse phonons they were able to find an empirical law: the attenuation of 9 GHz longitudinal and fast transverse phonons is 3 dB/cm when the temperature is $\approx 0.1\,\theta$.

Attempts were also made to calculate the absolute value of the attenuation for the region $\Omega\tau \gg 1$. A comparison of the temperature at which theory and experiment gave an attenuation of 3 dB/cm was made. For transverse waves along the [100] axis in Ge and Si it was found that if the formula of Landau and Rumer, which neglected

anisotropy, is used, then the theoretical results are approximately twice the experimental ones. A better agreement is obtained for the attenuation of longitudinal waves by three-phonon collinear interactions, particularly in the case of cubic materials. The results obtained by Pomerantz are given in table 4.5.

The temperature dependence of the hypersonic attenuation in rutile has been measured in detail by LANGE[1968] at frequencies of 3 and 1 GHz, particular attention being paid to the temperature range 7–30 K where the three-phonon processes dominate. These measurements provide a good example of how the anisotropy of the structure may influence the results. The observed frequency and temperature dependence of the absorption coefficients at the lower end of the temperature range for several directions of propagation and polarization are given in table 4.6. It will be noticed that there is a considerable degree of anisotropy in the attenuation reflecting the internal symmetry of the crystal. Any theory such as that described in this chapter which utilises an average relaxation time will be somewhat hard pressed to explain all the aspects of these results.

TABLE 4.5

Material	Axis	T_{calc} (K)	T_{expt} (K)
MgO	[100]	44	45
	[110]	77	62
	[111]	230	70
Ge	[100]	36	43
	[110]	27	44
CaF$_2$	[100]	34	43
	[110]	24	40
Si	[100]	76	62
	[110]	48	62
α-quartz	x	> 130	30
Al$_2$O$_3$	(a)	> 175	103
	(c)	> 180	100

TABLE 4.6

Propagation direction	Polarization direction	ω	T
[110]	[110]	$\omega^{0.5}$	T^9
[001] (c)	[001]	$\omega^{1.1}$	T^7
[010] (a)	[010]	$\omega^{0.75}$	T^7
[001] (c)	[010]	$\omega^{1.0}$	T^4
[110]	[001]	$\omega^{1.2}$	T^3
[110]	[1$\bar{1}$0]	$\omega^{0.55}$	T^2

Experimental measurements of the low-temperature hypersonic attenuation of transverse modes in quartz have been made by KING [1970]. Because of anisotropy the selection rules of eq. (4.15) which referred to an isotropic situation are considerably relaxed for certain transverse modes. In addition to (v) it is also found that other selection rules are possible that also lead to a $\omega\tau^4$ law. Let (θ, ϕ) be the polar angles that the thermal phonon wave vector q_2 makes with the ultrasonic wave vector q_1. Then from fig. 4.12 it is clear that for the situation of interest when $q_1 \ll q_2, q_3$, $q_3 \approx q_2 + q_1 \cos \theta$ and $q_2 \approx q_1 \sin \theta / \delta\theta$. Also, to satisfy energy conservation $\Omega \equiv \omega_1 + \omega_2 - \omega_3$ must be zero. Assuming q_1 and q_2 belong to the same branch it follows on writing $v_3 = v_2 - \delta\theta(\partial v_2/\partial\theta)$ that the process is allowed if $\Omega \equiv q_1(v_1 - v_2 \cos \theta + \sin \theta \, \partial v_2/\partial\theta) = 0$. Because of the last term it is found that in cases of severe anisotropy processes such as $S + S \to S$, $F + F \to F$ and $S + F \to F$ may occur, where S and F refer to the slow and fast transverse branches respectively.

The modes examined by King were the slow and fast X-directed and the degenerate Z-directed transverse modes. His paper contains computer plots showing the allowed values of θ and ϕ for which each process is allowed. In addition to the variation of velocity due to anisotropy, some attempt was made to include dispersion. On the basis of these plots it was found that the slow transverse mode in the X-direction interacted most strongly with slow transverse thermal phonons through the process $S + S \to S$. Good agreement with experiment was obtained. The allowed three-phonon processes were found to be insufficient to explain the attenuation of the fast transverse mode in the X-direction and the lifetime effects had to be included to give
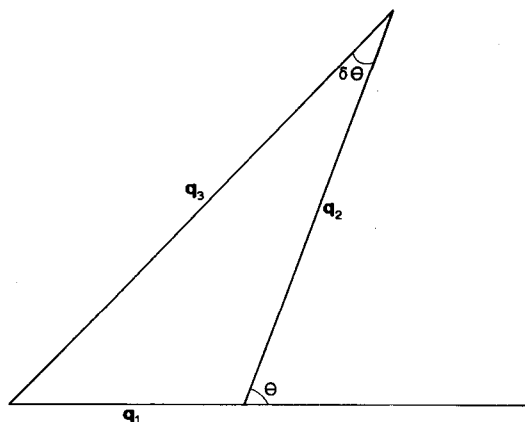
Fig. 4.12.

agreement with experiment. However interactions with fast transverse thermal phonons were responsible for the major part of the attenuation of the transverse modes in the Z-direction. The attenuation measurements at 1.01 GHz exhibited the usual plateau region above 60 K where the $\Omega\tau \ll 1$ regime applies. Below this temperature the attenuation fell sharply as a high power of the temperature and approached a T^4 law at very low temperatures.

KING and ROSENBERG [1970] reported measurements of the attenuation of 1 GHz ultrasonic waves in single crystal specimens of InSb and GaAs at low temperatures. InSb and GaAs are particularly good choices for the comparison of theory and experiment because the development of semiconductor technology has led to methods for producing large single crystals in a high state of perfection. Also the second- and third-order elastic constants are known and there is a good deal of information available on the phonon dispersion curves and the temperature dependence of the thermal conductivity.

The attenuation of the longitudinal modes which propagate in the $\langle 110 \rangle$ and $\langle 111 \rangle$ directions in GaAs was found to be proportional to T^4–T^5 at 20 K. Below this temperature the dependence of the attenuation on temperature was greater but the exact form could not be determined from the results. Above 20 K the dependence on temperature was reduced, being proportional to $T^{2.5}$ at about 75 K. The attenuation for these modes in InSb was found to be greater although measurements above 40 K were unreliable. At the lower temperature end the dependence was again between T^4 and T^5 and increasing at lower temperatures, while at the higher temperature end a T^2–T^3 law was observed. Measurements of the fast shear mode in the $\langle 110 \rangle$ direction in InSb also gave a T^4 law at low temperatures but the power of the temperature dependence decreased rapidly below 40 K. Comparisons were made of their results with predictions based on the work of SIMONS [1963] and MARIS [1964] which take into account the finite lifetimes of the thermal phonons with which the ultrasonic phonons interact, see the discussion of §2.6. Denoting longitudinal, fast transverse, slow transverse and degenerate transverse by L, F, S and T respectively they found that the main contributions to the attenuation of the longitudinal modes are as follows. In GaAs the main part of the attenuation for the $\langle 110 \rangle$ directed mode arises from the processes $L+L \rightarrow L$ and $L+S \rightarrow S$ with a contribution from the process $L+F \rightarrow F$ at high temperatures. In the $\langle 111 \rangle$ direction the process $L+L \rightarrow L$ dominates at all temperatures although the interaction with transverse thermal phonons through $L+T \rightarrow T$ plays a role at high temperatures. In the case of InSb all the processes, $L+L \rightarrow L$,

$L + S \rightarrow S$ and $L + F \rightarrow F$ can contribute to the attenuation of the $\langle 100 \rangle$ directed mode although the first of these again dominates except at the high temperature end. In the $\langle 110 \rangle$ direction $L + L \rightarrow L$ is found to be of less importance than $L + S \rightarrow S$ while the process $L + F \rightarrow F$ can be neglected. Finally for the $\langle 111 \rangle$ oriented wave the process $L + L \rightarrow L$ dominates over $L + T \rightarrow T$ at all temperatures.

ULTRASONIC WAVES IN FERROMAGNETIC MATERIALS

1. Resumé of the spin wave theory of ferromagnetism

In this chapter the propagation and the interaction of ultrasonic waves in ferromagnetic media will be described. In a magnetic medium the low-lying excited magnetic states have a wave-like nature and are known as spin waves. These can be coupled via magnetoelastic interactions to the elastic waves which are generated or excited thermally in the material. This coupling between the elastic and magnetic waves causes the velocity of the ultrasonic waves to depend upon the strength of externally applied magnetic fields and on the spontaneous magnetization of the material. It also provides a mechanism for the acoustic excitation of magnetic waves, or as described in ch. 3, a means whereby acoustic waves may be generated. In order to understand these phenomena the reader must be acquainted with the basic concepts of spin waves in ferromagnetic crystals. For completeness and in order to define the nomenclature this chapter will commence with an outline of the main features of ferromagnetism that are relevant to a discussion of these topics.

1.1. Concept of spin waves

In 1907 Weiss put forward his molecular field hypothesis to explain the phenomenon of ferromagnetism. He postulated the existence of regions, called domains, which were each spontaneously magnetized because of the presence of a very strong molecular field that tended to align the individual atomic magnetic moments in the domain. This hypothesis was successful in explaining the existence of spontaneous magnetization below the Curie temperature and the fact that the material could reach saturation magnetization by the application of only a very small external magnetic field. It was not until much later that the origin of the internal field was explained independently by Heisenberg and Dirac. Dirac showed that in a two-electron system,

because of the Pauli exclusion principle, spatial wave functions with different symmetries corresponded to different values of the total spin and consequently had different energy values associated with them. He showed that the interaction between the electrons could be written formally as $JS_1 \cdot S_2$ so that they behaved as if there existed a very strong magnetic-like coupling between the spin vectors. It should be emphasised that it is not a magnetic coupling in reality but a purely quantum effect related to the indistinguishability of the particles.

The Heisenberg exchange model of a ferromagnet is a generalization of this idea to an n-electron system. The Hamiltonian is written as

$$H = -\tfrac{1}{2} \sum_{n,m} J(R_{nm}) S_n \cdot S_m, \qquad (5.1)$$

where S_n and S_m are the total spins of the atoms at the lattice sites n and m and $J(R_{nm})$ may be regarded as an effective exchange coupling between them. In general the exchange parameter J will be a function of the separation vector R_{nm} of the two atoms. When or if this Hamiltonian is justified is still a matter of conjecture so we shall not attempt to justify it any further but merely regard it as a model Hamiltonian which in many instances yields results in favourable agreement with experiment. Even if the problem can be written in these simple terms the solution of eq. (5.1) is still a formidable problem and one has to resort to approximate techniques to solve it. In the presence of an external magnetic field H_0 there will be an additional term in the Hamiltonian, the Zeeman term. This is simply the sum of the energies of each spin in the magnetic field which will be taken to be directed along the z-axis. The total Hamiltonian is then

$$H = -\tfrac{1}{2} \sum_{n,m} J(R_{nm}) S_n \cdot S_m - g\beta H_0 \sum_n S_n^z \qquad (5.2)$$

g is the Landé g-factor and β is the Bohr magneton. It is recalled that the components of the spin operators satisfy the commutation rules

$$[S_n^x, S_m^y] = i\delta_{n,m} S_n^z,$$
$$[S_n^y, S_m^z] = i\delta_{n,m} S_n^x, \qquad (5.3)$$
$$[S_n^z, S_m^x] = i\delta_{n,m} S_n^y.$$

Rather than work with the x and y components of the spin operators it is convenient to introduce the operators S_n^+ and S_n^- defined through the relations

$$S_n^+ = S_n^x + iS_n^y, \qquad S_n^- = S_n^x - iS_n^y \qquad (5.4)$$

and satisfying the commutation rule

$$[S_n^+, S_m^-] = 2\delta_{n,m} S_n^z. \qquad (5.5)$$

If the eigenstates of S^z are denoted by $|m\rangle$ such that $S^z|m\rangle = m|m\rangle$ then S^+ and S^- operate on these states according to

$$S^+|m\rangle = [(S-m)(S+m+1)]^{1/2}|m+1\rangle,$$
$$S^-|m\rangle = [(S+m)(S-m+1)]^{1/2}|m-1\rangle. \tag{5.6}$$

In terms of these 'raising' and 'lowering' operators the scalar product $S_n \cdot S_m$ becomes $\tfrac{1}{2}(S_n^+S_m^- + S_n^-S_m^+) + S_n^zS_m^z$ so that the Hamiltonian of eq. (5.2) takes the form

$$H = -\tfrac{1}{2}\sum_{n,m} J(R_{nm})[\tfrac{1}{2}S_n^+S_m^- + \tfrac{1}{2}S_n^-S_m^+ + S_n^zS_m^z] - g\beta H_0\sum_n S_n^z. \tag{5.7}$$

In the ground state of the ferromagnet each spin will have its maximum allowable value of S_n^z, that is S. Above zero temperature, as the system is excited out of its ground state, deviations from maximum alignment of the spin will occur. Bloch demonstrated that the low-lying states of the system had wave-like properties giving rise to the concept of spin waves. A simple illustration of this is provided by a regular lattice in the form of a linear chain of spins each of magnitude $\tfrac{1}{2}$ coupled together by exchange forces which are restricted to nearest-neighbour inter- actions. The Hamiltonian for this lattice is

$$H = -J\sum_n [\tfrac{1}{2}(S_n^+S_{n+1}^- + S_n^-S_{n+1}^+) + S_n^zS_{n+1}^z] - g\beta H_0\sum_n S_n^z. \tag{5.8}$$

In the case of spin $\tfrac{1}{2}$ the z-component of spin can have two values, namely $m = \pm\tfrac{1}{2}$. At the absolute zero of temperature the ground state of eq. (5.8) corresponding to maximum alignment of spins may be written as

$$\phi_0 = |\tfrac{1}{2}\rangle_1 |\tfrac{1}{2}\rangle_2 \cdots |\tfrac{1}{2}\rangle_n \cdots |\tfrac{1}{2}\rangle_N$$

where N is the total number of spins on the lattice. By operating with the Hamiltonian operator of eq. (5.8) it is found by the use of the rules of eq. (5.6) that the energy of this state is

$$E_0 = -\tfrac{1}{4}JN - \tfrac{1}{2}g\beta H_0 N.$$

It might be expected that the first excited state is the situation where the spin on one site, say the nth site, has been reversed. That is the state $\phi_n = |\tfrac{1}{2}\rangle_1, |\tfrac{1}{2}\rangle_2 \cdots |-\tfrac{1}{2}\rangle_n \cdots |\tfrac{1}{2}\rangle_N$. Unfortunately, direct substitution shows that this state is in fact not an eigenstate of H for

$$H\phi_n = -J\left\{\tfrac{1}{2}\phi_{n+1} + \tfrac{1}{2}\phi_{n-1} + \left(\frac{N-2}{4} - \frac{2}{4}\right)\phi_n\right\} - g\beta H_0\left(\frac{N-1}{2} - \frac{1}{2}\right)\phi_n.$$

The Hamiltonian is seen to couple the state ϕ_n to the states ϕ_{n+1} and ϕ_{n-1}. However, instead of this state suppose that a linear combination of the ϕ_n's modulated by a wave-like factor $\exp(i\,kna)$ is taken. That is,

states of the type $\psi_k = N^{-1/2} \sum_n \phi_n \exp(ikna)$ are formed, a being the lattice spacing. The operation of the Hamiltonian on this state gives

$$H\psi_k = -JN^{-1/2} \sum_n \left\{ \tfrac{1}{2}\phi_{n+1} + \tfrac{1}{2}\phi_{n-1} + \frac{(N-4)}{4}\phi_n \right\} \exp(ikna)$$
$$- g\beta H_0 N^{-1/2} \left(\frac{N-2}{2}\right) \phi_n \exp(ikna).$$

If, in analogy with the one-dimensional phonon problem, periodic boundary conditions are now imposed on the wave functions such that the $(N+1)$th spin may be regarded as the first, then

$$H\psi_k = \{-\tfrac{1}{2}J(e^{ika} + e^{-ika}) - \tfrac{1}{4}(N-4)J - \tfrac{1}{2}g\beta H_0(N-2)\}\psi_k.$$

To satisfy this boundary condition k must be such that $\exp(ikNa)$ is unity, that is $k = 2\pi p/Na$ where p is an integer. It is seen that ψ_k is indeed an eigenfunction of the Hamiltonian having an eigenenergy

$$E_1 = -J \cos ka - \tfrac{1}{4}(N-4)J - \tfrac{1}{2}g\beta H_0(N-2).$$

Because of the wave-like nature of ψ_k it is referred to as a spin wave, and it has an energy relative to the ground state of

$$E_1 - E_0 = g\beta H_0 + J(1 - \cos ka). \tag{5.9}$$

The spin wave state considered above involving the reversal of one spin is an exact stationary state of the system. What happens if the treatment is extended to two 'reversals' of spin? Bloch proposed that at low temperatures the eigenstates of the ferromagnet would be very nearly a linear superposition of non-interacting spin waves. It is evident that this is only an approximation for clearly in the case of $S = \tfrac{1}{2}$ there must be some interaction between the spin wave states since it is not possible to have two spin deviations at a single site if the individual spins have only two states.

The interaction between spin waves was first investigated in detail by DYSON[1956]. Basically there are two types of interaction. The first is known as the kinematical interaction which is a repulsive interaction that prevents the spin waves from piling up at the same site, that is one cannot have more than $(2S + 1)$ spin deviations at a given lattice site. Mathematically it arises because spin wave states containing more than one spin wave are not members of an orthogonal set. The second interaction, the dynamical interaction, arises because these states do not diagonalize the exchange Hamiltonian. This interaction is attractive and gives rise to a shift of the spin wave energy because of the presence of other spin waves. It arises because the energy required to reverse a spin is lowered if the neighbouring spins are reversed. Dyson showed that at low temperatures the kinematical interactions

are negligible; this implies that any number of spin waves of a given vector k can be excited and thus Bose–Einstein statistics may be used. The theory of spin waves has been developed along three different lines: (a) a microscopic quantum mechanical approach; (b) a semi-classical method which starts with a microscopic model but then treats the spin moments as classical vectors; (c) a continuum theory which should be valid for spin waves of long wavelength. The latter approach may be regarded as the limiting case of the microscopic theory just as in ch. 2 it was seen that the long wavelength limit of lattice dynamics is intimately related to the classical theory of elasticity. An outline of the main features of these theories will now be given.

1.2. *The microscopic theory*

The Hamiltonian in the microscopic theory has already been given in the previous section, eq. (5.7). To obtain the solution of this Hamiltonian the approach developed by HOLSTEIN and PRIMAKOFF[1940] will be followed. The essential point in their treatment is that they replaced the spin operators S_n^+ and S_n^- by Bose operators by utilizing the following transformation

$$S_n^+ = (2S)^{1/2}(1 - a_n^* a_n/2S)^{1/2} a_n$$

$$S_n^- = (2S)^{1/2} a_n^* (1 - a_n^* a_n/2S)^{1/2} \qquad (5.10)$$

$$S_n^z = S - a_n^* a_n$$

where the Bose operators satisfy the usual relationship

$$a_n a_m^* - a_m^* a_n = \delta_{n,m}$$

$$a_n a_m - a_m a_n = a_n^* a_m^* - a_m^* a_n^* = 0. \qquad (5.11)$$

It is readily checked by direct substitution that this transformation of the spin operators to Bose operators satisfies the required commutation rules of eq. (5.5). It is noticed that the quantity $a_n^* a_n$ determines the deviation of the z-component of the spin of the nth atom from its maximum value S. The $(2S + 1)$-level spin system has been replaced by a Bose system which has an infinite set of states associated with it. Thus, although the transformation preserves the correct commutation rules it does not give the correct number of states. However Holstein and Primakoff argued that the approach is realistic at low temperatures where the deviation of the spins from their maximum projection is small. In mathematical terms the expectation value of $a_n^* a_n$ is small compared to S. In this region the authors proposed that one could expand the square-root sign in the expressions of eq. (5.10) and retain only the leading terms in the expansion. The transformation then

becomes

$$S_n^+ \approx (2S)^{1/2} a_n, \quad S_n^- \approx (2S)^{1/2} a_n^*, \quad S_n^z \approx S - a_n^* a_n. \quad (5.12)$$

With this substitution the Hamiltonian transforms to

$$H = -\tfrac{1}{2} \sum_{n,m} J(R_{nm}) [S(a_n a_m^* + a_n^* a_m) + (S - a_n^* a_n)(S - a_m^* a_m)]$$

$$- g\beta H_0 \sum_n (S - a_n^* a_n)$$

$$= -S \sum_{n,m} J(R_{nm})(a_n^* a_m - a_n^* a_n) + g\beta H_0 \sum_n a_n^* a_n + \text{constant}$$

if terms greater than quadratic in the Bose operators are ignored. The value of the constant is

$$-S^2 \sum_{n,m} \tfrac{1}{2} J(R_{nm}) - g\beta H_0 N S$$

where N is the total number of atoms. In order to introduce spin waves the Fourier transform of the operators defined by

$$a_k = N^{-1/2} \sum_n e^{-ik \cdot r_n} a_n; \qquad a_k^* = N^{-1/2} \sum_n e^{ik \cdot r_n} a_n^*$$

is introduced. These operators satisfy $[a_k, a_{k'}^*] = \delta_{k,k'}$ and are therefore also Bose operators. Direct substitution into the Hamiltonian gives

$$H = \sum_k \epsilon_k a_k^* a_k + \text{constant}$$

where

$$\epsilon_k = S \sum_h J(h)(1 - e^{ik \cdot h}) + g\beta H_0 \quad (5.13)$$

and h are the vectors connecting each atom to the atom regarded as the origin. For the linear chain considered earlier h has two values $\pm a$ and for that lattice eq. (5.13) reduces to

$$\epsilon_k = 2JS(1 - \cos ka) + g\beta H_0. \quad (5.14)$$

This agrees with eq. (5.9) if it is remembered that in that example S was $\tfrac{1}{2}$. In the long wavelength limit, $k \to 0$

$$\epsilon_k \approx JSk^2 a^2 + g\beta H_0. \quad (5.15)$$

If the small applied direct magnetic field is neglected then the energy of the spin excitation is proportional to k^2 in contrast to that of a phonon in the Debye limit which is proportional to k. It will be seen later, §2.2, that this is important because it allows the spin wave and phonon dispersion curves to intersect.

In the theory sketched above only the exchange and Zeeman energies have been treated. In magnetic materials other interactions are present, for example the magnetic dipole interaction between the

spins. In their classic paper, Holstein and Primakoff did include this interaction in the Hamiltonian. It has the form

$$H_d = \tfrac{1}{2} \sum_{\substack{n,m \\ \neq}} g^2 \beta^2 \left[\frac{S_n \cdot S_m}{R_{nm}^3} - \frac{3 (S_n \cdot R_{nm})(S_m \cdot R_{nm})}{R_{nm}^5} \right]. \quad (5.16)$$

The inclusion of this term gives rise to considerable complications. Nevertheless with certain assumptions the authors showed that the Hamiltonian can be reduced to

$$H = C + \sum_k A_k a_k^* a_k + \sum_k (\tfrac{1}{2} B_k a_k a_{-k} + \tfrac{1}{2} B_k^* a_k^* a_{-k}^*) \quad (5.17)$$

where the constant term C is

$$-\tfrac{1}{2} \sum_{n,m} J(R_{nm}) S^2 - g\beta N H_0 S + \tfrac{1}{2} \sum_{\substack{n,m \\ \neq}} \frac{g^2 \beta^2 S^2}{R_{nm}^3} \left(1 - \frac{3 z_{nm}^2}{R_{nm}^2} \right). \quad (5.18)$$

The first two terms are the same as before and correspond to the energy when all the atomic moments point in the direction of H_0. The last term is the mutual dipole–dipole interaction of the atomic moments. To unscramble the k's and $-k$'s in the last term of eq. (5.17) a further transformation is necessary to diagonalize the Hamiltonian. The final result is

$$H = C + \sum_k \{ [A_k^2 - |B_k|^2]^{1/2} (C_k^* C_k + \tfrac{1}{2}) - \tfrac{1}{2} A_k \} \quad (5.19)$$

C_k^* and C_k are again Bose operators and A_k and B_k are given by the following expressions

$$A_k = A_{-k} = JSk^2 a^2 + g\beta (H_0 - 4\pi N_z M_0) + 2\pi g \beta M_0 \sin^2 \theta_k,$$
$$B_k = B_{-k} = 2\pi g \beta M_0 \sin^2 \theta_k \exp(-2i\phi_k). \quad (5.20)$$

where $J = J(R_h)_{NN}$, M_0 is the saturation magnetization and θ_k and ϕ_k are the polar angles of k with the z-axis parallel to H_0. N_z is the demagnetization factor for the z-direction, see §1.3. In what follows $(H_0 - 4\pi N_z M_0)$ will be written as H_i. This result is valid for a cubic lattice with nearest neighbour exchange interactions. The expressions for A_k and B_k are valid only in a certain range which is discussed in the next paragraph.

In the derivation of A_k, B_k and the constant term in eq. (5.18) there are difficulties in the evaluation of dipole sums which have the form

$$S_{ij}(k) = \sum_n r_n^{-5} [3 r_n^i r_n^j - \delta_{i,j} (r_n)^2] \exp(ik \cdot r_n).$$

The superscripts indicate the cartesian components of the position vectors. Consider first the sums when k is zero. These terms reduce to

the usual dipole field factors which are discussed in the next section. In general the sums depend upon the origin unless the specimen is ellipsoidal. It is therefore usual to consider only ellipsoidal specimens since it is only samples of this shape that can have a uniform magnetization when placed in a magnetic field. To evaluate the lattice sums one introduces the concept of a Lorentz sphere. The volume is divided into two by considering a Lorentz sphere of radius R_L such that R_L is much larger than the atomic spacing and so contains many atomic sites, but at the same time it is much smaller than the total volume. The sum over the Lorentz sphere is treated directly taking into account the actual structure. For cubic symmetry $S_{ij}(0)$ is found to be zero. The remaining volume is treated by replacing the discrete summation by a volume integral. By integrating by parts this volume integral is converted to surface integrals over the surfaces S_1 and S_2 shown in fig. 5.1. The integration over S_1 gives rise to a factor $\frac{4}{3}\pi$, the Lorentz factor, whereas the integration over the surface gives rise to demagnetization factors. The dipole sums are therefore shape dependent because they have to satisfy the boundary conditions at the surface of the specimen.

Consider now the summations with non-zero k. For k greater than zero but less than about ten times the reciprocal of the sample dimensions, the solutions are very complicated because the boundary conditions at the surface can no longer be described in terms of simple demagnetization factors. Furthermore the dipole sums are found to be strongly position dependent. This constitutes the region of the magnetostatic modes and the simple spin wave picture breaks down. However for k greater than about ten times the reciprocal of the sample dimensions, the modulating factor $\exp(i\mathbf{k}\cdot\mathbf{r})$ has the effect of eliminating the problem of the cut-off at the surface of the sample since the dipole
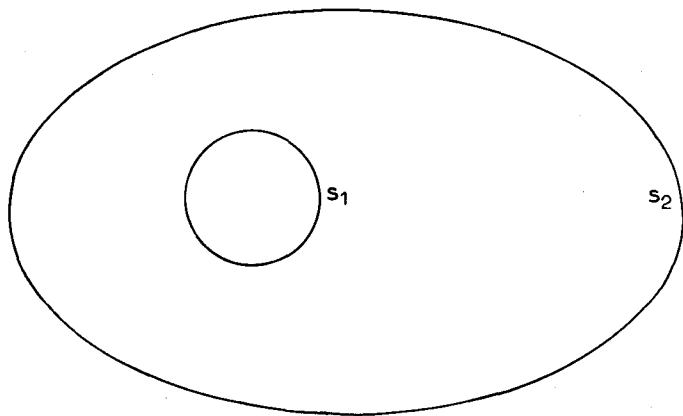
Fig. 5.1.

sums fluctuate across the specimen. In this region the surface effects disappear and the dipole sums are position independent. This is the region for which the result of eq. (5.20) is valid. It should be stated though, that it was assumed also that k was much less than a reciprocal lattice spacing. If this were not so the $S_{ij}(k)$ would have to be evaluated numerically since they would then be severely dependent upon the structure.

This completes the basic features of the microscopic spin wave model which will be needed in subsequent sections. It has been mentioned already that the spin wave theory may also be introduced in a purely phenomenological manner. This method will now be described.

1.3. *The phenomenological theory*

In the phenomenological theory it is assumed that the state of the magnetic crystal is described by its magnetic density $M(r)$, the magnetization per unit volume about the point at position r, which is regarded as a continuous function in space. Increase in energy of the magnetic crystal arises from departures from uniformity of $M(r)$. The basic assumption of the phenomenological theory is that only those oscillations are allowed for which the modulus of the vector remains constant, that is $M \cdot M = M_0^2$. Macroscopically the energy can be expressed in terms of the space derivatives of M. If the energy density $W(r)$ is expanded in a power series of the space derivatives of M, the leading term is

$$W(r) = A_{\alpha\beta\gamma\delta} \frac{\partial m_\alpha}{\partial r_\gamma} \frac{\partial m_\beta}{\partial r_\delta} \tag{5.21}$$

where $m_\alpha = M_\alpha(r)/M_0$. The form of the tensor components will be determined by the symmetry elements of the crystal. There is no linear term because there must be symmetry with respect to change in sign of time. Furthermore the isotropic exchange contribution of eq. (5.21) must be invariant with respect to reversal of m and therefore it has the form

$$W(r) = A_{\gamma\delta} \frac{\partial m_\alpha}{\partial r_\gamma} \frac{\partial m_\alpha}{\partial r_\delta}. \tag{5.22}$$

It might be thought that eq. (5.21) should include terms involving the components of m and their first derivatives. These terms, on integrating over the volume, would only give expressions depending on the properties of the surface of the body. Also it might be thought that terms involving the components of m and their second derivatives should appear; however, integration over the volume would give products of the first derivatives so they are in fact already included in eq. (5.21). From the symmetry properties of a cubic crystal the tensor components $A_{\gamma\delta}$ reduce to $A\delta_{\gamma\delta}$ so that for this symmetry the energy

density is

$$W(r) = A \left(\frac{\partial m_\alpha}{\partial r_\gamma} \right)^2 \tag{5.23}$$

or in terms of α_1, α_2 and α_3, the direction cosines of M

$$W(r) = A \left[(\nabla \alpha_1)^2 + (\nabla \alpha_2)^2 + (\nabla \alpha_3)^2 \right]. \tag{5.24}$$

This is the exchange energy of a cubic crystal on the macroscopic model. It is of interest to make contact with the microscopic approach by giving an argument that relates A to microscopic parameters. For a simple cubic crystal with only nearest-neighbour interactions the microscopic Hamiltonian of eq. (5.1) becomes $H = -\frac{1}{2} J \Sigma_n S_n \cdot \Sigma_h S_{n+h}$ where the sum over h is over the six vectors connecting n to its six nearest-neighbours. The spin vectors are now regarded as classical vectors and it is assumed that the variation from site to site can be regarded as forming a continuous field. Performing a Taylor expansion about the site n, $\Sigma_h S_{n+h} = 6 S_n + a^2 \nabla^2 S_n$ where a is the lattice spacing. If S_n is now replaced by $S M(r_n)/M_0$ and, as should be reasonable in the long wavelength limit, the summation approximated by an integral, then

$$H = \text{constant} - \frac{1}{2} J \int \frac{NS}{M_0} M(r) \cdot \frac{a^2 S}{M_0} \nabla^2 M(r) \, dr$$

where N is the number of magnetic ions per unit volume. The stiffness constant A can therefore be related to the exchange constant J by noting that the exchange contribution is

$$H_{ex} = -\frac{JNS^2 a^2}{2 M_0^2} \int M \cdot \nabla^2 M \, dr. \tag{5.25}$$

Integrating by parts this becomes

$$H_{ex} = \frac{1}{2} JNS^2 a^2 \int \left[(\nabla \alpha_1)^2 + (\nabla \alpha_2)^2 + (\nabla \alpha_3)^2 \right] dr \tag{5.26}$$

since the surface integral vanishes because of inversion symmetry. Comparison of eqs. (5.24) and (5.26) gives the result

$$A = \frac{1}{2} JNS^2 a^2. \tag{5.27}$$

In addition to the isotropic exchange term of eq. (5.23) there must be other terms in the Hamiltonian that reflect the fact that there exist directions of easy magnetization, that is to say preferred directions along which the magnetization vector would like to sit. On the microscopic scale these terms arise from magnetic dipole interactions and from the interaction between magnetic moments and the electric fields of the crystal lattice. Both of these effects are of relativistic origin and are consequently much smaller than the exchange interaction because they involve the factor $(v/c)^2$ where v is the electron velocity and c is

the velocity of light. Nevertheless, they must be included in the theory if anisotropy is to be accounted for. This is because the exchange energy by itself is a scalar product of the magnetization components and is therefore invariant to the rotation of the direction of M.

On the microscopic level the magnetic dipole interaction is given by the Hamiltonian of eq. (5.16). To effect a transition from the microscopic to the macroscopic model it is convenient to introduce a spin vector density $S(r)$ defined by

$$S(r) = \sum_n S_n \delta(r - r_n). \tag{5.28}$$

This operator represents the spin moment density at position r because its integral over a volume is equal to the total spin in the volume. The magnetization may then be introduced through the operator

$$\hat{M}(r) = g\beta S(r). \tag{5.29}$$

The average value of this operator over a physically infinitesimal volume element is the macroscopic magnetic moment density $M(r)$. Unfortunately, a difficulty arises in replacing the summations over discrete sites by integrals over space. For a fixed n it is necessary to divide the summation over m into two regions separated by a spherical boundary of radius R as described in §1.2. R is chosen to be much greater than the lattice spacing but at the same time very much less than the length over which there is an appreciable change in the magnetization. In this way the dipolar contribution is split into two parts

$$W_d^{(1)} = -\tfrac{1}{2}\Omega^2 \sum_{\substack{n,m \\ R_{nm} > R}} M_i(r_n) M_j(r_m) \frac{\partial^2}{\partial R_{nm}^i \partial R_{nm}^j} \frac{1}{R_{nm}}$$

and

$$W_d^{(2)} = -\tfrac{1}{2}\Omega^2 \sum_{\substack{n,m(+) \\ R_{nm} < R}} M_i(r_n) M_j(r_m) \frac{\partial^2}{\partial R_{nm}^i \partial R_{nm}^j} \frac{1}{R_{nm}}$$

Ω is the volume of the unit cell. Since the magnetization varies slowly from one lattice site to another, the summations in $W_d^{(1)}$ may be replaced by integrals

$$W_d^{(1)} = -\tfrac{1}{2} \iint_{|r-r'|>R} dr dr' M_i(r) M_j(r') \frac{\partial^2}{\partial r^i \partial r^j} \frac{1}{|r-r'|}.$$

In the expression for $W_d^{(2)}$ one replaces $M(r_n)$ by $M(r_m)$ but the summation over m is done explicitly

$$W_d^{(2)} = -\tfrac{1}{2}\beta_{ij} \int dr M_i(r) M_j(r)$$

where

$$\beta_{ij} = \Omega \sum_{\substack{n,m(\neq) \\ R_{nm}<R}} \frac{\partial^2}{\partial R_{nm}^i \partial R_{nm}^j} \frac{1}{R_{nm}}.$$

Now in magnetic materials the magnetic field H_d due to the magnetization M is given by

$$H_d(r) = -\operatorname{grad} \phi(r) \tag{5.30}$$

where $\phi(r)$ is the magnetostatic potential

$$\phi(r) = \int M(r') \operatorname{grad}_{r'} \left| \frac{1}{r-r'} \right| dr' \tag{5.31}$$

or in usual form

$$\phi(r) = -\int_V dr' \frac{\operatorname{div} M(r')}{|r-r'|} + \int \frac{dS \cdot M(r')}{|r-r'|}. \tag{5.32}$$

Using eq. (5.30) it may readily be verified that $W_d^{(1)}$ can be expressed in the form

$$W_d^{(1)} = -\tfrac{1}{2} \int_V dr \{\tfrac{4}{3}\pi M \cdot M + M \cdot H_d\}. \tag{5.33}$$

These dipolar terms which have been obtained give rise to anisotropy in the spin wave spectrum. Additional anisotropy arises from the interaction of the spin of the electrons with the electric field of the crystal lattice. This mechanism takes place through the orbit-lattice and the spin-lattice coupling. A general expression for this is very complicated and its derivation would certainly be out of place here but it is worth mentioning that the effect gives rise to terms in the energy density which depend on the products of the components of M. In the phenomenological theory the form of these terms is deduced merely by symmetry arguments, no explicit expressions being given for the tensor coefficients that occur. Because the term $W_d^{(2)}$ of the dipolar interaction is of the same form, this is usually regarded as being included in the anisotropy terms deduced from the crystal symmetry and the dipolar term is taken to be just the long-range part

$$W_d = -\tfrac{1}{2} \int M \cdot H_d \, dr \tag{5.34}$$

where H_d is the solution of Maxwell's equation of magnetostatics satisfying the boundary conditions at the surface of the specimen. In particular it is noted that if M is uniform

$$H_d(r) = \operatorname{grad} \left(M \cdot \int_V \operatorname{grad} \frac{dr'}{|r-r'|} \right) = -4\pi N(r) : M$$

where $N(r)$ is a tensor whose components are

$$N_{ij}(r) = -\frac{1}{4\pi}\frac{\partial^2}{\partial r^i \partial r^j}\int_V \frac{dr'}{|r-r'|}.$$ (5.35)

Only in the case of an ellipsoidal specimen is the field inside the specimen uniform. The tensor N is known as the demagnetization tensor. If the coordinates have axes lying along the principal axes of the ellipsoid then N has only diagonal elements, N_1, N_2, N_3 and their sum is equal to unity. (Sometimes the factor 4π is included in the definition of N.) The values of the components of the demagnetization factors for various symmetries are listed in table 5.1.

TABLE 5.1
Demagnetization factors for different symmetries

Shape	Direction of field	N	Uniform mode frequency ω_0 (eq. (5.51))
Sphere	any	$N_x = N_y = N_z = \frac{1}{3}$	γH_0
Long circular cylinder	longitudinal	$N_x = N_y = \frac{1}{2}, N_z = 0$	$\gamma(H_0 + 2\pi M_0)$
	transverse	$N_x = N_z = \frac{1}{2}, N_y = 0$	$\gamma[H_0(H_0 - 2\pi M_0)]^{1/2}$
Thin infinite disc	in plane of disc	$N_y = N_z = 0, N_x = 1$	$\gamma[H_0(H_0 + 4\pi M_0)]^{1/2}$
	normal to disc	$N_x = N_y = 0, N_z = 1$	$\gamma(H_0 - 4\pi M_0)$

The anisotropy terms on the macroscopic model are deduced with the aid of the symmetry operations of the crystal. The magnetocrystalline anisotropy is a power series of the magnetization components. Since the anisotropy energy must be invariant with respect to the change in sign of time, the anisotropy energy must be an even function of the direction cosine of M. This is because the magnetization changes sign under the reversal of time. It is usual to write

$$W_{\text{anis}} = K_{n_1 n_2 n_3} m_x^{n_1} m_y^{n_2} m_z^{n_3} = K(m)$$ (5.36)

where $n_1 + n_2 + n_3$ is an even integer and the non-zero components of K are determined from the crystal symmetry as will be shown below for the case of a cubic crystal. Unfortunately two slightly different expansions have appeared in the literature. In one, the magnetocrystalline anisotropy is expressed in terms of anisotropy *constants* while in the other anisotropy *coefficients* have been introduced. To avoid confusion we shall distinguish between the two. The problem is to find products of even powers of the components of M which are invariant with respect to the operations of crystal symmetry but are dependent

upon the direction of M. Let us specialize the argument to cubic symmetry. The only quadratic combination of the components of M which is invariant under cubic symmetry is $M_x^2 + M_y^2 + M_z^2$. However this is independent of the direction of M and therefore does not contribute to anisotropy. It is necessary to go to fourth order where there are two quartic invariants, $M_x^2 M_y^2 + M_z^2 M_x^2 + M_y^2 M_z^2$ or $\frac{1}{2}(M_x^4 + M_y^4 + M_z^4)$. These are not independent because their sum is $\frac{1}{2}(M_x^2 + M_y^2 + M_z^2)^2$ and so only one of them need be considered. The next term will be of sixth order. The term M^6 must be excluded together with functions that differ from the quartic invariants by a factor M^2. This leaves the single invariant which can be taken as $M_x^2 M_y^2 M_z^2$. In terms of the direction cosines of the magnetization the anisotropy can therefore be written in the form

$$W_{\text{anis}}^{\text{cubic}} = K_1(\alpha_1^2 \alpha_2^2 + \alpha_2^2 \alpha_3^2 + \alpha_3^2 \alpha_1^2) + K_2 \alpha_1^2 \alpha_2^2 \alpha_3^2 + \cdots. \qquad (5.37)$$

Similar arguments may be applied to obtain the anisotropy energies for other symmetries. The K's in the above expression are usually referred to as anisotropy constants. It was pointed out by ZENER[1954] that a more natural expansion would be in terms of linear combinations of spherical harmonics that satisfy the crystal symmetry. Such combinations are known as Kubic harmonics. The Kubic harmonics for cubic symmetry have been listed in cartesian coordinates by VON DER LAGE and BETHE[1947] and using the fact that $\alpha_1^2 + \alpha_2^2 + \alpha_3^2 = 1$ they may be rewritten in the form shown in table 5.2. In terms of these harmonics the anisotropy can be expressed in the form

$$W_{\text{anis}}^{\text{cubic}} = \kappa_0 + \kappa_4 g_4 + \kappa_6 g_6 + \kappa_8 g_8. \qquad (5.38)$$

The κ's have been referred to by CALLEN and CALLEN[1960] as anisotropy coefficients. It will be noted that in general the K's are linear combinations of the κ's. For instance, if only two anisotropy constants

TABLE 5.2

Kubic harmonics normalized to 4π for cubic symmetry

$g_0 = 1$

$g_4 = \frac{5}{2}\sqrt{21}\,(s - \frac{1}{5})$

$g_6 = \frac{231}{8}\sqrt{26}\,(p - \frac{1}{105} - \frac{1}{11}[s - \frac{1}{5}])$

$g_8 = \frac{65}{8}\sqrt{561}\,(s^2 - \frac{1}{21} - \frac{18}{65}[s - \frac{1}{5}] - \frac{4}{5}[p - \frac{1}{105}])$

with $s = \alpha_1^2 \alpha_2^2 + \alpha_1^2 \alpha_3^2 + \alpha_2^2 \alpha_3^2$

$\qquad p = \alpha_1^2 \alpha_2^2 \alpha_3^2$

These can be shown to agree with $\alpha_0 \ldots \alpha_8$ of Von der Lage and Bethe[a]) if it is remembered that $\alpha_1^2 + \alpha_2^2 + \alpha_3^2 = 1$.

---

[a]) There is a misprint in this reference. The last term of α_8 should be $-\frac{1}{3}\rho^8$ rather than $-\frac{1}{6}\rho^8$.

are adequate to describe the anisotropy, the connection between the constants and the coefficients is

$$22K_1 + 2K_2 = 55\sqrt{21}\,\kappa_4; \qquad 8K_2 = 231\sqrt{26}\,\kappa_6.$$

Sometimes the normalizing factors of the g's are incorporated in the κ's so as to minimize the difference between the K's and the κ's. General expressions for the anisotropy energy of all the 32 crystal classes have been tabulated by DORING[1958].

It is often convenient to express the effect of the anisotropy energy in terms of an equivalent magnetic field. The equivalent field is defined such that the torque exerted on the specimen by the field is equal to the torque exerted by the anisotropy energy. Frequently an additional advantage, particularly for directions of high symmetry, is to express these fields in terms of effective demagnetization factors, these are then additive to the demagnetization factors arising from the shape of the specimen.

1.4. *Oscillations of the magnetic moment*

The total classical energy of the ferromagnet is

$$W(r) = \frac{A_{\gamma\delta}}{M_0^2}\frac{\partial M_\alpha}{\partial r_\gamma}\frac{\partial M_\alpha}{\partial r_\delta} + K(M) - \tfrac{1}{2}M\cdot H_\mathrm{d} - M\cdot H_0. \qquad (5.39)$$

The leading two terms are the exchange and anisotropy energies, given by eqs. (5.22) and (5.36) respectively. The third term is the magnetostatic long-range part of the energy density related to the demagnetization fields of the volume and surface magnetic charges, see eq. (5.34), and the last term is the energy of the ferromagnet in the external magnetic field H_0. The demagnetization field H_d is given by

$$H_\mathrm{d} = \mathrm{grad}\int_V \frac{\mathrm{div}\,M(r')\,\mathrm{d}r'}{|r-r'|} - \mathrm{grad}\oint \frac{M(r')\,\mathrm{d}S'}{|r-r'|} \qquad (5.40)$$

where the surface integral is over the surface of the specimen. For a uniform magnetization in an ellipsoidal sample the first integral will be zero and the surface integral gives rise to the usual demagnetization factors for the specimen. The field H_d can be obtained with the aid of the Maxwell equations for magnetostatics

$$\mathrm{curl}\,H = 0 \quad \text{and} \quad \mathrm{div}\,H = -4\pi\,\mathrm{div}\,M. \qquad (5.41)$$

To consider oscillations of the magnetic moment about equilibrium one should, of course, use the complete Maxwell equation of electrodynamics

$$\mathrm{curl}\,H = \frac{4\pi}{c}\,j + \frac{1}{c}\frac{\partial D}{\partial t} \qquad (5.42)$$

where j is the current density and D the displacement current. For a dielectric, which is of interest in ultrasonic work, j is zero and neglect of the displacement current is permissible if the discussion is restricted to low frequency oscillations for which a magnetostatic approximation is valid.

The classical approach to the discussion of the oscillations is based on the equation of motion of the classical magnetization vector $M(r)$. Remembering the assumption that $M^2(r)$ is a constant M_0^2, implying rigidity of the magnetic moment, the equation of motion is the familiar torque equation

$$\dot{M} = +\gamma[M \times H_e] \tag{5.43}$$

where H_e is the effective magnetic field acting on the magnetization M and $\gamma = g\beta/\hbar$ is the reciprocal of the gyromagnetic ratio. The effective field may be regarded as the negative of the functional derivative of $W(r)$ with respect to M for fixed magnetic induction. Since the energy density may be regarded as a function of both the components of M and their spatial derivatives the effective field is given by, MacDonald[1951]

$$H_e = -\frac{\partial W}{\partial M} + \frac{\partial}{\partial r_\alpha} \frac{\partial W}{\partial(\partial M/\partial r_\alpha)}. \tag{5.44}$$

The equilibrium direction of the magnetization vector, is of course determined by the condition

$$M_S \times H_e = 0. \tag{5.45}$$

Operating with the operator of eq. (5.44) on the expression of eq. (5.39) it follows for a cubic crystal, where there is only one exchange constant, that

$$\frac{dM}{dt} = \gamma\left\{\frac{2A}{M_0^2} M \times \nabla^2 M + M \times (H_0 + H_a + H_d^0 + h)\right\}. \tag{5.46}$$

H_a is the effective anisotropy field given by $-\partial K/\partial M$, H_d^0 is the usual static demagnetization field determined by the shape of the sample and h is the demagnetization field due to the spin wave oscillation. It is convenient to consider both M and H_d to be split into a constant and oscillating part proportional to $\exp\{i(\omega t - k \cdot r)\}$

$$M = M_S + m; \qquad H_d = H_d^0 + h. \tag{5.47}$$

As has been remarked at low frequencies h may be determined from eq. (5.41) and is readily found to be given by

$$h = -\frac{4\pi}{k^2} m \cdot k\, k \tag{5.48}$$

for the region discussed in §1.2 where the boundary effects are washed

away. To compare the result with that of §1.2 the transverse static demagnetization field and the anisotropy will be neglected so that M_S is parallel to H_0 which is taken to be aligned along the z-direction. This leaves

$$\frac{dM}{dt} = \gamma \left\{ \frac{2A}{M_0^2} M \times \nabla^2 M + M \times H_1 - M \times 4\pi (k \cdot m) k/k^2 \right\}. \quad (5.49)$$

Assuming m is small and essentially at right angles to M_S so that $m_z \ll m_x \sim m_y \ll M_0$, this equation can be linearized to give for its x- and y-components equations

$$m_x \left(i\omega - \frac{4\pi}{k^2} \gamma M_0 k_x k_y \right) - \gamma m_y \left(\frac{2A}{M_0} k^2 + H_1 + \frac{4\pi}{k^2} M_0 k_y^2 \right) = 0,$$

$$\gamma m_x \left(\frac{2A}{M_0} k^2 + H_1 + \frac{4\pi}{k^2} M_0 k_x^2 \right) + m_y \left(i\omega + \frac{4\pi}{k^2} \gamma M_0 k_x k_y \right) = 0 .$$

The solution of these equations for the frequency of oscillation ω is

$$\omega^2 = \gamma^2 \left[\frac{2A}{M_0} k^2 + H_1 \right] \left[\frac{2A}{M_0} k^2 + H_1 + 4\pi M_0 \sin^2 \theta_k \right] \quad (5.50)$$

where θ_k is the angle between k and H_0. It is seen that the energy $\hbar\omega$ given by eq. (5.50) agrees with the spin wave energy $[A_k^2 - |B_k|^2]^{1/2}$ of eq. (5.19) if the following replacements are made: $\gamma \rightarrow g\beta/\hbar$, $M_0 \rightarrow Ng\beta S$ and $A \rightarrow \frac{1}{2}JNS^2a^2$, see eq. (5.27).

It is again stressed that the above result is only correct where a plane wave expansion is possible. In a small region near $k = 0$ the correct boundary conditions at the surface of the specimen must be satisfied. These are that the magnetic potential ϕ and the normal component of B must be continuous. The problem has been solved by WALKER[1957] for the case of a general ellipsoid of revolution about z. Each mode is labelled by three numbers (n, m, r) where n and m refer to a particular spherical harmonic P_n^m associated with ϕ and r labels the roots of the secular equation.

Of particular interest in ferromagnetic resonance work is the homogeneous magnetostatic mode in which the magnetization is uniform. In this case, see §1.3, the dipolar sums give rise to the static demagnetization factors. The exchange torques play no part and the torque equation gives for the uniform precessional mode

$$\omega^2 = \gamma^2 [H_1 + 4\pi N_x M_0][H_1 + 4\pi N_y M_0]. \quad (5.51)$$

It is noted that this solution is not the zero k limit of eq. (5.50). This is because the two regimes are separated by the region of inhomogeneous magnetostatic modes discussed above. These three regions are shown in fig. 5.2.
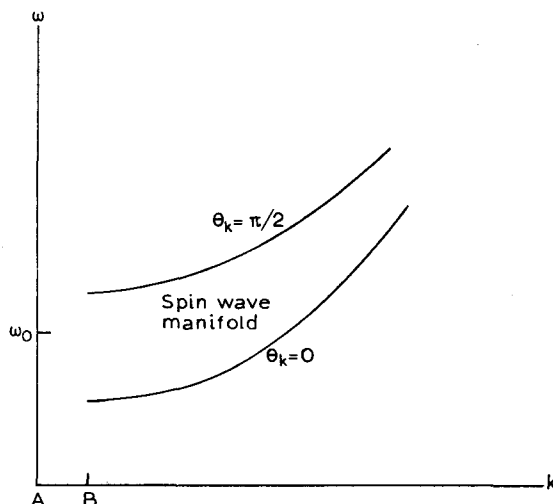
Fig. 5.2. The point labelled ω_0 is the ferromagnetic resonance mode (see table 5.1). For k-values in the range A to B, the magnetostatic modes of Walker exist. The spin-wave manifold at $k=0$ extends from $\omega = \gamma H_1$ to $\gamma[H_1(H_1+4\pi M_0)]^{1/2}$. The uniform mode ω_0 will be in this range if $H_1 > 4\pi M_0 N_x N_y/N_z$.

A quantum theory of spin waves can be obtained from the pheno-menological theory in the following way. The magnetization is thought of as arising from a distribution of electron spins at positions r_n. Then

$$\hat{M}(r) = \gamma\hbar \sum_n S_n \delta(r-r_n). \tag{5.52}$$

Making use of the commutation rules of the spins, the components of magnetic moment density $M(rt)$ satisfy the commutation rules

$$[\hat{M}_x(rt), \hat{M}_y(r't)] = i\gamma\hbar\hat{M}_z(rt)\delta(r-r'),$$

$$[\hat{M}_z(rt), \hat{M}_x(r't)] = i\gamma\hbar\hat{M}_y(rt)\delta(r-r'), \tag{5.53}$$

$$[\hat{M}_y(rt), \hat{M}_z(r't)] = i\gamma\hbar\hat{M}_x(rt)\delta(r-r').$$

Operators $a(rt)$ and $a^*(rt)$ can then be introduced by analogy with the discrete operators a_n and a_n^* of §1.2

$$\hat{M}^+ = (2\gamma\hbar M_0)^{1/2}\left(1-\frac{\gamma\hbar a^*a}{2M_0}\right)^{1/2} a,$$

$$\hat{M}^- = (2\gamma\hbar M_0)^{1/2}a^*\left(1-\frac{\gamma\hbar a^*a}{2M_0}\right)^{1/2}. \tag{5.54}$$

$$\hat{M}_z = M_0-\gamma\hbar a^*a,$$

where

$$a(rt)a^*(r't) - a^*(r't)a(rt) = \delta(r-r'). \qquad (5.55)$$

Near saturation of the magnetization the square-root sign can be expanded by the binomial theorem as before. After going over to the Fourier components of the a's, a diagonalization procedure similar to §1.2 can be followed and the energy spectrum of the spin waves obtained.

2. The interaction between magnons and phonons

2.1. *The magnetoelastic interaction*

A pioneering study of the magnon–phonon interaction was made by AKHIESER[1946]. He considered the modulation of the exchange and dipolar interactions by the lattice vibrations. The interaction arises because parameters, like the exchange constants, for example, are a function of the lattice spacing which, in the presence of vibrations, is varying. Mathematically the exchange parameters may be expanded in a Taylor series of the atomic displacements, which are then expressed in terms of Debye elastic waves giving rise to a coupling between the phonons and the magnons. Unfortunately, because the detailed form of the magnetic coupling on the interatomic spacing is not known the approach is not usually used but, rather, a phenomenological method is adopted based on the continuum model. In a saturated ferromagnetic insulator the magnetoelastic effects are treated phenomenologically by expanding the magnetocrystalline energy in a Taylor series expansion in terms of the strain components:

$$W_{\text{m-p}}(\alpha\epsilon) = W_{\text{anis}}(\alpha) + \sum_{ij} F_{ij}(\alpha)\epsilon_{ij} + \tfrac{1}{2}\sum_{ijkl} G_{ijkl}(\alpha)\epsilon_{ij}\epsilon_{kl}. \quad (5.56)$$

W_{anis} is the anisotropy energy of §1.3, α is a unit vector in the direction of the magnetization and ϵ_{ij} are the strain components of ch. 2, which describe the distortions of the crystal with respect to the unmagnetized state. Only the term linear in the strain components, which is the one leading to magnetostriction, will be retained here. The third term can be important when non-linear effects are discussed, §4.3. Of course, this is not the only term linear in the strain that couples the magnons and the phonons. This term is the one describing magnetoelastic effects which accompany homogeneous rotation of the magnetization vector. One can add to this other terms involving the spatial derivatives of the components of M. These terms, describing effects arising from the inhomogeneous magnetization, which were included by AKHIESER [1946] and in more detail by KAGANOV and TSUKERNIK[1959], arise

mainly from the isotropic exchange term. These will be included when the attenuation of sound is considered, §3. Because the magneto-crystalline energy must be invariant with respect to time reversal symmetry, the coefficients $F_{ij}(\alpha)$ given by $F_{ij}(\alpha) = (\partial W_{m-p}/\partial \epsilon_{ij})_{\epsilon_{ij}=0}$ must contain only even powers of the components of α. Suppose the term $\Sigma_{ij} F_{ij}(\alpha) \epsilon_{ij}$ is written in the tensor form $T : \epsilon$ where T is a second-rank tensor. Then from the symmetry operations of the crystal the form of the components of T can be determined. For example, BECKER and DORING[1939] have shown that for a cubic crystal

$$T_{11} = f(\alpha_1^2, s), \qquad T_{12} = \alpha_1 \alpha_2 g(\alpha_3^2, s),$$

where $s = \alpha_1^2 \alpha_2^2 + \alpha_1^2 \alpha_3^2 + \alpha_2^2 \alpha_3^2$ and the other non-zero components of T follow from symmetry. By expanding the functions F and G in a power series of the α-components they show that

$$T_{11} = b_0 + b_1(\alpha_1^2 - \tfrac{1}{3}) + b_3 s + b_4(\alpha_1^4 + \tfrac{2}{3}s - \tfrac{1}{3}) + \cdots,$$

$$T_{12} = b_2 \alpha_1 \alpha_2 + b_5 \alpha_1 \alpha_2 \alpha_3^2 + \cdots,$$

and therefore

$$
\begin{aligned}
W_{m-p} = {} & b_0[\epsilon_{11} + \epsilon_{22} + \epsilon_{33}] + b_1[(\alpha_1^2 - \tfrac{1}{3})\epsilon_{11} + (\alpha_2^2 - \tfrac{1}{3})\epsilon_{22} + (\alpha_3^2 - \tfrac{1}{3})\epsilon_{33}] \\
& + b_2[\alpha_1 \alpha_2(\epsilon_{12} + \epsilon_{21}) + \alpha_1 \alpha_3(\epsilon_{13} + \epsilon_{31}) + \alpha_2 \alpha_3(\epsilon_{23} + \epsilon_{32})] \\
& + b_3 s[\epsilon_{11} + \epsilon_{22} + \epsilon_{33}] + b_4[(\alpha_1^4 + \tfrac{2}{3}s - \tfrac{1}{3})\epsilon_{11} \\
& + (\alpha_2^4 + \tfrac{2}{3}s - \tfrac{1}{3})\epsilon_{22} + (\alpha_3^4 + \tfrac{2}{3}s - \tfrac{1}{3})\epsilon_{33}] \\
& + b_5[\alpha_1 \alpha_2 \alpha_3^2(\epsilon_{12} + \epsilon_{21}) + \alpha_1 \alpha_3 \alpha_2^2(\epsilon_{13} + \epsilon_{31}) \\
& + \alpha_2 \alpha_3 \alpha_1^2(\epsilon_{23} + \epsilon_{32})] + \cdots
\end{aligned}
\tag{5.57}
$$

The b_n's are known as the magnetoelastic constants. Sometimes, as in the case of the anisotropy constants, §1.3, rather than expand in a power series of the components of α, an expansion in combinations of the components having the symmetry of the crystal harmonics is more useful. The coefficients in this case are known as magnetoelastic coupling coefficients. The expression corresponding to eq. (5.57) is then, KITTEL and VAN VLECK[1960]

$$
\begin{aligned}
W_{m-p} = {} & \beta_0[\epsilon_{11} + \epsilon_{22} + \epsilon_{33}] + \beta_1[(\alpha_1^2 - \tfrac{1}{3})\epsilon_{11} + (\alpha_2^2 - \tfrac{1}{3})\epsilon_{22} + (\alpha_3^2 - \tfrac{1}{3})\epsilon_{33}] \\
& + \beta_2[2\alpha_1 \alpha_2 \epsilon_{12} + 2\alpha_2 \alpha_3 \epsilon_{23} + 2\alpha_3 \alpha_1 \epsilon_{13}] \\
& + \beta_3 s'(\epsilon_{11} + \epsilon_{22} + \epsilon_{33}) \\
& + \beta_4[p_4(\alpha_1)\epsilon_{11} + p_4(\alpha_2)\epsilon_{22} + p_4(\alpha_3)\epsilon_{33}] \\
& + \beta_5[(7\alpha_1 \alpha_2 \alpha_3^2 - \alpha_1 \alpha_2)\epsilon_{12} + (7\alpha_2 \alpha_3 \alpha_1^2 - \alpha_2 \alpha_3)\epsilon_{23} \\
& + (7\alpha_3 \alpha_1 \alpha_2^2 - \alpha_3 \alpha_1)\epsilon_{13}]
\end{aligned}
\tag{5.58}
$$

with

$$p_4(\mu) = \tfrac{8}{35}P_4(\mu) = \mu^4 - \tfrac{6}{7}\mu^2 - \tfrac{6}{70}$$

$$s' = \alpha_1^2\alpha_2^2 + \alpha_1^2\alpha_3^2 + \alpha_2^2\alpha_3^2 - \tfrac{1}{5}$$

and the relationships between the two sets of constants are

$$\beta_0 = b_0 + \tfrac{1}{5}b_3; \quad \beta_1 = b_1 + \tfrac{6}{7}b_4; \quad \beta_2 = b_2 + \tfrac{1}{7}b_5,$$

$$\beta_3 = b_3 + \tfrac{2}{3}b_4; \quad \beta_4 = b_4; \quad \beta_5 = \tfrac{2}{7}b_5.$$

2.2. *Macroscopic theory of magnetoelastic waves*

This subsection examines the influence of the magnon–phonon interaction on the propagation of elastic waves in a ferromagnetic dielectric. For simplicity the treatment will be applied to the particular case of crystals having cubic symmetry. The elastic energy density of a cubic crystal in the harmonic approximation is

$$W_{\text{L}}(r) = \frac{1}{2\rho}P(r) \cdot P(r) + \tfrac{1}{2}c_{11}[\epsilon_{xx}^2 + \epsilon_{yy}^2 + \epsilon_{zz}^2]$$

$$+ c_{12}[\epsilon_{xx}\epsilon_{yy} + \epsilon_{yy}\epsilon_{zz} + \epsilon_{zz}\epsilon_{xx}] + 2c_{44}[\epsilon_{xy}^2 + \epsilon_{xz}^2 + \epsilon_{yz}^2]. \quad (5.59)$$

To the elastic energy density must be added the magnetic energy density and the energy due to the magnon–phonon interaction. These are respectively

$$W_{\text{magn}} = \frac{A}{M_0^2}[(\text{grad } M_x)^2 + (\text{grad } M_y)^2 + (\text{grad } M_z)^2] - M_z H_0, \quad (5.60)$$

$$W_{\text{m-p}} = \frac{b_1}{M_0^2}[M_x^2\epsilon_{xx} + M_y^2\epsilon_{yy} + M_z^2\epsilon_{zz}]$$

$$+ \frac{2b_2}{M_0^2}[M_xM_y\epsilon_{xy} + M_yM_z\epsilon_{yz} + M_zM_x\epsilon_{zx}]. \quad (5.61)$$

The term in b_0 has been dropped since it only involves ϵ_{ii}. In the magnetic energy density only the isotropic exchange term and a Zeeman energy term for a magnetic field directed along the z-axis have been included. Effects of anisotropy and demagnetization will be treated later. In the magnon–phonon interaction only the terms quadratic in the components of $M(r)$ have been retained. We are now in a position to write down the coupled equations of motion for the combined system. To do this use is made of the fact that the equation of motion for the elastic displacement is

$$\rho\ddot{u}_i = \frac{\partial\sigma_{ik}}{\partial x_k} \quad (5.62)$$

where the components of the stress tensor are given by

$$\sigma_m = \frac{\partial W}{\partial \epsilon_m} \qquad (m = 1-6). \tag{5.63}$$

To these equations the equation of motion for the magnetization, eq. (5.43), must be added

$$\dot{M} = \gamma[M \times H_e], \tag{5.64}$$

where the effective field is given by eq. (5.44). In this way the following five equations are obtained

$$\rho \ddot{u}_x = c_{11} \frac{\partial^2 u_x}{\partial x^2} + c_{12} \left[\frac{\partial^2 u_y}{\partial x \partial y} + \frac{\partial^2 u_z}{\partial x \partial z} \right] + c_{44} \left[\frac{\partial^2 u_x}{\partial y^2} + \frac{\partial^2 u_y}{\partial x \partial y} + \frac{\partial^2 u_x}{\partial z^2} + \frac{\partial^2 u_z}{\partial x \partial z} \right]$$

$$+ \frac{b_1}{M_0^2} \frac{\partial}{\partial x} (M_x^2) + \frac{b_2}{M_0^2} \left[\frac{\partial}{\partial y} (M_x M_y) + \frac{\partial}{\partial z} (M_z M_x) \right]$$

$$\rho \ddot{u}_y = c_{11} \frac{\partial^2 u_y}{\partial y^2} + c_{12} \left[\frac{\partial^2 u_x}{\partial x \partial y} + \frac{\partial^2 u_z}{\partial y \partial z} \right] + c_{44} \left[\frac{\partial^2 u_y}{\partial x^2} + \frac{\partial^2 u_x}{\partial x \partial y} + \frac{\partial^2 u_y}{\partial z^2} + \frac{\partial^2 u_z}{\partial y \partial z} \right]$$

$$+ \frac{b_1}{M_0^2} \frac{\partial}{\partial y} (M_y^2) + \frac{b_2}{M_0^2} \left[\frac{\partial}{\partial x} (M_x M_y) + \frac{\partial}{\partial z} (M_y M_z) \right]$$

$$\rho \ddot{u}_z = c_{11} \frac{\partial^2 u_z}{\partial z^2} + c_{12} \left[\frac{\partial^2 u_y}{\partial y \partial z} + \frac{\partial^2 u_x}{\partial x \partial z} \right] + c_{44} \left[\frac{\partial^2 u_z}{\partial y^2} + \frac{\partial^2 u_y}{\partial y \partial z} + \frac{\partial^2 u_z}{\partial x^2} + \frac{\partial^2 u_x}{\partial x \partial z} \right]$$

$$+ \frac{b_1}{M_0^2} \frac{\partial}{\partial z} (M_z^2) + \frac{b_2}{M_0^2} \left[\frac{\partial}{\partial y} (M_y M_z) + \frac{\partial}{\partial x} (M_z M_x) \right]$$

$$\dot{M}_x = \gamma \left\{ \frac{2A}{M_0^2} [M_y \nabla^2 M_z - M_z \nabla^2 M_y] + M_y H_0 - \frac{2b_1}{M_0^2} M_y M_z (\epsilon_{zz} - \epsilon_{yy}) \right.$$

$$\left. - \frac{2b_2}{M_0^2} [M_y^2 \epsilon_{yz} - M_z^2 \epsilon_{yz} + M_y M_x \epsilon_{zx} - M_z M_x \epsilon_{xy}] \right\}$$

$$\dot{M}_y = \gamma \left\{ \frac{2A}{M_0^2} [M_z \nabla^2 M_x - M_x \nabla^2 M_z] - M_x H_0 - \frac{2b_1}{M_0^2} M_z M_x (\epsilon_{xx} - \epsilon_{zz}) \right.$$

$$\left. - \frac{2b_2}{M_0^2} [M_z^2 \epsilon_{zx} - M_x^2 \epsilon_{zx} + M_z M_y \epsilon_{xy} - M_x M_y \epsilon_{yz}] \right\}. \tag{5.65}$$

One is interested in the solutions of these equations that represent plane waves of the form

$$u_\alpha = u_\alpha^0 \exp \{i(\omega t - k \cdot r)\},$$
$$m_{x,y} = m_{x,y}^0 \exp \{i(\omega t - k \cdot r)\}. \tag{5.66}$$

To find a solution of this form it is necessary to linearize the equations of motion by dropping terms involving the square of the amplitudes. In

this approximation the equations are

$$\rho\omega^2 u_x = c_{11}k_x^2 u_x + c_{12}[k_x k_y u_y + k_x k_z u_z]$$

$$+ c_{44}[k_y^2 u_x + k_x k_y u_y + k_z^2 u_x + k_x k_z u_z] + \frac{ib_2}{M_0}k_z m_x$$

$$\rho\omega^2 u_y = c_{11}k_y^2 u_y + c_{12}[k_x k_y u_x + k_y k_z u_z]$$

$$+ c_{44}[k_x^2 u_y + k_x k_y u_x + k_z^2 u_y + k_y k_z u_z] + \frac{ib_2}{M_0}k_z m_y \qquad (5.67)$$

$$\rho\omega^2 u_z = c_{11}k_z^2 u_z + c_{12}[k_y k_z u_y + k_x k_z u_x]$$

$$+ c_{44}[k_y^2 u_z + k_y k_z u_y + k_x^2 u_z + k_x k_z u_x] + \frac{ib_2}{M_0}(k_y m_y + k_x m_x)$$

$$i\omega m_x = \gamma\left\{\frac{2A}{M_0}k^2 m_y + H_0 m_y - ib_2(k_z u_y + k_y u_z)\right\}$$

$$i\omega m_y = \gamma\left\{-\frac{2A}{M_0}k^2 m_x - H_0 m_x + ib_2(k_x u_z + k_z u_x)\right\}.$$

To illustrate the nature of the coupled modes a particular example is considered, that of wave propagation along the z-axis. This requires that $k_x = k_y = 0$ and $k_z = k$. The above equations then reduce to

$$\rho\omega^2 u_x = c_{44}k^2 u_x + \frac{ib_2}{M_0}km_x$$

$$\rho\omega^2 u_y = c_{44}k^2 u_y + \frac{ib_2}{M_0}km_y$$

$$\rho\omega^2 u_z = c_{11}k^2 u_z$$

$$i\omega m_x = \gamma\left\{\frac{2A}{M_0}k^2 m_y + H_0 m_y - ib_2 k u_y\right\}$$

$$i\omega m_y = \gamma\left\{-\frac{2A}{M_0}k^2 m_x - H_0 m_x + ib_2 k u_x\right\}. \qquad (5.68)$$

Defining $u_\pm = u_x \pm iu_y$ and $m_\pm = m_x \pm im_y$ these equations may be rearranged to give

$$\rho\omega^2 u_\pm = c_{44}k^2 u_\pm + \frac{ib_2}{M_0}km_\pm$$

$$\omega m_\pm = \gamma\left\{\mp\frac{2A}{M_0}k^2 m_\pm \mp H_0 m_\pm \pm ib_2 k u_\pm\right\} \qquad (5.69)$$

$$\rho\omega^2 u_z = c_{11}k^2 u_z.$$

The set of equations are compatible if the determinant of the coefficients of $u_\pm$, $m_\pm$ and u_z vanish.

$$
\begin{vmatrix}
(\rho\omega^2 - c_{44}k^2) & -\dfrac{ib_2}{M_0}k & 0 & 0 & 0 \\[2mm]
-i\gamma b_2 k & \omega + \gamma\left[\dfrac{2A}{M_0}k^2 + H_0\right] & 0 & 0 & 0 \\[2mm]
0 & 0 & (\rho\omega^2 - c_{44}k^2) & -\dfrac{ib_2}{M_0}k & 0 \\[2mm]
0 & 0 & i\gamma b_2 k & \omega - \gamma\left[\dfrac{2A}{M_0}k^2 + H_0\right] & 0 \\[2mm]
0 & 0 & 0 & 0 & (\rho\omega^2 - c_{11}k^2)
\end{vmatrix} \equiv 0
\tag{5.70}
$$

By combining the equations in this way, it is seen that the determinant conveniently factorizes to give three cubic equations for ω^2:

$$
\omega^2 - v_\ell^2 k^2 = 0, \tag{5.71}
$$

$$
(\omega^2 - v_t^2 k^2)(\omega + \omega_s) + \frac{|\gamma|b_2^2 k^2}{\rho M_0} = 0, \tag{5.72}
$$

$$
(\omega^2 - v_t^2 k^2)(\omega - \omega_s) - \frac{|\gamma|b_2^2 k^2}{\rho M_0} = 0, \tag{5.73}
$$

where $v_\ell^2 = c_{11}/\rho$, $v_t^2 = c_{44}/\rho$ and $\omega_s = |\gamma|H_0 + 2A|\gamma|k^2/M_0 \equiv \omega_0 + Yk^2$. It has been assumed that the gyromagnetic ratio γ is negative. The first dispersion relation arises from the equations involving just u_z and therefore corresponds to wave motion which is purely elastic. Since k is parallel to the z-direction it is a longitudinal wave and the velocity is identical to that which would occur in the absence of magneto-elastic coupling. Therefore for this particular direction of propagation the longitudinal part of the phonon spectrum is uncoupled from the spin wave spectrum. The third dispersion relation belongs to the equations containing m_+ and u_+ and therefore gives the frequency for wave propagation in which $m_y/m_x = +i$ and $u_y/u_x = +i$. In other words it refers to wave propagation in which the x- and y-components of the vibration vectors are equal in magnitude but the y-component leads that of x by a phase factor of $\frac{1}{2}\pi$. The wave is therefore circularly polarized in the positive sense, that is clockwise looking along the direction of propagation. Likewise, the second dispersion relation corresponds to vibrations circularly polarized in the negative sense. If b_2 is zero eq. (5.73) gives two positive values of ω, namely $v_t k$ and ω_s. These are the frequencies belonging to the unperturbed elastic and magnetic dispersion curves. Equation (5.72) on the other hand

has only one positive solution corresponding to the second transverse elastic branch. When b_2 is finite Descartes' rule of signs tells us that for $|\gamma| b_2^2/\rho M_0 < v_t^2 \omega_s$ there are still two positive roots to eq. (5.73) and one to eq. (5.72). Away from the crossover region the solutions of eq. (5.73) for ω are very near the unperturbed spin wave and elastic frequencies but near the crossover point the curves are split as in fig. 5.3. For the wave circularly polarized in the negative sense the departure from linearity is small and the curve is close to the unperturbed lattice frequencies.
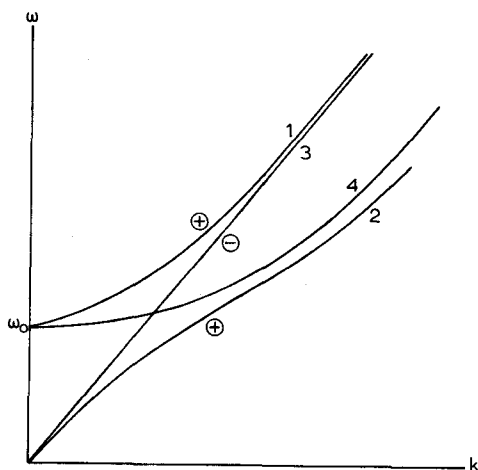
Fig. 5.3. Dispersion curves for magnetoelastic waves along the direction of the magnetic field. The $\oplus$ and $\ominus$ refer to the positive and negative circularly polarized waves. The $\ominus$ curve is drawn to coincide with the unperturbed elastic dispersion relation, labelled 3, since its departure from linearity is usually small. The curve labelled 4 is the unperturbed spin wave dispersion relation.

Sometimes, rather than consider the frequency as a function of the wave vector k, it is more convenient to consider k as a function of ω. To examine this it is better to rewrite eqs. (5.72) and (5.73) in the form

$$k_\pm^4 - k_\pm^2 \left[\frac{\omega^2}{v_t^2} - \frac{(\omega_0 \mp \omega)}{Y} + \frac{|\gamma| b_2^2}{Y M_0 \rho v_t^2} \right] - \frac{\omega^2}{v_t^2} \frac{(\omega_0 \mp \omega)}{Y} = 0, \quad (5.74)$$

For each positive value of ω there are four values of k, two for each sense of polarization. For zero frequency it is seen that each sense of polarization has a solution at $k^2 = 0$ and $-\omega_0/Y + |\gamma| b_2^2/\rho M_0 Y v_t^2$. If the magnetoelastic coupling constant is put equal to zero it is seen that the solutions starting at $k = 0$ go as ω^2 while the other two are linear in frequency. For non-zero values of b_2 the exact solutions have the form sketched in fig. 5.4.
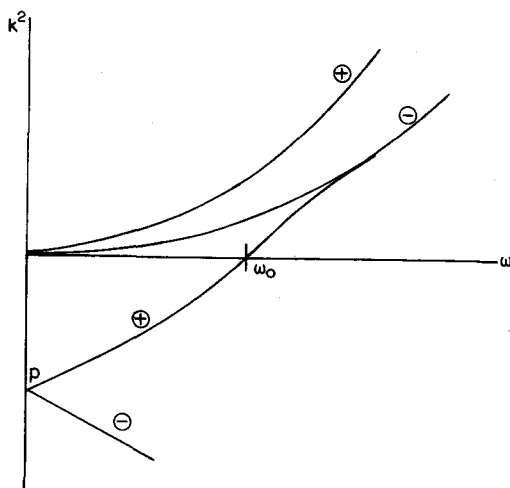
Fig. 5.4. Dispersion curves for magnetoelastic waves along the direction of the magnetic field. $\oplus$ and $\ominus$ refer to positive and negative circularly polarized waves. The point P is at

$$k^2 = -\frac{\omega_0}{Y} + \frac{|\gamma| b_2^2}{\rho M_0 Y v_t^2}.$$

2.3. *The quantum mechanical approach to the theory of magnetoelastic waves*

Instead of obtaining the equations of motion by using the classical equation of elasticity and the torque equation for the magnetic moment, one can proceed quantum mechanically. The elastic energy density may be regarded as the Hamiltonian density if the displacement u and the momentum P are interpreted as quantum mechanical operators satisfying the commutation rule

$$[u_\alpha(r), P_\beta(r')] = i\hbar\delta(r - r'). \tag{5.75}$$

Similarly the components of $M(r)$ are replaced by the components of the operator $\hat{M}(r)$ of eq. (5.52). Before replacing the components of $M(r)$ by their operator equivalents it is better to retain in W_{m-p} only the part of interest, namely $2b_2[M_y\epsilon_{yz} + M_x\epsilon_{zx}]/M_0$. This avoids the difficulty of having to say what the products like M_xM_y should be replaced by. A difficulty arises in the replacement of these products because of the non-commutability of their corresponding operators. Usually the symmetrized product $\hat{M}_x\hat{M}_y + \hat{M}_y\hat{M}_x$ has to be used. The equations of motion can be obtained directly from Heisenberg's equation of motion for a dynamical operator A. This is

$$i\hbar\dot{A} = [A, H]_- \tag{5.76}$$

where H is the Hamiltonian of the system. For example

$$i\hbar\dot{u}_\alpha(r) = \left[u_\alpha(r), \int H(r')\,dr'\right]. \tag{5.77}$$

In the analysis it is found that one has to evaluate quantities like $\int [P_x(r'),f(r)\,(\partial/\partial z)\,u_x(r)]\,dr$ where $f(r)$ commutes with u_x and P_x. This can be evaluated by integrating by parts and it is readily found to give $(\partial/\partial z)f(r')$. In this way the equations of motion can be obtained and one arrives at the same linearized equations as before. This is not surprising because if the Hamiltonian is such that the equations of motion are linear, then the expectation values obey the same equations.

2.4. Modifications arising from the presence of demagnetization fields

It has already been shown, eq. (5.49), how the demagnetization field of the spin waves enters into the equations of motion for the magnetization. To include this in the present work the terms

$$4\pi M_0[k_x k_y m_x + k_y^2 m_y]/k^2$$

and   (5.78)

$$-4\pi M_0[k_x^2 m_x + k_x k_y m_y]/k^2$$

must be added respectively to the right-hand side of the last two equations of eq. (5.67). These terms are the linearized parts of the x- and y-components of $M \times h$. For wave propagation along the z-axis they obviously drop out of the equations and the result is unchanged except for the inclusion of the static part of the demagnetization field which is easily accounted for by replacing H_0 by H_1. Consider now a general direction of propagation. For a cubic crystal it is known that it is only in a direction of high symmetry that there are one purely longitudinal and two degenerate transverse modes. Consequently even in the absence of any magnetoelastic coupling the dispersion relationships will be more complicated for arbitrary directions of the wave vector k. To remove this complication it will be assumed that the elastic behaviour of the crystal is isotropic. This implies, see ch. 2§1.4, that $c_{11} - c_{12} = 2c_{44}$. In this case there are only two independent elastic constants and there are always one longitudinal and two degenerate transverse modes. The polar angle that the direction of propagation makes with the z-axis will be denoted by θ. If there is elastic isotropy it is immaterial what the azimuthal angle is, so that without loss of generality k may be taken to be in the xz-plane. Putting $k_x = k \sin\theta$, $k_y = 0$ and $k_z = k \cos\theta$ into the equations of motion eq.

(5.67) one obtains

$$\rho\omega^2 u_x = c_{11}k^2 [u_x \sin^2\theta + u_z \sin\theta \cos\theta]$$

$$+ c_{44}k^2[u_x \cos^2\theta - u_z \cos\theta \sin\theta] + \frac{ib_2}{M_0} k m_x \cos\theta$$

$$\rho\omega^2 u_y = c_{44}k^2 u_y + \frac{ib_2}{M_0} k m_y \cos\theta$$

$$\rho\omega^2 u_z = c_{11}k^2 [u_z \cos^2\theta + u_x \cos\theta \sin\theta]$$

$$+ c_{44}k^2 [u_z \sin^2\theta - u_x \cos\theta \sin\theta] + \frac{ib_2}{M_0} k m_x \sin\theta \quad (5.79)$$

$$i\omega m_x = \gamma \left\{ \frac{2A}{M_0} k^2 m_y + H_1 m_y - ib_2 k u_y \cos\theta \right\}$$

$$i\omega m_y = \gamma \left\{ -\frac{2A}{M_0} k^2 m_x - H_1 m_x - 4\pi M_0 m_x \sin^2\theta \right.$$

$$\left. + ib_2 k(u_z \sin\theta + u_x \cos\theta) \right\}.$$

Now because it is known that in the absence of magnetoelastic coupling there are pure longitudinal and transverse modes, one suspects that it is more convenient to work with components of displacement that are parallel or at right angles to the direction of propagation. One works therefore with $u_\ell = u_z \cos\theta + u_x \sin\theta$ and $u_t = -u_z \sin\theta + u_x \cos\theta$ rather than with u_x and u_z. In terms of the components u_ℓ and u_t the equations of motion are

$$\rho\omega^2 [u_\ell \sin\theta + u_t \cos\theta] = c_{11}k^2 u_\ell \sin\theta + c_{44}k^2 u_t \cos\theta + \frac{ib_2}{M_0} k m_x \cos\theta$$

$$\rho\omega^2 u_y = c_{44}k^2 u_y + \frac{ib_2}{M_0} k m_y \cos\theta$$

$$\rho\omega^2 [u_\ell \cos\theta - u_t \sin\theta] = c_{11}k^2 u_\ell \cos\theta - c_{44}k^2 u_t \sin\theta + \frac{ib_2}{M_0} k m_x \sin\theta$$

$$i\omega m_x = \gamma \left\{ \frac{2A}{M_0} k^2 m_y + H_1 m_y - ib_2 k u_y \cos\theta \right\} \quad (5.80)$$

$$i\omega m_y = \gamma \left\{ -\frac{2A}{M_0} k^2 m_x - H_1 m_x - 4\pi M_0 m_x \sin^2\theta \right.$$

$$\left. + ib_2 k(u_\ell \sin 2\theta + u_t \cos 2\theta) \right\}.$$

Equating the determinant of the coefficients of u_ℓ, u_t, u_y, m_x and m_y to

zero gives the following condition for the equations to be self-consistent:

$$
\begin{vmatrix}
(\rho\omega^2-c_{11}k^2)\sin\theta\,; & (\rho\omega^2-c_{44}k^2)\cos\theta\,; & 0 & ;-\dfrac{ib_2}{M_0}k\cos\theta; & 0 \\[2mm]
0 & ; \quad 0 & ;(\rho\omega^2-c_{44}k^2); & 0 & ;-\dfrac{ib_2}{M_0}k\cos\theta \\[2mm]
(\rho\omega^2-c_{11}k^2)\cos\theta; & (-\rho\omega^2+c_{44}k^2)\sin\theta; & 0 & ;-\dfrac{ib_2}{M_0}k\sin\theta\,; & 0 \\[2mm]
0 & ; \quad 0 & ; i\gamma b_2 k\cos\theta; & i\omega & ;-\gamma\left[\dfrac{2Ak^2}{M_0}+H_i\right] \\[2mm]
-i\gamma b_2 k\sin 2\theta & ; \quad -i\gamma b_2 k\cos 2\theta & ; \quad 0 & ;\gamma\left[\dfrac{2A}{M_0}k^2+H_i; \atop +4\pi M_0\sin\theta\right] & i\omega
\end{vmatrix}=0. \quad (5.81)
$$

After some manipulation the following equation for the allowed values of ω may be obtained from the determinant.

$$(\rho\omega^2-c_{11}k^2)\left\{(\rho\omega^2-c_{44}k^2)^2(\omega^2-\omega_s\omega_m)-(\rho\omega^2-c_{44}k^2)|\gamma|\frac{b_2^2}{M_0}k^2\right.$$

$$\left.\times(\omega_m\cos^2\theta+\omega_s\cos^2 2\theta)-|\gamma|^2\frac{b_2^4}{M_0^2}k^4\cos^2 2\theta\cos^2\theta\right\}-(\rho\omega^2-c_{44}k^2)$$

$$\times\frac{b_2^2}{M_0}|\gamma|k^2\left[\omega_s(\rho\omega^2-c_{44}k^2)\sin^2 2\theta+\frac{|\gamma|}{M_0}b_2^2k^2\sin^2 2\theta\cos^2\theta\right]=0 \quad (5.82)$$

where

$$\omega_m=|\gamma|\left[\frac{2Ak^2}{M_0}+H_i+4\pi M_0\sin^2\theta\right]$$

$$\omega_s=|\gamma|\left[\frac{2Ak^2}{M_0}+H_i\right].$$

From this equation it is seen that for general values of θ the longitudinal elastic mode is also coupled to the magnon spectrum. It is however uncoupled in the two particular instances of θ being zero or $\frac{1}{2}\pi$, that is, when k is parallel or at right angles to the direction of the magnetic field. In the former case ω_m becomes equal to ω_s and the solutions are those obtained previously, eqs. (5.71)–(5.73). For $\theta=\frac{1}{2}\pi$.

$$(\rho\omega^2-c_{11}k^2)(\rho\omega^2-c_{44}k^2)\{(\rho\omega^2-c_{44}k^2)$$

$$\times(\omega^2-\omega_s\omega_m)-|\gamma|b_2^2k^2\omega_s/M_0\}=0. \quad (5.83)$$

From eq. (5.80) it is seen that with $\theta=\frac{1}{2}\pi$ both u_ℓ and u_y are uncoupled which means that both of these branches of the phonon spectrum are unaffected by the magnetoelastic coupling. The only branch that is coupled to the magnon spectrum is the one that is polarized parallel

to the magnetic field. The curly bracket in eq. (5.83) gives for the coupled modes in this case

$$\omega^2 = \tfrac{1}{2}\left\{ v_t^2 k^2 + \omega_s \omega_m \pm \left[(v_t^2 k^2 - \omega_s \omega_m)^2 + \frac{4|\gamma|}{\rho M_0} b_2^2 k^2 \omega_s \right]^{1/2} \right\}. \quad (5.84)$$

When b_2 is zero this equation gives the unperturbed transverse elastic and spin wave frequencies. For values of k such that the elastic and spin wave frequencies are significantly different, the magnetoelastic coupling will have little effect but near resonance this is not so. The presence of b_2 results in the two branches being split in the vicinity of the crossover frequency as shown in fig. 5.5.
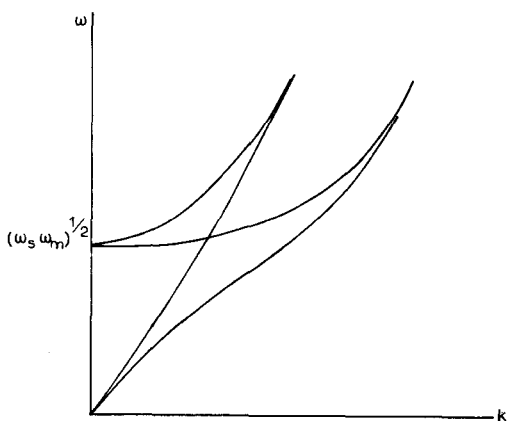
Fig. 5.5. Magnetoelastic waves perpendicular to the magnetic field. The elastic displacement vector is parallel to the magnetic field direction.

So far in the analysis it has been assumed that the magnetic field is along the z-axis, which is one of the cubic axes. To consider magneto-elastic wave propagation for other directions of the magnetic field it is convenient to change to a different set of coordinates in which the z'-axis is parallel to the d.c. magnetic field. In the primed coordinates the expression for the energy of the magnetoelastic interaction looks quite different. The expressions for two particular cases, namely those for which the magnetic field is parallel to a $\langle 110 \rangle$ or $\langle 111 \rangle$ axis has been given in the article by LeCraw and Comstock [1965] to which the reader is referred for details. It should be noted though that when using these expressions the non-diagonal components of the strain tensor differ by a factor two from our definition. After transforming to this new set of coordinates the coupled modes of the system can again be found if the equations are linearized by dropping the terms in $m_{x'}^2$ and $m_{y'}^2$.

2.5. *Acoustic wave rotation*

We now return to the discussion of magnetoelastic waves when the direction of wave propagation is parallel to the magnetic field in the z-direction. This is the situation for which the dispersion relations are those of eqs. (5.71)–(5.73). At high frequencies, very much greater than the frequency at which the spin wave and elastic dispersion curves intersect, the elastic energy of the transverse modes is carried mainly in the branches (1) and (3) of fig. 5.3, while for frequencies very much less than the crossover frequency it is carried in the branches (2) and (3). In both cases there are two branches available for the propagation of transverse elastic waves and these are circularly polarized in opposite senses. Wave motion of a definite frequency ω associated with the two branches may be described by displacement vectors

$$d_+ = A_+(\hat{i}+i\hat{j}) \exp [i(\omega t - k_+ z)],$$
$$d_- = A_-(\hat{i}-i\hat{j}) \exp [i(\omega t - k_- z)], \tag{5.85}$$

$\hat{i}$ and $\hat{j}$ are unit vectors parallel to the x and y cartesian axes. Since the displacement vector is a real physical quantity it is understood that the real part of these quantities should be used. Suppose that the amplitude of the two circularly polarized waves are equal, i.e. $A_+ = A_- = A$. Then the resultant disturbance at any point is given by the displacement components

$$d_x = A[\cos (\omega t - k_+ z) + \cos (\omega t - k_- z)]$$
$$= 2A \cos (\omega t - \tfrac{1}{2}(k_+ + k_-)z) \cos (\tfrac{1}{2}(k_+ - k_-)z) \tag{5.86}$$

and

$$d_y = A[-\sin (\omega t - k_+ z) + \sin (\omega t - k_- z)]$$
$$= 2A[\cos (\omega t - \tfrac{1}{2}(k_+ + k_-)z) \sin (\tfrac{1}{2}(k_+ - k_-)z)].$$

It is seen that the ratio d_y/d_x is a constant in time equal to $\tan [\tfrac{1}{2}(k_+ - k_-)z]$. Since this quantity is independent of time the resultant motion is a linearly polarized transverse wave making an angle $\theta = \tfrac{1}{2}(k_+ - k_-)z$ with respect to the x-axis. Since the angle is proportional to z, the distance the wave has travelled in the crystal, the plane of the polarization of the wave will rotate as the wave propagates. In other words, if a transverse plane polarized elastic wave is sent into the crystal along its cubic axis, it may be regarded as being split into two circularly polarized components of equal amplitudes but travelling with different velocities. A consequence of this difference in wave velocity for the two branches is that the plane of polarization of the elastic wave will rotate as it propagates. To find the degree of rotation per unit length an expression for k_+ and k_- is required. This may be

found from the dispersion relation of eq. (5.74). For a given frequency ω there are two values of k_+^2, and k_-^2. If interest is in elastic wave propagation well away from the crossover frequency, only solutions for k near ω/v_t are required. These two solutions are given by

$$k_\pm^2 = \frac{\omega^2}{v_t^2}\left\{1 + \frac{|\gamma|b_2^2}{YM_0\rho v_t^2[\omega^2/v_t^2 + (\omega_0 \mp \omega)/Y]}\right\} \qquad (5.87)$$

if terms involving b_2^4 etc. are neglected. Since $k_+ \approx k_-$ in this region, it follows that

$$k_+ - k_- \approx \frac{|\gamma|b_2^2\omega^2}{Y^2M_0\rho v_t^3[(\omega^2/v_t^2 + \omega_0/Y)^2 - \omega^2/Y^2]}. \qquad (5.88)$$

For small k the exchange term involving Y may be neglected so that

$$k_+ - k_- \approx \frac{|\gamma|b_2^2\omega^2}{M_0\rho v_t^3[\omega_0^2 - \omega^2]}. \qquad (5.89)$$

Thus the angle per unit length of propagation through which the plane of polarization of the wave rotates is

$$\frac{\theta}{z} = \tfrac{1}{2}(k_+ - k_-) = -\frac{|\gamma|b_2^2\omega^2}{2M_0\rho v_t^3[\omega^2 - \omega_0^2]}, \qquad (5.90)$$

where $\omega_0 = |\gamma|H_0$. If the demagnetization field of the specimen is taken into account H_0 should be replaced by $(H_0 - 4\pi N_z M_0)$.

In the analysis so far all loss effects have been excluded with the result that the sinusoidal wave propagates without attenuation. In practice spin wave damping and phonon collisions will contribute to attenuation. The presence of attenuation will not only diminish the amplitude of the resulting wave but may change the nature of its polarization. In the case of the two circularly polarized wave components of eq. (5.85) it is seen that one of them is more strongly coupled to the spin wave spectrum than the other because of the resonant denominator in the expression for the wave vector. Consequently it is to be expected that any spin wave damping will influence this component to a greater extent than the other. If this is so the plane transverse wave discussed above will not be propagated as a plane polarized wave but, rather, it will have an elliptical polarization. To demonstrate this, suppose that the positive polarized wave component suffers an attenuation $\exp(-\alpha z)$ as it propagates, whilst the attenuation associated with the negative polarized wave may be neglected. Then

$$d_+ = A \exp(-\alpha z)(\hat{i} + i\hat{j}) \exp[i(\omega t - k_+ z)],$$
$$d_- = A(\hat{i} - i\hat{j}) \exp[i(\omega t - k_- z)]. \qquad (5.91)$$

The x- and y-components of the resulting displacement are then, in the place of eq. (5.86)

$$d_x = A[e^{-\alpha z}\cos(\omega t - k_+z) + \cos(\omega t - k_-z)],$$
$$d_y = A[e^{-\alpha z}\cos(\omega t - k_+z + \tfrac{1}{2}\pi) - \cos(\omega t - k_-z + \tfrac{1}{2}\pi)]. \qquad (5.92)$$

These may be written in the form

$$d_x = R_1\cos(\omega t - \theta_1), \qquad d_y = R_2\cos(\omega t - \theta_2), \qquad (5.93)$$

where

$$R_1^2 = A^2[1 + e^{-2\alpha z} + 2e^{-\alpha z}\cos(k_+ - k_-)z],$$
$$R_2^2 = A^2[1 + e^{-2\alpha z} - 2e^{-\alpha z}\cos(k_+ - k_-)z]$$
$$\tan\theta_1 = \frac{e^{-\alpha z}\sin k_+z + \sin k_-z}{e^{-\alpha z}\cos k_+z + \cos k_-z} \qquad (5.94)$$
$$\tan\theta_2 = \frac{\cos k_-z - e^{-\alpha z}\cos k_+z}{e^{-\alpha z}\sin k_+z - \sin k_-z}.$$

It is seen that the displacement components d_x and d_y satisfy the equation

$$\frac{d_x^2}{R_1^2} + \frac{d_y^2}{R_2^2} - \frac{2d_xd_y}{R_1R_2}\cos(\theta_1 - \theta_2) = \sin^2(\theta_1 - \theta_2) \qquad (5.95)$$

for all time t. Now it is known that any general equation of the form $ax^2 + 2hxy + by^2 = 1$ is the equation of an ellipse if the solutions r_1 and r_2 of

$$r^2 = \{(a+b) \pm [(a-b)^2 + 4h^2]^{1/2}\}/[2(ab - h^2)]$$

are both positive. The ellipse has major and minor axes of lengths r_1 and r_2 and is inclined at an angle ψ equal to $\tfrac{1}{2}\tan^{-1}[2h/(a-b)]$ to the x-coordinate axis, see fig. 5.6. It follows that the end-point of the resultant displacement vector of the motion described by eq. (5.95) lies on an ellipse inclined at an angle ψ given by

$$\tan 2\psi = \frac{2R_1R_2\cos(\theta_1 - \theta_2)}{R_1^2 - R_2^2} \qquad (5.96)$$

to the x-axis. From the relations of eq. (5.94) it is found that

$$\psi = \tfrac{1}{2}(k_+ - k_-)z$$

so that the angle of inclination increases as the wave propagates. This is the same rate of rotation as for the plane polarized wave discussed above. Naturally this is to be expected as the plane polarized wave is the special case of the ellipse when its minor axis is zero. The lengths
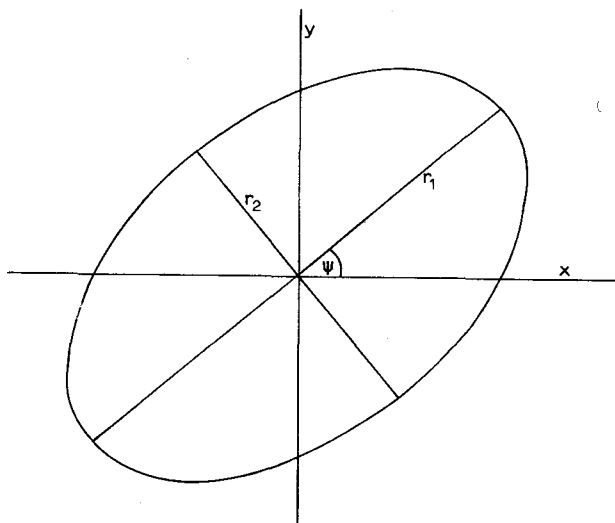
Fig. 5.6.

of the minor and major axes of the ellipse are in the ratio

$$\frac{r_2}{r_1} = \left\{ \frac{\cosh(\alpha z) - 1}{\cosh(\alpha z) + 1} \right\}^{1/2} \tag{5.97}$$

This ratio is also a function of z and implies that the ellipse changes gradually into a circle as the wave travels through the crystal.

Spin wave damping or finite phonon lifetimes that contribute to the attenuation coefficient are usually incorporated in the theory phenomenologically. In ferromagnetic relaxation theory the usual dynamic equation accounting for relaxation is taken to be the Landau–Lifshitz equation

$$\dot{M} = \gamma [M \times H] - \lambda [M \times (M \times H)]. \tag{5.98}$$

In the absence of magnetoelastic interactions the second equation of eq. (5.69) will have this form if γ is replaced by $(\gamma \pm i\lambda)$. That is $(\pm \omega_0)$ will be replaced by $(\pm \omega_0 + i/\tau_s)$ where the spin wave lifetime τ_s is $1/\lambda H_0$. In the same way phonon lifetimes τ_p may be included by adding a term $-2i\omega \rho u_{\pm}/\tau_p$ to the l.h.s. of the first equation.

The first observation of acoustic wave rotation by magnon–phonon interaction was observed by MATTHEWS and LECRAW[1962] in a specimen of yttrium iron garnet at room temperature. A cylindrical specimen whose axis was parallel to a $\langle 100 \rangle$ crystal axis was bonded onto an AC-cut quartz disc transducer and a d.c. magnetic field was directed along its axis. A 2 μsec long 528 MHz r.f. electric pulse

applied at right angles to the face of the quartz disc generated a trans-
verse acoustic wave which was polarized parallel to the $\langle 100 \rangle$ quartz
crystal axis in the plane of the transducer. The phonon pulse travelled
down the specimen and was reflected at its end. On its return part of
it passed through the bond–YIG interface but, because of the large
reflection coefficient at the junction, most of it was reflected back down
the YIG rod. This was subsequently reflected at the open end to form
a second echo and so on. As each echo reached the bond the part
transmitted to the quartz transducer generated an electric field pro-
portional to the transverse strain component in the $\langle 100 \rangle$ direction.
The nth echo arrived at the bond with its plane of polarization rotated
through an angle $n\theta$ where θ was the angle of rotation associated with
twice the length of the specimen. A measurement of the electric
field detected at each echo is thus a measure of the degree of rotation
of the plane of polarization. From eq. (5.86) it is clear that a cosine
variation of the pulse amplitude should occur. Nodes occurred when
the plane of polarization had been rotated through $\frac{1}{2}\pi$. Figure 5.7,
taken from the work of Matthews and LeCraw, shows the detected
amplitude of the echoes in their experiment for magnetic fields of
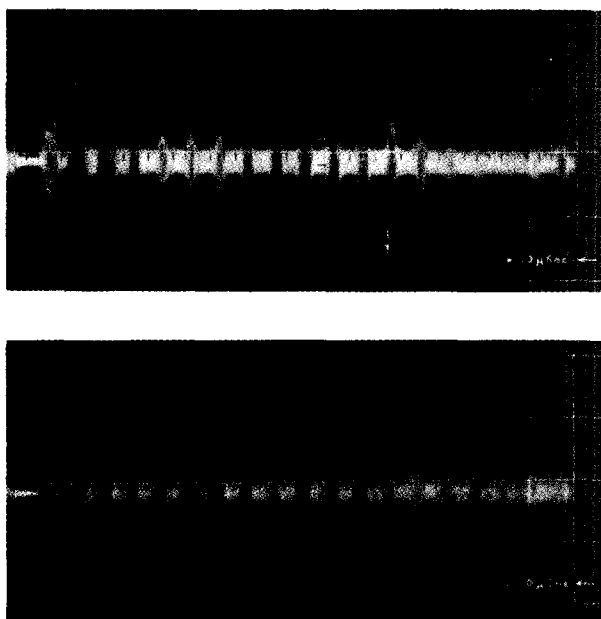
Fig. 5.7. (Reproduced from H. MATTHEWS and R. C. LeCRAW, Phys. Rev. Lett. **8**,
397 (1962) with permission.)

2000 and 1500 Oe. It is observed from these echo traces that exact nodes do not occur. This is because the presence of losses results in an elliptic rather than a plane polarized wave, see the discussion centred around eq. (5.95). By curve-fitting to a graph of θ/l against the applied magnetic field they determined the value of NM_0 which was found to be in good agreement with the theoretical demagnetization field of an ellipsoid of revolution with the same major and minor dimensions. The value of the magnetoelastic coupling coefficient b_2 was also determined. While it was to within a factor 2 of the value obtained from a strain gauge technique, it was about a factor 13 greater than that obtained by parametric excitation of microwave phonons at 17.4 GHz.

Because Matthews and LeCraw were only interested in the acoustic wave rotation they only studied the behaviour of waves propagating parallel to the magnetic field. Soon afterwards, experiments were performed by LUTHI[1963], at much lower frequencies, on specimens of yttrium iron garnet in which other geometries were used. In addition to the situation described above he considered the case when the saturation magnetization was perpendicular to the propagation direction of the sound wave. In this case he found that only the shear wave with the polarization vector parallel to the magnetic field was coupled to the spin waves. This is in accord with the result of eq. (5.82). When the magnetic field is inclined at some other angle to the axis of the specimen, longitudinal sound waves should also be coupled to the magnon spectrum. Luthi found experimentally that the coupling reached a maximum at 17° as opposed to the theoretical value of 45°. This difference was put down to the fact that not all the domains were removed because of the low field used.

Recently, LEWIS and SCOTTER[1968] have examined the interaction of longitudinal phonons with spin waves in YIG. They observe the interaction of 1 GHz pure-longitudinal phonons propagating in a [110] YIG rod when the applied magnetic field was swung in the $(1\bar{1}2)$ plane through the [110] axis parallel to the rod and the $[1\bar{1}1]$ axis perpendicular to it. As mentioned at the end of §2.4, for magnetic field directions not along a cubic axis it is convenient to define new coordinate axes such that z' is parallel to the direction of the saturation magnetization. It is seen from the expressions given by LeCraw and Comstock that when z' is along a $\langle 111 \rangle$ axis there is a linear term in the magnetoelastic energy proportional to $(b_1 - b_2)m_{x'}(\epsilon_{x'x'} - \epsilon_{y'y'})$ showing that a longitudinal wave can be coupled to the magnon spectrum provided b_1 is not equal to b_2. For z' along a $\langle 110 \rangle$ axis no such linear term exists. The experimental findings of Lewis and Scotter support these predictions.

3. Absorption of sound in ferromagnetic dielectrics

The absorption of sound in ferromagnetic crystals depends upon the frequency of the sound compared to the characteristic collision times between the elementary excitations of the system. There are four relaxation times that may enter the discussion, τ_{mm}, τ_{pp}, τ_{mp} and τ_{pm}. The subscripts m and p refer to the magnons and phonons respectively so that τ_{pp} is for example the mean relaxation time for the phonon–phonon collisions. Over a wide range of temperatures the interactions within each sub-system, the magnons and phonons, are considerably stronger than the interaction between the two systems. In other words $\tau_{mm} \ll \tau_{mp}$ and $\tau_{pp} \ll \tau_{pm}$. If these conditions prevail then the ferromagnet can be regarded as two loosely coupled systems.

The theory of sound absorption in ferromagnetic dielectrics is developed along two different lines depending on the frequency of the sound being used. For low frequencies Ω such that $\Omega\tau_{mm}$ and $\Omega\tau_{pp}$ are very much less than unity the acoustic field is regarded as a classical quasi-stationary field while at high frequencies, $\Omega\tau_{mm} \gg 1$, the acoustic waves may be regarded as causing transitions in the spin wave spectrum. This division of the sound-wave absorption into a quasi-static and quantum mechanical regime is similar to the division that occurred in ch. 4 where the absorption due to phonon–phonon interactions was treated. In the microwave ultrasonic region at temperatures of interest Ω is generally greater than $1/\tau_{mm}$ so only the high frequency regime will be treated.

It was mentioned in §2.1, where the form of the magnetoelastic interaction was discussed, that there were two types of term linear in the strain. The first is that describing magnetoelastic effects which accompany homogeneous rotation of the magnetization vector and the other arises from inhomogeneous magnetization. In general

$$W_{\text{m–p}} = \sum F_{ij}(\boldsymbol{\alpha})\epsilon_{ij} + \sum F_{ijklmn} \frac{\partial M_m}{\partial x_i} \frac{\partial M_n}{\partial x_j} \epsilon_{kl}. \qquad (5.99)$$

When the coupled magneto-acoustic waves were studied the second type of term was neglected because it is essentially of third order, being second order in the deviation from equilibrium of the magnetization components and first order in the strain. There are two contributions from this term, the main part coming from the exchange interaction and the rest from the relativistic interactions. This latter part is normally neglected. The part arising from the exchange interaction must be invariant with respect to rotations of the magnetic moment M and is therefore of the form

$$F_{ijkl} \frac{\partial M_n}{\partial x_i} \frac{\partial M_n}{\partial x_j} \epsilon_{kl} .$$

It is characterized by a fourth-rank tensor rather than by one of rank six. In the following discussion the case of an isotropic body will be treated for which F_{ijkl} will have the form

$$F_{ijkl} = \tfrac{1}{2}\lambda_1 (\delta_{ik}\delta_{jl} + \delta_{il}\delta_{jk}) + \lambda_2 \delta_{ij}\delta_{kl}.$$

This form for the non-zero components of the fourth-rank tensor can be written down from table A1.2 where the non-zero components of c_{ijkl} for an isotropic medium are given. The connection is seen if c_{11} is replaced by $\lambda_1 + \lambda_2$ and c_{12} by λ_2. In the literature on the magnon–phonon interaction it is customary to write the exchange parameter A/M_0^2 of eq. (5.23) for a cubic lattice in terms of a temperature θ_c defined through the relation $A/M_0^2 = K\theta_c a^2/2g\beta M_0$. This definition implies from eq. (5.27) that $K\theta_c = JS$. Because the term in F_{ijkl} comes from an expansion of the exchange interaction it is convenient to introduce the same factor by writing $\lambda_{1,2} = \beta'^{,''} K\theta_c a^2/2g\beta M_0$ where β' and β'' will be of the order of unity*. For an isotropic medium the first term of eq. (5.99) may be written as

$$\frac{b}{M_0^2} [M_x^2 \epsilon_{xx} + M_y^2 \epsilon_{yy} + M_z^2 \epsilon_{zz} + 2M_x M_y \epsilon_{xy} + 2M_x M_z \epsilon_{xz} + 2M_y M_z \epsilon_{yz}].$$

This follows from eq. (5.61) with $b_1 = b_2$. Near the ground state of the system we may put $M_z = M_0 + M_z'$ and assume $M_z' \ll M_x$, $M_y \ll M_0$. The leading terms in the magnon–phonon interaction are then

$$
\begin{aligned}
H_{m-p} = {}& \frac{2b}{M_0} \int (M_x \epsilon_{xz} + M_y \epsilon_{yz})\, dv \\
& + \frac{b}{M_0^2} \int (M_x^2 \epsilon_{xx} + M_y^2 \epsilon_{yy} + 2M_x M_y \epsilon_{xy} + 2M_0 M_z' \epsilon_{zz})\, dv \\
& + \frac{\beta' K\theta_c a^2}{2g\beta M_0} \int \left(\frac{\partial M_x}{\partial x_i}\frac{\partial M_x}{\partial x_j} + \frac{\partial M_y}{\partial x_i}\frac{\partial M_y}{\partial x_j} \right) \epsilon_{ij}\, dv \\
& + \frac{\beta'' K\theta_c a^2}{2g\beta M_0} \int \left(\frac{\partial M_x}{\partial x_i}\frac{\partial M_x}{\partial x_i} + \frac{\partial M_y}{\partial x_i}\frac{\partial M_y}{\partial x_i} \right) \epsilon_{jj}\, dv. \quad (5.100)
\end{aligned}
$$

The first term in this expression is the one that leads to the formation of the magneto-acoustic waves described in §2.2. It is not important when dealing with processes involving transitions between the phonon and magnon sub-systems and will consequently be neglected in this section. In order to express the Hamiltonian in second quantization, use is made of eqs. (5.54) and (4.21). It is found that†

$$
\begin{aligned}
H_{m-p} = {}& -\sum_{qskk'} \{ A_{qs} a_{qs} a_{k'}^* a_k^* + \delta_{k+k'-q} \\
& + (B_{qs} + C_{qs}) a_{qs} a_{k'}^* a_k \delta_{k-k'+q} + \text{c.c.} \} \quad (5.101)
\end{aligned}
$$

*A prime has been put on the β's to distinguish them from those of §2.1.

†The phonon operators are distinguished from the magnon operators by the addition of the polarization index s.

where

$$A_{qs} = \frac{bg\beta}{2M_0}\left(\frac{\hbar}{2\rho V\omega_{qs}}\right)^{1/2} q_+ e_+(qs)$$

$$B_{qs} = \frac{bg\beta}{2M_0}\left(\frac{\hbar}{2\rho V\omega_{qs}}\right)^{1/2} [q_+ e_-(qs) + q_- e_+(qs) - 4q_z e_z(qs)]$$

$$C_{qs} = \tfrac{1}{2}K\theta_c a^2 \left(\frac{\hbar}{2\rho V\omega_{qs}}\right)^{1/2} \{\beta'[(k\cdot e(qs))(k'\cdot q)$$

$$+ (k\cdot q)(k'\cdot e(qs))] + 2\beta''(k\cdot k')(e(qs)\cdot q)\}. \quad (5.102)$$

There are two types of processes resulting in phonon absorption. Those of the form $a_{qs}a_{k'}^* a_k^*$ which represent the dissociation of a phonon into two magnons and terms like $a_{qs}a_{k'}^* a_k$ representing the absorption of a phonon by a magnon to give a magnon of higher energy. The conjugate complex terms in the interaction Hamiltonian give rise to the reverse processes leading to the emission of a phonon.

It is relevant here to notice how an interaction Hamiltonian of the form of eq. (5.101) might be obtained from a microscopic model. For instance it has been seen that on a microscopic model the exchange interaction can be represented by a Hamiltonian of the form of eq. (5.1). In this Hamiltonian the exchange integral is a function of R_{mn}. In the presence of thermal vibrations R_{mn} is no longer the equilibrium vector R_{mn}^0 but rather $R_{mn}^0 + \Delta R_{mn}$ where ΔR_{mn} is the relative displacement from equilibrium of the two atoms at R_n and R_m. For small displacements $J(R_{mn})$ may be expanded in a Taylor series

$$J(R_{mn}) = J(R_{mn}^0) + [\Delta R_{mn}\cdot\nabla J(R_{mn})]_{R_{mn}^0}$$

$$+ [\Delta R_{mn}\cdot\nabla][\Delta R_{mn}\cdot\nabla J(R_{mn})]_{R_{mn}^0} + \cdots.$$

The second term in the series is the one leading to one-phonon processes. On substituting this into the Hamiltonian and using eq. (5.10) and eq. (2.56) an interaction similar to the exchange term of eq. (5.101) is obtained. This microscopic approach was the method adopted by AKHIESER[1946] in his fundamental paper on the subject.

In order to calculate the sound attenuation in the high frequency region the transition probabilities for these processes are required. By use of the standard result of time-dependent perturbation theory, appendix 3, it is found that the rate of change of the occupation number for the (q, s) phonon mode is given by

$$\frac{d}{dt}N_{qs} = \frac{2\pi}{\hbar}\left\{\sum_{kk'}|A_{qs}|^2[(N_{qs}+1)n_{k'}n_k - N_{qs}(n_{k'}+1)(n_k+1)]\right.$$

$$\times \delta(\hbar\omega_{qs} - \epsilon_{k'} - \epsilon_k) + |B_{qs} + C_{qs}|^2[(N_{qs}+1)n_{k'}(n_k+1)$$

$$- N_{qs}(n_{k'}+1)n_k]\delta(\hbar\omega_{qs} + \epsilon_k - \epsilon_{k'}) \quad (5.103)$$

N_{qs} and n_k are the occupation numbers of the phonon and magnon modes respectively and ϵ_k is the magnon energy. It is understood that the delta functions imply conservation of momentum as well as energy. If all the occupation numbers are replaced by their thermal equilibrium values then the right-hand side of this equation is identically zero as it should be. To calculate the attenuation of sound the method of ch. 4§2.3 is followed. The magnons are taken to be in equilibrium so the n's are replaced by their thermal equilibrium values whereas for the phonon mode of interest it is assumed that $N_{qs} = N_{qs}^0 + \Delta N_{qs}$. The attenuation is then given by the return of this non-equilibrium distribution function to zero. It is usual to define an attenuation coefficient $\delta = -\frac{1}{2} N_{qs}/\Delta N_{qs}$ per unit time which is consistent with the definition in appendix 4, eq. (A4.18).

The absorption of sound was calculated in this way by KAGANOV and CHIKVASHVILI [1961]. The summations over k and k' are replaced by integrations over dk and dk'. Because of the complicated nature of the delta functions and the structure of the coefficients A, B and C the integrations can only be performed for limiting cases. For thoses interested in the details the articles by AKHIESER [1946] and AKHIESER et al. [1959] should prove useful. Kaganov and Chikvashvili find that the part of the interaction arising from exchange, that is the part involving the coefficient C_{qs} leads to an attenuation for transverse waves of

$$\delta_t = \frac{\beta'^2 \theta_t^2 K T \Omega}{2^8 \pi \theta_c^3 \rho a^3 v_t^2} \exp\left[-\frac{\theta_t^2}{4\theta_c T}\right] \qquad T \ll \frac{\theta_t^2}{4\theta_c},$$

$$\delta_t = \frac{\beta'^2 \theta_t^3 K T \Omega}{2^8 \pi \theta_c^3 \rho a^3 v_t^2} \exp\left[1.3 + \log\frac{4\theta_c T}{\theta_t^2}\right] \qquad T \gg \frac{\theta_t^2}{4\theta_c}. \tag{5.104}$$

Ω is the frequency of the transverse wave with velocity v_t, and $\theta_t = \hbar v_t/Ka$. For longitudinal waves the corresponding results are

$$\delta_\ell = \frac{(\beta' + \beta'') K \theta_\ell^5 \Omega}{2^9 \pi \theta_c^4 \rho a^3 v_\ell^2} \exp\left[-\frac{\theta_\ell^2}{4\theta_c T}\right] \qquad T \ll \frac{\theta_\ell^2}{4\theta_c},$$

$$\delta_\ell = \frac{\beta''^2 \zeta(2) K \theta_\ell \Omega T^2}{2^4 \pi \theta_c^2 \rho a^3 v_\ell^2} \qquad T \gg \frac{\theta_\ell^2}{4\theta_c}. \tag{5.105}$$

They also gave expressions for the attenuation arising from that part of the interaction leading to the dissociation of phonons into spin waves. It was estimated that this process only contributed to the attenuation of frequencies much greater than those that could be produced experimentally.

In a recent paper, LORD [1968] has examined in detail the magnitude of the attenuation to be expected in YIG at several temperatures and

for different frequencies in the microwave ultrasonic range. To obtain numerical results he assumed that the magnon dispersion relation has the isotropic form $\epsilon_k = K\theta_c a^2 k^2 + g\beta H_0$ and from the literature he extracted what he believed to be the best data available for the following parameters, $\theta_c = 12.7$ K, $v_t = 3.87 \times 10^5$ cm/sec, $v_\ell = 7.18 \times 10^5$ cm/sec, $a = 12$ Å, $\beta' = \beta'' = 3.3$ and $g\beta = 1.86 \times 10^{-20}$ erg/Oe. On replacing the summations over k and k' by integrals the question arises as to what is the upper limit of integration. This is important at high temperatures when the upper region of the magnon spectrum will be active. At very low temperatures the upper limit may be taken as infinity but at higher temperatures a more realistic approximation to the upper limit of the acoustic branch is required. Lord estimates this to be $\epsilon_{max} = 101$ K in YIG. To show the extent to which this cut-off affects the results he gives results for both cases.

His results for the absorption of sound due to the exchange part of the interaction are summarized in table 5.3 where it is seen that the longitudinal waves suffer a greater attenuation than the transverse ones. At temperatures of 50 K the effect of using a realistic ϵ_{max} results in a reduction of 40% in the attenuation to that obtained with $\epsilon_{max} = \infty$.

TABLE 5.3

T (K)	ν (GHz)	δ_t (dB/μ sec)		δ_ℓ (dB/μ sec)
		$\epsilon_{max} = 101$ K	$\epsilon_{max} = \infty$	$\epsilon_{max} = \infty$
3	1	6×10^{-5}	6×10^{-5}	
3	10	6×10^{-4}	6×10^{-4}	
10	1		8.1×10^{-4}	5×10^{-3}
10	10		6.95×10^{-3}	4×10^{-2}
25	10	0.119	0.108	
50	1		5×10^{-2}	0.26
50	10	0.324	0.528	2.1

The results quoted in table 5.3 are for zero magnetic field H_0. Lord has also examined the magnetic field dependence of the attenuation and finds that at 3 K it is reduced to $\frac{1}{5}$ of the zero field value in a magnetic field of 35000 Oe. As the temperature increases the effect of the magnetic field is less marked.

Lord has also estimated the contribution from the magnetoelastic term in the interaction, that is the contribution from B_{q_v}. For YIG b/M_0^2 has the value 255. It was found that this contribution can be neglected because it is small compared to that from the exchange term. The ratio of b to β' in YIG is quite characteristic of most materials so a similar conclusion as regards the relative importance of the two terms can be drawn for these. However there are some excep-

tions in the rare earth garnets where this ratio of b to β' may be 100 times larger. In these cases the contribution from the magnetostrictive term will dominate.

The temperature and frequency dependence of the attenuation in the region of interest has been calculated by Lord. For temperatures in the range 10 to 50 K and for frequencies 1 to 50 GHz the temperature variation of the transverse attenuation arising from the exchange term lies between $T^{1.7}$ and $T^{1.9}$ if $\epsilon_{max} = \infty$ is used. For $\epsilon_{max} = 101$ K the dependence is $T^{1.15-1.35}$. The limits of integration therefore play an important role. The corresponding figures for the attenuation due to the magnetostrictive term are $T^{1.4-1.6}$ and $T^{1.35-1.5}$. The frequency dependences are more consistent and all lie in the range $\Omega^{0.97}$ to $\Omega^{1.015}$ at temperatures 10–50 K.

4. Non-linear effects at high power levels

4.1. *Parallel pumping of magnetoelastic waves*

The formation of magnetoelastic waves and the theory of acoustic wave rotation discussed in §2.5 depended on a linear coupling existing between the magnetization and the elastic strain. At high signal powers the non-linear terms in the coupled equations of motion become important and new effects can occur; in particular, parametric excitation of magnetic waves is possible.

The parametric excitation of very high frequency modes in ferrites has received much attention in recent years. Historically the impetus for this work at high power levels stems from ferromagnetic resonance studies by DAMON [1953] and by BLOEMBERGEN and WANG [1954] in which they observed the premature saturation of the main resonance line and the appearance of a subsidiary resonance at lower magnetic fields. These observations led SUHL [1957] to develop his instability theory in which he showed that the observations could be explained in terms of a process in which a uniform-precession magnon is annihilated and a pair of magnons with wave vectors k and $-k$ is created. Normally, these magnons each of energy $\frac{1}{2}\hbar\omega$ subsequently decay by relaxing into other modes. However above a certain critical r.f. field strength the transfer of energy from the uniform precession into k and $-k$ modes exceeds the loss of energy out of the pair by relaxation. There is thus a threshold field strength above which there can be a very large energy flow from the uniform precession into the k, $-k$ pair resulting in an exponential growth of these spin waves. This is referred to as the first-order Suhl instability. Because the frequency of these potentially unstable magnons is at $\frac{1}{2}\omega$ it can be shown that a subsidiary line at applied fields less than that for the main resonance should appear in

agreement with the experimental observations. This first-order insta-
bility can sometimes occur when ω is equal to the ferromagnetic reso-
nance frequency in which case it may contribute to the premature
saturation of the main resonance line. More often in order to explain
this saturation it is necessary to invoke a second process in which two
$k = 0$ magnons decay into a $k, -k$ pair each of frequency ω. This is
referred to as the second-order Suhl instability.

Following this work a new experiment was proposed independently
by MORGENTHALER[1960] and by SCHLOMANN et al.[1960] in which
the microwave field of frequency ω is applied parallel to the magnetiza-
tion, a technique now referred to as parallel pumping. Above a certain
threshold amplitude similar instabilities occur in which unstable spin
waves of frequency $\omega_k = \frac{1}{2}\omega$ are produced. The importance of this
technique is that in principle it allows one to excite magnon pairs of
any desired frequency. The nature of the process is as follows. It may
be observed from the equations following eq. (5.49) that unless $\sin \theta_k$ is
zero the amplitudes of the m_x and m_y oscillatory components are
different. The spins therefore execute elliptical rather than circular pre-
cessions. A standing wave of elliptically precessing spins can be formed
from two such spin waves with equal and opposite k-vectors. Because
the spin vector is of constant length the z-component has an oscillatory
part whose frequency is twice the precessional frequency ω_k. Applica-
tion of a microwave field at this frequency enables power to be fed con-
tinuously into the standing wave and instability occurs when the rate of
growth from the applied field exceeds that loss through relaxation.
Theory shows that the threshold of instability is reached when the
amplitude of the microwave field is

$$h_c = \left\{ \frac{2\omega_k [(\omega - 2\omega_k)^2 + \gamma^2/\tau_k^2]^{1/2}}{4\pi\gamma^2 M_0 \sin^2 \theta_k} \right\}_{\text{minimum}} \qquad (5.106)$$

τ_k is the relaxation time of a magnon in the mode k.

Two major methods of calculating this and other threshold fields
are available. The first is to use the equations of motion keeping non-
linear terms and evaluating the pump amplitude for which the damping
coefficients become zero. This approach is outlined in §4.2 for the case
of elastic pumping. An alternative procedure is the rate-equation
method which is useful when the second quantization formulation is
being used. The rate at which the pump transfers energy to the unstable
modes is equated to the energy loss by relaxation. The pump (ω_p, k_p)
transfers energy into the modes $(\omega_1, k_1 ; \omega_2, k_2)$ at a rate given by

$$\hbar\omega_p \left(\frac{dn_p}{dt} \right)_{\text{scattered}} = \Delta n_p \hbar\omega_p [T_{n_p \to n_p + \Delta n_p} - T_{n_p \to n_p - \Delta n_p}] \qquad (5.107)$$

where T is the transition probability and Δn_p depends on the order of the process (one for first order, two for second order etc.). The transition probability is calculated by perturbation theory, appendix 3, and involves the square of the matrix elements of the interaction, the occupation numbers of the states concerned and the density of final states. This latter quantity can usually be expressed as a Lorentzian involving the relaxation times of the final states. This is in fact mathematically equivalent to adding an imaginary part to the frequency in the equations of motion. The loss by relaxation is

$$(\hbar\omega_1 \dot{n}_1)_{\text{relax}} + (\hbar\omega_2 \dot{n}_2)_{\text{relax}} = \frac{\hbar\omega_1}{\tau_1}(n_1 - \bar{n}_1) + \frac{\hbar\omega_2}{\tau_2}(n_2 - \bar{n}_2) \quad (5.108)$$

where the bars signify thermal equilibrium values and the τ's are the relaxation times of the modes concerned in the process. The equation of these two expressions determines the threshold for instability.

Near the crossover region where the spin wave and phonon dispersion curves cross, magnetoelastic waves exist. Schlomann suggested that these magnetoelastic waves might be excited by this method, that is by the application of a uniform microwave magnetic field whose amplitude is above the threshold for non-linear excitation. In this region the threshold condition is modified because of the dispersion of the magnetoelastic waves and the losses associated with the elastic contribution. Schlomann showed that in the vicinity of the crossover frequency the power threshold for the instability rises sharply. This behaviour has been demonstrated by TURNER[1960] in the following way.

From the critical field condition given above it is expected that transverse, that is $\theta_k = \frac{1}{2}\pi$ directed spin waves, will become unstable first provided, of course, that they exist at the required frequency of $\frac{1}{2}\omega$. It is seen from eq. (5.50) that for excitation of these waves the pump frequency must satisfy

$$\omega = 2\omega_k = 2\gamma \left\{ \left[\frac{2A}{M_0} k^2 + H_i \right] \left[\frac{2A}{M_0} k^2 + H_i + 4\pi M_0 \right] \right\}^{1/2}. \quad (5.109)$$

For small H_i transverse spin waves will always exist at the frequency $\frac{1}{2}\omega$. As H_0 increases, the value of k needed to satisfy the above condition falls and reaches zero at H_m given by

$$\omega^2 = 4\gamma^2 H_m [H_m + 4\pi M_0]. \quad (5.110)$$

Over this range of H_i the threshold amplitude is proportional to τ_k^{-1} which is usually proportional to k. Above H_m there are no longer any $\theta_k = \frac{1}{2}\pi$ waves available to satisfy the required frequency condition, so spin waves with smaller θ_k become unstable. The critical field h_c is then

expected to increase rapidly because of the $\sin^2 \theta_k$ term in the denominator, becoming infinite when no spin waves can satisfy the frequency condition above. The theory is not quite correct of course in the vicinity of $k = 0$ where magnetostatic modes .rather than plane spin waves exist.

TURNER[1960] carried out measurements on a YIG sphere at 34 GHz to determine the r.f. field strength needed to excite spin wave pairs as a function of the d.c. applied magnetic field. His result is shown in fig. 5.8 for the case of the d.c. magnetic field being directed along the [111] axis. The curve to the left of H_m corresponds to the spin waves $\theta_k = \frac{1}{2}\pi$. Sharp peaks in this curve were found at H_1 and H_2. These are believed to arise from the sudden increase in the threshold field required due to phonon mixing as predicted by Schlomann. From the frequency condition it is seen that the k-value of the spin wave pair that becomes unstable is proportional to $(H_m - H)^{1/2}$. If this value occurs at the crossover between the phonon and spin wave dispersion curves it
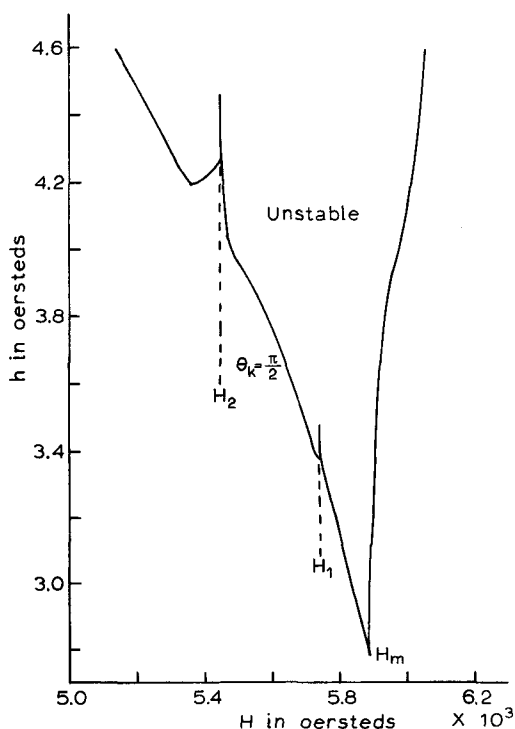
Fig. 5.8. The r.f. field strength required to excite spin wave pairs as a function of applied field. Pumping frequency is 34.627 GHz and the fields are along the [111] crystal axis. (After Turner.)

should also be inversely proportional to the phonon velocity. In Turner's experiment it was found that the ratio of $(H_m - H_2)^{1/2}$ to $(H_m - H_1)^{1/2}$ was the same as the ratio of the longitudinal and transverse velocities in support of the view that the kinks were due to the formation of magnetoelastic waves. The coupling of longitudinal as well as transverse phonons to the spin waves is due to the direction of propagation chosen, see §2.4.

4.2. Amplification of spin waves by phonon pumping

The preceding section has treated the parametric excitation of magneto-elastic modes by means of parallel magnetic pumping. From the viewpoint of this book a more interesting experiment would be the parametric amplification of two magnetic waves by an elastic pump wave, an experiment first suggested by GUREVICH [1964]. Unfortunately an error occurred in his work which led to the wrong conditions under which amplification is possible. This error was pointed out by HAAS [1966] who presented a corrected version of the theory.

The coupling between the pump wave and the spin waves to be excited is provided by the non-linear terms in the magnetoelastic coupling. For simplicity it will be assumed that the pump wave is a longitudinal wave travelling along the x-direction, that is perpendicular to the static magnetic field applied along the z cubic axis. Again it is assumed that the specimen is infinite and anisotropy and demagnetization fields will be ignored. Under these conditions the equations of motion for the transverse magnetization correct to second order in small deviations are, from eq. (5.65)

$$\dot{m}_x = \gamma \left[-\frac{2A}{M_0} \nabla^2 + H_0 \right] m_y$$

$$\dot{m}_y = \gamma \left[\frac{2A}{M_0} \nabla^2 - H_0 \right] m_x - \frac{2b_1}{M_0} m_x \frac{\partial u_x}{\partial x}.$$

(5.111)

Only the term in ϵ_{xx} has been retained because of the geometry of the pump wave. Differentiating the first equation with respect to time and substituting for $\dot{m}_y$ from the second it follows that

$$\ddot{m}_x = -\gamma^2 \left[\frac{2A}{M_0} \nabla^2 + H_0 \right]^2 m_x + \frac{2b_1}{M_0} \gamma \left[\frac{2A}{M_0} \nabla^2 - H_0 \right] \left(m_x \frac{\partial u_x}{\partial x} \right).$$

(5.112)

In the absence of b_1 the Fourier components of m_x oscillate with the usual spin wave frequency

$$\omega_k = |\gamma| \left[\frac{2A}{M_0} k^2 + H_0 \right].$$

(5.113)

Spin wave damping may be included phenomenologically by the addi-

tion of i/τ_k to ω_k, see eq. (5.98). Eq. (5.112) is now solved in the presence of a pump wave

$$u_x = u_x^0 \exp \left[i(\omega t - qx)\right] + u_x^{0*} \exp \left[-i(\omega t - qx)\right] \qquad (5.114)$$

of known amplitude. For the parametric excitation of two spin waves the solutions of interest are of the form

$$m_x = m_k + m_{k'} \qquad (5.115)$$

where

$$m_k = m_k(t) \exp \left[i(\omega_k t - k \cdot r)\right] + m_k^*(t) \exp \left[-i(\omega_k t - k \cdot r)\right].$$

It is noticed that in eqs. (5.114) and (5.115) u_x and m_x have been made real. A single complex exponential can no longer be used as the equations are non-linear. The frequencies ω_k and $\omega_{k'}$ are assumed to be the same as those in the absence of any pumping or loss, that is they are still given by eq. (5.113). This is essentially correct in the region of the threshold field where the loss is exactly compensated by the phonon pumping. The amplitudes $m_k(t)$ are taken to be slowly varying functions of time compared to the exponential time factors. It is then reasonable to take

$$\frac{\partial^2}{\partial t^2} \left[m_k(t) \exp \left(i\omega_k t\right)\right] \approx (2i\omega \, \dot{m}_k - \omega_k^2 m_k) \exp \left(i\omega_k t\right).$$

Substituting eqs. (5.114) and (5.115) into eq. (5.112) and equating to zero the coefficients of

$$\exp \left[i(\omega_k t - k \cdot r)\right] \quad \text{and} \quad \exp \left[-i(\omega_{k'} t - k' \cdot r)\right]$$

it is found that

$$\left(\dot{m}_k + \frac{m_k}{\tau_k}\right) = \frac{b_1}{M_0} q m_{k'}^* u^0, \qquad \left(\dot{m}_{k'}^* + \frac{m_{k'}^*}{\tau_{k'}}\right) = \frac{b_1}{M_0} q m_k u^{0*}. \qquad (5.116)$$

Use has been made of the conditions for the conservation of energy and momentum,

$$\omega_k + \omega_{k'} = \omega_q; \quad k + k' = q. \qquad (5.117)$$

Taking the 'amplitudes' to be of the form $m_k(t) = m_k^0 \exp \left(\Gamma t\right)$ it follows from eq. (5.116) that

$$\Gamma = -\frac{1}{2} \left(\frac{1}{\tau_k} + \frac{1}{\tau_{k'}}\right) \pm \left[\frac{1}{4} \left(\frac{1}{\tau_k} - \frac{1}{\tau_{k'}}\right)^2 + \frac{b_1^2}{M_0^2} q^2 u^0 u^{0*}\right]^{1/2}. \qquad (5.118)$$

When the amplitude of the pump wave is sufficiently large Γ is positive so that the spin wave amplitude grows exponentially. The threshold amplitude is given by

$$|u^0|_{\text{threshold}} = \frac{M_0}{b_1 q (\tau_k \tau_{k'})^{1/2}} \qquad (5.119)$$

in agreement with the result of Haas. Because of the restriction, eq. (5.117), on the wave vectors and frequencies there is an upper limit to the value of the d.c. field H_0 for which amplification can occur. The upper limit is reached when $k = k' = \frac{1}{2}q$ and $\omega_k = \omega_{k'} = \frac{1}{2}\omega_q$. For YIG at 9 GHz this would occur at $H_0 \approx 1500$ Oe. As pointed out by Haas the lower limit on H_0 is dictated only in that it must be sufficient to saturate the sample.

In his original paper Gurevich found that a longitudinal wave along the z-direction would cause parametric excitation of two spin waves. As Haas pointed out the component of magnetization coupled to ϵ_{zz}, see eq. (5.61), is M_z. As this commutes with the Zeeman and the exchange term no such process can occur in this model. It is possible however if dipolar interactions are taken into account. The modifications that the dipolar terms make to the theory have been discussed by Haas and also by MATTHEWS and MORGENTHALER[1964]. Haas has also considered the amplification by transverse phonons and finds that in the absence of dipolar interactions the threshold is the same as that given by eq. (5.119) if b_1 is replaced by b_2.

In YIG where the transverse phonon velocity is about 0.5 of the longitudinal velocity and $b_1 \approx b_2$, the threshold power for pumping of transverse phonons is about $\frac{1}{10}$ that for longitudinal phonons which Haas estimates as $0.1–1$ W/cm² at 9 GHz depending upon the spin wave line width. For lithium ferrite b_2 is very small so pumping by
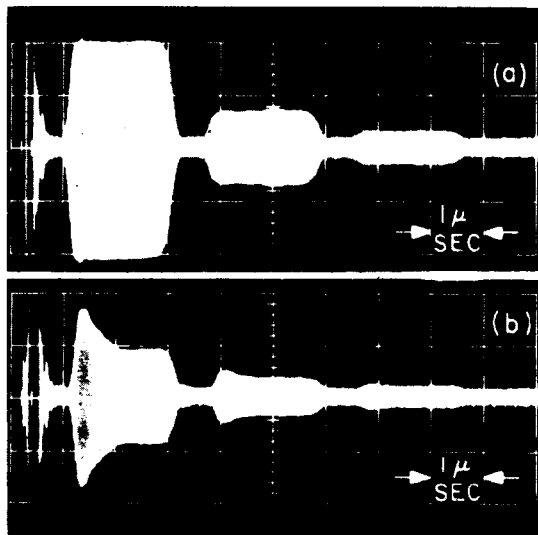
Fig. 5.9. (a) Normal propagation. (b) Breakdown. (Reproduced from H. MATTHEWS and F. R. MORGENTHALER, Phys. Rev. Lett. 13, 16 (1964) with permission.)

longitudinal phonons perpendicular to the d.c. field is more favorable. The corresponding threshold is about 10 mW/cm² at 9 GHz.

Experimental evidence for phonon pumping has been obtained by MATTHEWS and MORGENTHALER[1964]. A breakdown effect was observed consistent with their theoretical predictions. The propagation of 1 GHz longitudinal phonon pulses of $2\,\mu$sec duration was observed by a pulse-echo technique in a single crystal rod of gallium-substituted YIG. The direction of propagation and that of the d.c. magnetic field was along the $\langle 100 \rangle$ crystal axis. The echoes were observed as a function of the input power and the strength of the applied field. For a sufficiently large input power, breakdown as shown in fig. 5.9 occurred over a range of δH. They showed that the theory supported their view that the breakdown was due to the parametric excitation of $\frac{1}{2}\omega_q$ spin wave pairs near the top of the spin wave band.

4.3. *Other parametric processes*

MORGENTHALER[1962] and AULD[1962] independently suggested the possibility of producing phonons in a threshold process involving the uniform precession magnons excited by a transverse microwave field. Because the uniform precession magnons have $k = 0$ the process cannot arise from one-phonon processes since both energy and momentum cannot be conserved. Therefore the magnetoelastic interaction which arises from the term whose coefficient is F in eq. (5.56) does not contribute unless it is treated in second order in perturbation theory. The term quadratic in the strain in eq. (5.56) will provide a first-order contribution however. This is the term responsible for the intrinsic effect. By analogy with eq. (5.56) the elastic energy may be expanded in a Taylor series since the elastic constants will be functions of the magnetization.

$$W_e = \sum_{ijkl} c^0_{ijkl}\epsilon_{ij}\epsilon_{kl} + \sum_{ijkl} g_{ijkl}(\alpha)\epsilon_{ij}\epsilon_{kl} + \cdots .$$

The second term has the same form as the intrinsic term although its origin is quite different. It is referred to as the morphic effect. Both the intrinsic and morphic terms when written in second quantization can give rise to an interaction involving $(a_0 a^*_{qs} a^*_{qs} + c.c.)$. Whether this process is more important than that arising from the magnetoelastic term taken to second order in perturbation theory depends upon the relative magnitudes of the coupling constants.

So far spin waves which are propagating magnetoelastic oscillations of the magnetic moment have been investigated. The electric field was neglected and the magnetic field assumed to be irrotational, curl $H = 0$. However, electromagnetic waves can also propagate in magnetic crystals, so the full Maxwell's equations should be solved simul-
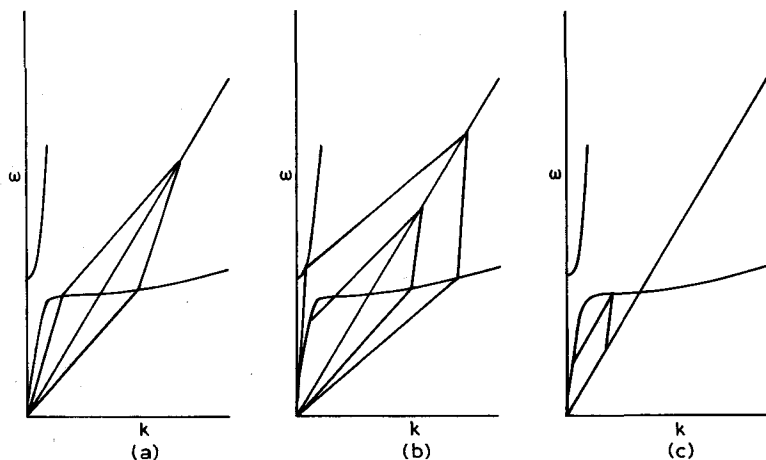
Fig. 5.10. Vector diagrams for parametric amplification of travelling waves discussed in text.

taneously with the magnetic moment equation. For k-values above $k_c = \omega(\mu\kappa)^{1/2}/c$ the electric field contribution is negligibly small and the magnetostatic region discussed above is applicable. c is the velocity of light in vacuo and μ and κ are the permeability and the permittivity of the medium respectively. When $k \approx k_c$ the electric and magnetic fields are of comparable magnitude and an electromagnetic region exists. In the vicinity of k_c the dispersion curve for the plane electromagnetic waves and the magnetic waves intersect and 'repel' as shown in fig. 5.10. Note that in this figure the extent of the electromagnetic region has been considerably exaggerated. Several types of parametric processes can be envisaged. The amplification of two spin waves by an elastic pump wave has just been treated, fig. 5.10(a). Alternatively an elastic pump wave might amplify a spin wave and an electromagnetic wave as illustrated, fig. 5.10(b). This process was considered by GURE-VICH[1964]. The theory is easily developed along the same lines as that described above. The reverse process, that of amplifying an elastic and an electromagnetic wave has been dealt with by COMSTOCK[1963]. fig. 5.10(c).

ACOUSTIC PARAMAGNETIC RESONANCE

1. Introduction

The study of the electron spin–lattice interaction using microwave ultrasonic waves has been a very fruitful area of research. It has often been called acoustic paramagnetic resonance – a.p.r. – to emphasize its similarities to conventional electron paramagnetic resonance – e.p.r. The discussion here will be restricted to electronic paramagnetism though nuclear paramagnetism has been studied using ultrasonic waves, BOLEF[1966], but only at much lower frequencies than the microwave frequency range with which this book is concerned.

The usual method employed in a.p.r. is to measure the attenuation of microwave ultrasound in a paramagnetic delay rod as a function of an applied magnetic field using a pulse-echo technique. An increased attenuation is observed at resonance when the paramagnetic ions scatter the ultrasonic waves. In addition there is dispersion at resonance: the phase velocity of the waves changes, which may result in an observable increase in the transit time of an ultrasonic pulse but the effect is more difficult to detect than the absorption.

The a.p.r. of a paramagnetic ion can be used to obtain information on its low-lying magnetic energy levels and on the coupling between the ion and the host crystal lattice. The resonant frequency and the applied magnetic field enable the separations between the energy levels to be found in the same way as in conventional e.p.r. experiments. A.p.r. has an advantage over e.p.r. in that the selection rules for the interaction between the ultrasonic wave and the electron spin are less restrictive and $\Delta M_S = \pm 2$ transitions can be observed as well as $\Delta M_S = \pm 1$. Thus it may happen that although a particular paramagnetic ion cannot be observed by e.p.r., it can be detected by a.p.r. This is especially true if the ion is strongly coupled to the lattice and gives a very intense a.p.r. absorption. Such an ion has a very rapid spin–lattice relaxation and may also have its resonance lines inhomogen-

eously broadened by random lattice strains. These broad weak lines are not easily detected by e.p.r.

The strength of the coupling between the ion and the lattice can be found from the magnitude of the change in ultrasonic attenuation at resonance. There are other methods of measuring this coupling–spin–lattice relaxation, e.p.r. with an applied static stress, low temperature magnetothermal resistance–and the results are complementary to a.p.r. but often more complex to interpret. Spin–lattice relaxation and magnetothermal resistance depend on thermal distributions of lattice vibrations, which makes interpretation difficult, while e.p.r. under static stress measures the coupling at zero frequency.

A further use of a.p.r. has been in the study of the passage of waves through a resonant system. Even though a path length of many wavelengths can readily be obtained a relatively long transit time compared with light waves is possible. A suitable paramagnetic ion can be chosen, strongly coupled to the lattice, to demonstrate phenomena only otherwise seen with very intense waves, SHIREN [1962b].

2. Experimental techniques

2.1. *Measurement of attenuation: — pulse-echo technique*

A typical a.p.r. X-band spectrometer using the pulse-echo method is shown diagrammatically in fig. 6.1. An ultrasonic pulse at about 9.5 GHz is generated using a piezoelectric transducer in the way described in ch. 3. The returning echoes from the paramagnetic delay rod are detected and the signal is taken to a box-car detector triggered to select a particular echo. The average detector output, proportional to the echo intensity, is applied to a chart recorder to plot out the a.p.r. spectrum.

The reasons for working at such a high frequency are the same as those which demand that e.p.r. be at microwave frequencies. Firstly, the absorption of energy is proportional to the frequency and so as high a frequency as possible is favoured. Secondly, the line-width of the resonances is such that at lower frequencies the lines could not be well resolved. The problems of a.p.r. increase rapidly at frequencies above 10 GHz because of the short wavelength of the ultrasonic waves which requires fine tolerances on orientation and polishing of the specimen delay rods. These problems have been considered in ch. 3, where it has also been shown that experiments must usually be made with the ultrasonic waves travelling along a high symmetry axis of the specimen. Experiments must usually be made at temperatures below 20 K because of the attenuation of the ultrasonic waves by scattering
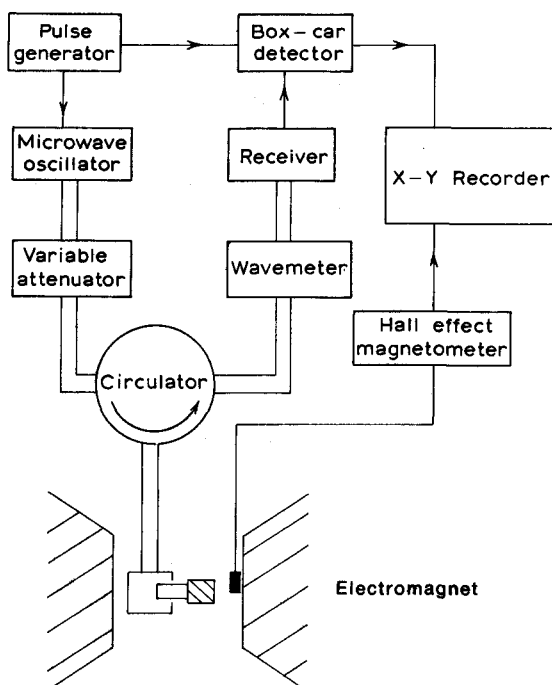
Fig. 6.1. Block diagram of acoustic paramagnetic resonance spectrometer.

by thermal phonons. If this background attenuation is too large the a.p.r. attenuation cannot be accurately measured.

If the coupling between the electron spins and the lattice depends linearly on the strain, then the probability per spin for a transition in the spin system due to a single oscillating strain component of amplitude ϵ produced by an ultrasonic wave can be written as $W\epsilon^2$ per unit time. The acoustic energy flux flowing through unit area of the crystal per unit time perpendicular to the propagation direction is $P = \frac{1}{2}cv\epsilon^2$ where c is an elastic stiffness constant and v the appropriate velocity of sound – ignoring the resonant dispersion. The energy absorbed per unit time by the spin system from the ultrasonic wave is $W\epsilon^2\hbar\omega\delta x n/V$ in a distance δx, where n is the population difference of the two spin energy levels involved in the transition and ω is the angular frequency of the wave. V is the volume of the crystal. Hence the change in the acoustic energy flux in the distance δx is $\delta P = - W\epsilon^2\hbar\omega\delta x n/V$. Substituting for ϵ^2 in terms of P and integrating it follows that

$$P = P_0 \exp\left(-\alpha x\right) \quad \text{with} \quad \alpha = 2W\hbar\omega n/cvV. \qquad (6.1)$$

The ultrasonic power decays exponentially with an attenuation

constant α, which can also be written in the form

$$\alpha = 2W\hbar\omega n/\rho v^3 V \qquad (6.2)$$

if the relationship between the sound velocity, v, the elastic constant c and the density ρ of the specimen is recalled. The extension to the case where the ultrasonic wave can be resolved into several strain components is straightforward. The expression for the transition probability W in terms of the spin–lattice coupling constant is considered later.

2.2. Measurement of dispersion

The dispersion of the ultrasonic waves at resonance can also be investigated experimentally. This can be done using the method of GUERMEUR et al. [1964] and which is shown diagrammatically in fig. 6.2. A transducer and paramagnetic delay rod are used in the same way as for attenuation measurements but a second quartz transducer acting as a delay rod is used to provide an echo that will coincide with a chosen echo from the paramagnetic specimen after both transducers have been excited with the same initial microwave pulse. The two echoes are detected separately and the microwave signals are brought together after the reference echo has passed a variable attenuator and variable phase shifter. These two controls can be adjusted to give
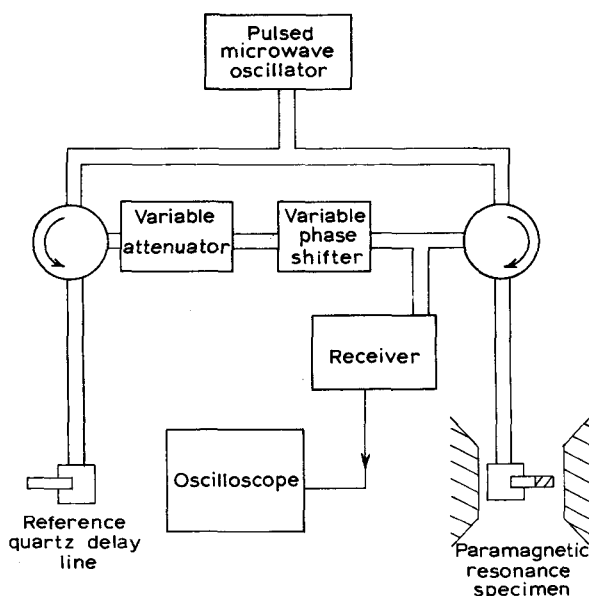
Fig. 6.2. Block diagram of acoustic paramagnetic resonance spectrometer for dispersion measurements.

complete destructive interference between the two echoes. This is done first with the magnetic field off resonance and then the change in phase setting needed for destructive interference with the magnetic field adjusted on resonance is noted. This gives the resonance dispersion in the specimen. The change in attenuator setting enables the absorption spectrum to be obtained in the same experiment.

2.3. Paramagnetic saturation

Another method of investigating the spin–lattice coupling is by the saturation of a conventional e.p.r. line using ultrasonic waves at the resonance frequency. In fact the first reported a.p.r. experiment was made in this way, JACOBSEN et al. [1959], using a specimen of irradiated quartz. The method has also been used by TUCKER [1961a] to study Cr^{3+} in corundum (Al_2O_3) and by LEWIS and STONEHAM [1967] to investigate Ni^{2+} and Fe^{2+} in magnesium oxide. The apparatus used is shown in fig. 6.3. The paramagnetic specimen is bonded to an ultrasonic transducer which is in a microwave resonant cavity for generation of the ultrasonic waves. The paramagnetic sample projects into another resonant cavity which forms part of an e.p.r. spectrometer. The e.p.r. signal is observed in the spectrometer and the change in its magnitude is measured when the ultrasonic waves are introduced. The change is due to the reduction in the population difference between the levels responsible for the resonance. Let δn be the change in the population
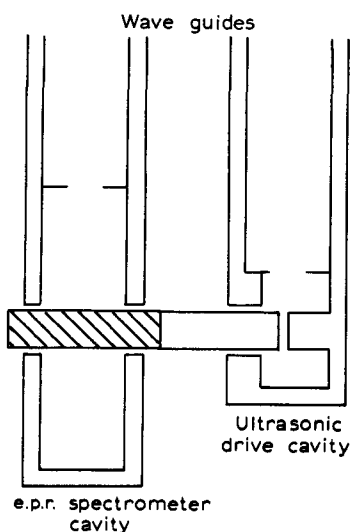
Fig. 6.3. Cavity system for e.p.r. saturation by ultrasonic waves.

difference n between the pair of levels. There are three contributions to δn, $-2U_E n\delta t$ and $-2U_A n\delta t$ due respectively to the incident electro-magnetic radiation and the incident ultrasonic waves and a contribution of $(n_0 - n)\delta t/T_1$ arising from spin–lattice relaxation. U_E and U_A are the transition probabilities for the interaction of the spin system with electromagnetic radiation and ultrasonic waves respectively. T_1 is the spin–lattice relaxation time and n_0 the thermal equilibrium value of n in the absence of any incident radiation. Thus the rate of change with time of the population difference n is given by

$$\frac{\mathrm{d}n}{\mathrm{d}t} = \frac{n_0 - n}{T_1} - 2U_E n - 2U_A n.$$

The factor 2 appears because in each transition the difference in population of the two levels changes by two. In the steady state $\mathrm{d}n/\mathrm{d}t = 0$ and so

$$\frac{n}{n_0} = \frac{1}{1 + 2(U_E + U_A)T_1}. \tag{6.3}$$

The e.p.r. signal obtained is proportional to n, the population difference. Initially, if the e.p.r. spectrometer is operated at very low power, $2U_E T_1 \ll 1$ and in the absence of ultrasonic waves, $U_A = 0$, the e.p.r. signal is proportional to $n \approx n_0$. Measurements of the ratio n/n_0 can then be made as the ultrasonic power is increased. An independent measurement of T_1 is needed to arrive at a value of U_A which depends on the spin–lattice coupling coefficients. TUCKER[1966b] avoided the need to measure T_1 by saturating his spins with electromagnetic radiation at the resonant frequency. This radiation was incoherent with his spectrometer signal so was thus not detected. After finding the amount of r.f. power required to give the same degree of saturation, a calculation of U_E enables U_A to be found.

2.4. Continuous wave technique

A c.w. technique for observing a.p.r. has been used by BOLEF et al. [1962]. Frequencies up to 1 GHz were employed. The reduced signal strength from the a.p.r. at this lower frequency was compensated by the greater sensitivity of the apparatus which used a synchronous detection system. The a.p.r. spectrometer was very similar to a conventional e.p.r. spectrometer but used the mechanical resonance of the specimen rod instead of a microwave cavity resonance. The applied magnetic field was modulated and a signal due to the increased acoustic loss was detected at the modulation frequency when the mean magnetic field tuned the ions to resonance.

3. The spin Hamiltonian

3.1. *Concept of the spin Hamiltonian*

Acoustic paramagnetic resonance is closely related to conventional electron paramagnetic resonance and many of the methods used to express the results of experiments and to describe the low-lying energy levels of a paramagnetic ion are common to them both. A particularly convenient method is to express the experimental results in terms of a spin Hamiltonian. An outline of this method will be given here together with an account of how the parameters in the spin Hamiltonian are determined from theory. For more detailed accounts the reader is referred to the works on e.p.r., for example BLEANEY and STEVENS [1953], LOW[1960], PAKE[1962], AL'TSHULER and KOZYREV[1964] and ABRAGAM and BLEANEY[1970].

Those energy levels of a paramagnetic ion in a solid which can be studied by a.p.r. are very close to the ground state because the energy of the ultrasonic phonons is small and because only low-lying energy levels are populated at the low temperatures which must be employed. These low-lying energy levels are usually small in number and can be described by an effective spin Hamiltonian, which is a polynomial in the components of an effective spin operator. The effective spin may or may not be the same as the real spin of the ion. The basic idea is to replace the Hamiltonian which describes all the states of the ion by another simpler Hamiltonian which only predicts these low-lying states accurately. This Hamiltonian will only contain a limited number of parameters whose values are deduced from experiment. Once these constants have been determined, the Hamiltonian can then be used to calculate other quantities and to predict other phenomena. The task of theory is to derive the parameters of the spin Hamiltonian from the full Hamiltonian of the ion in its host crystal lattice. An example of how this is done is given in §3.4. The spin Hamiltonian is thus essentially a stepping stone between theory and experiment.

As an example consider an ion that has two low-lying states well separated from any other populated state at low temperatures. Then as far as a.p.r. and e.p.r. experiments are concerned the ion is just a simple two-level system and its energy levels might appear to be much like those of a spin $\frac{1}{2}$ in a magnetic field. This suggests that the system should be described by a Hamiltonian involving spin operators for $S = \frac{1}{2}$. The most general form for this Hamiltonian is

$$H = AS_x + BS_y + CS_z + D. \tag{6.4}$$

In a representation in which S_z is diagonal the operators S_x, S_y and S_z are given by the Pauli matrices

$$S_x = \frac{1}{2}\begin{pmatrix} 0 & 1 \\ 1 & 0 \end{pmatrix}; \qquad S_y = \frac{1}{2}\begin{pmatrix} 0 & -i \\ i & 0 \end{pmatrix}; \qquad S_z = \frac{1}{2}\begin{pmatrix} 1 & 0 \\ 0 & -1 \end{pmatrix}$$

see for example the book by MANDL [1957]. These operators obey the usual spin commutation rules,

$$S_x S_y - S_y S_x = iS_z \text{ etc.} \qquad (6.5)$$

In addition, for $S = \frac{1}{2}$, other relationships hold as may be verified by direct matrix multiplication

$$S_x S_y + S_y S_x = 0 \qquad (6.6)$$

and

$$S_x^2 = S_y^2 = S_z^2 = \frac{1}{4}. \qquad (6.7)$$

It is clear then why the general spin Hamiltonian of eq. (6.4) for $S = \frac{1}{2}$ does not contain higher powers than the first in the components of the spin operators. Any higher power can be reduced by means of eqs. (6.6) and (6.7). For instance $S_x^3 S_y$ is readily reduced to $\frac{1}{8}iS_z$. The parameters A, B, C and D are not strictly constants but are chosen functions of, say, the magnitude and direction of the external magnetic field or other perturbation applied to the ion under consideration. Their values are adjusted until the energy level spectrum mapped out by the spin Hamiltonian agrees with experiment. It is noted that the matrix representation of any two-level system is a 2×2 hermitian matrix. Any 2×2 hermitian matrix can clearly be written as a linear combination of the three Pauli matrices above and the unit matrix $\begin{pmatrix} 1 & 0 \\ 0 & 1 \end{pmatrix}$. When one extends the theory to more complicated systems more independent matrices will be required. For instance in a three-level system 9 independent matrices are required to form an arbitrary 3×3 hermitian matrix. A convenient choice for these matrices is given in appendix 6. It is noted that now the spin Hamiltonian will contain terms quadratic in the components of S. Clearly on these arguments the spin of the spin Hamiltonian is such that $(2S + 1)$ is just the number of low-lying states. It is clear then that this spin need not have anything to do with the true spin of the ion, in fact the different states of the ion may contain different admixtures of orbital motion as well as spin.

3.2. *Energy levels of a paramagnetic ion*

The following sections will be mainly concerned with the ions of the iron group of transition metals as most a.p.r. work has been done on these ions. Some work has been reported on the rare earth ions and on uranium and these will be discussed more briefly. The main differences between the groups of ions stem from the relative magnitudes

of the different interactions affecting the paramagnetic electrons of the ions when they are embedded in their host lattice. In the iron group salts the interaction between the paramagnetic ion and its dia-magnetic neighbours is quite strong because the outermost 3d electrons are fully exposed to the crystal field of the surrounding atoms in the host lattice. The crystal field interaction is then usually stronger than the spin-orbit coupling. In the rare earth ions the paramagnetism is due to the 4f electrons which, because they are shielded by the 5s and 5p shells, do not interact to such a large extent with the electric field of their neighbours. The spin–orbit coupling is therefore stronger than the crystal field interaction in salts of these ions.

The full Hamiltonian for a paramagnetic ion in a dielectric crystal can be written as

$$H = V_{\text{free}} + V_{\text{crystal}} + V_{\text{spin-orbit}} + V_{\text{Zeeman}}. \tag{6.8}$$

The first term is the Hamiltonian of the free ion except for the spin-orbit coupling. One usually begins by treating the Coulomb interaction of the nucleus and the other electrons by a central field approximation in which the electrons move independently of each other within the restriction of the Pauli exclusion principle. This gives rise to the idea of configurations which are described by specifying the number of electrons in each orbit e.g. $3d^3 4s$. Next, account is taken of the cor-relations between the electrons due to the Coulomb repulsion and exchange. In the Russell–Saunders coupling scheme these inter-actions cause the configuration to be split up into terms each specified by the electron orbits and the total orbital and spin moments, e.g. $3d^2\,^1F$. (This nomenclature is explained in any elementary text-book on atomic spectroscopy.) The term separations are usually of the order of $10^4\ \text{cm}^{-1}$ so that in a.p.r. experiments interest is generally only in the lowest term of the configuration. The next two terms in the Hamil-tonian are the crystal field interaction due to the neighbouring ions and the spin–orbit coupling. In cases where the total orbital angular momentum L and the total spin S are reasonably good quantum numbers the spin–orbit coupling can be written as $\lambda L \cdot S$. Which of the two terms is treated first depends on their relative magnitudes. In the iron group salts where, as mentioned, the crystal field interaction is stronger than the spin–orbit coupling, one proceeds by finding out how the crystal field perturbs the orbital levels and then including the spin–orbit coupling as a secondary perturbation. This is known as the intermediate crystal field case. On the other hand, in the rare earth salts the effect of the spin–orbit interaction has to be treated first. This interaction may be thought of as a magnetic interaction between the magnetic moments associated with the orbital and spin motions.

This gives rise to a set of states characterized by the quantum number J, the total angular momentum. The crystal field is then a perturbation which acts on the degenerate states of J. This is the weak crystal field case. In the iron group salts the typical energies involved are $10^3 \, cm^{-1}$ and $10^2 \, cm^{-1}$ respectively for the crystal field and spin–orbit terms. In the rare earth salts these two numbers are interchanged. There is in fact a third case which can be considered. This is the strong field case which is relevant to the palladium and platinum group transition ions and to certain cyanides of the 3d group. In these situations the crystal field interactions are so strong that they are greater than the Coulomb interactions between the electrons in the unfilled shells. The crystal field interaction is then strong enough to prevent the formation of the resultant L and S in the first place.

The crystal field term is in fact composed of two parts, a static term which would be present for stationary ions and a smaller dynamic term due to the thermal motion of the crystal lattice ions or due to an incident ultrasonic wave. The static term, which is the part used to determine the energy levels of the ion in its surroundings, can be treated by crystal field theory. This is an approximation in which the chemical bonding is assumed to be purely ionic and the interaction of the neighbouring ions on the paramagnetic ion is represented by the electrostatic field of a set of point charges placed at the neighbouring sites. Although this approximation is rather crude it does appear to work and has been successful in several areas of research. A better approach would be to attempt a full molecular orbital calculation for a cluster of ions comprising the paramagnetic ion and its immediate neighbours. However only limited success has been achieved along these lines. Covalent bonding, which among other things reduces the orbital contribution to the magnetic moment, is sometimes accounted for by an orbital reduction factor, see for example Low[1960]. The dynamic term which gives rise to the spin–lattice interaction is treated later in this chapter. It provides the mechanism whereby energy transfer between the spin system and the phonon modes of the lattice can take place.

The lowest state of the free ion Hamiltonian, V_{free}, can be predicted using Hund's rule. This rule states that the lowest term is the one having maximum total spin and, secondly, maximum total orbital momentum consistent with the exclusion principle. The term is specified by its value of L and S and is $(2L+1)(2S+1)$ degenerate. When a free ion of the iron group is placed in a crystal field of a given symmetry the orbital degeneracy is completely or partially lifted because the Hamiltonian no longer has full rotation symmetry. The crystal field splitting in the iron group ions often leaves the ground

state with a smaller orbital magnetic moment than the free ion; this is the well known quenching phenomenon.

The final perturbation in the Hamiltonian is the Zeeman term, $\beta(L + 2S) \cdot H$, the interaction of the spin and orbital magnetic moments with an external magnetic field.* In many cases this may be represented by a spin Hamiltonian $\beta H \cdot g \cdot S$ where g is the effective g-value. Such a term has energies generally of the order of $10^{-2}\ \mathrm{cm}^{-1}$ and can therefore be treated as a very small perturbation after the spin–orbit coupling has been accounted for. If the crystal field leaves an orbital singlet lowest, that is to say quenching is complete, the effective spin is equal to the real spin and the g-value is close to the free electron value of 2. The admixture of higher levels by the spin–orbit coupling may reinstate a small orbital contribution to the magnetic moment and g then differs slightly from 2. If the crystal field leaves a degenerate lowest level, then the effective spin is different from the real spin and is chosen, as was mentioned above, such that $(2S + 1)$ is equal to the total number of states in the group of low-lying levels described by the spin Hamiltonian.

In trying to guess a particular form for a spin Hamiltonian two theorems prove useful. Kramers theorem states that in a system with an odd number of electrons the energy levels in an external electric field will be at least two-fold degenerate. Thus the energy levels of a paramagnetic ion with an odd number of electrons tend to be doublets when the ion is in the electric field of the crystal lattice. The theorem of Jahn and Teller states that, apart from linear complexes, a complex which has a degenerate ground state will spontaneously distort in such a way that the degeneracy is removed; the complex can reduce its energy in this way. In the case of a paramagnetic ion in a solid, the complex can be regarded as formed by the ion and its nearest neighbours. If the complex distorts, the elastic energy of the lattice is increased and equilibrium is reached when this is equal to the reduction in the electronic energy due to the distortion. For some ions, for example Cr^{2+} in magnesium oxide, a dynamic Jahn-Teller effect occurs. The energy reducing distortion can occur in one of three equivalent ways and quantum mechanical tunneling is possible between them. In this way the final energy level scheme and the states can be considerably modified.

3.3. Crystal field theory

An outline of crystal field theory will now be given. A more detailed account can be found in the excellent review article of HUTCHINGS

---

*The use of H in this chapter both for the Hamiltonian and for the magnetic field should not present difficulties.

[1964] which is particularly useful in that it systematizes the many different notations adopted by earlier researchers.

The crystal field potential on the basis of a point ion model is

$$V_{\text{crystal}} = \sum_i q_i V_i = \sum_{i,j} \frac{q_i q_j}{|\mathbf{R}_j - \mathbf{r}_i|}. \qquad (6.9)$$

q_i is the charge of the ith electron of the paramagnetic ion at position $\mathbf{r}_i$ and q_j the point charge representing the nearest neighbour ion at position $\mathbf{R}_j$. The sum over j is over neighbouring sites (usually only the nearest neighbours are considered) of the paramagnetic ion and the sum over i is over the electrons of the unfilled shell, the 3d electrons of the iron group ions or the 4f electrons of the rare earth ions. The crystal field potential $V^c = \sum_j q_j/|\mathbf{R}_j - \mathbf{r}|$, which of course is a solution of Laplace's equation, can be conveniently expanded in spherical harmonics, taking the position of the nucleus of the paramagnetic ion as origin

$$V^c = \sum_{n,m} A_n^m r^n Y_n^m(\theta\phi). \qquad (6.10)$$

The spherical harmonics $Y_n^m(\theta\phi)$ are normalized to unity and defined by

$$Y_n^m = (-1)^n \left\{ \frac{(2n+1)(n-|m|)!}{2(n+|m|)!} \right\} \frac{1}{(2\pi)^{1/2}} P_n^{|m|}(\cos\theta)\, e^{im\phi}, \qquad (6.11)$$

where

$$P_n^m(x) = \frac{(1-x^2)^{(1/2)m}}{2^n n!} \frac{d^{n+m}}{dx^{n+m}} (x^2 - 1)^n.$$

The non-zero coefficients A_n^m that occur in the expansion depend on the crystal symmetry. It might be thought that there is no limit to the value of n that can occur in the expression. However, it turns out that the expression for V^c can be terminated at a fairly early stage for the following reason. There is a useful theorem in mathematics which states that the integral of the product of three spherical harmonics is non-zero only if their three values of n can form a triangle. To calculate the energy splitting due to the crystal field the matrix element of V^c with respect to the appropriate electron wave function has to be taken. In the iron group ions these wave functions are those of the 3d electrons and it is well known that the angular part of these wave functions in the central field problem is described by spherical harmonics of order 2. Consequently when working out the matrix element of V^c only that part of V^c having spherical harmonics of order $n \leqslant 4$ can contribute because of the triangulation rule. Similarly for the rare earth ions, where the unpaired electrons are the 4f electrons, n must be less than or equal to six. A further reduction in the number of terms in V^c is dictated by symmetry. As an example consider an ion in a field

of octahedral symmetry and suppose that the polar axis of coordinates is chosen to be along one of the four-fold axes of symmetry. This means that $V^c(r, \theta, \phi)$ must be equal to $V^c(r, \theta, \phi + \frac{1}{2}\pi)$. Since $Y_n^m(\theta, \phi)$ depends on ϕ through $\exp(im\phi)$ this implies that m can be restricted to 0 or ± 4 when dealing with iron group ions. Also odd values of n cannot occur because there is a centre of inversion. In addition, because there is four-fold symmetry about the x-axis, A_2^0 must be zero and the ratio A_4^0 to A_4^4 is uniquely determined. Dropping the constant term A_0^0 which can only shift all energy levels equally, V^c for a field of octahedral symmetry will have the form

$$V_{\text{oct}}^c = A_4^0 r^4 \{Y_4^0(\theta\phi) + \sqrt{\tfrac{5}{14}}[Y_4^4(\theta\phi) + Y_4^{-4}(\theta\phi)]\} \qquad (6.12)$$

when dealing with iron group ions. For the ions of the rare earth group the additional term

$$A_6^0 r^6 \{Y_6^0(\theta\phi) - \sqrt{\tfrac{7}{2}}[Y_6^4(\theta\phi) + Y_6^{-4}(\theta\phi)]\} \qquad (6.13)$$

must be added. Note that the spherical harmonics that occur depend upon the choice of the polar axis. If the polar axis is not the four-fold cubic axis of symmetry a different combination of spherical harmonics will occur. The values of the parameters A_4^0 and A_6^0 depend on the details of the model adopted to represent the crystal field. For a point charge model in which the paramagnetic ion is surrounded by charges each of magnitude q at positions $(\pm a, 0, 0)$, $(0, \pm a, 0)$, $(0, 0, \pm a)$ with respect to the fourfold symmetry axes, it is found that

$$A_4^0 = \tfrac{7}{3}\sqrt{\pi} q/a^5 \quad \text{and} \quad A_6^0 = \tfrac{3}{2}\sqrt{\tfrac{1}{13}\pi} q/a^7. \qquad (6.14)$$

However for most purposes it is only the symmetry of the crystal field that is required, the parameters A_n^m being regarded as constants to be determined by experiment.

In order to calculate the matrix elements of V^c the radial part $f(r)$ of the single 3d (or 4f) electron wave function is required. This is not usually known very accurately. Parameters $\langle r^n \rangle$ defined by

$$\langle r^n \rangle = \int [f(r)]^2 r^n r^2 \mathrm{d}r \qquad (6.15)$$

are needed for each ion. Several theoretical calculations have been made to determine these and some of the values obtained are listed in table 6.1.

3.4. An example — Ni^{2+} in an octahedral field

In order to show how the crystal field energy splittings may be calculated we proceed by way of an example. An easy example to consider is the case of a Ni^{2+} ion in a cubic host crystal. This is an ion that gives a fairly strong a.p.r. absorption and it has been investigated by this technique in magnesium oxide by SHIREN [1962a] and in potassium

TABLE 6.1

$\langle r^2 \rangle$ and $\langle r^4 \rangle$ for 3d electrons of iron group ions[a]) in atomic units

Ion	Term	$\langle r^2 \rangle$	$\langle r^4 \rangle$
Ti^{3+}	^2D	1.911	7.307
V^{3+}	^3F	1.632	5.450
V^{2+}	^4F	2.028	9.112
Cr^{3+}	^4F	1.435	4.277
Cr^{2+}	^5D	1.760	7.003
Mn^{3+}	^5D	1.278	3.426
Mn^{2+}	^6S	1.528	5.325
Fe^{3+}	^6S	1.141	2.765
Fe^{2+}	^5D	1.391	4.530
Co^{2+}	^4F	1.262	3.861
Ni^{2+}	^3F	1.146	3.245
Cu^{2+}	^2D	1.044	2.671

$\langle r^2 \rangle$, $\langle r^4 \rangle$ and $\langle r^6 \rangle$ for 4f electrons of the rare earth ions[b]) in atomic units

Ion	$\langle r^2 \rangle$	$\langle r^4 \rangle$	$\langle r^6 \rangle$
Ce^{3+}	1.200	3.455	21.226
Pr^{3+}	1.086	2.822	15.726
Nd^{3+}	1.001	2.401	12.396
Sm^{3+}	0.883	1.897	8.775
Eu^{2+}	0.938	2.273	11.670
Gd^{3+}	0.785	1.515	6.281
Dy^{3+}	0.726	1.322	5.102
Er^{3+}	0.666	1.126	3.978
Yb^{3+}	0.613	0.960	3.104

[a]) From MICHEL-CALENDINI and KIBLER[1968].
[b]) From FREEMAN and WATSON [1962].

magnesium fluoride by ROSENBERG and WIGMORE[1967]. The model taken is of a Ni^{2+} ion surrounded by an octahedron of six O^{2-} ions (or F^- in the case of KMgF). These nearest neighbours produce a crystal field perturbation as given by eq. (6.12). The lowest term of the free ion configuration is found using Hund's rule and for Ni^{2+} which has eight 3d electrons in its unfilled shell it will be ^3F. Thus there are seven orbital states to consider. These are found to be split (see below) by the crystal field in the manner shown in fig. 6.4. This figure also shows the splitting of the orbital levels appropriate to the other iron group ions when placed in an octahedral field. The states of the free ion are labelled by the quantum numbers L and M_L and are written thus $|L, M_L\rangle$. Their wave functions will be denoted by $\psi(M_L)$.
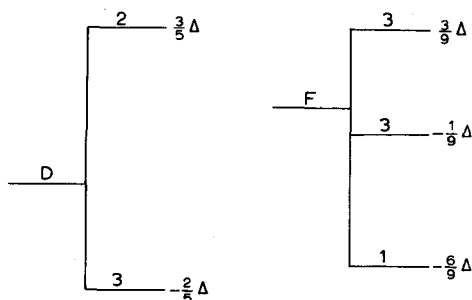
Fig. 6.4. Orbital energy levels of iron group ions in an octrahedral crystal field; showing the lowest term of the free ion and the energies in terms of the overall splitting. The degeneracy of each level is also shown. The D-term arises from $3d^1$ and $3d^6$ ions and from $3d^4$ and $3d^9$ ions for which the diagram is inverted. The F-term arises from $3d^3$ and $3d^8$ ions and from $3d^2$ and $3d^7$ ions for which the diagram is inverted.

To evaluate the matrix elements of the crystal field potential integrals of the type $\int \psi^*(M_L) Y_n^m \psi(M_L') \, dr$ have to be calculated. The number of matrix elements which have to be evaluated can fortunately be reduced in practice because it can be shown that when one matrix element for a particular n has been evaluated the other non-zero elements with the same n but with different m can be found from symmetry arguments. In the evaluation of the matrix elements the idea of operator equivalents due to STEVENS [1952] proves useful. To introduce these it is better to write the potential operator in cartesian coordinates

$$V_{\text{oct}}^c = \sum_{\text{electrons}} B_4^0 (35z^4 - 30r^2z^2 + 3r^4) + B_4^4(x^4 - 6x^2y^2 + y^4), \quad (6.16)$$

where

$$B_4^0 = \tfrac{1}{5}B_4^4 = \frac{3}{16\sqrt{\pi}} A_4^0.$$

Thus for the Ni^{2+} ion under consideration the matrix elements, for example of $\sum (35z^4 - 30r^2z^2 + 3r^4)$, are required between the states of the $(3d^8)^3F$ term. Stevens showed that the matrix elements of such operators are proportional to the matrix elements of similar operators in which x, y and z are replaced everywhere by L_x, L_y and L_z. In making the replacement care must be exercised because the angular momentum operators do not commute. For example $\sum xy$ must be replaced by the symmetrized combination $\tfrac{1}{2}(L_xL_y + L_yL_x)$. In this way the potential function of eq. (6.16) is replaced by an equivalent operator*

$$B_4^0 \beta' \langle r^4 \rangle [O_4^0 + 5O_4^4] \quad (6.17)$$

* A prime is placed on the parameter β' so that it is not confused with the Bohr magneton.

where the expressions for O_4^0 and O_4^4 are given in table 6.2. The proportionality constant is the same for all harmonics of a given n but different m. α, β' and γ are used when $n = 2$, 4 and 6 respectively. The matrix elements of this equivalent operator between the states $|3, 3\rangle$, $|3, 2\rangle$, $\cdots$ $|3, -3\rangle$ can then be readily evaluated by using the well-known rules for angular momentum operators, see for example MESSIAH [1961] (cf. eq. (5.6)).

$$L_+|L, M\rangle = [L(L+1) - M(M+1)]^{1/2}|L, M+1\rangle,$$
$$L_-|L, M\rangle = [L(L+1) - M(M-1)]^{1/2}|L, M-1\rangle. \quad (6.18)$$

The L_+ and L_- operators are defined in a similar manner to the S_+ and S_- operators of eq. (5.4). The proportionality constant β' depends on the particular ion under consideration and is determined by evaluating one matrix element explicitly as follows. First it is noted that instead of dealing with 8 3d electrons it is easier to consider the two holes remaining in the 3d shell. That is, the term $(3d^2)^3F$ may be considered and the sign of β' reversed to account for the change in sign of the charge. Consider the state $|3, 3\rangle$. This may be taken as a product of single electron states, suitably antisymmetrized, in which one 3d electron has $l_z = 2$ and the other $l_z = 1$. Such a state would have $L_z = 3$. The crystal field matrix element

$$\int \psi^*(3)\,(35z^4 - 30r^2z^2 + 3r^4)\psi(3)\,\mathrm{d}r$$

then breaks down into the sum of

$$\int \phi^*(2)\,(35z^4 - 30r^2z^2 + 3r^4)\phi(2)\,\mathrm{d}r$$

and

$$\int \phi^*(1)\,(35z^4 - 30r^2z^2 + 3r^4)\phi(1)\,\mathrm{d}r$$

where the 3d wavefunction $\phi(m)$ is $f(r)Y_2^m(\theta\phi)$. On evaluating the angular part of these integrals they are found to give $-\frac{8}{7}\langle r^4\rangle$. If now the matrix element $\beta'\langle r^4\rangle\langle 3, 3|O_4^0|3, 3\rangle$ is evaluated directly using eq. (6.18) it is found to give $180\beta'\langle r^4\rangle$. The constant β' must thus have the value $+\frac{2}{315}$ for Ni^{2+}.

To find the energy levels of the ion in the crystal field, all the matrix elements of the operator of eq. (6.17) between the states $|L, M_L\rangle$ are required. These are $60\beta' B_4^0\langle r^4\rangle$ times the matrix elements given below. Where there are blanks the matrix elements are zero. The secular equation can now be set up by subtracting E off the diagonal elements of the above matrix and equating the determinant to zero. Clearly, from the structure of the above matrix the secular determinant factor-

	$\lvert 3,0\rangle$	$\lvert 3,-1\rangle$	$\lvert 3,3\rangle$	$\lvert 3,1\rangle$	$\lvert 3,-3\rangle$	$\lvert 3,2\rangle$	$\lvert 3,-2\rangle$
$\langle 3,0\rvert$	6						
$\langle 3,-1\rvert$		1	$\sqrt{15}$				
$\langle 3,3\rvert$		$\sqrt{15}$	3				
$\langle 3,1\rvert$				1	$\sqrt{15}$		
$\langle 3,-3\rvert$				$\sqrt{15}$	3		
$\langle 3,2\rvert$						-7	5
$\langle 3,-2\rvert$						5	-7

izes into four parts giving one linear and three quadratic equations. The solution of these four equations is straightforward and leads to the states with the energies shown below.

$$
\begin{array}{cc}
\textit{State} & \textit{Energy}
\end{array}
$$

$$
\left.
\begin{aligned}
\lvert T_1,-1\rangle &\equiv \sqrt{\tfrac{3}{8}}\,\lvert 3,-1\rangle + \sqrt{\tfrac{5}{8}}\,\lvert 3,3\rangle \\[4pt]
\lvert T_1,1\rangle &\equiv \sqrt{\tfrac{3}{8}}\,\lvert 3,1\rangle + \sqrt{\tfrac{5}{8}}\,\lvert 3,-3\rangle \\[4pt]
\lvert T_1,0\rangle &\equiv \lvert 3,0\rangle
\end{aligned}
\right\} \quad 360\beta'\langle r^4\rangle B_4^0
$$

$$
\left.
\begin{aligned}
\lvert T_2,0\rangle &\equiv \sqrt{\tfrac{1}{2}}\,\lvert 3,2\rangle + \sqrt{\tfrac{1}{2}}\,\lvert 3,-2\rangle \\[4pt]
\lvert T_2,1\rangle &\equiv \sqrt{\tfrac{5}{8}}\,\lvert 3,1\rangle - \sqrt{\tfrac{3}{8}}\,\lvert 3,-3\rangle \\[4pt]
\lvert T_2,-1\rangle &\equiv \sqrt{\tfrac{5}{8}}\,\lvert 3,-1\rangle - \sqrt{\tfrac{3}{8}}\,\lvert 3,3\rangle
\end{aligned}
\right\} \quad -120\beta'\langle r^4\rangle B_4^0
$$

$$
\lvert A_2\rangle \equiv \sqrt{\tfrac{1}{2}}\,\lvert 3,2\rangle - \sqrt{\tfrac{1}{2}}\,\lvert 3,-2\rangle \quad -720\beta'\langle r^4\rangle B_4^0
$$

(6.19)

It is seen that the seven-fold orbital degenerate states of the free ion split into two triplets and a singlet in the presence of the octahedral crystal field. The states are labelled according to the irreducible representation of the cubic group to which they belong. Although group theory is outside the scope of this book it should be mentioned that it can be used to deduce directly the qualitative, but not quantitative, way in which the states split in the presence of a crystal field of a particular symmetry. The energies are quoted in terms of the parameters β', $\langle r^4\rangle$ and B_4^0. The first two of these as shown above depend upon the ion under consideration. For Ni^{2+} they are $+2/315$ and $3\cdot245$

TABLE 6.2

Equivalent operators[a]

$$\sum(3z^2 - r^2) \equiv \alpha\langle r^2\rangle O_2^0 = \alpha\langle r^2\rangle[3L_z^2 - L(L+1)]$$

$$\sum xy \equiv \alpha\langle r^2\rangle O_2^1 = \alpha\langle r^2\rangle(\tfrac{1}{4})[(2L_z-1)L_+ + (2L_z+1)L_-]$$

$$\sum yz \equiv \alpha\langle r^2\rangle O_2^1(s) = \alpha\langle r^2\rangle(-\tfrac{1}{4}i)[(2L_z-1)L_+ - (2L_z+1)L_-]$$

$$\sum(x^2-y^2) \equiv \alpha\langle r^2\rangle O_2^2 = \alpha\langle r^2\rangle(\tfrac{1}{2})[L_+^2 + L_-^2]$$

$$\sum 2xy \equiv \alpha\langle r^2\rangle O_2^2(s) = \alpha\langle r^2\rangle(-\tfrac{1}{2}i)[L_+^2 - L_-^2]$$

$$\sum(35z^4 - 30z^2\zeta^2 + 3r^2) \equiv \beta'\langle r^4\rangle O_4^0 = \beta'\langle r^4\rangle[35L_z^4 - 30L(L+1)L_z^2 + 25L_z^2 - 6L(L+1) + 3L^2(L+1)^2]$$

$$\sum xz(7z^2-3r^2) \equiv \beta'\langle r^4\rangle O_4^1 = \beta'\langle r^4\rangle(\tfrac{1}{4})\big[\{L_+(2L_z+1)+L_-(2L_z-1)+L_-(2L_z-1)\}\{7L_z^2-3L(L+1)+\tfrac{1}{2}\}+\{7L_z^2-3L(L+1)+\tfrac{1}{2}\}\{(2L_z-1)L_+\}$$
$$+ (2L_z+1)L_-\}\big]$$

$$\sum yz(7z^2-3r^2) \equiv \beta'\langle r^4\rangle O_4^1(s) = \beta'\langle r^4\rangle(-\tfrac{1}{4}i)\big[\{L_+(2L_z+1)-L_-(2L_z-1)-5\}\{L_+^2+L_-^2\}$$
$$- (2L_z+1)L_-\}\big]$$

$$\sum(7z^2-r^2)(x^2-y^2) \equiv \beta'\langle r^4\rangle O_4^2 = \beta'\langle r^4\rangle(\tfrac{1}{4})[\{7L_z^2-L(L+1)-5\}\{L_+^2+L_-^2\}+\{L_+^2+L_-^2\}\{7L_z^2-L(L+1)-5\}]$$

$$\sum(7z^2-r^2)2xy \equiv \beta'\langle r^4\rangle O_4^2(s) = \beta'\langle r^4\rangle(-\tfrac{1}{4}i)[\{7L_z^2-L(L+1)-5\}\{L_+^2-L_-^2\}+\{L_+^2-L_-^2\}\{7L_z^2-L(L+1)-5\}]$$

$$\sum z(x^3-3xy^2) \equiv \beta'\langle r^4\rangle O_4^3 = \beta'\langle r^4\rangle(\tfrac{1}{4})[L_z(L_+^3+L_-^3)+(L_+^3+L_-^3)L_z]$$

$$\sum z(3x^2y-y^3) \equiv \beta'\langle r^4\rangle O_4^3(s) = \beta'\langle r^4\rangle(-\tfrac{1}{4}i)[L_z(L_+^3-L_-^3)+(L_+^3-L_-^3)L_z]$$

$$\sum(x^4-6x^2y^2+y^4) \equiv \beta'\langle r^4\rangle O_4^4 = \beta'\langle r^4\rangle(\tfrac{1}{2})[L_+^4 + L_-^4]$$

$$\sum 4(x^3y-xy^3) \equiv \beta'\langle r^4\rangle O_4^4(s) = \beta'\langle r^4\rangle(-\tfrac{1}{2}i)[L_+^4 - L_-^4]$$

The factors α, β' are given by

$$\alpha = \pm\,\frac{2(2l+1-4S)}{(2l-1)(2l+3)(2L-1)}$$

$$\beta' = \pm\,\frac{3(2l+1-4S)[-7(l-2S)(l-2S+1)+3(l-1)(l+2)]}{(2l-3)(2l-1)(2l+3)(2l+5)(L-1)(2L-1)(2L-3)}$$

where the minus sign is used in the first half of the shell and the plus sign in the second half.

Thus for iron group ions:

$\alpha = -\tfrac{2}{21}$, $\beta' = \tfrac{2}{63}$ for $3d^1\ ^2D$ and $3d^6\ ^5D$

$\alpha = -\tfrac{2}{105}$, $\beta' = -\tfrac{2}{315}$ for $3d^2\ ^3F$ and $3d^7\ ^4F$

$\alpha = \tfrac{2}{21}$, $\beta' = -\tfrac{2}{63}$ for $3d^4\ ^5D$ and $3d^9\ ^2D$

$\alpha = \tfrac{2}{105}$, $\beta' = \tfrac{2}{315}$ for $3d^3\ ^4F$ and $3d^8\ ^3F$

[a] HUTCHINGS [1964].

a.u. as given in tables 6.2 and 6.1. The parameter B_4^0 depends upon the details of the model used to derive the crystal field and because of this and also the uncertainties in the calculation of $\langle r^4 \rangle$ the factor $\langle r^4 \rangle B_4^0$ is usually taken as a parameter to be found from experiment.

TABLE 6.3
Iron group ions in an octahedral crystal field

Ion	Configuration	Lowest term of free ion	Spin-orbit coupling of free ion in cm^{-1}	Symmetry of lowest level in crystal	Orbital degeneracy
Ti^{3+}	3d^1	$^2D_{3/2}$	154	T$_2$	3
V^{3+}	3d^2	$^3F_2$	104	T$_1$	3
V^{2+}	3d^3	$^4F_{3/2}$	55	A$_2$	1
Cr^{3+}	3d^3	$^4F_{3/2}$	87	A$_2$	1
Cr^{2+}	3d^4	$^5D_0$	57	E	2
Mn^{3+}	3d^4	$^5D_0$	85	E	2
Mn^{2+}	3d^5	$^6S_{5/2}$			
Fe^{3+}	3d^5	$^6S_{5/2}$			
Fe^{2+}	3d^6	$^5D_4$	-100	T$_2$	3
Co^{2+}	3d^7	$^4F_{9/2}$	-180	T$_1$	3
Ni^{2+}	3d^8	$^3F_4$	-335	A$_2$	1
Cu^{2+}	3d^9	$^2D_{5/2}$	-852	E	2

Now that the crystal field has been accounted for, the next step is to include the spin–orbit coupling term $\lambda L \cdot S$ and the Zeeman energy $\beta H \cdot (L + 2S)$. These perturbations depend upon the spin variables so the states must now be labelled by spin quantum numbers in addition to their orbital quantum numbers. For $S = 1$ S_z can have the three values ± 1 and 0. The states may be regarded as product states formed from the seven orbital states above and the spin states $|S_z = 1\rangle, |S_z = 0\rangle,$ $|S_z = -1\rangle$. In general the calculation now proceeds in one of two ways. The spin operators can be left as non-commuting algebraic variables and the result of the perturbation calculation is then the spin Hamiltonian with an effective spin equal to the real spin. This is possible, as is the case for Ni^{2+}, when the orbital ground state is a singlet. The states described by the spin Hamiltonian then arise from this singlet orbital state. When the orbital state is degenerate however, a full calculation of the perturbation including the spin operators must be carried out and the energy splittings so obtained compared with those predicted by an effective spin Hamiltonian.

The total perturbation is

$$H' = \lambda L \cdot S + \beta H \cdot (L + 2S).$$

(6.20)

This may be rewritten as

$$H' = \lambda[L_z S_z + \tfrac{1}{2}(L_+ S_- + L_- S_+)] + \beta H_z(L_z + 2S_z)$$

if it is assumed that the magnetic field is along one of the four-fold octahedral axes. The spectrum is in fact isotropic so this is not a serious restriction. Regarding the spin operators as algebraic variables H' has the following matrix elements between the seven orbital states above.

$$\langle A_2|H'|A_2\rangle = 2\beta H_z S_z$$

$$\langle T_2,0|H'|A_2\rangle = 2\beta H_z + 2\lambda S_z$$

$$\langle T_2,1|H'|A_2\rangle = \sqrt{2}\lambda S_+$$

$$\langle T_2,-1|H'|A_2\rangle = -\sqrt{2}\lambda S_- \qquad (6.21)$$

$$\langle A_2|H'|T_2,0\rangle = 2\beta H_z + 2\lambda S_z$$

$$\langle A_2|H'|T_2,1\rangle = \sqrt{2}\lambda S_-$$

$$\langle A_2|H'|T_2,-1\rangle = -\sqrt{2}\lambda S_+.$$

The matrix elements of H' between $|A_2\rangle$ and $|T_1\rangle$ are zero. Using the standard result of perturbation theory the shift in energy of the orbital ground state $|A_2\rangle$ to second order is given by

$$\Delta E = \langle A_2|H'|A_2\rangle + \sum_{n \neq A_2} \frac{\langle A_2|H'|n\rangle\langle n|H'|A_2\rangle}{-\Delta} \qquad (6.22)$$

where Δ is the splitting between the state $|A_2\rangle$ and the intermediate states $|n\rangle$ which in this case are those of $|T_2\rangle$. Thus it follows that

$$\Delta E = 2\beta H_z S_z - (1/\Delta)[(2\beta H_z + 2\lambda S_z)^2 + 2\lambda^2(S_+ S_- + S_- S_+)]$$

$$= \beta H_z S_z(2 - 8\lambda/\Delta) - 4\beta^2 H_z^2/\Delta - (4\lambda^2/\Delta)(S_x^2 + S_y^2 + S_z^2). \qquad (6.23)$$

The last two terms are constant for all the spin states belonging to the $|A_2\rangle$ orbital state so they need not be included in the spin Hamiltonian which becomes, for Ni^{2+} in an octahedral site

$$H_S = g\beta H \cdot S \qquad (6.24)$$

with $g = 2 - 8\lambda/\Delta$ where Δ is $600\beta'\langle r^4\rangle B_4^0$. The effective spin is of course equal to the real spin of one. An example when the effective spin is not equal to the real spin is Fe^{2+} in MgO discussed in §4.6.

It is seen that the expression of eq. (6.23) contains terms quadratic in the components of S and H. In a general case the spin Hamiltonian is thus of the form

$$H = \beta H \cdot g \cdot S + S \cdot D \cdot S - \beta^2 H \cdot \Lambda \cdot H$$

where g, D and Λ are tensors. The last term does not depend on S and so can be neglected as an additive constant. In addition to the crystal field, spin–orbit coupling and Zeeman terms, other interactions sometimes have to be included. For instance the interaction between the magnetic moments of the nuclear and electron spins are often important. When this interaction is accounted for it is found that there is an additional term in the spin Hamiltonian of the form $I \cdot A \cdot S$. It should be stressed that the derivation of the spin Hamiltonian above is based on the fact that the lowest orbital level in the cubic field is a singlet. However, it usually turns out for the iron group ions that even when this is not the case a similar spin Hamiltonian is satisfactory. In particular, when the ground orbital state is degenerate and the number of electrons is odd, a spin Hamiltonian with an effective spin of one-half is usually appropriate. An exceptional case is the S-state ions, that is those having an orbital state of the free ion which is non-degenerate. A suitable Hamiltonian for this case is given in the review article by BLEANEY and STEVENS [1953]. In many cases if the crystal field has trigonal or tetragonal symmetry the e.p.r. or a.p.r. spectrum has axial symmetry and the spin Hamiltonian above may take the form

$$H = \beta \left[g_{\parallel} H_z S_z + g_{\perp} (H_x S_x + H_y S_y) \right] + D S_z^2 + A I_z S_z + B (I_x S_x + I_y S_y)$$

$$(6.25)$$

where the z-axis is the tetragonal or trigonal axis of the crystal.

3.5. *The rare earth ions*

As mentioned earlier, for these ions the crystal field is weak compared to the spin–orbit coupling and is thus treated as a perturbation on states which are eigenstates of J, the total angular momentum. The calculation of the crystal field splittings proceeds in a similar way to that above and is again facilitated by the use of operator equivalents. In fact this was the situation to which Stevens originally applied his operator equivalents. In this case interest is in a manifold of states in which J, rather than L, is a constant. The crystal field calculation is again expressed in cartesian form but now x, y and z are replaced by J_x, J_y and J_z. Finding the constant of proportionality in this case is slightly more complicated because two steps are required. One has to go first from the (J, J_z)-representation to the (J, J_z, L, S)-representation before the transition from the (L, S)-representation to the individual $|l, l_z\rangle$ states can be made.

The a.p.r. work on the rare earth ions has mainly been carried out on trivalent rare earths in calcium fluoride, DOBROV [1966] and WETSEL *et al.* [1969]. In this case there is often a charge compensating fluorine ion in a nearby interstitial site giving a tetragonal or trigonal crystal

field. The energy levels can usually be represented by an effective spin Hamiltonian as given in eq. (6.25) with effective spin of $\frac{1}{2}$ if a doublet is the lowest level or one if a triplet is the lowest level. Some details of rare earth ions are given in table 6.4.

TABLE 6.4
Rare earth ions in eightfold co-ordination of CaF_2

Ion	Configuration	Lowest term of free ion	Symmetry of lowest level in CaF_2	Degeneracy of level
Ce^{3+}	$4f^1$	$^2F_{5/2}$	G	4
Pr^{3+}	$4f^2$	$^3H_4$	A_1 or T_2	1 or 3
Nd^{3+}	$4f^3$	$^4I_{9/2}$	G	4
Pm^{3+}	$4f^4$	$^5I_4$	A_1	1
Sm^{3+}	$4f^5$	$^6H_{5/2}$	G	4
Eu^{3+}	$4f^6$	$^7F_0$	A_1	1
Tb^{3+}	$4f^8$	$^7F_6$	A_2 or E	1 or 2
Dy^{3+}	$4f^9$	$^6H_{15/2}$	G	4
Ho^{3+}	$4f^{10}$	$^5I_8$	E or T_2	2 or 3
Er^{3+}	$4f^{11}$	$^4I_{15/2}$	$E_{5/2}$	2
Tm^{3+}	$4f^{12}$	$^3H_6$	A_2 or E	1 or 2
Yb^{3+}	$4f^{13}$	$^2F_{7/2}$	$E_{5/2}$	2

Taken from WEBER and BIERIG [1964]. See this reference for a discussion of the uncertainties associated with the alternatives for the lowest level in CaF_2.

4. The spin–lattice interaction

4.1. Introduction

The interaction coupling the electron spins to the lattice will now be discussed; this interaction is responsible for the spin–lattice relaxation in electron paramagnetic resonance experiments and for the attenuation of ultrasound in a.p.r. The current theory has been developed over a number of years by many authors among them Waller, Heitler and Teller, Kronig and Van Vleck. Originally WALLER [1932] suggested that the spin–lattice coupling was brought about by means of the magnetic forces acting between the ions in the crystal. He suggested that it was due to a modulation of the dipole energy between the spins of the type given in eq. (5.16). In ch. 5 it was seen that a similar modulation of the exchange interaction was responsible for the magnon–phonon interaction. The modulation arises because when the lattice is vibrating the interatomic separation R_{nm} will fluctuate. However when comparisons were made between his theory and experiment it was found that the theoretical results were an order of magnitude too

small. The discrepancy between theory and experiment was partially removed when it was realized first by HEITLER and TELLER[1936] and then by KRONIG[1939] that the main coupling between the spins and the lattice arose from a modulation of the crystal field. The vibrations of the lattice modulate the crystal field and hence produce a distortion of the orbital electron motion. This distortion is then felt by the spins because of the spin-orbit coupling. Before discussing in detail this interaction a phenomenological approach will be used to define a spin-lattice coupling tensor whose components can be measured by experiment, DOBROV[1964]. The task of theory is then to justify the form of this phenomenological Hamiltonian and to predict the values for the components of the coupling tensor.

4.2. *Phenomenological approach*

In the presence of lattice vibrations it is expected that the g, D and A tensors of the spin Hamiltonian of §3.4 will become modulated in some way. A total spin Hamiltonian including this modulation might therefore be written as

$$H = \beta H \cdot g \cdot S + S \cdot D \cdot S + I \cdot A \cdot S + \beta H \cdot h \cdot S + S \cdot d \cdot S + I \cdot a \cdot S$$
$$(6.26)$$

where the first three and the last three terms are the static and dynamic parts respectively. The parameters h, d and a depend upon the strain in the lattice. For a given paramagnetic ion only one of the terms in the dynamic part of the spin Hamiltonian is usually important. The interaction involving the nuclear spin is usually small and can be neglected. It has only been considered in the case of Co^{2+} by CULVAHOUSE *et al.* [1963] and by TUCKER[1966a]. If the ion has a spin of one half then the quadratic term disappears as its matrix elements are identically zero, see §3.1, and hence only the term $\beta H \cdot h \cdot S$ is important. For ions with spins greater than one half the term $S \cdot d \cdot S$ usually dominates. In the case of an iron group ion with an orbital singlet lowest this term can be shown to be larger by a factor $\lambda/\beta H$ than the term $\beta H \cdot h \cdot S$. The ratio of the spin-orbit coupling parameter λ to βH is usually of the order of 200 for typical iron group ions.

It has been stated that the parameters h, d and a depend on the lattice strain. It is perhaps worth noticing here that strain is defined on a continuum model of the crystal which is really inappropriate when discussing the mechanism of spin–lattice interaction where it is the relative displacements of the nearest neighbouring ions that are actually involved. Further it is found that the use of symmetry adapted modes is often convenient in the theory. The relation of these to conventional

strains is straightforward provided one is prepared to equate strain to relative displacement in spite of the inconsistency of the models.

Experiments have confirmed that the most important contributions to the spin–lattice interaction comes from terms linear in the strain so the spin–lattice coupling coefficients are defined in the following way:

$$d_{ij} = \sum G_{ijkl} \epsilon_{kl}, \tag{6.27}$$

$$h_{ij} = \sum F_{ijkl} \epsilon_{kl}, \tag{6.28}$$

$$a_{ij} = \sum Z_{ijkl} \epsilon_{kl}. \tag{6.29}$$

The fourth-rank tensors, the coupling coefficients G, F, Z are usually written in the contracted Voigt notation. In order for this to be possible the second-rank tensors ϵ_{ij}, d_{ij}, h_{ij} and a_{ij} must be symmetric. This is true of ϵ_{ij} and d_{ij} but not necessarily so for h_{ij}, BLACK and DONOHO [1968]. However in crystals of sufficiently high symmetry h_{ij} will be symmetric and so Voigt notation will be used in the following discussion.

The number of independent non-zero components of the coupling coefficient tensors depends upon the symmetry of the crystal containing the paramagnetic centres. The tensors must reflect the symmetry of the crystal, and in addition, in the case of G, an additional requirement that the trace of d shall vanish can be included. This is because the trace of d can only give a perturbation that affects all the energy levels equally and so cannot be observed in experiments which depend only on energy differences. The number of components of G can be reduced by choosing this trace to be zero. The non-zero elements of G, F and Z, previously listed by DOBROV [1964] and by TUCKER [1966b] are given in table A1.6. It should be remembered that when using the Voigt notation for the strains, the shear components have their engineering values, not their tensor values (see ch. 2).

4.3. *Determination of the spin–lattice coupling constants by experiment*

The values of the components of G, F and Z can be determined by experiment and also, at least in principle, calculated theoretically using a suitable model for the spin–lattice interaction. The theoretical treatment will be outlined in a subsequent section but first the experimental determination will be described.

There are essentially two methods, the use of an applied static stress in an electron spin resonance experiment or a dynamic method using acoustic paramagnetic resonance. The static stress method is really outside the scope of this book so the technique will only be outlined briefly for comparison with the ultrasonic method. The applied stress

causes a strain which shifts the energy levels of the paramagnetic ion in a way given by the Hamiltonian of eq. (6.26). This produces a change in the resonance frequency of the e.p.r. absorption. The shift in energy is usually measured as a change in the applied magnetic field needed for resonance at constant frequency in the conventional type of e.p.r. experiment. From the change in the magnitude of the magnetic field required the components of the appropriate spin–lattice coupling tensor G, F or Z can be determined. Such experiments have been performed by FEHER[1964], TUCKER[1966a] and by BLACK and DONOHO[1968].

In a.p.r. experiments using microwave ultrasonics the values of the components of G, F or Z are deduced from the attenuation of the ultrasonic wave that is at resonance with the spin system. The expressions for the attenuation of an ultrasonic wave have been given by DOBROV [1964] in terms of the components of G. In §1 the attenuation is discussed in terms of a transition probability $W\epsilon^2$ per unit time, where ϵ is the amplitude of a strain component produced by the ultrasonic wave. If the resonance is due to a transition between the states $|\alpha\rangle$ and $|\beta\rangle$ of the spin Hamiltonian the average transition probability per spin is given by

$$W\epsilon^2 = \frac{2\pi}{4\hbar^2} g(\omega) |\langle \alpha | H_{s-p} | \beta \rangle|^2, \qquad (6.30)$$

where H_{s-p} is the amplitude of the spin–phonon Hamiltonian $H_{s-p} \cos(\omega t)$ and $g(\omega)$ is the line-shape factor. H_{s-p} is the strain-dependent part of eq. (6.26). The formula of eq. (6.30) follows from the standard perturbation theory of appendix 3. If the above result is compared with Fermi's golden rule, eq. (A3.6) it is seen that there is an additional $4\hbar$ in the denominator. The $\hbar$ comes from the fact that $g(\omega)$ rather than $g(E)$ has been used and the factor 4 is due to the sinusoidal variation $\cos(\omega t)$. Equation (A3.6) was deduced on the assumption that the perturbation did not depend explicitly on time. From eqs. (6.30) and (6.2) the attenuation coefficient is therefore

$$\alpha = \frac{\pi n \omega g(\omega)}{\hbar \rho V v^3 \epsilon^2} |\langle \alpha | H_{s-p} | \beta \rangle|^2. \qquad (6.31)$$

It is noticed that the matrix element $\langle \alpha | H_{s-p} | \beta \rangle$ is proportional to the strain amplitude ϵ and so α is independent of ϵ.

It only remains to evaluate the matrix element to find the attenuation in a particular case. The interaction Hamiltonian contains linear and quadratic components of S and so the matrix elements may be non-zero for both $\Delta M_S = \pm 1$ and $\Delta M_S = \pm 2$ transitions of the spin system. For the case of a crystal of low symmetry and an ultrasonic wave with a general direction of propagation and polarization the evaluation of

the matrix elements can be a lengthy process. Experimentally only a few high symmetry directions are practicable for the propagation of ultrasonic waves because of the elastic anisotropy of the crystal. Most experiments have been made using longitudinal waves because it is difficult to make a satisfactory bond between the transducer and the specimen for the transmission of shear waves at microwave frequencies. To evaluate the components of d which are needed, the strain produced by the ultrasonic wave is best resolved into components with respect to the crystal lattice coordinate system. Thus a longitudinal wave of strain amplitude ϵ in a direction given by the direction cosines (l, m, n) with respect to the crystal axes has strain components

$$\epsilon_{xx} = l^2\epsilon \qquad \epsilon_{yz} = 2nm\epsilon$$
$$\epsilon_{yy} = m^2\epsilon \qquad \epsilon_{zy} = 2nl\epsilon \qquad (6.32)$$
$$\epsilon_{zz} = n^2\epsilon \qquad \epsilon_{xy} = 2lm\epsilon.$$

Similarly a shear wave of strain amplitude $\epsilon_{x''y''} = \epsilon$ such that x'' is in the direction (l, m, n) and y'' is in the direction (λ, μ, ν) referred to the crystal axes is equivalent to strains

$$\epsilon_{xx} = l\lambda\epsilon \qquad \epsilon_{yz} = (m\nu + \mu n)\epsilon$$
$$\epsilon_{yy} = m\mu\epsilon \qquad \epsilon_{zy} = (n\lambda + \nu l)\epsilon \qquad (6.33)$$
$$\epsilon_{zz} = n\nu\epsilon \qquad \epsilon_{xy} = (l\mu + \lambda m)\epsilon$$

referred to those axes. In order to evaluate the matrix elements of eq.
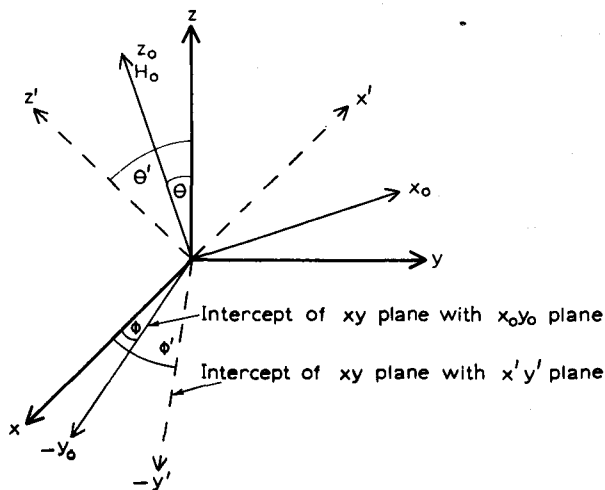
Fig. 6.5.

(6.31) the states $|\alpha\rangle$ and $|\beta\rangle$ are needed. If the magnetic field is along the z-axis of the spin Hamiltonian, or the term involving D is small, it proves useful to transform to a set of axes in which the Zeeman energy term of the Hamiltonian is diagonal. This was done by DOBROV[1964]. He chose a coordinate system as shown in fig. 6.5. x, y, z is the crystalline coordinate system in which the strains have been evaluated as described above. With respect to this set a coordinate system x', y', z' can be defined by Eulerian angles (θ', ϕ', ψ') in which the Zeeman energy is diagonal. A third system of coordinates x_0, y_0, z_0, the laboratory system, is required in which the applied magnetic field is along z_0 and the system is defined by the Eulerian angles (θ, ϕ, ψ) with respect to x, y, z. ψ' and ψ were put equal to $\frac{1}{2}\pi$ without loss of generality. The spin components then transform according to

$$S_x = -\frac{g_\parallel g_x}{g_\perp g} S_{x'} \cos\theta \sin\phi - \frac{g_y}{g_\perp} S_{y'} \cos\phi + \frac{g_x}{g} S_{z'} \sin\theta \sin\phi,$$

$$S_y = \frac{g_\parallel g_y}{g_\perp g} S_{x'} \cos\theta \cos\phi - \frac{g_x}{g} S_{y'} \sin\phi - \frac{g_y}{g} S_{z'} \sin\theta \cos\phi, \quad (6.34)$$

$$S_z = \frac{g_\perp}{g} S_{x'} \sin\theta + \frac{g_\parallel}{g} S_{z'} \cos\theta,$$

where

$$g = (g_\parallel^2 \cos^2\theta + g_\perp^2 \sin^2\theta)^{1/2} \qquad g_\perp = (g_x^2 \sin^2\phi + g_y^2 \cos^2\phi)^{1/2}.$$

In other cases, where D is appreciable the spin Hamiltonian may have to be exactly diagonalized in the crystalline coordinate system in order to evaluate the matrix elements. If experiments are made on crystals of high symmetry where the spectrum is isotropic or has axial symmetry about some axis the calculation is straightforward.

For an ion in a cubic crystalline host giving an isotropic spectrum the following expressions are obtained for the attenuation coefficient. (It is noted that when the g-factor is isotropic it drops out of the transformation expressions and then the diagonal and laboratory systems coincide.) A longitudinal ultrasonic wave travelling in a direction having direction cosines (l, m, n) relative to the cubic axes x, y, z is attenuated due to a $M_s \to M_s - 1$ transition in the spin system according to

$$\begin{aligned}
\alpha = C_1 &\{ [-\tfrac{1}{4}\sin 2\theta \,(3G_{11}[l^2 \sin^2\phi + m^2 \cos^2\phi - n^2] - 4G_{44}lm \sin 2\phi) \\
&+ 2G_{44} \cos 2\theta \,(mn \cos\phi - ln \sin\phi)]^2 + [\tfrac{1}{4}\sin\theta (-3G_{11}[l^2 - m^2] \\
&\times \sin 2\phi + 8G_{44}lm \cos 2\phi) - 2G_{44} \cos\theta \,(mn \sin\phi + ln \cos\phi)]^2 \}
\end{aligned}$$
$$(6.35)$$

where

$$C_1 = \frac{\pi n \omega g(\omega)}{4\hbar \rho V v^3} [(S + M_S)(S - M_S + 1)(2M_S - 1)^2].$$

Also for this longitudinal wave the $M_S \rightarrow M_S - 2$ transition leads to an attenuation coefficient given by

$$\alpha = C_2 \{\tfrac{1}{2}G_{11}[(l^2-1)\cos^2\theta\sin^2\phi + (m^2-1)\cos^2\theta\cos^2\phi + n^2$$
$$+ (3n^2-1)\sin^2\theta + (m^2-2l^2)\cos^2\phi + (l^2-2m^2)\sin^2\phi$$
$$+ 2(m^2\cos^2\phi + l^2\sin^2\phi)\cos^2\theta] + 2G_{44}(mn\cos\phi\sin 2\theta$$
$$- ln\sin\phi\sin 2\theta) - 2G_{44}\,lm(\cos^2\theta + 1)\sin 2\phi\}^2$$
$$+ 16C_2\{\tfrac{3}{8}G_{11}(l^2-m^2)\sin 2\phi\cos\theta - G_{44}(mn\sin\theta\sin\phi + nl\sin\theta$$
$$\times\cos\phi + lm\cos\theta\cos 2\phi)\}^2 \qquad\qquad (6.36)$$

where

$$C_2 = \frac{\pi n\omega g(\omega)}{16\hbar\rho V v^3} \left[(S+M_s)(S-M_s+1)(S+M_s-1)(S-M_s+2)\right].$$

The attenuation of the ultrasonic waves due to the dipolar term in the spin–phonon interaction is usually much less than that due to the quadrupolar term. However, as pointed out in §4.2 for systems with $S = \tfrac{1}{2}$ it is the only mechanism. The evaluation of the attenuation in terms of the spin–lattice coupling constant F is very similar to the discussion given above for G but of course the matrix elements are different. The only allowed transition is the $M_s \rightarrow M_s - 1$ and Dobrov finds that this produces an attenuation of the longitudinal wave considered above of

$$\alpha = C_3 H_0^2\{-\tfrac{1}{2}\sin 2\theta(\sin^2\phi[F_{11}l^2 + F_{12}m^2 + F_{12}n^2]$$
$$+ \cos^2\phi[F_{11}m^2 + F_{12}l^2 + F_{12}n^2] - F_{12}l^2 - F_{12}m^2 - F_{11}n^2$$
$$- 2F_{44}lm\sin 2\phi) + 2F_{44}\cos 2\theta(nm\cos\phi - nl\sin\phi)]^2$$
$$- \tfrac{1}{2}\sin\theta(F_{11}l^2 + F_{12}m^2 + F_{12}n^2)\sin 2\phi + \sin 2\phi(F_{11}m^2 + F_{12}l^2 + F_{12}n^2)$$
$$+ 4F_{44}lm\cos 2\phi - 2F_{44}\cos\theta(nm\sin\phi + nl\cos\phi)]^2\} \qquad (6.37)$$

with

$$C_3 = \frac{\pi n\omega g(\omega)\beta^2}{\hbar\rho V v^3} \left[(S+M_s)(S-M_s+1)\right].$$

Use of these formulae allows the magnitude of the spin–lattice coupling coefficients to be deduced from the measurement of attenuation of the ultrasonic wave at the paramagnetic resonance frequency.

4.4. *Microscopic theory of the spin–lattice interaction*

As mentioned in §4.1 the mechanism first put forward to explain spin–lattice relaxation was the modulation of the dipole–dipole interaction between the spins. In most instances this was too small to explain the measured spin–lattice relaxation times and it was later realized that a much stronger coupling arose from a modulation of the crystal field.

Nevertheless the Waller machanism can be important in substances
with large atomic magnetic moments and strong concentrations of
magnetic ions, for the relevant matrix elements are proportional to the
fourth power of the magnetic moment and inversely proportional to the
ninth· power of the ionic spacing. In ultrasonic studies however, only
lightly doped crystals have been used so the mechanism will not be
studied further. Instead we turn straight away to a discussion of the
crystal field modulation. As noted in §4.1 there are two links in the
chain coupling the phonons of the lattice to the spins of the spin system:
one from the phonons to the orbital motion of the electrons and the
other from the orbital motion to the spins. The theory was first de-
veloped in detail by VAN VLECK [1940] in the case of iron group salts
and it has more recently been extended by ORBACH [1961] to cover the
rare earth ions. The theory for the ion group salts was subsequently
reformulated by MATTUCK and STRANDBERG [1960] in a form which
allowed a spin Hamiltonian to be used. The use of dynamic spin
Hamiltonians has also been considered in detail by CULVAHOUSE *et al.*
[1963] and by RAY *et al.* [1966]. The paper by Culvahouse *et al.*
deals in particular with the importance of nuclear hyperfine interactions.
Reviews of the theory have been given with special reference to a.p.r.
by AL'TSHULER *et al.* [1961] and by TUCKER [1965] and a more general
survey has been presented by STEVENS [1967].

The crystal field acting on the electron of a paramagnetic ion is
determined by the position of the neighbouring ligands surrounding it.
The quantities which enter the calculation are the relative separations
of the paramagnetic ion and its neighbours. When the lattice vibrates,
either thermally or due to the passage of an ultrasonic wave, these
separations fluctuate and so the crystal field is modulated. It is usual to
expand the crystal field potential in a power series of these displace-
ments. For small displacements, only the term linear in the displace-
ments need be retained. These terms give rise to an interaction that is
the analogue of the term linear in the strain in the phenomenological
model of §4.2. As mentioned in that section, provided one is willing to
equate strain to relative displacement, the spin–lattice coupling con-
stants in the phenomenological model can be calculated.

The orbit–lattice Hamiltonian will be a product of two parts. A part
involving operators that act on the eigenstates of the paramagnetic ion
and a part depending upon the lattice displacements. The lattice dis-
placements are then expanded in terms of Debye waves to give a term
linear in the creation and annihilation operators of the phonon modes of
the lattice. If the ultrasonic wave is regarded as a highly excited phonon
mode a process can be envisaged in which a phonon is absorbed from
the mode by the spin system which then makes a transition to an

excited state. The transition probability can be calculated from the first-order transition theory of appendix 3 and clearly it can only be significant when the energy involved in the spin transition is equal to the phonon energy. Of course, the reverse process can also occur in which the paramagnetic ion makes a transition to a lower state with the simultaneous emission of a phonon. In thermal equilibrium the two transition probabilities are equal but when one mode is externally excited above its thermal equilibrium value, a net absorption of energy from this mode will occur. This one-phonon process is often referred to as the direct process. In addition two-phonon processes (Raman processes) are possible which involve the simultaneous absorption of one phonon and the emission of another of energy such that the difference in their energies is equal to the energy involved in the paramagnetic ion transition. Such a process can occur in second-order perturbation theory or could occur in first order if the terms quadratic in the lattice displacements were retained in the Hamiltonian. However, calculation shows that the former is the dominant mechanism and it is for this reason that only the linear terms are retained in the dynamical spin Hamiltonian.

The pioneering papers by Van Vleck and those of subsequent authors normally express the crystal field potential in a power series of the normal modes of the complex comprised of the paramagnetic ion and its neighbours. However in some cases a slightly different method of calculation is favoured which will be described first. The method is that given by STEVENS [1967]. The theory in this form has been used by STEVENS and WALSH [1968] and by CAOLA [1970].

4.4.1. *The orbit–lattice interaction.* As an example the case of an ion in a site of octahedral symmetry will be considered. A set of co-ordinate axes are chosen with the paramagnetic ion's nucleus as the origin. The crystal field will be taken as arising from six nearest neighbouring ligands arranged with octahedral symmetry at the positions $(\pm a, 0, 0)$, $(0, \pm a, 0)$, $(0, 0, \pm a)$. The electronic coordinates will be denoted by x, y, z and when the paramagnetic ion moves, the electron's coordinate axes are assumed to move with it. The neighbouring ions will be labelled 1 to 6 where the ions 1, 2, 3 lie along the positive x, y, z axes and 4, 5, 6 lie along the $-x, -y, -z$ axes respectively. The displacement of the paramagnetic ion will be denoted by ΔR_0 and that of its ith neighbouring ligand by ΔR_i (components X_i, Y_i, Z_i). The position vectors of these ions in the lattice will be denoted by R_0 and R_i (R_0^0 and R_i^0 in equilibrium). It is convenient to look at the potential arising from each neighbour separately. Consider what happens when the paramagnetic ion and its neighbour along the z-axis (labelled 3) are

displaced. The crystal field potential arising from this ligand obviously changes so that the electron at position (x, y, z) will now experience the potential which it would have previously felt if it were at the position $(x - X_3 + X_0,\ y - Y_3 + Y_0, z - Z_3 + Z_0)$. The potential $V_3(xyz)$ after this displacement is therefore related to the potential $V_3^c(xyz)$ before by

$$V_3(xyz) = V_3^c(x - X_3 + X_0, y - Y_3 + Y_0, z - Z_3 + Z_0)$$

which may be expanded in a Taylor series as

$$V_3(xyz) = V_3^c(xyz) + (X_0 - X_3)\frac{\partial V_3^c}{\partial x} + (Y_0 - Y_3)\frac{\partial V_3^c}{\partial y}$$
$$+ (Z_0 - Z_3)\frac{\partial V_3^c}{\partial z} + \cdots. \tag{6.38}$$

Note that in this form the expansion involves the derivatives with respect to the electronic coordinates x, y, z rather than with respect to the coordinates of the neighbouring ligand and that the V^c on the right-hand side is the static crystal field. As before, eq. (6.10), it is convenient to express the potential in spherical coordinates

$$V_3^c = \sum_{n,\,m} A_n^m r^n Y_n^m(\theta\phi). \tag{6.39}$$

In evaluating the derivatives of V^c the following relations prove useful

$$\frac{\partial}{\partial x}(r^n Y_n^m) = \tfrac{1}{2} r^{n-1}\{-f(n, m)\,Y_{n-1}^{m-1} + f(n, -m)\,Y_{n-1}^{m+1}\},$$

$$\frac{\partial}{\partial y}(r^n Y_n^m) = -\tfrac{1}{2}\mathrm{i} r^{n-1}\{f(n, m)\,Y_{n-1}^{m-1} + f(n, -m)\,Y_{n-1}^{m+1}\} \tag{6.40}$$

$$\frac{\partial}{\partial z}(r^n Y_n^m) = r^{n-1}g(n, m)Y_{n-1}^m,$$

for $n \geqslant m \geqslant -n$ where

$$f(n, m) = \left\{\frac{(2n+1)(n+m)(n+m-1)}{(2n-1)}\right\}^{1/2}$$

$$g(n, m) = \left\{\frac{(2n+1)(n^2 - m^2)}{(2n-1)}\right\}^{1/2}.$$

The advantage of these expressions is that they are now in just the right form for conversion to equivalent operators. Similar expressions to eq. (6.38) will result when the other neighbours of the paramagnetic ion are considered. In principle once the result for one neighbour is found expressions for the others can be obtained by simply applying the appropriate rotation but in practice this may prove tedious. Suggestions for reducing the labour involved have been put forward by

STEVENS[1967]. It is clear then that the dynamical crystal field calculation is no more difficult in principle than the static field case although in practice it is much longer as more matrix elements have to be evaluated. An explicit expression for the case of an octahedral coordination has been presented by CHALLIS and DE GÖER[1970]. The result will be given later in this section.

As discussed above only the term linear in the lattice displacements is retained in the expansion of V in eq. (6.38). The relative displacements of the paramagnetic ion and its neighbours can be expressed in terms of the creation and annihilation operators for the phonon modes of the lattice. Suppose that the displacement with respect to the paramagnetic ion of the ith ligand is required due to an excitation of the phonon mode (q,j). It follows from eq. (2.56), assuming all atoms have the same mass, that

$$\Delta R_i(qj) - \Delta R_0(qj) \approx -q \cdot (R_i^0 - R_0^0)\left(\frac{\hbar}{2Nm\omega_j(q)}\right)^{1/2}$$
$$\times e^*(qj)\, e^{iq \cdot R_0^0}[a_j(q) - a_j^*(-q)]. \quad (6.41)$$

$'$Therefore in the case of the octahedral complex the relative displacement of two ligands on opposite sides of the central ion is, in the long wavelength limit,

$$-\left(\frac{2\hbar\omega_j(q)}{\rho V}\right)^{1/2}\frac{a}{v}\cos\theta_j e(qj)\, e^{iq \cdot R_0^0}[a_j(q) - a_j^*(-q)], \quad (6.42)$$

θ_j is the angle between the propagation vector q and the line joining the two opposite ligands. A Debye model has been assumed for which $\omega_j(q) = vq$.

4.4.2. *Transition rates.* Suppose for simplicity that the spin-phonon interaction for the mode (q, j) is written as

$$H_{s-p} = H_{qj}(S)[a_j(q) - a_j^*(-q)], \quad (6.43)$$

where $H_{qj}(S)$ involves only operators that act on the states of the paramagnetic ion (the spin system). Consider two states of the ion $|\alpha\rangle$, $|\beta\rangle$ such that their energy difference is equal to $\hbar\omega_j(q)$. Then from standard first-order perturbation theory, appendix 3, the probability for the spin system to make a transition from the state $|\alpha\rangle$ to $|\beta\rangle$ with the absorption of a phonon from (q, j) is

$$T_{\alpha \to \beta} = (2\pi/\hbar^2) N_\alpha |\langle\beta|H_{qj}(S)|\alpha\rangle|^2 n_j(q) g(\omega), \quad (6.44)$$

where $n_j(q)$ is the number of phonons originally in the mode (q, j) and N_α is the number of spins in the lower state. $g(\omega)$ is the line-shape function describing the density of final states of the spin system.

Similarly the transition probability for the reverse process is

$$T_{\beta \to \alpha} = (2\pi/\hbar^2) N_\beta |\langle \alpha | H_{qj}(S) | \beta \rangle|^2 [n_j(q) + 1] g(\omega). \quad (6.45)$$

The factor $[n_j(q) + 1]$ arises from the use of eq. (2.36). Therefore the net absorption probability of a phonon from this mode is

$$T = (2\pi/\hbar^2) |\langle \alpha | H_{qj}(S) | \beta \rangle|^2 g(\omega) \{ N_\alpha n_j(q) - N_\beta n_j(q) - N_\beta \}. \quad (6.46)$$

If the occupation numbers N_α, N_β and $n_j(q)$ all have their thermal equilibrium value the factor in the curly brackets is clearly zero. When the mode (q, j) is externally excited above its equilibrium value, then the absorption is no longer zero for if $n_j(q)$ is written as $n_j^0(q) + \Delta n_j(q)$ it follows that

$$\dot{n}_j(q) = -(2\pi/\hbar^2) |\langle \alpha | H_{qj}(S) | \beta \rangle|^2 g(\omega) (N_\alpha - N_\beta) \Delta n_j(q). \quad (6.47)$$

Defining an absorption coefficient as in ch. 5§3 it follows that

$$\alpha = -\frac{\dot{n}_j(q)}{2\Delta n_j(q)} = \frac{2\pi}{\hbar^2} |\langle \alpha | H_{qj}(S) | \beta \rangle|^2 g(\omega) n \quad . \quad (6.48)$$

or if the absorption per unit distance is required

$$\alpha = \frac{2\pi}{\hbar^2 v} |\langle \alpha | H_{qj}(S) | \beta \rangle|^2 g(\omega) n \quad (6.49)$$

where n is the population difference introduced before. The connection with eq. (6.31) can be seen as follows. Consider the propagation of a longitudinal wave along the z-axis. Then it follows from eq. (6.42) that $(Z_3 - Z_6)/2a$, which in the limit of long wavelength may be thought of as the z-component of strain at the site of the paramagnetic ion, is

$$\frac{1}{2v} \left(\frac{2\hbar\omega(q)}{\rho V} \right)^{1/2} e^{iq \cdot R_0} [a(q) - a^*(-q)] \quad (6.50a)$$

so that

$$\alpha = \frac{\pi n \omega g(\omega)}{\hbar \rho V v^3} \left| 2a \left(\frac{\partial V^c}{\partial z} \right) \right|^2. \quad (6.50b)$$

The connection between the two formulae is then clear.

4.4.3. *The orbit–lattice interaction for an octahedral coordination.* It has been shown above how the attenuation of an ultrasonic wave due to paramagnetic resonance absorption can be calculated. As an example of a typical orbit–lattice Hamiltonian the results of CHALLIS and DE GÖER[1970] will now be presented. The results are applicable to an iron group ion in a site of octahedral symmetry. Challis and de Göer point out that although their Hamiltonian only applied rigorously to an ion in an octahedral site, it may be useful in cases where there is also

a small trigonal distortion as the difference expected in such instances will be small. In their expressions the magnetic field is taken along the z-axis and two choices of axes considered:

$$\text{(i) } z = [001], x = [100], y = [010]$$

$$\text{(ii) } z = [111], x = [\bar{1}\bar{1}2], y = [1\bar{1}0].$$

They find that the interaction Hamiltonian on the basis of a point ion model is given by

$$H_{s-p} = \frac{e e_{\text{eff}}}{v a^3} \left(\frac{2\hbar \omega_j(q)}{\rho V} \right)^{1/2} (a_j(q) - a_j^*(-q)) e^{i q \cdot R_i^0} W(0) \quad (6.51)$$

where e_{eff} is the charge on the nearest neighbours and a is the equilibrium separation of the paramagnetic ion from its nearest neighbours. $W(0)$ is an expression involving operator equivalents and is given below. If (l_1, m_1, n_1) and (l_2, m_2, n_2) are the direction cosines of the polarization and propagation vectors with respect to the chosen axes, it is found that in the first case with the magnetic field along [001] that

$$\begin{aligned}
W = \tfrac{1}{4}[\,&l_1 l_2 \{\alpha'(3O_2^0 - 9O_2^2) + \tfrac{5}{16}\beta''(-3O_4^0 + 20O_4^2 - 35O_4^4)\} \\
+ &l_1 n_2 \{\alpha'(6O_2^2(s)) + \tfrac{5}{4}\beta''(-2O_2^2(s) - 7O_4^4(s))\} \\
+ &l_1 n_2 \{\alpha'(12O_2^1) + \tfrac{5}{4}\beta''(8O_4^1)\} \\
+ &m_1 l_2 \{\alpha'(6O_2^2(s)) + \tfrac{5}{4}\beta''(-2O_4^2(s) + 7O_4^4(s))\} \\
+ &m_1 m_2 \{\alpha'(3O_2^0 + 9O_2^2) + \tfrac{5}{16}\beta''(-3O_4^0 - 20O_4^2 - 35O_4^4)\} \\
+ &m_1 n_2 \{\alpha'(12O_2^1(s)) + \tfrac{5}{4}\beta''(8O_4^1(s))\} \\
+ &n_1 l_2 \{\alpha'(12O_2^1) + \tfrac{5}{4}\beta''(-6O_4^1 + 14O_4^3)\} \\
+ &n_1 m_2 \{\alpha'(12O_2^1(s)) + \tfrac{5}{4}\beta''(-6O_4^1(s) - 14O_4^3(s))\} \\
+ &n_1 n_2 \{\alpha'(-6O_2^0) + \tfrac{5}{16}\beta''(-8O_4^0)\}\,], \qquad (6.52)
\end{aligned}$$

where $\alpha' = \alpha \langle r^2 \rangle$ and $\beta'' = \beta' \langle r^4 \rangle / a^2$ with α and β' the multiplication factors given in table 6.2. In the second case with the magnetic field and z-axis along [111] and the direction cosines defined with respect to the second choice of axes it is found that

$$\begin{aligned}
W = \tfrac{1}{4}[\,&L_1 L_2 \{\alpha'(-2O_2^0 + O_2^2 - 10\sqrt{2}O_2^1) + \tfrac{5}{8}\beta''(2O_4^0 - 4O_4^2 - 28\sqrt{2}O_4^3 - 7O_4^4)\} \\
+ &L_1 M_2 \{\alpha'(O_2^2(s) + 10\sqrt{2}O_2^1(s)) + \tfrac{5}{8}\beta''(-4O_4^2(s) - 28\sqrt{2}O_4^3(s) \\
& + 7O_4^4(s))\} + L_1 N_2 \{\alpha'(-8O_2^1 - 5\sqrt{2}O_2^2) + \tfrac{5}{24}\beta''(-8O_4^1 \\
& - 28\sqrt{2}O_4^2 + 7\sqrt{2}O_4^4)\} \\
+ &M_1 L_2 \{\alpha'(O_2^2(s) + 10\sqrt{2}O_2^1(s)) \\
& + \tfrac{5}{8}\beta''(-4O_4^2(s) + 28\sqrt{2}O_4^3(s) + 7O_4^4(s))\} \\
+ &M_1 M_2 \{\alpha'(-2O_2^0 - O_2^2 + 10\sqrt{2}O_2^1)
\end{aligned}$$

$$+ \tfrac{5}{8}\beta''(2O_4^0 + 4O_4^2 - 28\sqrt{2}O_4^3 + 7O_4^4)\}$$
$$+ M_1N_2\{\alpha'(-8O_2^1(s) + 5\sqrt{2}O_2^2(s))$$
$$+ \tfrac{5}{24}\beta''(-8O_4^1(s) + 28\sqrt{2}O_4^2(s) + 7\sqrt{2}O_4^4(s))\}$$
$$+ N_1L_2\{\alpha'(-8O_2^1 - 5\sqrt{2}O_2^2) + \tfrac{5}{8}\beta''(16O_4^1 - 7\sqrt{2}O_4^4)\}$$
$$+ N_1M_2\{\alpha'(-8O_2^1(s) + 5\sqrt{2}O_2^2(s)) + \tfrac{5}{8}\beta''(16O_4^1(s) - 7\sqrt{2}O_4^4(s))\}$$
$$+ N_1N_2\{\alpha'(4O_2^0) + \tfrac{5}{24}\beta''(2O_4^0 - 112\sqrt{2}O_4^3)\}]. \qquad (6.53)$$

The direction cosines have been given capital letters in eq. (6.53) to emphasize the change of axes. These expressions can be used to calculate the transition probabilities between states of the paramagnetic ion. Remembering that the operator equivalents act on orbital states, it is clear that the selection rule $\Delta M_s = 0$ must be obeyed.

4.4.4. *Normal mode analysis of Van Vleck.* An alternative procedure for the calculation of the orbit–lattice interaction is the approach described in the classic paper of VAN VLECK [1940]. In this the crystal field potential is expanded in a power series of the normal modes of the paramagnetic ion cluster

$$V = V_0^c + \sum_f \left(\frac{\partial V}{\partial Q_f}\right)_0 Q_f + \cdots . \qquad (6.54)$$

Once again only the linear terms are retained. The normal coordinates Q_f can be found from symmetry arguments. The method sometimes results in simplifications as it allows group theoretical methods to be employed directly. Only certain of the normal coordinates give displacements which can contribute to the orbit–lattice interaction and for a particular transition some of these can be neglected because of the symmetry of the states involved. As an example, the octahedral complex considered above has seven atoms and thus twenty-one normal modes of vibration. Only six of these normal modes can contribute however because nine of them change sign on inversion through the origin and so cannot contribute to the linear term in the Hamiltonian; the remaining six are merely translations or rotations and so can be neglected. The six modes of interest are

$$Q_1 = (1/\sqrt{6})[X_1 - X_4 + Y_2 - Y_5 + Z_3 - Z_6],$$
$$Q_2 = \tfrac{1}{2}[X_1 - X_4 - Y_2 + Y_5],$$
$$Q_3 = (1/\sqrt{3})[\tfrac{1}{2}(X_1 - X_4 + Y_2 - Y_5) - Z_3 + Z_6],$$
$$Q_4 = \tfrac{1}{2}[Y_1 - Y_4 + X_2 - X_5], \qquad (6.55)$$
$$Q_5 = \tfrac{1}{2}[Z_1 - Z_4 + X_3 - X_6],$$
$$Q_6 = \tfrac{1}{2}[Z_2 - Z_5 + Y_3 - Y_6].$$

The notation is that described earlier in this section. Sometimes the surrounding ions do not form a perfect octahedron but one which is slightly distorted. If the distortion is along a four-fold axis the Q_f's defined above are useful but in cases when the distortion is along a three-fold axis an alternative definition is more usefully employed. Of course these normal modes will just be linear combinations of the others. The six Q_f's defined in eq. (6.55) transform according to the following irreducible representations of the cubic group

$$Q_1 : A_1 \qquad Q_2, Q_3 : E \qquad Q_4, Q_5, Q_6 : T_2 \qquad (6.56)$$

The normal coordinates of the complex can then be expressed in terms of the normal modes of the lattice

$$Q_f = \sum_{fqj} B_f(qj) \frac{a}{v} \omega_j(q) \Delta R^0(qj), \qquad (6.57)$$

where from eqs. (6.42) and (6.55)

$$\Delta R^0(qj) = \left(\frac{\hbar \omega_j(q)}{2\rho V}\right)^{1/2} \exp(i q \cdot R_0^0)[a_j(q) - a_j^*(-q)] \qquad (6.58)$$

and

$$B_1 = \sqrt{\tfrac{2}{3}}(l_1 l_2 + m_1 m_2 + n_1 n_2), \qquad B_2 = l_1 l_2 - m_1 m_2,$$

$$B_3 = \sqrt{\tfrac{1}{3}}(l_1 l_2 + m_1 m_2 - 2 n_1 n_2), \qquad B_4 = l_1 m_2 + m_1 l_2, \qquad (6.59)$$

$$B_5 = n_1 l_2 + l_1 n_2, \qquad B_6 = m_1 n_2 + n_1 m_2.$$

(l_1, m_1, n_1) and (l_2, m_2, n_2) are again the direction cosines of the polarization and propagation vectors of the mode (q, j). $V_f \equiv \partial V/\partial Q_f$ is evaluated by writing it in the form

$$\sum_i \frac{\partial V}{\partial X_i} \frac{\partial X_i}{\partial Q_f} + \frac{\partial V}{\partial Y_i} \frac{\partial Y_i}{\partial Q_f} + \frac{\partial V}{\partial Z_i} \frac{\partial Z_i}{\partial Q_f}.$$

Because of the unitary nature of the transformation to normal co-ordinates, $\partial X_i/\partial Q_f$ is just $\partial Q_f/\partial X_i$ etc. $\partial V/\partial X_i$, which must of course be calculated for the unperturbed configuration, can be found once a model for V has been chosen. Since the ratio of r/a is small it is usual to perform an expansion in ascending powers of this parameter. For a point ion model in which the nearest neighbours have an effective charge e_{eff} it is found that the V_f's have the following form

$$\frac{\partial V}{\partial Q_1} = \frac{2}{\sqrt{6}} \{ A(x^2 + y^2 + z^2) + B(x^4 + y^4 + z^4) \} + \cdots$$

$$\frac{\partial V}{\partial Q_2} = \{ A(x^2 - y^2) + B(x^4 - y^4) \} + \cdots$$

$$\frac{\partial V}{\partial Q_3} = \frac{1}{\sqrt{3}} \{A(x^2 + y^2 - 2z^2) + B(x^4 + y^4 - 2z^4)\} + \cdots$$

$$\frac{\partial V}{\partial Q_4} = \{Cyz + E(y^3z + yz^3)\} + \cdots$$

$$\frac{\partial V}{\partial Q_5} = \{Cxz + E(x^3z + xz^3)\} + \cdots \tag{6.60}$$

$$\frac{\partial V}{\partial Q_6} = \{Cxy + E(x^3y + xy^3)\} + \cdots$$

where

$$A = -\tfrac{1}{4}e_{\text{eff}}\left(\frac{18}{a^4} - \frac{75r^2}{a^6}\right); \quad B = -\frac{175}{8a^6}e_{\text{eff}},$$

$$C = -e_{\text{eff}}\left(-\frac{6}{a^4} + \frac{15r^2}{a^6}\right); \quad E = +\frac{35}{2a^6}e_{\text{eff}}. \tag{6.61}$$

Once again the method of operator equivalents can be used to evaluate the matrix elements between the orbital states.

4.5. *An example–Ni²⁺ in MgO*

The theory will be illustrated by way of an example: Ni^{2+} in a cubic crystal such as MgO. Calculations for this ion have been made by ROSENBERG and WIGMORE[1967], AL'TSHULER *et al.*[1961] and SHIREN[1962c]. The spin–orbit coupling, the Zeeman interaction and the orbit–lattice interaction are regarded as a perturbation acting on the orbital states of the nickel ion in a cubic crystalline field. The unperturbed states in the cubic crystal field arising from the ^3F ground term of the free ion have already been considered in §3.4. The perturbation Hamiltonian is taken as

$$H' = \lambda L \cdot S + \beta H \cdot (L + 2S) + \sum_f V_f Q_f. \tag{6.62}$$

If the Q_f's were static the last term would be the perturbation appropriate to the distorted lattice problem. Because the ground state in the cubic field is an orbital singlet the spin operators can, as before, be regarded as non-commuting algebraic variables and the result of the perturbation calculation is an effective spin Hamiltonian which now includes the spin–orbit interaction. Thus by a comparison with the phenomenological Hamiltonian the components of the G-tensor can be found.

The perturbation calculation has to be taken to third order as the first-order term gives no contribution to the spin–lattice interaction and the second-order term is very small. Thus it is necessary to evaluate:

$$\Delta E = \langle 0|H'|0\rangle + \sum_{\alpha \neq 0} \frac{\langle 0|H'|\alpha\rangle\langle\alpha|H'|0\rangle}{E_0 - E_\alpha}$$

$$+ \sum_{\alpha,\beta \neq 0} \frac{\langle 0|H'|\beta\rangle\langle\beta|H'|\alpha\rangle\langle\alpha|H'|0\rangle}{(E_0 - E_\alpha)(E_0 - E_\beta)}$$

$$- \langle 0|H|0\rangle \sum_{\alpha \neq 0} \frac{\langle 0|H'|\alpha\rangle\langle\alpha|H'|0\rangle}{(E_0 - E_\alpha)^2} \qquad (6.63)$$

where $|0\rangle$ represents the state of the lowest orbital singlet with energy E_0 and the intermediate states $|\alpha\rangle$ and $|\beta\rangle$ are the higher orbital states with energy E_α and E_β. This is the standard formula of third-order non-degenerate perturbation theory, see for example Landau and LIFSHITZ[1965] p. 132. The matrix elements involving the spin–orbit coupling and the applied magnetic field (the Zeeman term) are evaluated as before (§3.4) and the matrix elements of V_f can be found using operator equivalents as explained above. The calculation of these matrix elements is, on the whole, more complicated than for the static crystal field, being long and tedious. The methods of group theory can help considerably here and an indication will be given of the technique though a complete account of group theoretical methods is outside the scope of this book. The irreducible representations of the cubic group to which the orbital states of the Ni^{2+} ion in an octahedral crystal field belong have been given in eq. (6.19) and those to which the normal coordinates Q_f's belong are as in eq. (6.56). The V_f's belong to the same irreducible representations as their corresponding Q_f's. The matrix elements $\langle\beta|V_f|\alpha\rangle$ will only be non-zero if the reduction of the product of the representations to which V_f and $|\alpha\rangle$ belong contains the representation to which $\langle\beta|$ belongs. Reduction of product representations is discussed for example in the book by HEINE[1960]. For the representations of the cubic group the reductions are as follows:

$$A_1 \times A_2 = A_2; \quad E \times A_2 = E; \quad T_2 \times A_2 = T_1$$

$$A_1 \times T_2 = T_2; \quad E \times T_2 = T_1 + T_2; \quad T_2 \times T_2 = A_1 + E + T_1 + T_2$$

$$A_1 \times T_1 = T_1; \quad E \times T_1 = T_1 + T_2; \quad T_2 \times T_1 = A_2 + E + T_1 + T_2.$$

$$(6.64)$$

Thus the only non-zero matrix elements of the V_f's are

$$\langle T_1|V_1|T_1\rangle \quad \langle T_1|V_{2,3}|T_1\rangle \quad \langle T_1|V_{4,5,6}|A_2\rangle$$

$$\langle T_2|V_1|T_2\rangle \quad \langle T_1|V_{2,3}|T_2\rangle \quad \langle T_1|V_{4,5,6}|T_1\rangle$$

$$\langle A_2|V_1|A_2\rangle \quad \langle T_2|V_{2,3}|T_1\rangle \quad \langle T_1|V_{4,5,6}|T_2\rangle$$

$$\langle T_2|V_{2,3}|T_2\rangle \quad \langle T_2|V_{4,5,6}|T_2\rangle$$

$$(6.65)$$

The first-order term in the perturbation expansion is zero because even though $\langle A_2|V_1|A_2\rangle$ is non-zero the spin–orbit interaction, as can be seen from eq. (6.21), has no effect so all the spin-states arising from the $|A_2\rangle$ ground state are shifted equally. The second-order term only gives a small contribution as there is no orbit–lattice matrix elements connecting the ground state to the $|T_2\rangle$ first excited state. The main contribution to the spin–lattice interaction comes from the third-order terms. H' is the sum of three separate interactions but to find the spin-lattice interaction which is linear in the strain, only one matrix element involving the $V_f Q_f$ is required. Also to couple the spins to the orbits at least one matrix element involving the spin–orbit coupling is needed. Therefore the important terms in ΔE are

$$\sum_{\alpha,\beta\neq0} \frac{\langle 0|\lambda L\cdot S|\beta\rangle\langle\beta|V_f Q_f|\alpha\rangle\langle\alpha|\lambda L\cdot S|0\rangle}{(E_0-E_\alpha)(E_0-E_\beta)}$$

and

$$\sum_{\alpha,\beta\neq0} \frac{\langle 0|\beta H\cdot(L+2S)|\beta\rangle\langle\beta|V_f Q_f|\alpha\rangle\langle\alpha|\lambda L\cdot S|0\rangle}{(E_0-E_\alpha)(E_0-E_\beta)}.$$

The first of these terms gives a coupling quadratic in the spin operators and is proportional to λ^2/Δ^2 where Δ is the static cubic field splitting. The second expression gives a coupling linear in both the spin and the magnetic field H and is proportional to $\beta H\lambda/\Delta^2$. Usually the first term is the dominant one as βH is usually much smaller than λ. If the calculation is performed and the results obtained compared to the phenomenological Hamiltonian it is found (ROSENBERG and WIGMORE [1967]) that

$$G_{11} = -\frac{100}{9}\frac{\lambda^2 e e_{\text{eff}}}{(E_{T_2}-E_{A_2})^2}\frac{\langle r^4\rangle}{a^5} \tag{6.66}$$

$$G_{44} = -\tfrac{4}{7}\lambda^2 e e_{\text{eff}}\left\{\frac{3\langle r^2\rangle/a^3+\tfrac{5}{3}\langle r^4\rangle/a^5}{(E_{T_2}-E_{A_2})^2}+\frac{6\langle r^2\rangle/a^3+5\langle r^4\rangle/2a^5}{(E_{T_2}-E_{A_2})(E_{T_1}-E_{A_2})}\right\}.$$

MATTUCK and STRANDBERG [1960] using the above method have obtained a general formula for the spin–lattice interaction Hamiltonian which is applicable to any iron-group ion with an orbital singlet ground state. This is

$$H_{s-L} = \sum_{fqjk>l} A_f(qj)[a_j(q)-a_j^*(-q)]\{2\beta\lambda\mathcal{L}_k^f[g_{mm'}S_k+g(S_k\xi-\xi S_k)]$$

$$+2\beta\lambda\mathcal{L}_{kl}^f(S_kH_l+S_lH_k)+\lambda^2\mathcal{L}_{kl}^f(S_kS_l+S_lS_k)\} \tag{6.67}$$

with

$$\mathcal{L}_k^f = \sum_{\alpha\neq0}\frac{\langle 0|V_f|\alpha\rangle\langle\alpha|L_k|0\rangle}{(E_\alpha-E_0)^2},$$

$$\mathcal{L}_{kl}^f = \sum_{\alpha, \beta \neq 0} \left\{ \frac{\langle 0|L_k|\alpha\rangle\langle\alpha|L_l|\beta\rangle\langle\beta|V_f|0\rangle + \langle 0|L_kV_fL_l|0\rangle\langle 0|V_fL_kL_l|0\rangle}{(E_\alpha - E_0)(E_\beta - E_0)} \right\},$$

$$g_{mm'} = (E_m - E_{m'})/\beta H, \quad \langle S'|\xi|S\rangle = \delta_{SS'}E_{S'}.$$

Apart from a phase factor,

$$A_f(qj) = \left(\frac{\hbar\omega_j(q)}{2\rho V v^2}\right) \sum_{i\gamma} B_{fi\gamma}\hat{q} \cdot (R_i^0 - R_0^0) e_\gamma(qj)$$

where $B_{fi\gamma}$ is the coefficient in the expansion of

$$Q_f = \sum_{fi\gamma} B_{fi\gamma} [\Delta R_i - \Delta R_0]_\gamma.$$

The sum over i is over the nearest neighbours and γ denotes the cartesian component of the vector. The R_i's etc. are as defined earlier in the text. $|0\rangle$ is the orbital ground state of energy E_0, and $|\alpha\rangle$, $|\beta\rangle$ are excited orbital states of energy E_α and E_β. $|m\rangle$ and $|m'\rangle$ with energy E_m and $E_{m'}$ are the eigenstates of the static spin Hamiltonian between which H_{s-L} gives the spin–lattice interaction. $|S\rangle$ and $|S'\rangle$ are eigenstates of $2\beta H \cdot S$.

An alternative approach to the calculation is to use the expressions of Challis and De Göer quoted above, eqs. (6.52) and (6.53). These expressions are immediately applicable to ions for which the lowest orbital state is degenerate. The static Hamiltonian including the effects of spin–orbit coupling and the Zeeman energy is treated to a sufficiently high order of perturbation and then the orbit–lattice interaction potential is regarded as inducing transitions between the states of this Hamiltonian. Once again, the Ni^{2+} ion in a site of octahedral coordination will be used as an example. The states of the static Hamiltonian are obtained in first-order perturbation theory from the matrix elements of eq. (6.21). Denoting the zero-order product states in the cubic crystalline field by $|A_2\rangle|M_S\rangle$ etc, it is found by first-order perturbation theory that the three lowest states are

$$|A_2\rangle|-1\rangle - (2\beta H_z/\Delta)[|T_2, 0\rangle|-1\rangle + |T_2, 0\rangle|0\rangle + |T_2, 0\rangle|+1\rangle]$$
$$- (2\lambda/\Delta)[|T_2, 1\rangle|0\rangle - |T_2, 0\rangle|-1\rangle],$$

$$|A_2\rangle|0\rangle - (2\beta H_z/\Delta)[|T_2, 0\rangle|-1\rangle + |T_2, 0\rangle|0\rangle + |T_2, 0\rangle|+1\rangle]$$
$$- (2\lambda/\Delta)[|T_2, 1\rangle|+1\rangle - |T_2, -1\rangle|-1\rangle], \tag{6.68}$$

$$|A_2\rangle|+1\rangle - (2\beta H_z/\Delta)[|T_2, 0\rangle|-1\rangle + |T_2, 0\rangle|0\rangle + |T_2, 0\rangle|+1\rangle]$$
$$- (2\lambda/\Delta)[|T_2, 0\rangle|+1\rangle - |T_2, -1\rangle|0\rangle].$$

The matrix elements of the orbit–lattice interaction between these states are now found. Because the orbit–lattice interaction does not

involve the spin operators, ΔM_S must clearly be zero. There are thus two main contributions, one proportional to $(\lambda/\Delta)^2$ and the other proportional to $\beta H_z \lambda/\Delta^2$. As already indicated the first of these terms is usually the larger. This is the typical situation that occurs when dealing with an iron group ion having an orbital singlet lowest. In the case of a Kramers doublet the term proportional to $\beta H_z \lambda/\Delta^2$ is the only one that can occur. This is because in the absence of a magnetic field no electric field can split the states of the pair so an ultrasonic wave cannot induce transitions between them. In the presence of a magnetic field there is a mixing in of other states to an extent determined by H. Transitions between them can then be induced.

4.6. Fe^{2+} in MgO

Ions of the iron group in which the lowest orbital level is degenerate are often more strongly coupled to the lattice than those already discussed which have an orbital singlet lowest. As an example, the case of a ferrous ion in an octahedral site such as is found in magnesium oxide will be considered. The lowest term of the $3d^6$ configuration of the free ion is $^5D_4$ as given by Hund's rule. The octahedral crystal field splits the five-fold orbital level into a triplet and a doublet with the former lowest. The splitting is calculated in exactly the same way as was described for the divalent nickel ion in §3.4. For the purposes of this discussion any Jahn–Teller effect that might be expected will be ignored. (A discussion of Fe^{2+} in MgO has been given by Low and Weger[1960].) The orbital states comprising the lowest triplet are found to be

$$|T_2, +1\rangle \equiv |2, -1\rangle,$$
$$|T_2, 0\rangle \equiv \{|2, 2\rangle - |2, -2\rangle\}, \qquad (6.69)$$
$$|T_2, -1\rangle \equiv -|2, 1\rangle,$$

where the states of the free ion are as before specified by their L and M_L quantum numbers and the resultant admixed states in the crystal field are labelled according to symmetry. Product states can be formed between these and the five spin states labelled by their M_S quantum numbers, $(M_S = 2, 1, 0, -1, -2)$, and so the lowest state is 15-fold degenerate. The splitting of these states by the spin–orbit coupling can then be calculated by perturbation theory which is found to give a 3-fold, a 5-fold and a 7-fold degenerate state at energies 3λ, λ and -2λ respectively. Remembering that in Fe^{2+} the spin–orbit coupling parameter is negative, the lowest level is therefore the triplet. This triplet can be represented by a spin Hamiltonian with an effective spin S' of unity. The zeroth-order approximation for the states of this triplet are

$$|M_{S'} = 1\rangle = \{|T_2, 1\rangle|0\rangle - \sqrt{3}|T_2, 0\rangle|1\rangle + \sqrt{6}|T_2, -1\rangle|2\rangle\}/\sqrt{10},$$

$$|M_{S'} = 0\rangle = \{-\sqrt{3}|T_2, 1\rangle|-1\rangle + \sqrt{4}|T_2, 0\rangle|0\rangle - \sqrt{3}|T_2, -1\rangle|1\rangle\}/\sqrt{10},$$

$$|M_{S'} = -1\rangle = \{-\sqrt{6}|T_2, 1\rangle|-2\rangle + \sqrt{3}|T_2, 0\rangle|-1\rangle - |T_2, -1\rangle|0\rangle\}/\sqrt{10}. \tag{6.70}$$

$M_{S'}$ is the z-component of the effective spin and on the right-hand side of these expressions the states are product states of the orbital states in the crystal field and the spin states labelled by the M_S value of the true spin. From the discussion centred around eq. (6.65) of the T_2 orbital states in Ni^{2+} it is clear that the orbit–lattice interaction can have matrix elements between these states. The matrix elements are proportional to numerical factors of the order of unity rather than to the much smaller factor $(\lambda/\Delta)^2$ which occurred in the case of Ni^{2+}. Thus it is to be expected that Fe^{2+} in MgO will give a much larger ultrasonic absorption than Ni^{2+} in the same crystal in agreement with experiment. The values of the spin–lattice coupling coefficients have been calculated in this way by GUERMEUR et al.[1965b] who obtained the following expressions:

$$G_{11} = -\tfrac{6}{35}a\beta_2 + \tfrac{10}{63}a\beta_4, \qquad G_{44} = -\tfrac{3}{35}a\beta_2 + \tfrac{1}{21}a\beta_4. \tag{6.71}$$

a is the equilibrium separation of the ferrous ion from its nearest-neighbour oxygen ion and the parameters β_2 and β_4 are $ee_{eff}\langle r^2\rangle/a^4$ and $ee_{eff}\langle r^4\rangle/a^6$ respectively where the notation is the same as before. Ions with orbitally degenerate ground states are therefore often more strongly coupled to the lattice than those having orbital singlets lowest. Unfortunately, it is just these ions that may suffer strong Jahn–Teller effects and so the theory in these interesting cases is more complicated. A good review of the Jahn–Teller effect is the article by STURGE[1967].

5. Dispersion

When an ultrasonic wave passes through a resonant paramagnetic crystal it suffers dispersion as well as attenuation. The experimental method which has been used for studying this phenomenon has already been mentioned in §2.2 and now a theoretical discussion of the effect will be given.

5.1. *Kramers–Kronig relation*

Using samples of potassium magnesium fluoride doped with Ni^{2+} ions ROSENBERG and WIGMORE[1967] demonstrated experimentally that for low intensity ultrasonic waves the Kramers–Kronig relations were

obeyed. These relations relate the attenuation and the dispersion of the wave. Consider an ultrasonic wave $u = u^0 \exp\{i[\omega t - (\beta - i\alpha)x]\}$ of frequency ω propagating along the x-axis through a resonant spin system. The propagation and attenuation constants, β and α will in general be functions of the magnetic field that is applied to the spin system and can be written thus

$$\alpha = \alpha_0 + \alpha(H) \qquad \beta = \beta_0 + \beta(H). \qquad (6.72)$$

α_0 amd β_0 are the magnetic field independent values due for example to phonon–phonon interactions. If the resonance line-shape is Lorentzian

$$\alpha(H) = A/[1 + (H - H_0)^2/\Delta^2]$$

and the Kramers–Kronig relations give

$$\beta(H) = \frac{A(H - H_0)/\Delta}{1 + (H - H_0)^2/\Delta^2}. \qquad (6.73)$$

The parameter A, related to the spin–phonon coupling coefficients, is a constant defining the maximum of the attenuation coefficient and Δ is the half-width of the resonance line centred at the magnetic field H_0. The Kramers–Kronig relations would only be expected to hold for low intensity ultrasonic waves as they essentially apply to a system of harmonic oscillators. The spin system has only a finite number of levels in contrast to the infinite number of equally spaced levels of a harmonic oscillator. The Kramers–Kronig relation will thus only hold if the wave is of sufficiently low intensity so that the spin system does not become saturated. The usual way of calculating the attenuation coefficient is by evaluating the transition probabilities along the lines indicated in §4.4.2. The dispersion function $\beta(H)$ is then deducible from $\alpha(H)$ using the Kramers–Kronig relations. A better method of obtaining the dispersion function, but one which is mathematically exceedingly complex, is to solve directly the equations of motion of the system.

5.2. *Equation of motion method*

In ch. 5§2.2 it was seen that, in the vicinity where the spin wave and the phonon dispersion curves intercepted, the dispersion curves were substantially modified because of the magnetoelastic interaction. In this region coupled excitations existed so that pure elastic wave propagation was no longer possible at those frequencies. The waves that could propagate were magnetoelastic waves which contained a mixture of both elastic and spin wave energy. In a paramagnetic crystal in which the spins are strongly coupled to the lattice, it is expected that coupled modes again exist. The first treatment of coupled spin–phonon modes was given by JACOBSEN and STEVENS[1963] whose method is

now presented. In their paper they considered model Hamiltonians for both $S = \frac{1}{2}$ and $S = 1$ spin systems. The motivation for this study of coupled spin–phonon modes was the experiments by SHIREN[1962b] which measured the velocity of ultrasound propagating through a sample of MgO containing Fe^{2+} or Ni^{2+} paramagnetic ions. Because of the existence of these experiments the model Hamiltonian chosen by Jacobsen and Stevens for their discussion of a $S = 1$ system was that appropriate to Ni^{2+} and Fe^{2+} in an octahedral coordination. It is this example which will be given here, although the analysis is some-what more complicated than for the $S = \frac{1}{2}$ situation. Ions with a spin of one half are usually weakly coupled to the lattice, so experimental confirmation of the theory is not easy in their case.

Jacobsen and Stevens considered a simple one-dimensional model in which a longitudinal wave was assumed to be propagating along the [100] four-fold cubic crystal axis. (Even though only a one-dimensional chain is considered the atoms are still assumed to be at sites of cubic symmetry.) The Hamiltonian is

$$H = \sum_n \left\{ \frac{p_n^2}{2m} + \tfrac{1}{2}K(u_n - u_{n+1})^2 + g\beta H \cdot S^n + \delta\left[(S_{x'}^n)^2 - \tfrac{2}{3}\right](u_{n+1} - u_{n-1}) \right\}.$$

$$(6.74)$$

The first two terms are the lattice Hamiltonian for a one-dimensional chain of atoms coupled by nearest-neighbour interactions p_n and u_n being respectively the momentum and displacement of the atom n, see eq. (2.27). The third term is the Zeeman energy of the spins in an applied magnetic field H. For Fe^{2+} and Ni^{2+} in a cubic environment this is the only term in the static spin Hamiltonian, see §3.4. The last term represents the coupling of the ultrasonic wave travelling in the x'-direction to the spin system. x', y', z' denote the four-fold cubic axes. Since S is greater than one half it is likely that the dominant interaction is through the crystal field tensor rather than through the g-factor. The coupling coefficient δ is related to the parameter d of the phenomeno-logical spin Hamiltonian, eq. (6.26) by $\delta(u_{n+1} - u_{n-1}) = d$ and hence δ is related to the coupling coefficient G, eq. (6.27) by $G = 2a\delta$ where a is the equilibrium spacing between the atoms. For a real three-dimensional crystal, G, of course has several components rather than one, as is appropriate to a linear chain. To simplify the mathematics Jacobsen and Stevens take the specific case when the magnetic field is applied at 45° to the x'-direction in the $x'z'$-plane. It is then convenient to rotate the coordinate system to a new frame (x, y, z) in which the Zeeman term is diagonal and the magnetic field is along the z-axis. The Hamiltonian in the new frame of reference for this direction

of the magnetic field is

$$H = \sum_n \left\{ \frac{p_n^2}{2m} + \tfrac{1}{2}K(u_n - u_{n+1})^2 + g\beta H S_z^n \right.$$

$$\left. + \tfrac{1}{2}\delta[(S_x^n)^2 + (S_z^n)^2 + S_z^n S_x^n + S_x^n S_z^n - \tfrac{4}{3}](u_{n+1} - u_{n-1}) \right\} \quad (6.75)$$

where the transformations

$$S_{x'} = (1/\sqrt{2})(S_x + S_z), \qquad S_{z'} = (1/\sqrt{2})(S_z - S_x),$$

$$S_{x'}^2 = \tfrac{1}{2}[S_x^2 + S_z^2 + S_z S_x + S_x S_z]$$

have been used. Using Heisenberg's equation of motion for a dynamical operator the following equations of motion for the coupled system are obtained:

$$\dot{p}_n = \frac{1}{i\hbar}[p_n, H] = K(u_{n+1} + u_{n-1} - 2u_n)$$

$$+ \tfrac{1}{2}\delta[S_x^2 + S_z^2 + S_z S_x + S_x S_z - \tfrac{4}{3}]_{n-1}^{n+1}$$

where the notation $[f(S)]_{n-1}^{n+1}$ meaning $f(S^{n+1}) - f(S^{n-1})$ has been introduced.

$$\dot{u}_n = \frac{1}{i\hbar}[u_n, H] = \frac{p_n}{m}$$

$$\frac{d}{dt}(S_x^n)^2 = -\omega_0(S_x^n S_y^n + S_y^n S_x^n) - \frac{\delta}{2\hbar}(u_{n+1} - u_{n-1})S_y^n$$

$$\frac{d}{dt}(S_y^n)^2 = \omega_0(S_x^n S_y^n + S_y^n S_x^n)$$

$$\frac{d}{dt}(S_z^n)^2 = \frac{1}{2}\frac{\delta}{\hbar}(u_{n+1} - u_{n-1})S_y^n \qquad (6.76)$$

$$\frac{d}{dt}(S_x^n S_y^n + S_y^n S_x^n) = 2\omega_0[2(S_x^n)^2 + (S_z^n)^2 - 2] - \frac{\delta}{2\hbar}(u_{n+1} - u_{n-1})(S_z^n + S_x^n)$$

$$\frac{d}{dt}(S_y^n S_z^n + S_z^n S_y^n) = \omega_0(S_x^n S_z^n + S_z^n S_x^n) - \frac{\delta}{2\hbar}(u_{n+1} - u_{n-1})(S_z^n - S_x^n)$$

$$\frac{d}{dt}(S_x^n S_z^n + S_z^n S_x^n) = -\omega_0(S_y^n S_z^n + S_z^n S_y^n)$$

where $\omega_0 = g\beta H/\hbar$. In deriving these equations the commutation rules $[u_n, p_m] = i\hbar\delta_{n,m}$ and those of eq. (5.3) are required. Besides using the commutation rules for the spins, explicit use has been made of other identities which hold for $S = 1$. For example $S_z^2 S_y + S_y S_z^2 = S_y$ as can be seen from the matrices given in appendix 6.

These equations are now linearized in much the same way as was

done in ch. 5 eq. (5.67) so that sinusoidal solutions can be obtained. This involves dropping all quadratic terms such as $u_n S_y^n$ and assuming that S_z^n remains constant in space and time so that where necessary it can be replaced by its mean value $\langle S_z \rangle$. This really amounts to assuming that the ultrasonic wave is of low amplitude or that the coupling is weak, so that the magnetization in the direction of the magnetic field is not changed appreciably by the absorption of the ultrasonic energy, that is, relaxation is sufficiently rapid to thermalize this energy. Using this procedure the following set of equations can be readily obtained.

$$m\ddot{u}_n = K(u_{n+1} + u_{n-1} - 2u_n) + \tfrac{1}{2}\delta[(S_x)^2 + \langle S_z \rangle^2 + S_z S_x + S_x S_z]_{n-1}^{n+1}$$

$$\frac{d^2}{dt^2}(S_x^n)^2 = -2\omega_0^2[2(S_x^n)^2 + \langle S_z \rangle^2 - 2] + \frac{\delta\omega_0}{2\hbar}(u_{n+1} - u_{n-1})\langle S_z \rangle,$$

$$\frac{d^2}{dt^2}(S_x^n S_z^n + S_z^n S_x^n) = -\omega_0^2(S_x^n S_z^n + S_z^n S_x^n) + \frac{\delta\omega_0}{2\hbar}(u_{n+1} - u_{n-1})\langle S_z \rangle.$$

$$(6.77)$$

Further the term $\langle S_z \rangle^2 - 2$ will be dropped since it does not contribute to the harmonic time dependence of $(S_x)^2$ but gives a term dependent on t^2. This approximation amounts to considering time intervals short enough such that the changes in spin population among the levels can be neglected. Sinusoidal solutions in the form of travelling waves are now assumed for u_n, $(S_x^n)^2$ and $(S_x^n S_z^n + S_z^n S_x^n)$ by writing for example $u_n = u_n^0 \exp[i(\omega t - qna)]$. After substitution into eq. (6.77) and equating the determinant of the coefficients of u_n, $(S_x^n)^2$ and $(S_x^n S_z^n + S_z^n S_x^n)$ to zero, the following secular equation is obtained for the dispersion relation.

$$\begin{vmatrix} (m\omega^2 - Kq^2a^2) & : & -i\delta qa & : & -i\delta qa \\[2mm] -\dfrac{i\delta}{\hbar}qa\omega_0\langle S_z \rangle & : & (\omega^2 - 4\omega_0^2) & : & 0 \\[2mm] -\dfrac{i\delta}{\hbar}qa\omega_0\langle S_z \rangle & : & 0 & : & (\omega^2 - \omega_0^2) \end{vmatrix} = 0 \qquad (6.78)$$

(The long wavelength approximation has been made which enables $\sin(qa)$ to be replaced by qa.) The determinant gives for the velocity, $v = \omega/q$, of the coupled waves

$$\left(\frac{v_0}{v}\right)^2 = \frac{Kq^2a^2}{m\omega^2} = \left\{1 - \frac{\delta^2\omega_0\langle S_z \rangle}{K\hbar}\left[\frac{1}{\omega^2 - \omega_0^2} + \frac{1}{\omega^2 - 4\omega_0^2}\right]\right\}^{-1} \quad (6.79)$$

$v_0 = (Ka^2/m)^{1/2}$ is the velocity of the ultrasonic wave in the absence of

any interaction with the spins. Equation (6.79) can be rewritten in the form

$$\left(\frac{v_0}{v}\right)^2 = 1 + \frac{\delta^2\omega_0\langle S_z\rangle}{K\hbar}\left\{\left((\omega^2-\omega_0^2)-\frac{\delta^2\omega_0}{K\hbar}\langle S_z\rangle\left[1+\frac{\omega^2-\omega_0^2}{\omega^2-4\omega_0^2}\right]\right)^{-1}\right.$$
$$\left. - \left((\omega^2-4\omega_0^2)-\frac{\delta^2\omega_0}{K\hbar}\langle S_z\rangle\left[1+\frac{\omega^2-4\omega_0^2}{\omega^2-\omega_0^2}\right]\right)^{-1}\right\}. \qquad (6.80)$$

In this form the equation clearly exhibits the fact that there are two resonances, one at $\omega = \omega_0$ and the other at twice this frequency. The resonances are of course associated with the $\Delta M_S = 1$ and $\Delta M_S = 2$ spin transitions that are possible in the $S = 1$ spin system. Figure 6.6 shows a plot of eq. (6.80) as given by Jacobsen and Stevens. So far losses due, for example, to spin–spin interactions have been neglected in the theory. Jacobsen and Stevens included damping in a pheno-menological way by assuming that in the absence of the spin–lattice interaction the spin system was described by the well-known relaxa-tion equations of Bloch in which the transverse components of the spin decay with a relaxation time τ. If this relaxation of the spin system is included in the equations of motion it is found that the dispersion relation is now complex so that the wave velocity has both a real and an imaginary part. For example in the vicinity of the frequency ω_0, where the second resonance in eq. (6.80) may be neglected, the in-clusion of τ leads to the modified dispersion law

$$\left(\frac{v_0}{v}\right)^2 = \left\{1 - \frac{\delta^2\omega_0}{K\hbar}\langle S_z\rangle\left[\frac{1}{\omega^2-\omega_0^2-\tau^{-2}-2i\omega/\tau}\right]\right\}^{-1}$$
$$= 1 - \frac{\delta^2\omega_0\langle S_z\rangle/K\hbar}{\omega_0^2-\omega^2+\tau^{-2}+(\delta^2\omega_0/K\hbar)\langle S_z\rangle+2i\omega/\tau}. \qquad (6.81)$$
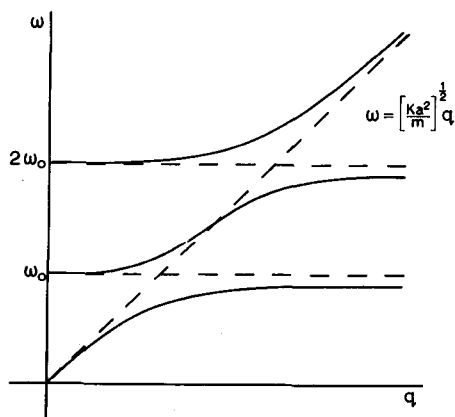
Fig. 6.6. Dispersion curve for $S = 1$.

Provided that the coupling between the spin system and the lattice is not too strong so that $|\delta^2\omega_0\langle S_z\rangle\tau/2\omega K\hbar| \ll 1$ the square root of eq. (6.81) can be taken and the real and imaginary parts of v obtained:

$$\frac{v_0}{v} = 1 - \frac{1}{2}\frac{\delta^2\omega_0\langle S_z\rangle/K\hbar}{\omega_0^2 + \tau^{-2} + (\delta^2\omega_0/K\hbar)\langle S_z\rangle - \omega^2 + 2i\omega/\tau}$$

$$= 1 - \frac{\delta^2\omega_0\langle S_z\rangle}{2K\hbar}\left\{\frac{\Omega_0^2 - \omega^2 - 2i\omega/\tau}{(\Omega_0^2 - \omega^2)^2 + (2\omega/\tau)^2}\right\} \tag{6.82}$$

where $\Omega_0^2 = \omega_0^2 + \tau^{-2} + (\delta^2\omega_0/K\hbar)\langle S_z\rangle$. Close to resonance when $\omega \approx \Omega_0$ the quantity $(\Omega_0^2 - \omega^2)$ may be approximated by $2\omega(\Omega_0 - \omega)$. Writing the propagation vector q as $q(\omega) = \beta_0 + \beta(\omega) - i\alpha(\omega)$ where $\beta_0 = \omega/v_0$ it is found that $\alpha(\omega)$ and $\beta(\omega)$ are given by

$$\alpha(\omega) = \frac{\delta^2\omega_0|\langle S_z\rangle|}{4K\hbar v_0}\left\{\frac{\tau}{(\Omega_0 - \omega)^2\tau^2 + 1}\right\}, \tag{6.83}$$

$$\beta(\omega) = \frac{\delta^2\omega_0|\langle S_z\rangle|}{4K\hbar v_0}\left\{\frac{\tau^2(\Omega_0 - \omega)}{(\Omega_0 - \omega)^2\tau^2 + 1}\right\}.$$

Remembering that the magnetic field for resonance is proportional to the frequency and that the line-width is the reciprocal of the lifetime, it is clear that eqs. (6.83) are consistent with eq. (6.73) at frequencies close to resonance.

5.3. Coupled spin–phonon modes

As mentioned in the introduction to this section Jacobsen and Stevens also considered a spin $\frac{1}{2}$ system. The model chosen was again a one-dimensional chain of atoms in which a longitudinal wave was propagating. The chain was taken to lie along the x-direction and a d.c. magnetic field was applied in the z-direction perpendicular to the chain. The spin–lattice interaction was represented by a term in which the relative displacement $(u_{n+1} - u_{n-1})$ was coupled just to the x-component of the spins through S_x^n. In this case the equations of motion required are those for $\ddot{u}_n$ and $\ddot{S}_z^n$. Assuming as before that S_z^n is a constant in space and time, the dispersion relation for the system is found to be given by

$$(\omega^2 - \omega_q^2)(\omega^2 - \omega_0^2) + 4\delta^2\omega_0\omega_q^2\langle S_z\rangle/K\hbar = 0, \tag{6.84}$$

where ω_q is the lattice mode frequency in the absence of coupling and ω_0 is $g\beta H/\hbar$ as before. The coupling parameter is again δ which this time would be related to h of eq. (6.26). A long wavelength approximation has also been made in the derivation of this dispersion law. Instead of finding the quantity $(v_0/v)^2$ as a function of frequency the dispersion

relation can be solved to give ω as a function of q. In this way coupled mode frequencies are found at

$$\omega^2 = \tfrac{1}{2}\{(\omega_0^2 + \omega_q^2) \pm [(\omega_0^2 - \omega_q^2)^2 - (16\delta^2/K\hbar)\omega_0\omega_q\langle S_z\rangle]^{1/2}\} \quad (6.85)$$

and these have been sketched in fig. 6.7. The dotted curves show the unperturbed lattice and spin frequencies. The dispersion curves are reminiscent of those in fig. 5.3 except for the fact that the parabolic spin wave curve is replaced by a constant frequency curve at ω_0. It is noticed that a stop-band exists over a small range of frequencies near to ω_0. This will disappear if losses in the spin system are included in the analysis but then ω will become complex so that the coupled waves are damped. It should also be pointed out that the stop-band on this model is really a consequence of taking the long wavelength limit. In thermal equilibrium $\langle S_z\rangle$ is negative but if the spin populations can be inverted in some way then it will have the opposite sign. A consequence of this is that amplification rather than attenuation can occur, see §7.1.

It might be expected that the anomalous dispersion associated with the coupled spin–phonon modes would manifest itself in the thermodynamic properties of the system. SEARS[1964] and TUCKER[1965] calculated by a Green's function method the energy of the spin–phonon system for this model Hamiltonian. In their analysis they employed a random phase approximation equivalent to the linearizing procedure of Jacobsen and Stevens which again led to coupled modes given by eq. (6.85). It was subsequently found by STEVENS and VAN EEKELEN[1967] that this simple decoupling approximation is not sufficiently accurate when calculating the energy of the system to second order in the coupling parameter. If the equations of motion are decoupled at a later stage a modified dispersion relation holds in which
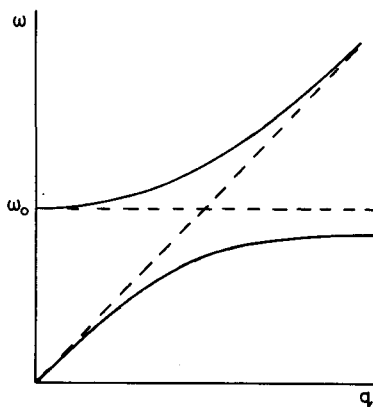
Fig. 6.7. Dispersion curve for $S = \tfrac{1}{2}$.

ω is complex, so that the excitations are damped in time. The lifetime of these coupled modes has also been examined by MILLS[1965], YOLIN[1965] and ELLIOTT and PARKINSON[1967]. The effect of the dispersion in the vicinity of the spin resonance frequency on the magnetic field dependent thermal conductivity of a spin–phonon system has been examined by MULLER and TUCKER[1966] and the theory has been extended by ELLIOTT and PARKINSON[1967] to account for the intrinsic lifetime of the coupled modes. Recently, ROUNDY and MILLS[1970] have modified the theory to allow for the difference in mass of the paramagnetic impurity ions and the host atoms of the crystal. Evidence in support of the theory can be found in the experimental measurements of CHALLIS et al.[1968]. Although thermal conductivity experiments can be used to study the coupling of paramagnetic spins to the lattice, the information is much more difficult to extract than in ultrasonic measurements because the analysis involves thermal distributions of phonons over many modes.

5.4. Rotatory dispersion

In the preceding section the discussion was based on a one-dimensional model in which longitudinal waves could propagate. When shear waves are considered a proper three-dimensional treatment is required and it is then expected that phenomena such as rotatory dispersion can occur similar to that found in ferromagnetic materials, ch. 5§2.5. The theory of acoustic wave rotation by spin–phonon interactions in paramagnetic crystals has been given by MULLER and TUCKER[1967] for the case of iron group ions with $S = \frac{1}{2}$ embedded in an octahedral complex. The Hamiltonian density appropriate to this situation is

$$\mathcal{H}(r) = \frac{1}{2\rho}P(r) \cdot P(r) + \tfrac{1}{2}(c_{11} - 2c_{44})\left\{\sum_{\alpha}\left(\frac{\partial u_{\alpha}}{\partial \alpha}\right)\right\}^2$$

$$+ \tfrac{1}{2}c_{44}\sum_{\alpha\beta}\left\{\left(\frac{\partial u_{\alpha}}{\partial \beta}\right)^2 + \left(\frac{\partial u_{\alpha}}{\partial \beta}\frac{\partial u_{\beta}}{\partial \alpha}\right)\right\} + g\beta H \cdot S(r)$$

$$+ A_1 H \cdot \dot{S}(r)\sum_{\alpha}\frac{\partial u_{\alpha}}{\partial \alpha} + A_2\sum_{\alpha}H_{\alpha}S_{\alpha}\frac{\partial u_{\alpha}}{\partial \alpha}$$

$$+ A_3\sum_{\alpha\beta}H_{\alpha}S_{\beta}\frac{\partial u_{\alpha}}{\partial \beta} + A_4\sum_{\alpha\beta}H_{\alpha}S_{\beta}\frac{\partial u_{\beta}}{\partial \alpha} \qquad (6.86)$$

where α and $\beta = x, y, z$, the cartesian coordinates with respect to the four-fold cubic crystal axes. The quantities $u_{\alpha}(r)$, $P_{\alpha}(r)$ and $S_{\alpha}(r)$ defined by $S_{\alpha}(r) = \sum_n S_{\alpha}^n\delta(r - r_n)$ are treated as operators obeying the commutation rules $[u_{\alpha}(r), P_{\beta}(r')] = i\hbar\delta_{\alpha,\beta}\delta(r - r')$ and $[S_{\alpha}(r), S_{\beta}(r')] = i\epsilon_{\alpha,\beta,\gamma}S_{\gamma}(r)\delta(r - r')$. The Hamiltonian density for the

elastic energy follows from eq. (5.59) if $c_{11} - c_{12}$ is put equal to $2c_{44}$. This is the assumption of elastic isotropy, see ch. 2§1.4, an approximation which is reasonable if the discussion is restricted to elastic waves propagating along a high symmetry axis of the crystal where pure longitudinal and degenerate transverse wave propagation can occur. In carrying out the analysis it was found convenient to define a new set of axes x', y', z' in which the Zeeman energy transformed to $HS_{z'}$. The equations of motion for $\dot{P}_x$, $\dot{P}_y$, $\dot{P}_z$, $\dot{S}_{x'}$ and $\dot{S}_{y'}$ were then obtained and linearized by replacing $S_{z'}$ by $\langle S_{z'} \rangle$. The term in the interaction which commuted with the Zeeman energy was also neglected since it did not represent a true dynamical coupling. Also relaxation of the spin system was again accounted for through Bloch's equations of motion. This procedure resulted in the following dispersion relation being obtained

$$(\omega^2 \rho - c_{11} q^2)\{(\omega^2 \rho - c_{44} q^2)^2 (\omega^2 - \omega_0^2 - 1/\tau^2 - 2i\omega/\tau)$$

$$+ (\omega^2 \rho - c_{44} q^2) H^2 \omega_0 q^2 \langle S_{z'} \rangle \hbar^{-1} [A_4^2 \cos^2 \theta (1 + \cos^2 \theta) - \tfrac{1}{2} A_3 A_4 \sin^2 2\theta$$

$$+ A_3^2 \sin^4 \theta] - A_4^2 H^4 q^4 \langle S_{z'} \rangle^2 \hbar^{-2} \cos^2 \theta \, [A_4^2 \cos^4 \theta - \tfrac{1}{2} A_3 A_4 \sin^2 2\theta$$

$$+ A_3^2 \sin^4 \theta]\} + \tfrac{1}{4} A_2^2 H^2 q^2 \langle S_{z'} \rangle \hbar^{-1} (\omega^2 \rho - c_{44} q^2) \sin^2 2\theta [\omega_0 (\omega^2 \rho - c_{44} q^2)$$

$$- A_4^2 H^2 \langle S_{z'} \rangle \hbar^{-1} q^2 \cos \theta] = 0. \tag{6.87}$$

θ and ϕ are the polar angles that the magnetic field makes with the cubic crystal axes. It is seen that when the direction of the magnetic field is such that $\theta = 0$ or $\tfrac{1}{2}\pi$ the secular determinant will factorize and pure transverse and longitudinal waves exist. When $\theta = 0$ the solutions are of the same form as those of eqs. (5.71)–(5.73) with ω_s replaced by ω_0 and $A_4^2 H^2 |\langle S_{z'} \rangle| \hbar$ playing the role of $|\gamma| b_2^2 / M_0$ in determining the difference in velocity of the two transverse waves. There is a slight difference however in that ω_0 is independent of q as opposed to ω_s, so that for a fixed frequency there are only two solutions for q instead of four. These values of q for the two transverse modes are given by

$$q_\pm^2 = \frac{\omega^2 \rho}{c_{44}} \left\{ 1 + \frac{A_4^2 H^2 |\langle S_{z'} \rangle|}{\hbar c_{44} [\Omega_0 \mp \omega \pm i/\tau]} \right\} \tag{6.88}$$

with $\Omega_0 = \omega_0 - A_4^2 H^2 |\langle S_{z'} \rangle| / \hbar c_{44}$. For these two modes it is found that $u_x / u_y = \pm i$. Thus when the magnetic field and the direction of propagation coincide with the crystal axis, two circularly polarized transverse waves may propagate with different velocities, leading to the phenomenon of rotatory dispersion. Well away from resonance where the effect of damping can be neglected, Muller and Tucker find that the rotation of the plane of polarization per unit distance is

$$\psi = \left(\frac{\omega^2 \rho}{c_{44}}\right)^{1/2} \frac{A_4^2 H^2 |\langle S_{z'} \rangle| \omega}{2\hbar c_{44} (\Omega_0^2 - \omega^2)}. \tag{6.89}$$

Rotation of the plane of polarization of an ultrasonic wave propagating in a paramagnetic crystal has been observed by GUERMEUR et al. [1968]. Their experiments were performed at a frequency of 9.375 GHz on a sample of MgO doped with Ni^{2+} ions (concentration 2×10^{-3}). A rotation of about 5°/cm was found at 4 K when the ultrasonic wave propagated parallel to the d.c. applied magnetic field. So far no experimental results have been reported for a spin $\frac{1}{2}$ system. Because the spin–phonon coupling constants are smaller for these ions it might be thought advantageous to work near resonance. Unfortunately the attenuation of the waves then has to be accounted for as discussed in ch. 5§2.5. Since one component of the wave will be more severely attenuated than the other elliptical polarization results. Muller and Tucker estimate from their theory that the ratio of the minor to major axes of the ellipse will be about 0.9 by the time ψ has reached the value of $\frac{1}{2}\pi$. In an experiment therefore, some compromise would have to be reached between the desirability of a large coupling and the disadvantage of a strong attenuation.

When θ is $\frac{1}{2}\pi$ only the transverse wave whose polarization vector is parallel to the magnetic field is coupled to the spin system. The equation for this orientation of the magnetic field is that of eq. (5.83) if $|\gamma| b_2^2 \omega_s / M_0$ is replaced by $A_3^2 H^2 \omega_0 |\langle S_{z'} \rangle| \hbar$ and $\omega_s \omega_m$ by ω_0^2. It is noted that two coupling constants, A_3 and A_4, occur in the present theory whereas only b_2 appeared in the ferromagnetic case. This is because the spin–phonon interaction is only linear in the spin components, not quadratic as for the magnetoelastic term, so that A_3 need not be equal to A_4. It is seen that the coupled spin–phonon mode for this orientation has a dispersion relation similar to that of Jacobsen and Stevens, eq. (6.85). In this three-dimensional model however it is a transverse mode, not the longitudinal mode, that has this dispersion.

5.5. High intensity waves

The discussion so far has concentrated on low intensity ultrasonic waves; a sufficiently intense ultrasonic wave travelling through a system of resonant spins strongly coupled to the lattice may exhibit non-linear effects. These effects are analogous to the self-induced transparency found by McCALL and HAHN [1969] in the case of light. The essential features of this phenomenon are a reduction in the ultrasonic attenuation at high intensities, an anomalously large delay in transmission of a pulse and a reshaping of a pulse during passage through the resonant medium. A theoretical account of this applied to acoustic paramagnetic resonance has been given by FLETCHER [1970] who shows that at a critical ultrasonic intensity an instability appears and an ultrasonic wave train will develop a series of oscillations which grow as the

wave propagates through the material. The conditions necessary for the observation of these oscillations are that the propagation distance is longer than the growth length and that the line-width of the resonance is sufficiently small. The growth length depends on the strength of the coupling between the spins and the lattice, the intensity of the ultrasonic wave and the spin–spin and spin–lattice relaxation times. The line-width condition is approximately that the strain amplitude of the ultrasonic wave is larger than the random static strain causing broadening of the line, assuming that the main contribution to the line-width is from this source, see §6.1. Some of these effects have been observed by SHIREN[1970] using Ni^{2+} ions in MgO.

A discussion of pulse propagation through a resonant medium together with experimental results on Ni^{2+} in MgO is given by SHIREN [1962b].

6. Line-widths in acoustic paramagnetic resonance

6.1. *Inhomogeneous broadening due to random strains*

The observed width of an acoustic paramagnetic resonance line may be due to several factors. Usually in the case of an ion which is very strongly coupled to the lattice the line-width observed is mainly due to an inhomogeneous broadening caused by the presence of random strains or random electric fields associated with defects in the host lattice. This is because an ion strongly coupled to the lattice is very sensitive to small distortions of its environment which may be produced by dislocations, vacancies, charged impurities and other defects at some distance from the paramagnetic ion. The resonance frequency of each ion is shifted slightly from the value that it would have in a perfect lattice and so the observed resonance lineshape is due to a distribution of local random strains.

The a.p.r. and e.p.r. lines of Fe^{2+} and Ni^{2+} in MgO consist of lines broadened in this way and will be used as an example, as it has been discussed extensively in the literature by McMAHON[1964], STONE-HAM[1966a] and LEWIS and STONEHAM[1967]. The spin Hamiltonian of this ion in the perfect unstrained lattice is $H = g\beta H \cdot S$ as was discussed earlier in §3.4. The perturbation due to random local strains is then, as in §4.2,

$$H_l = S \cdot d \cdot S$$
$$= G_{11}\left[\tfrac{1}{4}(2\epsilon_{zz} - \epsilon_{xx} - \epsilon_{yy})(2S_z^2 - S_x^2 - S_y^2) + \tfrac{3}{4}(\epsilon_{xx} - \epsilon_{yy})(S_x^2 - S_y^2)\right]$$
$$+ G_{44}\left[\epsilon_{yz}(S_zS_y + S_yS_z) + \epsilon_{rz}(S_xS_z + S_zS_x) + \epsilon_{xy}(S_yS_x + S_xS_y)\right]$$
$$(6.90)$$

where the x, y, z axes are the cubic axes of the MgO and the ϵ_{ij} are the components of the local strain at the site of the paramagnetic ion. The effective spins of both Fe^{2+} and Ni^{2+} are one and $\Delta M_S = 1$ and $\Delta M_S = 2$ transitions are possible. If a calculation is carried out it is found that the $\Delta M_S = 1$ resonance line is broadened by strains in first order so that the broadening is linear in the strain. This results in a symmetrically broadened line as positive and negative strains are equally probable. The $\Delta M_S = 2$ resonance line on the other hand is broadened by strains only in second order, giving a broadening that is quadratic in the strain and hence an asymmetric resonance line is produced. As an example, the resonance frequency for the $\Delta M_S = 1$ transition when the magnetic field is in the $(1\bar{1}0)$ plane making an angle θ with the [001] axis may be quoted. It is $\nu \pm \Delta\nu$ where the shift $\Delta\nu$ is given by

$$h\Delta\nu = G_{11}[\tfrac{1}{2}(3\cos^2\theta - 1)][\epsilon_{zz} - \tfrac{1}{2}(\epsilon_{xx} + \epsilon_{yy})]$$
$$+ G_{44}[\epsilon_{xy}\sin^2\theta + \sqrt{2}\sin\theta\cos\theta(\epsilon_{yz} + \epsilon_{zx})]. \qquad (6.91)$$

To obtain this expression it is first convenient to refer the spin coordinates to a new set of axes in which the magnetic field lies along the new z-axis (say z'). Then, using a representation in which $S_{z'}$ is diagonal, the difference in expectation value for the two states involved in the transition can be written down. It is clear that the line-shape depends both on the strain distribution and on the direction of the magnetic field. The line-widths observed due to strain broadening are usually specimen dependent and to calculate them some assumption has to be made about the strain distribution. STONEHAM[1966a] has given an example of how a strain distribution in MgO may be derived from an assumed distribution of dislocations. LEWIS and STONEHAM[1967] show that some conclusions can often be drawn about the ratio of G_{11}/G_{44} and about the possible sources of strain from measurements of the variation of line-shape as the direction of the magnetic field is changed (e.g. from eq. (6.91)).

6.2. *Line-width due to dipolar and exchange interactions*

There can be other contributions to the line-width of an a.p.r. line other than the strain broadening mechanism discussed above, although for an ion strongly coupled to the lattice and present in low concentration these contributions will be smaller. Of course, at sufficiently high temperatures broadening due to spin–lattice relaxation will always dominate as it is the main temperature dependent contribution to the line-width. This interaction is discussed below in §6.3. Here the homogeneous broadening of the resonance lines due to magnetic dipolar and exchange interactions between the paramagnetic ions will be discussed.

If there is more than one species of paramagnetic ion present in the crystal, the dipolar and exchange interactions between the resonant ions and the others are also a source of broadening. This interaction between unlike spins is really an inhomogeneous broadening mechanism; but SHIREN [1962b] has shown that it is properly treated with the homogeneous broadening in situations where the scale of the locally strained regions is large compared to the ultrasonic wavelength but where the average separation between the species is very much shorter than one wavelength.

Expressions for the second, $\langle \nu^2 \rangle$, and fourth moments $\langle \nu^4 \rangle$ of an a.p.r. line due to the dipolar and exchange interactions have been obtained by LOUDON [1960] in the high temperature limit. These moments are defined in the usual way by

$$\langle \nu^n \rangle = \int_{-\infty}^{\infty} g(\nu)(\nu - \nu_0)^n \, d\nu \qquad (6.92)$$

and the first two are usually sufficient to get a qualitative picture of the line-shape. $g(\nu)$ is the line-shape function normalized to unity,

$$\int_{-\infty}^{\infty} g(\nu) \, d\nu = 1,$$

and ν_0 is the resonance frequency at the centre of the line. If I represents that part of the spin–phonon interaction responsible for inducing the absorption, the moments can be calculated with the aid of the standard formulae

$$\langle \nu^2 \rangle = -\frac{\text{Trace } [H', I]^2}{h^2 \, \text{Trace } I^2}, \qquad (6.93)$$

$$\langle \nu^4 \rangle = \frac{\text{Trace } [H', [H', I]]^2}{h^4 \, \text{Trace } I^2}. \qquad (6.94)$$

These formulae hold only in the high temperature limit since they do not account for the population difference between the final and initial states of the spin system. H' is only that part of the Hamiltonian responsible for the line broadening which commutes with the Zeeman interaction. It is necessary to truncate H in this way in order not to include in the moments contributions from small satellite lines at frequencies $2\nu_0, 3\nu_0$ etc., far removed from the main line.

The sites in the host crystal will be labelled by i, j and it will be assumed that a magnetic field is applied in the z-direction. The Hamiltonian is

$$H = g\beta H \sum_i S_i^z + \sum_{i<j} J_{ij} S_i \cdot S_j + g^2\beta^2 \sum_{i<j} \left\{ \frac{S_i \cdot S_j}{R_{ij}^3} - \frac{3(S_i \cdot R_{ij})(S_j \cdot R_{ij})}{R_{ij}^5} \right\}. \qquad (6.95)$$

The first term is the Zeeman interaction due to the magnetic field H and this is taken as the unperturbed Hamiltonian. The second and third terms are respectively an isotropic exchange and dipolar interaction between the spins, see eqs. (5.2) and (5.16). The truncated Hamiltonian, the part needed in the calculation of the moments, is

$$H' = \sum_{i<j} C_{ij}[S_i^+ S_j^- + S_i^- S_j^+] + \sum_{i<j} D_{ij} S_i^z S_j^z, \qquad (6.96)$$

where

$$C_{ij} = \tfrac{1}{2} J_{ij} - \tfrac{1}{4} g^2 \beta^2 R_{ij}^{-3}(1 - 3\cos^2\theta_{ij}),$$
$$D_{ij} = J_{ij} + g^2 \beta^2 R_{ij}^{-3}(1 - 3\cos^2\theta_{ij}) \qquad (6.97)$$

and θ_{ij} is the angle between R_{ij} and the z-axis. The most general form for the spin–phonon interaction, quadratic in the components of the spin operators is

$$I = \sum_i [A(3S_i^z S_i^z - S_i^2) + B(S_i^z S_i^+ + S_i^+ S_i^z)$$
$$+ B^*(S_i^z S_i^- + S_i^- S_i^z) + CS_i^+ S_i^+ + C^* S_i^- S_i^-]. \qquad (6.98)$$

The terms in A, B and C give resonance lines at $\nu = 0$, $g\beta H/\hbar$ and $2g\beta H/\hbar$ respectively. A, B, C are linear in the strain and involve the spin–lattice coupling coefficients. This Hamiltonian is appropriate for $S > \tfrac{1}{2}$ when the dominant spin–lattice coupling is quadratic in the spin operators. For the case of $S = \tfrac{1}{2}$ it has been seen that the coupling due to this term vanishes, so in this case a coupling linear in the components of S has to be considered. This situation is considered later in the section.

Using eqs. (6.93), (6.94), (6.96) and (6.98) the following results are obtained: For the $\Delta M_S = 1$ resonance at $\nu = g\beta H/\hbar$

$$\langle \nu^2 \rangle = \frac{2}{3Nh^2} S(S+1) \sum_{i<j} [20C_{ij}^2 + D_{ij}^2], \qquad (6.99)$$

where N is the total number of spins,

$$\langle \nu^4 \rangle = \frac{1}{9Nh^4} S^2(S+1)^2 \sum_{i \neq j \neq k} \{624 C_{ij}^2 C_{ik}^2 - 32 C_{ij} C_{jk} C_{ki} D_{ij}$$
$$+ 112 C_{ij}^2 D_{ik}^2 - 32 C_{ij}^2 D_{ik} D_{jk} + 2 D_{ij}^2 D_{ik}^2 \} + \left(\frac{2}{105Nh^4} \right) S(S+1)$$
$$\times \sum_{i<j} \{8[1142S(S+1) - 569]C_{ij}^4 + 840[4S(S+1) - 3]C_{ij}^3 D_{ij}$$
$$+ 42[29S(S+1) - 13]C_{ij}^2 D_{ij}^2 - 14[4S(S+1) - 3]C_{ij} D_{ij}^3$$
$$+ 7[3S(S+1) - 1]D_{ij}^4 \} \qquad (6.100)$$

and for the $\Delta M_S = 2$ resonance at $\nu = 2g\beta H/\hbar$

$$\langle \nu^2 \rangle = \frac{8}{3Nh^2} S(S+1) \sum_{i<j} [2C_{ij}^2 + D_{ij}^2], \tag{6.101}$$

$$\langle \nu^4 \rangle = \frac{16}{9Nh^4} S^2(S+1)^2 \sum_{i \neq j \neq k} \{18C_{ij}^2 C_{jk}^2 - 8C_{ij}C_{jk}C_{ki}D_{ij} + 7C_{ij}^2 D_{ik}^2$$

$$+ C_{ij}^2 D_{ik}D_{jk} + 2D_{ij}^2 D_{ik}^2\} + \frac{16}{105Nh^4} S(S+1)$$

$$\times \sum_{i<j} \{8[26S(S+1) - 17]C_{ij}^4 + [452S(S+1) - 309]C_{ij}^2 D_{ij}^2$$

$$+ 14[3S(S+1) - 1]D_{ij}^4\}. \tag{6.102}$$

These expressions are considerably simplified if the exchange interaction can be neglected for then $D_{ij} = -4C_{ij}$. The exchange interaction is a short-range interaction and will probably be unimportant in a dilute crystal.

It is noted from the expressions given above that the exchange contributes to both the second and fourth moments. This is in contrast to a photon induced absorption line where it is well known that the exchange interaction does not contribute to the second moment but only to the fourth, giving rise to the phenomenon of exchange narrowing. The difference between the widths of the two absorption lines arises because, in the photon case, the coupling of the electromagnetic field to the spin is linear in the spin components of the paramagnetic ion whereas in the present case the interaction is quadratic in the spin components.

In a dilute crystal not every site is occupied by a paramagnetic ion so the lattice sums should have been restricted to the occupied sites only. KITTEL and ABRAHAMS [1953] have shown that if the available sites are randomly occupied then the sums over all lattice sites can be retained if $\Sigma'_{ij} C_{ij}^2$ and $\Sigma'_{ijk} C_{ij}^2 C_{jk}^2$ are replaced by $fN\Sigma'_j C_{ij}^2$ and $f^2N\Sigma'_{jk} C_{ij}^2 C_{jk}^2$ and so on. f is the probability that a given site is occupied and the prime on the summations means that the indices must not be equal.

If the specimen contains more than one species of paramagnetic ion the broadening of the resonances of one species by the interaction with the other can be calculated in a similar way. The interaction between the ions is

$$H' = \sum_{i<\mu} D_{i\mu} S_i^z S_\mu'^z. \tag{6.103}$$

This is the truncated Hamiltonian containing only those terms which commute with the Zeeman interaction. The prime refers to the spins not on resonance and the unprimed spins are the ones at resonance responsible for the transition being observed. The quantity $D_{i\mu}$ is

given by

$$D_{i\nu} = J_{i\nu} + \frac{gg'\beta^2}{R_{i\nu}^3}(1 - 3\cos^2\theta_{i\nu}). \qquad (6.104)$$

In this case the contributions to the second and fourth moments of the $\Delta M_s = 1$ resonance line are, GUERMEUR *et al.* [1965a],

$$\langle\nu^2\rangle = \frac{S'(S'+1)}{3N'h^2}\sum_{i\nu}D_{i\nu}^2,$$

$$\langle\nu^4\rangle = \frac{S'(S'+1)}{15N'h^4}[3S'(S'+1)-1]\sum_{i\nu}D_{i\nu}^4 + \frac{S'^2(S'+1)^2}{9N'h^4}$$

$$\times\sum_{i,p<q}[6D_{i\nu}^2D_{iq}^2 + 8C_{pq}^2(D_{i\nu}-D_{iq})^2] + \frac{S(S+1)S'(S'+1)}{9Nh^4}$$

$$\times\sum_{p,i<j}[(D_{i\nu}^2+D_{j\nu}^2)(6D_{ij}^2+80C_{ij}^2)+24C_{ij}^2(D_{i\nu}-D_{j\nu})^2]. \quad (6.105)$$

In these expressions the indices i,j refer to the spins on resonance and p, q to the other species of spins. The factor C_{pq} is defined similarly to C_{ij}

$$C_{pq} = \tfrac{1}{2}J_{pq} - \frac{1}{4}\frac{g'^2\beta^2}{R_{pq}^3}(1-3\cos^2\theta_{pq}). \qquad (6.106)$$

For the $\Delta M_s = 2$ resonance line the corresponding quantities for the second and fourth moments are

$$\langle\nu^2\rangle = \frac{S'(S'+1)}{3N'h^2}\sum_{i\nu}4D_{i\nu}^2,$$

$$\langle\nu^4\rangle = \frac{S'(S'+1)}{15N'h^4}[3S'(S'+1)-1]\sum_{i\nu}16D_{i\nu}^4 + \frac{S'^2(S'+1)^2}{9N'h^4}$$

$$\times\sum_{i,p<q}[96D_{i\nu}^2D_{iq}^2 + 32C_{pq}^2(D_{i\nu}-D_{iq})^2] + \frac{S(S+1)(S'+1)S'}{9N'h^4}$$

$$\times\sum_{p,i<j}[96(D_{i\nu}^2+D_{j\nu}^2)(2C_{ij}^2+D_{ij}^2)-48C_{ij}^2(D_{i\nu}-D_{j\nu})^2]. \quad (6.107)$$

In dilute systems where the spins S' do not occupy all the available remaining sites the same modifications to these expressions have to be made as discussed in the text above eq. (6.103).

The case of paramagnetic ions with spin $\frac{1}{2}$ will now be considered. Experimentally these are less easily detected because they are weakly coupled to the lattice and give a much smaller a.p.r. absorption. From the discussion following eq. (6.102) it is expected that because the coupling is linear in the spin components, the line-shape of the phonon

and photon induced lines will be the same. The moments are thus those derived by VAN VLECK [1948] for the photon induced resonance line.

$$\langle \nu^2 \rangle = \frac{1}{4Nh^2} \sum_{i \neq j} (D_{ij} - 2C_{ij})^2 + \frac{S'(S'+1)}{3N'h^2} \sum_{ip} D_{ip}^2,$$

$$\langle \nu^4 \rangle = \frac{1}{16Nh^4} \sum_{i \neq j \neq k} \{ 80C_{ij}^2 C_{ik}^2 - 32C_{ij}C_{ik}C_{jk}D_{ij}$$

$$+ 24C_{ik}^2 D_{ij}^2 + 3D_{ij}^2 D_{ik}^2 - 32C_{ij}^2 C_{ik}C_{jk} - 96C_{ik}^2 C_{ij}D_{ij}$$

$$+ 32C_{ik}^2 C_{ij}D_{jk} + 8C_{ik}C_{jk}D_{ij}^2 + 24C_{ik}C_{jk}D_{ik}D_{jk}$$

$$+ 16C_{ik}C_{jk}D_{ik}D_{ij} - 8C_{ij}D_{ij}D_{ik}D_{jk} - 16C_{ij}D_{ij}D_{ik}^2 \}$$

$$+ \frac{1}{8Nh^4} \sum_{i<j} \{ 16C_{ij}^4 + 24C_{ij}^2 D_{ij}^2 + D_{ij}^4 - 32C_{ij}^3 D_{ij} - 8C_{ij}D_{ij}^3 \}$$

$$+ \frac{S'(S'+1)[3S'(S'+1) - 1]}{15Nh^4} \sum_{ip} D_{ip}^4$$

$$+ \frac{S'^2(S'+1)^2}{9Nh^4} \sum_{ip<q} \{ 6D_{ip}^2 D_{iq}^2 + 8C_{pq}^2 (D_{ip} - D_{iq})^2 \}$$

$$+ \frac{S(S+1)S'(S'+1)}{9Nh^4} \sum_{pi<j} \{ 6(D_{ip}^2 + D_{jp}^2)(D_{ij} - 2C_{ij})^2$$

$$+ 64C_{ij}(D_{ij} - C_{ij})(D_{ip} - D_{jp})^2 \}. \qquad (6.108)$$

There is however one aspect that has not been accounted for, the fact that the wavelength of the ultrasonic waves can be quite short ($\sim$ 5000 Å). The coupling of the excitation to a particular spin, say the mth, involves the factor exp $(iq \cdot R_m)$ where R_m is the position vector of that spin. For electromagnetic radiation it is sufficient to replace this factor by unity, but in the case of ultrasonics, where the velocity is only $\sim 10^5$ cm/sec the approximation is no longer valid. Allowance for this fact has been made by STEVENS and TUCKER [1965] who gave expressions for the second and fourth moments. They considered just one type of spin and found that the second moment became

$$\langle \nu^2 \rangle = \frac{1}{4Nh^2} \sum_{i \neq j} \{ 4C_{ij}^2 - 4C_{ij}D_{ij} \cos q \cdot (R_i - R_j) + D_{ij}^2 \}. \quad (6.109)$$

The fourth moment was similarly modified, all terms except the first four in the first summation and the first three in the second summation of eq. (6.108) being multiplied by cos $[q \cdot (R_i - R_j)]$. The exchange interaction now contributes to the second moment as well as to the fourth, but more significantly the dependences on the magnitude and directions of the magnetic field will be altered. STONEHAM [1966b] has considered the problem further and shows that the moments are altered

by the appearance of weak satellite lines. These lines have not been observed directly using ultrasonics but he cites evidence for their existence from spin-lattice relaxation measurements.

As mentioned at the beginning of this section, the calculations quoted above all assume the high temperature approximation in which the Boltzmann factors are replaced by unity. The temperature dependence of the a.p.r. line-shape has been investigated by ALIEV[1967] who has calculated the first and second moments due to dipolar and isotropic exchange interactions. The dependence of the line-shape on temperature has also been investigated by PIROZHKOV and CHERNOV[1967] who have calculated the first two moments due to dipole–dipole and quadrupole–quadrupole interactions for the cases $S = 1$ and $S = \frac{3}{2}$.

Finally to conclude this account of a.p.r. line-widths due to dipolar and exchange interactions between the spins, the relationship between the line-width and the second and fourth moments of the line will be quoted. It is customary to introduce a half-width for the line defined by $\delta = \nu_{1/2} - \nu_0$ where ν_0 and $\nu_{1/2}$ are the frequencies corresponding to the points of maximum and half-maximum absorption. For a Gaussian line-shape, that is one for which

$$g(\nu) = (\sigma/\pi)^{1/2} \exp \left[-\sigma (\nu - \nu_0)^2 \right],$$

it can be shown that the following two relations hold.

$$\delta = [2\langle \nu^2 \rangle \log_e 2]^{1/2} \quad \text{and} \quad \langle \nu^4 \rangle = 3 \langle \nu^2 \rangle^2.$$

KITTEL and ABRAHAMS[1953] showed that a Gaussian e.p.r. line is expected for a concentrated paramagnetic specimen whose exchange effects are negligible but for concentrations of less than about 1% the line is better described by a cut-off Lorentzian. This has the form

$$g(\nu) = \{ \pi\delta [1 + (\nu - \nu_0)^2/\delta^2] \}^{-1}$$

for $(\nu_0 - \alpha) < \nu < (\nu_0 + \alpha)$ and is zero outside this range. Provided $\alpha \gg \delta$ it is found that for this line-shape $\langle \nu^2 \rangle = 2\alpha\delta/\pi$ and $\langle \nu^4 \rangle = 2\alpha^3\delta/3\pi$ so that the half-width δ is given by

$$\delta = \pi \left[\frac{1}{12} \frac{\langle \nu^2 \rangle^3}{\langle \nu^4 \rangle} \right]^{1/2}.$$

6.3. Broadening due to spin–phonon interactions

The final mechanism to be discussed is the broadening of the resonance lines arising from spin–phonon interactions. This has been treated in the case of dilute paramagnetic systems by MOROCHA[1967] and the extension to the case of concentrated systems has been given by FIDLER and TUCKER[1970]. In both cases a Green function theory is used to

calculate the line–shape function which enters the expression for the ultrasonic attenuation coefficient. In the work of Morocha the line-shape function depended only on the lifetime associated with a single ion. In concentrated paramagnetic materials ion–ion interaction through the phonon field produces additional contributions to the relaxation times and hence to the line-shape function in the coefficient of sound absorption. An expression was given by Fidler and Tucker for the absorption coefficient in the case of a paramagnetic ion of spin $\frac{1}{2}$ in a field of octahedral symmetry. The lifetime entering the expression was the same as that obtained by ELLIOTT and PARKINSON [1967] in their study of the magnetic field dependence of the thermal conductivity arising from strong spin–phonon coupling, see §5.3. Ultrasonic measurements may therefore be of help in testing this theory.

7. The phonon maser and double quantum detector

Two phenomena closely related to acoustic paramagnetic resonance are the phonon maser and the ultrasonic double quantum detector.

7.1. *The phonon maser*

The possibility of the production of phonons by maser action in a paramagnetic crystal was suggested by KITTEL [1961] and subsequently TUCKER [1961b, 1964] demonstrated amplification of an ultrasonic wave and then oscillation producing a beam of phonons. The material used was ruby, which consists of trivalent chromium ions doped into aluminium oxide. The low-lying energy levels of Cr^{3+} in ruby are two Kramers doublets separated, in zero magnetic field, by about 0.386 cm^{-1}. If a magnetic field is applied the doublets split and it is found that for a magnetic field orientation of 55° 44' to the c-axis (the trigonal axis) of the ruby, the splitting is such that the separation between the first and third energy levels is equal to that between the second and fourth. The levels are assumed to be labelled in order of decreasing energy. A pump frequency of 24 GHz can be used to saturate these transitions and maser action can occur due to the inversion of the populations between levels two and three. It is also found that with this orientation of the magnetic field there is a strong interaction between longitudinal ultrasonic waves along the c-axis and the spins responsible for the 2–3 transition. Thus amplification can occur. An increased pump power gives oscillation and an ultrasonic output can be detected in the absence of an ultrasonic input. This occurs when amplification due to stimulated emission has become greater than the losses due to the natural non-paramagnetic attenuation in the ruby – the transmission of

energy into the surrounding liquid helium and into the quartz transducer used as the detector.

The experimental apparatus is shown in fig. 6.8 taken from TUCKER's [1964] account. In his first experiments Tucker achieved a gain of about 10% per centimetre of path in pink ruby using a pump power of about 40 mW. The quartz transducer was a long non-resonant rod bonded to the ruby with indium. The maser oscillator used a thin resonant quartz transducer bonded to the ruby with grease and the improved performance enabled oscillations to be observed with an output electromagnetic power of about 10^{-11} W which corresponds to about 10^{-7} W of ultrasonic power incident on the transducer.

Wave guides

Silver plated
fused quartz
as maser pump
cavity

Ultrasonic
drive cavity
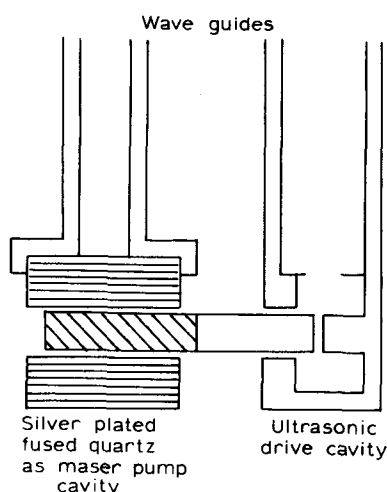
Fig. 6.8. Phonon maser apparatus of Tucker. The ruby maser is in a quartz pump cavity and is also bonded to a quartz ultrasonic transducer.

7.2. The double quantum detector

The double quantum detector was demonstrated by SHIREN [1961] and uses the three-level system of Fe^{2+} in MgO which has an effective spin of one. The diagram, fig. 6.9, shows the three levels of the Fe^{2+} ion when a magnetic field is applied. Four transitions can occur between these levels to give three resonances. The transitions between 1 and 2 or between 2 and 3 which occur at the same frequency ν_{12} give the $\Delta M_S = 1$ resonance in the language of effective spins. At twice this frequency, ν_{13}, the $\Delta M_S = 2$ transition can take place between the levels 1 and 3. Another resonance can also be observed between the levels 1 and 3 corresponding to the absorption of two quanta each with energy equal to the energy of the $\Delta M_S = 1$ transition. These three
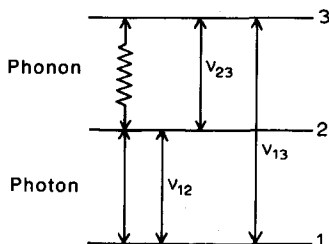
Fig. 6.9. Lowest three levels of Fe^{2+} in magnesium oxide used as a double quantum detector.

resonances can all be observed in a.p.r. and in e.p.r. experiments. The single quantum lines are broad due to the presence of strains while the double quantum line is a very narrow one superimposed on the $\Delta M_S = 1$ line at ν_{12}.

If a specimen of Fe^{2+} doped MgO is bonded to a quartz transducer for an ultrasonic experiment and is at the same time placed in a microwave resonant cavity of an e.p.r. spectrometer it is possible to observe a double quantum resonance corresponding to the simultaneous absorption of a phonon and a photon. This of course can only occur in the simultaneous presence of both electromagnetic and ultrasonic power. Thus if the e.p.r. spectrometer is operated continuously and the ultrasonic waves are pulsed an increased absorption will be observed in the e.p.r. spectrometer due to double quantum transitions when each ultrasonic pulse arrives.

The results achieved by SHIREN [1961] showed that the sensitivity was less than that obtained using a piezoelectric transducer but the output signal did not depend on the relative phase of the ultrasonic wave across the face of the specimen.

8. Experimental results

A short summary is now given of some of the experimental results and the spin–lattice coupling coefficients that have been obtained.

The results of experiments on the iron-group transition metals are given in table 6.5 with the exception of results on the Cr^{2+} ion which cannot be easily summarised in a table. This is one of the ions which gives a strong a.p.r. absorption but no e.p.r. signal because the transitions are forbidden for electromagnetic excitation but not for excitation by ultrasonic waves. The ion is subject to a dynamic Jahn-Teller effect and is very strongly coupled to the lattice (see FLETCHER et al. [1966], MARSHALL and RAMPTON [1968], GUERMEUR et al. [1967] and ANDERSON et al. [1970]). The isoelectronic ion Mn^{3+} has also been

TABLE 6.5

Acoustic paramagnetic resonance results from iron group ions

(Units: cm^{-1} per unit strain) Magnesium oxide host		
	$|G_{11}|$	$|G_{44}|$
Cr^{3+}	1.3	6.5
Fe^{3+}	5.0	0.65
a) Mn^{2+}	1.4	0.28
Fe^{2+}	650	380
Ni^{2+}	57	50
	$|G_{11}-G_{12}|$	$|G_{66}|$
b) V^{3+}	$\geqslant 1000$	$\leqslant 30$ spectrum had tetragonal symmetry.
Potassium magnesium fluoride host		
	$|G_{11}|$	$|G_{44}|$
c) Ni^{2+}	58	39
Aluminium oxide (corundum) host		
	$|G_{14}|$	$|G_{33}|$
d) Cr^{3+}	1.56	5.86

a) SHIREN [1962a].
b) BRABIN-SMITH and RAMPTON [1969].
c) ROSENBERG and WIGMORE [1967].
d) DOBROV [1964].

TABLE 6.6

Acoustic paramagnetic resonance results from rare earth ions

a) Eu^{2+} in calcium fluoride: $|G_{44}| \doteq 0.3$ cm^{-1} per unit strain
b) Dy^{3+} in calcium fluoride has been observed to give strong acoustic attenuation but no coupling coefficient given.
c) Pr^{3+} in calcium fluoride has been observed to give strong acoustic attenuation, no coupling coefficient given.

a) DOBROV [1964].
b) DOBROV [1966].
c) WETSEL et al. [1969].

observed in a.p.r. with results that are similar to Cr^{2+}, LOCATELLI et al. [1970].

There are fewer results available in table 6.6 for the rare-earth ions, most are from DOBROV [1966] who only found resonances from Eu^{2+} and Dy^{3+} in calcium fluoride. He did not observe a resonance from Pr^{3+} in calcium fluoride although WETSEL et al. [1969] have done so under apparently very similar conditions. This is another resonance that is much stronger in a.p.r. and was first found in this way although Wetsel et al. subsequently detected the weak e.p.r. signal.

ULTRASONIC WAVES IN SEMICONDUCTORS

1. Introduction

In chs. 4–6 the interaction of ultrasonic waves in insulating media was treated, a situation where the conductivity arising from the electron motion could be ignored. In this and the following chapter, the behaviour of ultrasonic waves in semiconductors and metals will be examined. In these cases the most interesting effects stem from the interaction of the wave with the moving carriers that are responsible for electronic conduction in the material. The extent to which the interaction with these carriers is important depends upon both the ultrasonic frequency and the mobility and number of the carriers. This interaction of acoustic phonons with conduction electrons has been of considerable interest for some time since it is this interaction which is responsible for the major part of the electrical resistance in a normal metal. In most semiconductors it is also the major mechanism whereby electrons are scattered in at least some range of temperature. The electron–phonon interaction can arise from a variety of sources, the relative importance of which depends on the type of material under consideration. The main types of coupling are electromagnetic coupling, deformation potential coupling, piezoelectric coupling and magnetoelastic coupling. This chapter will deal exclusively with semiconductors, in particular those which exhibit piezoelectricity. That these materials are of prime importance is clear from ch. 3 where it is shown that some of them, for example CdS, provide means whereby ultrasonic waves can be both generated and detected. The number of ultrasonic experiments performed in the gigahertz frequency range on metals is very much smaller and a discussion of these experiments will be deferred until a later chapter.

In piezoelectric materials ultrasonic waves are accompanied by electromagnetic waves and vice versa. The plane waves that propagate have to satisfy both the mechanical–piezoelectric equations of state and Maxwell's equations. It is shown in the next section that the prob-

lem reduces to solving a five-by-five secular determinant, the solutions of which correspond to two transverse electromagnetic waves and three acoustic waves. As far as the acoustic waves are concerned it is shown that the main effect is a modification of the effective elastic constants of the crystal which leads to a change in velocity of the waves. When the crystal is also semiconducting, attenuation and dispersion of the stress waves are found to occur due to their interactions with the space charges set up by the internal electric fields. The attenuation of the wave arises because energy is transferred between the wave and the carriers. As the carriers cannot completely follow the wave this energy is lost from it. It will be seen in §2.3.2 that under certain conditions the reverse situation can occur and the carriers can be made to give up their energy to the wave, thereby amplifying it.

In non-piezoelectric semiconductors an acoustic wave is also coupled to the charged carriers but this time the coupling occurs primarily through the deformation potential, see §3.1. Again attenuation will occur but the magnitude of the effect is by no means as large as that possible due to piezoelectric fields at frequencies currently used in ultrasonic experiments. For this reason attention will be centred on piezoelectric semiconductors. If piezoelectric semiconductors are to exhibit these properties, their conductivity must be small or the ultrasonic frequency high. This is essential because there must not be time for the carriers to redistribute themselves to create an electric field in opposition to the piezoelectric field.

In ch. 4 where the interaction of ultrasonic waves with thermal phonons was treated it was found convenient to formulate the problem in two parts depending upon the relative magnitude of the ultrasonic wavelength and the mean free path of the thermal phonons with which it interacted. Here a similar division of the problem is appropriate, the important parameter this time being the relative magnitude of the acoustic wavelength, $(\lambda = 2\pi/q)$, and the mean free path l of the carriers.

In the regime $ql \ll 1$ a macroscopic theory can be developed in which the acoustic wave is treated as a classical perturbation which perturbs the carrier distribution. This philosophy is similar to that of the low frequency regime of ch. 4. The problem reduces to a simultaneous solution of the piezoelectric equations together with Poisson's equation and the continuity equation governing the distribution of carrier charges. In the other limiting regime, $ql \gg 1$, the problem is formulated in terms of individual interactions brought about by the electron–phonon interaction. The treatment is analogous to the high frequency region described in ch. 4, the electron–phonon interaction replacing the role of the anharmonic terms in the potential energy expansion which lead to the phonon–phonon collisions.

2. Phenomenological theory

As was stated in the introduction, from the point of view of performing ultrasonic experiments interest is primarily in those materials which in addition to being semiconductors also exhibit piezoelectricity. This section therefore commences with a discussion of wave propagation in piezoelectric materials. In a piezoelectric material pure elastic wave propagation is not strictly possible because the piezoelectric equations of state couple the elastic displacement variables to those of the electromagnetic field. The dispersion relation governing plane wave propagation in such a material is obtained by solving simultaneously the piezoelectric equations with Maxwell's equations of electromagnetism. The resulting solutions will be coupled electromagnetic–elastic waves. This programme is carried out in §2.1 for a material having a constant conductivity and it is found that some solutions exist which to all intents and purposes correspond to pure elastic wave propagation but with wave velocities modified slightly from that which would occur in the absence of piezoelectricity. The theory is then extended in §2.2 to semiconductors, materials where the assumption of a constant conductivity is inappropriate.

2.1. *Wave propagation in a piezoelectric material having a constant conductivity*

The equations of state governing a piezoelectric material written in the form where the strain, the electric field and the temperature are the independent variables can be obtained from table 2.4. They are

$$
\begin{aligned}
\sigma_{ij} &= c_{ijkl}^{ET}\epsilon_{kl} - e_{kij}^{T}E_k - \lambda_{ij}^{E}\Delta T, \\
D_i &= e_{ikl}^{T}\epsilon_{kl} + \kappa_{ik}^{\epsilon T}E_k + p_i^{\epsilon}\Delta T, \\
\Delta S &= \lambda_{kl}^{E}\epsilon_{kl} + p_k^{\epsilon}E_k + (C^{\epsilon E}/T)\Delta T.
\end{aligned}
\tag{7.1}
$$

As pointed out in ch. 2§2 there can also be magnetic field variables in these equations. However for piezoelectric materials one is primarily concerned with the presence of electric rather than magnetic fields so the dependence of the equations on these variables will be dropped. As the waves are expected to propagate adiabatically ΔS may be equated to zero and the value of ΔT thereby obtained substituted into the other two piezoelectric equations. The result may be expressed in the form

$$
\begin{aligned}
\sigma_{ij} &= c_{ijkl}^{ES}\epsilon_{kl} - e_{kij}^{S}E_k, \\
D_i &= e_{ikl}^{S}\epsilon_{kl} + \kappa_{ik}^{\epsilon S}E_k,
\end{aligned}
\tag{7.2}
$$

where the coefficients are now the adiabatic coefficients of table 2.8. These piezoelectric equations of state have to be solved simultaneously

with the Maxwell's equations of electromagnetic theory, namely

$$\text{curl } H = \frac{\partial D}{\partial t} + J \tag{7.3}$$

$$\text{curl } E = -\frac{\partial}{\partial t} B \tag{7.4}$$

$$\nabla \cdot B = 0 \tag{7.5}$$

$$\nabla \cdot D = Q \tag{7.6}$$

Provided the piezoelectric material exhibits no appreciable piezomagnetic or pyromagnetic effect the magnetic induction can be related directly to the magnetic field through the permeability tensor

$$B_i = \mu_{ij} H_j. \tag{7.7}$$

In addition, the constitutive equation

$$J_i = b_{ji} E_j \tag{7.8}$$

will be required relating the current J to the electric field through the conductivity tensor. In all the equations above the indices i, j, k, l take values 1 to 3.

It will now be assumed that a set of axes is chosen such that x_1 coincides with the direction of the plane wave propagation in which we are interested. The partial derivatives $\partial/\partial x_2$, $\partial/\partial x_3$ of any field quantity will then, by definition, be zero. With this choice of coordinate axes, and remembering that $\epsilon_{ij} = \frac{1}{2}(\partial u_i/\partial x_j + \partial u_j/\partial x_i)$, the above piezoelectric equations can be written as follows

$$\sigma_{1j} = c_{1j1l} \frac{\partial u_l}{\partial x_1} - e_{k1j} E_k, \tag{7.9}$$

$$D_i = e_{i1l} \frac{\partial u_l}{\partial x_1} + \kappa_{ik} E_k. \tag{7.10}$$

From here on the superscripts on the coefficients will be dropped for ease of presentation. For spatial variations restricted to the x_1-direction the Maxwell relation, eq. (7.4), gives

$$\dot{B}_1 = 0. \tag{7.11}$$

Also, by taking the partial derivative with respect to x_1 of this Maxwell relation and substituting for the components of B from the constitutive relation, eq. (7.7), it follows that

$$\frac{\partial^2 E_2}{\partial x_1^2} = -\left[\mu_{32}' \frac{\partial \dot{H}_2}{\partial x_1} + \mu_{33}' \frac{\partial \dot{H}_3}{\partial x_1} \right] \tag{7.12}$$

and

$$\frac{\partial^2 E_3}{\partial x_1^2} = + \left[\mu_{22}' \frac{\partial \dot{H}_2}{\partial x_1} + \mu_{23}' \frac{\partial \dot{H}_3}{\partial x_1} \right] \tag{7.13}$$

where the dot signifies partial differentiation with respect to time and the components of μ' are defined by

$$\mu_{ij}' = \mu_{ij} - \mu_{i1}\mu_{1j}/\mu_{11}. \tag{7.14}$$

To eliminate the components of H another Maxwell relation, eq. (7.3), may be used. For the x-component equation this gives immediately

$$\dot{D}_1 + J_1 = 0 \tag{7.15}$$

and by taking the partial time-derivative of the other two component equations it follows upon substitution into eqs. (7.12) and (7.13) that

$$\frac{\partial^2 E_2}{\partial x_1^2} = - [\, \mu_{32}'(\ddot{D}_2 + \dot{J}_3) - \mu_{33}'(\ddot{D}_2 + \dot{J}_2)\,], \tag{7.16}$$

$$\frac{\partial^2 E_3}{\partial x_1^2} = + [\, \mu_{22}'(\ddot{D}_3 + \dot{J}_3) - \mu_{23}'(\ddot{D}_2 + \dot{J}_2)\,]. \tag{7.17}$$

The electric displacement components and the components of current density can now be eliminated by expressing them with the aid of the piezoelectric equation, eq. (7.10), and the constitutive relation, eq. (7.8) in terms of the elastic displacement and the electric field components. The necessary relations are

$$\ddot{D}_2 + \dot{J}_2 = e_{21l} \frac{\partial \ddot{u}_l}{\partial x_1} + \kappa_{2k}\ddot{E}_k + b_{j2}\dot{E}_j, \tag{7.18}$$

$$\ddot{D}_3 + \dot{J}_3 = e_{31l} \frac{\partial \ddot{u}_l}{\partial x_1} + \kappa_{3k}\ddot{E}_k + b_{j3}\dot{E}_j. \tag{7.19}$$

By plane-wave propagation along the x_1-direction it is meant that the components of u and E vary periodically according to

$$u_i = u_i^0 \exp\, [\mathrm{i}(\omega t - qx_1)],$$
$$E_i = E_i^0 \exp\, [\mathrm{i}(\omega t - qx_1)]. \tag{7.20}$$

For wave propagation of this type it follows from eqs. (7.15), (7.10) and (7.8) that

$$E_1 = \frac{\mathrm{i}qe_{11l}u_l - (\kappa_{1p} - \mathrm{i}b_{p1}/\omega)\,E_p}{\kappa_{11} - \mathrm{i}b_{11}/\omega} \tag{7.21}$$

where the suffix p takes only the values 2 and 3. In addition, the first

piezoelectric equation of state together with the force equation, see
eq. (2.6)

$$\rho\left(\frac{\partial^2 u_i}{\partial t^2}\right) = \frac{\partial \sigma_{ij}}{\partial x_j} \tag{7.22}$$

gives after the elimination of E_1

$$\rho\omega^2 u_i = q^2 c'_{1i1l} u_l - iq e'_{p1i} E_p \tag{7.23}$$

where

$$c'_{1i1l} = c_{1i1l} + \frac{e_{11i}e_{11l}}{\kappa_{11} - ib_{11}/\omega} \tag{7.24}$$

and

$$e'_{p1i} = e_{p1i} - \frac{e_{11i}(\kappa_{1p} - ib_{p1}/\omega)}{\kappa_{11} - ib_{11}/\omega}. \tag{7.25}$$

Furthermore the elimination of E_1 from eqs. (7.18) and (7.19) gives,
after substitution into eqs. (7.16) and (7.17)

$$q^2 E_2 = \mu'_{32}[iq\omega^2 e''_{31l}u_l - \omega^2 \kappa'_{3p}E_p] - \mu'_{33}[iq\omega^2 e''_{21l}u_l - \omega^2 \kappa'_{2p}E_p] \tag{7.26}$$

$$q^2 E_3 = -\mu'_{22}[iq\omega^2 e''_{31l}u_l - \omega^2 \kappa'_{3p}E_p] + \mu'_{23}[iq\omega^2 e''_{21l}u_l - \omega^2 \kappa'_{2p}E_p] \tag{7.27}$$

where

$$e''_{p1l} = e_{p1l} - \frac{e_{11l}(\kappa_{p1} - ib_{1p}/\omega)}{\kappa_{11} - ib_{11}/\omega} \tag{7.28}$$

$$\kappa'_{qp} = (\kappa_{qp} - ib_{pq}/\omega) - \frac{(\kappa_{q1} - ib_{1q}/\omega)(\kappa_{1p} - ib_{p1}/\omega)}{\kappa_{11} - ib_{11}/\omega}. \tag{7.29}$$

The problem thus reduces to solving the five coupled equations con-
tained in eqs. (7.23), (7.26) and (7.27) representing the propagation of
coupled electromagnetic and ultrasonic waves. These coupled equa-
tions contain the three components of the elastic displacement vector
and the two transverse components of the electromagnetic field. By
equating to zero the five-by-five determinant formed from the coeffi-
cients of these quantities, the dispersion relation connecting the fre-
quency ω and the wave vector q can be found. If the piezoelectric con-
stants are zero the determinant equation naturally factorizes to give
five solutions three of which correspond to pure acoustic wave propa-
gation and two to the propagation of pure transverse electromagnetic
waves. The problem is very similar to that of ch. 5§2.2 where magneto-
elastic wave propagation was treated. There it was the transverse
magnetization vectors which entered the equations rather than the

electric field components. The determinant equation in the present case is

$$
\begin{vmatrix}
(q^2c'_{1111}-\rho\omega^2) & q^2c'_{1112} & q^2c'_{1113} & \vdots & -iqe'_{211} & -iqe'_{311} \\
q^2c'_{1211} & (q^2c'_{1212}-\rho\omega^2) & q^2c'_{1213} & \vdots & -iqe'_{212} & -iqe'_{312} \\
q^2c'_{1311} & q^2c'_{1312} & (q^2c'_{1313}-\rho\omega^2) & \vdots & -iqe'_{213} & -iqe'_{313} \\
\hdashline
iq\omega^2a_{41} & iq\omega^2a_{42} & iq\omega^2a_{43} & (\omega^2a_{44}-q^2) & \omega^2a_{45} \\
iq\omega^2a_{51} & iq\omega^2a_{52} & iq\omega^2a_{53} & \omega^2a_{54} & (\omega^2a_{55}-q^2)
\end{vmatrix} \equiv 0
$$

(7.30)

where

$$
\begin{aligned}
a_{41} &= \mu'_{32}e''_{311} - \mu'_{33}e''_{211}; & a_{51} &= \mu'_{23}e''_{211} - \mu'_{22}e''_{311}, \\
a_{42} &= \mu'_{32}e''_{312} - \mu'_{33}e''_{212}; & a_{52} &= \mu'_{23}e''_{212} - \mu'_{22}e''_{312}, \\
a_{43} &= \mu'_{32}e''_{313} - \mu'_{33}e''_{213}; & a_{53} &= \mu'_{23}e''_{213} - \mu'_{22}e''_{313}, \\
a_{44} &= \mu'_{33}\kappa'_{22} - \mu'_{32}\kappa'_{32}; & a_{54} &= \mu'_{22}\kappa'_{32} - \mu'_{23}\kappa'_{22}, \\
a_{45} &= \mu'_{33}\kappa'_{23} - \mu'_{32}\kappa'_{33}; & a_{55} &= \mu'_{22}\kappa'_{33} - \mu'_{23}\kappa'_{23}.
\end{aligned}
$$

(7.31)

If the permeability tensor is taken to be isotropic so that $\mu_{11} = \mu_{22} = \mu_{33} = \mu$ and the off-diagonal components are zero, then this determinant equation reduces to that given by HUTSON and WHITE[1962] which was based on the earlier work of KYAME[1954]. In their paper Hutson and White showed that as far as acoustic wave propagation is concerned it is a very good approximation to solve just the 3×3 sub-determinant enclosed by the dotted line in the top left-hand corner of eq. (7.30). This sub-determinant is similar to that which would occur for the pure elastic problem in the absence of piezoelectric coupling if the c's are regarded as modified elastic constants. The modified elastic constants introduce terms in the solution of $(\omega/q)^2$ of the order of $\bar{e}^4/(\rho\bar{\kappa})^2$ where $\bar{e}$ and $\bar{\kappa}$ are some average values of the appropriate piezoelectric and permittivity constants. They showed that the result of considering the rest of the 5×5 determinant only gave corrections that were smaller by the square of the ratio of the velocity of sound to that of the electromagnetic wave.

2.2. *Wave propagation in extrinsic piezoelectric semiconductors*

It was seen in the last subsection that a plane wave propagating in a piezoelectric crystal was accompanied by a longitudinal electric field and that the coupling to the transverse electromagnetic waves could be neglected as far as the ultrasonic wave propagation was concerned. In that subsection a constant conductivity was assumed, the relationship between the current J and the electric field being given by the constitutive equation, eq. (7.8). In a semiconductor this relationship is

not appropriate since the number of carriers available for conduction can change. Because the coupling to the transverse electromagnetic waves may be neglected it is sufficient for the analysis to work with a one-dimensional problem. In this case eq. (7.2) reduces to

$$\sigma = c\epsilon - eE, \tag{7.32}$$

$$D = e\epsilon + \kappa E, \tag{7.33}$$

where all the tensor indices have been dropped, the coefficients now being regarded as scalar quantities. In the same way the force equation, eq. (7.22), and the Maxwell relation, eq. (7.6) become

$$\frac{\partial \sigma}{\partial x} = \rho \frac{\partial^2 u}{\partial t^2}, \tag{7.34}$$

$$\frac{\partial D}{\partial x} = -Q_e n'. \tag{7.35}$$

In the latter equation the space charge Q is written as $-n'Q_e$ where Q_e is the magnitude of the electronic charge. In an extrinsic semiconductor the relationship between the current density and the electric field is

$$J = Q_e \left[(n_0 + n')\mu_e E + \mathscr{D} \frac{\partial n'}{\partial x} \right] \tag{7.36}$$

where n' is the variation in the density of charge caused by the presence of the acoustic wave, n_0 is the unperturbed density, μ_e is the electronic mobility* and $\mathscr{D}$ is the diffusion constant. The sign of the charge has been chosen so that the equations refer to an n-type semiconductor. This equation for the current density has to be supplemented by the continuity equation expressing charge conservation

$$\frac{\partial J}{\partial x} = Q_e \frac{\partial n'}{\partial t}. \tag{7.37}$$

These equations will now be solved under the assumption that the electric and displacement fields have the following form

$$E = E_d + E_0 \exp[i(\omega t - qx)],$$
$$D = D_d + D_0 \exp[i(\omega t - qx)]. \tag{7.38}$$

The terms E_d and D_d have been added to account for the presence of any applied direct electric field. From the force, eq. (7.34), and eq. (7.32) it follows directly that

$$\rho \frac{\partial^2 u}{\partial t^2} = c \frac{\partial^2 u}{\partial x^2} - e \frac{\partial E}{\partial x}. \tag{7.39}$$

---

* μ_e and μ_v are reserved for the electronic and positive hole mobilities. They are not to be confused with μ which is the permeability tensor.

From the expression for the current density, eq. (7.36)

$$\frac{\partial J}{\partial x} = Q_e \left[n_0 \mu_e \frac{\partial E}{\partial x} + \mu_e \frac{\partial}{\partial x} (n'E) + \mathscr{D} \frac{\partial^2 n'}{\partial x^2} \right]. \tag{7.40}$$

In a *linear* theory this may be approximated by dropping terms involving the square of small quantities to

$$\frac{\partial J}{\partial x} \approx Q_e \left[n_0 \mu_e \frac{\partial E}{\partial x} + \mu_e E_d \frac{\partial n'}{\partial x} + \mathscr{D} \frac{\partial^2 n'}{\partial x^2} \right] \tag{7.41}$$

and by making use of the Maxwell condition, eq. (7.35) and the continuity equation, the following expression is obtained

$$\frac{\partial J}{\partial x} = -\frac{\partial^2 D}{\partial x \partial t} = n_0 Q_e \mu_e \frac{\partial E}{\partial x} - \mu_e E_d \frac{\partial^2 D}{\partial x^2} - \mathscr{D} \frac{\partial^3 D}{\partial x^3}. \tag{7.42}$$

Substitution of eq. (7.38) then gives an expression connecting the electric displacement with the electric field

$$\frac{\partial D}{\partial x} = \frac{i n_0 Q_e \mu_e}{\omega + q \mu_e E_d - i q^2 \mathscr{D}} \frac{\partial E}{\partial x} \tag{7.43}$$

and hence from eq. (7.33)

$$e \frac{\partial^2 u}{\partial x^2} = -\left[\kappa - \frac{i n_0 Q_e \mu_e}{\omega + q \mu_e E_d - i q^2 \mathscr{D}} \right] \frac{\partial E}{\partial x}. \tag{7.44}$$

Finally on substituting into eq. (7.39) an equation for the elastic displacement is obtained.

$$\rho \frac{\partial^2 u}{\partial t^2} = c \left[1 + \frac{e^2/c}{\kappa - i n_0 Q_e \mu_e/(\omega + q \mu_e E_d - i q^2 \mathscr{D})} \right] \frac{\partial^2 u}{\partial x^2}. \tag{7.45}$$

If the diffusion term and the applied field E_d are omitted the modified stiffness constant reduces to

$$c' = c + \frac{e^2}{\kappa - i b/\omega} \tag{7.46}$$

where a constant conductivity $b = n_0 Q_e \mu_e$ has been introduced. This should be compared with the result of eqs. (7.23) and (7.24).

Following HUTSON and WHITE[1962] and WHITE[1962] it will be found convenient to introduce a conductivity frequency $\omega_c = b/\kappa$ and a diffusion frequency $\omega_D = v^2/\mathscr{D}$, where v is the velocity ω/q. In addition they introduce a drift velocity $v_d = -\mu_e E_d$ due to the applied electric field and the parameter $\gamma = 1 - v_d/v$ which is a measure of the ratio of this electron drift velocity to the velocity of sound. That this parameter is of interest is clear if it is remembered that it enters the expression for the Doppler frequency shift of a source moving with velocity

v_d. Also it will be seen later that the physical importance of ω_D is that it determines the frequency above which the wavelength is short enough for the diffusion to smooth out the carrier density fluctuations having the periodicity of the acoustic wave. Because of dispersion ω/q is not a constant although it is found sufficient in ω_D and γ to replace it by v_0 the unperturbed sound velocity $(c/\rho)^{1/2}$. In this notation the modified elastic constant of eq. (7.45) is

$$c' = c\left[1 + \frac{e^2}{c\kappa}\frac{\gamma - i\omega/\omega_D}{\gamma - i(\omega_c/\omega + \omega/\omega_D)}\right]. \tag{7.47}$$

In this expression q has been replaced by ω/v_0. The alternating components of electric field, space charge and current can easily be related to the a.c. strain. From eq. (7.44)

$$E' = -\frac{e}{\kappa}\left[\frac{\gamma - i\omega/\omega_D}{\gamma - i(\omega_c/\omega + \omega/\omega_D)}\right]\epsilon' \tag{7.48}$$

and by eqs. (7.43) and (7.35)

$$n'Q_e = -\frac{b}{v}\frac{E'}{\gamma - i\omega/\omega_D} = \frac{\omega_c}{v}\frac{e\epsilon'}{\gamma - i(\omega_c/\omega + \omega/\omega_D)}. \tag{7.49}$$

Finally eq. (7.37) gives

$$J' = +\frac{bE'}{\gamma - i\omega/\omega_D} = -\omega_c\frac{e\epsilon'}{\gamma - i(\omega_c/\omega + \omega/\omega_D)}. \tag{7.50}$$

Interest lies in that solution of eq. (7.45) which represents a damped sinusoidal wave of definite frequency. That is, a solution of the form $u = u_0 \exp[i(\omega t - qx)]$ is sought where the wave vector q is now complex. If the coupling between the acoustic wave and the electrons is small it is possible to write q as

$$q = \frac{\omega}{v} - i\Gamma. \tag{7.51}$$

This is only meaningful if the attenuation constant is such that $|\Gamma| \ll \omega/v$. Direct substitution into eq. (7.45) gives, after equating the real and imaginary parts,

$$v = v_0\left\{1 + \frac{e^2}{2c\kappa}\frac{1 + \frac{1}{\gamma^2}\left(\frac{\omega_c}{\omega_D} + \frac{\omega^2}{\omega_D^2}\right)}{1 + \frac{1}{\gamma^2}\left(\frac{\omega_c}{\omega} + \frac{\omega}{\omega_D}\right)^2}\right\}, \tag{7.52}$$

$$\Gamma = \frac{e^2\omega_c}{2c\kappa\gamma v_0}\left[1 + \frac{1}{\gamma^2}\left(\frac{\omega_c}{\omega} + \frac{\omega}{\omega_D}\right)^2\right]^{-1}. \tag{7.53}$$

It has been assumed that $e^2/c\kappa$ is small.

2.3. *Acoustic dispersion and attenuation in a piezoelectric semi-conductor*

2.3.1. *In the absence of an external electromagnetic field.* In the absence of an applied electric field the drift velocity v_d is zero so that γ is unity. This was the situation treated by HUTSON and WHITE [1962]. It is seen from the equation above that the extent to which the acoustic wave will suffer dispersion and attenuation depends on the relative magnitudes of the frequency ω and the parameters ω_c and ω_D. Assuming that the actual velocity v is close to v_0 the loss in Np/rad is $\alpha = v_0 \Gamma / \omega$. A plot of this loss in units of $e^2/2c\kappa$ as a function of the dimensionless parameter ω/ω_c is shown in fig. 7.1 for several values of the ratio ω_D/ω_c. It is observed that the loss is greatest when ω_D/ω_c is large, that is when the diffusion constant is very small. In the limit of ω_D/ω_c becoming infinite the loss factor reaches a maximum of $0.5(e^2/2c\kappa)$ at the frequency ω equal to the conductivity frequency ω_c. When the effects of diffusion overwhelm those of conduction α decreases and its maximum value then occurs at a frequency much lower than ω_c. In fact it is readily found from eq. (7.53) that for $\omega_D \ll \omega_c$ the maximum value of α is $\frac{3}{16}(3\omega_D/\omega_c)^{1/2} e^2/2c\kappa$ and occurs around $\omega/\omega_c = (\omega_D/3\omega_c)^{1/2}$. Qualitatively the shape of the attenuation curves may be understood from
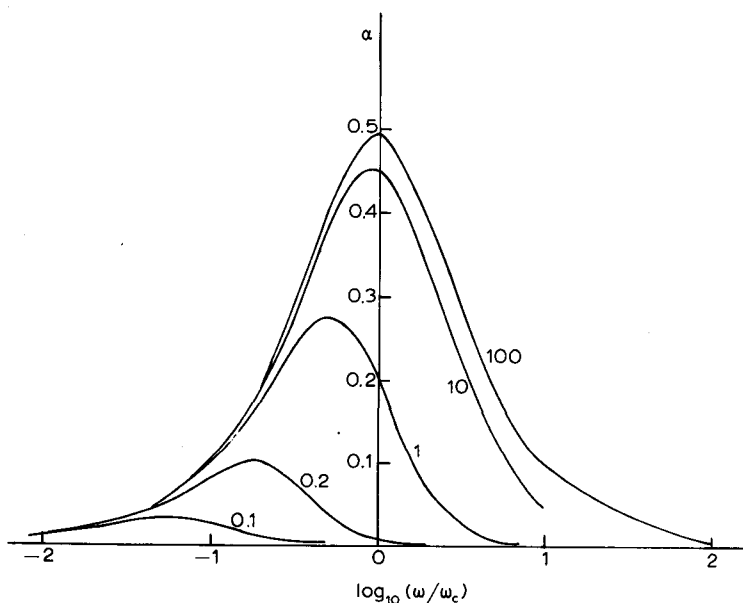
Fig. 7.1. Graph of α in units of $e^2/2c\kappa$ as a function of $\log_{10}(\omega/\omega_c)$ for different values of ω_D/ω_c $(= 0.1, 0.2, 1, 10, 100)$.

an examination of eqs. (7.48) and (7.50). The power dissipated to the electron distribution is proportional to $\mathbf{J} \cdot \mathbf{E}'$. When $\omega \ll \omega_c$ it is clear from eq. (7.48) that the magnitude of the electric field is small. Physically this arises because the current can flow for a long enough time to set up a space charge distribution that produces an electric field in opposition to the piezoelectric field. The dependence of the loss on ω_D is due to a slightly different cause. When $\omega \geq \omega_D$ the current and the electric field are no longer in phase, as is evident from eq. (7.50), so the power loss is reduced.

In addition to losses dispersion occurs. The dependence of this acoustic dispersion on ω, ω_c and ω_D is illustrated in fig. 7.2 where graphs of $(v - v_0)/v_0$ versus $\log_{10} (\omega/\omega_c)$ are given for several values of the ratio ω_D/ω_c. The dispersion, as described by this parameter, is zero at low frequencies and rises to reach a maximum of $e^2/(2c\kappa)$ in the high frequency limit. For situations where the diffusion frequency is comparable to, or greater than the conductivity frequency, the dispersion reaches half of its maximum value near frequencies close to the frequency ω_c. In cases where $\omega_D \ll \omega_c$ the dispersion curve retains the same shape but is shifted to lower frequencies. For example, it is noted from the graphs that when $\omega_D = 0.01\omega_c$ the 50% mark is reached as early as $\omega = 0.1\omega_c$. In fact, a quick examination of eq. (7.52) shows that in these situations the half-way mark occurs at $(\omega/\omega_c) = (\omega_D/\omega_c)^{1/2}$.
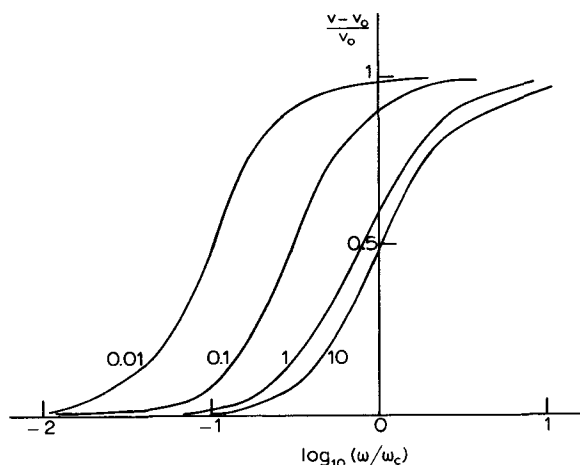
Fig. 7.2. Graph of $(v - v_0)/v_0$ against $\log_{10} (\omega/\omega_c)$ for different values of ω_D/ω_c (= 0.01, 0.1, 1, 10).

2.3.2. *In the presence of an applied electric field.* The attenuation discussed in the last subsection can be considerably modified by the application of a d.c. electric field. In fact not only can the magnitude

of the attenuation coefficient be affected but even its sign can be changed so that instead, amplification occurs. The experimental observation of the amplification of ultrasonic waves in piezoelectric semiconductors was first made by HUTSON *et al.*[1961] with a specimen of cadmium sulphide and the essential theoretical explanation was provided by WHITE[1962]. It is evident from eq. (7.53) that the necessary condition for amplification, Γ negative, is that γ should be less than zero. To achieve this an electric field E_d has to be applied such that the drift velocity of the electrons $v_d = -\mu_e E_d$ is greater than the velocity of the acoustic wave.

The variation of the attenuation (or amplification) Γ as a function of ω/ω_c is illustrated in fig. 7.3 for different values of the drift parameter $|\gamma|$. Although the curves are drawn for the specific case when ω_D/ω_c is unity they are quite characteristic of the family that would be obtained for other values of this parameter. The main points to be noted are that the family of curves will be centred about the frequency $\omega/\omega_c = (\omega_D/\omega_c)^{1/2}$ and that the value of $|\Gamma|$ at this frequency is

$$(e^2/2c\kappa)\,(\omega_c/v_0)\,\gamma\,[\gamma^2 + 4\omega_c/\omega_D]^{-1}.$$

Also, the value of $|\gamma|$ corresponding to maximum attenuation (or
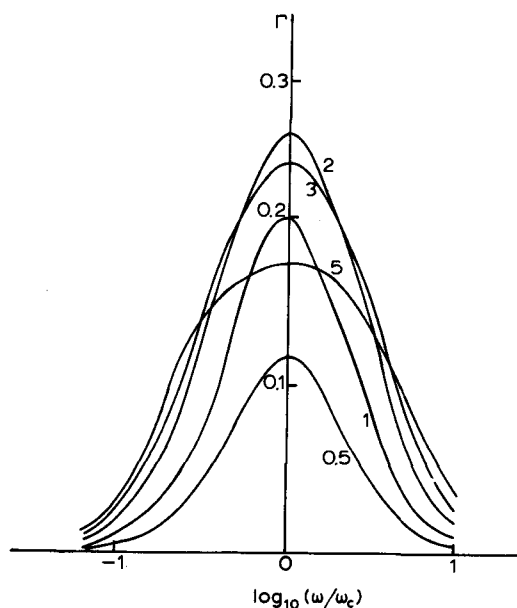
Fig. 7.3. Graph of Γ in units of $(e^2/2c\kappa)(\omega_c/v_0)$ against $\log_{10}(\omega/\omega_c)$ for different values of γ (= 0.5, 1, 2, 3, 5) when $\omega_D = \omega_c$.

amplification) at this frequency is found from eq. (7.53) to be given by
$|\gamma| = (\omega_c/\omega + \omega/\omega_D)$, at which point $|\Gamma|$ has the value $e^2\omega_c/(4c\kappa v_0\gamma)$.
Besides wishing to know the magnitude of the maximum amplification
that is possible, a knowledge of the bandwidth is desirable. For a given
value of ω_c, ω_D and γ frequencies $\omega_{1,2}$ may be introduced at which $|\Gamma|$
is one half of its maximum value. Denoting the frequency at which
$|\Gamma|$ is a maximum by ω_0 it can be shown that the bandwidth factor
defined by $(\omega_1 - \omega_2)/\omega_0$ is $(\gamma^2\omega_D/\omega_c + 4)^{1/2}$. When $\gamma^2 \gg \omega_c/\omega_D$ a large
bandwidth can result and the curve of $|\Gamma|$ against ω will be relatively
flat over a large frequency range. It is seen that this is beginning to
happen when $\gamma = 5$ in fig. 7.3.

2.3.3. *Effects due to the presence of bound states and carrier trapping.*
The expression that has been obtained for the amplification factor is
dependent upon the specific form that has been taken for the current
density J, eq. (7.36). In that equation it was assumed that all the
space charge produced by the acoustic wave was mobile. In actual fact
this need not be the case because some of it may be bound at the
crystal impurity levels in the energy gap. To allow for this Hutson and
White wrote n' and fn' where f was the fraction of the total acoustically
produced space charge that contributed to the conduction and diffu-
sion. If an n-type non-degenerate extrinsic semiconductor is considered
the electron space charge at temperature T is

$$Q = -Q_e\left\{K_e e^{E_f/KT} + \sum_j \frac{g_j N_j}{\exp\left[-(E_j + E_f)/KT\right] + g_j}\right\}. \quad (7.54)$$

The first term is the number of electrons n_e in the conduction band as
given by eq. (A7.5) and the second term results from the incomplete
ionization of N_j impurities of type j. For donors which can accept only
one electron in either of their two spin states the statistical degeneracy
factor is 2 as given by eq. (A7.19). The position of the Fermi level in
equilibrium is determined by the condition that total Q is zero. The
presence of the acoustic wave produces a periodic variation in E_f and
hence in Q. The fraction f of the acoustically produced space charge
that is mobile is given by

$$f = \left\{\left(\frac{\partial n_e}{\partial E_f}\right)\bigg/\frac{\partial}{\partial E_f}\left[n_e + \sum_j n_j\right]\right\}_0. \quad (7.55)$$

where the subscript 0 indicates evaluation at the unperturbed Fermi
energy. Strictly speaking only the states j should be included which
can equilibrate with the conduction band in a time short compared to
the sound wave frequency. As an example, consider the case of there
being a single type of impurity present, say, N_d donors with ionization

energy E_d. Then it is readily found that

$$f = \frac{n_e N_d}{N_d n_e + n_d (N_d - n_d)} = \frac{N_d}{N_d + n_d} \qquad (7.56)$$

since $n_e = (N_d - n_d)$ if the intrinsic carriers are neglected. For complete ionization n_d is zero and f is unity. The minimum value of f occurs when there is very little ionization $n_d \approx N_d$ for which $f = \frac{1}{2}$. Other cases when both donors and acceptors are present have been considered by Hutson and White. The expression derived above for the amplification factor is still valid if the parameters ω_D and γ are redefined so as to include f. The new definitions are $\omega_D = v^2/f\mathscr{D}$ and $\gamma = 1 - f\mu_e E_d/v$. It is seen that if f is less than unity there must be a corresponding increase in the value of the applied electric field before amplification can occur. This theory was subsequently extended in the work of UCHIDA et al. [1964] where the frequency dependence of f was considered. When the period of the ultrasonic wave is substantially greater than the relaxation time τ for electron trapping by empty donors the theory given above for f is correct. When $\omega\tau \approx 1$ however, the fraction f will be larger and a phase difference will exist between the mobile and trapped space charges. This is because the mobile space charge will pass through a point in the crystal before it has time to equilibrate completely. For situations where $\omega\tau \gg 1$ the total space charge is formed completely of mobile electrons because trapping cannot occur; f should then be unity. Since a phase difference can exist between the mobile and trapped space charges f must in general be complex. If the real and imaginary parts of f are denoted by f_r and f_i respectively the attenuation coefficient of eq. (7.53) becomes

$$\Gamma = \frac{e^2 \omega_c}{2c\kappa v_0} \frac{\left[1 - \frac{v_d}{v} f_r - \frac{\omega}{\omega_d} f_i\right]}{\left[1 - \frac{v_d}{v} f_r - \frac{\omega}{\omega_d} f_i\right]^2 + \left[\frac{\omega_c}{\omega} + \frac{\omega}{\omega_d} f_r - \frac{v_d}{v} f_i\right]^2} \qquad (7.57)$$

Uchida et al. considered a particular model for trapping which is appropriate to CdS. In their model they assumed that the rate of generation of carriers was equal to the rate of trapping. This assumption led to the following expressions for f_r and f_i

$$f_r = \frac{f_0 + \omega^2\tau^2}{1 + \omega^2\tau^2}; \quad f_i = \frac{\omega\tau(f_0 - 1)}{1 + \omega^2\tau^2} \qquad (7.58)$$

τ is the trapping time and f_0 the fraction of the excess carriers that are free in the equilibrium state. When $\omega\tau \ll 1$ f_r tends to f_0 and f_i tends to zero. The result for Γ is then that given by WHITE [1962]. In the

opposite limit, $\omega\tau \gg 1$, it is seen that f_r is unity and f_i is zero so all the space charge is mobile.

The effect of this carrier trapping is two-fold: it causes an asymmetry in the Γ versus drift velocity curve and an overall reduction in the amplification. From eq. (7.53) it is clear that the maximum magnitude in the attenuation and the amplification at a given frequency are the same. This is not so if f is complex, in fact examination of eq. (7.57) shows that

$$\frac{|\Gamma|_{\text{max amp.}}}{|\Gamma|_{\text{max atten.}}} = \frac{(1+a^2)^{1/2}+a}{(1+a^2)^{1/2}-a}, \tag{7.59}$$

where a is $f_i/f_r = \omega\tau(f_0-1)/(f_0+\omega^2\tau^2)$. The maximum amplification possible is therefore less than the maximum attenuation since f_i is negative. The curve of Γ as a function of the drift velocity v_d will therefore become asymmetric about the value of v_d corresponding to zero Γ. It is found that there is an overall drop in the amplification so the parameter a may be regarded as an attenuation factor. If the crystal is to be used as an ultrasonic amplifier it is desirable that $|a|$ should be small.

Recently KRISCHER and INGARD [1970] have considered the presence of trapping on the ultrasonic velocity. The result of WHITE [1962], eq. (7.52) shows that the range of possible phase velocities is bounded between the limits v_0 and the fully stiffened value $v_0(1 + e^2/c\kappa)^{1/2}$. Krischer and Ingard show that if a complex trapping factor of the form above is introduced, then for sufficiently large negative values of the electron drift parameter v_d, this upper limit of v may be exceeded.

3. Microscopic theory

3.1. *The electron–phonon interaction Hamiltonian*

In ch. 4 it was seen that in the high frequency regime acoustic attenuation could be described quantum mechanically in terms of phonon–phonon collisions brought about by the anharmonic terms in the expansion of the crystal potential. In metals and semiconductors an important contribution to the ultrasonic attenuation is the interaction of phonons with the conduction electrons. The electron–phonon interaction can be thought of in terms of collisions between phonons and electrons which result in the scatter of conduction electrons from one k-state to another with a consequent absorption or emission of a phonon. If the ultrasonic wave is regarded as a highly excited phonon mode the attenuation or amplification can be found by using perturbation theory to calculate the resultant loss or gain of phonons from the mode. The use of perturbation theory requires that the electron–

phonon interaction is small. The particular collision processes which can contribute to the attenuation are dictated by the momentum and energy conservation laws.

It was pointed out in the introduction to this chapter that the electron–phonon interaction can arise from a variety of sources, the relative importance of which depends on the type of material under consideration. In non-piezoelectric semiconductors the deformation potential concept of Bardeen and Shockley can be used to describe the electron–phonon interaction for the scattering of long wavelength acoustic waves. The idea is to find a slowly varying potential to represent the change in potential due to the wave. The method is best suited to semiconductors where the conduction electrons only have wave vectors near to the minimum of the conduction band and the effective mass approximation can be used. Also since the conduction electrons are few in number the screening effect of the carriers on each other is small. Suppose that in the unstrained crystal the conduction band is spherically symmetric so that the energy may be written as $E_0(k) = \hbar^2 k^2 / 2m_e^*$ where m_e^* is the effective mass of the conduction electron. If the crystal is given a small uniform static deformation it is expected that the new energy surfaces can be expressed in the form

$$E(k) = E_0(k) + C_{ij}\epsilon_{ij} + D_{ij}k_i k_j \epsilon_{ij} + \cdots \qquad (7.60)$$

where ϵ_{ij} are the components of the strain tensor (ch. 2§1.1). The first term gives a shift of all the energy levels while the one involving the components of k can be regarded as a change in the effective mass. This can be neglected since the values of k are usually small. For a spherical energy surface the shear components of the strain can be shown not to contribute so that only the dilatation components remain. In this case

$$E(k) \approx E_0(k) + C\Delta, \qquad (7.61)$$

where Δ is the dilatation. The constant C is given by $\partial E(0)/\partial \Delta$. If the dilatation is now a slowly varying function of position, as is the case for acoustic phonons of long wavelength, it is assumed that eq. (7.61) can be generalized to

$$E(k, r) = E_0(k, r) + C\Delta(r). \qquad (7.62)$$

That is, a local set of energy levels is defined with a constant energy shift. $\Delta E(r)$ equal to $C\Delta(r)$ is then used as a perturbing potential in the effective mass equation.

If the electron–phonon interaction is to be regarded as causing collisions between the electrons and phonons, it is convenient to express the interaction Hamiltonian in second quantization. To do this creation

and annihilation operators have to be introduced for the electron states. It is of course beyond the scope of this book to give an account of the formal aspects of second quantization. For those readers unfamiliar with the technique there are now several advanced text-books on quantum mechanics available that treat the subject in depth. Nevertheless to avoid unnecessary confusion it is perhaps worthwhile to digress briefly to define the nomenclature and basic rules of second quantization which need to be known.

The one-electron eigenfunctions are taken as Bloch functions, $\phi_k(r) = u_k(r) \exp(ik \cdot r)$, where $u_k(r)$ has the periodicity of the lattice. Field operators are introduced as follows

$$\Psi^*(r) = \sum_k c_k^* \phi_k(r), \qquad \Psi(r) = \sum_k c_k \phi_k(r), \qquad (7.63)$$

$\Psi^*(r)$ and $\Psi(r)$ are the operators that create or destroy an electron at the position r. The c_k's are the creation and annihilation operators of an electron in the state k. Because of the Pauli exclusion principle the c's are fermion operators and as such they satisfy the anti-commutation relations

$$c_k c_{k'}^* + c_{k'}^* c_k = \delta_{k,k'},$$
$$c_k c_{k'} + c_{k'} c_k = 0, \qquad (7.64)$$
$$c_k^* c_{k'}^* + c_{k'}^* c_k^* = 0,$$

cf. the creation and annihilation operators for the phonons, eq. (2.34). The field operators $\Psi(r)$ and the fermion operators c_k operate on state vectors Φ. The state vector is in the space of occupation numbers of the one-electron states. That is, it specifies whether each one-electron state is occupied or empty. Remember that the occupation number n_k for the state k in the case of fermions is limited to 1 or 0. It is found convenient to define a vacuum state Φ_{vac} in which all the one-electron states are empty. This may be written as

$$\Phi_{\text{vac}} = |0\,0\,0 \cdots 0\rangle. \qquad (7.65)$$

That is there are no particles present. The ground state of a system of N fermions in the independent particle approximation is in this notation

$$\Phi_0 = |1_1\,1_2\,1_3 \cdots 1_N\,0_{N+1}\,0_{N+2} \cdots\rangle. \qquad (7.66)$$

The one-particle states are assumed to be numbered in the order of increasing energy. In the ground state the first N one-particle states are filled and the rest are empty. A state Φ in which one one-electron state is occupied can be written alternatively as an operator acting on the vacuum state

$$\Phi \equiv |0\,0 \cdots 1_k\,0 \cdots\rangle = c_k^* \Phi_{\text{vac}}. \qquad (7.67)$$

Similarly the ground state Φ_0 defined above could have been written as

$$\Phi_0 = c_1^* c_2^* \cdots c_k^* \cdots c_{k_f}^* \Phi_{\text{vac}} \tag{7.68}$$

where k_f is the Fermi momentum. Care must be taken though when more than one one-particle state is occupied because of the complication of an additional minus sign. It is easy to show from the commutation rules that the creation and annihilation operators operate on these states according to

$$c_k | \cdots n_k \cdots \rangle = n_k (-1)^p | \cdots 0_k \cdots \rangle$$
$$c_k^* | \cdots n_k \cdots \rangle = (1 - n_k)(-1)^p | \cdots 1_k \cdots \rangle \tag{7.69}$$

where p is the number of occupied states to the left of k in the state vector $| \ \rangle$. Notice that $c_k^* c_k$ operating on the state vector gives the occupation number of the state k (cf. eq. (2.36)).

Besides expressing the states in the second quantization representation one must also transform the Hamiltonian. To do this it can be shown that for a one-particle operator, one simply multiplies to the left and the right by the field operators $\Psi^*(r)$ and $\Psi(r)$ respectively and integrates over all space.

After this digression the subject of the electron–phonon interaction will now be resumed. Using the prescription above the deformation potential in the second quantization representation is

$$H = \int \Psi^*(r) C\Delta(r) \Psi(r) \, dr$$
$$= C \sum_{kk'q} \left(\frac{\hbar}{2\rho V \omega_q} \right)^{1/2} c_k^* c_k \int e^{i(k-k') \cdot r} u_{k'} u_k$$
$$\times \{ |q| (a_q^* e^{-iq \cdot r} - a_q e^{iq \cdot r}) \, dr \}. \tag{7.70}$$

Here, use has been made of eq. (4.21) which expresses the elastic displacement in terms of normal mode coordinates

$$\Delta = \sum_i \frac{\partial u_i}{\partial x_i} = -\sum_q \left(\frac{\hbar}{2\rho V \omega_q} \right)^{1/2} e^{iq \cdot r} [a_q - a_{-q}^*] q \cdot e_q . \tag{7.71}$$

The factor $q \cdot e_q$ implies that the sum over q in eq. (7.70) is only over the longitudinal modes. Now $u_k(r)$ has the periodicity of the lattice so that on performing the integral over the spatial coordinates in eq. (7.70) it vanishes unless

$$k - k' \pm q = 0 \text{ or } G \tag{7.72}$$

where G is a reciprocal lattice vector. This is the same conservation law as for the three-phonon process in ch. 4 (see eq. (4.10)). Processes

for which G is zero are referred to as normal processes or N-type processes, while those for non-zero G are the Umklapp or U-processes. If the electrons are nearly free-electron like, $\int u_{k'}^* u_k \, dr$ approximates to unity. Also in a semiconductor at low temperatures the possibility of U-processes is remote. Under these conditions the electron–phonon interaction reduces to

$$H = C \sum_{kq} \left(\frac{\hbar}{2\rho V \omega_q} \right)^{1/2} |q| \, (a_q^* - a_{-q}) c_{k-q}^* c_k. \tag{7.73}$$

This interaction gives rise in first-order perturbation theory to the collision processes illustrated in fig. 7.4. The wavy lines refer to phonons and the straight lines to electrons.

As was stressed above the use of the deformation potential depends on being able to use the effective mass approximation to determine the wave functions. It is therefore more applicable to semiconductors than metals. In metals it can be used if the nearly free-electron picture is valid. Recent pseudo-potential calculations have shown that the range of applicability may be greater than had previously been thought. The value of C for a metal on the basis of a free-electron model can be obtained from a very simple argument. In a free-electron gas it is well known that the electron density and the density of states are given by

$$n_0 = \frac{8\pi}{3h^3} (2mE_f)^{3/2} \quad \text{and} \quad N(E) = \frac{4\pi}{h^3} (2m)^{3/2} E^{1/2}. \tag{7.74}$$

A varying dilatation $\Delta(r)$ will change the density of the electrons near position r from n_0 to $n_0(1 - \Delta)$. If Δ is small this means that the Fermi surface will change by an amount $n_0 \Delta(r)/N(E_f)$ which from eqs. (7.74) is $\frac{2}{3} E_f \Delta(r)$. To get back to a uniform Fermi level (this is essential since it is the chemical potential) electrons will have to flow out of the dense regions. This flow of electrons destroys local neutrality and produces an electric field whose potential is $-\frac{2}{3} E_f \Delta(r)$. This is the deformation potential. In a more sophisticated theory it can be shown that this result is only correct if the perturbing potential is slowly varying so it is only applicable to long wavelength acoustic phonons.

The electron–phonon interaction obtained above was based on the concept of a deformation potential. In a piezoelectric semiconductor there is another source of electron–phonon scattering because there is an electric polarization associated with the acoustic modes of vibration. This polarization may lead to a local charge accumulation and a periodic electric potential. It can be shown that there is a phase difference of $\frac{1}{2}\pi$ between the matrix elements for scattering by this mechanism and those of the deformation potential so the two can be treated independently. It is expected that the electron–phonon interaction will

have a similar form to that of eq. (7.73) but with a different constant. However there is one essential difference. In the deformation potential theory the lattice distortion produces a change in the potential energy of a conduction electron which is proportional to the strain. In a piezo-electric material it is the electric field that is proportional to the strain. Since $E = -\text{grad } V$ it follows that there will be an additional factor of $1/q$ in the coupling constant so that the frequency dependence of the interaction will be different. To be more explicit it is seen from eq. (7.48) that the electric field in a piezoelectric insulator is equal to $-(e/\kappa)\epsilon$. Thus when the strain arises from an ultrasonic wave the potential energy of an electron is proportional to $-Q_e(e/\kappa)(i/q)\epsilon$. The ratio of the magnitude of the deformation potential coupling constant C_d to that of the piezoelectric effect C_p in the electron–phonon interaction is therefore

$$\left|\frac{C_d}{C_p}\right| = \frac{\omega}{v}\frac{\kappa}{eQ_e}C_d. \tag{7.75}$$

It is seen from this ratio that the relative importance of the two mechanisms as a source of phonon scattering is dependent upon the frequency of the applied ultrasonic wave. At low frequencies the contribution from the deformation potential is considerably smaller than that from the piezoelectric coupling in a strong piezoelectric material. As an example the value $C_d(\text{Ge})/C_p(\text{CdS}) \approx 10^{-12}\,\omega$ may be quoted. The two effects are comparable for acoustic frequencies around 100 GHz.

3.2. *Quantum mechanical perturbation treatment of acoustic attenuation*

Quantum mechanical perturbation theory will now be used to calculate the acoustic attenuation arising from the electron–phonon interaction given in eq. (7.73). A quasi free-electron description of the conduction electrons will be assumed to be valid. The method is to regard the acoustic wave as a highly excited phonon mode and to calculate the loss and gain of phonons from this mode due to its interaction with the equilibrium electron distribution. The energy and wave number of a phonon in the acoustic mode will be denoted by $\hbar\omega_q$ and q respectively and the corresponding quantities for the electrons by E_k and k. If the electron-phonon interaction can be treated by the perturbation theory of appendix 3 the probability of emission of a phonon into the mode q due to a process of the type shown in fig. 7.4(a) will involve the squared matrix element

$$|\langle ..., N_q + 1, ...; ...1_{k-q}... 0_k ... |a_q^* c_{k-q}^* c_k| ...; n_{k-q} ... n_k ...; ... N_q ...\rangle|^2$$
$$= (N_q + 1)n_k(1 - n_{k-q}). \tag{7.76}$$

Phonon emission
(a)

Phonon absorption
(b)
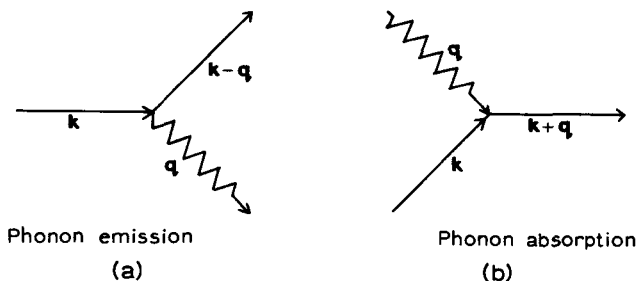
Fig. 7.4.

The occupation numbers of the phonon modes are designated by N and those of the electron states by n (note $n^2 = n$ since $n = 1$ or 0). Likewise the probability of absorption of a phonon in mode q by the process of fig. 7.4(b) involves the quantity $N_q n_k(1 - n_{k+q})$. Therefore the total net transition probability per second for the absorption of a phonon of mode q due to its interaction with a thermal distribution of electrons in all the modes k is, according to eq. (A3.6),

$$W = \frac{2\pi}{\hbar} \sum_k |C|^2 \left(\frac{\hbar}{2\rho V \omega_q}\right) |q|^2 \{N_q n_k^0 (1 - n_{k+q}^0) \delta(E_k + \hbar\omega_q - E_{k+q})$$
$$- (N_q + 1) n_k^0 (1 - n_{k-q}^0) \delta(E_k - \hbar\omega_q - E_{k-q})\} \tag{7.77}$$

where n^0 is the thermal equilibrium Fermi distribution function for the electrons. When the lattice mode q is highly excited ($N_q \gg 1$) this reduces to

$$W = \frac{2\pi}{\hbar} \sum_k |C|^2 \left(\frac{\hbar}{2\rho V \omega_q}\right) |q|^2 N_q (n_k^0 - n_{k+q}^0) \delta(E_k + \hbar\omega_q - E_{k+q}). \tag{7.78}$$

If the angle between the vectors k and q is denoted by θ, then the delta function for the conservation of energy implies that

$$\hbar\omega_q = \frac{\hbar^2}{2m^*} (q^2 + 2kq \cos\theta). \tag{7.79}$$

Changing from a summation over states to an integral over k according to the prescription $\sum_k \rightarrow 2V/(2\pi)^3 \int dk$ it follows that

$$W = \frac{2\pi}{\hbar} \left(\frac{2V}{8\pi^3}\right) |C|^2 \left(\frac{\hbar}{2\rho V \omega_q}\right) |q|^2 N_q \int dk (n_k^0 - n_{k+q}^0) \frac{m^*}{\hbar^2 q}$$
$$\times \delta\left(k \cos\theta + \tfrac{1}{2}q - \frac{m^* \omega_q}{\hbar q}\right). \tag{7.80}$$

It is convenient to evaluate this integral in cylindrical polar co-

ordinates (z, ρ, ϕ) in which the direction of q is the z-axis. The integral in eq. (7.80) then becomes

$$I = \int \int \int \rho\, d\rho\, dz\, d\phi\, (n_k^0 - n_{k+q}^0) \frac{m^*}{\hbar^2 q} \delta\left(z + \tfrac{1}{2}q - \frac{m^* \omega_q}{\hbar q}\right). \quad (7.81)$$

The integration is readily performed at the absolute zero of temperature when the distribution functions n^0 have a particularly simple form. n^0 is either zero or unity depending on whether its k-value is greater or less than the Fermi momentum k_f. That is

$$n_k^0 \text{ is 1 if } k^2 < k_f^2$$

$$n_{k+q}^0 \text{ is 1 if } k^2 + q^2 + 2kq \cos \theta < k_f^2$$

and zero otherwise. In terms of the cylindrical polar coordinates (z, ρ, ϕ) the conditions are

$$n_k^0 \text{ is 1 if } \rho^2 < k_f^2 - z^2$$

and

$$n_{k+q}^0 \text{ is 1 if } \rho^2 < k_f^2 - (z+q)^2.$$

After substituting these values into the integral I and completing the integration it is found that

$$W = \frac{|C|^2 (m^*)^2 N_q |q|}{2\pi\rho\hbar^3}. \quad (7.82)$$

In situations where the electrons have a drift velocity v_d in the direction of q a modification of the distribution function is required. This may be done by multiplying ω_q/q in the delta function of I by $(v - v_d)/v$ so that the distribution functions are in the moving frame of reference. If an attenuation coefficient α is defined as W divided by the phonon flux $N_q v$ then it follows that

$$\alpha = \frac{|C|^2 (m^*)^2 \omega}{2\pi\rho\hbar^3 v^2} \left(1 - \frac{v_d}{v}\right). \quad (7.83)$$

It is of interest to compare this result with that of §4.2 obtained by solving the Boltzmann equation in the relaxation time approximation. The present method is only applicable in the $ql \gg 1$ regime so the comparison should be made with the result of eq. (7.94). A quick glance at the two expressions shows that there is some fundamental difference. The reason for this is that the electron screening automatically included in the method of §4.2 has not been included here. No account has been taken of the fact that the electron distribution redistributes itself in an attempt to screen out the potential set up by the ultrasonic wave. The simplest way to include the effect of this redis-

tribution of electronic charge is to use the results of Thomas–Fermi theory. This semi-classical theory, see for example the book by MARCH et al. [1967], shows that the potential around a point charge ZQ_e in a free-electron gas is not the Coulomb potential $ZQ_e/4\pi\kappa r$ but the screened potential $(ZQ_e/4\pi\kappa r)$ exp $(-\Lambda r)$. Λ^{-1} is the Thomas–Fermi screening radius and in linear theory is given by

$$\Lambda^2 = \frac{4\pi}{h^3}\frac{Q_e^2}{\kappa}(2m)^{3/2}E_f^{1/2}. \tag{7.84}$$

The qth Fourier component of this potential is $(ZQ_e/\kappa)[q^2(1+\Lambda^2/q^2)]^{-1}$ and so it is reduced by the factor $(1+\Lambda^2/q^2)^{-1}$ to that which it would be in the absence of screening. To account for screening by the electrons in the present calculation it seems reasonable to replace C by $C/[1+\Lambda^2/q^2]$. If this is done, remembering n_0 is given by eq. (7.74), the result of eq. (7.83) then becomes identical to that of eq. (7.94).

In semiconductors with low electronic densities the electrons can usually be taken to be non-degenerate so Maxwell–Boltzmann statistics apply. In this situation the distribution function $n_k^0 - n_{k+q}^0$ is replaced by

$$\exp\left[-(\hbar^2/2m^*KT)(\rho^2+z^2)\right] - \exp\left[-(\hbar^2/2m^*KT)(\rho^2+[z+q]^2)\right].$$

That is, the -1 in the denominator of the Fermi distribution function can be dropped and the degeneracy factor A, which in Fermi–Dirac statistics is usually written as $\exp(E_f/KT)$, now takes the value $2h^3(2\pi m^*KT)^{-3/2}N/V$, (see for example the book by TOLMAN [1938]). This approximation is valid if $A \ll 1$ that is, it is best for low densities, large effective masses and at high temperature. Under these conditions the net transition probability per second is found to be*

$$W = \frac{A|C|^2|q|N_q(m^*)^2KT}{2\pi\rho\hbar\omega_q}\left\{\exp\left(-\frac{\hbar^2}{2m^*KT}\left[\frac{m^*\omega_q}{\hbar q}-\tfrac{1}{2}q\right]^2\right)\right.$$
$$\left.-\exp\left(-\frac{\hbar^2}{2m^*KT}\left[\frac{m^*\omega_q}{\hbar q}+\tfrac{1}{2}q\right]^2\right)\right\}. \tag{7.85}$$

In situations where the exponentials may be expanded and only the leading terms retained this reduces to

$$W = \frac{A|C|^2(m^*)^2N_q|q|}{2\pi\rho\hbar^3} \tag{7.86}$$

---

*
$$\int_0^\infty \rho\exp(-a\rho^2)\,d\rho = \frac{1}{2a}.$$

so the attenuation coefficient in this case in the presence of a drift velocity v_d is

$$\alpha = \frac{A|C|^2(m^*)^2\omega}{2\pi\rho\hbar^3 v^2}\left(1 - \frac{v_d}{v}\right). \qquad (7.87)$$

This expression for the absorption coefficient is just A times the result of eq. (7.83) for the case of degenerate statistics.

4. Boltzmann equation method

4.1. *The Boltzmann equation*

The method described in §2 is a phenomenological approach which assumes that a local relation, like that of eq. (7.36), exists for the electronic current. This assumption is valid if the wave number of the acoustic wave is very much less than the reciprocal of the mean free path of the electrons, $(ql \ll 1)$. This condition implies that an electron is scattered many times before travelling one acoustic wavelength, so that its motion under the influence of the external field is averaged out. When ql is of the order of unity or greater the method will fail, so a more general approach such as a complete Boltzmann equation treatment must be used.

A semi-classical approach based on the Boltzmann equation can be used to determine the electron distribution function in the presence of an acoustic wave. The method is quite general and can be applied to semi-metals and semiconductors as well as to metals. It is semi-classical in the sense that the electrons are treated classically except for the fact they they must obey the correct statistics. This means that in metals, semi-metals and degenerate semiconductors, Fermi–Dirac statistics will have to be used, while Boltzmann statistics are more appropriate for non-degenerate semiconductors. The motion of the electrons may be treated classically if their wave number is very much greater than that of the acoustic wave. This condition is violated for very high frequency acoustic waves, so the method then breaks down. Another condition, of course, is that the wavelength of the acoustic wave must be much larger than the lattice spacing. This is necessary if the deformation potential concept is valid and if the phenomenological constitutive equations of piezoelectricity can be used. It also allows the positive ions to be regarded as smeared out into a positive background. This condition, which is expected to be satisfied for all acoustic frequencies that can be generated experimentally, must also hold if the dispersion of the phonon mode frequencies can be ignored.

The Boltzmann transport equation for the system is set up in the

same way as was done in ch. 4§3.2 for the phonon gas. An electron distribution function $f(r v_e t)$ for electrons with velocity v_e at position r at time t is introduced, which satisfies the equation

$$\frac{\partial f}{\partial t} + v_e \cdot \frac{\partial f}{\partial r} + \frac{F}{m^*} \cdot \frac{\partial f}{\partial v_e} = \left[\frac{\partial f}{\partial t}\right]_{\text{collisions}}$$

This equation balances the change in distribution arising from its time dependence, spatial gradients and external forces with the change in distribution arising from collisions. In semiconductors where more than one type of carrier may be present a Boltzmann equation exists for each type. The mass which enters this equation is the effective mass m^* of the carrier, since it is this which determines the kinetic response of the particles to forces in the effective mass approximation. The force in the Boltzmann equation includes both the d.c. force acting on the electron because of the presence of the applied d.c. electric and magnetic fields, E_d and B_d, and the force arising from the passage of the acoustic wave. In general this latter contribution is made up of the Lorentz force due to the self-consistent electromagnetic fields E' and B' which satisfy both Maxwell's equations, eqs. (7.3)–(7.6), and the appropriate constitutive relations of the material, and a part due to the deformation energy discussed in §3.1. eq. (7.62). The constitutive relations appropriate to a piezoelectric semiconductor are given in eqs. (7.2) and (7.7). The force due to the deformation potential is

$$F = -\frac{\partial}{\partial r} C_{ij}\epsilon_{ij} = q(q \cdot C \cdot u).$$

If the Boltzmann equation is solved for the distribution function f, then the electronic current density can be readily obtained in the semi-classical limit from

$$j_e = -Q_e \int v_e f \, dv_e.$$

A major problem, of course, is solving the Boltzmann equation. The usual method of treating the collision term is to make the relaxation time 'ansatz' used in ch. 4. It is assumed that if all the external forces were removed, the distribution function would relax back to an appropriate equilibrium distribution in time τ. This enables the collision term to be replaced by $-(f-f_a)/\tau$. The equilibrium distribution to which the distribution function relaxes need not be the one that would occur in the absence of the acoustic wave. At low temperatures the major source of scattering of the electrons is from impurities while at high temperatures scattering from acoustic phonons usually dominates. The impurities are displaced from their equilibrium positions by the ultrasonic wave and consequently have a velocity $\dot{u}$. If the impurities

were at rest the electrons would scatter into a velocity distribution centred about the impurity velocity, namely zero. In this case f_a would be $f_0(v_e, E_f^0)$. When the impurities are moving with velocity $\dot{u}$ then the electrons will be scattered into a velocity distribution centred about this velocity. Also, because the scattering is local it cannot change the electron density; therefore

$$f_a(rv_e t) = f_0(v_e - \dot{u}, E_f(rt))$$

where the Fermi energy $E_f(rt)$ is chosen to give the correct electron density $n(rt)$. In this relaxation time approximation the Boltzmann transport equation becomes

$$\frac{\partial f}{\partial t} + v_e \cdot \frac{\partial f}{\partial r} - \frac{Q_e}{m^*} \left[(E_d + E') + v_e \right.$$

$$\left. \times (B_d + B') \right] \cdot \frac{\partial f}{\partial v_e} + \frac{1}{m^*} q(q \cdot C \cdot u) \cdot \frac{\partial f}{\partial v_e} = -\frac{(f - f_a)}{\tau}. \quad (7.88)$$

The relaxation time approximation to the collision time is generally believed to be satisfactory if the major scattering processes are elastic and if τ is independent of the electric and magnetic fields. Methods of solving the Boltzmann equation usually involve linearization at some stage, so that only terms linear in the acoustic displacement u appear. This can be done directly if the distribution function is split into two parts, $f = f_0 + f'$ ($rv_e t$) where f_0 is the equilibrium part and f' is the part linear in u. In this way the linearized Boltzmann equation

$$\frac{\partial f'}{\partial t} + v_e \cdot \frac{\partial f'}{\partial r} - \frac{Q_e}{m^*} \left[(E_d + v_e \times B_d) \cdot \frac{\partial f'}{\partial v_e} + (E' + v_e \times B') \cdot \frac{\partial f_0}{\partial v_e} \right]$$

$$+ \frac{1}{m^*} q(q \cdot C \cdot u) \cdot \frac{\partial f_0}{\partial v_e} = -\frac{1}{\tau} \left(f' + \dot{u} \cdot \frac{\partial f_0}{\partial v_e} - n' \frac{\partial f_0}{\partial n_0} \right) \quad (7.89)$$

is obtained where the expansion

$$f_a(v_e) = f_0(v_e - \dot{u}, n_0 + n') \approx f_0(v_e) - \dot{u} \cdot \frac{\partial f_0}{\partial v_e} + n' \frac{\partial f_0}{\partial n_e} \quad (7.90)$$

has been used. This self-consistent semi-classical treatment outlined above was developed by COHEN et al. [1960] to calculate the magnetic field dependence of the ultrasonic attenuation in metals and applied by HARRISON [1960] to semi-metals. It was subsequently applied to non-degenerate semiconductors by SPECTOR [1962c].

4.2. The attenuation coefficient

The quantity of interest is the absorption coefficient. This may be calculated either by finding the rate at which power is dissipated per

unit volume by the ultrasonic wave or, alternatively, by solving the equations of motion to find the real and imaginary parts of the frequency. The method adopted by COHEN *et al.* [1960] was the former. The sound wave feeds both kinetic and potential energy into the electron system as it propagates and the energy is dissipated to the positive background through collisions. Since an individual collision is a local event, only kinetic energy is changed after a collision. The average rate at which kinetic energy is dissipated per unit volume via collisions is

$$\left\langle j_e \cdot \left(E' - \frac{1}{Q_e} q(q \cdot C \cdot u) \right) \right\rangle_{av}.$$

Not all the kinetic energy is dissipated as heat because a part is fed coherently back into the sound wave. This is because the average electron velocity $\langle v_e \rangle$ before collision in general differs from that after collision, u. Energy is thus returned to the sound wave at an average rate $\langle \dot{u} \cdot n_0 m(\langle v_e \rangle - \dot{u})/\tau \rangle_{av}$. In this expression m is the free electron mass. The actual momentum transfer to the moving lattice in a collision is the change in expectation value of the linear momentum operator which is just the product of the free electron mass and the velocity operator. This term is related to the collision drag effect discussed by HOLSTEIN [1959]. The net power dissipated per unit volume is

$$P = \tfrac{1}{2} \mathrm{Re} \left\{ j_e^* \cdot \left(E' - \frac{1}{Q_e} q(q \cdot C \cdot u) \right) - \dot{u}^* \cdot n_0 m(\langle v_e \rangle - \dot{u})/\tau \right\}. \quad (7.91)$$

As far as attenuation is concerned the collision drag term is only important in metals at high frequencies when screening breaks down. It is then that the forces from purely electromagnetic coupling start to vanish. In metals this occurs for transverse waves in the microwave frequency range so for these waves the attenuation is determined solely by the collision drag term. In semi-metals or in piezoelectric semiconductors the collision drag term can be ignored since when screening breaks down the deformation potential or the piezoelectric coupling terms still dominate. Once P is known the attenuation coefficient α, which is the power dissipated per unit energy flux, is obtained from

$$\alpha = P/\tfrac{1}{2} \rho |\dot{u}|^2 v, \quad (7.92)$$

ρ being the mass density of the material and v the velocity of sound.

The formalism described above was applied by SPECTOR [1962c] to calculate the amplification of acoustic waves in the presence of a d.c. electric field. His results for the case when the deformation potential term is dominant and the electric field is parallel to the direction of

propagation are given below. When $ql \ll 1$,

$$\alpha = \frac{n_0 m^*}{2\rho} \omega \tau \gamma q \left(\frac{v_f}{v}\right)^4 \left(\frac{\omega}{\omega_p}\right)^4 \left(\frac{C}{m^* v_f^2}\right)^2$$

$$\times \left\{ \gamma^2 \left(\frac{\omega}{\omega_p}\right)^4 + (\omega\tau)^2 \left[1 + \frac{1}{3}\left(\frac{v_f}{v}\right)^2 \left(\frac{\omega}{\omega_p}\right)^2\right]^2 \right\}^{-1} \qquad (7.93)$$

when $ql \gg 1$,

$$\alpha = \frac{\pi n_0 m^*}{6\rho} \gamma q \left(\frac{v_f}{v}\right)^5 \left(\frac{\omega}{\omega_p}\right)^4 \left(\frac{C}{m^* v_f^2}\right)^2 \times \left\{ \left[1 + \frac{1}{3}\left(\frac{v_f}{v}\right)^2 \left(\frac{\omega}{\omega_p}\right)^2\right]^2 \right\}^{-1} \qquad (7.94)$$

$\omega_p = (n_0 Q_{el}^2 / m^* \kappa)^{1/2}$ is the plasma frequency for the electrons and v_f is the Fermi velocity. Note that the m.k.s. system of units is being used and that κ is the permittivity other than that arising from the free electrons. As before, $\gamma = 1 - v_d/v$ with v_d the drift velocity of the electrons in the electric field. C is the component of the deformation potential coupling constant appropriate to the directions of propagation and polarization of the wave that is propagating. In piezoelectric semiconductors where the piezoelectric coupling is dominant over that of the deformation potential, the same expressions hold if C is replaced by $Q_e e/\kappa q$. e is the appropriate piezoelectric constant. The results quoted are based on the use of Fermi–Dirac statistics. For semiconductors where the electron density is low enough to obey classical statistics, similar expressions are obtained except for some numerical factors that are of the order of unity.

The result for $ql \ll 1$ may be compared with the result of WHITE [1962] derived in eq. (7.53). The two results are found to be equivalent if the deformation potential coupling constant is replaced by the appropriate piezoelectric factor in the manner described above and the value of n_0 from eq. (7.74) is substituted. It is also necessary to recall that $\omega_c = b/\kappa = Q_e n_0 \mu_e/\kappa$ and $\omega_D = v^2/\mathscr{D}$. The equivalence between the two expressions then follows if the relations

$$\mu_e = Q_e \tau/m \quad \text{and} \quad \mathscr{D} = \tfrac{2}{3} E_f \mu_e / Q_e$$

are used (see for example the book by SMITH [1961], in particular pp. 97 and 236). In the latter expression the thermal energy KT in his formula has been replaced by the mean energy of a conduction electron, $\tfrac{3}{5} E_f$. In the opposite limit when $ql \gg 1$ the result is in agreement with the quantum mechanical treatment outlined in §3.2. The equivalence between the two methods is pointed out in the discussion following eq. (7.83) of that section.

In a later paper, SPECTOR [1968] solved the Boltzmann equation to obtain the conductivity tensor for electrons interacting with acoustic waves in the presence of *strong* electric fields. The work was an exten-

sion of his earlier work which was limited only to solutions correct to first order in the d.c. electric field. The presence of the d.c. electric field is two-fold. It leads to the introduction of a drifted d.c. distribution for the electrons and to a complex field-dependent effective temperature. In the limit $ql \ll 1$ the result of the calculation is the same as that reported earlier but it is clearer from this later work that the acoustic amplification arises from the field-dependent effective temperature. In the short wavelength regime $ql \gg 1$ it is the drifted distribution function that leads to the amplification of the acoustic waves. Experimental evidence to support the result of this theory is presented in §5.3.

5. Magnetic field effects

5.1. *Amplification in crossed electric and magnetic fields*

It has been seen that amplification of sound in a semiconductor is possible when the drift velocity of the conduction electrons in an external field exceeds the velocity of sound. So far in this chapter the only situation considered has been when the drift velocity of the conduction electrons is due to an applied d.c. electric field. Under these circumstances large acoustic gains can be obtained in strong piezoelectric semiconductors like CdS even though the number of free carriers is small. In principle there is no reason why the effect should not be observed in non-piezoelectric materials but with higher carrier concentrations. Practical difficulties occur, however, in these cases because by the time the carriers have drift velocities comparable to the velocity of sound, the current density is very large. Because of this difficulty DUMKE and HAERING[1962] proposed an alternative scheme for observing ultrasonic amplification. They suggested that crossed electric and magnetic fields should be used, a situation where the current density required for amplification is smaller since the magnetic field limits the current flowing in the electric field direction. Because the drift velocity in crossed electric and magnetic fields is independent of the sign of the charge, the method is suitable for semimetals having equal concentrations of holes and electrons. The theory for this situation was given by Dumke and Haering and subsequently applied to extrinsic semiconductors having only one type of carrier by SPECTOR[1963a].

Classically the motion of an electron in d.c. electric and magnetic fields can be obtained by solving the Lorentz force equation

$$F = -Q_e[E_d + v_e \times B_d] \qquad (7.95)$$

(m.k.s. unit are adopted.) In the special case when the electric and magnetic fields are at right angles it is found that the electron has a rotation of frequency $\omega_B = Q_e B_d/m$ and radius $r_B = mv_e/Q_e B_d$ in a clockwise direction about the direction of B_d together with a drift velocity $v_B = E_d/B_d$ in the direction of $E_d \times B_d$. This drift velocity is clearly independent of both the particle mass and its charge. The frequency ω_B is known as the cyclotron frequency. Spector considered the particular case of the amplification of a longitudinally polarized sound wave propagating along the x-direction, when the electric and magnetic fields were applied in the y- and z-directions respectively. For this geometry the electronic current density is

$$J_x = -nQ_e v_B + nQ_e \mu_e \left[E'_x - \omega_B \tau E'_y - \frac{q^2 C u_x}{Q_e} - \frac{m\dot{u}_x}{Q_e \tau} \right] + Q_e \mathscr{D} \frac{\partial n}{\partial x},$$

$$J_y = \frac{nQ_e v_B}{\omega_B \tau} + nQ_e \mu_e \left[E'_y + \omega_B \tau \left(E'_x - \frac{q^2 C u_x}{Q_e} - \frac{m\dot{u}_x}{Q_e \tau} \right) \right] + Q_e \omega_B \tau \mathscr{D} \frac{\partial n}{\partial x}.$$

$$(7.96)$$

It has been assumed that the ultrasonic wavelength is very much greater than the cyclotron radius of the electrons and that the cyclotron frequency ω_B is very much greater than the collision frequency $1/\tau$. The mobility μ_e is then given by $Q_e \tau/m(\omega_B \tau)^2$ and the diffusion constant by $\mathscr{D} = \frac{2}{3} E_f \mu_e/Q_e$. A derivation of these results may be found, for example, in the book by SMITH [1961] pp. 105. E' is the self-consistent electric field determined by Maxwell's equations and C is the deformation potential constant. If the effect of the sound wave on the electron density can be treated as a small perturbation n may be replaced by $n_0 + n'$ as in §2.2. These equations may then be combined with the equation of continuity and Maxwell's equations connecting the self-consistent electromagnetic field to the electronic and ionic currents. The solution of these equations enables the attenuation coefficient to be determined as before by calculating the rate of average power dissipated per unit time and unit volume to the incident energy flux. For n_0 less than about 10^{10} el/cm³ and ultrasonic frequencies greater than about a megahertz the screening of the ionic currents by the electronic currents breaks down. Under these conditions Spector finds that the absorption coefficient is the same as that of eq. (7.93) in the absence of a magnetic field if γ is replaced by $(1 - v_B/v)$ and ω_c and ω_D by $\phi \omega_c$ and ω_D/ϕ respectively, where $\phi = 1/(\omega_B \tau)^2$. The reason for the factor ϕ is obvious, the only difference in the present case is that μ and $\mathscr{D}$ are $(\omega_B \tau)^{-2}$ smaller. This fact had been noted by STEELE [1967] but in his work ϕ had the value $1/[1 + (\omega_B \tau)^2]$ because the high field

approximation was not assumed. Cf. eqs. (7.96) with those of SMITH [1961] p. 105. When $v_B > v$ amplification rather than attenuation occurs. The maximum amplification and attenuation occurs respectively when

$$\frac{v_B}{v} = 1 \pm \frac{\omega_p^2 \tau}{\omega (\omega_B \tau)^2} \left[1 + \frac{1}{3} \left(\frac{v_f}{v} \right)^2 \left(\frac{\omega}{\omega_p} \right)^2 \right] \tag{7.97}$$

and the maximum value of the coefficient is then

$$\alpha_{max} = \pm n_0 m \omega \left(\frac{\omega_p}{\omega} \right)^2 \left[1 + \frac{C}{mv^2} \left(\frac{\omega}{\omega_p} \right)^2 \right]^2$$

$$\times \left\{ 4\rho v \left[1 + \frac{1}{3} \left(\frac{v_f}{v} \right)^2 \left(\frac{\omega}{\omega_p} \right)^2 \right] \right\}^{-1}. \tag{7.98}$$

Thus as long as $\omega_B \tau \gg 1$, the maximum value of the absorption coefficient is independent of the relaxation time. It should be noticed though that the results are only valid when $\omega \tau < 1$ since the frequency dependence of the mobility and diffusion constants have not been accounted for. The amplification factor may be very large at high frequencies and low carrier densities. For example, in a typical semiconductor, $(C = 10 \text{ eV}, \tau = 10^{-11} \text{ sec}$ and $v = 10^5 \text{ cm/sec})$ α_{max} has values of 10 and 10^5 for carrier densities of 10^{14} el/cm³ at frequencies equal to 10^9 and 10^{11} sec^{-1} respectively when v_B/v is of the order of unity. For higher electron densities such as 10^{18} el/cm³ reasonable amplification can only be obtained at unattainable electric field strengths.

The above approach, which was based upon the assumption that a local relationship exists for the current density requires, in addition to the condition $\omega_B \tau \gg 1$ being satisfied, that $qr_B \ll 1$ holds. The former condition is necessary if the influence of the magnetic field on the motion of the electrons is not to be dominated by collisions. The second requirement prevents the electrons from moving more than a wavelength under the influence of the acoustically produced fields. These are the analogues of the requirements $\omega \tau \ll 1$ and $ql \ll 1$ for a local theory to be valid in the absence of a magnetic field. To obtain more general results which are not restricted to this regime a Boltzmann equation method can be used. ECKSTEIN [1963] used the method of the Boltzmann equation to study the amplification of sound in the presence of crossed electric and magnetic fields as a function of the angle between the drift velocity and the direction of propagation, but his results were again limited by the high field limit. About the same time SPECTOR [1963b] also carried out a Boltzmann equation treatment but this time it was valid for all magnetic field strengths within the

semi-classical limit. A number of interesting resonance phenomena can occur which will now be briefly discussed.

5.2. *Resonance phenomena in a magnetic field*

In the presence of a magnetic field resonance phenomena can occur for certain values of the acoustic wave frequency. One type of resonance is known as geometric or magneto-acoustic resonance and occurs whenever the diameter of the electron orbit is of the order of an odd integral number of half wavelengths of the acoustic wave. The condition $\omega_B \tau \gg 1$ is of course necessary for the resonance to be observed, since it is necessary that the electron traverses several orbits before suffering a collision. The resonance condition expressed in terms of frequencies and velocities is $\omega/\omega_B \approx (n + \frac{1}{2})\pi v/v_e$. For semiconductors the value of v/v_e for a conduction electron is typically of the order of $\frac{1}{100}$. A simple physical picture of how the resonance occurs is given in fig. 7.5. The acoustic wave may set up a transverse electric field which interacts with the cyclotron orbit of the electron in the magnetic field. In the diagram the magnetic field is directed out of the plane of the page, so the electron circulates anticlockwise as shown. In fig. 7.5(a) it is seen that the geometry is such that the electric field accelerates the electron in the same sense around the orbit at both the points P and Q while in fig. 7.5(b) the accelerations at P' and Q' are in opposite senses. Clearly, resonance occurs when the diameter of the orbit is an integral number of half-wavelengths and there is an increase in the conductivity. Since in a constant current system the absorption of energy is inversely proportional to the effective conductivity, there is a minimum in the ultrasonic attenuation. Consequently if the wavelength of the acoustic wave is fixed and the magnetic field strength varied, the absorption should oscillate with a period of $1/B$. The picture is not quite as simple as this because the electron orbit need not be circular and also the relationship between the elastic strain and the electric field needs to be treated properly. Even if the orbit were circular a complete integration around it would be needed to obtain the total energy
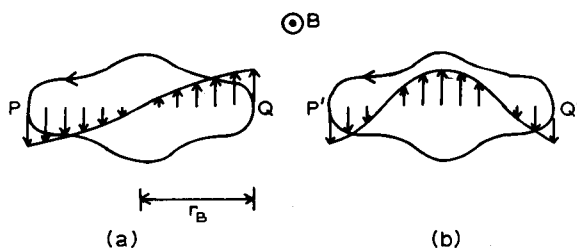
Fig. 7.5.

absorbed per cycle. If this is done the energy absorbed is found to be proportional to the Bessel function $J_1(qr_B)$ whose maxima are somewhat displaced from those of $(n+\frac{1}{2})\pi$.

A second type of resonance is cyclotron resonance. This occurs whenever ω is an integral multiple of ω_B. Again the condition $\omega_B\tau \gg 1$ is required so that the electron may complete at least one orbit before scattering. The resonance condition $\omega = n\omega_B$ implies that the acoustic wave remains in temporal resonance with the electron so that a resonance transfer of energy can take place. The condition is easily understood in the quantum treatment of the magnetic field problem. The Schrödinger equation for a free electron in a magnetic field is obtained by replacing the momentum operator $-i\hbar\nabla$ by $(-i\hbar\nabla - eA/c)$ where A is the vector potential. The solution to this equation, as is well known, see for example the book by KITTEL [1963], gives energy levels at

$$E = (n+\tfrac{1}{2})\hbar\omega_B + \frac{\hbar^2 k_z^2}{2m} \qquad (7.99)$$

rather than at the free electron energy $\hbar^2 k^2/2m$. z is the direction of the d.c. magnetic field. The energy of the electron states can therefore be divided into two parts, a translational energy along the magnetic field and a quantized energy of the cyclotron motion in the plane perpendicular to the field. The quantum number n specifies what are known as Landau levels. If an acoustic wave propagates perpendicular to the magnetic field, the cyclotron resonance condition is just the condition required for an electron to make a transition from one Landau level to another with the absorption or emission of a phonon. The restriction that $\omega_B\tau$ must be greater than unity for the resonance to be observed then arises naturally. It is just the condition imposed by the uncertainty principle in order that the energy levels may be sufficiently well defined for energy conservation in the transition process to be maintained.

Spector finds that geometric resonances and cyclotron resonances can occur in the sound wave intensity under conditions of amplification when crossed electric and magnetic fields are used. The detailed form of the expressions will not be given here; those interested should refer to his original paper on the subject. In the presence of crossed electric and magnetic fields it has been seen that amplification occurs when the drift velocity of the electrons in the direction of propagation is greater than the sound velocity. While the condition for geometric resonance remains unchanged, the frequency at which cyclotron resonance can occur is Doppler-shifted from its value in the absence of a d.c. field. This is because the electrons have an average velocity in the direction of propagation. The new condition is that $\omega - q \cdot v_B$ must equal $n\omega_B$. The occurrence of geometric resonances and cyclotron resonance

under conditions of amplification presents more favourable circumstances for studying them than would otherwise be possible. The observation of cyclotron resonance requires $\omega\tau$ greater than unity, that is, frequencies are needed in the range where the attenuation is usually too high to measure anything conveniently. This difficulty is removed under conditions of amplification.

5.3. *Experiments on InSb in the presence of a magnetic field*

The propagation of 9 GHz longitudinal ultrasonic waves in InSb at temperatures between 4.2 and 50K and in magnetic fields up to 25 kG has been studied by NILL and McWHORTER[1966]. Longitudinal waves propagating in the [111] direction are only coupled piezoelectrically to the electrons whereas for the [110] and [100] directions longitudinal waves are only coupled via the deformation potential. This means that measurements of the magnetic field dependent acoustic attenuation in different crystallographic directions allow the deformation potential constant and the piezoelectric coupling constant to be determined independently.

Measurements of the amplification of ultrasonic waves in InSb under d.c. operating conditions in the presence of a transverse magnetic field were made by HAYAKAWA and KIKUCHI[1968] at frequencies of 225 MHz and extended later by ROUTE and KINO[1969b] into the microwave region, 0.5 to 2.0 GHz. Measurements of the acoustic gain for shear wave propagation along the [110] direction were made since it is this orientation which gives the strongest interaction between the drifting carriers and the acoustic wave. Experiments in the microwave range are of interest because the frequency of maximum interaction for this material lies in this region. The material used by Route and Kino was high mobility InSb ($\mu = 6 \times 10^5 \text{ cm}^2/\text{V} \cdot \text{sec}$, $N = 10^{14}$ cm^{-3}) at 77K. The experimental arrangement is shown in fig. 7.6. The bar of InSb was 1 mm^2 in cross section and roughly 1 cm long in the
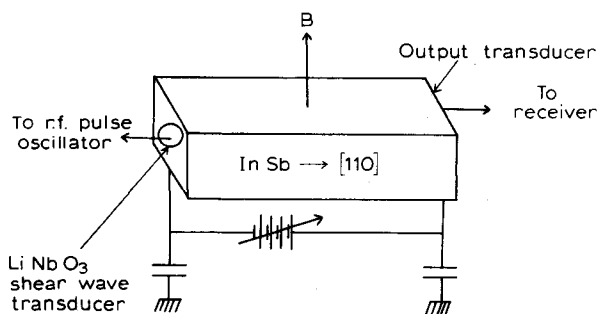
Fig. 7.6.

[110] direction and the opposite ends of the sample were polished optically flat and parallel. Bulk $LiNbO_3$ shear wave transducers and ohmic contacts to apply the drift field were then attached at each end. The acoustic gain was determined by placing the sample in a r.f. circuit and measuring the change in insertion loss as a function of the carrier drift velocity and magnetic field. For high magnetic fields the experimental results agreed well with the theory of White modified by the factor ϕ as described above, see fig. 7.7, but for magnetic fields lower than 3 kG the maximum gain appeared to decrease below that given by theory. A similar behaviour had been observed prior to these results by DOLAT *et al.*[1968]. The explanation is that for $B < 3$ kG the cyclotron radius (or in the case of $B = 0$, the mean free path) of the electrons l becomes comparable to the acoustic wavelength so that in this region, the $ql \gg 1$ theory of SPECTOR[1968] for strong electric fields has to be used. For zero magnetic field ql lies between 5 and 11 in the 1 to 2 GHz range. The degree of agreement between the theory of Spector and experiment is shown in fig. 7.8. It is found that the magnitude of the gain, its linear variation with drift velocity and its frequency dependence are all predicted to within 10%.
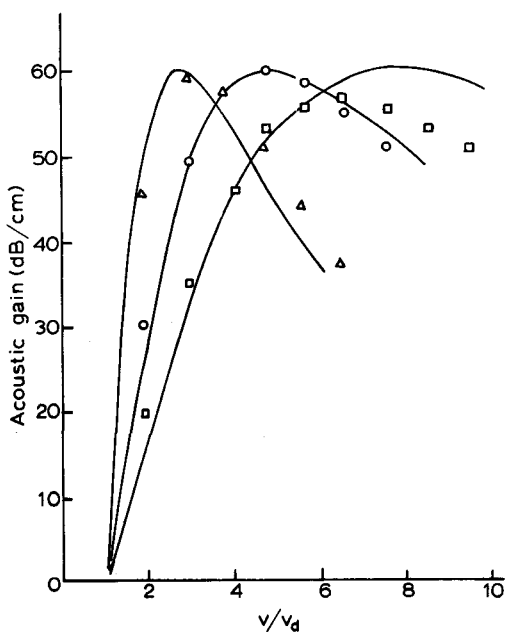
Fig. 7.7. Comparison between experiment and the theory of WHITE[1962] in the high magnetic field limit, $ql \ll 1$. $\triangle B = 6$ kG, $\bigcirc B = 4$ kG, $\square B = 3$ kG; Experimental results of ROUTE and KINO[1969b] at 1.525 GHz. — Theory of White modified by the factor ϕ.
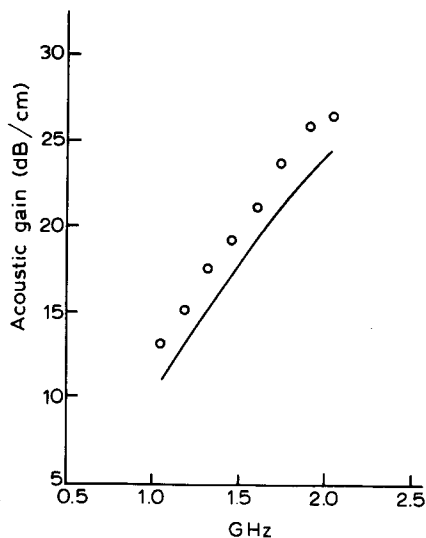
Fig. 7.8. Comparison between experiment and the theory of Spector for the zero magnetic field case, $ql \gg 1$. The results are for $(v/v_d - 1) = 30$. ○ Experiment of Route and Kino, — Theory.

HAYAKAWA and KIKUCHI[1970] have recently reported anomalous behaviour in the ultrasonic amplification of 465 MHz waves at high electric and low magnetic field strengths in InSb at 77K. In the absence of the magnetic field the amplification factor increased linearly as a function of the electric field. When the magnetic field was applied the acoustic gain was first linear for small electric fields but then saturated to give a maximum. For low magnetic fields $B < 2$ kG the gain increased again at higher electric field strengths whereas for $B > 2$ kG it decreased monotonically. The effect could not be observed in the frequency range below 0.3 GHz. The authors took the increase in gain at low magnetic fields to be attributed to Doppler-shifted amplification and in fact made a comparison of their results with the theory of ABE and MIKOSHIBA[1968], §6.4, to obtain qualitative but not quantitative agreement.

6. Non-linear effects

6.1. *Acoustoelectric current*

It was seen in §2.2 that the interaction of an ultrasonic wave with the charge carriers in a piezoelectric semiconductor has two effects. It produces a space charge bunching $n'Q_e$ and an alternating electric

field E' which in linear theory is given by eqs. (7.49) and (7.48) respectively. If the expression for the current density J is examined, eq. (7.36), it is observed that there is a non-linear contribution arising from the interaction of this space charge with the alternating electric field. This can give a d.c. component of current which is referred to as the 'acoustoelectric current'. This effect was first named and discussed by PARAMENTER[1953] but his discussion was centred on metals and non-piezoelectric semiconductors. Using the results of linear theory for n' and E' this d.c. acoustoelectric current is given by

$$J_{ae} = Q_e \mu_e \mathrm{Re}(n') \cdot \mathrm{Re}(E') = -\mu_e \Gamma c |\epsilon'|^2, \qquad (7.100)$$

where the expression of eq. (7.53) for the attenuation coefficient has been used. Now, the acoustic energy flux I is $\frac{1}{2}c|\epsilon'|^2 v$ so the acousto-electric current can be written alternatively as

$$J_{ae} = -2\mu_e \Gamma I / v. \qquad (7.101)$$

This relationship is known as Weinreich's relation after his work on non-piezoelectric semiconductors, WEINREICH[1956]. In his work the coupling of the ultrasonic wave to the carriers arose through the deformation potential. The acoustoelectric effect arises because the acoustic phonons give up momentum to the electrons in addition to their energy. The change in momentum leads to a d.c. force acting on the electrons which can be regarded as an acoustoelectric field. Since the absorption coefficient is proportional to the energy transfer between the acoustic wave and the electrons and the acoustoelectric field is proportional to the transfer of momentum this linear relation between them, according to the Weinreich relation, is only to be expected since the energy and momentum of a phonon are similarly related. The importance of the sign in the Weinreich relation should be noted. When the acoustic wave is being attenuated, Γ positive, the acoustoelectric component of the current is negative. If, on the other hand, conditions are such that amplification occurs, J_{ae} is positive, that is, it is in the direction of the ultrasonic wave. But it has been seen that the condition required for amplification is that the drift velocity of the carriers exceeds that of the wave, which implies that the current $J_0 \equiv Q_e n_0 \mu_e E_d$ must be in the reverse direction. It follows then, that as $|E_d|$ is increased from zero an ultrasonic wave propagating in an antiparallel direction to E_d will set up an acoustoelectric current which adds to J_0. This is so until the magnitude of E_d reaches the critical value v/μ_e, at which point J_{ae} changes direction and opposes J_0.

To account for the fact that not all the space charge produced by the acoustic wave is mobile, a factor f should be included as discussed in §2.3.3. There it was pointed out that f is in general complex because the

mobile and trapped charge bunches need not be in phase. As a consequence of this the simple Weinreich relation, eq. (7.101) breaks down as pointed out by SOUTHGATE and SPECTOR[1965]. The essential point is that J_{ae} is now given by $Q_e\mu_e$ Re (fn') Re (E') so that there is an additional contribution from the product of the imaginary parts of f and n'. In the notation of §2.3.3 the acoustoelectric current is now given by

$$J_{ae} = -\mu_e I \frac{e^2\omega_c}{c\kappa v^2}\left[f_r - \frac{v_d}{v}|f|^2\right]$$

$$\times\left\{\left[1 - \frac{v_d}{v}f_r - \frac{\omega}{\omega_d}f_i\right]^2 + \left[\frac{\omega_c}{\omega} + \frac{\omega}{\omega_d}f_r - \frac{v_d}{v}f_i\right]^2\right\}^{-1} \quad (7.102)$$

which when combined with eq. (7.57) for the attenuation coefficient gives the modified Weinreich relation

$$J_{ae} = -\frac{2\mu_e I\Gamma}{v}\left[f_r - \frac{v_d}{v}|f|^2\right]\Big/\left[1 - \frac{v_d}{v}f_r - \frac{\omega}{\omega_d}f_i\right]. \quad (7.103)$$

This reduces to the ordinary result, eq. (7.101), in the absence of trapping when f is 1 and f_i zero. It is seen that the basic effect of accounting for the trapping of carriers is that the proportionality constant between the acoustoelectric current and the attenuation coefficient is both frequency and drift field dependent. The difference arises because all the space charge contributes to the attenuation coefficient Γ whilst only the mobile part contributes to the acoustoelectric current. An obvious result of eqs. (7.57) and (7.102) is that the acoustoelectric current and the attenuation pass through zero at different electric field strengths. The trapping also affects the minimum and maximum values of J_{ae} and the values of the drift field at which these occur. Expressions for these quantities are given in the paper by Southgate and Spector quoted above. If the model of Uchida et al. is adopted, these authors show that the absorption coefficient changes sign at a higher value of drift field than that for the acoustoelectric current.

A non-linear theory of acoustoelectric gain and current in piezoelectric semiconductors which takes explicit account of the non-linearities in the derivation of the formulae for acoustic gain and acoustoelectric current has recently been developed by BUTCHER and OGG[1968]. Recalling from §2.2 that the expression for the total current density is

$$J(t) = Q_e\left[(n_0 + n')\mu_e E + \mathcal{D}\frac{\partial n'}{\partial x}\right] + \frac{\partial D}{\partial t} \quad (7.104)$$

it follows on substituting for n' from Poisson's equation $\partial D/\partial x = -Q_e n'$ that

$$E = \{J + \mathcal{D}(\partial^2 D/\partial x^2) - \partial D/\partial T\}/\{b[1 - (Q_e n_0)^{-1}\partial D/\partial x]\}. \quad (7.105)$$

It is assumed that $J(t)$ has a time independent value J. The non-linearity is contained in the denominator of this equation. To recover linear theory this denominator is expanded in powers of $(Q_e n_0)^{-1} \partial D / \partial x$ and only the linear terms retained. As Butcher and Ogg have pointed out this is clearly incorrect if the electron concentration approaches complete depletion as is expected to occur under conditions of strong electron bunching in the presence of large amplitude sound waves.

In the non-linear regime the electric displacement is assumed to have the form

$$D = D_d + \tfrac{1}{2} D_0 \exp \left[i(\omega t - qx) \right] + \text{c.c.}$$

but now D_d and D_0 are treated as functions of x and t which are slowly varying compared to the exponential. If this is substituted into eq. (7.105) it is found that the local d.c. and fundamental components of the electric field determined by

$$E_d = \frac{1}{2\pi} \int\limits_0^{2\pi} E d\theta, \qquad E_0 = \frac{1}{2\pi} \int\limits_0^{2\pi} E e^{-i\theta} d\theta \qquad (7.106)$$

are given by

$$E_d = E_s \left(\frac{\beta}{(1 - |a|^2)^{1/2}} - 1 \right), \qquad (7.107)$$

$$E_0 = - \frac{E_s a}{[1 + (1 - |a|^2)^{1/2}]} \left(\frac{\beta}{(1 - |a|^2)^{1/2}} + \frac{i\omega}{\omega_D} \right). \qquad (7.108)$$

θ is the phase $(qx - \omega t)$ and the parameter a is $-iqD_0/Q_e n_0$. E_s is the synchronous field v/μ_e and β is $1 + J/J_s$ with $J_s = n_0 Q_e v$. The integrations are best performed by contour integrating around a unit circle when $\exp(-i\theta)$ is replaced by z.

Equation (7.107) may be solved for the total current J to give the result

$$J = b E_d - J_s \gamma [1 - (1 - |a|^2)^{1/2}]. \qquad (7.109)$$

The last term is a corrected form of the Weinreich relation for the acoustoelectric current density. For small amplitude acoustic waves, when $|a|$ is small, the square-root may be expanded to give

$$J_{ae} = -\tfrac{1}{2} J_s \gamma |a|^2. \qquad (7.110)$$

Then by use of eqs. (7.43), (7.48) and (7.53) the usual expression relating the acoustoelectric current to the amplification factor, eq. (7.101), is recovered. Alternatively Butcher and Ogg point out that the total current density may be written as

$$J = b E_d (1 - F) - J_s F \qquad (7.111)$$

with $F = 1 - (1 - |a|^2)^{1/2}$. The interpretation of the factor F is clear. The total current behaves as if the factor F of the electrons were trapped at the sound velocity while the rest exhibits the normal ohmic response to the d.c. local electric field.

If eq. (7.107) is used to eliminate J from eq. (7.108) for E_0 it is found that

$$E_0 = \frac{i\omega D_0}{2\kappa\omega_c(F)} [\gamma + i\omega/\omega_D], \qquad (7.112)$$

where $\omega_c(F) = \omega_c(1 - \frac{1}{2}F)$. This result, together with the wave equation, eq. (7.39), and the constitutive relation, eq. (7.30), can be used to obtain the amplification coefficient and the shift in wave number. The results are in agreement with those of eqs. (7.52) and (7.53) if ω_c is replaced by $\omega_c(F)$. The frequency corresponding to maximum gain now occurs at $[\omega_c(F)\omega_D]^{1/2}$ which is a function of $|a|$. As $|a|$ is increased from zero to unity the peak gain frequency is reduced to 30%. When $(\omega_c(F)/\omega)^2 < (\omega/\omega_D)^2 + \gamma^2$ the magnitude of the gain will also decrease as $|a|$ increases.

The results of this work depend on the assumption that the space charge distribution is sinusoidal, which is certainly not the case under conditions of strong electron bunching. This restriction was lifted in a second paper by BUTCHER and OGG[1969] where the results were generalized to the case when the electron density associated with the acoustic wave is an arbitrary but nearly periodic wave, moving with a velocity close to the velocity of sound. This problem had previously been treated by TIEN[1968] who gave a numerical calculation of the acoustoelectric gain.

Recently, RIDLEY and WILKINSON[1969] in a series of papers have employed the Krylov–Bogoliubov method to obtain differential equations describing the growth of acoustic flux in the non-linear regime.

6.2. *Current saturation and oscillations*

A great deal of experimental and theoretical work on non-linear effects in piezoelectric semiconductors stems from the initial observation by SMITH[1962] of current saturation and oscillations in CdS. There was ample experimental evidence to suggest that the saturation arose from the bulk of the material and could not be associated with a contact phenomenon. In particular Smith observed that the current in semiconducting CdS saturated at an applied electric field whose value was such that the drift velocity of the electrons was comparable to the velocity of sound in the crystal. This suggested that the current saturation arose from a saturation of the drift velocity of the electrons due to energy transfer from the electron stream to a travelling wave of

phonons in the crystal. A typical current–voltage characteristic, shown in fig. 7.9 was obtained for a $0·1\ (\Omega \cdot \text{cm})^{-1}$ CdS crystal with the electric field parallel to the c-axis using voltage pulses of $10\ \mu\text{sec}$ duration. The specimen was $0·05$ cm long so that saturation occurred around an applied electric field 1600 V/cm. Since $\mu \approx 300\ \text{cm}^2/\text{V} \cdot \text{sec}$ the drift velocity of the electrons in this field is $\sim 5 \times 10^5$ cm/sec, close to the longitudinal acoustic wave velocity in CdS. For electric fields greater than the critical value, it was found that when the voltage pulse was applied the current rose to its initial ohmic value but then decayed in an oscillatory fashion to its saturated value. This behaviour is shown in fig. 7.10. The oscillations were thought to be shock excited since their frequency was about 2 MHz which corresponds to that expected if the fundamental mode was excited for the length of specimen used.
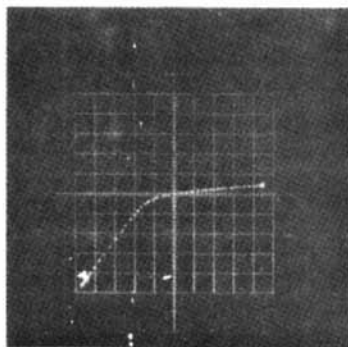
Fig. 7.9. (Reproduced from R. W. Smith, Phys. Rev. Lett. 9, 87 (1962) with permission.)

At about the same time, Esaki[1962] performed an experiment on bismuth in which he observed a sharp change in the shape of the current–voltage characteristic. In his experiment a d.c. magnetic field at right angles to the electric field was also present. As discussed in §5.1 these crossed fields produce in addition to a cyclotron motion a drift of the electrons and holes in the direction of $E \times B$. In addition, if the electron lattice collisions interfere with the cyclotron motion there is also a current in the direction of the applied electric field. Esaki observed that this current increased sharply as a function of the magnitude of the electric field when the drift velocity exceeded a value near to the acoustic wave velocity in bismuth. The similarity of the observations in the experiments of Esaki and Smith was noted by Hutson [1962] who proposed an explanation in terms of acoustoelectric currents accompanying an acoustic flux produced in a traveling wave
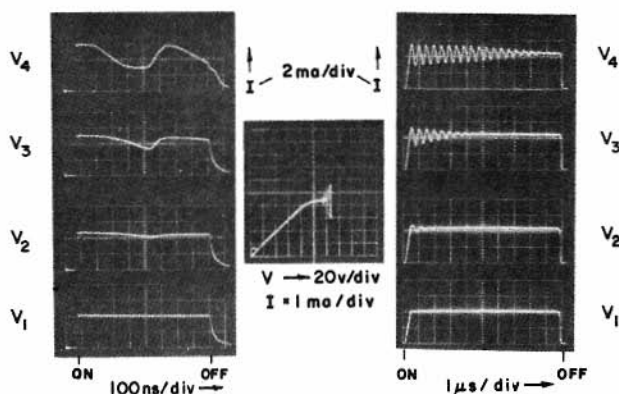
Fig. 7.10. Time dependence of current for d.c. voltage pulses. V_1 corresponds to a voltage just below the knee of the $V-I$ curve while V_2, V_3 and V_4 correspond to increasing increments in voltage going over the knee. Left: Current pulses due to 1 ns rise time voltage pulses; decay time of voltage pulse $\sim$ 100 ns. Centre: $V-I$ characteristic. Right: Current pulses due to essentially equivalent amplitude voltage pulses as left curves but of 10 μs duration. Voltage pulse rise time here $\sim$ 30 ns. Pulse repetition rate $\sim$ 60 pulses/sec in both cases. (Reproduced from R. W. SMITH, Phys. Rev. Lett. 9, 89 (1962) with permission.)

amplification process. Hutson proposed that in a certain frequency range a build up of acoustic flux might occur through the mechanism proposed by White. A stationary state for the acoustic flux under amplifying conditions would occur when the amplitude of the amplified waves was sufficiently great to bring a non-linear loss mechanism into equality with the gain. In the case of Smith's experiment, when the electric field is above the amplification threshold an acoustoelectric current will be produced parallel to the acoustic flux that is built up and hence is in opposition to the ohmic current as described in §6.1. This is illustrated in the vector diagram of fig. 7.11(a). In Esaki's experiment on bismuth the electrons and holes drift at right angles to both
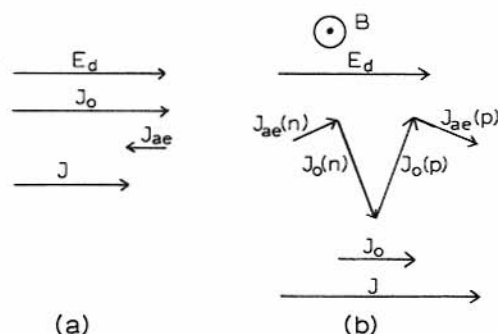
Fig. 7.11.

the electric and magnetic fields so that their ohmic currents are inclined at their respective Hall angles (assumed equal) as shown in fig. 7.11(b). When the drift velocity exceeds the velocity of sound and an acoustic flux is set up, the electrons and holes will be driven in the reverse direction to the flux but because of the magnetic field the acoustoelectric currents will be rotated through the appropriate Hall angle as shown. In this case it is seen that the acoustoelectric currents add to the ohmic currents in agreement with the experimental observation by Esaki of a sudden increase in the current–voltage characteristic.

Current instabilities of acoustoelectric origin have now been observed in several groups of piezoelectric semiconductors. For example in the group II–VI semiconductors in addition to CdS, oscillations have been observed in CdSe and CdTe, KIKUCHI [1964], and in ZnO, McFEE [1963] and MEYER and JORGENSEN [1966]. In the III–V group, instabilities have been reported in p-type GaSb, SILVA and BRAY [1965], p-type InSb, ROSS and BRAY [1966] and in n-type GaAs, HERVOUET et al. [1965]. Also the measurements of QUENTIN and THUILLIER [1966] on Te may be quoted as an example of a group VI semiconductor where oscillations have been observed. One form of instability consists of continuous oscillations of current between an ohmic and high resistance state. This arises from the build up of successive domains of high resistance which propagate through the sample with the velocity of sound in the direction of the carrier drift. In a second type of instability, ISHIDA et al. [1966], the current changes from ohmic to a steady high resistance state which corresponds to the eventual formation of a stationary domain at the down stream electrode. The demarcation between the two types of behaviour is somewhat confused; frequently damped oscillations of the current, culminating in a steady high resistive state, can be observed.

6.3. *Observation of acoustic domains*

Several workers have carried out investigations to demonstrate the formation of acoustic domains in piezoelectric crystals using a variety of methods. For example SILVA and BRAY [1965], HAYDL and QUATE [1966] and McFEE et al. [1967] among others have employed surface probes to detect the high electric field which accompanies the domains while other workers, ZUCKER and ZEMON [1966], have adopted optical, and HOBSON and PAIGE [1966], transmission methods. An acoustic pulse generated when the voltage pulse is applied to the crystal is amplified as it travels towards the anode. Because the acoustoelectric current is in a direction opposite to the drift current, when the carrier velocity exceeds the sound velocity the total current decreases as the acoustic pulse is amplified. At some point the pulse amplitude will in-

crease to a value such that the acoustoelectric current increases with electric field faster than the drift current. The differential conductivity within the bulk of the material becomes negative at this point and the electric field through the crystal becomes non-uniform. HAYDL and QUATE employed tungsten probes to examine this field in n-type semi-conducting CdS samples having resistivities of 8 and $1.5 \, \Omega \cdot cm$ at 300 and 77 K respectively. Above a certain threshold field the current remained ohmic for a time t_0 and then decayed to a value J_a where it remained for a time $(\tau - t_0)$. τ was the oscillation period. Both the time τ and the current J_a were independent of field and temperature. The current J_a was given by $nQ_e v_0$ and the period τ by L/v_0 with L the electrode separation. The velocity v_0 agreed with the velocity of shear waves in CdS. Evidence for the domains is clearly seen in fig. 7.12(a). These figures show various probe voltages (the anode is grounded and V_1 is nearest the cathode) as a function of time. When the domain enters the region between the probe and the anode the probe voltage increases rapidly, showing that the domain is a high resistive region. The velocity of the domain can be obtained from the probe spacing and is found to be v_0. The character of the domain as it is formed at t_0 and travels to the anode is shown in fig. 7.12(b).

ZUCKER and ZEMON[1966] used the photoelastic scattering of light to investigate the frequency spectrum of acoustic shear wave packets generated in semiconducting CdS by high electric fields. They found that the frequencies were in the range 10^8—1.5×10^9 Hz which is at least an order of magnitude lower than the predicted frequency for maximum gain on the linear theory.

A particularly interesting experiment was reported by MOORE[1968] who used a modification of the optical strain birefringent method which enabled the acoustic domains to be made directly visible to the eye or to be photographed. The principle of the method is quite standard: the strain accompanying the acoustic flux produces a local change in the birefringence which is detected by placing the crystal between crossed polarizers. However instead of illuminating the sample with a c.w. laser beam focussed at a given spot through which the fully formed domain was expected to pass, Moore illuminated the whole crystal from anode to cathode with light from a pulsed laser. It was found that when the light pulse is sufficiently short and the time delay between the start of the electric field or drift pulse and the light flash is properly adjusted the domain could be caught in mid-flight and made visible in two dimensions. This optical stroboscopic method has the advantage over potential probing that the spatial distribution of acoustic energy within the crystal and even within the domain could be observed either during or after the pulse, all without any influence on the potential distribution.
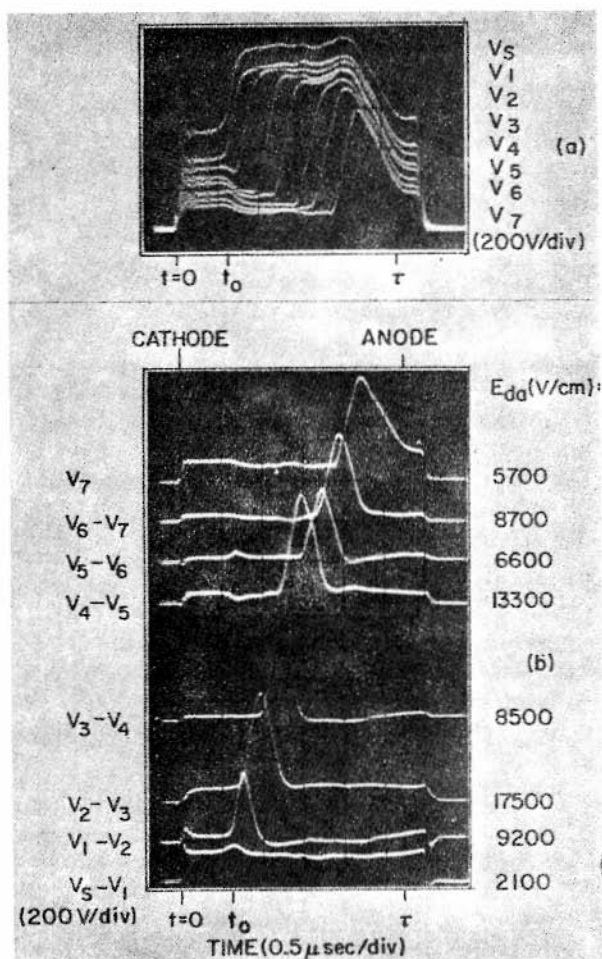
Fig. 7.12. (Reproduced from W. H. HAYDL and C. F. QUATE, Phys. Lett. 20, 464 (1966) with permission.)

Potential probing has the disadvantage that it is confined to the surface and so may not give a true picture of what is happening in the bulk of the sample. A schematic diagram of the experimental arrangement used by Moore is shown in fig. 7.13. The light source was a GaAsP injection laser operated at 78 K driven by a pulse generator which results in a 20 nsec light pulse at 6440 Å. During the flash the domain moved about 25 μm. The crystal was illuminated uniformly as far as possible by projecting onto it an enlarged. but slightly out of focus, image of the laser line. Between the source and the crystal the light passed through a polarization rotator to set the polarization plane at
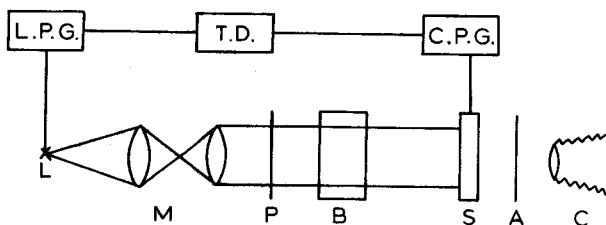
Fig. 7.13. L.P.G.–laser pulse generator; T.D.–time delay; C.P.G.–crystal pulse generator; L–injection laser light source; M–microscope; P–polarizer and polarization rotator; B–Babinet–Soleil compensator; S–crystal sample of CdS; A–analyzer; C–camera.

45° to the c-axis of the sample. A Babinet–Soleil compensator was also employed to correct for the natural birefringence of the CdS so that the crossed analysers at the other end of the specimen could extinguish the transmitted beam. All the CdS semiconducting samples used by Moore exhibited current oscillation which was characteristic of domain formation and drift, that is ohmic incubation time, decay of the current to its acoustically saturated value $nQ_e v_0$, drift time, and current rise back to ohmic to restart the cycle. Fig. 7.14 shows a composite photograph of 14 steps in the time evolution of a domain. The pictures were taken in $\frac{1}{4}\mu$sec intervals and begin at the top at the time when the drift pulse was first applied. The pictures are for a specimen 5 mm long and 1×1 mm in cross section with the c-axis oriented perpendicular to the electric field. The photographic method is best suited for measuring the velocity of the domains and for determining their shape. It is not very good for accurate measurements of the strain amplitudes.

6.4. *Magnetic field dependence of acoustoelectric oscillations*

A curious transverse magnetic field dependence of the current oscillation in InSb at 77 K was reported by KIKUCHI *et al.* [1966]. A graph of the threshold electric field for the onset of current oscillation as a function of the applied transverse magnetic field is shown in fig. 7.15. In the absence of a magnetic field the current oscillations were quickly damped, but when the magnetic field was increased the threshold electric field was found to decrease and the oscillations were greatly enhanced. This reduction in the threshold electric field continued up to a magnetic field value of about 400 G. At this point the curve passed through a minimum. For higher magnetic field strengths the threshold electric field is increased until at about 3 kG the oscillations disappeared. However, it was found at around the 2kG mark that a second branch became operative whose threshold field value was very low. For this branch the threshold field at first decreased monotonically with increasing magnetic field and then saturated. An explanation of
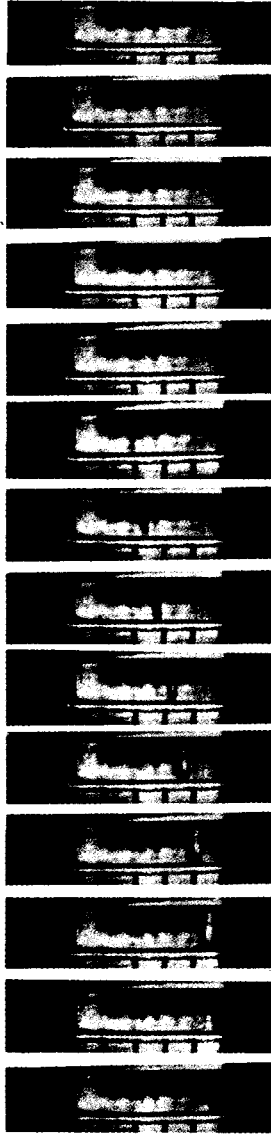
Fig. 7.14. (Reproduced from A. R. MOORE, Appl. Phys. Lett. **13**, 128 (1968) with permission.)

the mode II behaviour was put forward by KINO and ROUTE[1967] who repeated the experiments of KIKUCHI *et al.*[1966] with similar results. They assumed that the acoustoelectric domains resulted from a growth of acoustic noise excited at the cathode. If it is assumed that the
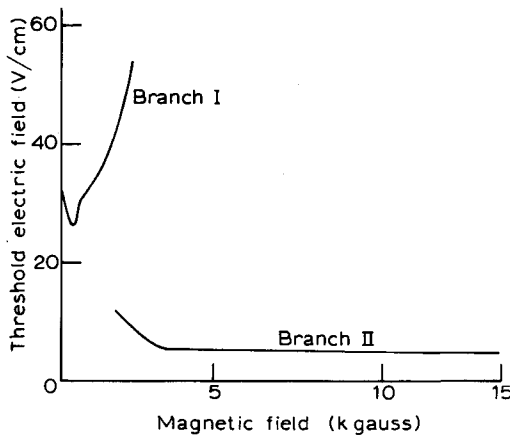
Fig. 7.15. Threshold electric field for acoustoelectric current oscillation in InSb at 77 K as a function of the transverse magnetic field. (After Kikuchi *et al.*)

samples cross section is much greater than the wavelength of the sound waves involved, the one-dimensional theory of White for sound propagation in a piezoelectric semiconductor is appropriate. Because the wavelength was much less than the sample dimensions it was assumed that the r.f. Hall fields could be neglected, so that the effect of the transverse magnetic field was to reduce the effective r.f. mobility and diffusion constant by the factor $\phi = [1 + (\omega_B \tau)^2]^{-1}$ as discussed in §5.1. The amplification factor is then given by the result of White, see eq. (7.53), suitably modified by this factor. The frequency of maximum gain is still at $\omega_{max} = (\omega_c \omega_D)^{1/2}$ at which frequency the gain is a maximum when the electron drift velocity v_d is

$$v_d = v[1 + 2\phi(\omega_c/\omega_D)^{1/2}]. \tag{7.113}$$

The effect of the transverse magnetic field is to cause the factor ϕ to be small and hence the electron drift velocity for maximum gain to be greatly reduced. To obtain a threshold condition for domain formation it was assumed that the first component of thermal noise (given by ω_{max}) to reach a certain critical amplitude would precipitate a domain. Since the net acoustic gain in InSb is small, it is thus to be expected that the threshold condition for domain formation would correspond roughly to the electron velocity for maximum gain at the frequency of maximum gain. Thus the threshold for domain formation would be when the drift velocity v_d assumes the value given by eq. (7.113). The agreement between theory and experiment on the basis of this theory is quite good for mode II operation as shown in fig. 7.16. The authors also attempted an explanation of mode I operation based on the effect of
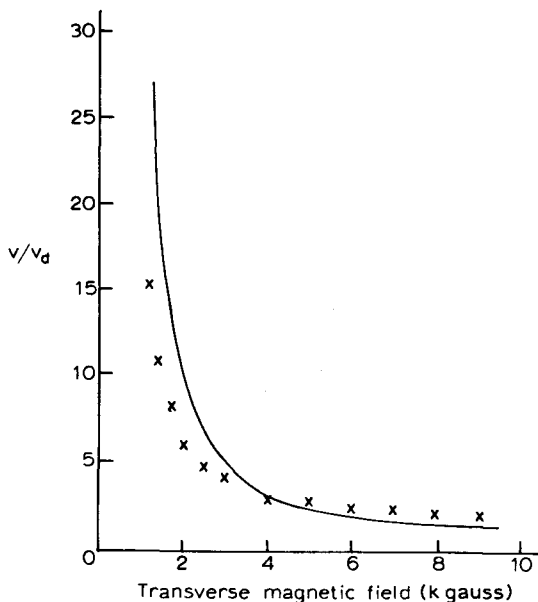
Fig. 7.16. Threshold for domain formation for mode II operation. × Experiment. — Theory.

inertial terms in the equation of motion but it was not entirely satisfactory. It was suggested that a more accurate analysis based on a quantum mechanical theory might give a better result.

An explanation of mode I operation was subsequently put forward by ABE and MIKOSHIBA[1968]. In branch 1 it is to be noted that the drift velocity v_d of the electrons becomes much larger than the sound velocity. This is important for two reasons. Firstly, the extent to which the transverse magnetic field affects the ultrasonic amplification depends on the magnitude of the screening which occurs. A large drift velocity of the electrons may change the situation from one of nearly complete screening to one of incomplete screening. In the nearly complete screening case $\omega \ll \omega_c$ the amplification coefficient is proportional to $1/\omega_c$ and hence to the inverse of the conductivity. The transverse magnetic field then increases the amplification by decreasing the a.c. conductivity. On the other hand, when $\omega \gg \omega_c$ the amplification factor is proportional to ω_c and hence decreases with magnetic field. This decrease in amplification has been observed in GaAs with low carrier concentrations and low mobility. Secondly, as pointed out by Kino and Route the apparent frequency of the ultrasonic waves is Doppler shifted to a value of the order of the inverse electron relaxation time. To account for the Doppler shift Abe and Mikoshiba used

the following expression for the electronic current J

$$\frac{\partial J}{\partial t} + v_e \nabla J - \frac{n}{m} Q_e^2 E - \frac{Q_e}{B} B \times J = -\frac{J}{\tau} - Q_e \frac{\mathcal{D} \nabla n}{\tau} \qquad (7.114)$$

and then used the equation of continuity and the small signal analysis of White to obtain an expression for the a.c. conductivity tensor, including dispersion. This was then used to obtain the amplification factor. Finally, by introducing the somewhat arbitrary criterion that the threshold electric field for acoustoelectric current oscillation is determined by the condition $|\Gamma_{max}| = \Gamma_{loss}$, fair agreement between theory and the experiment of Kikuchi *et al.* was obtained for both modes of operation. Γ_{max} is the amplification factor for the frequency of maximum gain and Γ_{loss} is ten times the loss computed for an Akhieser-type mechanism.

ROUTE and KINO[1969a] have recently reported further measurements on InSb in the microwave frequency range, in the presence of a transverse magnetic field. To include the effect of a drifting carrier distribution they simply modified the microscopic theory of SPECTOR [1962b] by shifting to a moving frame of reference. This microscopic theory clearly accounted for the two-mode behaviour but the numerical agreement was still only moderate.

6.5. *The present theoretical situation*

On the theoretical side several detailed theories have now been put forward to account for non-linear phenomena. It is beyond the scope of this book to describe these theories in any detail so no more than a brief reference to a few of them will be made. Theories based on the classical approach, and thus limited to the $ql < 1$ regime have been given by GUREVICH[1963] and by ABE[1964]. In these phenomenological approaches the lattice vibrations of long wavelength are regarded as setting up a potential field which acts on the electrons. Abe studied the steady state solution of the non-linear one-dimensional coupled equations for electrons and one acoustic wave. Non-linearities were taken into account by the expressions for the current, in the piezoelectric coupling and in the anharmonic terms of the lattice vibrations. He was able to obtain a steady state solution for the amplitude of the acoustic wave and to obtain the kink character of the current. It is doubtful, though, whether his solution can correspond to any real physical situations because it is unlikely that a single wave will propagate through the crystal without harmonic generation occurring.

A second approach is based on the quantum treatment and involves setting up coupled Boltzmann equations for the phonons and electrons. PROHOFSKY[1964] and YAMASHITA and NAKAMURA[1965] were the

first to set up a theory along these lines. The method which may be applied to the $ql > 1$ regime treats the lattice vibrations of short wavelength as particles, phonons, which interact with the electrons. This approach is sometimes referred to as the Čerenkov emission mechanism, while the phenomenological approach is termed the bunching mechanism. Recently NAKAMURA and YAMASHITA[1968] have presented a treatment of non-ohmic conduction in piezoelectric semiconductors which unifies the two approaches on the basis of the electron–phonon interaction from the quantum point of view. OZAKI and MIKOSHIBA[1966], (see also MIKOSHIBA and OZAKI[1968]) have also given a theory for the $ql < 1$ regime to describe the current saturation in cadmium sulphide. Their constitutive equations consisted of coupled Boltzmann equations for the conduction electrons and the amplified phonons. A three-phonon process via a non-linear interaction with the electrons was accounted for by introducing a non-linear relaxation time involving a variable parameter. When a suitable choice of this parameter was made, a semi-quantitative explanation of the current–voltage characteristics, the decay time of the current from ohmic to its saturation value and the characteristic features of the acoustoelectric after-current was obtained. On the basis of this work OZAKI and MIKOSHIBA[1968] have derived a simple criterion for the onset of acoustoelectric current oscillation. They propose that the threshold drift velocity of the carriers for oscillation is determined by the condition that the decrease of drift velocity due to amplified phonons during the one-way transit time of the phonons through the sample becomes an appreciable factor (say 10%) of the difference between the ohmic drift velocity and the velocity of sound. Numerical estimates for Te, CdS, GaAs, InSb and the non-piezoelectric semiconductor Ge give a fair agreement with experiment.

MICROWAVE ULTRASONIC PROPAGATION IN METALS

1. Introduction

Because of the very high attenuation due to the presence of the con-
duction electrons, very few experiments have been performed in
metals using ultrasonic waves in excess of 1 GHz. The majority of
experiments that have been carried out involve the use of super-
conductors below the transition temperature, where the high attenua-
tion is substantially reduced.

   In a metal, of course, attenuation mechanisms similar to those dis-
cussed in ch. 4 also occur, in which the ultrasonic waves are attenuated
by the anharmonic forces in the lattice. At high frequencies and at
high temperatures this will be the dominant mechanism of attenuation.
As the temperature is reduced the lattice contribution to the attenua-
tion falls whereas the electron attenuation, for high frequencies,
remains constant. The electronic contribution to the attenuation thus
becomes dominant in the low temperature range for high frequency
waves. At low frequencies the electron attenuation depends on the
mean free path of the electrons and this results in an increase in
attenuation with decreasing temperature. It is clear that an important
parameter of the material that needs to be considered is the mean free
path l of the conduction electrons and the related relaxation time τ.
As was discussed in ch. 7, it is convenient to divide the ultrasonic
frequency range into two regions depending on whether the product
ql is less or greater than unity. q denotes the wave number of the
ultrasonic wave. In a reasonably pure material at low temperatures, it
will be found that ql is unity for ultrasonic frequencies much less than
1 GHz. For example, using a typical value of 10^{-3} cm for l at 4 K and
an ultrasonic velocity of 5×10^5 cm/sec it is found that $ql = 1$ at a
frequency of only 80 MHz. Thus it is not necessary to use microwave
frequencies to investigate the region for which $ql > 1$ in pure metals.
It may be necessary, though, in impure and alloy materials where the

mean free path of the electrons is much less. This was true in the work of TITTMANN [1970] where a frequency of 1 GHz was used yet the value of ql was estimated to be only 0.01. The experiment was on a single crystal of the alloy vanadium – 5.6 at.% tantalum at temperatures in the liquid helium range. On the other hand it is not yet possible to reach frequencies where $\omega\tau > 1$ because of the great difference in the ultrasonic velocity v and the Fermi velocity v_f. Typically the ratio v/v_f is about 10^{-3} and thus at a given frequency $\omega\tau \approx 10^{-3} ql$. Experiments by DOOLEY and TEPLEY [1969a] have almost reached this region. They worked at 9.3 GHz using bismuth specimens for which $\omega\tau$ was 0.175 to 0.3 in the liquid helium temperature range.

The high attenuation in metals gives rise to experimental difficulties, in particular a very short specimen must be used and then it is more convenient to use a transmission system rather than a pulse-echo reflection system. Figure 8.1 shows the apparatus used by FAGEN and GARFUNKEL [1967] in which two quartz rods in microwave cavities act as transmitter and receiver and a thin metal specimen is sandwiched between them.

Ultrasonic attenuation in metals is magnetic field dependent and many experiments have been made at frequencies below 1 GHz in studying the shape of the Fermi surface. It is usually sufficient to work in the region $ql > 1$ to do this and the added complication of microwave frequencies is unnecessary except in materials with very short electron mean free paths. The other area in which the study of ultrasonic attenuation in metals has proved particularly fruitful has been in the study of superconductors where such measurements have provided strong support for the Bardeen–Cooper–Schriefer (BCS)

Waveguides
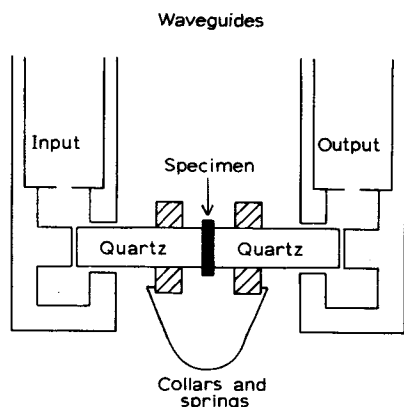
Fig. 8.1. Apparatus used by FAGEN and GARFUNKEL [1967] to study ultrasonic attenuation at 9.3 GHz in aluminium.

theory of superconductivity. Most aspects of this can be adequately studied at frequencies in the range 10 to 100 MHz. An exception is the observation of the creation by phonons of quasi-particles having energies greater than the energy gap, a phenomenon that can only convincingly be observed at microwave frequencies and above. Other experiments which require microwave ultrasonic waves are those which concern type II superconductors. Dirty type II materials have a short electron mean free path and microwave frequencies are needed to reach the region $ql > 1$. Type II materials in the mixed state contain an array of flux lines and it is possible that anomalies in the ultrasonic attenuation may occur when the wavelength of the ultrasound is equal to the flux line spacing. This requires the use of high frequencies.

In the following sections, a brief review of the effects which are most easily observed below the microwave frequency range will be given, together with an account of those phenomena for which microwave frequencies are necessary.

2. Normal metals

2.1. Acoustic attenuation in the absence of a magnetic field

The reasons for the very high attenuation in normal metals will now be considered. This topic has been discussed in the books by TRUELL et al. [1969] and BEYER and LETCHER [1969] while a useful review is due to MACKINTOSH [1964].

The mechanism of the electron–phonon interaction has been considered at some length in ch. 7 where it was applied to a discussion of the ultrasonic attenuation in semiconductors. Thus for a metal to which the free-electron model with a spherical Fermi surface is applicable, eq. (7.83) and the result of the discussion following eq. (7.74) can be applied to give

$$\alpha = \frac{2m^2 E_f^2 \omega}{9\pi \rho \hbar^3 v^2}, \qquad (8.1)$$

where α is the intensity attenuation coefficient for longitudinal waves in the regime $ql > 1$, m is the electron mass, E_f the Fermi energy, ρ the density and v the ultrasonic wave velocity. The attenuation is linearly dependent on the frequency $\omega/2\pi$ but is independent of l and thus is independent of temperature so long as the condition $ql > 1$ holds. As a typical set of values for the parameters in eq. (8.1), $E_f = 7.0$ eV, $\rho = 8.89$ g $\cdot$ cm^{-3}, $v = 5 \times 10^5$ cm $\cdot$ sec^{-1} may be quoted which are approximately those pertaining to copper. These figures give an attenuation at frequency f of $17.8 \times 10^{-9} f$ cm^{-1}. At 1 GHz and 10 GHz the attenuation is thus about 77.3 dB $\cdot$ cm^{-1} and 773 dB $\cdot$ cm^{-1} respectively.

The expression of eq. (8.1) which was deduced in ch. 7, was obtained by PIPPARD [1955] as the limiting case, when $ql \gg 1$, of a more general treatment valid for all values of ql. His treatment which was a semi-classical one has been summarised by MACKINTOSH [1964] and has been extended to the case of a metal in the presence of a magnetic field by COHEN et al. [1960]. An account of their theory is given in ch. 7§4.1. The coupling between the electrons and the ultrasonic wave is of electromagnetic origin. As the ultrasonic wave passes through the metal the positive ions move and if the electrons do not quite follow them, electric fields are generated which act on the electrons to produce an electron current. In the case of a longitudinal wave the changes in density cause a space charge to be built up which generates the electric fields directly. In the case of a transverse wave there is no density change but the positive ion current gives rise to an oscillating magnetic field which produces an electric field to drive the electrons. The electrons thus gain energy from the ultrasonic wave and lose energy by the collision processes responsible for electrical resist-ance. These collision processes can frequently be described by a relaxation time τ or a mean free path l. COHEN et al. [1960] expresses the ultrasonic attenuation in terms of a generalized electrical con-ductivity tensor which describes the loss of energy by the electrons. It should be noted that the electron system is relaxing by collisions with the positive ion lattice – impurities, thermal phonons etc. – and thus there is a 'collision drag' effect whereby some energy is fed back into the ultrasonic wave carried by the positive ion lattice.

The final expression obtained by PIPPARD [1955] is now quoted. In the case of longitudinal waves the attenuation coefficient for the energy is given by

$$\alpha = \frac{n_0 m}{\rho v_\ell \tau} \left[\frac{1}{3} \frac{q^2 l^2 \tan^{-1}(ql)}{ql - \tan^{-1}(ql)} - 1 \right], \tag{8.2}$$

where n_0 is the number of free electrons per unit volume and the other symbols are as defined above. It is seen that in the high frequency limit when $ql \gg 1$ eq. (8.2) becomes

$$\alpha \approx \frac{\pi n_0 m q l}{6 \rho v_\ell \tau} = \frac{\pi n_0 m v_f \omega}{6 \rho v_\ell^2} \tag{8.3}$$

where $v_f = l/\tau$ is the Fermi velocity and v_ℓ the longitudinal sound velocity. In the case of a spherical Fermi surface when n_0 is given by eq. (7.74) and v_f is $(2E_f/m)^{1/2}$, eq. (8.3) becomes

$$\alpha \approx \frac{2m^2 E_f^2 \omega}{9\pi \rho \hbar^3 v_\ell^2}$$

and thus the result of eq. (8.1) is recovered. For the case of transverse

waves, Pippard finds that

$$\alpha = \frac{n_0 m (1 - g)}{\rho v_t \tau g} \tag{8.4}$$

where v_t is the velocity appropriate to transverse ultrasonic waves and g is the function

$$g = \frac{3}{2q^2 l^2} \left[\frac{q^2 l^2 + 1}{ql} \tan^{-1}(ql) - 1 \right].$$

When ql attains the value unity but with $\omega \tau$ still very small, eq. (8.4) takes the form

$$\alpha = \frac{4 n_0 m v_f \omega}{3 \pi \rho v_t^2} \tag{8.5}$$

which is very similar to the expression of eq. (8.3) for longitudinal waves. However it is found that when ql becomes much larger, the value of α at the highest frequencies is independent of frequency and inversely proportional to the relaxation time. When ql is very much less than unity Pippard finds that both the longitudinal and transverse attenuation constants are proportional to $\omega^2 \tau$. It should be stressed, though, that these expressions were derived using the free electron model of a metal with a spherical Fermi surface. To sum up, the attenuation is a function of frequency, quadratic in frequency at low frequencies and becoming linear at higher frequencies. At very high frequencies the attenuation of the longitudinal waves increases in proportion to the frequency without limit, while that of the transverse waves tends to a constant value. The low frequency attenuation is temperature dependent through the temperature variation of the mean free path, l, but at very low temperatures the attenuation should tend to a limiting value when ql becomes greater than unity.

These expressions have not been tested in the microwave frequency range because, as indicated, the attenuation is very large in that case. An outline of the quantum mechanical treatment of ultrasonic attenuation is given by MACKINTOSH [1964] and by TRUELL et al. [1969] to which the reader is referred in addition to ch. 7 of this book.

2.2. Magnetic field dependent effects

Much information on the Fermi surfaces of metals has been obtained by investigating the attenuation of radio-frequency ultrasonic waves in metals as a function of the applied magnetic field. Very little work has been reported for the microwave region because of the experimental problems associated with the high attenuation and because it seems unlikely that information can be obtained which cannot be gained at frequencies of tens or hundreds of megahertz. Therefore

only an outline of the effects observed will be presented here; for a fuller account reference should be made to MACKINTOSH[1964] or PEVERLEY[1966].

As seen in ch. 7§5, when a magnetic field is applied to a metal or semiconductor the motion of the conduction electrons is modified. In the presence of a magnetic field there is a Lorentz force $-Q_e v_e \times B$ acting on the electrons which causes their wave vector to change at a rate

$$\hbar \frac{dk}{dt} = Q_e v_e \times B. \tag{8.6}$$

The motion of the electron is thus a helix about the magnetic field direction and the frequency with which the electron traces out a circular path is $\omega_B = Q_e B/m$, the cyclotron frequency. In a quantum treatment the motion is quantized and the electron states have energies determined by the Landau formula, eq. (7.99),

$$E = (n + \tfrac{1}{2})\hbar\omega_B + \hbar^2 k_z^2/2m. \tag{8.7}$$

k_z is the component of the electron wave vector along the direction of B taken as the z-axis. For a real metal in which the Fermi surface is not spherical, the path traced out by the tip of the electron wave vector k is not usually a circle. The path of the k-vector lies in the Fermi surface– only electrons at the Fermi surface are involved in ultrasonic attenuation and need to be considered–and the orbit of the electron in real space can be found on integrating eq. (8.6) thus

$$\hbar k = Q_e r \times B + \text{constant}. \tag{8.8}$$

It is seen that the electron orbit in real space is the same shape as that in k-space but rotated by $\tfrac{1}{2}\pi$ about the direction of B and scaled by the factor $\hbar/Q_e B$. Investigations of the ultrasonic attenuation as a function of magnetic field can give information about the electron orbits and thus about the shape of the Fermi surface.

The case when the magnetic field lies perpendicular to the direction of propagation will be considered first. As discussed in ch. 7§5.2 a geometric resonance occurs when the size of the electron orbit matches the wavelength of the ultrasonic wave. In fact, if the electron orbit diameter is an even number of half-wavelengths there will be a maximum attenuation since the electron remains in a region of constant phase and continues to draw energy from the ultrasonic wave. If the orbit is an odd number of half-wavelengths the attenuation is a minimum. Thus a series of oscillations is observed in the ultrasonic attenuation as a function of frequency. The observed oscillations are due to certain dominant electron orbits which are those of extreme dimen-

sions of the Fermi surface. If Δ_k is the dimension of the Fermi surface perpendicular to both B and q, then eq. (8.8) shows that the condition for geometric resonance is $n\lambda = (\hbar/Q_e B)\Delta_k$ where λ is the ultrasonic wavelength and n is an integer. The attenuation shows a periodicity in $1/B$ given by

$$\Delta(1/B) = \frac{2\pi Q_e}{q\hbar\Delta_k}. \tag{8.9}$$

It must be stressed that this discussion is rather simplified and a consideration of the dominant orbits responsible for attenuation is necessary; this shows that n may not be integral but depends on the detailed shape of the Fermi surface. Usually the attenuation is dominated by orbits for which Δ_k is a maximum or minimum, since the effect of other orbits will be cancelled by neighbouring orbits making contributions of slightly differing phase. The geometric resonance oscillations thus give information on the extremal dimensions of the Fermi surface in a direction perpendicular to both q and B. However, n changes by integral values between resonances and thus eq. (8.9) is retained. A detailed calculation of ultrasonic attenuation has been given by COHEN *et al.* [1960] for a spherical Fermi surface.

A related spatial resonance effect can sometimes be observed when the shape of the Fermi surface allows a periodic open orbit for the electrons in k-space. In that case an increased attenuation can be observed when the periodicity of the orbit matches the wavelength of the ultrasonic wave.

A temporal resonance when the ultrasonic frequency is equal to the cyclotron frequency has also been predicted, MIKOSHIBA [1958] (see ch. 7§5.2). The condition $\omega\tau > 1$ is necessary for this to be observed and as has been discussed above, it is not easy to satisfy. Very pure materials are needed and a high frequency is required. No report of an observation of acoustic cyclotron resonance at microwave frequencies has been made as yet, though clearly this might be the most promising frequency range. Observation of the effect has been made for example in gallium at 115 MHz, ROBERTS [1961]. COHEN *et al.* [1960] have shown that the attenuation of longitudinal waves due to cyclotron resonance is proportional to $ql \operatorname{Re} \coth[(1 - i\omega\tau)/\omega_B\tau]$ and thus the attenuation maxima are observed at ω_B and its harmonics. The attenuation is therefore periodic in $1/B$ and

$$\Delta(1/B) = Q_e/m\omega, \tag{8.10}$$

where m is the cyclotron effective mass of the electrons.

The situation when the magnetic field is applied parallel to the direction of propagation of the ultrasonic waves will now be considered. In

this case absorption edges discussed by KJELDAAS[1959] can be observed. Electrons moving in cyclotron orbits and drifting along the magnetic field see a Doppler-shifted ultrasonic wave so that the resonance condition becomes

$$\omega_B = \omega \left(1 - \frac{v_z}{v}\right), \tag{8.11}$$

where v_z is the component of electron velocity along the magnetic field and v as before is the ultrasonic velocity. Transverse waves can couple to the electrons in this way and are attenuated if there is a range of values of v_z for which eq. (8.11) can be satisfied. When eq. (8.11) is satisfied with $v_z = v_m$, the maximum value of v_z on the Fermi surface, an absorption edge should occur since at higher magnetic field strengths and thus at higher values of ω_B, attenuation by this mechanism is not possible. It is interesting to note that eq. (8.11) can be obtained from a quantum mechanical point of view by considering the conservation of energy and momentum in an electron–phonon collision. If the electron initially has a wave vector k_z along the magnetic field, it will, after the absorption of a phonon, have a wave vector $k_z + q$. Thus from eq. (8.7)

$$(n + \tfrac{1}{2})\hbar\omega_B + \frac{\hbar^2 k_z^2}{2m} + \hbar\omega = (n' + \tfrac{1}{2})\hbar\omega_B + \frac{\hbar^2 (k_z + q)^2}{2m} \tag{8.12}$$

or

$$(n' - n)\hbar\omega_B = \hbar\omega - \frac{\hbar^2 k_z q}{m} - \frac{\hbar^2 q^2}{2m}.$$

Since $\hbar k_z / m = v_z$ and $q = \omega/v$ it follows on putting $(n' - n)$ equal to unity that

$$\omega_B = \omega \left(1 - \frac{v_z}{v}\right) - \frac{\hbar q^2}{2m}. \tag{8.13}$$

The last term is very small however since q is very much less than k_z for most of the electrons, and thus it can be neglected. When $v_z \approx v_m$ the factor v_z/v is very much greater than unity and eq. (8.11) can be written as $\omega_B = (v_m/v)\omega$ to give the position of the absorption edge. When the Fermi surface is not spherical KJELDAAS[1959] has shown that the cyclotron frequency at the extremal point is given by

$$\frac{\omega_B}{v_m} = \frac{BQ_e K_G^{1/2}}{\hbar}, \tag{8.14}$$

where v_m is the maximum electron velocity and K_G the Gaussian curvature of the Fermi surface (i.e. the product of the reciprocals of the principal radii of curvature at the point in question).

Geometric resonances and geometric oscillations can sometimes be observed when the magnetic field is parallel to the direction of propaga-

tion of the ultrasonic waves for some particular shapes of Fermi surfaces, MACKINTOSH [1964].

Another effect which can be observed in the ultrasonic attenuation of metals in a magnetic field and which is due to the quantization of the electronic motion into Landau levels, is known as quantum oscillations. These are similar in origin to the de Haas–van Alphen oscillations in the magnetic susceptibility and the Shubnikov–de Haas oscillations in the electrical conductivity. The density of states is of course zero between the Landau levels, while at the Landau levels it is greater than the density of states corresponding to zero magnetic field. The cyclotron frequency increases with increasing magnetic field and thus there is a corresponding increase in the energy of the Landau levels. The Landau levels therefore successively pass through the Fermi surface as the magnetic field is increased and the density of states at the Fermi surface fluctuates. Since the attenuation of the ultrasonic wave depends on this density of states at the Fermi surface, it will exhibit oscillations as a function of magnetic field strength. Some account of the theory of these quantum oscillations in ultrasonic attenuation has been given for example by TOXEN and TAUSAL [1965] and by SHAPIRA and LAX [1965]. From eq. (8.12) for the conservation of energy in an electron–phonon collision where the z-component of the wave vector of the electron changes from k_z^0 to $k_z^0 + q_z$, it is noticed that

$$(n - n')\omega_B + \omega = \hbar k_z^0 q_z / m. \tag{8.15}$$

In a sufficiently strong magnetic field when $\omega_B > \hbar k_z^0 q_z / m$ this can only be satisfied when $n = n'$. In these circumstances $\omega = \hbar k_z^0 q_z / m$ and since $\omega = qv$

$$k_z^0 = \frac{mvq}{\hbar q_z} = \frac{mv}{\hbar \cos \theta} \tag{8.16}$$

where $\cos \theta$ is the cosine of the angle between the magnetic field and the ultrasonic propagation direction. If v_z^0 is the drift velocity of the electron along the magnetic field direction it follows, since $v_z^0 = \hbar k_z^0 / m$, that

$$v_z^0 = v / \cos \theta. \tag{8.17}$$

This demonstrates that the electrons responsible for the attenuation are those that drift along in phase with the ultrasonic wave. The electrons that participate in the attenuation are those from the Fermi surface so the condition

$$E_f = (n_i + \tfrac{1}{2}) \frac{\hbar Q_e B_i}{m} + \frac{\hbar^2 k_z^{02}}{2m} \tag{8.18}$$

has to be satisfied for some integer n_i and field value B_i. Thus quantum

oscillations of this type can only appear if $k_z^0 < k_f$ which implies that $v/\cos\theta < v_f$ or that $\cos\theta > 10^{-3}$. The oscillations are again periodic in $1/B$ with periodicity given by

$$\Delta(1/B) = \frac{\hbar Q_e}{m}\left[E_f - \frac{\hbar^2 k_z^{02}}{2m}\right]^{-1}. \tag{8.19}$$

Other types of quantum oscillations can occur in which n changes by ± 1 and they are also periodic in $1/B$ and give information about the area of the Fermi surface in a particular plane. It should be noticed that the periodicity of quantum oscillations is independent of the ultrasonic frequency – except through the value of k_z^0, the wave vector of the electrons responsible – but that the periodicities of geometric and cyclotron resonance oscillations are inversely proportional to the ultrasonic frequency (c.f. eqs. (8.19), (8.9) and (8.10)). For a spherical Fermi surface and with q parallel to B, the $\Delta n = 0$ oscillations appear with longitudinal waves and $\Delta n = \pm 1$ oscillations with shear waves. However in a real metal these selection rules may not apply. Under certain conditions the quantum oscillations may have a very large amplitude and these are then referred to as giant quantum oscillations. The conditions for the presence of these large oscillations are discussed for example in the article by TOXEN and TAUSAL [1965].

Finally, another magnetic effect should be mentioned. This is the tilt effect, SPECTOR [1962a]. Equation (8.17) above shows that the electrons responsible for the attenuation of the ultrasonic wave are those that drift along the magnetic field at such a velocity that the component of their velocity along the direction of propagation is equal to the ultrasonic velocity. At sufficiently small values of $\cos\theta$ this condition cannot be achieved by any electrons at the Fermi surface and thus the attenuation is low. As θ is decreased from $\frac{1}{2}\pi$ an angle of tilt is reached at which the attenuation rises rapidly, namely when $v/\cos\theta$ is equal to the Fermi velocity in the magnetic field direction. Unfortunately the angle of tilt is very small except in materials such as bismuth, a semimetal with a low Fermi velocity.

Experimental observation of the ultrasonic attenuation at microwave frequencies in metals has been made by DOOLEY and TEPLEY [1969 a,b]. Experiments were performed on bismuth using longitudinal waves at a frequency of 9.3 GHz. Because the Fermi velocity is low in bismuth, the experiments approached the $\omega\tau > 1$ regime. Geometric resonance oscillations were observed, and are reproduced in fig. 8.2 and the tilt effect was also found. From these experiments estimates of the electronic relaxation time τ were made.

An extensive bibliography up to 1965 and an account especially concerned with the magnetic effects is given by TEPLEY [1965].
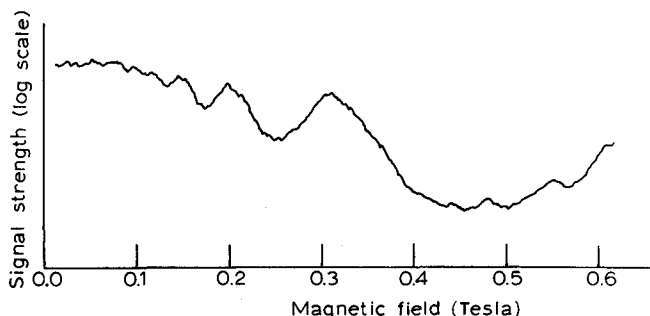
Fig. 8.2. Geometric resonances observed at 9.3 GHz in bismuth by DOOLEY and TEPLEY[1969a].

3. Superconducting metals

3.1. *BCS theory*

The most successful microscopic theory of superconductivity is the Bardeen–Cooper–Schrieffer theory (BCS) which has proved to be one of the major successes of the quantum theory of solids. A detailed account of the theory of this many-body problem is certainly beyond the scope of this book but it is worthwhile to indicate the basic ideas upon which it is founded. For a detailed discussion of the theory of superconductivity the reader is referred to the account of RICKAYZEN [1965].

It was found that in many superconducting elements the transition temperature T_c varied as the inverse of the square-root of the isotropic mass. This demonstrated conclusively, as had been realized by Fröhlich, that the electron–phonon interaction was responsible for superconductivity. The form of the electron–phonon interaction is, as discussed in ch. 7§3.1, quadratic in the electron creation and annihilation operators and linear in the corresponding operators for the phonons. The total Hamiltonian of the electron–phonon system has the form $H = H_0 + H'$ where

$$H_0 = \sum_k \epsilon_k c_k^* c_k + \sum_q \hbar \omega_q a_q^* a_q \qquad (8.20)$$

is the sum of the electron and phonon energies and

$$H' = D \sum_{k,q} (a_q^* - a_{-q}) c_{k-q}^* c_k. \qquad (8.21)$$

For simplicity it will be assumed that D is independent of q. If one has a Hamiltonian consisting of an unperturbed part H_0 and a perturbation λV, then a standard approach to removing the interaction linear in λ is to make a canonical transformation to a new Hamiltonian $\tilde{H} =$

$e^{-X}He^X$. If X is chosen to satisfy $[X, H_0] = \lambda V$ then

$$\tilde{H} = H_0 + \tfrac{1}{2}\lambda [V, X] + \text{terms of order } \lambda^3. \tag{8.22}$$

When this technique is applied to the electron–phonon interaction H' of eq. (8.21) at $T = 0$ it is found that the transformed Hamiltonian is $H_0 + H''$ where

$$H'' = D^2 \sum_{q,k,k'} \frac{\hbar\omega_q}{(\epsilon_k - \epsilon_{k-q})^2 - (\hbar\omega_q)^2}\, c^*_{k'+q} c_{k'} c^*_{k-q}\, c_k. \tag{8.23}$$

The matrix elements over the phonon operators have been taken using eq. (2.36) but the fermion operators have been explicitly displayed. In this way the electron–phonon interaction has been recast into an effective electron–electron interaction. The important point to note is that when the change in electron energies is such that $|\epsilon_{k\pm q} - \epsilon_k| < \hbar\omega_q$, H'' is negative and represents an attractive interaction. The attractive interaction is of course opposed by the screened Coulomb repulsion between the electrons but if the interaction constant D is sufficiently large the indirect interaction through the phonon field will dominate. Since most of the zero point phonons are near the Debye limit the attraction may be taken as dominant when ϵ_k and $\epsilon_{k\pm q}$ come from within a distance $\hbar\omega_D$ of the Fermi surface. That is

$$\epsilon_f - \hbar\omega_D < \epsilon_k, \quad \epsilon_{k\pm q} < \epsilon_f + \hbar\omega_D. \tag{8.24}$$

The total Hamiltonian of the electrons and the phonons can therefore be recast into the form

$$H = H_0 - V \sum_{q,k,k'} c^*_{k'+q}\, c_{k'} c^*_{k-q}\, c_k, \tag{8.25}$$

where the sum over q is only over those modes for which eq. (8.24) is satisfied.

Having seen that the phonon field can produce an attractive interaction between the electrons, the important step which stimulated the interest of Bardeen, Cooper and Schrieffer was the realization by Cooper than unusual properties would result from having this attractive term in a Fermi gas. He considered what would happen if two additional electrons were added to a system filling a Fermi sea. It was assumed that the states within the Fermi sea were held rigid so that they were forbidden to the two electrons by the exclusion principle. If the Fermi sea is filled, the two electrons must be in a superposition of states above the Fermi sea, one possibility being that they are just above the Fermi level. This was the problem solved by Cooper who found that in the presence of the attractive potential the lowest eigenvalue was given by $2\epsilon_f - \Delta_C$ with

$$\Delta_C = \frac{2\hbar\omega_D}{\exp(1/N_f V) - 1} \tag{8.26}$$

N_f being the density of states at the Fermi surface. This calculation therefore showed that the two electrons could take advantage of the attractive interaction to form a bound state lower in energy than that obtained by simply adding them to the top of the Fermi sea. It is noticed from eq. (8.26) that this conclusion is true even when V is very weak. This suggested that in the presence of an attractive potential such as H'' the energy of the electron system would be lowered by exciting pairs of electrons above the Fermi level, i.e. the Fermi sea is unstable.

The next step is to consider the full many-body problem and to study the ground state of the Fermi gas in the presence of the interaction of eq. (8.25). This was the problem tackled by BCS. The work of Cooper suggested that to obtain a state of low energy states should be considered in which the individual Bloch states are paired and only those configurations need be considered for which the two members of the pairs are either occupied or unoccupied. Since the interaction conserves momentum, see eq. (8.25), one chooses the pairs in such a way that they all have the same momentum, that is $k + k' = K$. Because the ground state is expected to have zero momentum the pairs are k and $-k$. Because of this pairing idea BCS considered the reduced Hamiltonian

$$H_{\text{red.}} = \sum_k \epsilon_k (c_k^* c_k + \underline{c}_{-k}^* c_{-k}) - V \sum_k c_{k'}^* c_{-k'} c_{-k}^* c_k \qquad (8.27)$$

which only operated within the pair subspace. The solution of this Hamiltonian led to an excitation spectrum given by

$$E_k = 2(\epsilon_k^2 + \Delta^2)^{1/2} \qquad (8.28)$$

with

$$\Delta = \frac{\hbar \omega_D}{\sinh (1/N_f V)}.$$

An energy gap thus occurs in the excitation spectrum of a superconductor and the minimum excitation energy is 2Δ.

This is the situation at $T = 0$. At a finite temperature quasi-particles are excited so the number of states occupied in pairs decreases and the pairing energy decreases. Hence the energy gap which is a measure of the pairing energy decreases with increasing temperature until it vanishes at the transition temperature T_c. On the basis of the theory outlined above it can be shown that the gap at $T = 0$ is related to T_c by $\Delta = 1.76 \, KT_c$. For temperatures up to about $\frac{1}{2}T_c$ the gap only changes very slightly but then falls off much more rapidly with increasing temperature. In the vicinity of T_c it falls steeply according to $\Delta(T) = 3.2 \, KT_c (1 - T/T_c)^{1/2}$.

In the treatment of the theory due to Bogoliubov, new creation and annihilation operators are introduced which create and annihilate the quasi-particles. These are defined by

$$b_k = u_k c_k - v_k c^*_{-k}, \qquad b^*_k = u_k c^*_k - v_k c_{-k},$$
$$b_{-k} = u_k c_{-k} + v_k c^*_k, \qquad b^*_{-k} = u_k c^*_{-k} + v_k c_k,$$

(8.29)

and it is found that the values of u_k and v_k are given by

$$u^2_k = \tfrac{1}{2}[1 + \epsilon_k/\lambda_k], \qquad v^2_k = \tfrac{1}{2}[1 - \epsilon_k/\lambda_k]$$

with $\lambda_k = (\epsilon^2_k + \Delta^2)^{1/2}$. These operators create and destroy excitations of the vacuum just as the original c-operators create and destroy electrons. b^*_k has the effect of creating an electron in the state k with amplitude u_k and at the same time destroying an electron in the state $-k$ with amplitude v_k. When $u^2_k \approx 1$ and $v^2_k \approx 0$ the quasi-particle excitation will look like an electron, whereas when $v^2_k \approx 1$ and $u^2_k \approx 0$ it will look like a hole. In the intermediate range each quasi-particle is a mixture of an electron with wave-vector k and a hole in the state $-k$. There is thus a correlation between electrons and holes of opposite momenta. The ground state of the system in terms of these quasi-particle operators is $\phi_0 = \Pi_k b_{-k} b_k \phi_{vac}$. Single particle excitations can then occur in which two single particles are excited and a virtual pair is destroyed from ϕ_0, $\phi_s = b^*_k b^*_{k'} \phi_0$. This involves an energy $\lambda_{k'} + \lambda_{k'}$. If a real pair excitation $\phi_p = b^*_{k'} b^*_{-k'} \phi_0$ occurs the excitation energy is $2\lambda_{k'}$. The minimum energy required for an excitation is thus 2Δ in both cases in agreement with the result stated above, eq. (8.28).

3.2. *Acoustic attenuation in the absence of a magnetic field*

The change in ultrasonic attenuation as a superconductor is cooled through its transition temperature was one of the first indications that there was a large attenuation in the normal material due to the conduction electrons, BÖMMEL [1954]. This early observation and subsequent experiments were made using ultrasonic waves in the radio frequency range. As yet very few experiments have been performed at microwave frequencies, so the theory will be briefly summarized with special reference to the high frequency effects expected.

As discussed in the last section, because of the electron–phonon interaction, the excitations in the superconducting state are quasi-particles which can be regarded as a mixture of an electron and a hole with opposite momentum, and an energy gap appears between the excited and ground states. Attenuation of ultrasonic waves can occur in two ways: the wave can either excite quasi-particles across the energy gap or it can be scattered by quasi-particles above the energy gap. The first possibility can usually only occur with high frequency waves because the phonon energy must be larger than that associated with the energy gap. The energy gap is in fact temperature dependent, increasing from zero at the transition temperature to its largest value

at the absolute zero. The frequency of the ultrasonic wave needed to excite a quasi-particle across the gap is therefore temperature dependent.

To calculate the ultrasonic attenuation due to the second mechanism – the scattering by quasi-particles above the energy gap – two factors have to be considered. The first point is that the matrix elements for the interaction between a phonon and the quasi-particles will differ from those, eq. (7.78), for the interaction between a phonon and normal electrons by a factor $(1 - \Delta^2/E_k E_{k'})$. E_k and $E_{k'}$ are the energies of the quasi-particle in the initial and final states and Δ is one-half of the energy gap. Of course the conservation of energy requires that $E_{k'} = E_k + \hbar\omega$. This factor appears in the matrix elements because of the parameters u_k and v_k appearing in the definition of the creation and annihilation operators for the quasi-particles in terms of the usual electron operators c_k^* and c_{-k}. The second point to remember is that when the sum over wave vectors is replaced by an integral, the density of states enters and this will be different from that in the normal metal because of the energy gap. In the superconducting state the density of states above the gap is given by,

$$N_S(E) = N_N(E) E / (E^2 - \Delta^2)^{1/2},$$

where $N_N(E)$ is the density of states per unit energy for electrons in the normal metal, BARDEEN et al. [1957]. The probability of absorption of a phonon in the superconducting state will therefore involve an integral of the form

$$2 \int_\Delta^\infty \left(1 - \frac{\Delta^2}{E_k E_{k'}}\right) \{f(E_k)[1 - f(E_{k'})]$$
$$- f(E_{k'})[1 - f(E_k)]\} N_S(E_k) N_S(E_{k'}) \, dE \qquad (8.30)$$

where the f's are the Fermi functions for the thermal distribution of the quasi-particles. Substituting for the density of states and taking $\hbar\omega \ll 2\Delta$ this gives

$$2 \int_\Delta^\infty N_N^2 \{f(E_k) - f(E_k + \hbar\omega)\} \, dE$$
$$= -2 \int_\Delta^\infty N_N^2 \frac{df}{dE} \hbar\omega \, dE = 2\hbar\omega N_N^2 f(\Delta).$$

It is observed that the coherence factor which enters the matrix element exactly cancels the density of states factor. The corresponding integral for the normal metal is, see eq. (7.78),

$$2 \int_0^\infty N_N^2 \{f(E_k) - f(E_k + \hbar\omega)\} \, dE = 2\hbar\omega N_N^2 f(0) = \hbar\omega N_N^2,$$

The other factors that enter the calculation of the attenuation will be the same for the normal and superconducting states so the ratio of the two attenuation coefficients is simply given by

$$\alpha_S/\alpha_N = 2f(\Delta). \tag{8.31}$$

This extremely useful relationship was first given in the original paper by Bardeen, Cooper and Schrieffer.

Eq. (8.31) has been verified at microwave frequencies by FERGUSON and BURGESS[1967] using ultrasonic waves at 9.3 GHz in mercury at temperatures between 1.5 and 4.2 K. The normal metal attenuation was of the order of 2000 dB · cm^{-1} and the superconducting attenuation was fitted by the BCS equation, eq. (8.31), with an energy gap given by $2\Delta(0)/KT_c = 4.0 \pm 0.3$ which compares with the value 4.6 from tunneling and infra-red absorption experiments and the value 3.95 from specific heat and critical field measurements. $\Delta(0)$ is the energy gap at the absolute zero of temperature.

The attenuation of longitudinal ultrasonic waves is adequately represented by eq. (8.31) when $\hbar\omega \ll \Delta(T)$ the temperature dependent energy gap. However in the case of transverse waves a rapid drop in attenuation is observed at the transition temperature. This is because the electromagnetic part of the interaction, which for transverse waves is through the magnetic fields generated by the moving positive ions, is shielded out by the superconducting electrons leaving only the collision drag effect.

We return now to the discussion of high ultrasonic frequencies where the condition $\hbar\omega \gg \Delta(T)$ is satisfied and the creation of quasi-particles by the breaking of Cooper pairs is possible. This case has been treated theoretically by BOBETIC[1964]. Unfortunately the results do not have such a simple form as that of eq. (8.31) because the integrals cannot be evaluated analytically. Again the ratio of the ultrasonic attenuation in the superconducting and normal states is given by

$$\frac{\alpha_S}{\alpha_N} = \frac{1}{\hbar\omega} \int_{-\infty}^{\infty} \left(1 - \frac{\Delta^2}{E_k E_{k'}}\right) [f(E_k) - f(E_{k'})] \rho_S(E_k)\rho_S(E_{k'}) \, dE_k \tag{8.32}$$

where $\rho_S(E_k)$, the relative density of states N_S/N_N, is given by

$$\rho_S(E_k) = 0, \qquad |E_k| < \Delta$$

$$\rho_S(E_k) = \frac{|E_k|}{(E_k^2 - \Delta^2)^{1/2}}, \quad |E_k| > \Delta.$$

For this equation to hold, it is required that Δ and KT are much less than $\hbar q v_f$ where q is the wave vector of the ultrasonic wave and v_f is

the Fermi velocity. It is also required that $ql > 1$ where l is the mean free path of the electrons. The integral to be evaluated can be written in two parts

$$\frac{\alpha_S}{\alpha_N} = \frac{2}{\hbar\omega} \int_\Delta^\infty [f(E) - f(E + \hbar\omega)] \frac{[E(E + \hbar\omega) - \Delta^2]\,dE}{\{(E^2 - \Delta^2)[(E + \hbar\omega)^2 - \Delta^2]\}^{1/2}}$$

$$- \frac{1}{\hbar\omega} \int_{\Delta - \hbar\omega}^{-\Delta} [1 - 2f(E + \hbar\omega)] \frac{[E(E + \hbar\omega) - \Delta^2]\,dE}{\{(E^2 - \Delta^2)[(E + \hbar\omega)^2 - \Delta^2]\}^{1/2}} \quad (8.33)$$

where the first term is the one already discussed for the case $\hbar\omega \ll \Delta(T)$. The second term corresponding to the creation of a pair of quasi-particles cannot be evaluated analytically but Bobetic has given the results of a numerical integration. This integral contributes even when $\hbar\omega$ is only infinitesimally greater than 2Δ, so a discontinuity in the attenuation versus temperature curve should appear when the energy gap becomes equal to the ultrasonic frequency. Thus, as the material is cooled through the superconducting transition temperature, the ultra-sonic attenuation at first rises until the energy gap becomes equal to the ultrasonic phonon energy when there is a discontinuous drop; this is then followed by a smooth fall towards zero as the temperature tends to the absolute zero. Fig. 8.3, taken from Bobetic's article
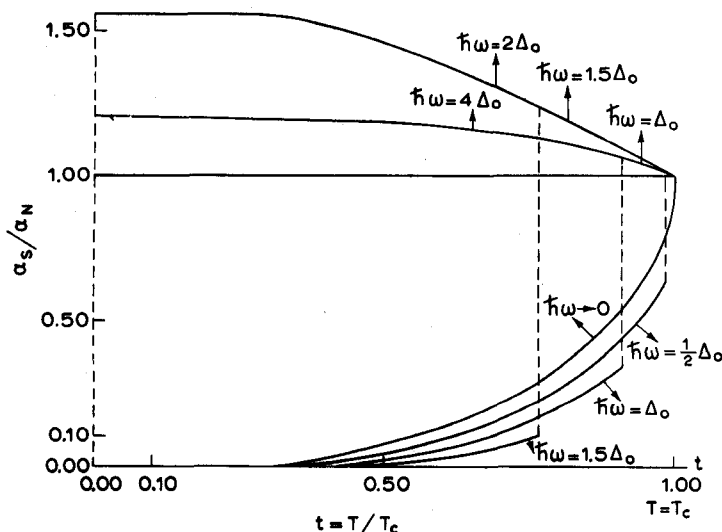
Fig. 8.3. Ratio of attenuations in superconducting and normal states as a function of temperature for different frequencies. (Reproduced from V. M. BOBETIC, Phys. Rev. 136, A1538 (1964) with permission.)

shows the theoretical curves for the attenuation as a function of temperature.

The effect of quasi-particle creation has been observed by FAGEN and GARFUNKEL [1967] using longitudinal ultrasonic waves at 9.3 GHz in aluminium. A discontinuity of 7.5 dB in the attenuation through about 0.05 mm of aluminium was found at a temperature 0.005 K below the transition temperature. It occurred in a temperature range less than about 5×10^{-4} K.

3.3. *Type II superconductors in a magnetic field*

Superconductors of the second type – type II – can exist in the so-called mixed state in a magnetic field between two critical values H_{c_1} and H_{c_2} the latter being greater than the thermodynamical critical field value $H_c(T)$. This situation is energetically favorable for superconductors with a negative surface energy between the normal and superconducting states. The material splits into some fine scale mixture of superconducting and normal regions whose boundaries are parallel to the applied magnetic field, the configuration of normal regions threading the superconducting material being such that the ratio of the surface to the volume of normal material minimizes the energy. Within each normal core threading the diamagnetic material there is a magnetic flux–flux line – generated by a persistent current that circulates through the core with a sense of rotation opposite to that of the diamagnetic surface current. This mixed state is an intrinsic feature of type II superconductors and must not be confused with the intermediate state that can exist in type I materials which have a non-zero demagnetization factor. The intermediate state is relatively coarse grained and can be made visible to the eye, whereas in the mixed state the periodicity is less than about 1000 Å.

The behaviour of these materials in a magnetic field is usually discussed in terms of the Landau–Ginzburg equations in which two characteristic lengths are introduced, the temperature dependent coherence length $\xi(T)$ and the temperature dependent penetration depth $\lambda(T)$. $\xi(T)$ gives the distance in which the superconducting order parameter changes – roughly speaking the extent of a Cooper pair, and $\lambda(T)$ gives the distance in which the magnetic field falls to zero in going from a normal to a superconducting region. Both $\xi(T)$ and $\lambda(T)$ have the same temperature dependence so a temperature independent Landau–Ginzburg parameter κ can be defined as $\kappa = \lambda(T)/\xi(T)$. The condition for the existence of type II superconductivity is then that $\kappa > 1/\sqrt{2}$ while for $\kappa < 1/\sqrt{2}$ the material is a type I superconductor. The original Landau–Ginzburg treatment of superconductivity was applicable to temperatures near T_c but it has been extended to all temperatures

and magnetic fields by subsequent workers. For a fuller discussion see for example LYNTON[1969], DE GENNES[1966]. In terms of the parameter κ the critical fields are given by

$$H_{c_2} = \sqrt{2}\kappa H_c \quad \text{and} \quad H_{c_1} \approx \frac{1}{\sqrt{2}\kappa} H_c [\log (\kappa + 1.18) + 0.08].$$

κ can be expressed in terms of other parameters of the superconductor. In particular it can be written as

$$\kappa^2 = 2\mu_0^2 \epsilon^2 H_c^2 \lambda_0^4 / \hbar^2,$$

where ϵ is the effective charge of the current carriers which is known from BCS theory to be twice the electronic charge and H_c is the critical magnetic field. λ_0 is the penetration depth defined as

$$\lambda_0^2 = m/\mu_0 \epsilon^2 \psi_0^2$$

m is a mass usually taken as the electronic mass and ψ_0 is the order parameter of the Landau–Ginzburg theory. Finally Gorkov, see DE GENNES[1966], has derived the Landau–Ginzburg equations from first principles and then it is found that $\kappa = 0.96\lambda_0/\xi_0$ where ξ_0 is the coherence length of the pure material. The coherence length is a function of the electronic mean free path and thus the properties of a type II material depend on its purity. Two situations are considered, the clean limit $l \gg \xi_0$, which applies to the elements niobium and vanadium and the so-called dirty limit $l \ll \xi_0$ which applies to the alloy and compound materials which form type II superconductors. Of course, these materials are only dirtied in the sense that the electronic mean free path is relatively short; by chemical standards they are of high purity.

The main difference between the cases now discussed, of a type II superconductor in the mixed state between H_{c_1} and H_{c_2}, and the pure superconductor described in §3.2 above, is that the order parameter and hence the energy gap are not constant throughout the material. Thus the expression for the ultrasonic attenuation eq. (8.31) cannot be applied. The fact that the ultrasonic attenuation is markedly different in the superconducting phase from the normal phase led to the suggestion by COOPER et al.[1965] that a resonance effect might be observed in the attenuation when the flux line spacing was equal to the ultrasonic wavelength. Clearly, the microwave region where the wavelength is short is the most likely range to use to observe the effect. However subsequent theoretical work, MCLEAN and HOUGHTON[1968], has suggested that the resonance effect might be undetectably small and experiments have not revealed it, BUISSON and CHEEKE[1969], GUERMEUR et al.[1970].

The theory in the dirty limit $l \ll \xi_0$ has been presented by McLean and Houghton [1967] who find that the ratio of the ultrasonic attenuation in the superconducting phase α_S to that in the normal phase α_N is given, for longitudinal waves, by

$$\frac{\alpha_S}{\alpha_N} = 1 - \frac{Q_e}{4\pi b \alpha} \left[\frac{H_{c_2} - H_0}{\beta \{2\kappa_2^2(T) - 1\}} \right] [1 + L(\rho)]. \qquad (8.34)$$

Q_e is the electronic charge, b the d.c. conductivity of the normal material, α the Ginzburg–Landau eigenvalue and H_0 is the applied magnetic field. β equal to 1.16 is the ratio $\langle |\Delta|^4 \rangle_{av} / \langle |\Delta|^2 \rangle_{av}^2$ where Δ is the order parameter. The parameters b and α are given by $b = nQ_e^2\tau/m$ and $\alpha = \frac{1}{3}\tau v_f^2 Q_e H_{c_2} \mu_0$ with v_f the Fermi velocity and n the electron density. $\kappa_2(T)$ is the temperature dependent Ginzburg–Landau parameter introduced by Maki [1964] and is defined through the relation

$$-\frac{4\pi M}{H_{c_2} - H_0} = \frac{1}{\beta \{2\kappa_2^2(T) - 1\}}, \qquad (8.35)$$

where ψ' is the trigamma function and $\rho = \alpha/2\pi KT$. The function $L(\rho)$ of κ_2 is discussed by Caroli et al. [1966]. $L(\rho)$ is the function

$$-\rho(\partial/\partial\rho) \log_e \psi'(\rho + \tfrac{1}{2})$$

where ψ' is the trigamma function and $\rho = \alpha/2\pi kT$. The function $L(\rho)$ has been plotted for values of ρ between 0 and 2 by McLean and Houghton [1967].

The opposite limit, the clean limit, $l \gg \xi_0$ has been considered by Maki [1967] and by McLean and Houghton [1968]. The ratio of the ultrasonic attenuations in the superconducting and normal phases is given, for longitudinal waves and with the applied magnetic field parallel to q, by

$$\frac{\alpha_S}{\alpha_N} = 1 - \frac{\Delta}{2KT} \int_{-\infty}^{\infty} \phi_1 \left(\frac{\alpha}{\epsilon}, y \right) \cosh^{-2} \left(\frac{\alpha}{2KT} \right) \frac{d\alpha}{\epsilon} \qquad (8.36)$$

with

$$\phi_1(x, y) = \frac{1}{\pi^{1/2} I_0} \int_0^1 dz \frac{(1 - 3z^2)}{(1 - z^2)^{1/2}} \exp \left(-\frac{x^2}{1 - z^2} \right)$$

$$\times \left\{ [1 + (yz)^2]^{-1} (1 - y^{-1} \arctan y)^{-1} - \frac{3z^2}{y^2} \right\}$$

and

$$y = ql, \quad I_0 = \frac{\arctan y}{y - \arctan y} - \frac{3}{y^2},$$

$$\epsilon(T) = \frac{v_f}{\sqrt{2}} [\mu_0 Q_e \hbar H_{c_2}(T)]^{1/2}.$$

Δ is the average order parameter for the material and is given by

$$\Delta^2 = \frac{m(2\pi KT)^2}{6\pi Q_e H_{c_2} \mu_0} \frac{[H_{c_2} - H_0]}{\beta(2\kappa_2^2 - 1)} g^{-1}(\rho)$$

where $g(\rho)$ is a function defined by MAKI and TSUZUKI [1965] and $\rho = [v_f(\hbar Q_e \mu_0 H_0)^{1/2}/2\pi KT]^2$.

The important difference between the clean limit and the dirty limit is thus shown to be the dependence on the average of the order parameter. This gives a variation with applied magnetic field of the form $[H_{c_2} - H_0]$ in the dirty limit and $[H_{c_2} - H_0]^{1/2}$ in the clean limit. The temperature dependence enters in several ways, both explicitly and through the temperature dependence of κ_2, H_{c_2} etc.

Experiments have been performed in the microwave region by GUERMEUR et al. [1970] and by TITTMANN [1970] which have shown the magnetic field dependence in the dirty limit. Tittmann also showed that in zero magnetic field the temperature dependence of the attenuation in vanadium–tantalum alloys followed the BCS expression, eq. (8.31) given in §3.2. He found too that the attenuation varied as $[H_{c_2} - H_0]$ only for small values of $[H_{c_2} - H_0]$.

No experiments have been reported in the microwave frequency range using transverse ultrasonic waves, probably because of the difficulty of making satisfactory bonds for transmitting transverse waves. Bonds will be necessary if a pulse-echo method is used, as a dielectric delay rod is needed when only a very thin metal specimen can be used on account of the high attenuation. However, theoretical treatments of the attenuation of transverse ultrasonic waves have been made by McLEAN and HOUGHTON [1967] and MAKI [1966] for the dirty limit and by MAKI [1967] for the clean limit.

THE INTERACTION OF LIGHT WITH MICROWAVE
ULTRASONIC WAVES

1. Introduction

The diffraction of light was one of the first ways by which microwave ultrasonic waves were detected, BARANSKII [1957a, b], BÖMMEL and DRANSFELD [1958]. In these early experiments the ultrasonic waves were generated by a quartz transducer and the diffraction of the light caused by these waves as they travelled through the quartz was taken as evidence of their existence.

Three aspects of the interaction of light with lattice vibrations will be considered here. First, the diffraction of light by a beam of microwave ultrasonic waves generated by one of the methods discussed in ch. 3 will be treated. Secondly, the scattering of light from the thermal vibrations of the crystal lattice will be considered, and finally, the generation of intense beams of microwave ultrasonic waves by parametric amplification of the thermal vibrations will be treated. These last two phenomena are frequently called Brillouin scattering and stimulated Brillouin scattering respectively, after the author who first discussed the scattering of light by thermal fluctuations, BRILLOUIN [1922]. The phenomenon was independently studied about the same time by Mandel'shtam and is therefore sometimes called Mandel'shtam scattering or Mandel'shtam–Brillouin scattering. For brevity in what follows it will be referred to as Brillouin scattering. Extensive accounts of the subject appear in the book by FABELINSKII [1968] and in the review article by the same author, FABELINSKII [1957].

The advantage of light diffraction as a method of detecting ultrasound is that the wave can be studied at various points along its path by varying the point of incidence of the light. The preparation of the end face and transducer for detection is unnecessary, though the sides of the specimen delay-rod have to be optically finished.

The scattering of light from thermal vibrations permits the investigation of lattice waves in the microwave frequency range under condi-

tions where ultrasonic generation techniques cannot be used;–for example at temperatures where the attenuation is too high to give a sufficiently long path for detection of the coherent ultrasonic wave.

2. Photo-elasticity

The coupling between the lattice vibrations and the incident light wave is through the photoelastic effect. The refractive index of a transparent material is in general not only a function of the applied electric field but is also a function of the stress applied to the crystal. The application of a stress causes a strain in the crystal which may change the polarization and hence the refractive index. Thus the optical properties of a crystal are affected by the application of a stress. General discussions of photoelasticity can be found for example in the books by BORN and WOLF [1965] and NYE [1957].

In an anisotropic medium the dielectric properties are described by the permittivity tensor, ch. 2§2, $D_i = \kappa_{ij} E_j = \kappa_0 K_{ij} E_j$ where K is the dielectric constant. (Remember though, that the values of κ_{ij} at optical frequencies are not the same as those measured statically.) The inverse relation is $E_i = \beta_{ij} D_j = \beta_0 B_{ij} D_j$ where the β_{ij}'s are given by

$$\beta_{ij} = (-1)^{i+j} \Delta^{ij} / \Delta$$

with

$$\Delta = \begin{vmatrix} \kappa_{11} & \kappa_{12} & \kappa_{13} \\ \kappa_{12} & \kappa_{22} & \kappa_{23} \\ \kappa_{13} & \kappa_{23} & \kappa_{33} \end{vmatrix}$$

and Δ^{ij} is the minor obtained by suppressing the ith row and the jth column. It is convenient to utilize the six independent coefficients of B to define an ellipsoid called the index ellipsoid or indicatrix by writing its equation as

$$B_{ij} x_i x_j = 1.$$

If axes are used which are the principal axes of the B tensor this has the simpler form

$$B_1 x_1^2 + B_2 x_2^2 + B_3 x_3^2 = 1. \tag{9.1}$$

For a transparent crystal (low conductivity) which is not ferromagnetic ($\mu = \mu_0$) the principal components of the dielectric tensor are related to the components of the refractive index by $n_1 = \sqrt{K_1}$, $n_2 = \sqrt{K_2}$, $n_3 = \sqrt{K_3}$. Therefore B_1 is $1/n_1^2$ etc. and the indicatrix becomes

$$\frac{x_1^2}{n_1^2} + \frac{x_2^2}{n_2^2} + \frac{x_3^2}{n_3^2} = 1. \tag{9.2}$$

This indicatrix ellipsoid is important for the following reason. For a

given wave normal it provides an elegant construction for the refractive index and the direction of the electric displacements. To find the wavefronts that can propagate through the crystal normal to a given direction one simply has to draw the section through the centre of the ellipsoid perpendicular to this direction. Then the wavefronts that can propagate have refractive indices equal to the major and minor axes of this ellipse, and the electric displacement vector D in each plane polarized wave vibrates parallel to the axis of the ellipse that gave its refractive index.

An applied stress σ_{kl} will cause a small change in the size, shape or orientation of this indicatrix. This change can be specified by giving the changes in the coefficients B_{ij}

$$\Delta B_{ij} = \pi_{ijkl}\sigma_{kl}, \tag{9.3}$$

where the π_{ijkl} are the components of a fourth-rank tensor known as the piezo-optical coefficient. Since $\Delta B_{ij} = \Delta B_{ji}$ it follows that $\pi_{ijkl} = \pi_{jikl}$ and furthermore, if body-torques are ignored ($\sigma_{kl} = \sigma_{lk}$), $\pi_{ijkl} = \pi_{ijlk}$. These relations allow the contracted matrix notation to be used

$$\Delta B_m = \pi_{mn}\sigma_n \qquad m, n = 1 \text{ to } 6. \tag{9.4}$$

The π_{mn} are related to the π_{ijkl} by the rules

$$\begin{aligned} \pi_{mn} = \pi_{ijkl} \qquad & n = 1, 2 \text{ or } 3 \quad m = 1 \text{ to } 6, \\ \pi_{mn} = 2\pi_{ijkl} \qquad & n = 4, 5 \text{ or } 6 \quad m = 1 \text{ to } 6, \end{aligned} \tag{9.5}$$

(cf. the corresponding relations for the elastic compliances ch. 2§1.3). In the case of the elastic constants it will be recalled, ch. 2§1.3, that it followed from the uniqueness of the energy function that $c_{ij} = c_{ji}$. However no similar condition holds for the components of π so that in general $\pi_{nm} \neq \pi_{mn}$. It is more convenient to work with the elasto-optical coefficients p_{ijrs} which relate the change in B to the strain ϵ_{ij} produced by the stress

$$\Delta B_{ij} = p_{ijrs}\epsilon_{rs}. \tag{9.6}$$

It follows that the piezo-optical and elasto-optical coefficients are related through the elastic stiffness constants

$$p_{ijrs} = \pi_{ijkl}c_{klrs}. \tag{9.7}$$

Some values of the elasto-optical coefficients are given in table 9.1. These components are dimensionless and because of the symmetry of ΔB_{ij} and ϵ_{ij} the contracted matrix notation can again be used

$$\Delta B_n = p_{nm}\epsilon_m \qquad n, m = 1 \text{ to } 6 \tag{9.8}$$

but this time

$$p_{mn} = p_{ijrs} \text{ for all } m \text{ and } n. \tag{9.9}$$

TABLE 9.1
Elasto-optical coefficients for some solids

Material	p_{11}	p_{12}	p_{44}	p_{31}	p_{13}	p_{33}	p_{41}	p_{14}
(1) α-quartz	0.138	0.250	−0.067	0.258	0.259	0.098	−0.044	−0.035
(2) fused quartz	0.121	0.270	−0.075					
(3) α-Al$_2$O$_3$	∼0.20	∼0.08	0.085	∼0	∼0	0.252		
(4) LiNbO$_3$	0.036	0.072		0.178	0.092	0.088	0.155	
(5) CaF$_2$	0.056	0.228	0.0236					
(6) LiF	0.020	0.130	−0.045					
(7) NaCl	0.137	0.178	−0.0108					
(8) KCl	0.215	0.159	−0.024					

(1) and (5) LANDOLT and BORNSTEIN [1966] quoting POCKELS [1889, 1894].
(2), (3) and (4) DIXON [1967].
(6) and (8) LANDOLT and BORNSTEIN [1966] quoting IYENGAR [1955].
(7) NYE [1957] quoting POCKELS [1906].
Many more values for other materials are given in LANDOLT and BORNSTEIN [1966].

Again there is no reason why p_{mn} is equal to p_{nm}. The numbers of independent components of both p and π are limited by symmetry as in the case of the elastic constants and these are shown in tables A1.5.

In the discussion of light scattering that follows, expressions for $\Delta K/K$ will be needed, where ΔK is the amplitude of the wave-like variation in the dielectric constant due to the presence of an ultrasonic wave. For a general direction of propagation and polarization of the ultrasonic wave and of the light used, the expressions may be quite long especially for crystals of low symmetry. Instead of giving these general expressions simple examples required later will be given. Consider a longitudinal ultrasonic wave travelling in the x_3 direction along the [001] axis of a cubic crystal and subjected to light polarized in the x_2 direction along the [010] axis. From table A1.5 for full cubic symmetry it is seen that for this particular ultrasonic wave $\Delta B_4 = \Delta B_5 = \Delta B_6 = 0$. The component ΔB_2 is equal to $p_{23}\epsilon_3$ and the other two components are not required when dealing with light polarized along x_2. Since $B_2 = 1/K_2$ it follows that $\Delta B_2 = -\Delta K_2/K_2^2$ so that the required relation is

$$\frac{\Delta K_2}{K_2} = -\Delta B_2 K_2 = -K_2 p_{23}\epsilon_3. \qquad (9.10)$$

If the incident light is polarized along x_3 rather than along x_2 (as it might be if it were incident parallel to the ultrasonic wavefront) the required expression is then

$$\frac{\Delta K_3}{K_3} = -K_3 p_{33}\epsilon_3. \qquad (9.11)$$

Of course, for a material with full cubic symmetry there is only one dielectric constant, $K_2 = K_3$ and eqs. (9.10) and (9.11) become

$$\frac{\Delta K_2}{K} = -Kp_{23}\epsilon_3 \quad \text{and} \quad \frac{\Delta K_3}{K} = -Kp_{33}\epsilon_3. \qquad (9.12)$$

These equations show how this crystal becomes optically uniaxial along the direction of ultrasonic propagation as p_{23} is in general not equal to p_{33}.

3. The detection of ultrasonic waves by light scattering

The diffraction of visible light has been used for many years in the study of ultrasonic waves. Much of the early work at low frequencies is described by BERGMAN[1938] and an account of the theory can be found in the book by BORN and WOLF[1965].

3.1. *Raman–Nath scattering*

At low frequencies – that is lower than the microwave region of interest in this book – the diffraction takes place according to the Raman–Nath theory, RAMAN and NATH[1935, 1936]. This occurs when $q^2L/k < \pi$, see the quantitative discussion in §3.2. q and k are the wave numbers of the ultrasonic and light waves respectively and L is the width of the ultrasonic beam transversed by the light. The light beam is incident in a direction parallel to, or at a very small angle to the ultrasonic wavefronts. The ultrasonic wave acts as a phase diffraction grating and the light emerges with a sinusoidally varying phase in the plane across the beam. The light is thus diffracted into a number of orders on either side of the zero order beam. The intensity of the l-order beam is approximately given by BORN and WOLF[1965],

$$I_l = E_0^2 J_l^2 \left[\frac{1}{2} \frac{\Delta K}{K} kL \sec \theta \right]. \qquad (9.13)$$

In this formula E_0 is the amplitude of the incident light wave and θ is the angle measured in the medium between the incident light beam and the ultrasonic wavefronts. J_l is a Bessel function of order l. The other quantities are as defined before, but it should be noticed that k is the wave number of the light measured in the medium. Raman–Nath diffraction is of little importance in the microwave frequency region because the inequality above is not satisfied unless the ultrasonic beam is impracticably narrow; it will therefore not be discussed further.

3.2. *Bragg scattering*

At high frequencies, that is when the inequality $q^2L/k > \pi$ is satisfied,

only the zero-order and first-order diffracted light beams are obtained. This is the Bragg scattering region, so called as the angle at which the first-order beam appears is given by the usual Bragg law for diffraction

$$2\Lambda \sin \theta = \lambda. \qquad (9.14)$$

Λ and λ are the wavelengths of the ultrasonic and the light waves respectively and θ is the angle between the incident light and the ultrasonic wavefronts. The scattered light also appears at the angle θ to the ultrasonic wavefronts as it is specularly reflected from them. The angle θ and the wavelength λ must either both be measured in the medium or both outside it. The diagram of fig. 9.1 shows the arrangement and it is clear that $\sin \theta_{out} = n \sin \theta_{in}$ and also $\lambda_{out} = n\lambda_{in}$ where n is the refractive index.
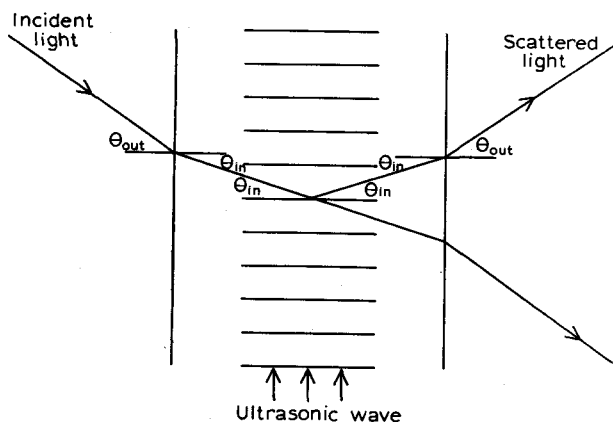
Fig. 9.1. Light scattered from ultrasonic wavefronts in a crystal.

The ultrasonic wavefronts from which the light is scattered are moving with the velocity of sound in the medium and thus there is a Doppler shift in the frequency of the scattered light. The frequency ω_s of the scattered light is given by

$$\omega_s = \omega_i \pm \Omega, \qquad (9.15)$$

where ω_i is the frequency of the incident light and Ω is the frequency of the ultrasonic waves. The positive sign applies to the $+l$ order scattered beam shown in fig. 9.1 while the negative sign applies to the $-l$ order scattered beam obtained if the direction of the ultrasonic waves is reversed in fig. 9.1.

Before a detailed theory leading to eqs. (9.14) and (9.15) and to an expression for the intensity of the scattered light is given it is worth indicating the relative magnitudes of the effects being considered. As

typical examples the materials quartz and sapphire will be considered. Transverse ultrasonic waves propagating along the trigonal axis in quartz travel at 4.7×10^3 m/sec and the longitudinal wave velocity along the trigonal axis of sapphire is 12×10^3 m/sec. Consider first the condition for Bragg scattering, $q^2 L/k > \pi$. Taking an ultrasonic beam width L of 5 mm and the light from a helium–neon laser ($\lambda =$ 6328 Å) it is found that $q^2 L/k$ reaches the value π at a frequency of 59 MHz for the transverse waves in quartz and at 151 MHz for longitudinal waves in sapphire when propagation is along the trigonal axis. Thus in the microwave frequency range Bragg diffraction is more important than Raman–Nath diffraction. The maximum frequency at which Bragg diffraction can be obtained is determined by the condition $\sin \theta = 1$ that is when $\Lambda = \frac{1}{2}\lambda$. For helium–neon laser light at 6328 Å the maximum ultrasonic frequency occurs at 15 GHz for transverse waves in quartz or 38 GHz for longitudinal waves in sapphire. The Bragg angles at an ultrasonic frequency of 1 GHz are approximately 1.5° for the longitudinal waves in sapphire and 4° for the transverse waves in quartz. Finally it is to be noted that the frequency shift of the light is very small, the maximum change being about 1 part in 10^4 for the longitudinal wave in sapphire but more typical changes are of course much less. These figures demonstrate that in the microwave frequency region Bragg diffraction is the dominant effect expected. A semi-quantitative discussion of the conditions necessary for Bragg diffraction is given by WILLARD[1949] who suggests that it becomes important when the light passes more than one wavefront in crossing the ultrasonic beam. This is why the width of the beam in addition to the ultrasonic wavelength occurs in the inequality statement.

There are two approaches to the theory of light diffraction by ultrasonic waves. In one approach a wave equation obtained from Maxwell's relations is used to calculate the passage of light through the material when the parameters of the materials are altered by the presence of the ultrasonic waves. The second approach is to regard the combined effects of the incident light and the ultrasonic wave as producing an oscillating polarization at each point of the material. The emerging light is then taken as being due to the addition of the radiation re-emitted by all these dipole moments. To illustrate both methods, the former will be used in this section to describe the scattering of light by an externally generated ultrasonic wave and the latter approach will be used when the scattering by thermal vibrations is discussed. The calculations are classical and treat the solid as a continuum. This is justifiable as the wavelength of the light is long compared to the interatomic spacing. For example, a cube whose edge is one wavelength long contains about 10^9 atoms. Nevertheless it is sometimes more con-

venient to interpret the interaction between the light and the ultra-
sonic wave as a collision between a photon and a phonon. Eqs. (9.14)
and (9.15) can then be regarded as expressing the conservation of
quasi-momentum and the conservation of energy in the interaction
between these two particles. However fig. 9.2 shows that the small
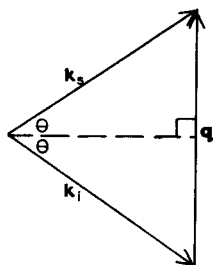
Fig. 9.2. Light scattering as a photon–phonon collision, k_i is the incident photon wave-
vector and k_s the scattered photon wave-vector. q is the phonon wave-vector.

change in the magnitude of the light wave-vector must be neglected to
obtain the first of these two equations. Conservation of quasi-
momentum gives

$$k_i + q = k_s \qquad (9.16)$$

where k_i and k_s are the wave vectors of the incident and scattered
photons and q is the wave number of the phonon. From the diagram
of fig. 9.2 it is seen that if $|k_i| \approx |k_s| = k$ then

$$2k \sin \theta = q$$

or alternatively in terms of the wavelengths

$$2\Lambda \sin \theta = \lambda. \qquad (9.17)$$

A detailed classical theory will now be given following the treatment
of COHEN and GORDON [1965].

An ultrasonic wave of wave vector q and frequency Ω is assumed to
be travelling in the x-direction to produce a variation in permittivity
given by

$$\Delta\kappa(xyt) = [\Delta\kappa(y)]_c \cos (\Omega t - qx) + [\Delta\kappa(y)]_s \sin (\Omega t - qx). \quad (9.18)$$

The beam is assumed to be of finite extent in the y-direction but to
extend to infinity in the z-direction with constant amplitude. Thus the
amplitude of κ is just a function of the coordinate y. The incident light
of frequency ω and wave vector k travels in the xy-plane at an angle
θ_0 to the y-axis. Here the polarization of the incident light can be left
unspecified since it does not enter the calculation at this stage. It does

of course control the components of $\Delta\kappa$ that are needed and thus determines the polarization of the scattered beam. This will be considered later. Figure 9.3 shows the geometry of the interaction. The propagation of the light beam is determined by Maxwell's equations and the constitutive relations for the material which for a non-magnetic, non-conducting medium are

$$\text{div } D = 0 \qquad \text{div } B = 0, \qquad (9.19)$$

$$\text{curl } E = -\frac{\partial B}{\partial t} \qquad \text{curl } H = \frac{\partial D}{\partial t},$$

with

$$D = \kappa E \quad \text{and} \quad B = \mu_0 H. \qquad (9.20)$$

Combining these equations it follows that

$$\text{curl curl } E \equiv -\nabla^2 E + \text{grad div } E = -\mu_0 \frac{\partial^2}{\partial t^2} (\kappa E). \qquad (9.21)$$
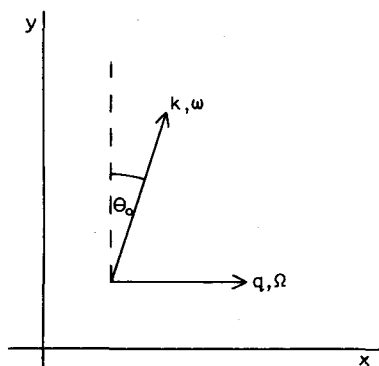
Fig. 9.3.

It is to be remembered that in the presence of the ultrasonic wave κ is not a constant and so cannot be removed outside the differential operator. Suppose for the moment that κ is a scalar quantity as it would be for an isotropic medium. Then

$$\text{div } E = \text{div } \left(\frac{D}{\kappa}\right) \equiv \frac{D}{\kappa_0} \cdot \text{grad } \left(\frac{1}{K}\right) + \frac{1}{K} \text{div } \left(\frac{D}{\kappa_0}\right). \qquad (9.22)$$

The last term is zero by Maxwell's equation and grad $(1/K)$ can be written as $-(1/K)$ grad log K. Therefore

$$\text{grad div } E = -\text{grad } \{E \cdot \text{grad log } K\} \qquad (9.23)$$

so that eq. (9.21) becomes

$$\nabla^2 E + \text{grad } \{E \cdot \text{grad log } K\} = \mu_0 \frac{\partial^2}{\partial t^2} (\kappa E). \qquad (9.24)$$

Now if E and κ are sinusoidal functions it is clear that the first term involves a factor like $1/\lambda^2$ coming from the second differential in ∇^2 while the second term will contain a factor $\Delta\kappa/\kappa\lambda\Lambda$. The ratio of the second term to the first is thus $(\Delta\kappa/\kappa)(\lambda/\Lambda)$. From eq. (9.17) the largest value of λ/Λ is 2 and typically is much less while $\Delta\kappa/\kappa$ is always very much less than unity. Thus the second term in eq. (9.24) is small and so may be neglected compared to the first. The equation thus reduces to

$$\nabla^2 E = \mu_0 \frac{\partial^2}{\partial t^2} (\kappa E). \qquad (9.25)$$

For the geometry considered in the present example this equation has the form

$$\frac{\partial^2 E}{\partial x^2} + \frac{\partial^2 E}{\partial y^2} = \frac{1}{c'^2} \frac{\partial^2}{\partial t^2} \left[\left(1 + \frac{\Delta\kappa}{\kappa} \right) E \right] \qquad (9.26)$$

where c' is the velocity of light in the medium. In the absence of any ultrasonic wave, $\Delta\kappa$ is zero and E is a plane wave of wave vector $k = \omega/c'$. The perturbed E is expanded in a set of plane waves corresponding to the various diffracted waves thus:

$$E(xyt) = \sum_{l=-\infty}^{\infty} \{ V_l(y) \exp (i[(\omega+l\Omega)t - (k \sin \theta_0 + lq)x - ky \cos \theta_0]) $$

$$+ \text{complex conjugate}\}. \qquad (9.27)$$

$V_l(y)$ is the amplitude of the lth deflected beam which has a frequency $(\omega + l\Omega)$. The zero-order beam is naturally parallel to the incident beam and therefore makes an angle θ_0 with the y-axis. $\Delta\kappa$ as given by eq. (9.18) can be written in the alternative form

$$\Delta\kappa = \tfrac{1}{2}[\Delta\kappa_c(y) - i\Delta\kappa_s(y)] \exp [i(\Omega t - qx)] + \text{c.c.}$$

and so

$$\frac{\Delta\kappa}{\kappa} E = \sum_{l=-\infty}^{\infty} \left\{ \frac{1}{2\kappa} [(\Delta\kappa_c + i\Delta\kappa_s)V_{l+1} + (\Delta\kappa_c - i\Delta\kappa_s)V_{l-1}] \right.$$

$$\left. \times \exp \{i[(\omega+l\Omega)t - (k \sin \theta_0 + lq)x - ky \cos \theta_0]\} + \text{c.c.} \right\}.$$

Direct substitution of this and the expansion for E into eq. (9.26) yields the following equation for the amplitudes V_l:

$$\frac{d^2 V_l}{dy^2} - 2ik \cos \theta_0 \frac{dV_l}{dy} - \left[k^2 + 2lkq \sin \theta_0 + l^2 q^2 - \frac{(\omega+l\Omega)^2}{c'^2} \right] V_l$$

$$= -\frac{1}{2\kappa c'^2} (\omega+l\Omega)^2 [(\Delta\kappa_c + i\Delta\kappa_s)V_{l+1} + (\Delta\kappa_c - i\Delta\kappa_s)V_{l-1}]. \quad (9.28)$$

Finally using $\omega = c'k$ and $\Omega = vq$ where v is the velocity of the ultrasonic waves this equation can be written as

$$\frac{d^2V_l}{dy^2} - 2ik\cos\theta_0\frac{dV_l}{dy} + 2k\beta_l\cos\theta_0 V_l$$

$$= -\frac{k^2}{2\kappa}\left(1+\frac{l\Omega}{\omega}\right)^2[(\Delta\kappa_c+i\Delta\kappa_s)V_{l+1}+(\Delta\kappa_c-i\Delta\kappa_s)V_{l-1}],\qquad(9.29)$$

where

$$\beta_l = \left[2lkq\left(\frac{v}{c'}-\sin\theta_0\right)-l^2q^2\left(1-\frac{v^2}{c'^2}\right)\right]\bigg/2k\cos\theta_0.\qquad(9.30)$$

When $\Delta\kappa/\kappa$ is very much less than unity — the usual practical situation — V_l varies very slowly with y so d^2V_l/dy^2 can be neglected in comparison to the other terms in eq. (9.29). Also the ultrasonic frequency is very much less than the optical frequency so $l\Omega/\omega$ is much less than unity for any reasonable value of l. Introducing the parameter

$$\xi(y) = \frac{k}{2\kappa\cos\theta_0}\left[\Delta\kappa_c(y)+i\Delta\kappa_s(y)\right]\qquad(9.31)$$

eq. (9.29) can therefore be approximated to

$$\frac{dV_l}{dy}+i\beta_l V_l = -\tfrac{1}{2}i\left[\xi V_{l+1}+\xi^*V_{l-1}\right]\qquad(9.32)$$

where the asterisk denotes the complex conjugate. It will be assumed that $|\int_{-\infty}^{\infty}\xi(y)\,dy| \ll 1$, which implies that the percentage change in the permittivity due to the ultrasonic wave is small, and also that θ_0 is not so large as to give a very small value for its cosine. In addition the ultrasonic beam must be of limited width. In most experimental situations these conditions are satisfied except at the highest frequencies with very large Bragg angles. Eq. (9.32) can be integrated to give

$$V_l = \exp(-i\beta_l y)\int_{-\infty}^{y}\{-\tfrac{1}{2}i[\xi(y')V_{l+1}(y')+\xi^*(y')V_{l-1}(y')]\}$$

$$\times\exp(i\beta_l y')\,dy'\qquad(9.33)$$

Because of the smallness of $|\int_{-\infty}^{\infty}\xi(y)\,dy|$ it is clear that $V_{l+1}\leqslant V_l$ so this equation may be approximated to give

$$V_l = \exp(-i\beta_l y)\int_{-\infty}^{y}-\tfrac{1}{2}i\xi^*(y')V_{l-1}(y')\exp(i\beta_l y')\,dy'\qquad(9.34)$$

for positive values of l and

$$V_l = \exp\left(-i\beta_l y\right) \int_{-\infty}^{y} -\tfrac{1}{2} i\xi(y') V_{l+1}(y') \exp\left(i\beta_l y'\right) dy' \quad (9.35)$$

for negative l. If $\xi(y)$ is a function that is not changing rapidly it follows from eq. (9.34) that V_1 involves something like $[\exp\left(i\beta_1 L\right)]/\beta_1$ where L is the interaction length of the light with the acoustic beam. Thus V_1 and hence all other V_l's except V_0 will be small unless $\beta_1 L < \pi$. From eq. (9.30) it can be seen that even if $\beta_1 L$ is small the rest of the $\beta_l L$'s cannot be less than π unless $q^2 L/k < \pi$. If this equality is satisfied many different orders can be excited. This is the Raman–Nath regime. If $q^2 L/k > \pi$ then only $\beta_1 L$ can be less than π so only V_1 (or V_{-1}) and V_0 can be non-zero. This is the Bragg regime. The first-order beam appears for the particular value of θ_0 that makes β_1 small. β_1 can be written as

$$\beta_{\pm 1} = \pm\frac{q}{\cos\theta_0}\left[\sin\vartheta_{\pm 1} - \sin\theta_0\right], \quad (9.36)$$

where

$$\sin\vartheta_{\pm 1} = \frac{v}{c'} \mp \frac{q}{2k}\left(1 - \frac{v^2}{c'^2}\right). \quad (9.37)$$

Thus β_1 is zero when $\vartheta_1 = \theta_0$, that is

$$\sin\theta_0 = \frac{v}{c'} - \frac{q}{2k}\left(1 - \frac{v^2}{c'^2}\right). \quad (9.38)$$

Noting that v/c' is very small, eq. (9.38) is to all intents and purposes identical to the Bragg law, eq. (9.14) if the diffracted beam moves in the direction making an angle $(-\theta_0)$ with the y-axis. That this is so can be seen from eq. (9.27) where the lth beam travels in a direction making an angle with the y-axis as given by

$$\sin\theta_l = \frac{\sin\theta_0 + lq/k}{1 + l\Omega/\omega}. \quad (9.39)$$

When l is unity and $\Omega/\omega \ll 1$ it follows from eq. (9.37) that $\sin\theta_l \approx \sin\theta_0 - 2\sin\vartheta_1$ so that when $\theta_0 = \vartheta_1$, θ_1 is equal to $-\theta_0$ thus establishing the full Bragg relation. The terms neglected in eqs. (9.38) and (9.39) are those giving the change in frequency and the magnitude of the wave vector of the scattered wave. This is most clearly seen if the interaction is regarded as a collision between a photon and a phonon. If the conservation laws given earlier are derived without the assumption $|k_i| \approx |k_s|$, eqs. (9.37) and (9.39) result.

We return to a consideration of the expression for V_l given by eq. (9.34) under the conditions for Bragg scattering:

$$V_1 = -\tfrac{1}{2}iV_0 \exp\left(-i\beta_1 y\right) \int\limits_{-\infty}^{\infty} \xi^*(y') \exp\left(i\beta_1 y'\right) dy'. \qquad (9.40)$$

It has been assumed that V_0 is approximately a constant and has been removed from the integral. The loss of intensity of the incident beam is small because $\left|\int_{-\infty}^{\infty}\xi(y')\,dy\right| \ll 1$. The upper limit of integration can be extended to infinity as it is assumed that the observation is made outside the scattering region. Substitution of eq. (9.36) into eq. (9.40) gives

$$V_1 = -\tfrac{1}{2}i\,V_0 \exp\left[-iqy\,\frac{(\sin\vartheta_1 - \sin\theta_0)}{\cos\theta_0}\right] \int\limits_{-\infty}^{\infty} \xi^*(y')$$

$$\times \exp\left[-iqy'\,\frac{(\sin\theta_0 - \sin\vartheta_1)}{\cos\theta_0}\right] dy'. \qquad (9.41)$$

This expression gives the amplitude of the Bragg diffracted beam and it is the Fourier transform of the function $\xi(y')$ which is proportional to the ultrasonic amplitude function. Noting that $\xi(y')$ is a function of $y'/\cos\theta_0$ and making the substitution $y'' = y'/\cos\theta_0$, the integral can be recognized as having the form of a Fraunhofer diffraction pattern for the ultrasonic wave. This is not surprising because as COHEN and GORDON[1965] show, the expression can be interpreted in another way by considering the effect of ultrasonic beams moving at small angles relative to the x-axis. The deflected light always corresponds to ultrasonic waves moving at an angle $(\theta_0 - \vartheta)$ with the x-axis. Thus the deflected light plots out the angular distribution of the ultrasonic wave which is another way of describing the Fraunhofer diffraction pattern. Thus light diffraction can be used to investigate the size and shape of the ultrasonic beam.

As an example consider an ultrasonic beam of width L and of constant amplitude, $\xi(y) = \xi_0$, a constant for $-\tfrac{1}{2}L \leqslant y \leqslant \tfrac{1}{2}L$. The deflected light amplitude is by eq. (9.41)

$$V_1 = -\tfrac{1}{2}iV_0 \exp\left[iqy\,\frac{(\sin\theta_0 - \sin\vartheta)}{\cos\theta_0}\right]$$

$$\times \frac{2\xi_0 \sin\left[\tfrac{1}{2}qL(\sin\theta_0 - \sin\vartheta)/\cos\theta_0\right]}{q(\sin\theta_0 - \sin\vartheta)/\cos\theta_0}$$

so the relative intensity of the diffracted beam is

$$\left|\frac{V_1}{V_0}\right|^2 = \xi_0^2 \cos^2\theta_0 \frac{\sin^2\left[\tfrac{1}{2}qL(\sin\theta_0 - \sin\vartheta)/\cos\theta_0\right]}{q^2(\sin\theta_0 - \sin\vartheta)^2}$$

$$\approx \xi_0^2 \frac{\sin^2\left[\tfrac{1}{2}qL(\theta_0 - \vartheta)\right]}{q^2(\theta_0 - \vartheta)^2} \qquad (9.42)$$

where θ_0 is near ϑ. The maximum intensity of the diffracted light occurs when $\theta_0 = \vartheta$ and from eq. (9.42) it is given by

$$\left|\frac{V_1}{V_0}\right|^2_{\max} = \tfrac{1}{4}L^2|\xi_0|^2$$

which from eq. (9.31) is

$$\frac{I_{\max}}{I_0} = \left|\frac{V_1}{V_0}\right|^2_{\max} = \frac{L^2 k^2}{16\cos^2\theta_0}\left[\left(\frac{\Delta\kappa_c}{\kappa}\right)^2 + \left(\frac{\Delta\kappa_s}{\kappa}\right)^2\right]. \qquad (9.43)$$

The relative changes in permittivity appearing in eq. (9.43) can be related through the elasto-optical coefficients to the components of the strain tensor. For the geometry appropriate to eq. (9.10)–a cubic crystal with longitudinal ultrasonic wave propagation along the [001] axis and an incident light beam polarized along the [010] axis–the maximum intensity of the diffracted light is given by

$$\frac{I_{\max}}{I_0} = \frac{L^2 k^2}{16\cos^2\theta_0}K_2^2 p_{23}^2 \epsilon_3^2. \qquad (9.44)$$

This shows that the diffracted light intensity is proportional to the intensity of the ultrasonic wave as eq. (9.44) involves the square of the strain. The intensity, I_s, of the ultrasonic wave is $\tfrac{1}{2}\rho v_3^3 \epsilon_3^2$ where ρ is the density of the crystal and v_3 the appropriate ultrasonic velocity. Hence

$$\left(\frac{I_{\max}}{I_0}\right)_{\text{light}} = \frac{L^2 k^2 K_2^2 p_{23}^2}{8\rho v_3^3 \cos^2\theta_0}I_s. \qquad (9.45)$$

Note that in this equation the wave vector k of the incident light is measured inside the scattering medium. A factor $n^2 = K$ has to be introduced if k is measured outside the material.

3.3. *Polarization of the diffracted light*

The polarization of the diffracted light can be found by considering the elasto-optical coefficients which enter in eq. (9.45). The light scattered by the crystal is due to the oscillating electrical polarization in it. The components of the electrical polarization are related to those of the electric field through the susceptibility tensor

$$P_i = \kappa_0 \chi_{ij} E_j, \qquad (9.46)$$

κ_0 is the permittivity of free space. The susceptibility tensor is connected to the dielectric tensor by

$$K_{ij} = \delta_{ij} + \chi_{ij}. \qquad (9.47)$$

Thus the changes in the dielectric constant due to the strain give corresponding changes in the susceptibility $\Delta\chi_{ij} = \Delta K_{ij}$ and hence an

electrical polarization

$$P_i = \kappa_0 \Delta K_{ij} E_j. \tag{9.48}$$

E_j is the component of the electric field due to the incident light. Hence in terms of the displacement components D_k due to the incident light, the combined effect of the ultrasonic wave and the incident light is to produce a polarization

$$P_i = \Delta K_{ij} (K^{-1})_{jk} D_k. \tag{9.49}$$

Because of the smallness of the elements of ΔK compared to those of K, $\Delta K_{ij}(K^{-1})_{jk}$ is approximately equal to $-K_{ij}(\Delta K^{-1})_{jk}$ so that eq. (9.49) can be put in the more useful form

$$P_i = -K_{ij}(\Delta K^{-1})_{jk} D_k \tag{9.50}$$

and hence from eq. (9.6)

$$P_i = -K_{ij} p_{jkrs} \epsilon_{rs} D_k. \tag{9.51}$$

The polarization of the diffracted light is given by the direction of P. For a low symmetry crystal and for a general direction of propagation and polarization of the ultrasonic waves the number of terms contributing to the summation in eq. (9.51) can be large. However, in normal experimental situations the ultrasonic waves are directed along a symmetry axis and the expressions will simplify.

GAMMON[1968] has suggested a rule of thumb which although not always rigorous appears to hold for high symmetry materials. He states that a longitudinal ultrasonic wave diffracts a light beam polarized in the scattering plane as a beam polarized in that plane. If, on the other hand, the light beam is polarized perpendicular to the scattering plane then the diffracted light beam is also so polarized. In the case of an ultrasonic shear wave polarized perpendicular to the scattering plane, light beams polarized in and perpendicular to the scattering plane are diffracted as beams polarized perpendicular to and in the scattering plane respectively. On the other hand an ultrasonic shear wave polarized in the scattering plane diffracts a light beam polarized in this plane as a beam also polarized in the scattering plane provided the scattering angle (that is twice the Bragg angle) is not $\frac{1}{2}\pi$. A light beam polarized perpendicular to the scattering plane is not diffracted by such an ultrasonic wave. A further discussion of these topics is given by BORN and HUANG[1954].

When more than one term contributes to the summation in eq. (9.51) the situation can be more complicated. For instance, COHEN and GORDON[1965] using an isotropic material—fused quartz—obtained a rotation of the plane of polarization of the light scattered by longi-

tudinal ultrasonic waves by adjusting the plane of polarization of the incident light to an angle of 45° with the scattering plane. The presence of the longitudinal ultrasonic wave causes the quartz to become uniaxial with an optic axis along the direction of propagation of the ultrasonic waves. There are two components to the scattered beam— two terms in the sum of eq. (9.51) contribute—and these components travel with different velocities causing the observed beam to have a polarization rotated from that of the incident beam. The zero-order light beam of course retains the incident polarization and so the zero-order and first-order beams can easily be distinguished using a crossed analyser even if the Bragg angles are small.

3.4. *Determination of acoustic attenuation*

The effect of ultrasonic losses will now be discussed. In particular it will be shown how the attenuation constant of the ultrasonic waves can be found using optical Bragg scattering techniques. In §3.2, it has already been demonstrated that the intensity of the diffracted beam is proportional to the ultrasonic intensity (see eq. (9.44)) so it is only to be expected that the ultrasonic attenuation can be determined from the intensity of the diffracted light beam at various points along the ultrasonic path. Also it happens, as Cohen and Gordon show, that a narrow light beam is not necessary since when the light beam is translated in a direction parallel to the ultrasonic path, the scattered light energy will change by an amount independent of the width of the light beam.

The theory given above is modified to account for the ultrasonic losses as follows. A decay factor $\exp(-\alpha x)$ has to be inserted into eq. (9.18) to give

$$\Delta\kappa(xyt) = \exp(-\alpha x)\{[\Delta\kappa(y)]_c \cos(\Omega t - qx) + [\Delta\kappa(y)]_s \sin(\Omega t - qx)\}.$$

$$(9.52)$$

Now provided the condition $|\int \xi(y)\,dy| \ll 1$ is still met the solution can be written as

$$E(xyt) = \sum_{l=-\infty}^{\infty} \{V_l(y) \exp(i[|l|\alpha x + (\omega + l\Omega)t - (k\sin\theta_0 + lq)x$$

$$- ky\cos\theta_0]) + \text{c.c.}\}. \qquad (9.53)$$

Strictly this is not a true solution because when substituted into eq. (9.26) it leaves a factor involving x in the equation for $V_l(y)$

$$\frac{\partial^2 V_l}{\partial y^2} - 2ik\cos\theta_0 \frac{\partial V_l}{\partial y} - [k^2 + 2lkq\sin\theta_0 + l^2q^2 - l^2\alpha^2$$

$$- 2i|l|\alpha(k\sin\theta_0 + lq) - \frac{1}{c'^2}(\omega + l\Omega)^2]V_l$$

$$= -\frac{(\omega + l\Omega)^2}{2\kappa c'^2}[\exp(-2\alpha x)(\Delta\kappa_c + i\Delta\kappa_s)V_{l+1} + (\Delta\kappa_c - i\Delta\kappa_s)V_{l-1}] \quad (9.54)$$

when $l > 0$. For the case when $l < 0$, the factor $\exp(-2\alpha x)$ multiples the term in V_{l-1} instead of that in V_{l+1}. This solution is a good enough approximation however when $V_{l+1} \ll V_{l-1}$ since it is these unwanted terms that are dropped in going to eqs. (9.34) and (9.35). The only difference that occurs therefore is that the β_l's, defined in eq. (9.30) are modified to give

$$\beta_l' = \beta_l + \frac{2i|l|\alpha(k\sin\theta_0 + lq) + l^2\alpha^2}{2k\cos\theta_0} \approx \beta_l + i|l|\alpha(\sin\theta_0 + lq/k)/\cos\theta_0 \quad (9.55)$$

where it has been assumed that $\alpha \ll q$ so that the term in α^2 has been neglected. It is seen from this expression that β_l' can never be zero if α is non-zero even at the optimum angle, the Bragg angle, for θ_0.

The maximum intensity of the first-order diffracted beam for a rectangular uniform ultrasonic wave can be written down from eq. (9.42) and the reasoning immediately preceding it. At the Bragg angle $\sin\theta_0$ is $-\frac{1}{2}q/k$ and hence from eq. (9.55)

$$\beta_1' = \beta_1 - i\alpha\tan\theta_0. \quad (9.56)$$

Thus, remembering that ξ_0 is now multiplied by a factor $\exp(-\alpha x)$, see eqs. (9.31) and (9.52), it is found that

$$V_1 = -\frac{1}{2}iV_0\xi_0\exp[-(\alpha x + i\beta_1 y)]\int_{-\infty}^{\infty}\exp(i\beta_1 y')\,dy' \quad (9.57)$$

which gives

$$\left|\frac{V_1}{V_0}\right|^2 = \xi_0^2\exp(-2\alpha x - \alpha L\tan\theta_0)\frac{|\sin\frac{1}{2}[q(\theta_0 - \vartheta) + i\alpha\tan\theta_0]L|^2}{q^2(\theta_0 - \vartheta)^2 + \alpha^2\tan^2\theta_0} \quad (9.58)$$

where the approximation $(\sin\theta_0 - \sin\vartheta)/\cos\theta_0 \approx \theta_0 - \vartheta$ has been used. At the Bragg angle it follows that

$$\left|\frac{V_1}{V_0}\right|^2 = \xi_0^2\exp(-2\alpha x - \alpha L\tan\vartheta)\frac{\sinh^2(\frac{1}{2}\alpha L\tan\vartheta)}{\alpha^2\tan^2\vartheta}. \quad (9.59)$$

Several useful conclusions can be drawn from this equation. First, that if the point of observation is moved along the ultrasonic beam, the diffracted light intensity falls off as $\exp(-2\alpha x)$ independent of the width of the incident light beam. Thus the attenuation coefficient α for the ultrasonic beam can be measured. Because of the decay of the

ultrasonic wave there is a limit to the angular resolution. The ratio of V_1 to V_0 falls off exponentially by an amount determined by $\alpha L \tan \theta_0$. There is thus a limit, which may be taken as $1/\alpha \tan \theta_0$, to the useful width of the beam. COHEN and GORDON[1965] go on to show that the ultrasonic attenuation coefficient can also be measured by studying the far-field shape of the scattered light beam. They show that if the incident beam has a Gaussian profile, as might be obtained from a laser, the scattered beam is also very nearly Gaussian in shape with the same spot size. However, if half of the incident Gaussian beam is blocked and its width is much greater than the ultrasonic decay length $1/\alpha$, then the distant scattered beam is Lorentzian in shape with an angular width at half intensity given by

$$\Delta\theta = 2\alpha/k \cos \vartheta. \qquad (9.60)$$

Thus the attenuation coefficient can be measured without moving the light source or scattering crystal.

3.5. Experimental measurements.

Methods for generating ultrasonic waves for light scattering experiments are described in ch. 3. The diagram, fig. 9.4, shows the arrangement needed to observe light diffraction. It is essentially the method
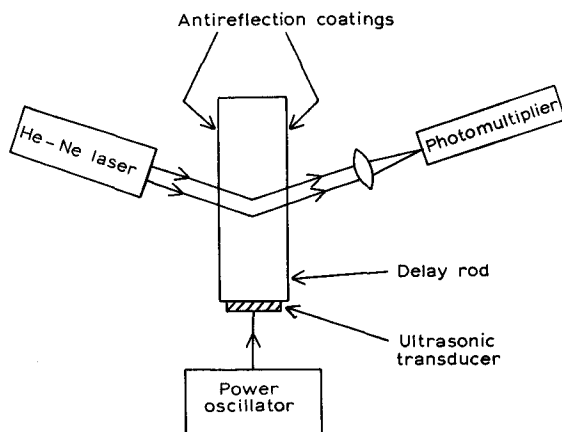
Fig. 9.4. Light scattering apparatus of COHEN and GORDON[1965]. The diagram is simplified omitting the facilities for rotating the specimen.

used by COHEN and GORDON[1965] to demonstrate their theory given above. A specimen crystal with polished sides and anti-reflection coatings is illuminated by a helium–neon laser and the scattered beam is detected with a photomultiplier.

The anti-reflection coatings are necessary to prevent loss of light by reflection away from the detector. If the side faces of the specimen are polished to be accurately parallel, it can act as a Fabry–Perot resonator and a large enhancement in the scattering of light can be observed when the Bragg angle corresponds to the Fabry–Perot transmission maximum. This is discussed by COHEN and GORDON [1966]. The effect of Fabry–Perot interferences can be avoided either by anti-reflection coatings or by polishing the surfaces of the specimen at a slight angle to each other so that the multiple reflected beams are separated from each other. This method involves a loss of light and a reduction in the intensity of the scattered beam.

A modification of these experimental methods is given by GORDON and COHEN [1967] for a situation where the ultrasonic attenuation is very high. They examined the attenuation in water by scattering light at the Bragg angle very close to the quartz transducer generating the waves. The Bragg scattered light mixed with light specularly reflected off the transducer at a photo-detector. The ultrasonic frequency – the difference frequency – could be observed in the photo-current. Thus increased sensitivity was obtained for examining the rapidly decaying waves.

4. Brillouin scattering by thermal vibrations

4.1. *Introduction*

Light is scattered by thermal vibrations of a solid in the same way as by an ultrasonic wave and therefore Brillouin scattering of light by the crystal provides a means whereby the acoustic modes of the solid can be studied. From the discussion of §3 it is clear that the frequency range of interest is the microwave range. Thermally excited phonon modes enable investigations to be made in regions where the use of ultrasonic waves is impossible, for example at temperatures where the mean free path of the acoustic phonons is very short. However the intensity of the Brillouin scattered light is low and so careful experiments are needed to observe it.

When a light beam is incident on a crystal, light is scattered in all directions. Some of this scattering is due to crystal imperfections and the light is scattered without change of frequency; this is the so-called Rayleigh scattering. Brillouin scattering by the thermal vibrations of the crystal lattice occurs with a change in the frequency of the light. Hence in order to observe the Brillouin components a high resolution spectroscopic technique is required. Two Brillouin components can be seen: the Stokes line, corresponding to the creation of a phonon, has a

lower frequency than the incident light and is in accordance with Stokes' law of fluorescence; the other component, the anti-Stokes line, corresponds to the annihilation of a phonon and has a higher frequency than the incident light. The change in frequency of the light enables the frequency of the phonons to be found. The wave-vector of the phonon is determined from the scattering angle and from the frequency of the light (see eq. (9.17)) and thus the phonon velocity in a particular direction can be found. As implied by the discussion of §3.4 the life-time of the phonon can be determined from the spectral width of the Brillouin scattered light. This is discussed below in §4.2.

4.2. *Theory of Brillouin scattering*

The mechanism of the interaction between the light and the thermal vibrations in a solid is of course exactly the same as the interaction with an impressed ultrasonic wave discussed in §3. The main differ-ence is that there is now no well defined ultrasonic beam and so light scattering occurs in all directions. The spectral distribution of the scattered light in a specific direction has to be calculated. As stated in the discussion of §3.2 both situations can be treated in exactly the same way but to illustrate the various methods that are available, the scatter-ing by thermal vibrations will be treated by a different approach to that used above. The theory of Brillouin scattering which will be given here follows the work of BENEDEK and FRITSCH[1966] on cubic crystals. It has more recently been extended to birefringent materials by HOPE[1968].

The crystal is treated as a continuum as the optical wavelength is much longer than the atomic spacing. The incident light passing through the material produces a polarization $P(rt)$ at each point r of the material and this oscillating dipole moment re-radiates light in all directions. In those directions where the scattered waves from all parts of the material reinforce each other, a scattered light beam is observed. The electric field $dE'(R, t)$ at a distant point R due to the scattering polarization in a volume element $|dr| \ll \lambda^3$ is

$$dE'(Rt) = \frac{1}{4\pi\kappa_0} \frac{\{(\widehat{R-r}) \times (\widehat{R-r}) \times (\partial^2 P(rt')/\partial t'^2) \, d|r|\}}{c^2 |R-r|} \quad (9.61)$$

where t' is the retarded time $t - |R-r|/c_m$. c_m is the velocity of light in the medium, c/n, where n is the refractive index. The carets over a vector denote unit vectors. The formula is proved in many books on electromagnetic theory, for example, BORN and WOLF[1965] p. 82 eq. (53). The polarization P is due to the electric field

$$E(rt) = E_0 \exp[i(\omega_0 t - k_0 \cdot r)]$$

of the incident light wave, where the wave vector k_0 is related to the frequency ω_0 by $k_0 = n\omega_0/c$. For small amplitude fields it is assumed that there is a linear relationship between E and P in the crystal. The two are connected by the susceptibility tensor which consists of two parts, a static time-averaged susceptibility χ and a space–time varying part $\delta\chi(rt)$ produced by the thermal vibrations of the crystal. Thus

$$P(rt) = \kappa_0[\chi + \delta\chi(rt)] \cdot E_0 \exp[i(\omega_0 t - k_0 \cdot r)]. \qquad (9.62)$$

Note that χ is a tensor so that $\chi \cdot E_0$ must not be confused with the ordinary scalar product between two vectors. Because the dielectric constant K of the material is related to the susceptibility through eq. (9.47) the space–time varying part of the susceptibility $\delta\chi$ is equal to the varying part of the dielectric constant $\delta K(rt)$ and can thus be related to the elasto-optical constants of the material as described in §2. In what follows $\delta\chi$ will be replaced by δK to emphasize this relation to the earlier discussion. The frequency of the thermal vibrations is much less than that of the light which implies that the variation in δK is slow compared to that of the electric field vector E. It is thus sufficient to ignore the variation in δK when writing the time-derivatives of P. That is it is sufficient to assume that

$$\frac{\partial^2 P(rt)}{\partial t^2} \approx -\omega_0^2 P(rt) \qquad (9.63)$$

so that eq. (9.61) takes the form

$$dE'(Rt) = -\frac{1}{4\pi}\left(\frac{\omega_0}{c}\right)^2 \frac{\widehat{(R-r)} \times \widehat{(R-r)} \times [(\chi + \delta K) \cdot E_0]}{|R-r|}$$
$$\times d|r| \exp i(\omega_0 t - k_0 \cdot r). \qquad (9.64)$$

From fig. 9.5 it is seen that if $R \gg r$ then $\widehat{(R-r)} \approx \hat{k}$ and $|R-r|n\omega_0/c \approx \hat{k} \cdot (R-r)n\omega_0/c$. Introducing $k_0' \equiv n\omega_0\hat{k}/c$ and approximating $|R-r|$ by R in the determinant of eq. (9.64) it follows that

$$dE'(Rt) = -\frac{1}{4\pi}\left(\frac{\omega_0}{c}\right)^2 \frac{\{\hat{k} \times \hat{k} \times [(\chi + \delta K) \cdot E_0]\}}{R}$$
$$\times \exp[i(\omega_0 t - k_0' \cdot R)] \exp[i(k_0' - k_0) \cdot r] |dr|. \qquad (9.65)$$
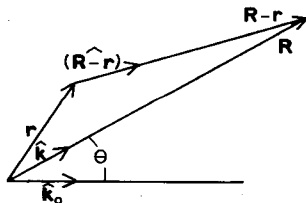
Fig. 9.5. Brillouin scattering geometry.

To obtain the total electric field at R eq. (9.65) must be integrated over the whole illuminated volume V

$$E'(Rt) = -\frac{1}{4\pi}\left(\frac{\omega_0}{c}\right)^2 \frac{\exp\left[i(\omega_0 t - k'_0 \cdot R)\right]}{R} \hat{k} \times \hat{k}$$

$$\times \int_V \left[(\chi + \delta K) \cdot E_0\right] \exp\left[i(k'_0 - k_0) \cdot r\right] |dr|. \qquad (9.66)$$

This expression for E' consists of two parts. One part depends on χ, which is a constant, and gives a scattered beam in the forward direction. The other part depending on $\delta K(rt')$ gives scattering in all directions and includes the Brillouin components. In order to account for scattering in a specified direction it is convenient to take a spatial Fourier transform of $\delta K(rt')$ so as to express the variation in terms of components having a definite wave vector.

$$\delta K(rt') = \frac{1}{(2\pi)^{3/2}} \sum_j \int \delta K(qj) \exp\left[i(\pm\omega_j(q)t' - q \cdot r)\right] |dq|. \qquad (9.67)$$

$\omega_j(q)$ is the frequency of the thermal mode labelled by its wave-vector q and branch number j. The double sign $\pm$ before the frequency is to allow for the presence of running waves in either direction. Damping of waves is included if $\omega_j(q)$ is allowed to become complex. If $\delta K(rt')$ had been taken as a monochromatic plane wave – due to the presence of an ultrasonic wave – the results of §3 would be obtained. Account must be taken in eq. (9.67) of the retarded time $t' \approx t - (n/c)\hat{k} \cdot (R-r)$. The results are simplified by defining a vector $k(q)$ by

$$k(q) \equiv \frac{n}{c}\left[\omega_0 \pm \omega_j(q)\right]\hat{k} \qquad (9.68)$$

from which it follows that

$$\omega_j(q)t' = \omega_j(q)t \mp (k-k'_0) \cdot (R-r). \qquad (9.69)$$

Eq. (9.66) then becomes, apart from the part involving the constant χ which will be dropped,

$$E'(Rt) = -\frac{1}{4\pi}\left(\frac{\omega_0}{c}\right)^2 \sum_j \hat{k} \times \hat{k} \times \int \left[\delta K(qj) \cdot E_0\right] |dq|$$

$$\times \frac{\exp i[(\omega_0 \pm \omega_j(q))t - k \cdot R]}{R} \frac{1}{(2\pi)^{3/2}}$$

$$\times \int_V \exp\left[i(k-k_0-q) \cdot r\right] |dr|. \qquad (9.70)$$

Provided that the linear dimensions of V are much larger than the wave-

length of light the last factor in this expression is the Dirac delta function

$$\int \exp\left[i(k-k_0-q)\cdot r\right]|dr| = (2\pi)^3\delta[q-(k-k_0)]. \quad (9.71)$$

The electric field given by eq. (9.70) thus only has an appreciable value if $q = k(q) - k_0$. It is clear from this equation that k is the wave vector of the scattered light, the frequency of which is $\omega_0 \pm \omega_j(q)$. These expressions are equivalent to the Bragg scattering law, eq. (9.17). Thus because of the delta function eq. (9.70) reduces to

$$E'(qt) = -\left(\frac{\omega_0}{c}\right)^2 \frac{(2\pi)^{3/2}}{4\pi R} \sum_j \hat{k}\times\hat{k}\times[\delta K(qj)\cdot E_0]$$

$$\times \exp\{i[(\omega_0 \mp \omega_j(q))t - k\cdot R]\}, \quad (9.72)$$

where $E'(Rt)$ has been written as $E'(qt)$ to emphasize the direction of scattering. This equation is similar to those derived in §3, the only difference being that now δK is determined by the thermal fluctuations rather than by the presence of an ultrasonic wave of a definite wave vector. In an experiment the spectral distribution of the light scattered in a particular direction is examined and so it is useful to recast the Bragg law in a form that involves the frequency shift of the light. Introducing the phase velocity $v_j(q)$ of the acoustic waves eq. (9.17) is

$$\frac{2\dot{v}_j(q)\sin\theta}{\omega_j(q)} = \frac{c}{n\omega_0} \quad (9.73)$$

so that

$$\frac{\omega' - \omega_0}{\omega_0} = \pm\frac{\omega_j(q)}{\omega_0} = \pm\frac{2n}{c}v_j(q)\sin\theta$$

$$= \pm\frac{2n}{c}v_j(q)\sin\tfrac{1}{2}\phi. \quad (9.74)$$

ω' is the frequency of the scattered light and ϕ is the angle through which it is scattered. Equation (9.74) is the equation obtained by BRILLOUIN[1922]. The velocity of sound in a particular direction can be obtained from the position of the Brillouin doublets.

The intensity and spectral distribution of the scattered light will now be calculated. The information required is contained in the auto-correlation function for the scattered electric field defined by

$$\langle E'(q, t+\tau)\cdot E'(qt)\rangle \equiv \underset{T\to\infty}{\mathrm{Lt}}\frac{1}{2T}\int_{-T}^{T} E'(q, t+\tau)\cdot E'^*(q, t)\,dt. \quad (9.75)$$

(A general discussion of auto-correlation functions is given, for example, in the books by COX and MILLER[1965] and SCHWARTZ [1970].) From the auto-correlation function a spectral density function

$S(q, \omega')$ can be defined as

$$S(q, \omega') = \frac{1}{2\pi} \frac{\int\limits_{-\infty}^{\infty} \langle E'(q, t+\tau) \cdot E'(qt) \rangle e^{i\omega'\tau} d\tau}{\langle |E'(q, t)|^2 \rangle} \tag{9.76}$$

which is normalized to unity thus: $\int_{-\infty}^{\infty} S(q\omega') d\omega' = 1$. In terms of this spectral density function, the power which lies in the frequency range ω' to $\omega' + d\omega'$ and is scattered into a solid angle $d\Omega$ at the point R is

$$dP'(q\omega') d\omega' = [dP'(qR)] S(q\omega') d\omega' \tag{9.77}$$

where

$$dP'(qR) = \tfrac{1}{2} c\kappa_0 \langle |E'(qt)|^2 \rangle R^2 d\Omega \tag{9.78}$$

is the total power of all frequencies scattered into this angle. It now remains to find an expression for the auto-correlation function of the electric field E'. This is related via the dielectric constant and the elasto–optical coefficients to the strain and hence to the auto-correlation function for the elastic displacement vector of the crystal. First, eq. (9.72) is rewritten to restore the time dependence in the dielectric constant

$$E'(qt) = -\left(\frac{\omega_0}{c}\right)^2 \frac{(2\pi)^{3/2}}{4\pi R} \sum_j \hat{k} \times \hat{k} \times [\delta K(qjt) \cdot E_0]$$

$$\times \exp\{i[\omega_0 t - k \cdot R]\} \tag{9.79}$$

where $\delta K(qjt) = \delta K(qj) \exp[i\omega_j(q)t]$. For simplicity the discussion will be restricted to cubic crystals which are electrically isotropic having only a single dielectric constant. The change in dielectric constant is related to the components of the strain through the elasto-optical coefficients (see §2)

$$\delta K_i = -K^2 p_{ij}\epsilon_j \tag{9.80}$$

which for cubic crystals takes the form

$$-\frac{\delta K_{ij}(rt)}{K^2} = 2p_{44}\epsilon_{ij}(rt) + (p_{11} - p_{12} - 2p_{44})\delta_{ij}\epsilon_{ii}(rt)$$

$$+ p_{12}\left(\sum_l \epsilon_{ll}(rt)\right)\delta_{ij}. \tag{9.81}$$

In eq. (9.79) the Fourier components of $\delta K_{ij}(qjt)$ are required. These involve the Fourier components of the strain $\epsilon(rt)$ which in terms of the elastic displacement vectors are given by

$$\epsilon_{lm}(qt) = \frac{1}{(2\pi)^{3/2}} \int \frac{1}{2}\left(\frac{\partial u_l(rt)}{\partial x_m} + \frac{\partial u_m(rt)}{\partial x_l}\right) e^{-iq\cdot r}|dr|. \tag{9.82}$$

Writing the displacement vector $u(rt)$ in terms of its Fourier components defined by

$$u_\alpha(rt) = \frac{1}{(2\pi)^{3/2}} \int \sum_j u(qjt) e_\alpha(qj)\, e^{iq\cdot r} |dq| \qquad (9.83)$$

eq. (9.82) gives

$$\epsilon_{lm}(qt) = \tfrac{1}{2}i \sum_j u(qjt)[e_l(qj)q_m + e_m(qj)q_l]. \qquad (9.84)$$

$e(qj)$ is the unit polarization vector for the mode (qj) (see ch. 2). The change in the electric displacement vector $\delta D(qt)$ produced by the sound waves in conjunction with E_0 is by eqs. (9.81) and (9.84)

$$\delta D(qjt) \equiv \delta K(qjt) \cdot E_0$$
$$= - K^2 i u(qjt)|E_0|\,|q|E(qj) \qquad (9.85)$$

where $E(qj)$ is a vector given by

$$E(qj) = p_{44}[(\hat{q}\cdot\hat{E}_0)e(qj) + (e(qj)\cdot\hat{E}_0)]$$
$$+ (p_{11} - p_{12} - 2p_{44}) \sum_i e_i(qj)\hat{q}_i(\hat{E}_0)_i\hat{i} + p_{12}(e(qj)\cdot\hat{q})\hat{E}_0. \quad (9.86)$$

$\hat{i}$ is a unit vector parallel to the ith coordinate axis. Now by eq. (9.79) it is seen that the scattered light depends on the vector

$$\Xi(qj) = \hat{k} \times \hat{k} \times E(qj). \qquad (9.87)$$

Introducing this vector and using eq. (9.79) the auto-correlation function of eq. (9.75) assumes the form

$$\langle E'(q, t+\tau) \cdot E'^*(qt) \rangle$$
$$= \left(\frac{\omega_0}{c}\right)^4 \cdot \frac{(2\pi)^3}{(4\pi)^2 R^2} K^4 E_n^2 q^2 \sum_j |\Xi(qj)|^2 \langle u(qj, t+\tau) \cdot u^*(qjt) \rangle e^{i\omega_0\tau}. \quad (9.88)$$

This follows if it is remembered that the polarization vectors belonging to the different acoustic branches are orthogonal to each other. The calculation of the intensity of the scattered light therefore involves finding the auto-correlation function of the lattice displacements. BENEDEK and FRITSCH[1966] obtain an expression for this based on a classical argument and point out the modifications required in a quantum treatment. The classical and quantum mechanical results differ only at very low temperatures. The Fourier component of the displacement $u(qjt)$ has essentially two types of time dependence, a rapid oscillation at frequency $\omega_j(q)$ and a slower statistical variation in its amplitude. To separate these two parts $u(qjt)$ is written as

$$u'(qjt) \exp[\pm i\omega_j(q)t].$$

The slower variation in the amplitude can be characterized by a correlation rate $1/\Gamma_j(q)$. If the correlation function for the amplitude is assumed to fall off exponentially in time, then it can be identified with the decay rate for the sound wave of wave vector q or in a quantum treatment as the lifetime of a phonon. In mathematical terms

$$\langle u(qj, t+\tau) \cdot u^*(qjt) \rangle = \langle u'(qj, t+\tau) \cdot u'(qjt) \rangle \exp \pm i\omega_j(q)\tau]$$

$$= \langle |u'(qjt)|^2 \rangle \exp \pm i\omega_j(q)\tau] \exp [-\Gamma_j(q)\tau].$$

$$(9.89)$$

In classical theory an expression for $\langle |u(qjt)|^2 \rangle$ can be obtained from a consideration of the energy of the vibrational modes of the solid. By the equipartition theorem for harmonic oscillators the total vibration energy is twice the kinetic energy:

$$\langle E \rangle = \left\langle \int \rho |\dot{u}(rt)|^2 |dr| \right\rangle \tag{9.90}$$

where ρ is the density of the material. By eq. (9.83)

$$u(rt) = \frac{1}{(2\pi)^{3/2}} \sum_j \int u'(qjt) \exp i[\pm \omega_j(q)t - q \cdot r] |dq| \tag{9.91}$$

so

$$\langle E \rangle = 2 \sum_j \int \rho \omega_j^2(q) |u'(qj)|^2 |dq| \tag{9.92}$$

where the factor 2 arises as there are two waves for each wave vector q moving in opposite directions. Alternatively, the total energy of the lattice can be expressed as a sum of the energies of all the modes each of which has a mean thermal energy $\langle E_j(q) \rangle$. Hence

$$\langle E \rangle = \sum_j \int \frac{V}{(2\pi)^3} \langle E_j(q) \rangle |dq|, \tag{9.93}$$

V is the total volume of the solid and the factor $V/(2\pi)^3$ is the density of states required when converting the sum over q to an integral over $|dq|$. When $\hbar\omega \ll KT$ the average energy per mode, $\langle E_j(q) \rangle$, is KT so from eqs. (9.92) and (9.93)

$$\langle |u'(qj)|^2 \rangle = \frac{VKT}{2(2\pi)^3 \rho \omega_j^2(q)}. \tag{9.94}$$

Thus the auto-correlation function of the scattered field is by eq. (9.88)

$$\langle E'(q, t+\tau) \cdot E'^*(qt) \rangle = \left(\frac{\omega_0}{c} \right)^4 \frac{E_0^2 K^4}{R^2} \frac{V}{(4\pi)^2} \frac{KT}{2\rho} \sum_j \frac{|\Xi(qj)|^2 q^2}{\omega_j^2(q)}$$

$$\times \exp \left(-i[\pm \omega_j(q) + \omega_0]\tau \right)$$

$$\times \exp [-\Gamma_j(q)\tau] \tag{9.95}$$

and hence

$$\langle |E'(qt)|^2\rangle = \left(\frac{\omega_0}{c}\right)^4 \frac{E_0^2 K^4}{R^2} \frac{V}{(4\pi)^2} \frac{KT}{\rho} \sum_j \frac{|\Xi(qj)|^2 q^2}{\omega_j^2(q)}. \qquad (9.96)$$

Therefore, from the definition of eq. (9.76) the spectral density function is

$$S(q\omega') = \sum_j \frac{|\Xi(qj)|^2}{\omega_j^2(q)} \left\{ \frac{\Gamma_j(q)}{[\omega' - (\omega_0 + \omega_j(q))]^2 + \Gamma_j^2(q)} \right.$$
$$\left. + \frac{\Gamma_j(q)}{[\omega' - (\omega_0 - \omega_j(q))]^2 + \Gamma_j^2(q)} \right\} \bigg/ 2\pi \sum_j \frac{|\Xi(qj)|^2}{\omega_j^2(q)}.$$
$$(9.97)$$

The Brillouin components of the scattered light have a Lorentzian shape whose width $\Gamma_j(q)$ gives the acoustic phonon lifetime. There are in general three doublets corresponding to the three values of the polarization index j. In this 'classical derivation' the assumption that $\hbar\omega_j(q) \ll KT$ was made, an assumption which is valid if $T \gg 3$ K. In a quantum treatment the Fourier components of the displacement are expanded in terms of the phonon creation and annihilation operators, see for example eqs. (2.51) and (2.56). It is seen that $u(qjt)$ involves both $a_j(-q)$ and $a_j^*(q)$. From Heisenberg's equation of motion and the Hamiltonian, eq. (2.55) it is seen that the time dependence of $a_j(q)$ is $\exp(-i\omega_j(q)t)$ and that of $a_j^*(q)$ is $\exp(i\omega_j(q)t)$. In addition the thermal average value of $a_j(q)a_j^*(q)$ is $n_j(q) + 1$ and that of $a_j^*(q)a_j(q)$ is $n_j(q)$ where the occupation number $n_j(q)$ is given by the Bose–Einstein factor $\{\exp[\hbar\omega_j(q)/KT] - 1\}^{-1}$. Therefore in eq. (9.94) the classical thermal energy per mode, KT, is replaced by $\hbar\omega_j(q)\{[n_j(q) + 1]$ or $n_j(q)\}$ depending on whether $u'(qj)$ is the amplitude of the running wave with frequency $\omega_j(q)$ or $-\omega_j(q)$. This modification results in $S(q\omega')$ being given by

$$S(q\omega') = \sum_j \frac{|\Xi(qj)|^2}{\omega_j(q)} \Gamma_j(q)$$
$$\times \left(\frac{n_j(q) + 1}{[\omega' - (\omega_0 - \omega_j(q))]^2 + \Gamma_j^2(q)} + \frac{n_j(q)}{[\omega' - (\omega_0 + \omega_j(q))]^2 + \Gamma_j^2(q)} \right)$$
$$\times \left[2\pi \sum_j \frac{|\Xi(qj)|^2}{\omega_j(q)} (2n_j(q) + 1) \right]^{-1}. \qquad (9.98)$$

It is clear that in the quantum regime the intensities of the Brillouin doublets become asymmetric at low temperatures. The low frequency (Stokes) line becomes independent of temperature as $T \to 0$, because

even at the lowest temperatures phonons can be created as the light is scattered. The high frequency (anti-Stokes) line gets weaker in intensity as the temperature is lowered because of the exponential factor $\exp\left[-\hbar\omega_j(q)/KT\right]$. This is because the number of phonons available to scatter the light decreases.

An added complexity arises when the crystal used for Brillouin scattering is birefringent. This situation will not be considered in detail but the main consequences of anisotropy will be indicated. The Bragg scattering law is now modified because the refractive index of the material depends on the direction of propagation and polarization of the scattered light. Thus it can no longer be assumed that the magnitude of the scattered wave vector is approximately equal to the magnitude of the incident wave vector. Although the frequency change is small the change in direction and polarization can cause a larger change in the magnitude of the wave vector. This has been considered theoretically by HOPE [1968] who gives expressions for the light intensity scattered from a birefringent crystal for a number of particular geometries. A study of the scattering from calcite has been made by GRECHUSHNIKOV et al. [1969] who show that due to the birefringence of the material each Brillouin component may split, depending on the polarization of the light, into as many as four parts.

It has been shown that in principle the velocity and decay rate of acoustic phonons in the microwave frequency range can be found by Brillouin scattering. The limitations of the method are set by the need to use a source of very narrow spectral linewidth and a detector of very high resolving power.

4.3. Experiments

A typical experimental arrangement for studying Brillouin scattering is shown in fig. 9.6. The requirements of this apparatus have been discussed by DURAND and PINE [1968]. The narrow spectral line source is a laser which has now become universal in this type of work. A Fabry–Perot interferometer with a photomultiplier acts as the detector. The separation of the Fabry–Perot interferometer plates is varied by means of a piezoelectric transducer and thus scans the spectrum. A multichannel analyser is triggered by the intense elastic Rayleigh scattered light thus allowing an accumulation of counts in spite of the small drift of the apparatus. Other workers have used pressure scanned Fabry–Perot interferometers – the gas pressure between the interferometer plates is varied to scan across the spectrum. BENEDEK and FRITSCH [1966] used a high resolution grating spectrograph to observe the Brillouin scattering from alkali halides. To avoid the problem of scattering from the rough crystal surfaces they immersed their speci-
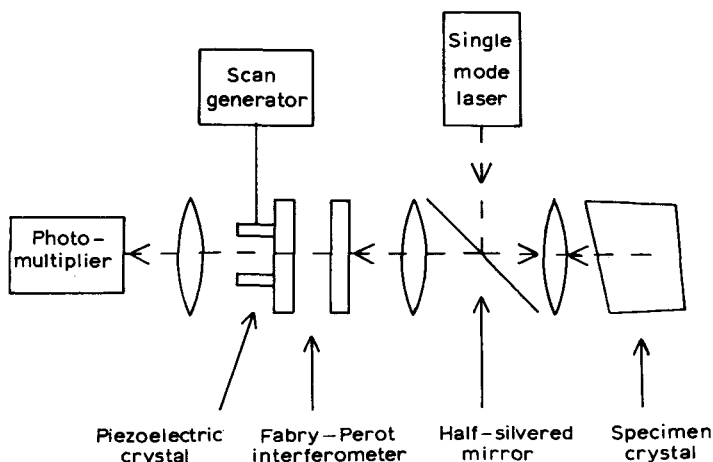
Fig. 9.6. Apparatus of DURAND and PINE [1968] for Brillouin scattering, observed with a piezo-electrically scanned Fabry–Perot interferometer.

mens in liquids with matching refractive index. Care must be taken with this method to avoid strong Brillouin scattering from the liquid itself.

Electronic spectrometers have been briefly discussed by FLEURY [1970] in a useful review which surveys several experimental methods. The majority of the experimental results obtained so far have been concerned with the determination of ultrasonic velocities from the positions of the Brillouin doublets. Early work is described in the review by FABELINSKII [1957]. In the work of Benedek and Fritsch cited above, the Brillouin scattering from potassium chloride, rubidium chloride and potassium iodide was observed. They obtained values for the ultrasonic velocities in agreement with those found at low frequencies. However KAPLAN et al. [1970] using potassium bromide found that the values of the elastic constants determined from their Brillouin scattering data were lower than those of the low frequency measurements and exhibited greater anisotropy.

The ultrasonic attenuation in fused quartz has been found by PINE [1969] from Brillouin scattering data. This is a case that could not be handled by ultrasonic pulse echo techniques as the attenuation is too great. Pine gives a useful discussion of deconvolution procedures needed to obtain the true Brillouin line width from data obtained with instruments of finite resolving power. The linewidth due to the source and the detector is not much less than that of the Brillouin scattering that is being observed and so great care is needed in the interpretation of the results.

5. Stimulated Brillouin scattering

5.1. *Theory of stimulated Brillouin scattering*

When a light beam incident on a solid has an intensity greater than a certain threshold value, a rapid increase in the Stokes scattered light can occur accompanied by the generation of an intense ultrasonic wave. From a quantum point of view this is easily understood as follows. If the scattering of light is regarded as the destruction of a photon in the mode 1 and the creation of another in the mode 2 the scattering rate will involve a factor $n_1(n_2 + 1)$ where the n's are the occupation numbers for these two modes. Normally n_2 is small, of the order of zero, but when the incident intensity is high it may grow exponentially at the point when the rate at which photons are created in this mode exceeds the rate at which they are lost by relaxation. The intensity of light will then increase until the depletion of n_1 calls a halt.

An alternative way of looking at the phenomenon, and the one that will be adopted here, is as a parametric amplifying system. Accounts of the theory have been given by KROLL[1965], whose treatment follows below, and by BOBROFF[1965] and reviews of the subject by QUATE *et al.*[1965] and by STARUNOV and FABELINSKII[1969]. Only the collinear system where the geometry is such that the scattered light travels in the opposite direction to the incident light will be discussed. The scattering angle is π and the ultrasonic wave generated in the process travels in the same direction as the incident light. Eqs. (9.17) and (9.74) show that the frequency change suffered by the light and hence that of the ultrasonic wave is the largest that is possible. The system is a backward wave parametric amplifier. Other geometries have also been considered by KASTLER[1964a, b and 1965] who discussed the case of crossed laser beams in a crystal and also the case of an incident laser beam with a Fabry–Perot resonator at the appropriate Bragg angle for the scattered beam. The collinear system is the one that has been employed experimentally, for example by CHIAO *et al.*[1964].

Consider an incident light wave travelling in the $+z$ direction – the forward direction – given by

$$E_f = \tfrac{1}{2}E_1 \exp\left[i(\omega_1 t - k_1 z)\right] + \tfrac{1}{2}E_1^* \exp\left[-i(\omega_1 t - k_1 z)\right] \quad (9.99)$$

and assume that it is polarized in the y-direction. The scattered wave in the backward direction is likewise given by

$$E_b = \tfrac{1}{2}E_2 \exp\left[i(\omega_2 t + k_2 z)\right] + \tfrac{1}{2}E_2^* \exp\left[-i(\omega_2 t + k_2 z)\right] \quad (9.100)$$

and is accompanied by an ultrasonic wave having associated with it a strain of the form

$$\epsilon = \tfrac{1}{2}\epsilon_1 \exp\left[i(\Omega t - qz)\right] + \tfrac{1}{2}\epsilon_1^* \exp\left[-i(\Omega t - qz)\right]. \quad (9.101)$$

The relationship between the frequencies and wave numbers of the three waves has been discussed above and is

$$\omega_1 = \omega_2 + \Omega, \qquad k_1 = -k_2 + q. \tag{9.102}$$

The usual vector relation connecting the three wave vectors reduces to a simple scalar equation for their magnitudes when the three waves are collinear. The coupling between the waves can be expressed either in terms of the photoelastic constants discussed in §2 or in terms of the constants that describe electrostriction. When an electric field is applied it has been seen that a material becomes strained and for small electric fields only the linear effect, the piezoelectric effect discussed in ch. 2, need be considered. When the field is larger quadratic terms appear and this is known as electrostriction. Since the strain is proportional to the square of the electric field electrostriction can occur in all materials in contrast to the piezoelectric effect which is destroyed by a centre of inversion. Neglecting the piezoelectric term the strain arising from the presence of the electric field can be written as

$$\epsilon_{ij} = \gamma_{klij} E_k E_l, \tag{9.103}$$

where γ_{klij} is the fourth-rank tensor known as the electrostriction tensor. A relationship between γ and the piezo-optical tensor is obtained as follows. In terms of the electric displacement tensor the strain can be written as

$$\epsilon_{ij} = \gamma_{klij} \beta_{kp} \beta_{lq} D_p D_q.$$

Now from the definition of the piezo-optical tensor

$$\frac{\partial \beta_{ij}}{\partial \sigma_{kl}} = \beta_0 \frac{\partial B_{ij}}{\partial \sigma_{kl}} = \beta_0 \pi_{ijkl}.$$

But

$$\frac{\partial \beta_{ij}}{\partial \sigma_{kl}} = \frac{\partial}{\partial \sigma_{kl}} \left(\frac{\partial E_i}{\partial D_j} \right)_\sigma = \frac{\partial}{\partial D_j} \left(\frac{\partial E_i}{\partial \sigma_{kl}} \right)_D = \frac{\partial}{\partial D_j} \left(-\frac{\partial \epsilon_{kl}}{\partial D_i} \right)_\sigma$$

the last step following from the use of table 2.5. Therefore

$$\beta_0 \pi_{ijkl} = -2\gamma_{pqkl} \beta_{pi} \beta_{qj}. \tag{9.104}$$

Again, to simplify the discussion cubic symmetry will be assumed so that there is only one dielectric constant and because of the geometry only one electrostrictive coefficient γ_{23} occurs. Thus the strain, ϵ_E, due to electrostriction in the presence of the light wave is

$$\epsilon_E = \gamma_{23}(E_f + E_b)^2$$
$$= \tfrac{1}{2}\gamma_{23} E_1 E_2^* \exp\left[i(\Omega t - qz)\right] + \text{c.c.} + \text{other terms.} \tag{9.105}$$

On the right-hand side only the term having the correct frequency and

the wave number satisfying eq. (9.102) has been written explicitly. The other terms are of no interest. This strain contributes a driving term in the equation of motion for longitudinal wave propagation along the z-axis in the crystal. The electrostrictive strain is equivalent to a stress $c_{33}\epsilon_E$ where c_{33} is the appropriate elastic stiffness constant. Thus the wave equation for longitudinal wave propagation in this direction is

$$\rho \frac{\partial^2 u}{\partial t^2} - c_{33} \frac{\partial^2 u}{\partial z^2} = c_{33} \frac{\partial^2 u}{\partial z^2}, \tag{9.106}$$

where ρ is the density and u the displacement in the z-direction. Denoting the longitudinal sound velocity in the z-direction in the absence of the electric field by v_ℓ the equation takes the form

$$\frac{1}{v_\ell^2} \frac{\partial^2 \epsilon}{\partial t^2} - \frac{\partial^2 \epsilon}{\partial z^2} = \frac{\partial^2 \epsilon_E}{\partial z^2}. \tag{9.107}$$

Substitution of ϵ and ϵ_E as given by eqs. (9.101) and (9.105) into this equation enables a relationship between the amplitudes of the elastic and light waves to be found. Under the assumption that the incident amplitude E_1 remains constant and that the amplitudes E_2 and ϵ_1 are functions of z but not of time, it is found that

$$\frac{\partial \epsilon_1}{\partial z} = \tfrac{1}{2} i \gamma_{23} q E_1 E_2^*$$

or in terms of the piezo-optical coefficient

$$\frac{\partial \epsilon_1}{\partial z} = \tfrac{1}{4} i q \kappa_0 K^2 \pi_{23} E_1 E_2^*. \tag{9.108}$$

In obtaining this result it is assumed that the second derivatives with respect to z of E_2 and ϵ_1 can be ignored. A similar equation can be obtained for E_2^*. Applying eq. (9.25) to the geometry that is now being considered

$$\frac{1}{c'^2} \frac{\partial^2 E}{\partial t^2} - \frac{\partial^2 E}{\partial z^2} = -\frac{1}{c'^2} \frac{\partial^2}{\partial t^2} \left(\frac{\Delta \kappa}{\kappa} E \right)$$

or

$$\frac{1}{c'^2} \frac{\partial^2 E}{\partial t^2} - \frac{\partial^2 E}{\partial z^2} = \frac{K p_{23}}{c'^2} \frac{\partial^2}{\partial t^2} (\epsilon E). \tag{9.109}$$

The electric field E is the sum of the fields due to the forward and backward light waves. The driving term on the right-hand side of eq. (9.109) is required to give the scattered wave E_b so it is only necessary to consider in the product ϵE the part which has the correct frequency and wave number to satisfy eq. (9.102). Thus only the term involving E_1, the incident wave, is needed on the right-hand side. With similar

approximations to those leading to eq. (9.108) it is found that

$$\frac{\partial E_2^*}{\partial z} = \tfrac{1}{4} i k_2 K p_{23} E_1^* \epsilon_1 + \text{c.c.} \tag{9.110}$$

Equations (9.108) and (9.110) can now be solved for ϵ_1 and E_2^*

$$\frac{\partial^2 \epsilon_1}{\partial z^2} = -\tfrac{1}{16} q k_2 \kappa_0 K^3 \pi_{23} p_{23} E_1 E_1^* \epsilon_1 \tag{9.111}$$

with a similar equation for E_2^*. The solutions are of the form exp $(\pm i\Gamma z)$ with the constant given by

$$\Gamma = \tfrac{1}{4} (q k_2)^{1/2} K (\pi_{23} p_{23})^{1/2} (\kappa_0 K E_1 E_1^*)^{1/2}$$

$$= \tfrac{1}{2} (q k_2)^{1/2} K (\pi_{23} p_{23}/c')^{1/2} (\tfrac{1}{2} P_1)^{1/2}, \tag{9.112}$$

where $P_1 = \tfrac{1}{2} c' \kappa_0 K E_1 E_1^*$ is the incident light power and c' is the phase velocity of the light in the crystal. The general solution for ϵ_1 is

$$\epsilon_1(z) = A \exp(i\Gamma z) + B \exp(-i\Gamma z), \tag{9.113}$$

where the coefficients A and B have to be determined from the boundary conditions. For example, suppose the crystal is of length L stretching from $z = 0$ to $z = L$. Then the appropriate boundary condition is $E_2^*(L) = 0$. From eqs. (9.108) and (9.113)

$$\frac{\partial \epsilon_1(z)}{\partial z} = \tfrac{1}{4} i q \kappa_0 K^2 \pi_{23} E_1 E_2^*$$

$$= i\Gamma [A \exp(i\Gamma z) - B \exp(-i\Gamma z)] \tag{9.114}$$

and so if both A and B are non-zero the boundary condition implies that $A \exp(i\Gamma L) = B \exp(-i\Gamma L)$, from whence it follows that

$$\epsilon_1(z) = \frac{\epsilon_1(0) \cos[\Gamma(z-L)]}{\cos(\Gamma L)}. \tag{9.115}$$

Also by eq. (9.110)

$$E_2^* = i \left(\frac{k_2}{q}\right)^{1/2} \left(\frac{p_{23}}{\kappa_0 K \pi_{23}}\right)^{1/2} \left(\frac{E_1^*}{E_1}\right)^{1/2} \epsilon_1(0) \frac{\sin[\Gamma(z-L)]}{\cos(\Gamma L)}. \tag{9.116}$$

Even if $\epsilon_1(0)$ is zero, that is there is no initial input at the end of the specimen, it is seen that $\epsilon(z)$ and $E_2(z)$ can be finite when $\Gamma L = \tfrac{1}{2}\pi$. Thus at this threshold both ultrasonic waves at a frequency Ω and light at frequency ω_2 are generated.

The analysis presented above has been simplified in that several factors have been neglected. Among these is the neglect of optical and acoustic losses in the crystal due to other processes and also the change in the incident light amplitude due to conversion of the energy

into the ultrasonic and scattered light beam. The changes which arise from the inclusion of all these factors have been discussed by KROLL [1965] but only the effect of acoustic loss will be mentioned here. If the ultrasonic wave amplitude is attenuated according to $\exp(-\alpha z)$ then eq. (9.114) is modified to

$$\frac{\partial \epsilon_1}{\partial z} + \alpha \epsilon_1 = \tfrac{1}{4} i q \kappa_0 K^2 \pi_{23} E_1 E_2^*. \tag{9.117}$$

The solutions now take the form $\exp(\Gamma' z)$ with

$$\Gamma' = -\tfrac{1}{2}\alpha \pm (\tfrac{1}{4}\alpha^2 - \Gamma^2)^{1/2}. \tag{9.118}$$

There is only a build up of acoustic energy provided $2\Gamma' > \alpha$ and then the threshold occurs when the imaginary part of $\Gamma' L$ is equal to $\tfrac{1}{2}\pi$. This a much more stringent requirement than the previous result.
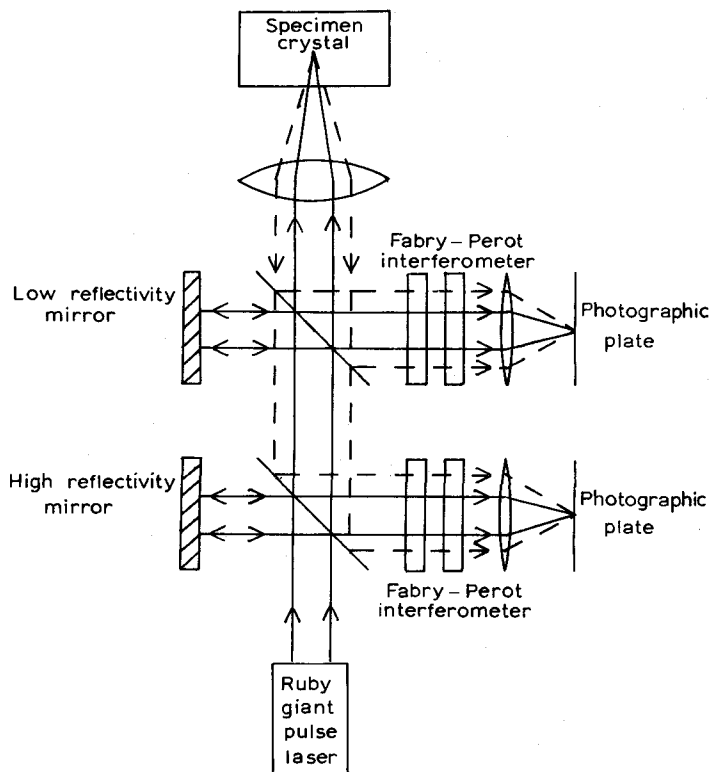
Fig. 9.7. Apparatus for the observation of stimulated Brillouin scattering due to CHIAO *et al.* [1964]. The incident beam and scattered beam are both observed. The incident beam is identified in the interference patterns by the different intensities caused by the different reflectivities of the mirrors.

5.2. *Experiments*

The apparatus used in the first reported stimulated Brillouin scattering experiment is shown in fig. 9.7 taken from the account by CHIAO *et al.*[1964]. Back scattered light from quartz and sapphire was observed when excited by a ruby laser. Back scattered light was similarly observed from benzene and water by BREWER and RIECKHOFF[1964].

Direct evidence of the generation of ultrasonic waves was obtained by HSU and KAVAGE[1965]. By using X-cut quartz as the scattering medium they were able to use a forward scattering geometry and low frequency ultrasonic waves. The incident light was polarized to form the ordinary ray in quartz and the scattering occurred into the extra-ordinary ray travelling in the same direction. Because of the different velocities of light the frequency and wave number matching conditions could be met by ultrasonic waves of 75 MHz travelling in the reverse direction. These were detected piezoelectrically.

The microwave ultrasonic waves generated by stimulated Brillouin scattering have been used by WINTERLING *et al.*[1969] to investigate the ultrasonic absorption in quartz at 29 GHz. A laser pulse was sent into the quartz to generate the waves and a weaker light pulse sent in after a delay of 50 nsec to examine the decaying ultrasonic waves by observing the light scattered from them. A knowledge of the decay that occurred in 50 nsec allowed the attenuation coefficient to be found in a range very difficult to measure by other methods.

TABLE A1.1 Crystal symmetry

System	Class	
	International	Schönflies
Triclinic	1	C_1
	$\bar{1}$	$C_i(S_2)$
Monoclinic	m	$C_s(C_{1h})$
	2	C_2
	2/m	C_{2h}
Orthorhombic	2mm	C_{2v}
	222	$D_2(V)$
	mmm	$D_{2h}(V_h)$
Tetragonal	4	C_4
	$\bar{4}$	S_4
	4/m	C_{4h}
	4mm	C_{4v}
	$\bar{4}2m$	$D_{2d}(V_d)$
	422	D_4
	4/mmm	D_{4h}
Trigonal	3	C_3
	$\bar{3}$	$C_{3i}(S_6)$
	3m	C_{3v}
	32	D_3
	$\bar{3}m$	D_{3d}
Hexagonal	$\bar{6}$	C_{3h}
	6	C_6
	6/m	C_{6h}
	$\bar{6}m2$	D_{3h}
	6mm	C_{6v}
	622	D_6
	6/mmm	D_{6h}
Cubic	23	T
	m3	T_h
	$\bar{4}3m$	T_d
	432	O
	m3m	O_h

TABLE A1.2: Non-vanishing independent elastic stiffness coefficients

Triclinic

c_{11}	c_{12}	c_{13}	c_{14}	c_{15}	c_{16}
	c_{22}	c_{23}	c_{24}	c_{25}	c_{26}
		c_{33}	c_{34}	c_{35}	c_{36}
			c_{44}	c_{45}	c_{46}
				c_{55}	c_{56}
					c_{66}

Monoclinic

c_{11}	c_{12}	c_{13}	0	0	c_{16}
	c_{22}	c_{23}	0	0	c_{26}
		c_{33}	0	0	c_{36}
			c_{44}	c_{45}	0
				c_{55}	0
					c_{66}

x_3 is the unique axis

Orthorhombic

c_{11}	c_{12}	c_{13}	0	0	0
	c_{22}	c_{23}	0	0	0
		c_{33}	0	0	0
			c_{44}	0	0
				c_{55}	0
					c_{66}

Axes along the normals to the symmetry planes

Tetragonal 4, $\overline{4}$, 4/m

c_{11}	c_{12}	c_{13}	0	0	c_{16}
	c_{11}	c_{13}	0	0	$-c_{16}$
		c_{33}	0	0	0
			c_{44}	0	0
				c_{44}	0
					c_{66}

$x_3 \parallel$ 4-fold axis. By a judicial choice of the x_1 axis (which cannot be determined from symmetry) the c_{16} element can be eliminated.

Tetragonal 4mm, $\overline{4}$2m, 422, 4/mmm

c_{11}	c_{12}	c_{13}	0	0	0
	c_{11}	c_{13}	0	0	0
		c_{33}	0	0	0
			c_{44}	0	0
				c_{44}	0
					c_{66}

$x_3 \parallel$ 4-fold axis
$x_1 \parallel$ 2-fold axis

Trigonal 3, $\overline{3}$

c_{11}	c_{12}	c_{13}	c_{14}	c_{15}	0
	c_{11}	c_{13}	$-c_{14}$	$-c_{15}$	0
		c_{33}	0	0	0
			c_{44}	0	$-c_{15}$
				c_{44}	c_{14}
					$\tfrac{1}{2}(c_{11}-c_{12})$

$x_3 \parallel$ 3-fold axis. By a judicial choice of the x_1 axis the c_{15} element can be eliminated.

TABLE A1.2 (*continued*)

Trigonal 3m, 32, $\overline{3}$m

c_{11}	c_{12}	c_{13}	c_{14}	0	0
	c_{11}	c_{13}	$-c_{14}$	0	0
		c_{33}	0	0	0
			c_{44}	0	0
				c_{44}	c_{14}
					$\frac{1}{2}(c_{11}-c_{12})$

$x_3 \parallel$ 3-fold axis
$x_1 \parallel$ 2-fold axis

Hexagonal

c_{11}	c_{12}	c_{13}	0	0	0
	c_{11}	c_{13}	0	0	0
		c_{33}	0	0	0
			c_{44}	0	0
				c_{44}	0
					$\frac{1}{2}(c_{11}-c_{12})$

$x_3 \parallel$ 6-fold axis.

Cubic

c_{11}	c_{12}	c_{12}	0	0	0
	c_{11}	c_{12}	0	0	0
		c_{11}	0	0	0
			c_{44}	0	0
				c_{44}	0
					c_{44}

$x_1, x_2, x_3 \parallel$ cubic axes

Isotropic

c_{11}	c_{12}	c_{12}	0	0	0
	c_{11}	c_{12}	0	0	0
		c_{11}	0	0	0
			$\frac{1}{2}(c_{11}-c_{12})$	0	0
				$\frac{1}{2}(c_{11}-c_{12})$	0
					$\frac{1}{2}(c_{11}-c_{12})$

TABLE A1.3: Non-vanishing third-order elastic constants

1 / 1̄	2 / 2/m / m	2mm / 222 / mmm	4 / 4̄ / 4/m	4mm / 4̄2m / 422 / 4/mmm	3 / 3̄	3m / 32 / 3̄m	6 / 6̄ / 6/m	6̄m2 / 6mm / 622 / 6/mmm	23 / m3	4̄3m / 432 / m3m
111	111	111	111	111	111	111	111	111	111	111
112	112	112	112	112	112	112	112	112	112	112
113	113	113	113	113	113	113	113	113	113	112
114	0	0	0	0	114	114	0	0	0	0
115	0	0	0	0	115	0	0	0	0	0
116	116	0	116	0	116	0	116	0	0	0
122	122	122	112	112	111−222+112	111−222+112	111−222+112	111−222+112	113	112
123	123	123	123	123	123	123	123	123	123	123
124	0	0	0	0	124	124	0	0	0	0
125	0	0	0	0	125	0	0	0	0	0
126	126	0	0	0	−116	0	−116	0	0	0
133	133	133	133	133	133	133	133	133	112	112
134	0	0	0	0	134	134	0	0	0	0
135	0	0	0	0	135	0	0	0	0	0
136	136	0	136	0	0	0	0	0	0	0
144	144	144	144	144	144	144	144	144	144	144
145	145	0	145	0	145	0	145	0	0	0
146	0	0	0	0	$-\frac{1}{4}(115)-\frac{3}{4}(125)$	0	0	0	0	0
155	155	155	155	155	155	155	155	155	155	155
156	0	0	0	0	$\frac{1}{4}(114)+\frac{1}{2}(124)$	$\frac{1}{2}(114)+\frac{1}{2}(124)$	0	0	0	0
166	166	166	166	166	$\frac{3}{4}(222)-\frac{1}{2}(111)-\frac{1}{4}(112)$	$\frac{3}{4}(222)-\frac{1}{2}(111)-\frac{1}{4}(112)$	$\frac{3}{4}(222)-\frac{1}{2}(111)-\frac{1}{4}(112)$	$\frac{3}{4}(222)-\frac{1}{2}(111)-\frac{1}{4}(112)$	166	155
222	222	222	111	111	222	222	222	222	111	111
223	223	223	113	113	113	113	113	113	112	112
224	0	0	0	0	$-114-2(124)$	$-114-2(124)$	0	0	0	0
225	0	0	0	0	$-115-2(125)$	0	0	0	0	0

(The following is a rotated numerical coupling-coefficient table. Rows are labelled by the triples listed at the left; blank cells are 0.)

226	226	226			116		116		0	0
233	233	233	−116	233	133	133	133	133	113	112
234					−134	−134				
235			−136		−135					
236	236	244	155	244	0	0	0	0	166	155
244	244		−145		155	155	155	155		
245	245	255	144	255	−145	144	−145	0	144	144
246					$\frac{1}{2}(125-115)$	$\frac{1}{2}(114-124)$	144	144	155	155
255	255	266	166	266	144	333	0	0	111	111
256		333	333	333	$\frac{1}{2}(114-124)$		$\frac{1}{3}(222+112)$	$\frac{1}{2}(111)-\frac{1}{3}(222+112)$		
266	266				$\frac{1}{2}(111)-\frac{1}{3}(222+112)$	$\frac{1}{2}(111)-\frac{1}{3}(222+112)$	333	333	0	0
333	333				333	333			0	0
334									0	0
335		344	344	344	0	0	0	0	155	155
336	336				344	344	344	344		
344	344	344	344	344	0	0	0	0	166	0
345	345				−135	344				
346		355	366	366	344	134	344	344	144	144
355	355				134	$\frac{1}{2}(113-123)$	$\frac{1}{2}(113-123)$	$\frac{1}{2}(113-123)$	0	0
356					$\frac{1}{2}(113-123)$	444	0			
366	366	366	366	456	444	0	0	0	0	0
444					445	0	0		0	0
445			446		145	0	145		0	0
446	446		456		−444	0	0		456	456
455					$\frac{1}{2}(155-144)$	$\frac{1}{2}(155-144)$	$\frac{1}{2}(155-144)$	$\frac{1}{2}(155-144)$		
456	456	456	456		124	124	0	0	0	0
466					−445	0	−145	0	0	0
555			−446		−145	0	0		0	0
556	556				125	0	−116		0	0
566					−116				0	0
666	666	666							0	0

TABLE A1.4
Non-vanishing independent piezoelectric constants

Triclinic 1

d_{11}	d_{12}	d_{13}	d_{14}	d_{15}	d_{16}
d_{21}	d_{22}	d_{23}	d_{24}	d_{25}	d_{26}
d_{31}	d_{32}	d_{33}	d_{34}	d_{35}	d_{36}

Monoclinic m

d_{11}	d_{12}	d_{13}	0	0	d_{16}
d_{21}	d_{22}	d_{23}	0	0	d_{26}
0	0	0	d_{34}	d_{35}	0

Monoclinic 2

0	0	0	d_{14}	d_{15}	0
0	0	0	d_{24}	d_{25}	0
d_{31}	d_{32}	d_{33}	0	0	d_{36}

Orthorhombic 2mm

0	0	0	0	d_{15}	0
0	0	0	d_{24}	0	0
d_{31}	d_{32}	d_{33}	0	0	0

Orthorhombic 222

0	0	0	d_{14}	0	0
0	0	0	0	d_{25}	0
0	0	0	0	0	d_{36}

Tetragonal 4

0	0	0	d_{14}	d_{15}	0
0	0	0	d_{15}	$-d_{14}$	0
d_{31}	d_{31}	d_{33}	0	0	0

Tetragonal $\bar{4}$

0	0	0	d_{14}	d_{15}	0
0	0	0	$-d_{15}$	d_{14}	0
d_{31}	$-d_{31}$	0	0	0	d_{36}

Tetragonal 4mm

0	0	0	0	d_{15}	0
0	0	0	d_{15}	0	0
d_{31}	d_{31}	d_{33}	0	0	0

Tetragonal $\bar{4}$2m

0	0	0	d_{14}	0	0
0	0	0	0	d_{14}	0
0	0	0	0	0	d_{36}

Tetragonal 422

0	0	0	d_{14}	0	0
0	0	0	0	$-d_{14}$	0
0	0	0	0	0	0

Trigonal 3

d_{11}	$-d_{11}$	0	d_{14}	d_{15}	$-2d_{22}$
$-d_{22}$	d_{22}	0	d_{15}	$-d_{14}$	$-2d_{11}$
d_{31}	d_{31}	d_{33}	0	0	0

Trigonal 3m

0	0	0	0	d_{15}	$-2d_{22}$
$-d_{22}$	d_{22}	0	d_{15}	0	0
d_{31}	d_{31}	d_{33}	0	0	0

Trigonal 32

d_{11}	$-d_{11}$	0	d_{14}	0	0
0	0	0	0	$-d_{14}$	$-2d_{11}$
0	0	0	0	0	0

Hexagonal $\bar{6}$

d_{11}	$-d_{11}$	0	0	0	$-2d_{22}$
$-d_{22}$	d_{22}	0	0	0	$-2d_{11}$
0	0	0	0	0	0

Hexagonal $\bar{6}$m2

0	0	0	0	0	$-2d_{22}$
$-d_{22}$	d_{22}	0	0	0	0
0	0	0	0	0	0

Hexagonal 6
Same as class 4
Hexagonal 6mm
Same as class 4mm
Hexagonal 622
Same as class 422

Cubic 23, $\bar{4}$3m

0	0	0	d_{14}	0	0
0	0	0	0	d_{14}	0
0	0	0	0	0	d_{14}

TABLE A1.5
Non-vanishing independent elasto-optical coefficients

Triclinic

p_{11}	p_{12}	p_{13}	p_{14}	p_{15}	p_{16}
p_{21}	p_{22}	p_{23}	p_{24}	p_{25}	p_{26}
p_{31}	p_{32}	p_{33}	p_{34}	p_{35}	p_{36}
p_{41}	p_{42}	p_{43}	p_{44}	p_{45}	p_{46}
p_{51}	p_{52}	p_{53}	p_{54}	p_{55}	p_{56}
p_{61}	p_{62}	p_{63}	p_{64}	p_{65}	p_{66}

Monoclinic

p_{11}	p_{12}	p_{13}	0	0	p_{16}
p_{21}	p_{22}	p_{23}	0	0	p_{26}
p_{31}	p_{32}	p_{33}	0	0	p_{36}
0	0	0	p_{44}	p_{45}	0
0	0	0	p_{54}	p_{55}	0
p_{61}	p_{62}	p_{63}	0	0	p_{66}

Orthorhombic

p_{11}	p_{12}	p_{13}	0	0	0
p_{21}	p_{22}	p_{23}	0	0	0
p_{31}	p_{32}	p_{33}	0	0	0
0	0	0	p_{44}	0	0
0	0	0	0	p_{55}	0
0	0	0	0	0	p_{66}

Tetragonal 4, $\bar{4}$, 4/m

p_{11}	p_{12}	p_{13}	0	0	p_{16}
p_{12}	p_{11}	p_{13}	0	0	$-p_{16}$
p_{31}	p_{31}	p_{33}	0	0	0
0	0	0	p_{44}	p_{45}	0
0	0	0	$-p_{45}$	p_{44}	0
p_{61}	$-p_{61}$	0	0	0	p_{66}

Tetragonal 4mm, $\bar{4}$2m, 422, 4/mmm

p_{11}	p_{12}	p_{13}	0	0	0
p_{12}	p_{11}	p_{13}	0	0	0
p_{31}	p_{31}	p_{33}	0	0	0
0	0	0	p_{44}	0	0
0	0	0	0	p_{44}	0
0	0	0	0	0	p_{66}

Trigonal 3, $\bar{3}$

p_{11}	p_{12}	p_{13}	p_{14}	p_{15}	$-p_{61}$
p_{12}	p_{11}	p_{13}	$-p_{14}$	$-p_{15}$	p_{61}
p_{31}	p_{31}	p_{33}	0	0	0
p_{41}	$-p_{41}$	0	p_{44}	p_{45}	$-p_{51}$
p_{51}	$-p_{51}$	0	$-p_{45}$	p_{44}	p_{41}
p_{61}	$-p_{61}$	0	$-p_{15}$	p_{14}	$\frac{1}{2}(p_{11}-p_{12})$

Trigonal 3m, 32, $\bar{3}$m

p_{11}	p_{12}	p_{13}	p_{14}	0	0
p_{12}	p_{11}	p_{13}	$-p_{14}$	0	0
p_{31}	p_{31}	p_{33}	0	0	0
p_{41}	$-p_{41}$	0	p_{44}	0	0
0	0	0	0	p_{44}	p_{41}
0	0	0	0	p_{14}	$\frac{1}{2}(p_{11}-p_{12})$

Hexagonal $\bar{6}$, 6, 6/m

p_{11}	p_{12}	p_{13}	0	0	$-p_{61}$
p_{12}	p_{11}	p_{13}	0	0	p_{61}
p_{31}	p_{31}	p_{33}	0	0	0
0	0	0	p_{44}	p_{45}	0
0	0	0	$-p_{45}$	p_{44}	0
p_{61}	$-p_{61}$	0	0	0	$\frac{1}{2}(p_{11}-p_{12})$

TABLE A1.5 (*continued*)

Hexagonal $\bar{6}$m2, 6mm, 622, 6/mmm						Cubic 23, m3					
p_{11}	p_{12}	p_{13}	0	0	0	p_{11}	p_{12}	p_{13}	0	0	0
p_{12}	p_{11}	p_{13}	0	0	0	p_{13}	p_{11}	p_{12}	0	0	0
p_{31}	p_{31}	p_{33}	0	0	0	p_{12}	p_{13}	p_{11}	0	0	0
0	0	0	p_{44}	0	0	0	0	0	p_{44}	0	0
0	0	0	0	p_{44}	0	0	0	0	0	p_{44}	0
0	0	0	0	0	$\frac{1}{2}(p_{11}-p_{12})$	0	0	0	0	0	p_{44}
Cubic $\bar{4}$3m, 432, m3m						Isotropic					
p_{11}	p_{12}	p_{12}	0	0	0	p_{11}	p_{12}	p_{12}	0	0	0
p_{12}	p_{11}	p_{12}	0	0	0	p_{12}	p_{11}	p_{12}	0	0	0
p_{12}	p_{12}	p_{11}	0	0	0	p_{12}	p_{12}	p_{11}	0	0	0
0	0	0	p_{44}	0	0	0	0	0	$\frac{1}{2}(p_{11}-p_{12})$	0	0
0	0	0	0	p_{44}	0	0	0	0	0	$\frac{1}{2}(p_{11}-p_{12})$	0
0	0	0	0	0	p_{44}	0	0	0	0	0	$\frac{1}{2}(p_{11}-p_{12})$

The tables for the coefficient π are identical to those for p except in the following cases. For trigonal and hexagonal systems the coefficients in the last column must be multiplied by a factor 2. Also in the isotropic case the factor $\frac{1}{2}$ in p_{44}, p_{55}, p_{66} should be omitted.

TABLE A1.6

Components of spin–lattice coupling tensor allowed by symmetry

The non-vanishing independent components of the tensor F for different symmetries are the same as those for the elasto-optical coefficient p in table A1.5. For the tensor G the following additional relations hold:

Triclinic

  The same as F

Monoclinic

  $G_{31} = -(G_{11}+G_{21}), \quad G_{32} = -(G_{12}+G_{22})$

  $G_{33} = -(G_{13}+G_{23}), \quad G_{36} = -(G_{16}+G_{26})$

Orthorhombic

  $G_{31} = -(G_{11}+G_{21}), \quad G_{32} = -(G_{12}+G_{22})$

  $G_{33} = -(G_{13}+G_{23})$

Tetragonal 4, $\bar{4}$, 4/m

  $G_{13} = -\frac{1}{2}G_{33}, \quad G_{31} = -(G_{11}+G_{12})$

Tetragonal 4mm, 42m, 422, 4/mmm

  $G_{13} = -\frac{1}{2}G_{33}, \quad G_{31} = -(G_{11}+G_{12})$

Trigonal 3, $\bar{3}$

  $G_{13} = -\frac{1}{2}G_{33}, \quad G_{31} = -(G_{11}+G_{12})$

Trigonal 3m, 32, $\bar{3}$m

  $G_{13} = -\frac{1}{2}G_{33}, \quad G_{31} = -(G_{11}+G_{12})$

Hexagonal 6, $\bar{6}$, 6/m

  $G_{13} = -\frac{1}{2}G_{33}, \quad G_{31} = -(G_{11}+G_{12})$

Hexagonal $\bar{6}$m2, 6mm, 622, 6/mmm

  $G_{13} = -\frac{1}{2}G_{33}, \quad G_{31} = -(G_{11}+G_{12})$

Cubic 23, m3

  $G_{13} = -(G_{11}+G_{12})$

Cubic 43m, $\bar{4}$32, m3m

  $G_{12} = -\frac{1}{2}G_{11}$

APPENDIX 2

TABLE A2.1

Elements of Christoffel's equation for different symmetries

Isotropic

$$\rho\Lambda_{11} = \tfrac{1}{2}c_{11}(1 + \hat{q}_1^2) - \tfrac{1}{2}c_{12}(\hat{q}_2^2 + \hat{q}_3^2)$$

$$\rho\Lambda_{22} = \tfrac{1}{2}c_{11}(1 + \hat{q}_2^2) - \tfrac{1}{2}c_{12}(\hat{q}_1^2 + \hat{q}_3^2)$$

$$\rho\Lambda_{33} = \tfrac{1}{2}c_{11}(1 + \hat{q}_3^2) - \tfrac{1}{2}c_{12}(\hat{q}_1^2 + \hat{q}_2^2)$$

$$\rho\Lambda_{23} = \tfrac{1}{2}(c_{11} + c_{12})\hat{q}_2\hat{q}_3$$

$$\rho\Lambda_{31} = \tfrac{1}{2}(c_{11} + c_{12})\hat{q}_1\hat{q}_3$$

$$\rho\Lambda_{12} = \tfrac{1}{2}(c_{11} + c_{12})\hat{q}_1\hat{q}_2$$

Cubic

$$\rho\Lambda_{11} = c_{11}\hat{q}_1^2 + c_{44}(\hat{q}_2^2 + \hat{q}_3^2)$$

$$\rho\Lambda_{22} = c_{11}\hat{q}_2^2 + c_{44}(\hat{q}_1^2 + \hat{q}_3^2)$$

$$\rho\Lambda_{33} = c_{11}\hat{q}_3^2 + c_{44}(\hat{q}_1^2 + \hat{q}_2^2)$$

$$\rho\Lambda_{23} = (c_{12} + c_{44})\hat{q}_2\hat{q}_3$$

$$\rho\Lambda_{31} = (c_{12} + c_{44})\hat{q}_1\hat{q}_3$$

$$\rho\Lambda_{12} = (c_{12} + c_{44})\hat{q}_1\hat{q}_2$$

Hexagonal

$$\rho\Lambda_{11} = c_{11}\hat{q}_1^2 + \tfrac{1}{2}(c_{11} - c_{12})\hat{q}_2^2 + c_{44}\hat{q}_3^2$$

$$\rho\Lambda_{22} = \tfrac{1}{2}(c_{11} - c_{12})\hat{q}_1^2 + c_{11}\hat{q}_2^2 + c_{44}\hat{q}_3^2$$

$$\rho\Lambda_{33} = c_{44}(\hat{q}_1^2 + \hat{q}_2^2) + c_{33}\hat{q}_3^2$$

$$\rho\Lambda_{23} = (c_{13} + c_{44})\hat{q}_2\hat{q}_3$$

$$\rho\Lambda_{31} = (c_{13} + c_{44})\hat{q}_1\hat{q}_3$$

$$\rho\Lambda_{12} = \tfrac{1}{2}(c_{11} + c_{12})\hat{q}_1\hat{q}_2$$

<div align="center">TABLE A2.1 (continued)</div>

Trigonal 3m, 32, $\overline{3}$m

$$\rho\Lambda_{11} = c_{11}\hat{q}_1^2 + \tfrac{1}{2}(c_{11} - c_{12})\hat{q}_2^2 + c_{44}\hat{q}_3^2 + 2c_{14}\hat{q}_2\hat{q}_3$$
$$\rho\Lambda_{22} = \tfrac{1}{2}(c_{11} - c_{12})\hat{q}_1^2 + c_{11}\hat{q}_2^2 + c_{44}\hat{q}_3^2 - 2c_{14}\hat{q}_2\hat{q}_3$$
$$\rho\Lambda_{33} = c_{44}(\hat{q}_1^2 + \hat{q}_2^2) + c_{33}\hat{q}_3^2$$
$$\rho\Lambda_{23} = c_{14}(\hat{q}_1^2 - \hat{q}_2^2) + (c_{13} + c_{44})\hat{q}_2\hat{q}_3$$
$$\rho\Lambda_{31} = (c_{13} + c_{44})\hat{q}_1\hat{q}_3 + 2c_{14}\hat{q}_1\hat{q}_2$$
$$\rho\Lambda_{12} = 2c_{14}\hat{q}_1\hat{q}_3 + \tfrac{1}{2}(c_{11} + c_{12})\hat{q}_1\hat{q}_2$$

Trigonal 3, $\overline{3}$

$$\rho\Lambda_{11} = c_{11}\hat{q}_1^2 + \tfrac{1}{2}(c_{11} - c_{12})\hat{q}_2^2 + c_{44}\hat{q}_3^2 + 2c_{14}\hat{q}_2\hat{q}_3 + 2c_{15}\hat{q}_1\hat{q}_3$$
$$\rho\Lambda_{22} = \tfrac{1}{2}(c_{11} - c_{12})\hat{q}_1^2 + c_{11}\hat{q}_2^2 + c_{44}\hat{q}_3^2 - 2c_{14}\hat{q}_2\hat{q}_3 - 2c_{15}\hat{q}_1\hat{q}_3$$
$$\rho\Lambda_{33} = c_{44}(\hat{q}_1^2 + \hat{q}_2^2) + c_{33}\hat{q}_3^2$$
$$\rho\Lambda_{23} = c_{14}(\hat{q}_1^2 - \hat{q}_2^2) + (c_{13} + c_{44})\hat{q}_2\hat{q}_3 - 2c_{15}\hat{q}_1\hat{q}_2$$
$$\rho\Lambda_{31} = c_{15}(\hat{q}_1^2 - \hat{q}_2^2) + (c_{13} + c_{44})\hat{q}_1\hat{q}_3 + 2c_{14}\hat{q}_1\hat{q}_2$$
$$\rho\Lambda_{12} = 2c_{14}\hat{q}_1\hat{q}_3 - 2c_{15}\hat{q}_2\hat{q}_3 + \tfrac{1}{2}(c_{12} + c_{11})\hat{q}_1\hat{q}_2$$

Tetragonal 4mm, $\overline{4}$2m, 422, 4/mmm

$$\rho\Lambda_{11} = c_{11}\hat{q}_1^2 + c_{66}\hat{q}_2^2 + c_{44}\hat{q}_3^2$$
$$\rho\Lambda_{22} = c_{66}\hat{q}_1^2 + c_{11}\hat{q}_2^2 + c_{44}\hat{q}_3^2$$
$$\rho\Lambda_{33} = c_{44}(\hat{q}_1^2 + \hat{q}_2^2) + c_{33}\hat{q}_3^2$$
$$\rho\Lambda_{23} = (c_{13} + c_{44})\hat{q}_2\hat{q}_3$$
$$\rho\Lambda_{31} = (c_{13} + c_{44})\hat{q}_1\hat{q}_3$$
$$\rho\Lambda_{12} = (c_{12} + c_{66})\hat{q}_1\hat{q}_2$$

Tetragonal 4, $\overline{4}$, 4/m

$$\rho\Lambda_{11} = c_{11}\hat{q}_1^2 + c_{66}\hat{q}_2^2 + c_{44}\hat{q}_3^2 + 2c_{16}\hat{q}_1\hat{q}_2$$
$$\rho\Lambda_{22} = c_{66}\hat{q}_1^2 + c_{11}\hat{q}_2^2 + c_{44}\hat{q}_3^2 - 2c_{16}\hat{q}_1\hat{q}_2$$
$$\rho\Lambda_{33} = c_{44}(\hat{q}_1^2 + \hat{q}_2^2) + c_{33}\hat{q}_3^2$$
$$\rho\Lambda_{23} = (c_{13} + c_{44})\hat{q}_2\hat{q}_3$$
$$\rho\Lambda_{31} = (c_{13} + c_{44})\hat{q}_1\hat{q}_3$$
$$\rho\Lambda_{12} = c_{16}(\hat{q}_1^2 - \hat{q}_2^2) + (c_{12} + c_{66})\hat{q}_1\hat{q}_2$$

<p align="center">TABLE A2.1 (*continued*)</p>

Orthorhombic

$$\rho\Lambda_{11} = c_{11}\hat{q}_1^2 + c_{66}\hat{q}_2^2 + c_{55}\hat{q}_3^2$$
$$\rho\Lambda_{22} = c_{66}\hat{q}_1^2 + c_{22}\hat{q}_2^2 + c_{44}\hat{q}_3^2$$
$$\rho\Lambda_{33} = c_{55}\hat{q}_1^2 + c_{44}\hat{q}_2^2 + c_{33}\hat{q}_3^2$$
$$\rho\Lambda_{23} = (c_{23} + c_{44})\,\hat{q}_2\hat{q}_3$$
$$\rho\Lambda_{31} = (c_{13} + c_{55})\,\hat{q}_1\hat{q}_3$$
$$\rho\Lambda_{12} = (c_{12} + c_{66})\,\hat{q}_1\hat{q}_2$$

Monoclinic

$$\rho\Lambda_{11} = c_{11}\hat{q}_1^2 + c_{66}\hat{q}_2^2 + c_{55}\hat{q}_3^2 + 2c_{16}\hat{q}_1\hat{q}_2$$
$$\rho\Lambda_{22} = c_{66}\hat{q}_1^2 + c_{22}\hat{q}_2^2 + c_{44}\hat{q}_3^2 + 2c_{26}\hat{q}_1\hat{q}_2$$
$$\rho\Lambda_{33} = c_{55}\hat{q}_1^2 + c_{44}\hat{q}_2^2 + c_{33}\hat{q}_3^2 + 2c_{45}\hat{q}_1\hat{q}_2$$
$$\rho\Lambda_{23} = (c_{23} + c_{44})\,\hat{q}_2\hat{q}_3 + (c_{45} + c_{36})\,\hat{q}_1\hat{q}_3$$
$$\rho\Lambda_{31} = (c_{45} + c_{36})\,\hat{q}_2\hat{q}_3 + (c_{13} + c_{55})\,\hat{q}_1\hat{q}_3$$
$$\rho\Lambda_{12} = c_{16}\hat{q}_1^2 + c_{26}\hat{q}_2^2 + c_{45}\hat{q}_3^2 + (c_{12} + c_{66})\,\hat{q}_1\hat{q}_2$$

Triclinic

$$\rho\Lambda_{11} = c_{11}\hat{q}_1^2 + c_{66}\hat{q}_2^2 + c_{55}\hat{q}_3^2 + 2c_{56}\hat{q}_2\hat{q}_3 + 2c_{15}\hat{q}_1\hat{q}_3 + 2c_{16}\hat{q}_1\hat{q}_2$$
$$\rho\Lambda_{22} = c_{66}\hat{q}_1^2 + c_{22}\hat{q}_2^2 + c_{44}\hat{q}_3^2 + 2c_{24}\hat{q}_2\hat{q}_3 + 2c_{46}\hat{q}_1\hat{q}_3 + 2c_{26}\hat{q}_1\hat{q}_2$$
$$\rho\Lambda_{33} = c_{55}\hat{q}_1^2 + c_{44}\hat{q}_2^2 + c_{33}\hat{q}_3^2 + 2c_{34}\hat{q}_2\hat{q}_3 + 2c_{35}\hat{q}_1\hat{q}_3 + 2c_{45}\hat{q}_1\hat{q}_2$$
$$\rho\Lambda_{23} = c_{56}\hat{q}_1^2 + c_{24}\hat{q}_2^2 + c_{34}\hat{q}_3^2 + (c_{23} + c_{44})\,\hat{q}_2\hat{q}_3 + (c_{45} + c_{36})\,\hat{q}_1\hat{q}_3 + (c_{46} + c_{25})\,\hat{q}_1\hat{q}_2$$
$$\rho\Lambda_{31} = c_{15}\hat{q}_1^2 + c_{46}\hat{q}_2^2 + c_{35}\hat{q}_3^2 + (c_{45} + c_{36})\,\hat{q}_2\hat{q}_3 + (c_{13} + c_{55})\,\hat{q}_1\hat{q}_3 + (c_{14} + c_{56})\,\hat{q}_1\hat{q}_2$$
$$\rho\Lambda_{12} = c_{16}\hat{q}_1^2 + c_{26}\hat{q}_2^2 + c_{45}\hat{q}_3^2 + (c_{46} + c_{25})\,\hat{q}_2\hat{q}_3 + (c_{14} + c_{56})\,\hat{q}_1\hat{q}_3 + (c_{12} + c_{66})\,\hat{q}_1\hat{q}_2$$

TIME-DEPENDENT PERTURBATION THEORY

Because of its frequent use in this book for calculating the transition rates of various phonon processes we have felt it worthwhile to present the derivation of the basic equation of time-dependent perturbation theory.

Consider a Hamiltonian $H(xt) = H^0(x) + V(xt)$ made up of two parts, an unperturbed Hamiltonian H^0 whose eigenvalues E_n and eigenfunctions ϕ_n are known and $V(xt)$ a time-dependent perturbation. For the unperturbed Hamiltonian $H^0\phi_n = E_n\phi_n$. The problem is to find the solutions of the Schrödinger equation

$$i\hbar \frac{\partial \psi(xt)}{\partial t} = H\psi(xt) \qquad (A3.1)$$

given at some instant of time, say $t = 0$, $\psi(x0)$. To do this it is convenient to expand $\psi(xt)$ in terms of the time-dependent eigenfunctions $\phi_n \exp[-iE_nt/\hbar]$. That is,

$$\psi(xt) = \sum_n a_n(t)\phi_n(x) \exp[-iE_nt/\hbar],$$

where the time-dependent coefficients $a_n(t)$ are to be determined. Substitution into eq. (A3.1) gives

$$i\hbar \sum_n \frac{da_n(t)}{dt} \phi_n(x) \exp[-iE_nt/\hbar] = \sum_n a_n(t)V(xt)\phi(x) \exp[-iE_nt/\hbar].$$

Multiplying on the l.h.s. of the equation by $\phi_m^* \exp[iE_mt/\hbar]$ and integrating it follows that

$$i\hbar \frac{da_n(t)}{dt} = \sum_n \int dx \phi_m^* V\phi_n a_n(t) \exp[i(E_m - E_n)t/\hbar]$$

or in short-hand notation

$$i\hbar \dot{a}_m(t) = \sum_n V_{mn}a_n(t) \exp[i(E_m - E_n)t/\hbar] \qquad (A3.2)$$

with

$$V_{mn} = \int \phi_m^*(x) V(xt) \phi_n(x) \, dx.$$

This equation is now solved by successive approximations. It will be assumed that V does not depend explicitly on time. The first approximation is obtained by putting $a_n(t) = a_n(0)$ on the r.h.s. of eq. (A3.2)

$$a_m(t) = a_m(0) + \frac{1}{i\hbar} \sum_n \int V_{mn} a_n(0) \exp\left[i(E_m - E_n)t/\hbar\right]$$

$$= a_m(0) - \sum_n \left[V_{mn} a_n(0) \exp\left[i(E_m - E_n)t/\hbar\right]\right]_0^t$$

$$= a_m(0) + \sum_n \frac{V_{mn} a_n(0)}{E_m - E_n}\left[1 - \exp\left[i(E_m - E_n)t/\hbar\right]\right].$$

It is now assumed that at $t = 0$ the system is in the state $\phi_{m'}(x)$ that is, $a_m(0) = \delta_{m,m'}$. This boundary condition gives

$$a_m(t) = \delta_{m,m'} + \frac{V_{mm'}}{E_m - E_{m'}}\left[1 - \exp\left[i(E_m - E_{m'})t/\hbar\right]\right].$$

It follows that the probability that the system will be in the state ϕ_m at time t is

$$|a_m(t)|^2 = \frac{|V_{mm'}|^2}{(E_m - E_{m'})^2} 2[1 - \cos(E_m - E_{m'})t/\hbar]. \qquad (A3.3)$$

Since the system was initially in the state $\phi_{m'}$ the expression given in eq. (A3.3) may be regarded as being the transition probability for a transition from the state m' to m. That is

$$T_{m' \to m} = \frac{4|V_{mm'}|^2}{(E_m - E_{m'})^2} \sin^2(E_m - E_{m'})t/2\hbar. \qquad (A3.4)$$

The summation over states implies that we are dealing with a discrete set of states. Quite frequently we have to deal with a continuous set of states, or at any rate states that are very close together. The summations must then be replaced by integrals. In that case we are not interested in transitions to a single state but only to a narrow range of states. To indicate that m is now a continuous variable E_m will be written as $E \equiv E(m)$. Consider now the group of states in the range defined by $(E - \Delta E) \leqslant E(m) \leqslant (E + \Delta E)$. The probability of a transition to one of these states in time t is

$$\int dm |a_m(t)|^2 = \int_{E-\Delta E}^{E+\Delta E} dE \frac{dm}{dE} |a_m(t)|^2 = \frac{2\pi t}{\hbar} \int_{E-\Delta E}^{E+\Delta E} dE \frac{dm}{dE} |V_{mm'}|^2 f.$$

where

$$f = \frac{\sin^2\left[(E - E_{m'})t/2\hbar\right]}{\pi(E - E_{m'})^2 t/2\hbar}.$$

It has been assumed that initially the system was in a definite state and that at some instant of time the perturbation was suddenly switched on. In order to neglect 'end effects' only times long enough for $E_{m'}t$ to be very much greater than $\hbar$ must be considered. The function f is plotted in fig. A3.1. It is seen that the function is strongly peaked in the
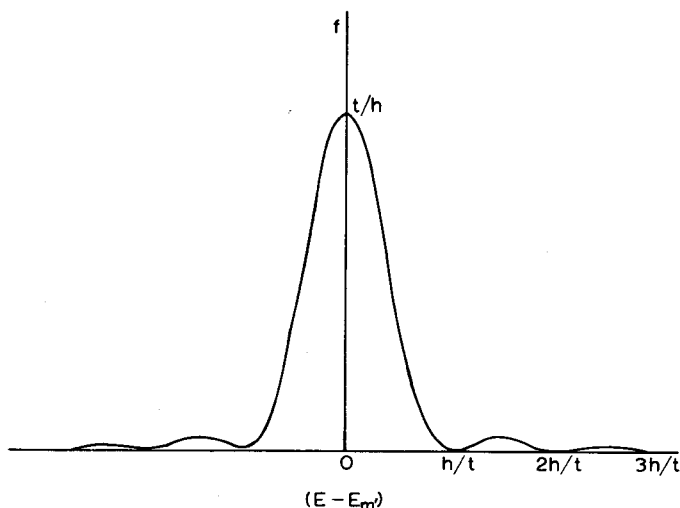
Fig. A3.1.

range $|E - E_{m'}|t \leq h$. Hence the transition probability is only appreciable if the energy is conserved within the limit of the uncertainty principle. Further it is noted that $\int_{-\infty}^{\infty} f \, dE = 1$ so that if $|V_{mm'}|^2 dm/dE$ is a slowly varying function compared to f in the range $|E - E_{m'}|t \leq h$, f behaves as a delta function and

$$T_{m' \to m} = \frac{2\pi t}{\hbar} \int dE \frac{dm}{dt} |V_{mm'}|^2 \delta(E - E_{m'}). \qquad (A3.5)$$

In this case a transition probability per unit time can be defined by

$$W_{m' \to m} = \frac{T_{m' \to m}}{t} = \frac{2\pi}{\hbar} \int dE |V_{mm'}|^2 \frac{dm}{dE} \delta(E - E_{m'})$$

where dm/dE is the density of states function. $\qquad\qquad$ (A3.6)

THERMOELASTIC EFFECT IN AN ISOTROPIC MEDIUM

One of the ways whereby sound may be absorbed in a solid is by the thermoelastic effect, the theory of which for an isotropic medium will now be presented. The energy loss arises because different points in the body will be at different temperatures, the compressed regions being slightly hotter than the expanded regions. The associated temperature gradients give rise to irreversible processes of thermal conduction whereby heat is transferred from the hotter to cooler regions.

For an isotropic elastic medium it has been seen, table A1.2, that there are only two independent elastic constants. The free energy of the material is often written in the form*

$$F = \tfrac{1}{2}\lambda'\epsilon_{ii}^2 + \mu\epsilon_{ik}^2, \tag{A4.1}$$

where λ', μ, the Lamé coefficients, are related to the elastic moduli of eq. (2.7) by $\lambda' = c_{12}$, $\mu = \tfrac{1}{2}(c_{11} - c_{12})$. From the discussion of ch. 2§1.1 it is easy to see by considering an infinitesimal volume element dV that the volume change after deformation is given by $dV' = dV(1 + \epsilon_{ii})$. That is, the relative volume change is just the trace of the strain tensor. An elastic modulus of interest is the bulk modulus B defined as the ratio of the hydrostatic pressure P to the change in volume of the material. For an isotropic medium it follows, on putting the stress components $\sigma_1, \sigma_2, \sigma_3$ equal to P in eq. (2.7), that $\epsilon_{ii} = 3P/(3\lambda' + 2\mu)$ and hence the bulk modulus B is $\lambda' + \tfrac{2}{3}\mu$. The free energy of eq. (A4.1) can therefore be written alternatively as

$$F = \mu(\epsilon_{ij} - \tfrac{1}{3}\delta_{ij}\epsilon_{kk})^2 + \tfrac{1}{2}B\epsilon_{kk}^2. \tag{A4.2}$$

If account is taken of the temperature changes during deformation then the relevant stress–strain relations, from table 2.6, are with

---

* A prime has been put on λ' to distinguish it from the thermal stress coefficient.

neglect of the electric variables

$$\sigma_{ij} = c^T_{ijkl}\epsilon_{kl} - \lambda_{ij}\Delta T, \qquad (A4.3)$$

$$\Delta S = \lambda_{kl}\epsilon_{kl} + C_v\Delta T/T. \qquad (A4.4)$$

The latter equation gives for adiabatic conditions

$$\Delta T = -\frac{T}{C_v}\lambda_{kl}\epsilon_{kl}. \qquad (A4.5)$$

If this is substituted into eq. (A4.3) it follows that $\sigma_{ij} = c^S_{ijkl}\epsilon_{kl}$ where the adiabatic constant c^S_{ijkl} is $c^T_{ijkl} + (T/C_v)\lambda_{kl}\lambda_{ij}$ as given in table 2.8. Also it is noted from the definitions of α and λ in tables 2.4 and 2.6 that

$$\lambda_{kl} = \alpha_{ij}c^T_{ijkl} \qquad (A4.6)$$

where α is the thermal expansion coefficient. Now λ and α transform like second-rank tensors so that for an isotropic medium only their diagonal components are non-zero and are all equal

$$c^S_{ijkl} = c^T_{ijkl} + \frac{T}{C_v}\lambda^2\delta_{k,l}\delta_{i,j}$$

so that $c^S_{11} = c^T_{11} + (T/C_v)\lambda^2$ and $c^S_{12} = c^T_{12} + (T/C_v)\lambda^2$ implying that $\mu^S = \mu^T$ and $B^S = B^T + (T/C_v)\lambda^2$. In addition from eq. (A4.6)

$$\lambda_{11} = \lambda = \alpha_{ii}c^T_{ii11} = \alpha[c_{11} + 2c_{12}] = 3\alpha B^T$$

so that

$$B^S = B^T + \frac{T}{C_v}9\alpha^2(B^T)^2 \qquad (A4.7)$$

which on rearrangement and by use of the thermodynamic relation $B^S/B^T = C_p/C_v$ gives

$$\frac{1}{B^S} = \frac{1}{B^T} - \frac{9\alpha^2 T}{C_p}.$$

Also from eq. (A4.5) the temperature change ΔT associated with adiabatic conditions is

$$\Delta T = -\frac{3T}{C_v}\alpha B^T\epsilon_{ii}. \qquad (A4.8)$$

In the literature dealing with thermal expansion a parameter known as Gruneisen's constant is frequently introduced. This constant characterises the anharmonic properties of solids in much the same way as the Debye temperature is a useful concept in the theory of the harmonic thermal properties such as the specific heat.

The partition function for a collection of harmonic oscillators is

$$Z = \sum_{q} \sum_{n=0}^{\infty} \exp\left[-(n+\tfrac{1}{2})\hbar\omega(q)/KT\right].$$

From the free energy given by $F = -KT \log Z$ the pressure and internal energy may be evaluated from the relations $P = -(\partial F/\partial V)_T$ and $U = \partial(\beta F)/\partial \beta$, respectively, where $\beta = 1/KT$. These differentials involve knowing the value of the partial derivatives

$$\gamma(q) = -\left(\frac{\partial \log \omega(q)}{\partial \log V}\right). \qquad (A4.9)$$

In his treatment, Gruneisen put $\gamma(q)$ equal to some value γ which was assumed to be independent of q. This parameter is known as Gruneisen's constant. Provided this approximation can be made it follows directly that $P = \gamma U/V$ so that

$$3\alpha = \frac{1}{V}\left(\frac{\partial V}{\partial T}\right)_P = \frac{1}{B}\left(\frac{\partial P}{\partial T}\right)_V = \frac{1}{B}\frac{\gamma}{V}\left(\frac{\partial U}{\partial T}\right)_V.$$

Therefore

$$\alpha = \frac{\gamma C_v}{3B}, \qquad (A4.10)$$

where C_v is the specific heat per unit volume. In a Debye model the above relation follows when γ is defined as $-(\partial \log \theta/\partial \log V)$, θ being the Debye temperature. This relationship between the coefficient of expansion and Gruneisen's constant allows the temperature change on adiabatic deformation to be expressed in the form

$$\Delta T = -\gamma T \epsilon_{ii}. \qquad (A4.11)$$

A further expression for ΔT may be obtained by relating the bulk modulus to the velocity of sound in the crystal. It was seen in ch. 2§1.4 that the velocities of longitudinal and transverse waves in an isotropic medium are given by $v_\ell^2 = c_{11}/\rho$, $v_t^2 = (c_{11} - c_{12})/2\rho$. If it is assumed that sound vibrations occur so rapidly that the conditions are essentially adiabatic, then the adiabatic bulk modulus may be expressed in terms of the velocity of sound: $B^S = \rho(v_\ell^2 - \tfrac{4}{3}v_t^2)$. Then

$$\Delta T = -\frac{3T\alpha\rho}{C_v}(v_\ell^2 - \tfrac{4}{3}v_t^2)\epsilon_{ii}. \qquad (A4.12)$$

Because of this temperature difference irreversible processes of heat conduction may occur. To obtain the rate of increase of the total entropy of the body due to these irreversible processes the amount of heat absorbed per unit time in unit volume of the body must be equated to $-\mathrm{div}\, Q$ where Q is the heat flux density. This heat flux is related to the

temperature gradient through the relation

$$Q_i = - \kappa_{ij} \frac{\partial T}{\partial x_j} \tag{A4.13}$$

where κ is the thermal conductivity tensor of rank 2. For an isotropic crystal the heat flux will be parallel to the temperature gradient so that

$$Q = - \kappa \, \text{grad} \, T. \tag{A4.14}$$

Therefore the rate of entropy production is given by

$$\dot{S} = - \int \frac{1}{T} \, \text{div} \, Q \, dV = - \int \, \text{div} \frac{Q}{T} \, dV + \int Q \cdot \text{grad} \frac{1}{T} \, dV.$$

The first integral on the right-hand side can be converted into a surface integral and is seen to give zero. Rearrangement of the last integral leads to the expression

$$\dot{S} = - \int \frac{1}{T^2} \{Q \cdot \text{grad} \, T\} \, dV.$$

Therefore for an isotropic medium the entropy change due to conduction is

$$\dot{S} = - \kappa \int \frac{1}{T^2} [\text{grad} \, T]^2 dV. \tag{A4.15}$$

If the temperature varies slowly throughout the crystal T may be taken outside the integral so that the energy dissipation arising from thermal conduction is

$$\dot{E}_d = - \frac{\kappa}{T} \int [\text{grad} \, T]^2 dV, \tag{A4.16}$$

where grad T may be obtained from eq. (A4.12). From that equation it is clear that ΔT is zero for transverse waves; thus thermal conduction cannot contribute to the absorption of these sound waves. In the case of a longitudinal wave, for example one propagating along the z-axis when $u_x = u_y = 0$, $u_z = u_0 \exp[i(qz - \omega t)]$, an absorption does occur. After substituting into the expression for ΔT, grad T may be calculated and it is found that

$$\frac{\bar{E}_d}{V} = - \frac{\kappa}{2T} \left(\frac{3T\alpha\rho}{C_p} \right)^2 [v_\ell^2 - \tfrac{4}{3}v_t^2]^2 u_0^2 q^4, \tag{A4.17}$$

where the bar indicates a time average over a cycle. The time-averaged energy $\bar{E}$ in the solid is twice the average kinetic energy so that $\bar{E}/V = \tfrac{1}{2}u_0^2\rho\omega^2$. It is usual to define a coefficient of sound absorption A as the ratio of the mean energy dissipation to twice the mean energy

flux. That is

$$A = \tilde{\bar{E}}_\mathrm{d}/2v\bar{E}. \qquad (A4.18)$$

This definition is such that the wave amplitude falls off with the distance as $\exp(-Az)$, see appendix 5. For the absorption of longitudinal sound waves by the thermoelastic effect it follows that

$$A = \kappa \left(\frac{3\alpha}{C_\mathrm{p}}\right)^2 \rho T [v_\ell^2 - \tfrac{4}{3}v_t^2]^2 \frac{\omega^2}{2v_\ell^5} \qquad (A4.19)$$

showing that the absorption is proportional to the square of the frequency.

INTERNAL FRICTION

In addition to the thermoelastic effect there is another source of sound attenuation which might be described as internal friction. This is a viscous effect due to internal motions in the body and can be described phenomenologically in terms of viscous coefficients. The process of deformation is only thermodynamically reversible if it takes place so slowly that thermodynamic equilibrium is established in the body at every instant. Because the motions take place with finite velocities there must therefore be processes which occur to restore thermal equilibrium. The motion is consequently irreversible and so dissipation of mechanical energy into heat occurs.

Dissipation in a mechanical system can be accounted for by adding to the forces in the equations of motion frictional forces which are linear functions of velocities. These frictional forces can be expressed as the velocity derivative of a function ϕ, known as the dissipative function, which is a quadratic function of the velocities. The rate at which mechanical energy is dissipated is then twice this quantity. To determine the general form for ϕ in the case of an isotropic continuous medium it is noted that it must be zero for pure translation or rotary motion since these motions do not give rise to internal friction. Thus ϕ must be zero if the time derivative of the displacement vector, $\dot{u}$, is a constant or if $\dot{u} = \Omega \times r$ where Ω is an angular velocity. To satisfy the first condition ϕ must not depend on the velocities $\dot{u}_i$ but rather on their spatial gradients. The correct combinations of these gradients to fulfill the second condition are those of the time derivatives $\dot{\epsilon}_{ij}$ of the strain tensor. The general form of the dissipative function is therefore*

$$\phi = \tfrac{1}{2} \eta'_{ijkl} \dot{\epsilon}_{ij} \dot{\epsilon}_{kl}, \qquad (A5.1)$$

where the fourth-rank tensor η' is the viscosity tensor. Because of

---

* A prime is put on η' to distinguish it from the deformation tensor.

symmetry there are only two independent non-zero viscosity co-efficients for an isotropic medium so the dissipative function takes the form

$$\phi = \eta_1' (\dot{\epsilon}_{ij} - \tfrac{1}{3}\delta_{ij}\dot{\epsilon}_{kk})^2 + \tfrac{1}{2}\eta_2'\dot{\epsilon}_{kk}^2. \tag{A5.2}$$

This is clearly the analogue of the expression given in eq. (A4.2) for the elastic energy. The rate of energy dissipation due to internal friction is therefore

$$\dot{E}_d = -2\eta_1' (\dot{\epsilon}_{ij} - \tfrac{1}{3}\delta_{ij}\dot{\epsilon}_{kk})^2 dV - \eta_2'\dot{\epsilon}_{kk}^2 dV. \tag{A5.3}$$

In contrast to the thermoelastic effect described in the preceding appendix it is seen that $\dot{E}_d$ will be non-zero for transverse as well as for longitudinal waves since ϕ contains off-diagonal as well as diagonal components of the strain tensor. On evaluating the sound absorption coefficient in the same way as was done for the thermoelastic effect it is readily found that

$$A_t = \eta_1'\omega^2/2\rho v_t^3,$$
$$A_\ell = [\tfrac{4}{3}\eta_1' + \eta_2']\,\omega^2/2\rho v_\ell^3. \tag{A5.4}$$

From the dissipative function a friction stress tensor may be obtained

$$\sigma_{ij}' = 2\eta_1' (\dot{\epsilon}_{ij} - \tfrac{1}{3}\delta_{ij}\dot{\epsilon}_{kk}) + \eta_2'\dot{\epsilon}_{kk}\delta_{i,j}. \tag{A5.5}$$

The total stress is then given by the addition of the ordinary elastic stress and this frictional stress

$$\sigma_{ij} = 2\mu (\epsilon_{ij} - \tfrac{1}{3}\delta_{ij}\epsilon_{kk}) + B\epsilon_{kk}\delta_{ij} + 2\eta_1' (\dot{\epsilon}_{ij} - \tfrac{1}{3}\delta_{ij}\dot{\epsilon}_{kk}) + \eta_2'\dot{\epsilon}_{kk}\delta_{ij}. \tag{A5.6}$$

The total stress is a function of the strain and strain rate. This type of expression used to describe viscous effects was first put forward by MEYER [1874] and by VOIGT [1892]. Solids which are described by this type of equation are often referred to in the literature as Voigt solids. As observed above the theory leads to a dissipation of energy at a rate proportional to the square of the frequency, which is not always in accord with experiment. Because of this ZENER [1948] proposed a more general extension to the elasticity equations. He defined a standard linear solid as one obeying the more general equations

$$(\sigma_{ij} - \tfrac{1}{3}\delta_{ij}\sigma_{kk}) + \tau_1 (\dot{\sigma}_{ij} - \tfrac{1}{3}\delta_{ij}\dot{\sigma}_{kk})$$
$$= 2\mu (\epsilon_{ij} - \tfrac{1}{3}\delta_{ij}\epsilon_{kk}) + 2\eta_1' (\dot{\epsilon}_{ij} - \tfrac{1}{3}\delta_{ij}\dot{\epsilon}_{kk}), \tag{A5.7}$$
$$\sigma_{kk} + \tau_2\dot{\sigma}_{kk} = 3B\epsilon_{kk} + 3\eta_2'\dot{\epsilon}_{kk}.$$

These equations have a greater range of applicability then the Voigt equation for describing relaxation in a solid. τ_1 and τ_2 are the shear and bulk relaxation times. η_1'/τ_1 and η_2'/τ_2 are often referred to as the un-relaxed shear modulus and bulk modulus respectively. μ and B are

the relaxed shear and bulk moduli. The calculation of the attenuation coefficients is as follows. Consider the example of a shear wave represented by $u_i = u_0 \exp[i(\omega t - \Gamma x_j], \ i \neq j$. Combining eq. (A5.7) with the equation of motion $\rho \ddot{u}_i = \partial \sigma_{ij}/\partial x_j$ it is found that the complex propagation vector Γ must satisfy

$$\Gamma^2 = \omega^2 \rho \frac{1 + i\omega \tau_1}{\mu + i\eta_1'\omega}. \qquad (A5.8)$$

To find the attenuation per unit distance the complex part of the propagation constant Γ is required. Putting Γ in the form $\alpha + i\beta$ it is found that

$$\beta = -\left\{ \frac{\omega^2 \rho}{2|F|} \left[1 - \frac{\text{real part } (F)}{|F|} \right] \right\}^{1/2}, \qquad (A5.9)$$

where

$$F = \frac{\eta_1'}{\tau_1} \left\{ \left(\frac{\mu \tau_1}{\eta_1'} + \omega^2 \tau_1^2 \right) + i \left(1 - \frac{\mu \tau_1}{\eta_1'} \right) \omega \tau_1 \right\} \Big/ \{1 + \omega^2 \tau_1^2\}. \qquad (A5.10)$$

If the relaxed and unrelaxed moduli are denoted by M_R and M_U respectively and if the condition $(M_U - M_R)/M_U \ll 1$ is satisfied it is seen that

$$\beta \approx -\frac{1}{2} \frac{\Delta M}{M} \frac{\omega^2 \tau_1}{1 + \omega^2 \tau_1^2} \frac{1}{v_t}. \qquad (A5.11)$$

The amplitude of the wave falls off as $\exp(-\beta x)$ so that the energy carried by the wave which is proportional to the square of the amplitude varies like $K \exp(-2\beta x)$. In a distance Δx the amount of energy dissipated is $[\partial \{K \exp(-2\beta x)\}/\partial x]\Delta x$ that is, it is dissipated at a rate equal to $v\partial [K \exp(-2\beta x)]/\partial x$. Thus from its definition, eq. (A4.18), the absorption coefficient A is seen to be identical to β. Sometimes the absorption coefficient is expressed in terms of the quality factor defined as

$$Q = 2\pi \frac{\text{energy stored}}{\text{energy dissipated/cycle}}. \qquad (A5.12)$$

From this definition and that of A it follows that

$$A = \beta = \omega/2vQ \qquad (A5.13)$$

and

$$Q = \alpha/2\beta. \qquad (A5.14)$$

An example of where the formula of eq. (A5.11) might be applied is to the thermoelastic effect treated in appendix 4. The basic equations are

$$\sigma_{ij} = c_{ijkl}^T \epsilon_{kl} - \lambda_{ij} \Delta T, \qquad (A5.15)$$

$$\Delta S = \lambda_{kl} \epsilon_{kl} + \frac{C_v}{T} \Delta T. \qquad (A5.16)$$

In appendix 4 the temperature gradient for use in the conductivity equation was calculated from the second of these equations assuming adiabatic conditions. To go beyond this approximation ΔT should be calculated from the heat conduction equation

$$\frac{d\Delta T}{dt} = D\nabla^2(\Delta T) - \frac{T}{C_v}\lambda_{kl}\dot{\epsilon}_{kl}, \qquad (A5.17)$$

where D is the diffusion constant equal to the ratio of the thermal conductivity coefficient to the specific heat. On taking the time derivative of eq. (A5.15) and substituting for ΔT it is found that

$$\dot{\sigma}_{ij} - D\nabla^2\sigma_{ij} = -Dc_{ijkl}^T\nabla^2\epsilon_{kl} + \left(c_{ijkl}^T + \frac{T}{C_v}\lambda_{ij}\lambda_{kl}\right)\dot{\epsilon}_{kl}. \qquad (A5.18)$$

This equation is of the same form as the general equation, eq. (A5.7). For longitudinal wave propagation along the x-axis, the relaxation time is $1/D\Gamma^2$ and the relaxed and unrelaxed moduli are c_{11}^T and c_{11}^S respectively. The propagation constant Γ is of course complex with real and imaginary parts α and β respectively. From the general result of eq. (A5.11)

$$\beta \approx -\frac{1}{2\rho v_\ell^3}(c_{11}^S - c_{11}^T)\frac{\omega^2}{D\Gamma^2}\frac{1}{1 + \omega^2/D^2\Gamma^4}. \qquad (A5.19)$$

The diffusion constant may be replaced by $v^2\tau_{th}$ where τ_{th} is the thermal relaxation time. Neglecting damping of the wave $\Gamma^2 = \alpha^2 = \omega^2/v_\ell^2$ so that

$$\beta = \frac{c_{11}^S - c_{11}^T}{2\rho v_\ell^3}\frac{\omega^2\tau_{th}}{1 + \omega^2\tau_{th}^2}. \qquad (A5.20)$$

It is seen that for $\omega\tau_{th} \ll 1$, β reduces to the classical expression obtained for A in appendix 4.

Matrices for $S = 1$ in a representation in which S_z is diagonal

$$S_z = \begin{pmatrix} 1 & 0 & 0 \\ 0 & 0 & 0 \\ 0 & 0 & -1 \end{pmatrix} \qquad\qquad S_z^2 = \begin{pmatrix} 1 & 0 & 0 \\ 0 & 0 & 0 \\ 0 & 0 & 1 \end{pmatrix}$$

$$S_x = \frac{1}{\sqrt{2}} \begin{pmatrix} 0 & 1 & 0 \\ 1 & 0 & 1 \\ 0 & 1 & 0 \end{pmatrix} \qquad\qquad S_y = \frac{i}{\sqrt{2}} \begin{pmatrix} 0 & -1 & 0 \\ 1 & 0 & -1 \\ 0 & 1 & 0 \end{pmatrix}$$

$$S_x S_z + S_z S_x = \frac{1}{\sqrt{2}} \begin{pmatrix} 0 & 1 & 0 \\ 1 & 0 & -1 \\ 0 & -1 & 0 \end{pmatrix} \qquad S_y S_z + S_z S_y = \frac{i}{\sqrt{2}} \begin{pmatrix} 0 & -1 & 0 \\ 1 & 0 & 1 \\ 0 & -1 & 0 \end{pmatrix}$$

$$S_x^2 - S_y^2 = \begin{pmatrix} 0 & 0 & \sqrt{2} \\ 0 & 0 & 0 \\ \sqrt{2} & 0 & 0 \end{pmatrix} \qquad S_x S_y + S_y S_x = \begin{pmatrix} 0 & 0 & -\sqrt{2} \\ 0 & 0 & 0 \\ \sqrt{2} & 0 & 0 \end{pmatrix}$$

RÉSUMÉ OF SEMICONDUCTOR THEORY

1. Intrinsic semiconductors

Many pure semiconductors exhibit intrinsic behaviour except at very low temperatures. An intrinsic semiconductor is one in which the effects of impurities on the conductivity are negligible. The conductivity is explained solely in terms of the conduction and valence bands, impurity levels playing no part. At zero temperature there is a filled valence band separated by an energy gap E_g from the empty conduction band. As the temperature is raised electrons are excited from the valence band to the conduction band. Both the electrons in the conduction band and the positive holes left behind in the valence band contribute to the conductivity b:

$$b = Q_e(n_e\mu_e + n_p\mu_p). \tag{A7.1}$$

Q_e is the magnitude of electronic charge and μ_e and μ_p the electronic and positive hole mobilities (drift velocities/electric field). It is noted that for intrinsic behaviour the number of electrons n_e and positive holes n_p must be equal. The simplest calculation of these numbers proceeds as follows. The conduction band and valence band are assumed to have a single minimum and maximum respectively in E–k space and to be spherically symmetric. In effective mass theory the density of states is then that for the free electron model of a metal with the electronic mass replaced by the appropriate effective mass m^*

$$g_c(E)\,dE = \frac{4\pi}{h^3}(2m_e^*)^{3/2}E^{1/2}dE, \tag{A7.2}$$

$$g_v(E)\,dE = \frac{4\pi}{h^3}(2m_p^*)^{3/2}(-E - E_g)^{1/2}dE \quad. \tag{A7.3}$$

In these equations the energy is measured from the bottom of the

conduction band. The number of electrons in the conduction band at temperature T is then by Fermi–Dirac statistics

$$n_e = \int g_c(E) f_e(E) \, dE, \tag{A7.4}$$

where $f_e(E)$ is the Fermi function $\{\exp[(E-E_f)/KT]+1\}^{-1}$. If it is assumed that $(E-E_f) \gg KT$ then $f_e(E) \approx \exp[-(E-E_f)/KT]$ so that the Fermi function goes over to the classical Boltzmann distribution. Under these conditions the semiconductor is said to be non-degenerate. Strictly speaking the particular form of the density of states given in eq. (A7.2) is only valid for E in the vicinity of the conduction band minimum but because of the exponential factor in the integral it can be assumed to hold for all E. Furthermore the upper limit on the integral can safely be taken as infinity. Under these approximations

$$n_e = 2h^{-3}(2\pi m_e^* KT)^{3/2} \exp(E_f/KT)$$

$$= K_e \exp(E_f/KT). \tag{A7.5}$$

In obtaining this result the standard integral

$$\int\limits_0^\infty \exp(-ax^2) x^2 dx = \tfrac{1}{4}(\pi/a^3)^{1/2}$$

has been used. Similarly the number of positive holes in the valence band is given by

$$n_p = \int\limits_{-\infty}^{-E_g} g_v(E) f_p(E) \, dE. \tag{A7.6}$$

Since the presence of a positive hole indicates the absence of an electron $f_p = 1-f_e$. Therefore if $(E_f - E) \gg KT, f_p \approx \exp[(E-E_f)]/KT]$. It follows that

$$n_p = 2h^{-3}(2\pi m_p^* KT)^{3/2} \exp[-(E_f+E_g)/KT]$$

$$= K_p \exp[-(E_f+E_g)/KT]$$

so that the product $n_p n_e$ is

$$n_p n_e = 4h^{-6}(2\pi KT)^3 (m_e^* m_p^*)^{3/2} \exp[-E_g/KT]. \tag{A7.8}$$

Since $n_p = n_e$ either of them is equal to the square-root of this quantity. The Fermi energy E_f can be found by taking the logarithm of n_p/n_e as given by eqs. (A7.5) and (A7.7)

$$E_f = -\tfrac{1}{2}E_g + \tfrac{3}{4}KT \log_e(m_p^*/m_e^*). \tag{A7.9}$$

If m_e^* and m_p^* are equal the Fermi level lies at the centre of the energy gap. For most semiconductors at normal temperatures deviations from

this point are small. The validity of the non-degenerate approximation can be tested by carrying out an exact numerical calculation using the correct statistics. It is found that the assumption of non-degeneracy is valid provided the Fermi level is at least KT below the conduction band.

2. Impurity semiconductors

In impure or compound semiconductors impurity levels exist that lie between the conduction and valence bands. These levels can be divided into two types, donors and acceptors. An acceptor level is a vacant electronic state usually situated just above the valence band. With a small amount of energy it is possible to excite an electron from the valence band to occupy this available state leaving behind a positive hole for conduction. A donor on the other hand is an impurity level situated just below the conduction band. Usually only a small ionization energy is required to excite an electron from the impurity atom to the conduction band.

Provided the Fermi level is still, say, about $2KT$ below the conduction band the electrons in the band are non-degenerate and the concentration of electrons is still given by eq. (A7.5) but with a different Fermi energy. A change in Fermi energy is to be expected since it will be remembered that eq. (A7.9) was obtained under the assumption that $n_e = n_p$. Similarly for non-degenerate behaviour condition (A7.7) still applies but again with a different Fermi energy. The important point though is that eq. (A7.8) still holds, that is, the product $n_e n_p$ is independent of impurity concentration.

2.1. *Donor impurities*

Suppose that there are N_d donor levels/unit volume with ionization energy $|E_d| \ll |E_g|$ and that the Fermi level lies well below the conduction band, $E_F \ll -KT$. Under these conditions, except at very low temperatures nearly all the impurities will be ionized, see §2.4. If the number of intrinsic electrons n_i (equal to the number of intrinsic holes) excited from the valence band is small compared to N_d the total number of electrons in the conduction band is $\approx N_d$. Since N_d is a constant the number of electrons in the conduction band is practically independent of temperature. Such a semiconductor is called an n-type extrinsic semiconductor. Under these conditions the Fermi level, by eq. (A7.5) is

$$E_f = KT \log (N_d/K_e). \qquad (A7.10)$$

Since this equation was based on the assumption $E_f \ll -KT$ it is clear

that it is only valid if $N_d/K_e \lesssim \frac{1}{2}$. Of course N_d must not be so small so as to violate the condition $N_d \gg n_i$. When $N_d \to K_e$ the Fermi level moves towards the conduction band and so for larger values of N_d degenerate statistics would have to be used.

If the condition $N_d \gg n_i$ is relaxed the intrinsic carriers have to be accounted for. Provided the Fermi level is well away from the conduction band and all the impurities are ionized the total number of carriers is $n_e = n_p + N_d$. But by eq. (A7.8) $n_p n_e = n_i^2$ so that

$$n_e \atop p = \frac{1}{2}[(N_d^2 + 4n_i^2)^{1/2} \pm N_d]. \qquad (A7.11)$$

Thus the limiting values n_e and n_p are

$$\left. \begin{array}{l} n_e = N_d + n_i^2/N_d \\ n_p = n_i^2/N_d \end{array} \right\} \quad \begin{array}{l} \text{when } N_d \gg n_i \\ \text{(but } < K_e) \end{array} \qquad (A7.12)$$

$$n_e \atop p = n_i \pm \frac{1}{2}N_d \qquad \text{when } N_d \ll n_i . \qquad (A7.13)$$

In the former case the number of holes is very much less than that for the intrinsic material. The electrons and holes are called the majority and minority carriers respectively.

2.2. Acceptor impurities

Similar arguments to those given for donor impurities apply. Provided the Fermi level is several KT above the valence band all the acceptors will be occupied and eq. (A7.7) becomes

$$-(E_f + E_g) = KT \log (N_a/K_p) \qquad (A7.14)$$

which is the analogue of eq. (A7.10) and is only valid if $N_a/K_p \lesssim \frac{1}{2}$. If intrinsic carriers are accounted for, $n_p - n_e = N_a$ and the analogue of eq. (A7.11) is

$$n_e \atop p = \frac{1}{2}[(N_a^2 + 4n_i^2)^{1/2} \mp N_a]. \qquad (A7.15)$$

This time the limiting values are

$$\left. \begin{array}{l} n_e = n_i^2/N_a \\ n_p = N_a + n_i^2/N_a \end{array} \right\} \quad N_a \gg n_i \qquad (A7.16)$$

$$n_e \atop p = n_i \mp \frac{1}{2}N_a \quad \text{when} \quad N_a \ll n_i. \qquad (A7.17)$$

2.3. Semiconductors with both donors and acceptors present

In semiconductors where both types of impurities are present the position of the Fermi level will be determined by the difference in numbers of donors and acceptors. In the presence of donors only the Fermi level will be in the upper half of the energy gap. As acceptors are

added electrons will drop down from the donor levels and from the conduction band to ionize them. The effective number of donors having electrons available for excitation to the conduction band is thus $N_d - N_a$ and the Fermi level will fall. When $N_a = N_d$ the Fermi level reaches the intrinsic position at the centre of the gap. For N_a greater than N_d the Fermi level will be in the lower half of the gap and there will then be $(N_a - N_d)$ effective acceptors present.

2.4. *Incomplete ionization*

At very low temperatures complete ionization of the impurities may not occur. If each donor can have two electrons, one of either spin, the average number of electrons in the donor level is given by Fermi–Dirac statistics as

$$n_d = \frac{2N_d}{\exp\left[-(E_d + E_f)/KT\right] + 1}, \qquad (A7.18)$$

where E_d is the appropriate ionization energy. In semiconductors however this formula needs modifying. The reason for this is that each donor, although it has two spin states, never has two electrons. It either has a single electron in either one of the two spin states or no electrons. In these circumstances it is easily verified by the usual method of deriving eq. (A7.18) that

$$n_d = \frac{2N_d}{\exp\left[-(E_d + E_f)/KT\right] + 2}. \qquad (A7.19)$$

In the case of acceptors, each acceptor has one electron of either spin or two paired electrons. In this situation the number of un-ionized acceptors is found to be

$$n_a = \frac{2N_a}{\exp\left[(E_f + E_g - E_a)/KT\right] + 2}. \qquad (A7.20)$$

BIBLIOGRAPHY

ABE, R., 1964, Progr. Theor. Phys. **31**, 957.

ABE, Y. and N. MIKOSHIBA, 1968, Appl. Phys. Lett. **13**, 241.

ABRAGAM, A. and B. BLEANEY, 1970, Electron Paramagnetic Resonance of Transition Ions (Clarendon Press, Oxford).

AKHIESER, A. I., 1939, J. Phys. USSR **1**, 277.

AKHIESER, A. I., 1946, J. Phys. USSR **10**, 217.

AKHIESER, A. I., V. G. BAR'YAKHTAR and S. V. PELETMINSHII, 1959, Zh. Eksp. Teor. Fiz. **36**, 216. (Sov. Phys. JETP. **9**, 146 [1959].)

ALIEV, M. N., 1967, Fiz. Tverd. Tela. **9**, 1304 (Sov. Phys. Solid State **9**, 1020 [1967]).

AL'TSHULER, S. A., B. I. KOCHELAEV and A. M. LEUSHIN, 1961, Usp. Fiz. Nauk **75**, 459 (Sov. Phys. Uspkh. **4**, 880 [1962]).

AL'TSHULER, S. A. and B. M. KOZYREV, 1964, Electron Paramagnetic Resonance (Academic Press, New York).

ANDERSON, R. S., R. G. BRABIN-SMITH and V. W. RAMPTON, 1970, J. Phys. C, **3**, 2379.

ANDREWS, J. M. and M. W. P. STRANDBERG, 1967, J. Appl. Phys. **38**, 2660.

AULD, B., 1962, see R. M. WHITE and E. SCHLOMANN, Microwave Laboratory Report No. 909, Stanford Univ. 1962 (unpublished).

BARANSKII, K. N., 1957a, Kristallografiya **2**, 299 (Sov. Phys. Crystallog. **2**, 296 [1957]).

BARANSKII, K. N., 1957b, Dokl. Akad. Nauk (USSR) **114**, 517 (Sov. Phys. Dokl. **2**, 237 [1958]).

BARDEEN, J., L. N. COOPER and J. R. SCHRIEFFER, 1957, Phys. Rev. **108**, 1175.

BATEMAN, T., W. P. MASON and H. J. McSKIMIN, 1961, J. Appl. Phys. **32**, 928.

BATEMAN, T. B., 1962, J. Appl. Phys. **33**, 3309.

BATEMAN, T. B., 1967, J. Acoust. Soc. Amer. **41**, 1011.

BECHMANN, R., 1955, IRE Trans. Ultrason. Eng. PGUE-3, 43.

BECHMANN, R., 1958, Phys. Rev. **110**, 1060.

BECKER, R. and W. DORING, 1939, Ferromagnetismus (Springer, Berlin).

BENEDEK, G. B. and K. FRITSCH, 1966, Phys. Rev. **149**, 647.

BENNETT, G. A. and R. B. WILSON, 1966, J. Sci. Instrum. **43**, 669.

BERGMAN, L., 1938, Ultrasonics, translated by H. S. Hatfield (Bell, London).

BERLINCOURT, D., H. JAFFE and L. R. SHIOZAWA, 1961, Phys. Rev. **129**, 1009.

BERLINCOURT, D. A., D. R. CURRAN and H. JAFFE, 1964, Piezoelectric and piezomagnetic materials and their function in transducers. In: Mason, W. P., Ed., Physical acoustics, vol. 1A, 1964 (Academic Press, London) pp. 170–271.

BEYER, R. T. and S. V. LETCHER, 1969, Physical Ultrasonics, (Academic Press, New York).

BIALAS, H. and O. WEIS, 1968, Appl. Phys. Lett. 13, 81.

BIRCH, F., 1947, Phys. Rev. 71, 809.

BLACK, T. D. and P. L. DONOHO, 1968, Phys. Rev. 170, 462.

BLEANEY, B. and K. W. H. STEVENS, 1953, Rep. Progr. Phys. 16, 108.

BLOEMBERGEN, N. and S. WANG, 1954, Phys. Rev. 93, 72.

BLOUNT, E. I., 1959, Phys. Rev. 114, 418.

BOBETIC, V. M., 1964, Phys. Rev. 136A, 1535.

BOBROFF, D. L., 1965, J. Appl. Phys. 36, 1760.

BOGARDUS, E. H., 1965, J. Appl. Phys. 36, 2504.

BOLEF, D. I., 1966, Interaction of acoustic waves with nuclear spins in solids. In: Mason, W. P., ed., Physical acoustics, vol. 4A, 1966. (Academic Press, London) pp. 113–182.

BOLEF, D. I., J. DE KLERK and R. B. GOSSER, 1962, Rev. Sci. Instrum. 33, 631.

BÖMMEL, H. E., 1954, Phys. Rev. 96, 220.

BÖMMEL, H. E. and K. DRANSFELD, 1958, Phys. Rev. Lett. 1, 234.

BÖMMEL, H. E. and K. DRANSFELD, 1959a, J. Acoust. Soc. Amer. 31, 837.

BÖMMEL, H. E. and K. DRANSFELD, 1959b, Phys. Rev. Lett. 2, 298.

BÖMMEL, H. E. and K. DRANSFELD, 1959c, Phys. Rev. Lett. 3, 83.

BÖMMEL, H. E. and K. DRANSFELD, 1960, Phys. Rev. 117, 1245.

BOND, W. L., 1961, J. Sci. Instrum. 38, 63.

BOND, W. L. and E. J. ARMSTRONG, 1943, Bell. Syst. Tech. J. 22, 293.

BORN, M. and K. HUANG, 1954, Dynamical theory of crystal lattices (Oxford University Press).

BORN, M. and E. WOLF, 1965, Principles of optics, 3rd ed. (Pergamon Press, Oxford).

BOZORTH, R. M., 1954, Phys. Rev. 96, 311.

BOZORTH, R. M. and R. W. HAMMING, 1953, Phys. Rev. 89, 865.

BRABIN-SMITH, R. G. and V. W. RAMPTON, 1969, J. Phys. C. 2, 1759.

BREWER, R. G. and K. E. RIECKHOFF, 1964, Phys. Rev. Lett. 13, 334a.

BRILLOUIN, L., 1922, Ann. Phys. (Paris) 17, 88.

BRUGGER, K., 1965, Phys. Rev. 137A, 1826.

BUISSON, R. and J. D. N. CHEEKE, 1969, Phys. Lett. 29A, 200.

BUTCHER, P. N. and N. R. OGG, 1968, Brit. J. Appl. Phys. ser. 2, 1, 1271.

BUTCHER, P. N. and N. R. OGG, 1969, Brit. J. Appl. Phys. ser. 2, 2, 333.

CALLAWAY, J., 1959, Phys. Rev. 113, 1046.

CALLEN, E. R. and H. B. CALLEN, 1960, J. Phys. Chem. Solids 16, 310.

CAOLA, M. J., 1970, J. Phys. C, 3, 27.

CAROLI, C., M. CYROT and P. G. DE GENNES, 1966, Solid State Commun. 4, 17.

CARR, P. H., 1965, J. Acoust. Soc. Amer. 37, 927.

CARR, P. H., 1967, J. Acoust. Soc. Amer. 41, 75.

CARR, P. H. and M. W. P. STRANDBERG, 1962, J. Phys. Chem. Solids 23, 923.

CARR, W. J. and R. SMOLUCHOWSKI, 1951, Phys. Rev. 83, 1236.

CHALLIS, L. J., M. A. McCONACHIE and D. J. WILLIAMS, 1968, Proc. Roy. Soc. A308, 355.

CHALLIS, L. J. and A. M. DE GÖER, 1970, Phys. Lett. 31A, 461.

CHANG, Z.-P., 1965, Phys. Rev. 140A, 1788.

CHIAO, R. Y., C. H. TOWNES and B. P. STOICHEFF, 1964, Phys. Rev. Lett. 12, 592.

CICCARELLO, I. S. and K. DRANSFELD, 1964, Phys. Rev. 134A, 1517.

COHEN, M. G. and E. I. GORDON, 1965, Bell. Syst. Tech. J. 44, 693.

COHEN, M. G. and E. I. GORDON, 1966, Bell. Syst. Tech. J. 45, 945.

COHEN, M. H., M. J. HARRISON and W. A. HARRISON, 1960, Phys. Rev. 117, 937.

COMSTOCK, R. L., 1963, J. Appl. Phys. **34**, 1465.

COOPER, L. N., A. HOUGHTON and H. J. LEE, 1965, Phys. Rev. Lett. **15**, 584.

COX, D. R. and H. D. MILLER, 1965, The theory of stochastic processes (Methuen, London).

CULVAHOUSE, J. W., W. P. UNRUH and D. K. BRICE, 1963, Phys. Rev. **129**, 2430.

DAMON, R. W., 1953, Rev. Mod. Phys. **25**, 239.

DE GENNES, P. G., 1966, Superconductivity of metals and alloys, translated by P. A. Pincus (Benjamin, New York).

DE KLERK, J., 1965, Phys. Rev. **139A**, 1635.

DE KLERK, J., 1966a, J. Appl. Phys. **37**, 4522.

DE KLERK. J., 1966b, Fabrication of vapor-deposited thin film piezoelectric transducers for the study of phonon behaviour in dielectric materials at microwave frequencies. In: Mason, W. P., ed., Physical acoustics, vol. 4A, (Academic Press, London) pp. 195–223.

DE KLERK, J., 1968, Appl. Phys. Lett. **13**, 102.

DE KLERK, J. and E. F. KELLY, 1965, Rev. Sci. Instrum. **36**, 506.

DE KLERK, J., P. G. KLEMENS and E. F. KELLY, 1965, Appl. Phys. Lett. **7**, 264.

DICKINSON, C. S., 1968, J. Sci. Instrum. **1**, 365.

DIXON, R. W., 1967, J. Appl. Phys. **38**, 5149.

DOBROV, W. I., 1964, Phys. Rev. **134A**, 734.

DOBROV, W. I., 1966, Phys. Rev. **146**, 268.

DOLAT, V., J. Ross and R. BRAY, 1968, Appl. Phys. Lett. **13**, 60.

DOOLEY, J. W. and N. TEPLEY, 1969a, Phys. Rev. **181**, 1001.

DOOLEY, J. W. and N. TEPLEY, 1969b, Phys. Rev. **187**, 781.

DORING, W., 1958, Ann. Phys. (Leipzig) **7**, 102.

DRABBLE, J. R. and M. GLUYAS, 1963, The third-order elastic moduli of germanium and silicon. In: Wallis, R. F., ed., Lattice dynamics, Int. Conference on lattice dynamics, Copenhagen, 1963 (Pergamon, Oxford) pp. 607–613.

DRANSFELD, K. and E. SALZMANN, 1970, Excitation, detection, and attenuation of high-frequency elastic surface waves. In: Mason, W. P. and R. N. Thurston, Eds., Physical acoustics, vol. 7, 1970 (Academic Press, London), pp. 219–272.

DUMKE, W. P. and R. R. HAERING, 1962, Phys. Rev. **126**, 1974.

DURAND, G. and A. S. PINE, 1968, IEEE J. Quantum Electron. **QE-4**, 523.

DYSON, F. J., 1956, Phys. Rev. **102**, 1217 and 1230.

EASTMAN, D. E., 1965, Ultrasonic symposium of the sonics and ultrasonics group, IEEE, Boston, Dec. 1965 (unpublished).

ECKSTEIN, S. G., 1963, Phys. Rev. **131**, 1087.

ELLIOTT, R. J. and J. B. PARKINSON, 1967, Proc. Phys. Soc., London, **92**, 1024.

ESAKI, L., 1962, Phys. Rev. Lett. **8**, 4.

FABELINSKII, I. L., 1957, Usp. Fiz. Nauk, **63**, 355.

FABELINSKII, I. L., 1968, Molecular scattering of light, translated by R. T. Beyer (Plenum Press, New York).

FAGEN, E. A. and M. P. GARFUNKEL, 1967, Phys. Rev. Lett. **18**, 897.

FARNELL, G. W., 1961, Can. J. Phys. **39**, 65.

FEHER, E. R., 1964, Phys. Rev. **136A**, 145.

FERGUSON, R. B. and J. H. BURGESS, 1967, Phys. Rev. Lett. **19**, 494.

FIDLER, F. B. and J. W. TUCKER, 1970, J. Phys. C. **3**, 1877.

FLETCHER, J. R., 1970, J. Phys. C, **3**, 1349.

FLETCHER, J. R., F. G. MARSHALL, V. W. RAMPTON, P. M. ROWELL and K. W. H. STEVENS, 1966, Proc. Phys. Soc., London, **88**, 127.

FLEURY, P. A., 1970, Light scattering as a probe of phonons and other excitations. In: Mason, W. P. and R. N. Thurston, eds., Physical acoustics, vol. 6, 1970 (Academic Press, London) pp. 1–64.

FOSTER, N. F., 1963, J. Appl. Phys. **34**, 990.

FOSTER, N. F., 1964, IEEE Trans. Sonics. Ultrason. SU-11, 63.

FOSTER, N. F., 1965, Proc. IEEE **53**, 1400.

FOSTER, N. F., 1967, J. Appl. Phys. **38**, 149.

FOSTER, N. F., G. A. COQUIN, G. A. ROZGONYI and F. A. VANNATTA, 1968, IEEE Trans. Sonics Ultrasonics SU-15, 28.

FRASER, D. B., J. T. KRAUSE and A. H. MEITZLER, 1967, Appl. Phys. Lett. **11**, 308.

FREEMAN, A. J. and R. E. WATSON, 1962, Phys. Rev. **127**, 2058.

FRY, W. J. and F. DUNN, 1962, J. Acoust. Soc. Amer. **34**, 188.

FYNN, G. W., 1950, J. SCI. INSTRUM. **27**, 229.

FYNN, G. W. and W. J. A. POWELL, 1966, Ind. Diamond Rev. **26**, 284.

FYNN, G. W. and W. J. A. POWELL, 1967, R.R.E. Tech. note 709.

GAMMON, R. W., 1968, Solid State Commun. **6**, no. 10, p. xx.

GORDON, E. I. and M. G. COHEN, 1967, Phys. Rev. **153**, 201.

GRACE, M. I., R. W. KEDZIE, M. KESTIGIAN and A. B. SMITH, 1966, Appl. Phys. Lett. **9**, 155.

GRECHUSHNIKOV, B. N., O. V. KACHALOV, N. M. KREINES and M. A. TALALAEV, 1969, Zh. Eksp. Teor. Fiz. **57**, 1570 (Sov. Phys. JETP **30**, 850 [1970]).

GUERMEUR. R., J. JOFFRIN and A. LEVELUT. 1970, Phys. Rev. **B1**, 4304.

GUERMEUR, R., J. JOFFRIN, A. LEVELUT and J. PENNÉ, 1964, Phys. Lett. **13**, 107.

GUERMEUR, R., J. JOFFRIN, A. LEVELUT and J. PENNÉ, 1965a, C.R. Acad. Sci. (Paris) **261**, 4705.

GUERMEUR, R., J. JOFFRIN, A. LEVELUT and J. PENNÉ, 1965b, C.R. Acad. Sci. (Paris) **261**, 5412.

GUERMEUR, R., J. JOFFRIN, A. LEVELUT and J. PENNÉ, 1967, C.R. Acad. Sci. (Paris) **264**, 407.

GUERMEUR, R., J. JOFFRIN, A. LEVELUT and J. PENNÉ, 1968, Solid State Commun. **6**, 519.

GUREVICH, A. G., 1964, Fiz. Tverd. Tela. **6**, 2376 (Sov. Phys. Solid State **6**, 1885 [1965]).

GUREVICH, V. L., 1963, Fiz. Tverd. Tela. **5**, 1222 (Sov. Phys. Solid State **5**, 892 [1963]).

HAAS, C. W., 1966, J. Phys. Chem. Solids **27**, 1687.

HARRISON, M. J., 1960, Phys. Rev. **119**, 1260.

HAYAKAWA, H. and M. KIKUCHI, 1968, Appl. Phys. Lett. **12**, 251.

HAYAKAWA, H. and M. KIKUCHI, 1970, Appl. Phys. Lett. **17**, 73.

HAYDL. W. H.. K. BLOTEKJAER and C. F. QUATE, 1964, J. Acoust. Soc. Amer. **36**, 1670.

HAYDL, W. H. and C. F. QUATE, 1966, Phys. Lett. **20**, 463.

HEARMON, R. F. S., 1953, Acta. Crystallogr. **6**, 331.

HEINE, V., 1960, Group theory in quantum mechanics (Pergamon, London).

HEITLER, W. and E. TELLER, 1936, Proc. Roy. Soc. A155, 629.

HERRING. C., 1954, PHYS. REV. **95**, 954.

HERVOUET, C., J. LEBAILLY, P. L. HUGON and R. VEILEX, 1965, Solid State Commun. **3**, 413.

HICKERNELL, F. S., 1968, Diffusion layer transduction in piezoelectric semiconductors (Sendai Symposium on Acoustoelectronics, preprints, pp. 1–10).

HICKERNELL, F. S. and D. E. ALLEN, 1965, Proc. IEEE 53, 1735.

HOBSON, G. S. and E. G. S. PAIGE, 1966, J. Phys. Soc. Jap., Supplement to vol. 21, 465.

HOGARTH, C. A., 1964, Brit. J. Appl. Phys. 15, 121.

HOLLAND, L., 1961, Vacuum deposition of thin films (Chapman and Hall, London).

HOLSTEIN, T., 1959, Phys. Rev. 113, 479.

HOLSTEIN, T. and H. PRIMAKOFF, 1940, Phys. Rev. 58, 1098.

HOPE, L. L., 1968, Phys. Rev. 166, 883.

HSU, H. and W. KAVAGE, 1965, Phys. Lett. 15, 207.

HUTCHINGS, M. T., 1964, Point-charge calculations of energy levels of magnetic ions in crystalline electric fields. In: Seitz, F. and D. Turnbull, eds., Solid State Physics, vol. 16, 1964 (Academic Press, London) pp. 227–273.

HUTSON, A. R., 1962, Phys. Rev. Lett. 9, 296.

HUTSON, A. R., J. H. McFEE and D. L. WHITE, 1961, Phys. Rev. Lett. 7, 237.

HUTSON, A. R. and D. L. WHITE, 1962, J. Appl. Phys. 33, 40.

ISHIDA, A., C. HAMAGUCHI and Y. INUISHI, 1966, J. Phys. Soc. Jap. 21, 186.

IYENGAR, K. S., 1955, Nature (London) 176, 1119.

JACOBSEN, E. H., 1960, J. Acoust. Soc. Amer. 32, 949.

JACOBSEN, E. H., N. S. SHIREN and E. B. TUCKER, 1959, Phys. Rev. Lett. 3, 81.

JACOBSEN, E. H. and K. W. H. STEVENS, 1963, Phys. Rev. 129, 2036.

JEFKINS, D. M. and R. E. HINES, 1968, J. Sci. Instrum. 1, 690.

KAGANOV, M. I. and YA. M. CHIKVASHVILI, 1961, Fiz. Tverd. Tela. 3, 275 (Sov. Phys. Solid State 3, 200).

KAGANOV, M. I. and V. M. TSUKERNIK, 1959, Zh. Eksp. Teor. Fiz. 36, 224 (Sov. Phys. JETP 9, 151 [1959]).

KAPLAN, H., J. SHAHAM and W. LOW, 1970, Phys. Lett. 31A, 201.

KASTLER, A., 1964a, C.R. Acad. Sci. (Paris) 259, 4233.

KASTLER, A., 1964b, C.R. Acad. Sci. (Paris) 259, 4535.

KASTLER, A., 1965, C.R. Acad. Sci. (Paris) 260, 77.

KIKUCHI, M., 1964, Jap. J. Appl. Phys. 3, 448.

KIKUCHI, M., H. HAYAKAWA and Y. ABE, 1966, Jap. J. Appl. Phys. 5, 1259.

KING, P. J., 1970, J. Phys. C, 3, 500.

KING, P. J. and H. M. ROSENBERG, 1970, Proc. Roy. Soc. A315, 369.

KINO, G. S. and R. ROUTE, 1967, Appl. Phys. Lett. 11, 312.

KIRCHHOFF, B., 1868, Poggend. Ann. 134, 177.

KITTEL, C., 1961, Phys. Rev. Lett. 6, 449.

KITTEL, C., 1963, Quantum theory of solids (Wiley and Sons, New York).

KITTEL, C. and E. ABRAHAMS, 1953, Phys. Rev. 90, 238.

KITTEL, C. and J. H. VAN VLECK, 1960, Phys. Rev. 118, 1231.

KJELDAAS, T., 1959, Phys. Rev. 113, 1473.

KLEIN, R., 1967, Phys. Condens. Matter 6, 38.

KOBYAKOV, I. B., 1966, Kristallografiya, 11, 419 (Sov. Phys. Crystallog. 11, 369 [1966]).

KOOI, C. F., 1963, Phys. Rev. 131, 1070.

KRISCHER, C. and U. INGARD, 1970, Phys. Lett. 32A, 41.

KROLL, N. M., 1965, J. Appl. Phys. 36, 34.

KRONIG, R., 1939, Physica 6, 33.

KWOK, P. C. and P. B. MILLER, 1966, Phys. Rev. 146, 592.

KYAME, J. J., 1954, J. Acoust. Soc. Amer. 26, 990.

LAMB, J., M. REDWOOD and Z. SHTEINSHLIEFER, 1959, Phys. Rev. Lett. 3, 28.

LAMB, J. and J. RICHTER, 1967, J. Acoust. Soc. Amer. 41, 1043.

LANDAU, L. D. and E. M. LIFSHITZ, 1965, Quantum mechanics, 2nd. ed. (Pergamon Press, Oxford) p. 132.

LANDAU, L. and G. RUMER, 1937, Phys. Z. Sowjetunion 11, 18.

LANDOLT, H. and R. BORNSTEIN, 1966, Landolt–Bornstein New Series, Group III, vol. 1, K.-H. Hellwege, ed. (Springer-Verlag, Berlin) pp. 136–139.

LANGE. J. N., 1968, Phys. Rev. 176, 1030.

LAVAL, J., 1951, C.R. Acad. Sci. (Paris) 232, 1947.

LECRAW, R. C. and R. L. COMSTOCK, 1965, Magnetoelastic interactions in ferromagnetic insulators. In: Mason, W. P., ed., Physical acoustics, vol. 3B, 1965 (Academic Press, London) pp. 127–199.

LEE, E. W., 1955, Rep. Progr. Phys. 18, 184.

LEWIS, M. F., 1965, Phys. Lett. 17, 183.

LEWIS, M. F., 1968, J. Acoust. Soc. Amer. 44, 713.

LEWIS, M. F. and D. G. SCOTTER, 1968, Phys. Lett. 28A, 303.

LEWIS, M. F. and A. M. STONEHAM, 1967, Phys. Rev. 164, 271.

LOCATELLI, M., P. JAUSSAUD and A-M. DE GÖER, 1970, C.R. Acad. Sci. (Paris) 270, 620.

LORD, A. E., 1968, Phys. Kondens. Mater. 7, 232.

LOUDON, R., 1960, Phys. Rev. 119, 919.

LOW. W., 1960, Paramagnetic resonance in solids. In: Seitz, F. and D. Turnbull, Solid state physics, supplement 2, 1960 (Academic Press, London).

LOW, W. and M. WEGER, 1960, Phys. Rev. 118, 1119.

LUTHI, B., 1963, Phys. Lett. 3, 285.

LYASHENKO. S. P. and V. K. MILOSLAVSKII. 1964, Opt. and Spectrosc. (USSR) 16, 80.

LYNTON, E. A., 1969, Superconductivity, 3rd. ed. (Methuen, London).

MACDONALD, J. R., 1951, Proc. Phys. Soc. (London) A64, 968.

MACKINTOSH, A. R., 1964, The interaction of long-wavelength phonons with electrons. In: Bak, T. A., ed., Phonons and phonon interactions, 1964 (Benjamin, New York) pp. 181–220.

MAKI, K., 1964, Physics (Long Island City, N.Y.) 1, 21.

MAKI, K., 1966, Phys. Rev. 148, 370.

MAKI, K., 1967, Phys. Rev. 156, 437.

MAKI, K. and T. TSUZUKI, 1965, Phys. Rev. 139A, 868.

MALBON, R. M., D. J. WALSH and D. K. WINSLOW, 1967, Appl. Phys. Lett. 10, 9.

MANDL, F., 1957, Quantum mechanics (Butterworths Scientific Publications, London).

MARCH, N. H., W. H. YOUNG and S. SAMPANTHAR, 1967, The many-body problem in quantum mechanics (Cambridge Univ. Press).

MARIS, H. J., 1964, Phil. Mag. 9, 901.

MARIS, H. J., 1965, Phys. Lett. 17, 228.

MARSHALL, F. G. and V. W. RAMPTON, 1968, J. Phys. C, 2, 594.

MASON, W. P. and T. B. BATEMAN, 1964, J. Acoust. Soc. Amer. 36, 644.

MASON, W. P. and T. B. BATEMAN, 1966, J. Acoust. Soc. Amer. 40, 852.

MATTHEWS, H. and R. C. LECRAW, 1962, Phys. Rev. Lett. 8, 397.

MATTHEWS, H. and F. R. MORGENTHALER, 1964, Phys. Rev. Lett. 13, 614.

MATTUCK, R. D. and M. W. P. STRANDBERG, 1960, Phys. Rev. 119, 1204.

MCCALL, S. L. and E. L. HAHN, 1969, Phys. Rev. 183, 457.

MCFEE, J. H., 1963, J. Appl. Phys. 34, 1548.

MCFEE, J. H., P. K. TIEN and H. L. HODGES, 1967, J. Appl. Phys. 38, 1721.

MCLEAN, F. B. and A. HOUGHTON, 1967, Phys. Rev. 157, 350.

MCLEAN, F. B. and A. HOUGHTON, 1968, Ann. Phys. (New York) 48, 43.

MCMAHON. D. H., 1964, Phys. Rev. 134A, 128.

MERKULOV, L. G., 1959, Akust. Zh. 5, 432 (Sov. Phys. Acoust. 5, 444 [1960]).

MESSIAH, A., 1961, Quantum mechanics (North-Holland, Amsterdam).

MEYER, N. I. and M. H. JORGENSEN, 1966, Phys. Lett. 20, 450.

MEYER, O., 1874, J. Rein. Angew. Math. 78, 130.

MICHEL-CALENDINI, F. M. O. and M. R. KIBLER, 1968, Theor. Chim. Acta. 10, 367.

MIKOSHIBA, N., 1958, J. Phys. Soc. Jap. 13, 759.

MIKOSHIBA, N. and H. OZAKI, 1968, J. Phys. Soc. Jap. 24, 514.

MILLS, D. L., 1965, Phys. Rev. 139A, 1640.

MOORE, A. R., 1968, Appl. Phys. Lett. 13, 126.

MORENO, T., 1958, Microwave transmission design data (Dover reprints, New York).

MORGENTHALER, F. R., 1960, J. Appl. Phys. 31, 95 S.

MORGENTHALER, F. R., 1962, see White, R. M. and E. Schlomann, Microwave Laboratory Report, no. 909, Stanford Univ., 1962 (unpublished).

MOROCHA, A. K., 1967, Zh. Eksp. Teor. Fiz. 53, 1835 (Sov. Phys. JETP 26, 1046 [1968]).

MULLER, E. R. and J. W. TUCKER, 1966, Proc. Phys. Soc. (London) 88, 693.

MULLER, E. R. and J. W. TUCKER, 1967, Can. J. Phys. 45, 2443.

MURNAGHAN, F. D., 1951, Finite deformation of an elastic solid (Wiley and Sons, New York).

NAKAMURA, K. and J. YAMASHITA, 1968, Progr. Theor. Phys. 39, 545.

NAVA, R., I. AZRT, I. CICCARELLO and K. DRANSFELD, 1964, Phys. Rev. 134A, 581.

NILL, K. W. and A. L. MCWHORTER, 1966, J. Phys. Soc. Jap., Supplement to vol. 21, 755.

NYE, J. F., 1957, Physical properties of crystals (Oxford Univ. Press).

ORBACH, R., 1960, Thesis, Univ. of California, Berkeley.

ORBACH, R., 1961, Proc. Roy. Soc. A264, 458.

ORBACH, R. and L. A. VREDEVOE, 1964, Physics (Long Island City, New York) 1, 91.

OZAKI, H. and N. MIKOSHIBA, 1966, J. Phys. Soc. Jap. 21, 2486.

OZAKI, H. and N. MIKOSHIBA, 1968, Jap. J. Appl. Phys. 7, 1305.

PAKE, G. E., 1962, Paramagnetic resonance (Frontiers in Physics Series), (Benjamin, New York).

PARAMENTER, R. H., 1953, Phys. Rev. 89, 990.

PEVERLEY, J. R., 1966, Ultrasonics and the Fermi surfaces of the monovalent metals. In: Mason, W. P., ed., Physical acoustics, vol. 4A, 1966 (Academic Press, London) pp. 353–378.

PINE, A. S., 1969, Phys. Rev. 185, 1187.

PIPPARD, A. B., 1955, Phil. Mag. 46, 1104.

PIROZHKOV, M. I. and V. M. CHERNOV, 1967, Akust. Zh. 13, 251. (Sov. Phys. Acoust. 13, 215, [1967]).

POCKELS, F., 1889, Ann. Phys. Chem. 37, 144, 267 and 372.

POCKELS, F., 1894, Abhandl Ges. Wiss. Gottingen 39, 1.

POCKELS, F., 1906, Lehrbuch der Kristalloptik (Teubuer, Leipzig).

POMERANCHUK, I., 1942, J. Phys. (USSR) 6, 237.

POMERANTZ, M., 1961, Phys. Lett. 7, 312.

POMERANTZ, M., 1965, Phys. Rev. 139A, 501.

PROHOFSKY, E. W., 1964, Phys. Rev. 134A, 1302.

QUATE, C. F., C. D. W. WILKINSON and D. K. WINSLOW, 1965, Proc. IEEE 53, 1604.

QUENTIN, G. and J. M. THUILLIER, 1966, J. Phys. Soc. Jap., Supplement to vol. 21, 493.

RAMAN, C. V. and N. S. N. NATH, 1935, Proc. Indian Acad. Sci. A2, 406 and 413.
RAMAN, C. V. and N. S. N. NATH, 1936, Proc. Indian Acad. Sci. A3, 75 and 119.
RAMAN, C. V. and K. S. VISWANATHAN, 1955, Proc. Indian Acad. Sci. A42, 1 and 51.
RAY, D. K., T. RAY and P. RUDRA, 1966, Proc. Phys. Soc, London 87, 485.
RICKAYZEN, G., 1965, Theory of superconductivity (Wiley and Sons, New York).
RIDLEY, B. K. and J. WILKINSON, 1969, J. Phys. C, 2, 1299.
RINGO, G. R., J. W. FITZGERALD and B. G. HURDLE, 1947, Phys. Rev. 72, 87.
ROBERTS, B. W., 1961, Phys. Rev. Lett. 6, 453.
ROSENBERG, H. M. and J. K. WIGMORE, 1967, Proc. Roy. Soc. A302, 69.
ROSS, J. B. and R. BRAY, 1966, Bull. Amer. Phys. Soc. 11, 173.
ROUNDY, V. and D. L. MILLS, 1970, Phys. Rev. B1, 3703.
ROUTE, R. K. and G. S. KINO, 1969a, IBM J. Res. Develop. 13, 507.
ROUTE, R. K. and G. S. KINO, 1969b, Appl. Phys. Lett. 14, 97.
ROZGONYI, G. A. and W. J. POLITO, 1966, Appl. Phys. Lett. 8, 220.

SABISKY, E. S. and C. H. ANDERSON, 1968, Appl. Phys. Lett. 13, 214.
SCHLOMANN, E., J. J. GREEN and U. MILANO, 1960, J. Appl. Phys. 31, 386 S.
SCHWARTZ, M., 1970, Information transmission, modulation and noise, 2nd. ed. (McGraw Hill, New York).
SEARS, V. F., 1964, Proc. Phys. Soc., London 84, 951.
SEAVEY, M. H., 1963, IRE Trans. Ultrason. Eng. 10, 49.
SHAPIRA, Y. and B. LAX, 1965, Phys. Rev. 138A, 1191.
SHIREN, N. S., 1961, Phys. Rev. Lett. 6, 168.
SHIREN, N. S., 1962a, Bull. Amer. Phys. Soc. 7, 29.
SHIREN, N. S., 1962b, Phys. Rev. 128, 2103.
SHIREN, N. S., 1962c, Comparison of ultrasonic spin resonance measurements with paramagnetic relaxation theory. In: Smidt, J., ed., Magnetic and electric resonance and relaxation, 1963, The Eleventh Colloque Ampère, Eindhoven, 1962 (North-Holland, Amsterdam) pp. 114–122.
SHIREN, N. S., 1966, Phys. Lett. 20, 10.
SHIREN, N. S., 1970, Phys. Rev. B2, 2471.
SILVA, P. O. and R. BRAY, 1965, Phys. Rev. Lett. 14, 372.
SIMONS, S., 1963, Proc. Phys. Soc. (London) 82, 401.
SIMONS, S., 1964, Proc. Phys. Soc. (London) 83, 749.
SLONIMSKII, G. L., 1937, Zh. Eksp. Teor. Fiz. 7, 1457.
SMITH, H. I., 1965, J. Acoust. Soc. Amer. 37, 928.
SMITH, R. A., 1961, Semiconductors (Cambridge Univ. Press).
SMITH, R. W., 1962, Phys. Rev. Lett. 9, 87.
SOUTHGATE, P. D. and H. N. SPECTOR, 1965, J. Appl. Phys. 36, 3728.
SPECTOR, H. N., 1962a, Phys. Rev. 125, 1192.
SPECTOR, H. N., 1962b, Phys. Rev. 125, 1880.
SPECTOR, H. N., 1962c, Phys. Rev. 127, 1084.
SPECTOR, H. N., 1963a, Phys. Rev. 130, 910.
SPECTOR, H. N., 1963b, Phys. Rev. 131, 2512.
SPECTOR, H. N., 1968, Phys. Rev. 165, 562.
STARUNOV, V. S. and I. L. FABELINSKII, 1969, Usp. Fiz. Nauk 98, 441 (Sov. Phys. Uspkh. 12, 463 [1970]).
STEELE. M. C., 1967, RCA Rev. 28, 58.
STEPHENSON, J. G., 1963, Electronics 36, 46.
STEVENS, K. W. H., 1952, Proc. Phys. Soc. (London) LXV, 209.
STEVENS, K. W. H., 1967, Rep. Progr. Phys. XXX, 189.
STEVENS, K. W. H. and J. W. TUCKER, 1965, Phys. Lett. 14, 291.
STEVENS, K. W. H. and H. A. M. VAN EEKELEN, 1967, Proc. Phys. Soc. (London) 92, 680.

STEVENS, K. W. H. and D. WALSH, 1968, J. Phys. C, 1, 1554.

STONEHAM, A. M., 1966a, Proc. Phys. Soc. (London) 89, 909.

STONEHAM, A. M., 1966b, Phys. Lett. 21, 621.

STURGE, M. D., 1967, The Jahn-Teller effect in solids. In: Seitz, F., D. Turnbull and H. Ehrenreich, eds., Solid State Physics, vol. 20 (Academic Press, London) pp. 91–211.

SUHL, H. J., 1957, J. Phys. Chem. Solids 1, 209.

SUSSE, C., 1955, J. Phys. Radium 16, 348.

TEPLEY, N. 1965, Proc. IEEE 53, 1586.

TER HAAR, D., 1954, Elements of statistical mechanics, (Holt, Rinehart and Winston, New York).

TIEN, P. K., 1968, Phys. Rev. 171, 970.

TITTMANN, B. R., 1970, Phys. Rev. B2, 625.

TITTMANN, B. R. and H. E. BÖMMEL, 1967, Rev. Sci. Instrum. 38, 1491.

TITTMANN, B. R. and H. E. BÖMMEL, 1968, Rev. Sci. Instrum. 39. 614.

TOLMAN, R. C., 1938, The principles of statistical mechanics (Oxford Univ. Press, London) p. 390.

TOXEN. A. M. and S. TAUSAL. 1965, Phys. Rev. 137A, 211.

TRUELL, R. and C. ELBAUM, 1962, High frequency ultrasonic stress waves in solids. In: Flugge, S., ed., Handbuch der Physik, band X 1/2, 1962, (Springer-Verlag, Berlin), pp. 154–258.

TRUELL, R., C. ELBAUM, and B. B. CHICK, 1969, Ultrasonic methods in solid state physics, (Academic Press, New York).

TRUELL, R. and W. OATES, 1963, J. Acoust. Soc. Amer. 35, 1382.

TUCKER, E. B., 1961a, Phys. Rev. Lett. 6, 183.

TUCKER, E. B., 1961b, Phys. Rev. Lett. 6, 547.

TUCKER, E. B., 1964, The phonon maser. In: Grivet, P. and N. Bloembergen, eds., Quantum Electronics, Paris 1963 Conference, vol. 2 (Columbia Univ. Press, New York) pp. 1787–1800.

TUCKER, E. B., 1965, Proc. IEEE 53, 1547.

TUCKER, E. B., 1966a, Phys. Rev. 143, 264.

TUCKER, E. B., 1966b, Paramagnetic spin–phonon interaction in crystals. In: Mason, W. P., ed., Physical acoustics, vol. 4A (Academic Press, London) pp. 47–112.

TUCKER, J. W., 1965, Proc. Phys. Soc. (London) 85, 559.

TURNER, E. H., 1960, Phys. Rev. Lett. 5, 100.

TWYMAN, F., 1952, Prism and lens making (Hilger and Watts Ltd., London).

UCHIDA, I., T. ISHIGURO, Y. SASAKI and T. SUZUKI, 1964, J. Phys. Soc. Jap. 19, 674.

VAN VLECK, J. H., 1940, Phys. Rev. 57, 426.

VAN VLECK, J. H., 1948, Phys. Rev. 74, 1168.

VOIGT, W., 1892, Ann. Phys. (Leipzig) 47, 671.

VON DER LAGE, F. C. and H. A. BETHE, 1947, Phys. Rev. 71, 612.

VON GUTFELD, R. T. and A. H. NETHERCOT, 1964, Phys. Rev. Lett. 12, 641.

WALKER, J. G., H. J. WILLIAMS and R. M. BOZORTH, 1949, Rev. Sci. Instrum. 20, 947.

WALKER, L. R., 1957, Phys. Rev. 105, 390.

WALLER, I., 1932, Z. Phys. 79, 370.

WAUK, M. T. and D. K. WINSLOW, 1968, Appl. Phys. Lett. 13, 286.

WEBER, M. J. and R. W. BIERIG, 1964, Phys. Rev. 134A, 1492.

WEINREICH, G., 1956, Phys. Rev. 104, 321.

WETSEL, G. C., C. G. ROBERTS. E. L. KITTS and P. O'HAGAN, 1969, Phys. Lett. 30A, 35.

WHITE. D. L.. 1961, IRE Int. Con. Rec., part 6, 304.

WHITE, D. L., 1962, J. Appl. Phys. 33, 2547.

WHITE, D. L., 1964, The depletion layer and other high frequency transducers using fundamental modes. In: Mason, W. P., ed., Physical acoustics, vol. 1B (Academic Press, London) pp. 321–352.

WIGEN, P. E., W. I. DOBROV and M. R. SHAUBARGER, 1965, Phys. Rev. 140A, 1827.

WIGMORE, J. K., 1968, Appl. Phys. Lett. 13, 73.

WILLARD, G. W., 1949, J. Acoust, Soc. Amer. 21, 101.

WILSON, R. B., 1967, J. Sci. Instrum. 44, 159.

WINSLOW, D. K., 1968, IEEE Trans. Sonics Ultrasonics SU-15, 64.

WINTERLING, G., W. HEINICKE and K. DRANSFELD, 1969, Optical determination of the ultrasonic absorption in quartz at 29 GHz. In: Wright, G. B., ed., Light scattering spectra in solids (Springer-Verlag, New York) pp. 589–591.

WOODRUFF, T. O. and H. EHRENREICH, 1961, Phys. Rev. 123, 1553.

YAMASHITA, J. and K. NAKAMURA, 1965, Progr. Theor. Phys. 33, 1022.

YOLIN, E. M., 1965, Proc. Phys. Soc. (London) 85, 759.

ZENER, C., 1948, Elasticity and anelasticity of metals (Univ. of Chicago Press, Chicago, Illinois).

ZENER, C., 1954, Phys. Rev. 96, 1335.

ZUCKER, J. and S. ZEMON, 1966, Appl. Phys. Lett. 9, 398.

ZYLBERSZTEJN, A., 1967, Phys. Rev. Lett. 19, 838.

AUTHOR INDEX

This index includes those authors implied by 'et al.' in the text.

TUCKER
RAMPTON

MICROWAVE ULTRASONICS IN SOLID STATE PHYSICS